Interior Columbia Basin Life-Cycle Modeling

May 23, 2017

Table of Contents

1. Intro (Rich Zabel, Tom Cooney, Chris Jordan)
2. Habitat
    a. Estimating the fish rearing capacity of freshwater systems: a review of approaches for salmonids in the Columbia River basin (Morgan H. Bond, Corey Phillis, Michael Beakes, Nicolaas Bouwes, J. Ryan Bellmore, Joe Benjamin, Seth M. White, Kevin See, Correigh M. Greene, Tim Beechie, Chris Jordan, Richard W. Zabel)
    b. A habitat expansion approach to estimating parr rearing capacity of spring and summer Chinook in the Columbia River Basin (Morgan H. Bond, Tyler G. Nodine, Tim Beechie, Rich Zabel)
    c. Modeling juvenile Chinook production in 22 Columbia River stream locations (Martin Liermann, Morgan H. Bond)
    d. Movement & Survival based on Mark-Recapture data (W. Carl Saunders, Kevin See, Shubha Pandit, Eric Buhle, Nicolaas Bouwes, Pamela Nelle, Tom Degroseiller, Keith VanDenBroek, Chris Jordan)
    e. Habitat Actions and Chinook parr-adult survival (Charlie Paulsen, Tim Fisher)
3. Ocean/Estuary survival based on PIT-TAG data (Brian Burke, Lisa Crozier, Jeff Jorgensen, Tom Cooney, Rich Zabel)
4. Hydro Modeling
    a. Integrated Population Model of Grande Ronde Basin (Bob Lessard)
    b. The COMPASS Model for Assessing Juvenile Salmon Passage through the Hydropower Systems on the Snake and Columbia Rivers (James R. Faulkner, Daniel L. Widener, and Richard W. Zabel)
5. Toxics as an obstacle to salmon recovery in the Columbia River Basin (Jessica Lundin, Lyndal Johnson, Julann Spromberg, Cathy Laetz, David Baldwin, Nathaniel L. Scholz)
    a. Introduction
    b. Spatial Vulnerability Analysis for Pesticides in the Columbia River Basin
    c. Impacts of persistent organic pollutants (POPs) on ESA-listed fish
    d. Industrial and municipal wastewater and untreated stormwater: increased risks for salmonids
    e. Population-scale benefits from pollution remediation strategies
    f. Successes and next steps
6. Ecological Interactions
    a. Population-specific migration timing affects en route survival of adult Chinook salmon through the Lower Columbia River (Mark Sorel, A. Michelle Wargo Rub, Rich Zabel)
    b. Avian predation management effects (Charlie Paulsen)
    c. Incorporating food web dynamics into life cycle modeling (Joseph R. Benjamin, J. Ryan Bellmore, Emily Whitney, and Jason Dunham)
7. Simple Population Model
    a. Using integrated population models to evaluate natural and anthropogenic risk factors for Pacific salmon (Eric R. Buhle, Mark D. Scheuerell, James T. Thorson)
8. Intermediate Model

    a. Building A State-Space Life Cycle Model for Naturally Produced Snake River Fall Chinook Salmon (Russel W. Perry., John M. Plumb, Kenneth F. Tiffan, William P. Connor, Thomas D. Cooney, William Young)
9. Full Model
    a. Grande Ronde Spring Chinook Populations: Juvenile Based Models (Thomas D. Cooney, Brian C. Jonasson, Edwin W. Sedell, Timothy L. Hoffnagle, Richard W. Carmichael)
    b. Wenatchee River spring-run Chinook salmon life-cycle model: hatchery effects, calibration, and sensitivity analyses (Jeff Jorgensen, Andrew Murdoch, Jeremy Cram, Mark Sorel, Tracy Hillman, Greer Maier, Charlie Paulsen, Tom Cooney, Rich Zabel, and Chris Jordan)
    c. Themes of climate impacts on Salmon River Basin Salmon: multiple limiting factors, correlation in climate drivers, and cumulative life cycle effects (Lisa Crozier, Rich Zabel, Brian Burke)
    d. ISEMP/CHaMP Life-cycle models– Entiat, John Day, Lemhi, Habitat Actions (W. Carl Saunders, Nick Weber, Nicolass Bouwes, Pete McHugh, Eric Buhle, Kevin See, Braden Lott, Chris Beasely, Jody White, Shubha Pandit, Pamella Nelle, Tom Desgroseillier, Keith van den Broek, Mark Armour, Matt Nahorniak, and Chris Jordon)
    e. Yakama R *Oncorhynchus mykiss* populations (Neala Kendall, Chris Frederiksen)
    f. Catherine Creek spring Chinook Life Cycle Model (Peter McHugh, Casey Justice, Seth White, Dale McCullough, and Nicolaas Bouwes)
10. Meta Population
    a. Assessing salmon spatial structure and metapopulation dynamics (Aimee Fullerton, Chris Jordan, Tom Cooney, Rich Zabel and Mike Ford)
11. Communication with Managers (Greg Seiglitz)

CHAPTER 1. INTRODUCTION

Rich Zabel (NWFSC), Tom Cooney (NWFSC), Chris Jordan (NWFSC)

This document is the second document on Life-Cycle modeling that is being reviewed by the Independent Scientific Advisory Board (ISAB). The first review took place in 2013 (Zabel et 2013, ISAB 2013), and this document is a follow up to that one. We have made many improvements since 2013. Here are some highlights:

We have developed several methods to estimate habitat capacity (Bond et al. Chapter 2a, 2b, Liermann et al. Chapter. 2c, Jordan et al Chapter 9d). The ISAB recommended working with our Watershed program, and this is partially in response. Overall, we have gotten closer to establishing relationships between fish performance and habitat restoration. We provide several examples of this (e.g., Bond et al. Chapter 2a, 2b; Benjamin et al., Chapter 6c; Cooney et al., Chapter 9a; Jordan et al., Chapter 9d).

We have improved out modeling of ocean/estuary survival (Burke et al., Chapter 3). We have adopted an approach that utilizes PIT-tag data instead of using dam counts. This has improved accuracy because PIT tags are detected at Bonneville Dam, for both juveniles and adults, so we don't need to "back out" survival through the hydrosystem. Further, because the modeling is based on individuals, we can incorporate the effect of arrival timing in our estimates.

In hydro modeling, both CSS and COMPASS have improved. Lessard (Chapter 4a) has developed an integrated life-cycle model for the Grande Ronde basin that incorporates a covariate related to powerhouse exposure. With COMPASS, Faulkner et al. (Chapter 4b) have calibrated the model to the most recent data and have developed population-specific estimates for survival through the hydrosystem.

In the last review, the ISAB recommended that we consider exposure to toxics as an impact on salmon populations. Chapter 5 (Scholz et al., Chapter 5) represents a comprehensive treatment of this topic. The chapter deals with the spatial location of various sources of toxics to the response of populations to toxic loads. It also presents a population model of the impacts of toxic exposure on population performance.

In regard to ecological interactions, we have expanded our modeling substantially. The avian predation section (Paulsen, Chapter 6b) has been updated with recent analyses. California Sea

Lions have expanded their presence in the Columbia River estuary to become a major threat. Accordingly, we have developed a module that covers population-specific mortality due to predation by sea lions (Sorel et al., Chapter 6a). And finally, the Methow food web model (Benjamin, Chapter 6c) has improved greatly.

Types of Models

We developed models of varying degrees of complexity to help us address issues of data availability to inform various actions. We are working on three classes of life cycle models – Simple, Intermediate and Complex – that vary in their data needs, spatial and temporal resolution and complexity, but most importantly, are designed for specific management applications. The modeling approaches are distinct, but complementary, and it is our plan to continue their development, eventually hybridizing the methods to optimize model design and performance.

Simple Model

For our uses, we define the "simple" model as a spawner-to-spawner model with just enough information (e.g., harvest rates, age-composition data, hatchery releases) to represent key drivers that affect population dynamics (Buhle et al., chapter 7). We developed Integrated Population Models (IPMs), which are Bayesian and state-space, to represent this type of model. These models are useful for capturing the overall population dynamics and for assigning risk to populations under current conditions.

Intermediate Model

These models still use Integrated Population Modeling. However they expand upon the simple models to add additional factors and/or life stages. The Snake River fall chinook model (Perry et al., Chapter 8) and the Grande Ronde Integrated Population Models (Lessard, Chapter 4a) are examples of this. In addition, we envision several other models that focus on particular drivers such as hydro, harvest, parr production, or pinniped predation. With these models, we can examine the effects of one to a few impacts on populations.

Complex model

These models represent a number of different life stages and drivers. They are too complex to be represented by an integrated population model; however, they are still very reliant on data. Their main purposes are to look at a "portfolio" of actions and to serve as 'test beds' for evaluating less data intensive methods for simulating action effects with intermediate models that can be applied to populations with less data. Chapter 9 provides several examples of this type of model.

We are developing methods (e.g., Jorgensen et al., Chapter 9) to calibrate these models such that their "baseline" scenarios have the same statistical properties as current conditions.

Synergistic Interactions

One of the benefits of having models of different levels of complexity is that we can compare results across models and foster the development of hybrid approaches. For example, the Integrated Population Model approach of simultaneously estimating population processes and population behavior is a much more statistically robust method than the purely simulation based stage-based models. Unfortunately, the biological complexity of salmonid life cycles that account for spatially and temporally explicit management actions are beyond the capacity of IPMs. However, using IPMs to estimate population process values where possible and incorporating these as parameters in more complex simulation models makes the best advantage of the available data. Also, we can "borrow" relationships from one population and apply it to another population.

Spatial Modeling

Interrelationships within and among populations

It is quite clear that salmon populations are not independent units; however, it is not always clear when and where demographic isolation occurs. It is also clear that basic fish-habitat relationships exist by species; but again, it is not always clear the degree to which these relationships can be applied broadly within and across populations and ESUs. These constraints may imply that to apply life cycle based management tools, every salmonid population requires a complete and locally specific parameterization effort. We take, however, a somewhat moderated view, by assuming that there are broad commonalities to salmonid biology, watershed processes, and their interactions, across populations within the interior Columbia River Basin. As such, "borrowing" data within and among populations is a reasonable approach to allow the development of complex life cycle models in what may appear to be data "poor" population areas.

Also, we plan to use spatial or meta-population models to help prioritize among populations.

Collaborative Effort

As was the case when the ISAB first reviewed this project, all of the work resulting from this project represents an extensive collaborative effort among scientists from federal, state, and tribal agencies and universities. We also acknowledge and are encouraged that each model is quite different, with each model development process following a different trajectory. We believe that this approach encourages creativity and results in more robust products with increased collective understanding and buy-in.

The collaborative effort has been distributed across participating entities, but also across the geographic domains that the participants represent. For example, the following life cycle model sectors have advanced particular features of the overall project

Grande Ronde – timing of actions; supplementation

Wenatchee – Model calibration and sensitivity analysis

Salmon River Basin – climate change

Middle Fork John Day – reach-scale restoration actions to watershed impact

ISEMP/CHaMP – habitat assessment toolkit

Yakama River steelhead – flow management, life-history diversity.

Communication with Managers

Because scientists are notoriously bad at communicating with non-scientist, we have asked some managers to provide us with the type of information they need in the decision-making process. This has led to the final chapter in our report – *Communication with Managers*. We have begun to compile some useful information (e.g., maps and fact sheets) that can help managers better understand what types of products we are producing.

What are we missing?

Climate change

Due to resource limitations, we were not able to comprehensively deal with climate change, beyond what is covered in the Salmon River basin model (Crozier et al., Chapter 9). Climate and climate change can affect multiple life stages of the salmon life history: pre-spawn mortality, parr survival, downstream migration through the hydrosystem, ocean/estuary survival, and upstream survival.

NOAA Fisheries is currently conducting a vulnerability analysis for West Coast fish species, including salmon. They identified five life stages – egg, juvenile freshwater, estuary, ocean, and adult freshwater – and a life-cycle component and assessed the vulnerability of each salmon Evolutionarily Significant Unit (ESU) to climate change in each life stage. We plan to take the information on vulnerability of each life stage and compare that to opportunities for action to develop a comprehensive plan to deal with climate change.

Non-indigenous species.

In our previous review, the ISAB identified non-indigenous species as a threat that we should consider. Unfortunately, this is the one area we did not get to. There has been little research to connect NIS to salmon survival, and this is one of the problems.

Portfolio of life-stage specific actions

One of the advantages of Life-Cycle modeling is the ability to assess impacts at multiple life stages by translating changes in life-stage demographic rates to changes in viability metrics. In this way, we can put together a portfolio of actions to compare across different portfolios. We are proposing an adaptive management strategy where we use life-cycle models to design and assess alternative suites of actions. Prospective life-cycle models are used to develop alternative portfolios of actions. Alternative portfolios can be compared with a variety of performance metrics, such as in a cost-benefit or extinction risk framework. The life cycle models also play a critical role in an adaptive management context as they make testable, quantitative predictions.

These predictions are treated as hypotheses, and an appropriately designed monitoring program can assess the predicted outcome and can be used to evaluate and improve the analytical framework when the outcomes differ from expected.

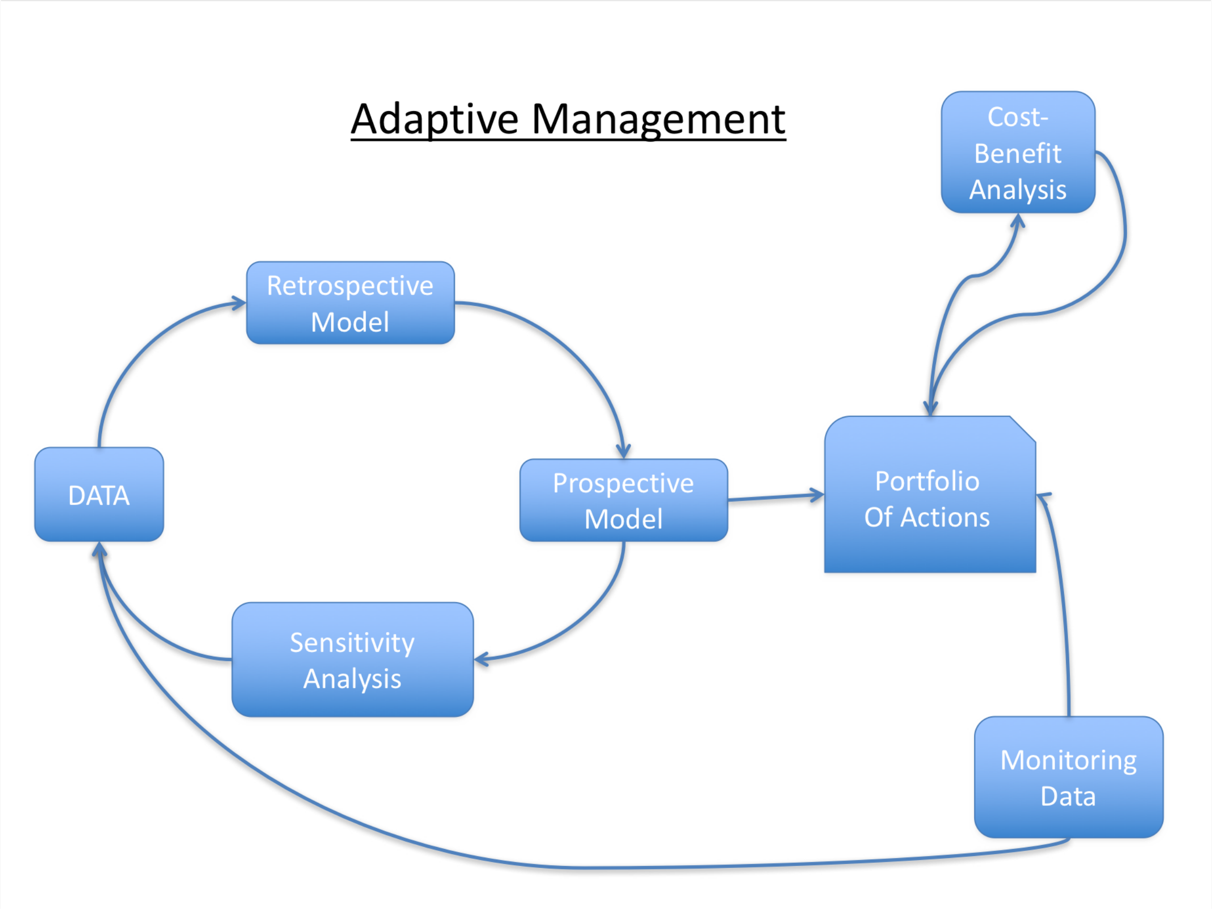

Figure 1. Adaptive Management scheme. Prospective life-cycle models are used to develop alternative portfolios of actions. Alternative portfolios can be compared in a cost-benefit analysis. Once a portfolio is chosen, we will use monitoring data to assess whether actions were effective.

Promote consistent use if available info & assumptions

Developing a suite of analytical tools to support decision-making around salmonid recovery actions in the Columbia River basin is critical given the scale of the region (3 species, 6 ESUs, more than 100 populations) and diversity of potential management actions (Hydro, Hatchery, Habitat….). Life cycle models are the obvious choice in this situation because they enforce consistent use of population and habitat data and constrain how management actions impacts are evaluated. As such, life cycle models represent a template that explicitly accounts for the diversity of population settings and management actions.

Applications (inform status assessments, strategic planning etc)

All assessments of salmon population management in an ESA (and MSFMA) context can be supported by life cycle modeling. Simple life cycle models are currently used in stock forecasting for most ocean salmon harvest. More complex life cycle models that are spatially explicit or have finer temporal resolution are used to support water management in the Sacrament River delta system. All ESA listing and status decisions are supported with full life cycle evaluations of extinction risk or population persistence. Consultations on reach-scale single habitat alterations may appear to be too small and too isolated to be applicable to a life cycle modeling based evaluation; however, the methods could be applied in a regional context if consultations were bundled spatially to a larger-scale.

Systematic framework for setting rme priorities

In the context of Adaptive Management, life cycle models both form the analytical framework for making quantitative, testable predictions of management action outcomes, but also form the basis for the data or monitoring needs. The data needs of a life cycle model based decision support system are both to parameterize the population processes represented in the model (e.g., stage specific abundance, survival and capacity), and to test the population response to management actions (e.g., fish-habitat relationships, mainstem project survival, hatchery-wild interactions). In either case, the life cycle model is the use-case for the monitoring data and as such should be used to set the spatial and temporal resolution of sampling, choice of monitoring metrics, and ultimately the data quality in terms of sampling and measurement uncertainty. Having an analytical tool as the consumer of monitoring data allows direct assessments of the consequence of variation in data quality since the impact of data quality can be immediately translated into the quality of decision-making in terms of risk of making an incorrect decision.

Output of life cycle models

With this round of modeling, we plan to express model outputs in terms of VSP scores.

Productivity and Abundance

Here we present the idea of "risk plots", which characterize the risk and uncertainty of populations. The plots can represent current risk (measured as probability of falling below QET), as well as risk under a variety of alternatives. Because the plots essentially summarize model outputs (abundance and recruits per spawner), they can be applied to an class of model, from simple to complex. They allow for comparison across alternatives, models and populations.

Before we describe our approach to estimating VSP based on productivity and abundance, we provide some definitions:

Run: A single iteration of the model with a given set of parameters for a set number of years (usually fifty or a hundred years). For each run we keep track of the population trajectory so we can calculate a suite of model metrics. To capture uncertainty in model outputs, we conduct a large number of runs per scenario.

Scenario: A specific set of parameters that represent a particular management scenario. The "Baseline" alternative represent current conditions. All other alternatives represent a proposed future management scenario.

To represent productivity and abundance, we produce the following outputs:

Productivity: In keeping with previous analyses (e.g., Interior Columbia Technical Recovery Team and Zabel, 2007), we calculate productivity as recruits (R, measured as returning spawners referenced to a brood year) per spawner (S) measured at relatively low abundance. This represents the ability of a population to rebound at low abundance. At higher abundances, populations tend to hover about an equilibrium level, so recruits per spawner approaches unity, and does not distinguish among alternatives. We measured productivity for each run as R/S at 50 spawners. We determined this by fitting a Gompertz model to each model run. The Gompertz equation is:

$$\log\left(\frac{R}{S}\right) = a + b \cdot \log\,(S)$$

where a and b are parameters. We chose this equation (over a Beverton Holt equation) because it is linear (and does not have convergence issues), and it strongly resembles a Beverton-Holt equation, particularly at low abundance. Figure 2 demonstrates this for nine runs of for the Wenatchee Spring Chinook population.

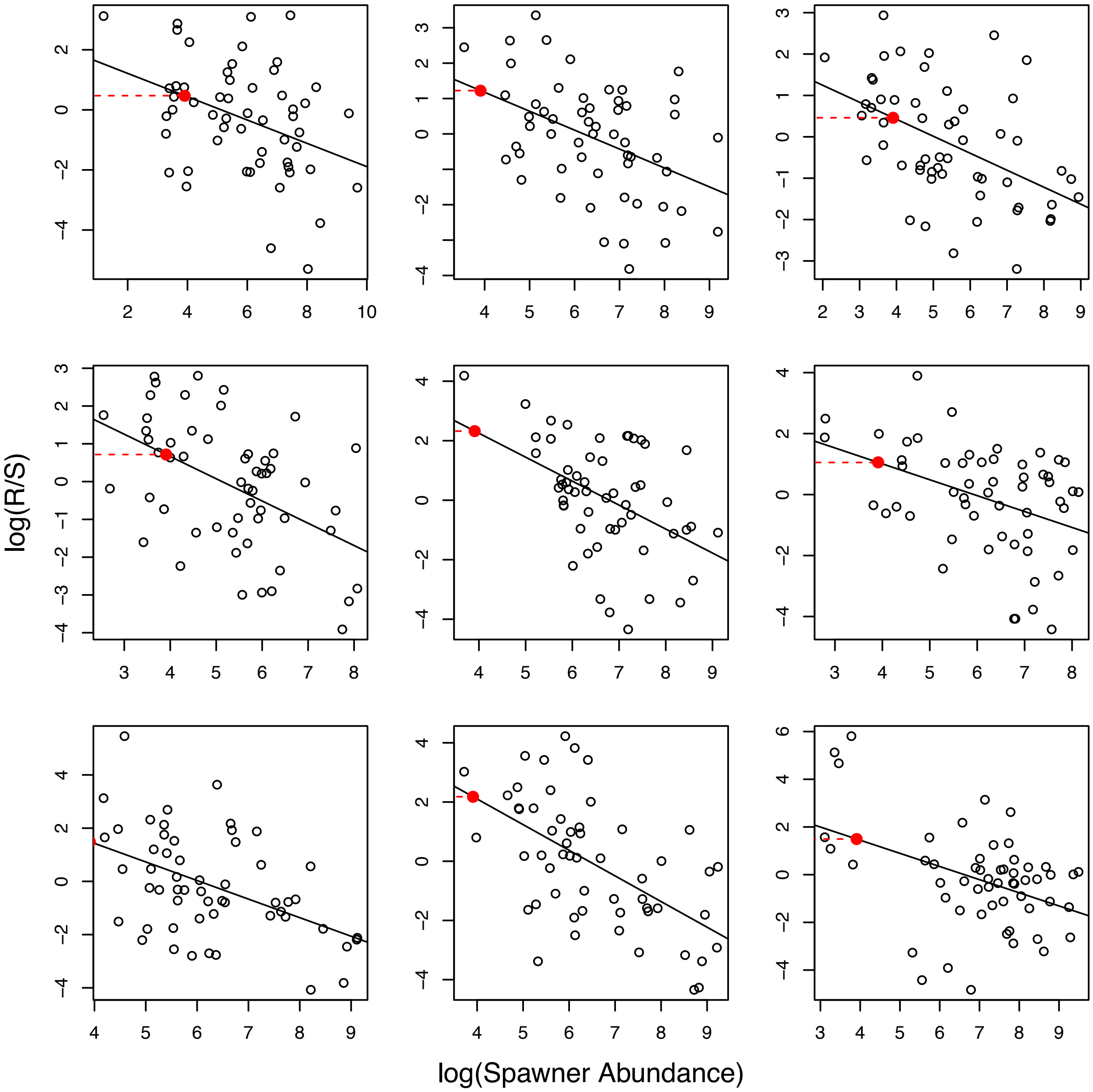

Figure 2. Gompertz model (solid line) fit to nine different runs of the baseline model for Wenatchee River Chinook. Each point represents the relationship between log(R/S) versus log(Spawner Abundance). The red point represents log (R/S) for 50 spawners for each model run.

Abundance: With this measure, we are capturing population abundance at equilibrium. Accordingly, we measured abundance for years 26-50. In keeping with precedent (e.g., Interior Columbia Technical Recovery Team and Zabel, 2007), we calculated the geometric mean of abundance across each run. Geometric mean was used because population abundances tend to have a logarithmic distribution, characterized by peaks in abundance, and the geometric mean down-weights the peaks.

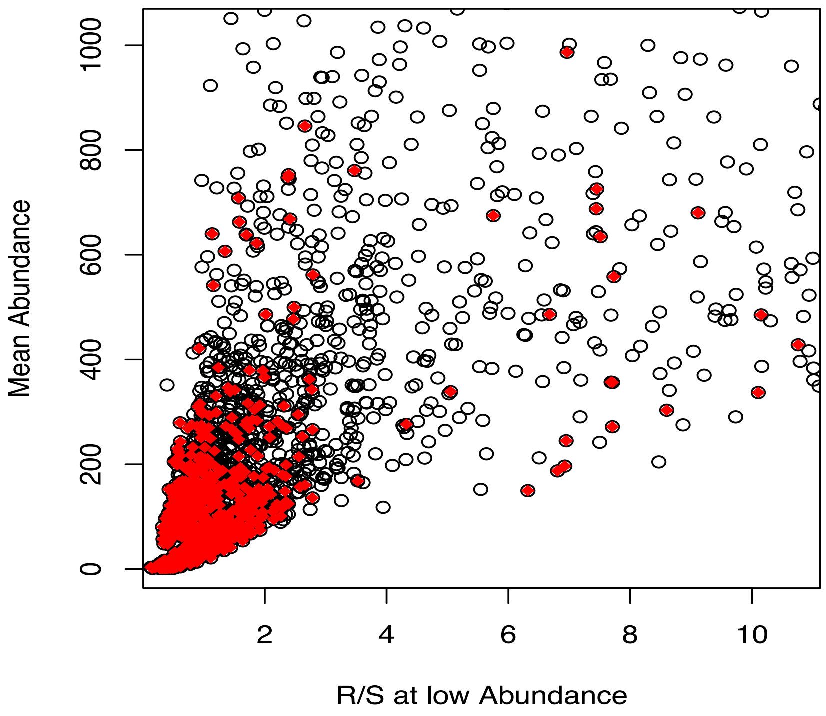

Figure 3. Mean Abundance versus R/S at low Abundance for Wenatchee Spring Chinook. Each point represents results for a single model run, and a range of scenarios are represented in the plot. Red points represent runs where the population fell below the quasi-extinction threshold.

We ran the model across several scenarios (Figure 3) and plotted Mean Abundance versus Productivity.

Consistent with the TRT, we calculated the abundance and productivity VSP score as measure of risk, as defined as probability of following below extinction thresholds. Below we describe the methods to do this.

Probability extinction: We adopted the definition of quasi-extinction that was established by the TRT. P(QET) is the probability of falling below the quasi-extinction threshold (QET) within T years, where $T = 50$. A population is considered to have fallen below the threshold if it drops below the QET threshold, on average per year, over a four-year period. We computed P(QET) for each alternative by compiling the proportion of 500 runs that fell below the QET threshold. We chose 500 runs because our estimates of P(QET) stabilized after that number of runs. The quasi-extinction threshold is determined for a population based on its historical size and complexity of subpopulations. The TRT set a QET of 50 spawners per year for Snake River spring/summer Chinook.

To generate a response surface, we used logistic regression to relate P(QET) to the Productivity and Abundance metrics, described above. For each of the 500 runs within an alternative, we determined whether the individual run fell below QET. If it did, we designated it as 0 (red points in Figure 3); otherwise it was designated as 1. We did this across all alternatives to create a data file with each line indicting whether the run fell below QET or not, and also the mean Productivity and Abundance for the run. We then performed a logistic regression to develop a response surface for probability of extinction versus Productivity and Abundance using the following equation:

$$logit(Prob(QET)) = P + N$$

where P is Productivity and N is abundance. Figure 4 demonstrates a response surface based on Wenatchee River spring Chinook.

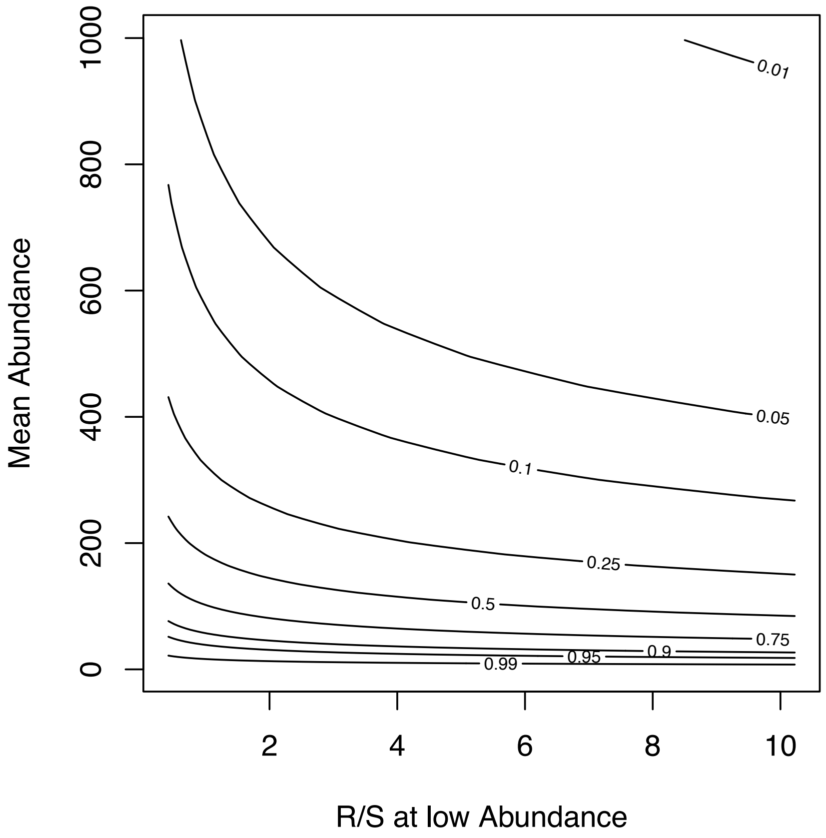

Figure 4. Isoclines of extinction probability on a plot of mean abundance versus mean productivity for the Wenatchee River spring Chinook population.

McElhany et al. (2003) provide guidelines on how to convert P(QET) into VSP scores (Table 1), with 0 indicating a population is either extinct or at a very high risk of extinction, and 4 indicating a population is at very low risk of extinction.

Table 1 Population persistence probabilities associated with persistence categories (copied from 2003 viability report).

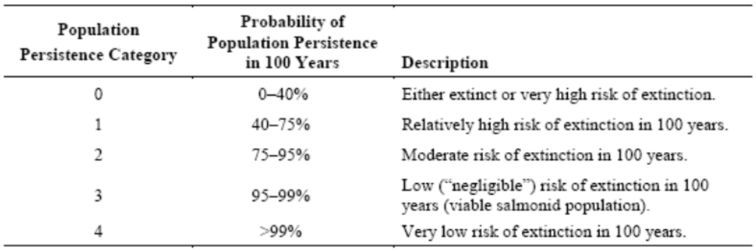

Population Persistence Category	Probability of Population Persistence in 100 Years	Description
0	0–40%	Either extinct or very high risk of extinction.
1	40–75%	Relatively high risk of extinction in 100 years.
2	75–95%	Moderate risk of extinction in 100 years.
3	95–99%	Low ("negligible") risk of extinction in 100 years (viable salmonid population).
4	>99%	Very low risk of extinction in 100 years.

Based on the Table 1, we developed a piecewise linear translation between VSP score and probability of extinction (Figure 5). Thus, to estimate VSP scores for productivity and abundance $VSP_{P\&A}$, we first calculated P(QET) based on 500 runs of a specified alternative. We then used the piecewise linear equation to convert P(QET) to $VSP_{P\&A}$.

Next, we translate the response surface for P(QET) to $VSP_{P\&A}$ scores using the equation depicted in Figure 5.

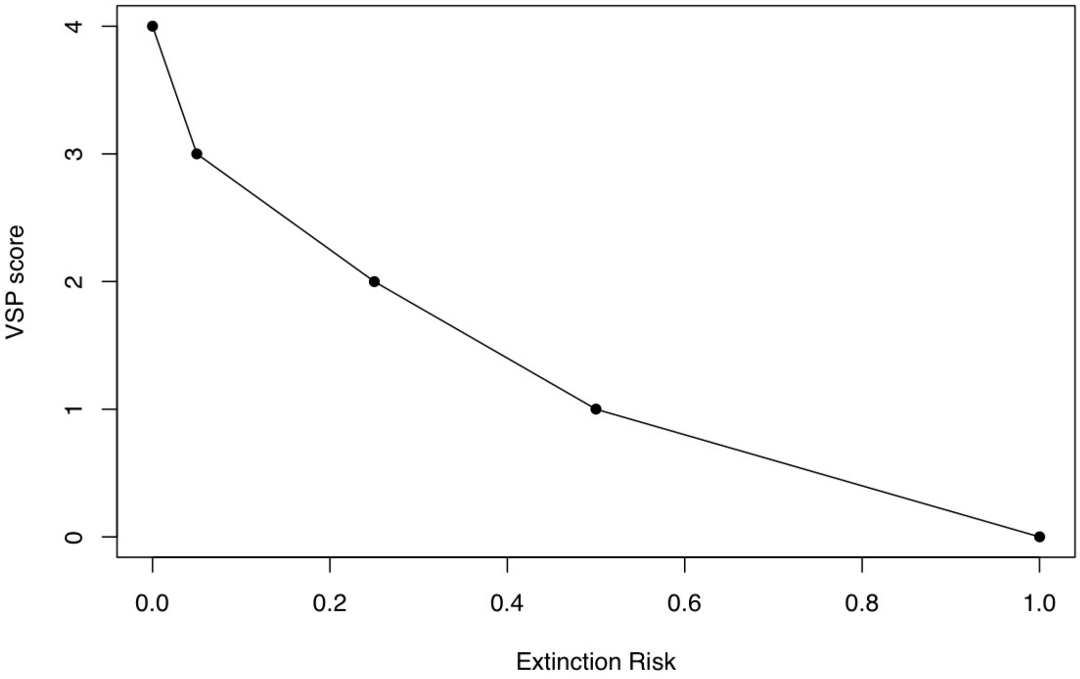

Figure 5. Relationship between VSP score (for productivity and abundance) versus extinction risk. From McElhany (2003).

For a single alternative, we can then plot mean productivity and abundance for individual runs on the response surface, along with the grand mean for all runs.

Based on Figure 4, we can then determine a $VSP_{P\&A}$ score for each run, and then determine the distribution of these scores (Figure 5). From this distribution of scores, we can derive uncertainty measures (variance, confidence intervals) for each alternative.

We note that the Interior Columbia Basin TRT (ICBTRT, 2007) used a slightly different approach to scoring the VSP metrics of Abundance and Productivity. They adopted a similar risk-based approach as we did here. However, they instituted a lower bound to abundance that varied by population size and complexity. If the mean population abundance fell below the threshold, they considered the population to be not viable. See Cooney et al. (Chapter 9a) for an illustration and further discussion of this approach.

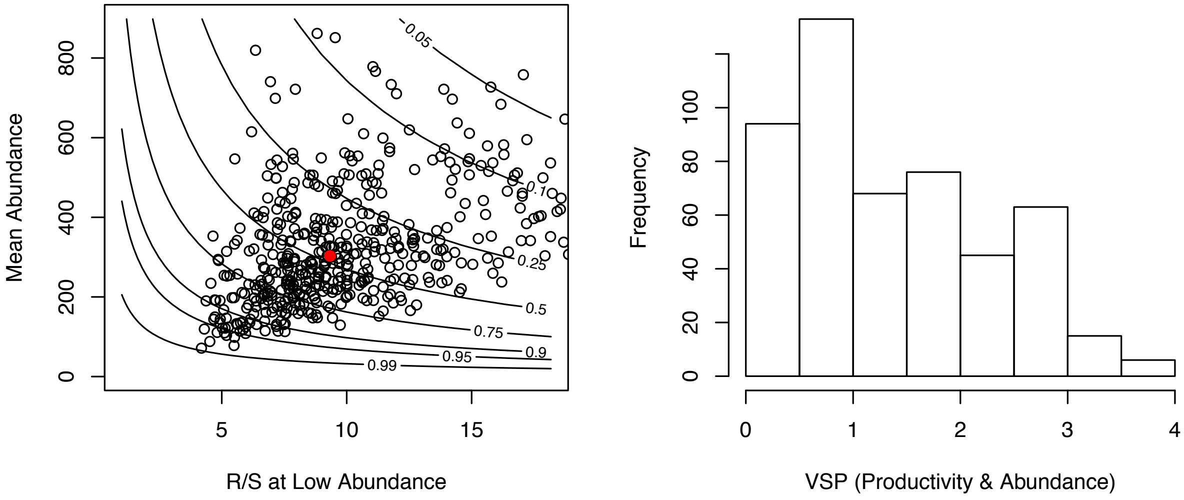

Figure 6. Response surface (left plot) with individual runs (points) of the model for the baseline scenario for Wenatchee Spring Chinook. The red point is the median run. Translation (right plot) of points on the response surface to a histogram of VSP scores for Productivity and Abundance.

Other VSP metrics.

We also calculate VSP scores for Diversity (VSP_D) and spatial structure (VSP_S). To combine scores, McElhany et al. (2003) suggested the following weighting:

$$VSP_T = \frac{4 \cdot VSP_{P\&A} + VSP_D + VSP_S}{6}$$

We are still exploring ways to incorporate diversity and spatial structure into overall scoring. At this point, we are looking at scoring life-history diversity on an MPG level.

Overview of report and chapters

We have tried to be comprehensive in our treatment of factors throughout the salmon life history. In particular, we responded to the ISAB review of our previous document by including a chapter on toxics and a chapter on habitat capacity involving our watershed program.

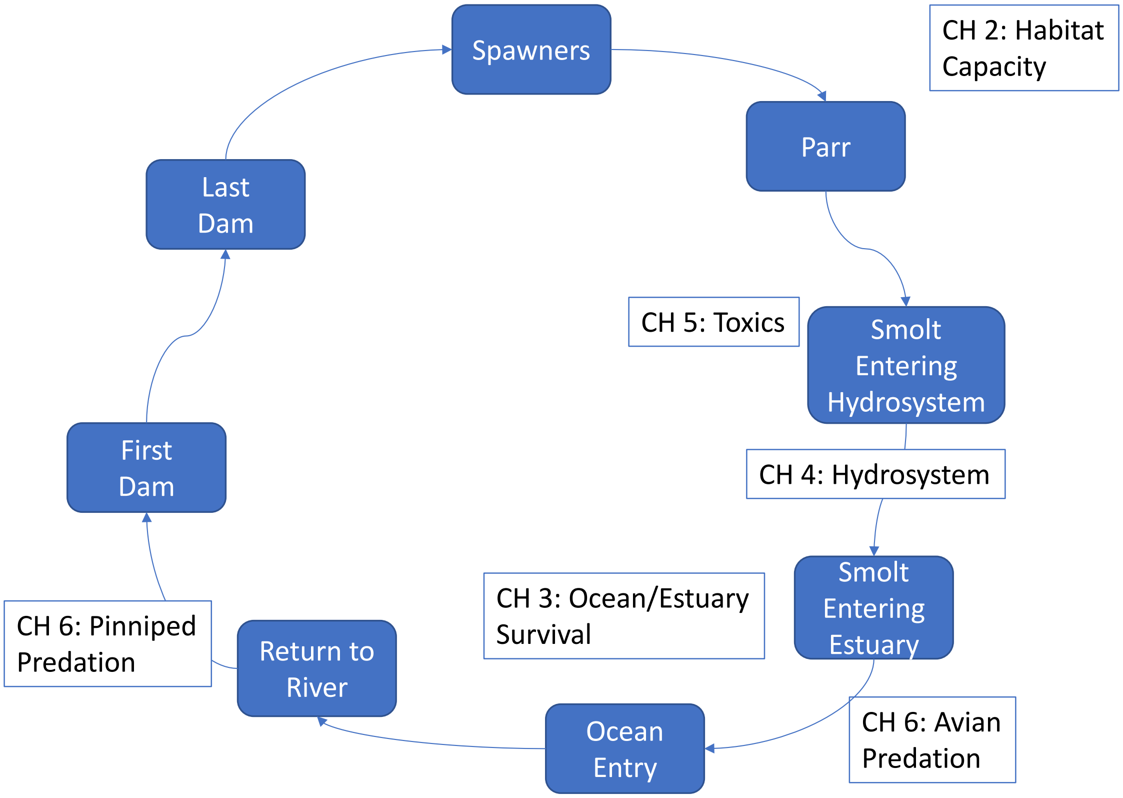

Figure 7. Chapters from this report and how they fit into the salmon life cycle.

References

ICTRT (Interior Columbia Basin Technical Recovery Team). 2007. Viability criteria for application to interior Columbia basin salmonid ESUs. Review draft, 3/1/2007. https://www.nwfsc.noaa.gov/research/divisions/cb/genetics/trt/col/trt_viability.cfm

McElhany, P., M. Ruckelshaus, M. Ford, T. Wainwright, and E. Bjorkstedt. 2000. Viable salmonid populations and the recovery of evolutionarily significant units. U.S. Dept. Commer., NOAA Tech. Memo. NMFS-NWFSC-42,156 p.

McElhany, P., T. Backman, C. Busack, S. Heppell, S. Kolmes, A. Maule, J. Myers, D. Rawding, D. Shively, A. Steel, C. Steward, and T. Whitesel. 2003. Viability status of Oregon salmon and steelhead populations in the Willamette and Lower Columbia Basins. Part 6: Upper Willamette Chinook. Oregon Department of Fish and Wildlife and National Marine Fisheries Service. 54 pp.

McElhany, P., C. Busack, M. W. Chilcote, S. Kolmes, B. A. McIntosh, J. Myers, D. Rawding, E. A. Steel, C. Steward, D. L. Ward, T. Whitesel, and C. Willis. 2006. Revised viability criteria for salmon and steelhead in the Willamette and Lower Columbia Basins. Willamette/Lower Columbia Technical Recovery Team and Oregon Department of Fish and Wildlife. Pp. 178.

CHAPTER 2: HABITAT

2.a Estimating the fish rearing capacity of freshwater systems: a review of approaches for salmonids in the Columbia River basin

Morgan H. Bond (Ocean Associates, contracted to NOAA Fisheries, NWFSC, Seattle), Corey C. Phillis (Ocean Associates, contracted to NOAA Fisheries, NWFSC, Seattle), Michael P. Beakes (NRC postdoc, NOAA Fisheries, NWFSC, Seattle), Nicolaas Bouwes (Utah State University), J. Ryan Bellmore (USFS), Joe Benjamin (QCI), Seth M. White (CRITFC), Kevin See (QCI), Correigh M. Greene (NOAA Fisheries, NWFSC, Seattle), Tim Beechie (NOAA Fisheries, NWFSC, Seattle), Chris Jordan (NOAA Fisheries, NWFSC, Seattle), Richard W. Zabel (NOAA Fisheries, NWFSC, Seattle)

Abstract

Life-cycle models are increasingly employed in an effort to better predict the outcome of various management scenarios on Pacific Northwest salmonids. By modeling multiple stages and transitions, life-cycle models can determine where bottlenecks in survival limit recovery, or make projections about population abundance under various scenarios of future conditions. However, modeling efforts can be hampered by uncertainties in key parameters, including stage-specific capacity. Depending on the estimation technique, capacity can refer to either the long-term average maximum or absolute maximum number or biomass of individuals that can occupy a habitat. Recently, focus has returned to estimating the capacity of freshwater habitats for rearing juvenile salmonids because of the restoration potential in freshwater habitats compared to marine waters. Additionally, changes in capacity under scenarios of management or restoration can be used outside of life cycle modeling exercises to evaluate the efficacy of alternative practices. In the Columbia River Basin there are seven different methods currently being used to estimate rearing capacity at several spatial grains and extents. These approaches range from empirical fitting of stock-recruit data, to geomorphic estimates of habitat availability, to food web models. Our aim is to review and compare all seven methods to benefit those using capacity estimates in modeling exercises or evaluating the benefits of restoration or management scenarios, as well as those collecting the data used to estimate capacity.

Introduction

A primary goal of conservation biologists is determining the potential population response of various restoration or management actions. Implied in these conservation efforts is that habitat restoration will promote a positive demographic response in imperiled populations. However, evaluating the efficacy of alternative restoration or management strategies requires an estimate of how populations will likely respond to various types or intensities of actions, if at all. To do this, researchers often attempt to estimate how many organisms a system might support under historical, contemporary, or proposed conditions. However, there are myriad techniques to make these estimates, and their data needs, assumptions, and applicability vary widely among systems, taxa, and life stage. Researchers and managers must therefore decide which technique will most adequately assess the capacity of a system.

Implicit in the ecology of organisms and ecosystems is a limit in the number of individuals that can occupy a given habitat, which emerges from the strength of density dependence in the environment. Although in an ecological sense carrying capacity is the maximum number of organisms that a habitat can support (Odum 1953), a more useful generalization for managers is the long term average asymptotic production of a given life stage that a population may be expected to maintain when fully seeded (i.e. not limited by propagules). Without commensurate increases in resource availability, elevation of a parent population beyond capacity will not result in additional surviving offspring, and at high enough parent abundances populations may suffer declines. The term “carrying capacity” to refer to maximum supported animal abundance gained widespread use in the 20th century as resource managers acquired time-series of population dynamics and grappled with managing populations in a changing environment (Sayre 2008). Thus, capacity is a key demographic characteristic that researchers and managers have used to understand how and why populations are limited in abundance across spatial scales.

In fisheries, the gold standard for estimating capacity has been fitting various stock-recruit (S-R) models to estimates of parent abundance (e.g. spawners, redds), and offspring abundance at the life stage of interest (recruit) (Ricker 1954, Beverton and Holt 1957, Barrowman and Myers 2000). These approaches assume that the number of recruits will increase logarithmically until the strength of density dependence creates an asymptotic limit on additional recruitment as capacity. However, estimating capacity in natural systems is a particular challenge because estimates of the number or biomass of fish at any life stage is often difficult to assess. As John Sheperd famously said: “Managing fisheries is hard: it’s like managing a forest, in which the trees are invisible and keep moving around.” Therefore, in fisheries we often employ limited and imprecise data when estimating capacity as the unfished equilibrium population size; used as a reference point when setting catch quotas.

While estimating biomass or abundance for marine fishes is challenging, the necessary movement between marine and freshwater environments of anadromous fishes provides additional opportunities for enumeration. During their migration anadromous fishes move through structures (e.g. weirs, dams, counting towers, sonar), or become conspicuous and ephemeral inhabitants of rivers and streams (spawner or redd counts). Therefore the biphasic life history of anadromous fishes facilitates a more accurate estimate of abundance, but ensures challenges in management and conservation as bottlenecks in population capacity may vary between freshwater, marine and migratory portions of the life history. Indeed, widespread declines in many anadromous fishes of cultural, ecological, and economic importance (Lichatowich et al. 1999, Gustafson et al. 2007) have led to conservation concerns and extensive mitigation and restoration actions. However, the expense of such actions necessitates an analysis of the potential resulting increase in capacity. Consequently, most of our knowledge and research into freshwater capacities comes from studies of salmonids because of the pressing need to inform management actions that will recover these culturally and commercially important populations (Kareiva et al. 2000, Upper Columbia Salmon Recovery Board 2007).

Estimates of salmonid capacity at fine spatial scales within freshwater habitats can be realized and separated from density dependence in the marine environment; made possible by several aspects of salmon life histories. First, with few exceptions, all fish migrating from marine to freshwater habitats are mature individuals, allowing for enumeration of the parent population. Second, most mature salmon home to their natal stream, which creates a metapopulation structure across the landscape that allows the population dynamics of adjacent streams to operate independently (Rogers and Schindler 2008). Third, burial of embryos ensures that juveniles emerge and rear, at least initially, in the same location where their parents spawned. Freshwater capacity can therefore be estimated with S-R models from time-series of spawner and juvenile abundances.

Although S-R models can allow managers to estimate contemporary capacity and harvest targets, the conservation utility of fitting approaches is limited, as there is no mechanistic basis for capacity implied in the model. Additionally, many monitored populations are monitored because of concern for population abundance, leading to a narrow range of spawner abundances with which to fit S-R models. Further, the long time-series required to fit S-R models ensures that estimates will span a range of environmental conditions, adding unwanted noise to the resulting relationship. In some cases where data are extensive researchers have retrospectively included environmental co-variates in S-R models to estimate the factors that may be limiting population abundance across an environmental gradient (Liermann et al. 2010) or estimate whether multiple S-R relationships exist among alternative environmental regimes (Neuswanger et al. 2015). However, S-R methods are costly in both data needs and the time required to obtain those data; a long time series is often required to estimate S-R parameters with even a single covariate because of the long generation time of anadromous fishes.

Recently, alternative methods for estimating freshwater capacity have been developed (e.g. Bellmore et al. 2013, Rosenfeld et al. 2014, Beechie et al. 2015). However, there are key trade-offs among methods regarding the spatiotemporal inference of capacity we can gain from each. Particular methods may be more or less appropriate depending on the management or conservation needs and resources available (e.g. data, time, funds, etc.) to execute each method. In addition, capacity estimates should include uncertainty in their prediction so that it can be accounted for and propagated in subsequent applications (e.g. life cycle models), and communicated to managers implementing policy. Although several reviews have discussed various methods for estimating capacity in freshwater fishes (Rosenfeld 2003, Minns et al. 2011, Wurtsbaugh et al. 2014), there has been no formal study contrasting the pros and cons of various approaches in their application to conservation efforts. Ideally, an approach would allow managers to estimate capacity under alternative scenarios of biotic and abiotic conditions in the environment at appropriate spatial and temporal scales. Therefore, in this study we aim to help guide the execution of the most appropriate method for estimating capacity given different management and conservation needs.

Defining capacity

The term “capacity” indicates a limit in the number of organisms supported by abundance, yet among researchers there is complementary terminology related to capacity or synonymous for it. Therefore, we provide a summary of commonly used terms and definitions:

Production/yield: Biomass produced per habitat unit per unit time (Ricker 1975, Wurtsbaugh et al. 2014).

Productivity/Productive capacity: “the sum of all production accrued by all stock during the time they spend any part of their life history in that area” (Minns 1997, Minns et al. 2011). Minns et al. (2011) separate productive capacity into two states: a historical state without anthropogenic influence (P_{MAX}), and contemporary capacity (P_{NOW}).

Density index: Primarily used in fish hatchery operations as the maximum number of fish that can occupy a unit of space (Piper 1982).

Carrying capacity: Often represented by the parameter K, and defined here by del Monte-Luna et al. (2004) carrying capacity is “the limit of growth or development of each and all hierarchical levels of biological integration, beginning with the population, and shaped by processes and interdependent relationships between finite resources and the consumers of those resources.”

Capacity: The long term average asymptotic production of a given life stage that a population may be expected to maintain when fully seeded (i.e. not limited by the number of spawners, although spawning habitat may be limiting). In other words, the unfished equilibrium population size that may be sustained indefinitely under a given set of conditions (Liermann et al. 2010).

Capacity as the unfished equilibrium populations size, that is, the long-term average maximum provides the most reasonable management target, often estimated from the fitting of S-R models and incorporated into life-cycle models. However, in other modeling exercises, capacity as a density index or carrying capacity where full seeding of the habitat is assumed, may be more useful as a tool to compare the relative gains or losses achieved by restoration or management actions. As discussed below, additional methods (e.g. taking the 90th percentile from model estimates) may further restrict the capacity to produce more realistic capacity targets for inclusion in life-cycle models.

Estimating Capacity

There are two broad classes of approaches currently employed to estimate capacity in freshwater systems. The first, which includes S-R models, is statistical fitting. In this approach measures of biotic and abiotic conditions are related to a dependent variable of abundance, biomass or density (Fausch et al. 1988). More recently, machine learning approaches (e.g. random forest) have been used to deal with the complex, often nonlinear, relationships between species and their habitat. The second broad class of approaches involves construction of mechanistic models that employ a set of functional responses to estimate fish occupancy of an area of interest. These approaches include bioenergetic models that estimate maximum occupancy of fish with species specific bioenergetic parameters and stream conditions (e.g. temperature, food, flow). Other approaches include estimates of fish biomass under varying primary productivity. Each of these approaches has advantages, drawbacks, and different data needs.

One of the most critical challenges of estimating capacity is matching the spatial grain and extent of interest with an appropriate method for estimating capacity at that extent, or extrapolating local estimates to larger spatial scales relevant to management. Data used to populate models are collected at discrete locations and times, yet estimates of capacity must be extrapolated to some larger spatial scale of interest. Here, we focus on comparing alternative methods for estimating the capacity of freshwater environments for fishes. Although these methods apply to a variety of organisms, for comparative purposes, we will review techniques applied to salmonids. The aim is to compare the data needs and application of different approaches to provide a framework for researchers and managers seeking to estimate capacity in their system. What are the options, data needs, limitations, and utility of various approaches?

Process and Empirical Models

As previously mentioned, S-R models are fit to estimates of the parent and offspring abundances. However, these models do not inherently imply which factors may be limiting populations. Therefore, researchers have long sought relationships between fish abundance and various habitat variables encompassing the biotic and abiotic environment; often explored in a multiple regression framework (Fausch et al. 1988). Although these models may be useful for explaining abundance at small spatial scales, the linear relationships employed often suffer from shortcomings that cannot be overcome with standard linear regression techniques. For example, although abundance may be correlated with any number of discrete or continuous habitat metrics, the monitored populations may never be observed at or near capacity. In addition, at larger spatial scales the non-linear or threshold effects, as well as higher order interactions may cause difficulties in expanding the relationships to the spatial or temporal grain and extent that is relevant to management. Logistical challenges prevent ecologists from performing large scale testing of models generated at small spatial scales, leading to a lack of validation for many of the models that attempt to explain variation in abundance. Finally, because of the previously mentioned difficulties in measuring the abundance of fish and the complexity of stream habitats, the data are often extremely noisy, even at small spatial. To overcome these limitations alternative approaches focus on estimation of habitat type and amount (process models), or where fish abundance data are extensive, fitting fish densities to landscape scale variables that can be extrapolated to larger stream networks.

Process based models (Habitat expansion)

Unlike previously mentioned S-R approaches for fitting fish abundance to local measurement of habitat characters, habitat expansion operates at the watershed or larger spatial scale. Capacity can be directly extrapolated at any spatial scale by multiplying the amount of available habitat by the maximum density at which animals occur. In the simplest form, estimating habitat capacity (C) for a life stage or for smolt production employs an equation

$$\mathrm{C} = \sum_{i=0}^{n} a_i d_i \qquad \text{(Eq. 1)}$$

where a_i is the area or volume (e.g., in terms of m^2 or m^3) and d_i is the maximum density (e.g., individuals per area or volume) of the *i*th habitat type (Beechie et al. 2003). This expansion of the maximum density across the set of habitat areas results in an estimate with units in terms of the number of individuals, although additional modifications (e.g., a known distribution of individual biomass at high densities) could modify this function into units of mass or other summary value. This calculation assumes that maximum densities are constant across different units of the same habitat type.

For example, spawning habitat capacity can be based on area of suitable spawning gravel for a species, multiplied by the density of adults (or divided by the area occupied for each redd) (Hanrahan et al. 2004). While this formula is simple, in many applications its use is made more complicated by (1) adding parameter uncertainty to the estimate (Beechie et al. 2006), (2) increasing the number of habitat types and life stages available (Scheuerell et al. 2006), or (3) incorporating the wide range of fish densities observed for each habitat type and life stage (Beakes et al. in prep). The basic equation remains the same, but as the calculation is parsed out among more life stages and habitat types the mechanics of the analysis become increasingly complex.

As suggested by Eq. 1, habitat expansions require three essential steps: 1) classify a given habitat into appropriate types, 2) estimate area of each habitat type, and 3) estimate maximum density of each type. While each of these steps is conceptually simple, they each involve some level of interpretation and uncertainty.

Habitat classification. One of the most important considerations in developing habitat-based capacity estimates is the habitat typing system used. Two key attributes of a habitat typing system that is useful for capacity estimation are that (1) the habitat types are predictive of fish production and (2) they are sensitive to land use or restoration (Beechie et al. 2003, Beechie et al. 2013). This facilitates analyses of habitat change (either past degradation or future restoration) and estimation of the change in fish populations as a function of that change. There are many habitat classification systems in use, and most are broadly similar in their hierarchical structure and utility for predicting changes in fish abundance as a function of habitat change (Beechie et al. 2013). Notably, there are more habitat typing systems for small streams than for large rivers, perhaps in part due to the fact that more research and monitoring efforts focus on small, wadable streams. Differences among habitat typing systems are most often in the level of detail in classifying units. In general, coarser resolution habitat units are more reliably identified and measured (i.e., there is less observer error), while finer resolution habitat units may elucidate more subtle responses of habitat to land use or restoration.

Amount of habitat. Quantifying the available area of each habitat type in a river basin is straightforward, but often time consuming. Field surveys are the most reliable means of measuring habitat areas, although some habitat types (e.g., large river habitat units) can be measured from aerial photography (Reeves et al. 1989). In either case, individual habitat units are typed and measured, and then total areas of each habitat type are summed for the river basin (or population). Where the analysis focuses on estimating historical or natural habitat areas, the area each habitat type must be estimated using historical data (e.g., side channels on historical maps), contemporary reference site data (e.g., pools and riffles in near-natural streams), or models (e.g., estimating total beaver pond area based on literature values for dam frequency and mean pond area) (Beechie et al. 1994). By contrast, if the analysis is focused on estimating restoration outcomes, future habitat areas can be estimated based on the natural potential habitat conditions in each reach, as well as on estimates of the new habitats created by individual restoration actions (Beechie et al. 2015).

Habitat-specific maximum densities. The most theoretically challenging aspect of the habitat capacity calculation is the estimation of maximum densities by habitat type. Maximum densities might be expected to depend upon habitat complexity and primary and secondary productivity, so estimates are likely region- or system-specific. Furthermore, estimation of maximum densities is highly dependent on measurements of fish habitat use, and different methods have their own associated variability and biases in estimation. Estimates can be complicated by the mobility of fish and dynamic use of different habitat units over time. Perhaps most importantly, estimates of fish densities are potentially subject to shifting baselines (Pauly 1995, Pinnegar and Engelhard 2008), whereby current estimates of density for a particular species reflect poor utilization due to recent trends toward low population size. In such cases, any estimate of maximum density would be biased toward low estimates of capacity. These biases could lead to an expectation that populations would reach capacity at lower levels of abundance than they naturally do.

With recognition of these potential biases, estimation of maximum density has proceeded in two ways. First, maximum density could be estimated using experimental observations of territory size, movement, or growth. For example, Grant and Kramer (1990) compiled data from experimental studies of individual territory size and body size for a variety of salmonids, and found a strong power function (Figure 1). This relationship was inverted to estimate a maximum population density as a function of body size, which was then compared to studies with experimental or natural observations by incorporating the frequency of various size classes observed in each study. The results supported the allometric territory size hypothesis, although numerous observations in natural populations were observed to be below the maximum density relationship, suggesting that in these cases other limiting factors were operating. Hence, in applying this broadly applicable relationship to particularly systems, care should be taken to determine whether species-specific or system-specific variation might result in strong departures from this upper threshold.

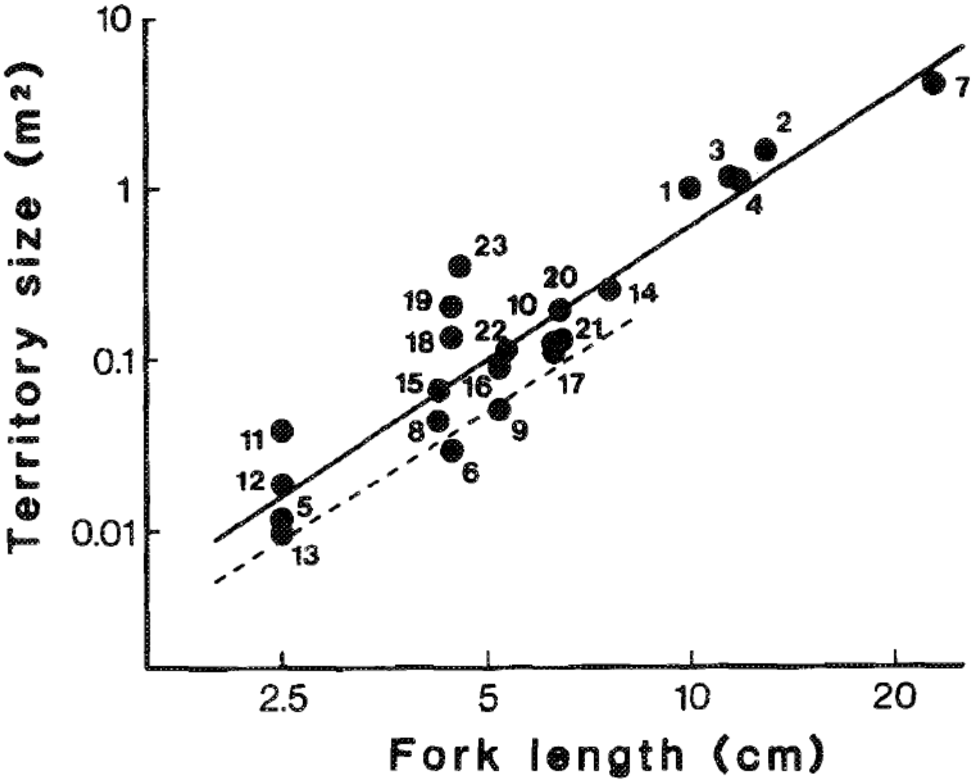

Figure 1. Relationship between $\log_{10}$(territory size) and fork length (cm) for fish from a variety of studies reported by Grant and Kramer (1990), including a separate regression for brook trout (dashed line) which falls within the 95th% confidence interval of the overall regression (solid line). See Grant and Kramer (1990) for description of individual studies (numbered points).

While experimental observations are not always possible to obtain for particular systems, natural observations as part of monitoring programs provide a second way to estimate maximum density. When numerous estimates of local density are available for particular habitat types, the upper percentiles can be used as a measure of maximum density (see quantile regression section). For example, Beechie et al. (2005) used data from boat electrofishing surveys on mainstem units of the Skagit River in Washington State to determine habitat preferences for various wild salmonids. These data could be used to estimate habitat capacity in mainstem reaches. One of the most prevalent species is Chinook salmon (*Oncorhynchus tshawytscha*), which may utilize mainstem environments for days, weeks, or months before migrating as sub-yearling fry or yearling smolts. While movements of older fish into tributaries might preclude use of these data to estimate long-term freshwater rearing capacity, the data are appropriate for estimating habitat capacity at the fry life stage. This stage represents the most populous life stage for Chinook salmon (millions in the Skagit River), and the sampling captures the habitat types most relevant for this stage (mainstem habitats used following emergence from redds). Electroshocking was performed throughout the Skagit mainstem, including lower reaches to which migrant fry might move after rearing upstream. Any estimation of maximum density might be sensitive to density-dependent migration (sensu Greene and Beechie 2004), so use of these data to estimate capacity should be restricted to data points most closely associated with spawning reaches.

Upon filtering data in this way, a broad distribution of densities of Chinook salmon fry were obtained (Figure 2A), illustrating a huge range in density estimates (0.5- 15.5 fry/m^2). Two estimates of high density were obtained using the 90th and 95th percentile of the distribution of densities, thereby eliminating the highest values which could represent outliers, non-equilibrium values, or recording errors. When these data were put in the context of a habitat classification, the 90th and 95th percentile scores increased as a function of habitat complexity and size-specific habitat utilization: maximum density doubled as functions of cover class, preferred depth, and preferred velocity (Figure 2B). Consequently, maximum density varied over eight-fold as a function of these three axes describing habitat variation.

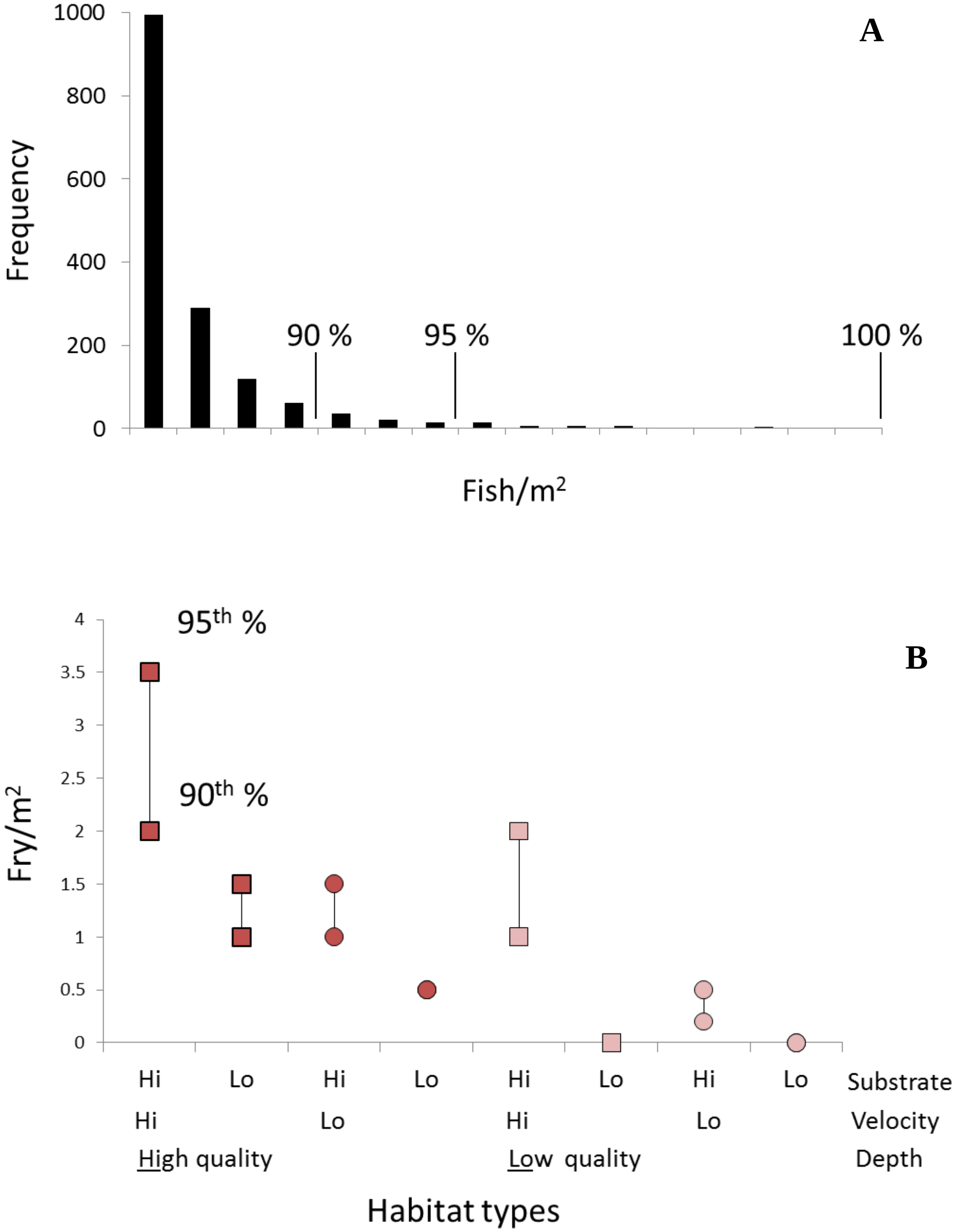

Figure 2. A) Distribution of electroshocking data for Chinook salmon fry in the Skagit River, and definition of high densities used to calculate maximum density. B) 90th and 95th percentile maximum density as functions of cover type, flow velocity (m/s), and unit depth (m).

Variation and uncertainty. Each parameter in the habitat expansion calculation may be subject to variation both in terms of uncertainty in observations and temporal variation in the processes influencing amount of habitat or maximum density. Capacity estimation via habitat expansions can factor these in if care is taken to incorporate observation or temporal variation. For example, Beechie et al. (2006) incorporated parameter uncertainty for number of redds per kilometer in small streams and redd size and adults per redd in large rivers into Chinook salmon spawning capacity estimates in the Skagit River basin, which produced spawner capacity estimates ranging four orders of magnitude.

The estimate of capacity may be relatively static or dynamic depending upon what parameters are used to differentiate habitat types. For example, if the habitat classification includes units whose area varies with river flow (see below), capacity estimates can likewise vary temporally as river flow increases or decreases. Estimates of capacity using habitat expansions are more sensitive to uncertainty in maximum density estimates as opposed to habit area values (Beakes et al. in prep), primarily because habitat area estimates do not vary significantly compared to densities of fish occupying those habitats.

Applications. On their own, habitat expansions to estimate capacity may be used to document whether particular life stages or habitats are likely limiting production. For example, Beechie et al. (2006) estimated spawning capacity for six populations in the Skagit River. Spawning capacity was calculated based on areal estimates of spawning habitat in mainstems and tributaries, and estimating maximum number of adults that could spawn in this habitat based on redd density, redd area, and adults per red. Each of these estimates is subject to variation, so Monte Carlo simulations incorporating multiple estimates of these parameters were used to estimate the range of possible spawning capacity. These values were compared to annual estimates of the number of spawners by population, and only one of the six populations exhibited > 1% overlap between capacity-level and observed number of spawners. These results provided strong support for the idea that spawning habitat is not limiting population dynamics in this system.

Two additional applications of habitat expansions take advantage of multiple estimates of capacity to deduce habitat-based limitations across the life cycle. One of the most common uses recently is ascertaining which freshwater habitats and life stages limit population sizes of salmon. For this purpose, the equation takes the form

$$C_{LS} = \sum_{i=0}^{n} a_i d_i s_{i,LS} \qquad \text{(Eq. 2)}$$

where *LS* indicates a specific life stage and *s* indicates survival from that life stage to smolt. This formula can be used to compare capacities across life stages without linking life stages in a life-cycle model (Reeves et al. 1989, Beechie et al. 1994). Using this approach, Beechie et al. (1994) deduced that summer rearing habitat availability likely limited coho salmon production in the Skagit River basin. However, current summer and winter rearing capacities were similar (980,000 potential smolts from summer rearing habitat and 1,170,000 potential smolts from winter rearing habitats), indicating that restoration of summer rearing habitat might soon result in winter rearing habitats becoming the limiting factor. The analysis also showed that the greatest restoration potential was in floodplain and delta habitats, and that restoring wood and pools in small streams would likely result in a relatively small benefit to the coho salmon population. Removing migration barriers would also provide a relatively small benefit, although it may be more cost effective than wood restoration because there are relatively few barriers to remove compared to hundreds of kilometers of wood and pool habitat to restore.

Habitat-based expansions of capacity may also be used in dynamic life cycle models. In this way, a life-cycle model estimates habitat capacity at each life stage, and links the life stages using survival to the next life stage or migration to new habitats (e.g. Moussalli and Hilborn 1986, Greene and Beechie 2004). Habitat expansions represent capacity parameters in Beverton-Holt models determining patterns of mortality or movement in the system. For example, Greene and Beechie (2004) used capacity estimates from habitat expansions at different life stages to parameterize a life cycle model for Skagit River Chinook salmon. These results revealed that under assumptions of density-dependent movement, restoration in the tidal delta maximized benefits to adult production.

Habitat expansions are used in a similar context for a life cycle model evaluating the California Water Fix (nee Bay-Delta Conservation Plan) for Winter-run Chinook salmon (Hendrix et al. 2014). This model evaluates transitions of salmon through several habitats for which productivity and capacity estimates are computed by multiple sub-models. It conceptualizes life history variation (fry and parr using freshwater, floodplain, delta, and nearshore habitats) as an outcome of density-dependent movement, which are determined in part by habitat expansions of freshwater, delta, and nearshore rearing habitat capacity. Due to the life history and model complexity, productivity and capacity parameters are estimated on a monthly time step. Capacity of floodplain and mainstem habitats are calculated based on habitat expansions using classification of high and low quality depths and velocities from the Sacramento HEC-RAS model (Singer and Dunne 2004). Habitat classifications of tidal delta habitats are based on river gage height, channel type, and cover class, while classifications of bay habitats are based on salinity level (a function of river flow), shoreline habitat type, and depth. Maximum density values were derived from analysis of capacity in Skagit River, delta, and nearshore habitats, recognizing that the Skagit may under-represent capacity compared to Sacramento given much lower primary productivity, but that the Sacramento system may be biased high due to inputs of hatchery fish. Areal estimates of capacity in the delta were further limited by applying the results of an occupancy model that predicted probability of presence using data from beach seines in the Sacramento delta based on river system (Sacramento R. or San Joaquin R.), distance of sampling site to its mainstem (m), physical channel depth (m), physical channel width (m), and DSM2 water stage (m).

Because capacity was estimated for each habitat using time-varying parameters such as river flow, gage height, and salinity, capacity could be predicted on a monthly and annual basis. Habitat capacity increases as a function of flow within river, delta, and and nearshore environments, although capacity within particular habitat types (e.g., mainstem rearing habitat) can decline as a function of flow because of the increased availability of shallower habitat types. The resulting habitat expansions suggest that substantial capacity exists for juveniles within the Sacramento River and delta regardless of whether 90th and 95th percentiles of maximum density are used (Figure 3), although the vast majority of capacity is of lower quality. This pattern is particularly pronounced in the delta, for which 0.3% of the capacity on average was high quality on all three axes.

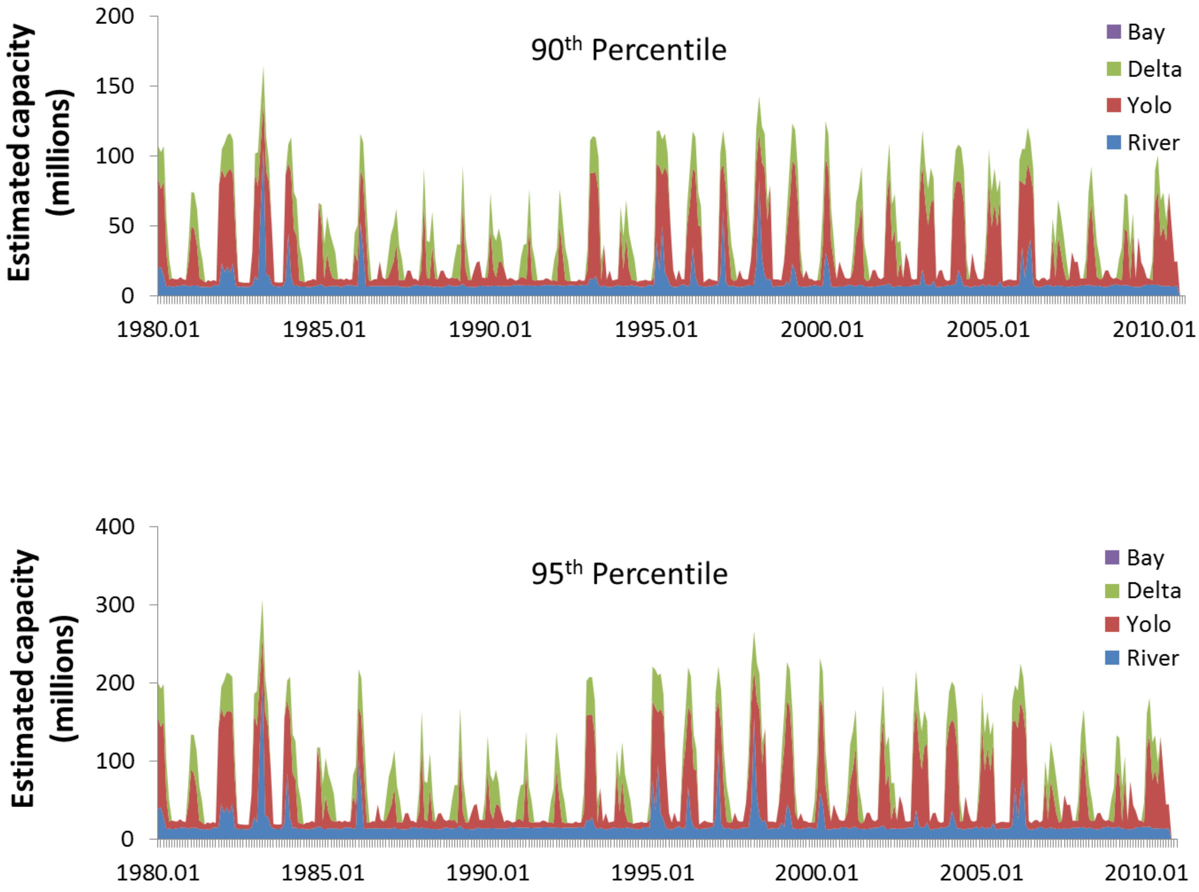

Figure 3. Estimated habitat capacity in mainstem, floodplain (Yolo Bypass), delta, and nearshore habitats of the Sacramento River by month (01 = January) and year (1980-2010) using 90th and 95th percentiles of maximum density. Bay capacity is extremely low compared to capacity in other habitats, which is why it is not readily observed on the graph.

Quantile regression

Advances in empirical modeling combined with widespread computing power now allow ecologists to deal with many of the shortcomings of standard linear regression approaches that have been employed for decades. Quantile regression approaches to estimating carrying capacity are an empirical approach to soliciting fish-habitat relationships from observed data, and using those relationships to predict capacity at the reach scale (Valavanis et al. 2008, Hegel et al.

2010). It relies on observations of abundance, density or biomass, and a variety of habitat metrics as covariates. For stream-dwelling juvenile fishes, these habitat metrics might include pool frequency, large woody debris density, substrate size, riparian cover, or a myriad of other possible metrics. Typical regression estimates how the mean of the response variable changes as various covariates shift, but quantile regression estimates how each quantile (e.g. 10th, 50th, 90th, etc.) shifts, in essence providing a predicted distribution of the response variable for a given set of habitat covariates (Koenker and Bassett Jr 1978). Selecting an upper quantile (e.g. 90th percentile) of this distribution as a proxy for carrying capacity provides a means for predicting capacity from a suite of habitat covariates.

The theory behind using quantile regression to estimate carrying capacity is that although capacity may be influenced by some components of the habitat that we can measure and incorporate into a quantile regression, there are often other, unmeasured, factors that limit the abundance or density of fish from reaching that capacity (e.g. presence of competitors, predators, spawner abundance, prior temperature, etc.). For a set of measured sites, only a subset may be near capacity, and how that upper quantile of fish density responds to changes in habitat characterizes the relationship between carrying capacity and habitat. Therefore, the upper quantiles may have a different relationship with a particular habitat metric than the mean. Viewed through the lens of quantile regression approaches, carrying capacity represents the maximum number or density of fish that sites with a particular suite of habitat characteristics can support. Therefore, quantile regression predictions pertain to the spatial scale at which fish densities are made. Once a quantile regression model is fit with data, predictions can be made anywhere the same set of habitat metrics have been collected, regardless of whether fish abundance data are available or not. However, predictions of capacity at the stream reach scale may not be useful in a management or life-cycle model context. Using some form of extrapolation model (e.g. linear regression model with covariates, spatial stream network model, etc.) the reach-scale capacity estimates can be scaled up to the stream or watershed scale.

An example of the power of quantile regression to solicit empirical fish-habitat relationships is found in Dunham et al. (2002), and summarized in (Cade and Noon 2003). The authors investigated the functional relationship between densities of cutthroat trout (*O. clarki*) and the ratio of stream width to depth using data from 71 sites across 13 streams and 7 years. That ratio was chosen as a measure of the integrity of stream habitat. Quantile regression analysis estimated a negative relationship for the upper quantiles (70th percentile), while a weighted least squares model indicated no relationship between the mean cutthroat trout density and stream width to depth ratio (Cade and Noon 2003) (See Figure 4). Without the quantile regression approach, the authors would have found no fish-habitat relationship. Other examples include quantile regression being used to determine the distribution of sole (*Solea solea*) nursery grounds (Eastwood et al. 2003), and to investigate the limiting effect of temperature on carrying capacity for three life stages of brown trout (*Salmo trutta*) (Ayllón et al. 2013).

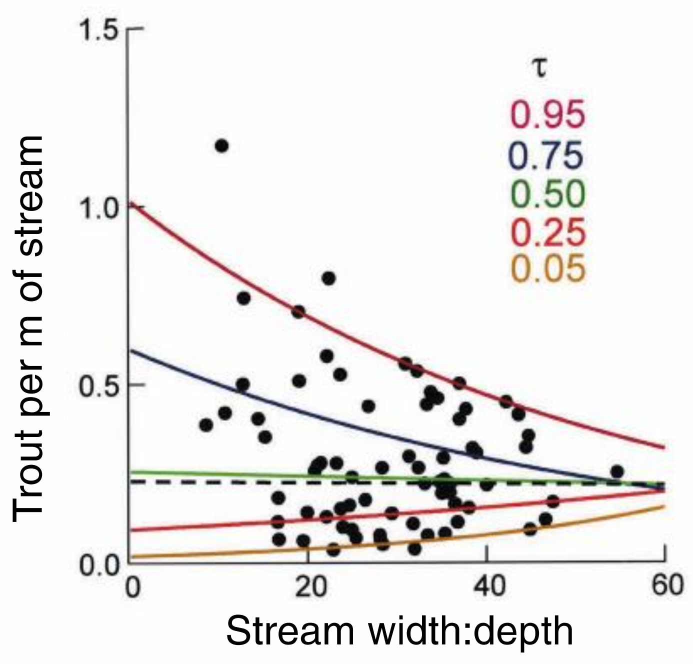

Figure 4. From Cade and Noon (2003), the points depict data from Dunham et al. (2002) with 0.95, 0.75, 0.50, 0.25 and 0.05 quantile estimates (solid lines) and least squares regression estimates (dashed line).

In the same way that quantile regression is an extension of least-squares regression, quantile regression forests (Meinshausen 2006) are an extension of random forest models (Breiman 2001), which are themselves an alternative to standard regression approaches. Random forests is a machine-learning technique, based on classification and regression tree models, which while fairly new to the ecological community is gaining traction (Prasad et al. 2006, Cutler et al. 2007, Olden et al. 2008, Kampichler et al. 2010, Knudby et al. 2010, Evans et al. 2011). A random forest model consists of an ensemble of many (>500 or 1000) individual classification and regression trees, each built on a subset of the list of possible predictor variables. Within each tree, the data are partitioned into successively smaller sets by selecting split points among the subset of predictors found in that tree. These split points are chosen to maximize the homogeneity between each group with respect to the response variable. As part of the random forest algorithm, all possible split points are examined across all possible predictors, and the best one chosen at each step in the algorithm. Random forests can account for non-linear relationships between the response and predictor variables, and naturally incorporate interactions between the predictor variables, two common features of ecological datasets (Breiman 2001). Although the mean predicted response is found by averaging the results of all trees, various quantiles of the predicted response can also be extracted from the distribution of tree predictions (Meinshausen 2006). While quantile regression has been used to solicit the effects of limiting factors on carrying capacity, and random forests have been employed to investigate animal-habitat relationships, to our knowledge an example of using quantile regression forests to estimate carrying capacity has not been described in the ecological literature, although they were used to describe suspended sediment concentration within a stream network (Francke et al. 2008).

Data Requirements. The data requirements for quantile regression include some form of fish abundance, density or biomass (fish, fish/m, fish/m^2, fish/m^3, etc.) as the dependent variable, and a suite of habitat covariates (e.g. pool frequency, large woody debris density, median substrate size, temperature, etc.) as the independent variables. The choice of whether to apply a quantile regression or a quantile regression forest model may be influenced by the dataset. Standard quantile regression requires the analyst to make some assumptions about the form of the fish-habitat relationship (e.g. linear, quadratic, exponential, etc.) and whether to include possible interactions between predictor variables. In return, quantile regression models can be fit with relatively little data. Quantile regression forests on the other hand, like other machine-learning methods, are more “data-hungry”. In return for automatically incorporating predictor interactions, and allowing the analyst to not specify the form of each fish-habitat relationship, they require more data points to provide reliable estimates (e.g. 50 – 500+, depending on how many predictor variables are included). Both of these methods do not require any borrowed parameters, all parameters are estimated through this approach.

To extrapolate to larger spatial scales than the reach, some information about the length or area (or volume) of the stream network is needed. In addition, an extrapolation model may benefit from including covariates that are available across the entire stream network.

The quantile regression approach makes several assumptions. The first is that fish densities respond to habitat characteristics in similar ways across the study sites. The second is that there exists some unmeasured limiting factor preventing many of the sites from reaching capacity. For stream-dwelling fishes, this could include the presence or abundance of other species, spawner abundance in the previous year, other factors that impact egg-to-juvenile survival, temperature, etc. Related to this is the assumption that at least some of the study sites are at or near capacity. If this assumption is not met, then whatever upper quantile is chosen as a proxy for capacity will underestimate the carrying capacity. The quantile chosen is also important. The higher the quantile, the better it is as a proxy of carrying capacity, but this also leads to more uncertainty in the predictions, because the highest quantiles are being estimated from only the top few percent of the data points. In our experience, the 90th quantile can be reliably estimated while providing a good, if slightly conservative, estimate of carrying capacity.

<u>Incorporating Uncertainty, Method Validation, & Future Work.</u> When using quantile regression, standard errors of the coefficients for a particular quantile can be calculated in several ways, including an appeal to asymptotic theory or bootstrapping (Koenker and Hallock 2001), although

bootstrapping is preferred due to the necessity for fewer assumptions. Because quantile regression forests, like random forests, are non-parametric, there is no asymptotic theory to apply, but bootstrap estimates of standard errors are available (Sexton and Laake 2009). Because these methods rely on estimates of fish abundance or density, which are often generated with their own standard errors; an additional bootstrapping step may be applied to account for the uncertainty in the abundance estimation.

Validating estimates of carrying capacity at the reach scale are difficult, since capacity is rarely observed. However, comparisons with other methodologies can be useful. For example, reach scale estimates of capacity can be produced by bioenergetics models such as NREI, and be directly compared to the estimates of quantile regression. For some systems, where reliable, long time-series of spawners and parr or smolts exist, estimates of quantile regression reach scale capacities that have been extrapolated to the stream or watershed scale can be compared with S-R model fits.

Quantile regression as an approach to estimate carrying capacity has been applied rarely to date, but the method is full of potential. Although data must be collected from a number of sample sites, it can be collected within a year or several years, rather than requiring a long time-series as fitting spawner-recruit curves does. With enough data, it allows investigators to derive fish-habitat relationships without making many assumptions. Capacity estimates can then be scaled up and utilized by management or in life-cycle models.

Structural equation models

<u>Introduction.</u> A general approach to most fish habitat monitoring programs is to measure a suite of habitat conditions and infer how those conditions change (a) over space and time and (b) in

response to alternative management strategies or policies. The importance of habitat condition to fish can either be gleaned from extensive literature on fish-habitat relationships (Jackson et al. 2001) or empirically determined by relating fish response to habitat conditions in a statistical model (Fausch et al. 1988). Most fish habitat monitoring programs occur as observational studies in natural systems rather than as controlled experiments, making it challenging to predict how management decisions directly translate into habitat conditions, or how habitat conditions influence fish response. This exemplifies the "correlation does not imply causation" problem of observational studies, where observed correlations among predictors (e.g., habitat conditions) and responses (e.g., fish performance) cannot be relied upon to infer mechanisms or direct causal effects (Shipley 2002).

Structural equation modeling (SEM) is a multivariate approach that emerged from various scientific disciplines and builds upon numerous statistical techniques such as regression, path analysis, factor analysis, and latent variables (Grace 2006). The SEM approach can help address the problems mentioned above, and is one potential approach to estimating tributary habitat carrying capacity. To our knowledge, SEMs have not been employed to estimate carrying capacity of individual fish species. However, the approach has been used by aquatic ecologists for understanding patterns in biodiversity (Belovsky et al. 2011, Duffy et al. 2016), water quality and temperature (Zou and Yu 1994, Isaak and Hubert 2001), ecosystem indicators (Arhonditsis et al. 2006, Maloney and Weller 2011, Irvine et al. 2015) and fish performance (i.e., growth) (Budy et al. 2011).

The advantages of SEM for observational studies and differences from conventional univariate and multivariate approaches are reviewed in (Grace 2008). SEMs graphically relay complex hypotheses about how system components interrelate in a manner easily comprehended by stakeholders (Figure 5). Theoretical knowledge is typically used to develop models, which represent alternative hypotheses about processes leading to observed patterns in the data. The approach is based on the analysis of covariance relations, with maximum-likelihood estimation being the most common method for obtaining solutions; however numerous procedures can be used including Bayesian estimation. Several recent advances to SEMs make it an ideal approach for non-normal or nonlinear data, categorical responses, and hierarchical data structure. Overall, the approach is well suited to elucidating how different processes work in concert, how effects propagate through as system, and evaluating the relative importance of different stimuli (Figure) (Wu and Zumbo 2008, Grace et al. 2010).

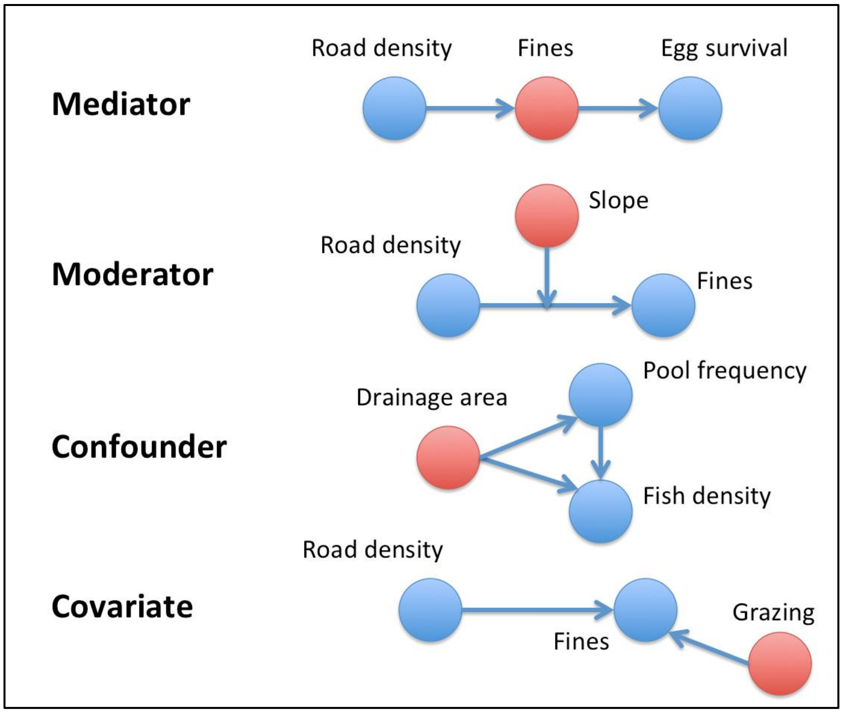

Figure 5. Language for causal models with an example of salmon habitat and resulting fish densities. Paths (arrows) between variables (circles) represent the direction of influence. Terms on the left in bold type relate to the variable in red in the adjacent diagram. Mediators influence how an independent variable affects a dependent variable. Moderators alter the direction or strength of an effect of one variable on another. Confounders are associated with both independent and dependent variables. Covariates are associated with a dependent variable only. Structural equation modeling (SEM) is well suited to analysis of these complex relationships.

In the Upper Grande Ronde River subbasin, SEMs are one potential approach to estimating tributary rearing capacity of juvenile Chinook Salmon. For this purpose, capacity is defined as the upper limit of abundance or density of a particular life stage under current conditions. As such, approaches that estimate the uppermost distribution of fish density should be used. Traditional SEMs, like most other regression-based approaches, estimate the influence of predictor variables (e.g., habitat condition) on the average value of a response variable (e.g., fish abundance). However, recent advances in ‘piecewise SEM’ permit non-normal distributions, random effects, and different correlation structures using local estimation (Lefcheck 2016); piecewise SEM could employ quantile regression to estimate the upper 90th percentile of fish density as a proxy for carrying capacity (see quantile regression section of this report). Alternative proxies for carrying capacity could include modeling the maximum observed fish densities in years with highest previous-year spawner returns; standardizing fish density estimates by previous-year spawner returns when that information is known; or using an SEM describing mean rearing density as a scalar to capacity estimates derived from other methods, such as a Beverton-Holt curve fit to empirical data. Because aquatic habitats across the Columbia River basin have been in a state of degradation for several decades (McIntosh et al. 2000), and because it is problematic for migratory species to navigate over man-made barriers (Humphries and Winemiller 2009), values of carrying capacity based on contemporary, empirical data should be considered conservative estimates at best.

<u>Application</u>. In the Upper Grande Ronde River, we developed a fish-habitat SEM (Figure 6) using data from the Columbia Habitat Monitoring Program (CHaMP 2016) coupled with snorkel surveys of salmonid densities (McCullough et al. 2015). Snorkel counts at each site were expanded using a correction factor developed from paired mark-recapture and snorkel survey

data to account for fish that were not observed by snorkelers (Jonasson et al. 2015). Higher frequencies of large woody debris and pool availability positively influenced Juvenile Chinook Salmon densities as expected. Large wood had both a *direct* influence on fish density and an *indirect* effect through its positive association with pools. To evaluate the total effect of wood on fish relative to other factors in the model, the sum of the direct standardized path coefficient between wood and fish (0.20) and product of the path of wood on pools (0.47) and pools to fish (0.19) yields a coefficient of 0.29, which is greater than the direct effect of wood on fish, underlining the importance of the indirect role of wood in forming pools used by fish. Landscape context was also an important consideration in this model: reaches with larger cumulative drainage area were strongly associated with higher fish densities, more pools, and lower wood frequency. The effects of local-scale habitat conditions on fish density would have been obscured without incorporating a variable accounting for the position of reaches in the stream network. Mossop and Bradford (2006) used a similar conceptual model explaining associations among juvenile Chinook salmon density, wood, pools, and reach gradient in small tributaries of the upper Yukon River, Canada. Their study was based on visualizing pairwise correlation coefficients, however, and did not account for the variance-covariance structure inherent in modern SEM.

SEM’s provide a flexible structure that allows for more data types and structures than habitat expansion or QRF methods. For example, the combination of continuous, categorical, and latent variables can be used in a single SEM. Because models are developed using *a priori* ecological knowledge—often in concert with local land managers—predictions of capacity estimates can be developed for relevant, real-world management applications. The value of SEM’s becomes most apparent when increasingly complex data are available, particularly at multiple spatial scales.

Under those conditions SEM's can incorporate interactions and covariance that habitat expansion or QRF cannot, while producing appealing and approachable visualizations of factors driving or limiting fish abundance. However, many watersheds currently lack the habitat and fish data needed to utilize the SEM approach and habitat expansion or QRF may suffice.

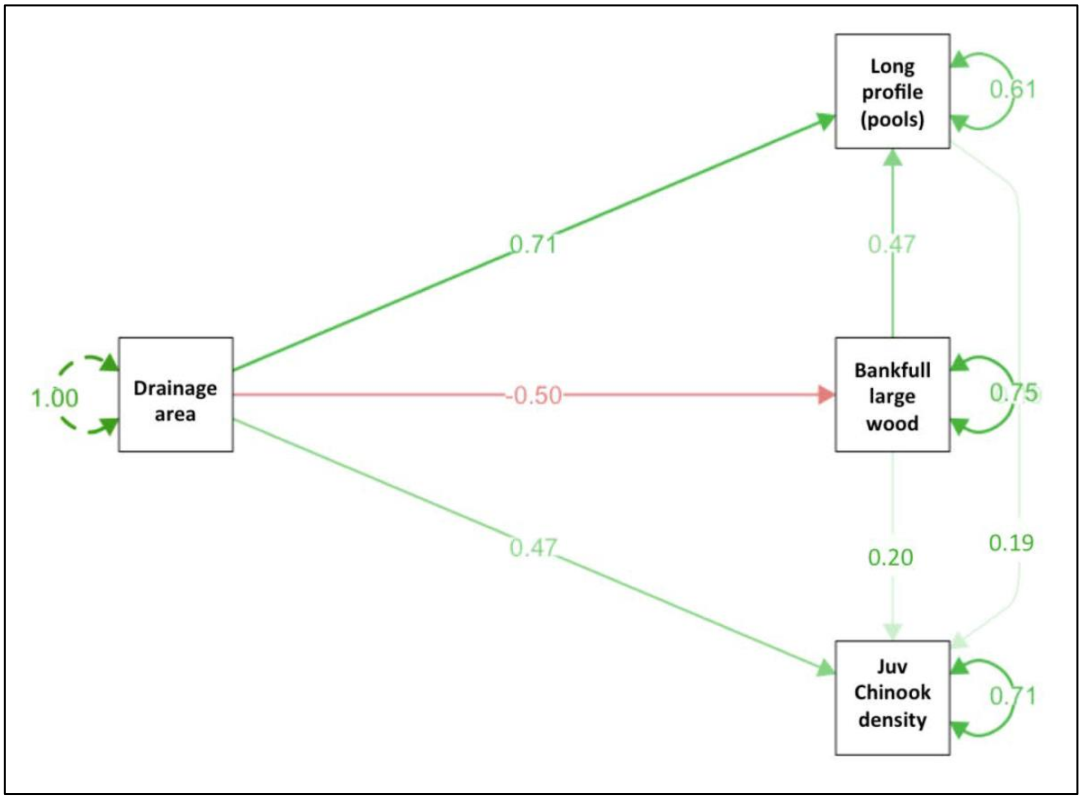

Figure 6. SEM results linking cumulative drainage area with longitudinal thalweg depth profile (a proxy for pool frequency), large wood frequency within the bankfull channel, and juvenile Chinook density (fish/m). Direction of arrows indicates the hypothesized direction of causal effect; whereas the color, shade, sign, and magnitude of the standardized path coefficients indicate the direction and strength of the relationship (green is positive, red is negative, coefficients closer to |1| and darker shade of arrow are stronger). Values in double-headed arrows are amount of variance explained for dependent variables (analogous to R^2 in linear regression).

Ecohydraulic and mechanistic habitat models

Introduction. A limitation of empirical models is the difficulty of scaling in both data collection and prediction. Empirical models are only useful to estimate the capacity of a system if observations of fish abundances have been made at or near capacity, a fact that may hamper many systems where contemporary abundances are low or non-existent (e.g. impounded by a dam). Although empirical estimates allow for some estimate in the uncertainty of predictions, they are limited by the extent of the data, and cannot make predictions for novel conditions. However, by definition mechanistic approaches employ a series of functional responses to predict fish abundance under a range of conditions. For stream fishes, two types of mechanistic models are generally employed: habitat suitability index (HSI) and net rate of energy intake (NREI). Historically, the term HSI has been cast broadly to include models which may be more empirical or even qualitative (e.g. expert opinion) as a way of relating habitat characteristics to capacity. In this context however, HSI will be used to describe models that employs applies suitability curves for a range of habitat characteristics with estimates (either modeled or measured) of those characteristics at the scale of interest. In these instances a habitat suitability index model is constructed from an understanding of the basic habitat requirements of a species, forming a “bottom up” approach by placing a floor on the capacity of a habitat that can be further reduced through additional habitat requirements. For salmonids, most HSI models are constructed from a hydrodynamics model (e.g. PHABSIM) that breaks the available habitat into cells, the grain of which is determined by the resolution of the hydrodynamics model. Hydrodynamics models can therefore provide estimates of basic habitat parameters (velocity, depth, etc.) under various flow regimes for each modeled cell.

Relationships between the abundance of fish and their habitat have most commonly been established through empirical methods (Rosenfeld 2003). These models are only useful for estimating carrying capacity when abundances are near their limits, although approaches like quantile regressions (see Quantile regression, above) may be able to establish these relationships when carrying capacity is at least occasionally reached. While empirical based models are an efficient approach to quantifying relationships and detecting patterns, their strength is generating hypotheses about variables of importance rather than being used in predictions and testing hypotheses. Empirical models often lack predictive ability because: they often contain many variables yet are based on low samples sizes; assume no measurement error of the predictor variables; relate to fish abundance estimates that are also often very imprecise; and often lack validation (Fausch et al. 1988). Commonly used multiple regression approaches assume linear relationships, do not contain higher order interactions, cannot identify threshold effects, or effectively deal with missing data. However, machine learning approaches are gaining popularity because of their ability to overcome many of these issues (see quantile regression) Empirical models also typically lack the experimental manipulations needed to identify and validate causal mechanisms, and thus understanding why these complex assemblages of variables interact to describe fish habitat requirements is extremely difficult. Drift-foraging bioenergetics models, however, are often based on experimental or comparative studies confirming patterns described by mathematical models based on ecological theory (Fausch 1984, Hughes and Dill 1990). Therefore, these models are not only potentially more robust for predictions, but they allow for the evaluation of alternative management scenarios (Nislow et al. 1999, Hayes et al. 2016, Wall et al. 2016). However, due to their complexity, they can be data intensive and difficult to calibrate and validate (Piccolo et al. 2014, Rosenfeld et al. 2014). Microhabitat models, such as habitat suitability models, straddle empirical and drift-foraging bioenergetics approaches (Rosenfeld et al. 2016). Proximate cues that fish are responding to such as depth, velocity, and substrate, describe habitat quantity and quality and can in part be driven by mechanistically based hydraulic models. However, the rule sets used in building these relationship are based on fish preferences of these variables which are often site-specific, making extrapolation difficult or uncertain (Rosenfeld 2003). Here we describe two ecohydraulic approaches to evaluate carrying capacity of adult and juvenile salmonids.

Hydraulics as the habitat template

Much of the fish habitat information used to develop empirical fish capacity models is coarsely resolved, often based on surrogate variables for the actual environmental cues to which fish are responding. For example, correlations between fish density and geomorphic units (e.g. pools, riffles) are commonly used to estimate fish abundance (Fausch et al. 1988). Fish are likely not responding to the geomorphic units, but rather to spatial patterns of depths and velocities. Additionally, relationships between these coarser habitat features and discharge are difficult to quantify and thus cannot inform evaluations flow or restoration alternatives. Therefore, ecohydraulic fish habitat models have been developed to potentially allow more detailed or mechanistic questions to be addressed (Hayes et al. 2007, Wall et al. 2016).

Hydraulic models provide spatially explicit estimates of depth and velocity across a reach. One-dimensional (1D) models provide longitudinal estimates of velocity and depth and are very commonly used when channel cross-sectional data is collected to describe channel morphology. While 1D hydraulic models are commonly used in fish habitat applications, 2D (adds lateral velocities), and 3D (adds depth and lateral velocities) models increase realism by providing more detail on the velocity vectors to which fish respond (Dunbar et al. 2012). In order to develop reach-level hydraulic models, spatially explicit information on channel planform, channel roughness, discharge, and surface water elevation is required. Few fish habitat monitoring programs collect the data necessary for developing 1D hydraulic models, much less higher dimensional models. One exception is the Columbia Habitat Monitoring Program, where topographically stratified XYZ data points are collected, via a total station or real-time kinematic GPS, that are interpolated to create high resolution (i.e. 10 cm) digital elevation models (DEMs) of the water surface and stream channel (Bangen et al. 2014a). These data are used to create 2 and 3D hydraulic models, which produce depth and velocity estimates with equal or less error than field-measured values (Pasternack et al. 2006) thereby creating a valuable high resolution tool for fish habitat assessments. The reach DEMs, and therefore subsequent hydraulic models, can also be manipulated to represent expected changes due to restoration (Wall et al. 2016).

Microhabitat Models

Habitat suitability index models (HSI) in conjunction with hydraulic models have been used extensively to evaluate how changes in stream discharge influence the availability of usable microhabitats for several species of fish across multiple life stages (Rosenfeld 2003). PHABSIM is the most popular of these models (Souchon and Capra 2004). Generally, frequencies of fish use (e.g., observed through snorkeling) of particular depth, velocity, substrate, and occasionally cover values, are divided by the available distributions for these variables to develop preference or habitat suitability curves. While these curves represent preferences rather than factors directly linked to fitness, these are the microhabitat environmental cues which are likely responsible for the behavior observed in fish. The habitat suitability curves are then used to weigh measured or modeled habitat features in a reach to estimate weighted usable area (WUA). As higher resolution data within reaches become increasingly more feasible to collect, models can describe detailed spatial patterns of microhabitat quantity and quality (Figure 7). Further, the carrying capacity of a modeled reach can be estimated by dividing WUA by the territory size required by an individual (Keeley and Slaney 1996, Ayllón et al. 2012, Cramer and Ceder 2013).

A criticism of HSI models is that they are site-specific, making extrapolation to other locations unreliable. For example, if observations of depths used by salmonids to develop habitat suitability curves come from a larger stream, this might incorrectly suggest that salmonids cannot use smaller streams where maximum depths are less than the minimum depths used by fish in the larger stream. A more robust approach is to develop more generalized habitat suitability curves using fuzzy inference systems (Ahmadi-Nedushan et al. 2008). Fuzzy inference systems (FIS) are founded on fuzzy set theory and fuzzy logic (Zadeh 1965). FIS are intuitive, flexible in adjusting model parameters and variables, are more robust with imprecise data, can incorporate expert knowledge, and can represent more complex multivariate relationships than traditional HSI models (Jang and Gulley 2014). When combined with high resolution hydraulic model outputs, FIS-based habitat models also provide a spatially explicit depiction of habitat suitability and an estimate of WUA, which can be used to estimate carrying capacity as described for traditional HSI models above.

Another criticism of HSI models, is that they do not include important variables such as temperature and food availability. For example, (Rosenfeld et al. 2005) found that habitat suitability curves derived in artificial stream channels poorly predicted habitat use in the same channels after prey resources were experimentally manipulated. However, bioenergetics model predictions that included prey and temperature variables accurately predicted habitat use across the prey resources tested. Because spawning salmon are no longer feeding while occupying redds, HSI models can provide accurate predictions of potential redd locations (Wheaton et al. 2010, Kammel et al. 2016).

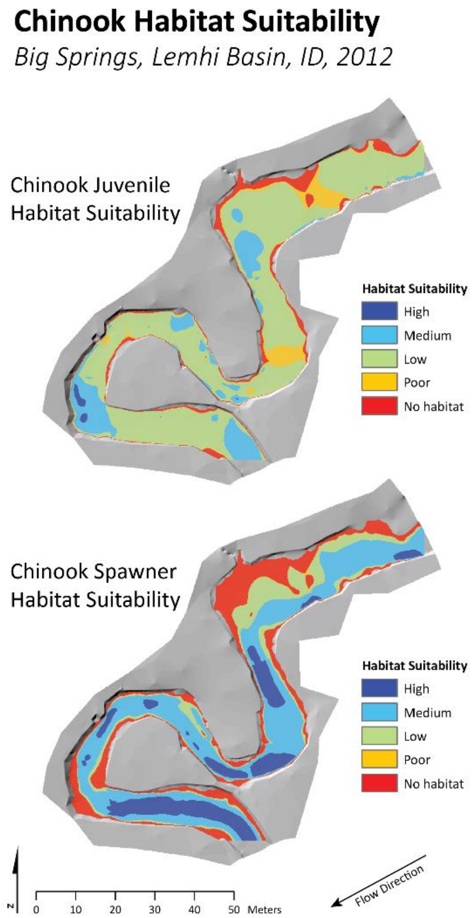

Figure 7. Maps of Chinook salmon juvenile rearing (upper) and adult spawning (lower) HSI model output. Data are for 2012 site visit of Big Springs Creek, Lemhi River basin, Idaho.

Drift-foraging models

Drift foraging models were originally developed based on optimal foraging theory to describe the feeding behavior and location position of drift feeding salmonids, positing that fish choose locations with optimal energetic value (Hughes and Dill 1990, Hill and Grossman 1993). A drift-feeding fish's net energy intake (NEI) or net rate of energy intake (NREI) is energy gains through capture and consumption of drifting invertebrates minus energy cost through swimming to maintain a foraging position. These models were initially validated with intensive observations of feeding locations (Fausch 1984, Hughes and Dill 1990, Addley 1993, Hill and

Grossman 1993, Guensch et al. 2001), but have also been used to successfully predict growth and abundance (Nislow et al. 2000, Hayes et al. 2007, Urabe et al. 2010, Wall et al. 2015).

The NEI model incorporates data on depth, focal velocity, prey abundance (drifting invertebrates) to predict prey encounter rates, capture success, and consumption rates at locations throughout the modeled environment. These variables can simply be measured throughout a reach and converted to NEI (Guensch et al. 2001, Urabe et al. 2010). Alternatively, depth and velocity results from hydraulic models (described above) can also be used to estimate these inputs (e.g. Wall et al. 2015), and additionally drift transport rates (e.g. Hayes et al. 2007). Bioenergetics models estimate gross energy input (GEI) from prey consumed and swimming costs (SC) at the focal velocity under a given temperature, with GEI-SC=NEI.

Many NEI-type foraging models follow the approach described by Hughes and Dill (1990). Foraging volumes at all focal points, or every location in a grid of hydraulic model output, are estimated using the reaction distance of the foraging fish (often determined in the laboratory) as the radius of the search area in a stream cross section times the velocity. This search area can be truncated by either water depth, or the maximum capture distance as a function of water velocity to produce a capture area (Hughes and Dill 1990, Hayes et al. 2007). The capture volumes multiplied by the drift density provides the instantaneous prey capture rates and, along with the energy content of the prey, a GEI at each modeled cell within the stream.

To estimate carrying capacity, the highest NEI value on each modeled cross section is compared to a user-defined NEI threshold and locations meeting or exceeding the NEI threshold (e.g. NREI>0) receive a fish (Hayes et al. 2007, Wall et al. 2015). A minimum distance between fish is set by the fish territory size. Fish are placed at upstream cross sections first and downstream drift predictions are then augmented to reflect consumption of drifting invertebrates by fish placed at upstream cross sections (Hayes et al. 2007). Placement proceeds downstream until the last cross section has been evaluated for fish placement, with carrying capacity equal to the sum of all fish in the reach.

NEI models have also been used to evaluate the effects of flow management and stream restoration on distribution, growth and abundance of drift foraging salmonids (Nislow et al. 1999, Hayes et al. 2016, Wall et al. 2016). Wall et al. (2016) recently demonstrated how a NEI model could be used to describe both a predicted and observed response to woody structures on energy availability and abundance changes for steelhead. They first conducted a topographic survey (Bangen et al. 2014b) and hydraulic model-based NREI assessment on a reach pre-restoration. They next manipulated the initial DEM to represent the intended restoration design. Woody structures were then added to the reach and surveyed the subsequent year and the same analyses were repeated. Following the restoration, both the predicted and observed changes to the DEM from the wood addition created energetically favorable areas, and an increase in average NREI and carrying capacity. As example of how this approach can be up-scaled to address population level predictions, this same approach was recently used in overall life-cycle assessment of steelhead population persistence following a large-scale restoration effort in the Middle Fork of the John Day River in Central Oregon (McHugh et al. *in revision* or Wheaton et al. in press).

Both microhabitat and drift-foraging bioenergetics models are limited by their complexity and sensitive to large number of assumptions and inputs. The input data can be labor intensive to collect and subject to observer variability. Recent advances in technology and methodologies have greatly reduced both labor costs and observer variability in collecting river bathymetry

(Bangen et al. 2014a, Bangen et al. 2014b) allowing the use of higher order hydraulic models. Remote sensing approaches are beginning to allow for large scale development of DEMs and hydraulic models (Kammel et al. 2016) that can rival efficiencies of even traditional rapid fish habitat assessments (Hankin and Reeves 1988).

Samples of invertebrate drift are inherently noisy and are generally not included in fish habitat monitoring protocols. However, this habitat metric was recently demonstrated to be highly relevant to salmonids (Weber et al. 2014), and of moderate repeatability (Weber et al. *in press*) to other habitat metrics commonly collected and used in empirical models. Estimates of gross primary production over reaches and even networks may be used as a surrogate or predictor of invertebrate drift (see above Ryan's section; Saunders et al. submitted) allowing for potential greater efficiencies in data collection or estimation for model input information.

The computation power required to run both the hydraulic models and drift-foraging bioenergetics models, until recently, limited model evaluations to relatively limited model domains (e.g., a single pool, Hayes et al. 2007). Wall et al. (2015) were able to increase the spatial extent of this approach to several reaches containing multiple geomorphic units. Slight mathematical changes, changes in the programing language, and use of low cost, high volume cloud computing services has allowed this model to be implemented across hundreds of reaches with about the same effort as previously for a single channel unit (Bouwes, *personal obs*.). Overcoming computational limitation greatly expands the potential for the improvement, validation, and widespread use of such models.

While ecohydraulic models summarize hugely important features of fish habitat, they obviously do not include other biotic or abiotic considerations that can limit carrying capacity. For example, inter- and intra-specific competition can reduce resources that might not be accounted for in certain models. However, some of this is partially implicit when using empirical estimates of territory sizes and drift data. Additionally, predators can have large influences on fish behavior or abundance and therefore consideration of the effects of cover and the presence of predators could potentially influence carrying capacity. More complex models have been developed to incorporate some of these concepts (Railsback et al. 2013). Some of these variables have been or could be added to microhabitat models to develop of habitat suitability or FIS functions. Finally, these models could be used to synthesize multiple habitat feature into an interpretable single metric that could then subsequently be used in multivariable empirical models. For example, (Kawai et al. 2014) found that while NEI predicted fish abundance, the addition of cover as a separate variable improve model predictive ability. Whether ecohydraulic models are powerful enough to describe the most important features of fish habitat that limit carrying capacity in most situations or if other mechanisms or variables must also be incorporated is currently being pursued and a fruitful area of fisheries science (Rosenfeld et al. 2014)

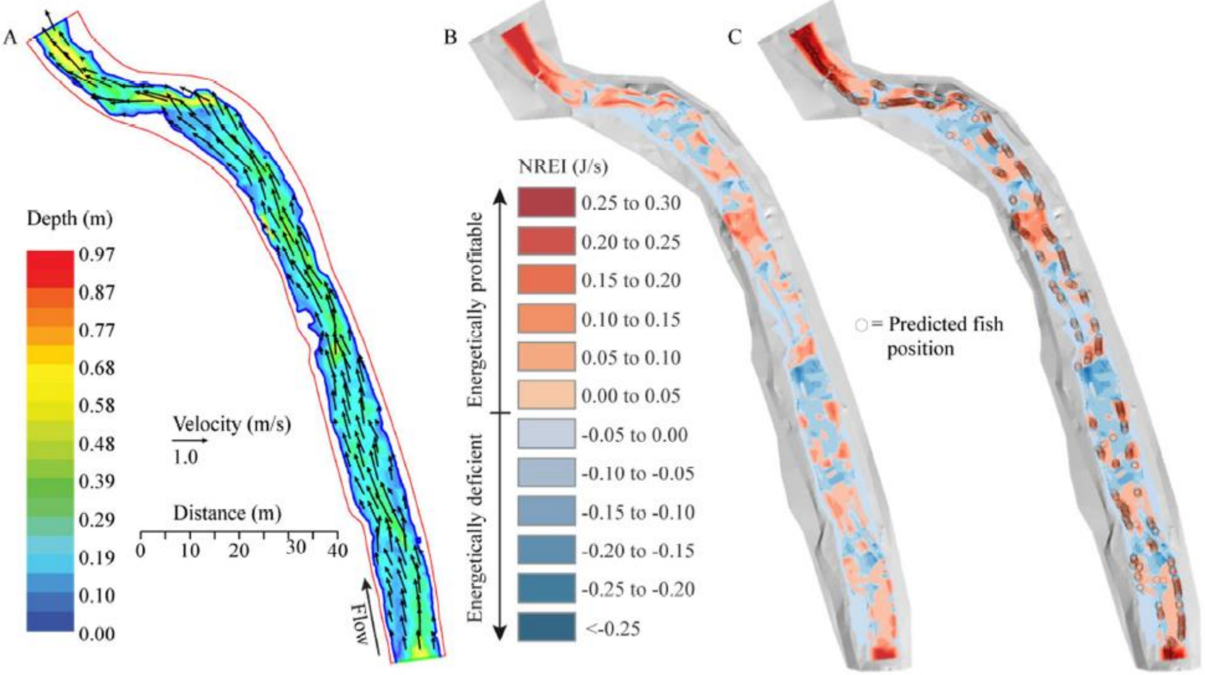

Figure 8. From Wall et al. 2015. (A) Depth and velocity estimated from a 2.5D hydraulic model (B) spatially explicit prediction of NREI based on foraging and swim cost models (C) predicted locations of fish based on NREI values greater than zero and territory size.

Dynamic Food Web Models

Introduction and Application. Food web approaches to estimating capacity are rooted in the fundamental laws of thermodynamics and mass balance (Gotelli 2001, Odum and Barrett 2005). In other words, the production of any population cannot exceed the production and availability of that populations prey (First Law of Thermodynamics). This upper bound is further constrained by the reality that the some of the energy from this food is lost as it is transformed into consumer biomass (Second Law of Thermodynamics). Food web approaches to estimating biological capacity take advantage of these fundamental bounds. Consequently, if food or prey availability is known, as well as the efficiency by which consumers can convert that prey to biomass (assimilation and production efficiencies), an "energetic" estimate of capacity can be determined.

There are three main approaches for synthesizing this information into a capacity estimate for fish. First, are simple trophic level fractionation models (Elton 1927, Lindeman 1942, Odum and Barrett 2005). This approach assumes that capacity at a given trophic level is some fraction of the production at a lower trophic level. Many studies, for instance, assume that 10% of the biomass produced at a given trophic level is passed on the next higher level. For instance, if only basal algal production was known and fish were two trophic levels above this, then fish production capacity would be 1% that of primary production (i.e., 10% X 10%).

The second approach is the trophic basis of production (Benke and Wallace 1980, Cross et al. 2011, Bellmore et al. 2013), which is an extension of the simple trophic level fractionation model. The trophic basis of production approach embraces the reality that food webs are complex, and that consumers may feed on a variety of prey items that vary in both quality and quantity. By combining empirical information on prey specific production estimates with information on consumer dietary proportions, as well as prey-specific assimilation efficiencies, this approach allows for the quantification of the consumptive energy flows that exist between predators and their prey. These quantitative food webs can not only be used to visualize energy flow through the food web, but it can also be used to quantify energetic carrying capacity, and how competitors influence this capacity (Bellmore et al. 2013).

Third, is dynamic food web modeling (Mcintire and Colby 1978, Yodzis and Innes 1992, Power et al. 1995). Unlike the other methods this approach acknowledges that predators and prey are dynamically linked, and that the availability of prey is also a function of consumption by predators. Unlike the previous two approaches, this approach does not require estimates of food availability. Instead, prey availability and consumer carrying capacity emerge from the predator-prey dynamics included in the model. In their simplest form, these food web models are a series of linked Lotka-Voltera predator/prey equations (Getz 1993). By mechanistically linking the demographics of web members (e.g., rate of consumption, mortality and respiration) to local environmental conditions (e.g., water temperature, channel hydraulics), these models can be used to predict equilibrium fish biomass dynamics for streams, which can be interpreted as an "energetic" carrying capacity estimate.

Below, we describe a dynamic stream food web model termed the Aquatic Trophic Productivity (ATP) model that can be used to estimate fish carrying capacity (Bellmore et al. 2017 , Figure 9). Within the ATP model, capacity is defined as the maximum amount of fish a system can support given available food resources and the efficiency at which fishes can convert those food resources to biomass. Because this is an energetic estimate of capacity, output metrics could be presented in unit of production (e.g., kg/year), biomass (e.g., kg), or abundance (#), depending on the user/manager needs.

The ATP model mechanistically links the dynamics of the river food webs, and the resultant performance of stream fishes, to (1) the physical and hydraulic conditions of the stream, (2) the structure and composition of the adjacent riparian zone, and (3) marine derived nutrient delivered by adult salmon (Figure 9). The modeling framework is founded on the assumption that the general dynamics of stream food webs can be simulated if the dynamics of these environmental factors are known (Vannote et al. 1980, Power and Dietrich 2002, Woodward and Hildrew 2002).

Specifically, the model allows energy to flow from the bottom-up, from basal resources (e.g., in-stream primary producers, terrestrially derived organic matter) to aquatic invertebrates, and aquatic invertebrates to fish. Reciprocally, these "bottom-up" organic matter flows represent losses of biomass imposed from the “top-down” (i.e., consumption). As with all ecosystems, the modeled food web is an “open” system, in that energy and materials enter the system from external locations (referred to as “subsidies”). In this case, these external inputs represent the raw ingredients and subsidies that fuel the productivity of the food web, and include: (1) light and nutrients, which provide the energy and materials necessary for the production of periphyton; (2) lateral inputs from the riparian zone, which provide detrital organic matter (leaf litter) as well as direct food resources for fish (terrestrial invertebrates); and (3), returning adult salmon, which represent a source of marine carbon and nutrients (marine derived nutrients).

The ATP model was designed to explore how stream salmonids (specifically salmon and steelhead) respond to alternative restoration strategies. That said, the approach is flexible and can be adjusted to confront numerous problems and potential applications (e.g., climate change, invasive species, local restoration goals, and watershed scale management). It can also be used to identify and rank factors limiting fish capacity.

Data Requirements. Because the food web component of the ATP model is founded on basic ecological (predator prey dynamics; Gotelli 2001) and thermodynamic (mass-balance) principles, the framework of the model should be transferable across study locations. Moreover, it is assumed that environmental factors mediate the dynamics within the food web. Thus, to simulate food web dynamics at specific sites will simply require information about local environmental conditions that are generally available (Table 1). This includes river discharge (m3/s), water temperature (C), distribution of substrate size on the river bed (cm), proportion of the stream shaded, total solar input (i.e. photosynthetically active radiation; µmol photons/m^2/s), proportion of the vegetation cover to account for allochthonous inputs, 1-dimensional channel hydraulics, number of the adult salmon returning to spawn, and water quality measures (e.g., turbidity, nitrogen and phosphorus concentration). In addition, it is useful to have estimates of biomass for fish, aquatic invertebrates, periphyton, and terrestrial detritus to corroborate model simulations. This information also allows model users to adjust the most sensitive model parameters (e.g., parameters that control the predator/prey functional responses, assimilation efficiencies, and strengths of self-interaction) to "fine tune" the model to better mimic food web dynamics in the study location.

Although the ATP is a food web model, it is not assumed that food or any other specific factor is limiting capacity. In fact, implicit in this approach is the idea that numerous things (both direct and indirect) may limit the capacity of rivers to sustain fish. Instead, it is assumed that the simplified structure of our food web model represents the most important processes of the stream in enough detail so that it can be used to evaluate which factors are most limiting. This is a critical assumption because the ATP model is simplified compared to the complex dynamics of real food webs (see Bellmore et al. 2013). However, incorporating more complexity may not make the model more predictive or useful (Ford 2010). Although important for furthering ecological theory, complex food web models often produce results that are extremely difficult to interpret, introduce numerous parameters of unknown value, and frequently exhibit behavior that is chaotic or unstable; all of these things serve as justification for a more simplified approach.

Methods/Products. The ATP model produces estimates of capacity for a fish population or the entire fish community. Given that the foundation of the ATP model is based on food web interactions, the model can easily be adjusted to evaluate a variety of food web structures, such as the presence of other fish competitors and/or predators. To date, the primary focus is on juvenile Chinook salmon. However, the model is capable of including other fishes to explore how changes in the fish community influence carrying capacity (Bellmore et al. 2017).

The ATP model can be used to estimate fish capacity across a range of temporal and spatial scales. Capacity estimates are produced on a daily time step, but these daily estimates can be summarized at different temporal scales, such as seasonal or annual. The advantage of daily estimates is that potential bottlenecks or temporal limitations to capacity can be identified, as well as the associated underlying mechanisms responsible for the observed limitation. From a spatial perspective, the model is currently being used to estimate capacity at the reach or segment scale (100 meters to 10 kilometers). That said, the model could be run at any spatial scale. However, given that habitat conditions are averaged within the model (i.e., the model is not spatially explicit), it may not make ecological sense to model areas that are either much smaller (e.g., channel units) or larger (e.g., entire tributaries). Current development on approaches for scaling up model results to larger spatial domains (e.g., floodplain mosaics and entire watersheds) is underway. This can be done by linking different modeled units together; whereby different modeled reaches would interact with one another via downstream transport of organic matter (periphyton, detritus, invertebrates), and the bi-direction movement of organisms (fishes). This type of network scale view of food webs may result in emergent dynamics could greatly contribute to our understanding (Polis et al. 2004) of how local restoration efforts interact to influence capacity at the watershed scale.

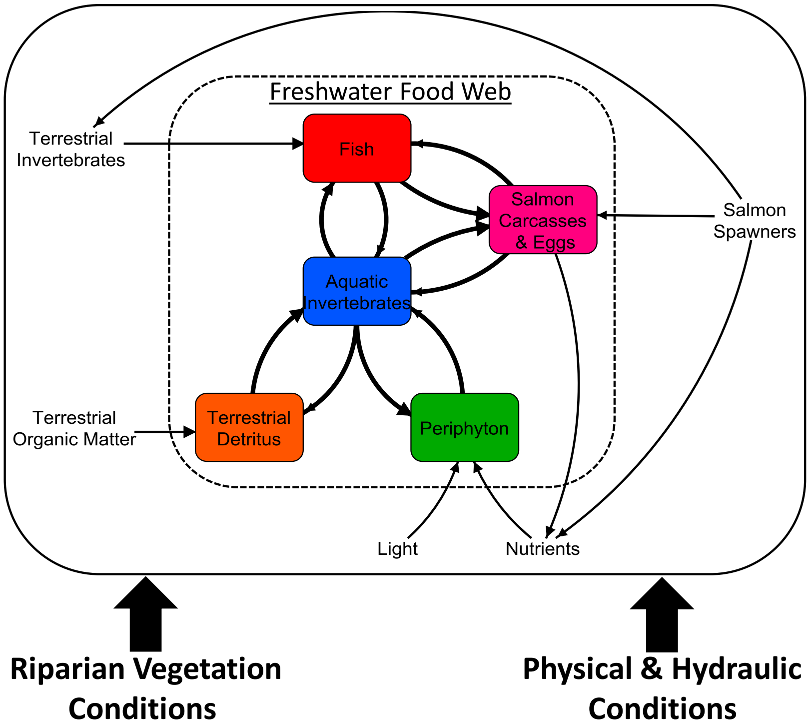

Figure 9. Conceptual representation of the Aquatic Trophic Productivity (ATP) model. The backbone of the model contains four stocks; terrestrial detritus, periphyton, aquatic invertebrates, and fish. Energy is transferred through each stock from the bottom-up, whereas top-down control (i.e., consumption) is also present. For periphyton, energy is provided from solor input (i.e., light) and nutrients. In situ energy is subsidized by terrestrial organic matter in the form of leaf litter and terrestrial insects that fall in the stream, and marine derived nutrients from adult salmon returning to spawn. For example, adults provide nutrients via excretion and carcass decomposition, and fish and invertebrates can directly consume organic carbon from carcasses. Ultimately, the food web dynamics and subsidies are mediated by physical, hydraulic, and riparian conditions. Figure taken from Bellmore et al. 2017.

<u>Incorporating Uncertainty, Method Validation, and Future Work.</u> To incorporate uncertainty into ATP model predictions, a global sensitivity analyses is used (Bellmore et al. 2014, Bellmore et al. 2017), which takes into account the interactive effects of multiple uncertain variables. In addition, we can add stochasticity to model runs by adding distributions (e.g., uniform, normal) around model parameters and environmental conditions.

Results of the ATP model have been corroborated at a single site (Bellmore et al. 2017). Full model validation will require correlating modeled fish biomass to empirical fish biomass across several sites. To fully validate the model, biomass dynamics for periphyton, invertebrate, and fish, as well as dietary proportions for invertebrates and fish would be needed. However, having all of this data at any site is rare because it can be expensive to collect and process. Collection of this extensive data is underway at six sites within the Methow River (J.R. Bellmore and J. R. Benjamin unpublished data). That said, it is not expected the model will produce fish abundance estimates that accurately predict observed fish biomass at a site. Instead, the goal of this modeling effort is to be able to represent relative differences in fish abundance, either across different sites, or at a single site, by comparing baseline conditions to those expected with restoration. For example, the model could be used to ask questions such as: "which locations in a watershed might have the greatest capacity to sustain fish production?", or "which set of management actions might lead to the greatest increase in carrying capacity?"

Future directions include using the ATP model to estimate fish capacity across the watershed, which will require a suite of movement rules for fish (Railsback et al. 1999). The ATP model is being linked to a full Chinook salmon life cycle model in order to account for out of basin effects on Chinook salmon, as well as to make better estimates of long term population trajectories. In addition, the model is linked to a habitat suitability index (J.R. Bellmore and J.R. Benjamin unpublished data) that accounts for the proportion of habitat that is unsuitable for juvenile Chinook salmon. Lastly, multiple components of a salmon life cycle model are being developed such as dam passage, ocean conditions and survival, climate change, habitat relationships. In the future, it may be possible to link the ATP model, along with these different components into a "global model" that can provide a more holistic view of salmon recovery.

Table 1. Location, species and life stage where each capacity method is currently being applied, or is proposed.

Method	MPG	ESU	Sub-Basin	(sub)watershed	species	life stage	Chapter
Empirical (spawner-recruit)	Upper Columbia	Upper Columbia	Entiat R.	Entiat R.	spring/summer Chnk.	parr/smolt	2c
	Wenatchee-Methow R.	Upper Columbia	Wenatchee R.	Chiwawa R.	spring/summer Chnk.	parr/smolt	
	Wenatchee-Methow R.	Upper Columbia	Methow R.	Methow R.	spring/summer Chnk.	parr/smolt	
	Wenatchee-Methow R.	Upper Columbia	Methow R.	Twisp R.	spring/summer Chnk.	parr/smolt	
	John Day Middle Fork	Middle Columbia	John Day R.	John Day Middle Fork	spring/summer Chnk.	parr/smolt	
	John Day Upper Mainstem	Middle Columbia	John Day R.	John Day Upper Mainstem	spring/summer Chnk.	parr/smolt	
	Umatilla-Walla Walla	Middle Columbia	Umatilla R.	Umatilla R.	spring/summer Chnk.	parr/smolt	
	Lower Snake	Snake R.	Tucannon R.	Tucannon R.	spring/summer Chnk.	parr/smolt	
	Grande Ronde-Imnaha	Snake R.	Grande Ronde	Catherine Creek	spring/summer Chnk.	parr/smolt	
	Grande Ronde-Imnaha	Snake R.	Grande Ronde	Lostine R.	spring/summer Chnk.	parr/smolt	
	Grande Ronde-Imnaha	Snake R.	Grande Ronde	Upper Grande Ronde R.	spring/summer Chnk.	parr/smolt	
	Grande Ronde-Imnaha	Snake R.	Imnaha R.	Imnaha R.	spring/summer Chnk.	parr/smolt	
	Dry Clearwater	Snake R.	Clearwater R.	Red R.	spring/summer Chnk.	parr/smolt	
	Wet Clearwater	Snake R.	Clearwater R.	Crooked Fork Creek	spring/summer Chnk.	parr/smolt	
	Middle Fork Salmon R.	Snake R.	Salmon R.	Marsh Creek	spring/summer Chnk.	parr/smolt	
	South Fork Salmon R.	Snake R.	Salmon R.	East Fork Salmon R.	spring/summer Chnk.	parr/smolt	
	South Fork Salmon R.	Snake R.	Salmon R.	Secesh R.	spring/summer Chnk.	parr/smolt	
	South Fork Salmon R.	Snake R.	Salmon R.	South Fork Salmon R.	spring/summer Chnk.	parr/smolt	
	Upper Salmon R.	Snake R.	Lemhi R.	Hayden Creek	spring/summer Chnk.	parr/smolt	
	Upper Salmon R.	Snake R.	Lemhi R.	Upper Lemhi R.	spring/summer Chnk.	parr/smolt	
	Upper Salmon R.	Snake R.	Salmon R.	Pahsimeroi R.	spring/summer Chnk.	parr/smolt	
	Upper Salmon R.	Snake R.	Salmon R.	Upper Salmon R.	spring/summer Chnk.	parr/smolt	
Habitat expansion	CRB-wide				spring/summer Chnk.	parr	2b
Quantile Random Forests	CRB-wide				spring/summer Chnk.	parr	NA
Structural Equation Models	Grande Ronde-Imnaha	Snake R.	Grande Ronde	Catherine Creek	spring Chnk.	parr	NA
	Grande Ronde-Imnaha	Snake R.	Grande Ronde	Upper Grande Ronde R.	spring Chnk.	parr	NA
HSI	John Day R.	Middle Columbia	John Day R.	MF John Day R.	spring/summer Chnk., sthd.	adult	9d
	Upper Columbia	Upper Columbia	Entiat R.	Entiat R.	spring/summer Chnk., sthd.	adult	9d
	Wenatchee-Methow R.	Upper Columbia	Wenatchee R.	all subwatersheds	spring/summer Chnk., sthd.	adult	9d
	Wenatchee-Methow R.	Upper Columbia	Methow R.	multiple	spring/summer Chnk., sthd.	adult	9d
	South Fork Salmon R.	Snake R.	Salmon R.	Secesh R.	spring/summer Chnk., sthd.	adult	9d
	Upper Salmon R.	Snake R.	Yankee Fork R.	Yankee Fork R.	spring/summer Chnk., sthd.	adult	9d
	Upper Salmon R.	Snake R.	Lemhi R.	multiple	spring/summer Chnk., sthd.	adult	9d
	Grande Ronde-Imnaha	Snake R.	Grande Ronde	Lower Grande Ronde R.	spring/summer Chnk., sthd.	adult	9d
	Grande Ronde-Imnaha	Snake R.	Grande Ronde	Upper Grande Ronde R.	spring/summer Chnk., sthd.	adult	9d
	Grande Ronde-Imnaha	Snake R.	Grande Ronde	Catherine Creek	spring/summer Chnk., sthd.	adult	9d
	Grande Ronde-Imnaha	Snake R.	Minam R.	Minam R.	spring/summer Chnk., sthd.	adult	9d
	Lower Snake	Snake R.	Asotin R.	Asotin R.	spring/summer Chnk., sthd.	adult	9d
	Lower Snake	Snake R.	Tucannon R.	Tucannon R.	spring/summer Chnk., sthd.	adult	9d
NREI	John Day R.	Middle Columbia	John Day R.	MF John Day R., SF John Day R. limted lower and upper mainstem John Day	spring/summer Chnk., sthd.	parr	9d
	Upper Columbia	Upper Columbia	Entiat R.	Entiat R.	spring/summer Chnk., sthd.	parr	9d
	Wenatchee-Methow R.	Upper Columbia	Wenatchee R.	all subwatersheds	spring/summer Chnk., sthd.	parr	9d
	Wenatchee-Methow R.	Upper Columbia	Methow R.	all subwatersheds	spring/summer Chnk., sthd.	parr	9d
	South Fork Salmon R.	Snake R.	Salmon R.	Secesh R.	spring/summer Chnk., sthd.	parr	9d
	Upper Salmon R.	Snake R.	Yankee Fork R.	Yankee Fork R.	spring/summer Chnk., sthd.	parr	9d
	Upper Salmon R.	Snake R.	Lemhi R.	multiple subwatersheds	spring/summer Chnk., sthd.	parr	9d
	Grande Ronde-Imnaha	Snake R.	Grande Ronde	Lower Grande Ronde R.	spring/summer Chnk., sthd.	parr	9d
	Grande Ronde-Imnaha	Snake R.	Grande Ronde	Upper Grande Ronde R.	spring/summer Chnk., sthd.	parr	9d
	Grande Ronde-Imnaha	Snake R.	Grande Ronde	Catherine Creek	spring/summer Chnk., sthd.	parr	9d
	Grande Ronde-Imnaha	Snake R.	Minam R.	Minam R.	spring/summer Chnk., sthd.	parr	9d
	Lower Snake	Snake R.	Asotin R.	Asotin R.	spring/summer Chnk., sthd.	parr	9d
	Lower Snake	Snake R.	Tucannon R.	Tucannon R.	spring/summer Chnk., sthd.	parr	9d
Dynamic food web	Wenatchee-Methow R.	Upper Columbia	Methow R.	Methow R.	Chnk.		NA

Table 2. Comparison of data needs and resolution of capacity approaches.

Approach	Local parameters	Borrowed parameters	Spatial grain	Spatial and temporal extent	Output metric	References
Stock-recruit	Estimates of independent (stock, e.g. Spawners, redds, females, eggs) and dependent (recruits, e.g. fry, parr, smolts, adult offspring) abundances	None	None	Area encompassed in surveys of spawners and recruits. Annual time-step	Abundance	Liermann et al. 2010, Schnute and Kronlund 2002, Walters et al. 2013, Neuswanger et al. 2015.
Habitat expansions	Maximum fish densities, area of habitat units. Dynamic parameters (e.g., flow) can be used if habitats are defined by these parameters.	Maximum fish density estimates are often borrowed across systems.	Habitat unit (e.g. pools) Density estimates are usually estimated at the scale of habitat units (e.g., pools). Relevant temporal scale is normally life-stage specific (e.g., fry, summer parr).	extent is limited only by the availbility of habitat units. Estimates vary by life stage rather than time,	Capacity is normally estimated as abundance, but biomass could be estimated based on individual biomass estimates.	Beechie et al. 2006, Hendrix et al. 2014
Quantile regression/random forests	Fish densities (e.g. fish/m), landscape characters (e.g. D50, elevation, CV of thalweg, LWD, pool frequency, etc.)	None	200-500 m stream reaches. Limited by the grain of landscape estimates.	Spatial extent is limited only by the availbility of landscape characters. Estimates vary by the life stage at which density data are collected rather than time.	Fish density or abundance	Haire et al. 2000, Dunham et al. 2002, Cade and Noon 2003, Eastwood et al. 2003, Sweka and Mackey 2010
Structural equation modeling (SEM)	Fish densities (e.g., fish/m, fish/m^2, etc.) and habitat metrics (e.g. substrate D50, elevation, CV of thalweg profile, LWD, pool frequency, etc.)	None	Spatial scale: 120-600 m reaches of stream	Extent is limited only by the availbility of landscape characters. Estimates vary by the life stage at which density data are collected rather than time.	Density (e.g. fish/m2), could be translated to abundance	Mossop and Bradford 2006, McCullough et al. 2015
Habitat suitability index (HSI)	Fish density by habitat attribute and estimates or measurements of attributes that limit habitat use (e.g. depth, velocity, substrate)	Habitat suitability curves may be borrowed or locally derived	limited only by resolution of habitat measurments or models to estimate attributes	Limited by the spatial coverage of habitat attribute models or measurements. Can track varying stream conditions at the temporal scale of hydraulic models.	Abundance at the estimated conditions	Keeley and Slaney 1996, Ayllón et al. 2012
Net rate of energy intake (NREI)	habitat attribute and estimates or measurements of attributes that limit habitat use (e.g. depth, velocity, substrate) and estimates of food availability.	Bioenergetics parameters for focal species	limited only by resolution of habitat measurments or models to estimate attributes	Limited by the spatial coverage of habitat attribute models or measurements. Can track varying stream conditions at the temporal scale of hydraulic models and drift estimates.	Abundance at the estimated conditions	Hughes and Dill 1990, Hayes et al. 2007, Wall et al. 2016
Dynamic food web	Discharge (m3/s), Water temperature, Particle size distribution, % stream shaded and total solar input (PAR to stream), % vegetation cover – allochthonous inputs (leaf litter and invertebrates), 1d hydraulic model, Salmon spawner abundance, Water turbidity, Nutrient concentrations (DIN and SRP)	Bioenergetics parameters for biomass stocks (e.g. consumption and respiration rates)	Scale irrelevant	Estimates are made at the scale of the data. Temoral extent is limited by the temporal update scheudle of the inputs	Biomass in ash-free-dry-mass	DeAngelis et al. 1975; McIntire and Colby 1978; Power et al. 1995; Power and Dietrich 2002; Bellmore et al. in review

Discussion

In this review of capacity estimation tools, the simplest approach is the process based habitat expansion where the grain and extent of the estimates are set by the availability of habitat or landscape characteristics, as fish densities need not be locally derived and may serve primarily as an index of benefit for a given life stage. Habitat expansion also benefits from versatility in creating restoration scenarios (e.g. restoring hydromodified bank to natural bank) (Beechie et al. 2015). A substantial drawback to the expansion approach is the difficulty of incorporating environmental components that may have non-linear effects on the resulting population. For example, determining how capacity might be affected by changes in temperature or flow would be better suited to a mechanistic model where the functional response of fish or habitat is formally incorporated. The largest benefit to the habitat expansion approach however, comes from the widespread availability of stream networks and digital elevation models that can be used to estimate landscape scale habitat estimates in the absence of higher resolution data (Hall et al. 2007, Beechie et al. 2012, Beechie and Imaki 2014). As additional data become available, estimation of capacity can be populated with more locally derived data through habitat expansion, QRF, or SEM. QRF has the added advantage of potentially making capacity estimates directly from the landscape attributes (e.g. slope, sinuosity, valley confinement) associated with measured fish abundances, rather than using those variables to estimate habitat type as an intermediate step. However, QRF requires extensive fish data over a range of conditions and abundances as only a percentile of the data are fitted in the model. QRF and SEM also require that some measurements are made at or near capacity, which may be unlikely. Extrapolation of SEM and QRF to areas outside of those measured may also be difficult if novel conditions are encountered. Empirical or process based approaches assume that fish densities are transferrable to unmeasured areas. This may not always be so (e.g. the Pahsimeroi R. tends to be very productive compared to other nearby watersheds, but geomorphology would not indicate this, see Thorson et al. 2014), and would be better dealt with in a mechanistic model where difference in primary productivity or invertebrate production would be accounted for explicitly. Mechanistic models therefore, may give more realistic results and are more flexible with respect to scenarios that involve interactions with other species, or temporal changes to the system that are not encompassed in landscape characters (e.g. temperature, light availability, flow, species interactions). The drawbacks to mechanistic models are the high resolution data required to populate them. In addition, mechanistic models are difficult to extrapolate to larger stream networks where hydraulic models are not available. Dynamic food webs ultimately provide the most flexibility and can be incorporated into other modeling exercises, but require extensive data collection (e.g. light, nutrient nutrients, species interactions) that may not be feasible in all areas.

One criticism of capacity models in general, is that they tend to focus on production while streams are not fish factories, but natural systems which vary in habitat and environment. In this sense, S-R models may produce a more realistic look at how many fish may be expected of a system by integrating the seasonal variation of a stream into a single output. Therefore, where data are available S-R models may be useful tools for estimating contemporary management targets, but they do suffer from limitations in interpretability and context. In a life-cycle model context, we are interested in producing not only contemporary estimates of capacity, but an understanding of how capacity has changed or is likely to change from different management scenarios, an area where S-R models are generally insufficient. In addition, S-R models may underestimate capacity. In part, this comes from fitting models to often noisy perennial data. We can always find support for one S-R model over another, but we must be sure to fully explore the potential for density independence in systems with extremely depressed abundances. When evaluating S-R models, we often find support for paradoxical density dependence in freshwater life stages at historically low population abundances. This may be interpreted as a sign of freshwater habitat limitation. While in many areas floodplain disconnection and channel simplification may have greatly reduced the rearing capacity of the habitat, caution should be exercised in light of the spawning and rearing behavior of salmonids. Salmon often exhibit strong philopatry, which can lead to high local spawning densities, while other areas remain unoccupied (Atlas et al. 2015). This phenomenon is particularly prominent as a legacy of hatchery release practices, and may result in density dependent effects despite low reach or watershed scale abundances. Fortunately, both habitat degradation and behavior can be accounted for with the alternative modeling approaches we have outlined here. Thus, the value in capacity estimates comes not from the absolute abundance estimate (although abundance may be required for life-cycle models), but when outputs are treated as an index that is flexible to the scenarios of a changing environment and landscape. Therefore, maximum occupancy capacity in isolation may seem unrealistic as it assumes full seeding of the preceding life stage (e.g. eggs to fry), which may never be achieved. But, assuming full seeding allows for a direct comparison of capacity to evaluations of alternative restoration where the percent change in capacity is likely more important than the value of abundance. In this context capacity modeling has great value outside of life cycle modeling exercises.

Capacity is not static, even though our estimates of it may be. The capacity of a system will fluctuate as rapidly as the changes in conditions that drive the limiting factor. However, from a management perspective we generally choose discrete reference points to make comparisons among scenarios or systems. A key question then is whether we are estimating capacity at the life stage that is limiting the population. The pitfall of evaluating capacity in isolation is why capacity is being incorporated into life cycle models, often with several capacities at different life stages. In this way, alternative restoration scenarios can be incorporated into life cycle models to estimate the demographic response of such actions.

Choosing an approach to estimate capacity is dependent upon data availability and the output needs (Table 3). For example, S-R models are appropriate for estimating contemporary capacity when extensive S-R data are available, but are not informative to estimate restoration scenarios. Similarly, habitat expansion models may be effective for evaluating the effects of large scale restoration actions (e.g. watershed-scale reconnection of floodplain habitats), but are less appropriate for evaluating alternative flow regimes, riparian plantings, or small-scale wood installations. For those actions, SEM's or mechanistic models may be more informative if the data to parameterize them are available at the scale needed. Nearly all models described above can be used to make direct estimates of metrics at unmeasured reaches within watersheds, or into watersheds for which no data exist. However, caution must be exercised, especially when extrapolating models into un-sampled watersheds, as we must assume that the empirical relationships observed are constant within and external to measured reaches which may not be true in many cases. The more our empirical relationships describe spatially constant underlying physical laws, the less risk there is in this assumption. However, cross validation and residual analysis has suggested many of the empirical models do an excellent job of describing populations at the watershed spatial level; thus extrapolating watershed level distribution estimates into un-sampled watersheds may indeed be useful and appropriate in many cases. Another approach that has been shown to greatly increase the predictive ability of site level monitoring and extrapolate this to areas of the watershed not sample are statistical approaches that include spatial autocorrelation, which simply suggests that sites closer to each other tend to be more similar to each other, and that the degree of similarity as a function of distance can then be used to extrapolate across areas not sampled to improve predictions. These approaches have also incorporated simple rules of a watershed network, such as water can only move downhill or that sites on the same tributary might be more similar to each other than sites an equal distance apart but on a different tributary. For example, Isaak et al. (2010) compiled stream temperature data from a variety of monitoring programs to make spatially continuous temperature estimates throughout a watershed. By including a degree of similarity based on the distance between sites and where they are located in the watershed, they greatly improve the prediction of temperature throughout the watershed.

Table 3. Qualitative comparison of the data needs and scale of outputs for freshwater capacity estimation techniques.

Approach	Habitat data requirements	Fish data requirements	Scalability	Resolution
Stock-recruit	None or low	Temporally extensive	Low	None
Habitat expansion	Variable	None to low	High	Scale of habitat data
Quantile regression/random forests	High	High	Intermediate	Scale of habitat data
Structural equation modeling (SEM)	High	High	Intermediate	Scale of habitat data
Habitat suitability index (HSI)	High	None to low	High	High
Net rate of energy intake (NREI)	High	None to low	Low	High
Dynamic food web	High	None to low	Low	None

References

Addley, R. C. 1993. A mechanistic approach to modeling habitat needs of drift feeding salmonids. Utah State University, Logan, Utah.

Ahmadi-Nedushan, B., A. St-Hilaire, M. Berube, T. Ouarda, and E. Robichaud. 2008. Instream flow determination using a multiple input fuzzy-based rule system: a case study. River Research and Applications **24**:279-292.

Arhonditsis, G. B., C. A. Stow, L. J. Steinberg, M. A. Kenney, R. C. Lathrop, S. J. McBride, and K. H. Reckhow. 2006. Exploring ecological patterns with structural equation modeling and Bayesian analysis. Ecological Modelling **192**:385-409.

Atlas, W. I., T. W. Buehrens, D. J. F. McCubbing, R. Bison, and J. W. Moore. 2015. Implications of spatial contraction for density dependence and conservation in a depressed population of anadromous fish. Canadian Journal of Fisheries and Aquatic Sciences **72**:1682-1693.

Ayllón, D., A. Almodóvar, G. G. Nicola, I. Parra, and B. Elvira. 2012. Modelling carrying capacity dynamics for the conservation and management of territorial salmonids. Fisheries Research **134**:95-103.

Ayllón, D., G. G. Nicola, B. Elvira, I. Parra, and A. Almodóvar. 2013. Thermal Carrying Capacity for a Thermally-Sensitive Species at the Warmest Edge of Its Range. Plos One **8**.

Bangen, S., J. Wheaton, N. Bouwes, C. Jordan, C. Volk, and M. B. Ward. 2014a. Crew variability in topographic surveys for monitoring wadeable streams: a case study from the Columbia River Basin. Earth Surface Processes and Landforms **39**:2070-2086.

Bangen, S. G., J. M. Wheaton, N. Bouwes, B. Bouwes, and C. Jordan. 2014b. A methodological intercomparison of topographic survey techniques for characterizing wadeable streams and rivers. Geomorphology **206**:343-361.

Barrowman, N. J., and R. A. Myers. 2000. Still more spawner-recruitment curves: the hockey stick and its generalizations. Canadian Journal of Fisheries and Aquatic Sciences **57**:665-676.

Beechie, T., E. Beamer, and L. Wasserman. 1994. Estimating Coho Salmon Rearing Habitat and Smolt Production Losses in a Large River Basin, and Implications for Habitat Restoration. North American Journal of Fisheries Management **14**:797-811.

Beechie, T., and H. Imaki. 2014. Predicting natural channel patterns based on landscape and geomorphic controls in the Columbia River basin, USA. Water Resources Research **50**:39-57.

Beechie, T., G. Pess, and H. Imaki. 2012. Estimated changes to Chinook salmon (*Oncorhynchus tshawytscha*) and steelhead (*Oncorhynchus mykiss*) habitat carrying capacity from rehabilitation actions for the Trinity River, North Fork Trinity to Lewiston Dam.

Beechie, T., G. Pess, S. Morley, L. Butler, P. Downs, A. Maltby, P. Skidmore, S. Clayton, C. Muhlfeld, and K. Hanson. 2013. Chapter 3: Watershed assessments and identification of restoration needs. Pages 50-113 *in* P. Roni and T. Beechie, editors. Stream and Watershed Restoration: A Guide to Restoring Riverine Processes and Habitats. Wiley-Blackwell, Chichester, UK.

Beechie, T. J., C. M. Greene, L. Holsinger, and E. M. Beamer. 2006. Incorporating parameter uncertainty into evaluation of spawning habitat limitations on Chinook salmon (*Oncorhynchus tshawytscha*) populations. Canadian Journal of Fisheries and Aquatic Sciences **63**:1242-1250.

Beechie, T. J., M. Liermann, E. M. Beamer, and R. Henderson. 2005. A classification of habitat types in a large river and their use by juvenile salmonids. Transactions of the American Fisheries Society **134**:717-729.

Beechie, T. J., G. Pess, E. Beamer, G. Lucchetti, and R. E. Bilby. 2003. Role of watershed assessments in recovery planning for salmon. Pages 194-225 *in* D. Montgomery, S. Bolton, D. Booth, and L. Wall, editors. Restoration of Puget Sound Rivers. . University of Washington Press, Seattle, WA.

Beechie, T. J., G. R. Pess, H. Imaki, A. Martin, J. Alvarez, and D. H. Goodman. 2015. Comparison of potential increases in juvenile salmonid rearing habitat capacity among alternative restoration scenarios, Trinity River, California. Restoration Ecology **23**:75-84.

Bellmore, J. R., C. V. Baxter, K. Martens, and P. J. Connolly. 2013. The floodplain food web mosaic: a study of its importance to salmon and steelhead with implications for their recovery. Ecological Applications **23**:189-207.

Bellmore, J. R., J. R. Benjamin, M. Newsom, J. A. Bountry, and D. Dombroski. 2017. Incorporating food web dynamics into ecological restoration: a modeling approach for river ecosystems. Ecological Applications **27**:814-832.

Bellmore, J. R., A. K. Fremier, F. Mejia, and M. Newsom. 2014. The response of stream periphyton to Pacific salmon: using a model to understand the role of environmental context. Freshwater Biology **59**:1437-1451.

Belovsky, G. E., D. Stephens, C. Perschon, P. Birdsey, D. Paul, D. Naftz, R. Baskin, C. Larson, C. Mellison, J. Luft, R. Mosley, H. Mahon, J. Van Leeuwen, and D. V. Allen. 2011. The Great Salt Lake Ecosystem (Utah, USA): long term data and a structural equation approach. Ecosphere **2**.

Benke, A. C., and J. B. Wallace. 1980. Trophic Basis of Production among Net-Spinning Caddisflies in a Southern Appalachian Stream. Ecology **61**:108-118.

Beverton, R. J., and S. J. Holt. 1957. On the dynamics of exploited fish populations. Fish. Invest. Ministry Agric. Fish. Food (GB) Ser. II.

Breiman, L. 2001. Random forests. Machine Learning **45**:5-32.

Budy, P., M. Baker, and S. K. Dahle. 2011. Predicting Fish Growth Potential and Identifying Water Quality Constraints: A Spatially-Explicit Bioenergetics Approach. Environmental Management **48**:691-709.

Cade, B. S., and B. R. Noon. 2003. A gentle introduction to quantile regression for ecologists. Frontiers in Ecology and the Environment **1**:412-420.

Cramer, S. P., and K. Ceder. 2013. Stream flows and potential production of spring-run Chinook salmon and steelhead in the Upper South Fork of Battle Creek, California. . Report submitted to Tetra Tech: 96.

Cross, W. F., C. V. Baxter, K. C. Donner, E. J. Rosi-Marshall, T. A. Kennedy, R. O. Hall, H. A. W. Kelly, and R. S. Rogers. 2011. Ecosystem ecology meets adaptive management: food web response to a controlled flood on the Colorado River, Glen Canyon. Ecological Applications **21**:2016-2033.

Cutler, D. R., T. C. Edwards Jr, K. H. Beard, A. Cutler, K. T. Hess, J. Gibson, and J. J. Lawler. 2007. Random forests for classification in ecology. Ecology **88**:2783-2792.

del Monte-Luna, P., B. W. Brook, M. J. Zetina-Rejon, and V. H. Cruz-Escalona. 2004. The carrying capacity of ecosystems. Global Ecology and Biogeography **13**:485-495.

Duffy, J. E., J. S. Lefcheck, R. D. Stuart-Smith, S. A. Navarrete, and G. J. Edgar. 2016. Biodiversity enhances reef fish biomass and resistance to climate change. Proceedings of the National Academy of Sciences of the United States of America **113**:6230-6235.

Dunbar, M. J., K. Alfredsen, and A. Harby. 2012. Hydraulic-habitat modelling for setting environmental river flow needs for salmonids. Fisheries Management and Ecology **19**:500-517.

Dunham, J. B., B. S. Cade, and J. W. Terrell. 2002. Influences of spatial and temporal variation on fish-habitat relationships defined by regression quantiles. Transactions of the American Fisheries Society **131**:86-98.

Eastwood, P. D., G. J. Meaden, A. Carpentier, and S. I. Rogers. 2003. Estimating limits to the spatial extent and suitability of sole (*Solea solea*) nursery grounds in the Dover Strait. Journal of Sea Research **50**:151-165.

Elton, C. 1927. Animal Ecology. Macmillan Co., New York, NY.

Evans, J. S., M. A. Murphy, Z. A. Holden, and S. A. Cushman. 2011. Modeling species distribution and change using random forest. Pages 139-159 Predictive Species and Habitat Modeling in Landscape Ecology. Springer.

Fausch, K. D. 1984. Profitable stream positions for salmonids: Relating specific growth rate to net energy gain. Can. J. Zool. **62**:441-451.

Fausch, K. D., C. L. Hawkes, and M. G. Parsons. 1988. Models that predict standing crop of stream fish from habitat variables: 1950-85. U.S. Department of Agriculture, Forest Service, Pacific Northwest Research Station, Portland, OR.

Ford, A. 2010. Modeling the Environment, 2nd Edition. Island Press, Washington DC.

Francke, T., J. López-Tarazón, and B. Schröder. 2008. Estimation of suspended sediment concentration and yield using linear models, random forests and quantile regression forests. Hydrological processes **22**:4892-4904.

Getz, W. M. 1993. Metaphysiological and Evolutionary Dynamics of Populations Exploiting Constant and Interactive Resources - R-K Selection Revisited. Evolutionary Ecology **7**:287-305.

Gotelli, N. J. 2001. A Primer of Ecology, 3rd Edition. Sinauer Associates, Sunderland, MA.

Grace, J. B. 2006. Structural Equation Modeling and Natural Systems. Cambridge University Press, Cambridge, NY.

Grace, J. B. 2008. Structural equation modeling for observational studies. Journal of Wildlife Management **72**:14-22.

Grace, J. B., T. M. Anderson, H. Olff, and S. M. Scheiner. 2010. On the specification of structural equation models for ecological systems. Ecological Monographs **80**:67-87.

Grant, J. W., and D. L. Kramer. 1990. Territory size as a predictor of the upper limit to population density of juvenile salmonids in streams. Canadian Journal of Fisheries and Aquatic Sciences **47**:1724-1737.

Greene, C. M., and T. J. Beechie. 2004. Consequences of potential density-dependent mechanisms on recovery of ocean-type chinook salmon (*Oncorhynchus tshawytscha*). Canadian Journal of Fisheries and Aquatic Sciences **61**:590-602.

Guensch, G. R., H. T. B., and R. C. Addley. 2001. Examining feeding strategies and position choice of drift-feeding salmonids using an individual-based, mechanistic foraging model. Canadian Journal of Fisheries and Aquatic Sciences **58**:446-457.

Gustafson, R. G., R. S. Waples, J. M. Myers, L. A. Weitkamp, G. J. Bryant, O. W. Johnson, and J. J. Hard. 2007. Pacific salmon extinctions: quantifying lost and remaining diversity. Conservation Biology **21**:1009-1020.

Hall, J. E., D. M. Holzer, and T. J. Beechie. 2007. Predicting river floodplain and lateral channel migration for salmon habitat conservation. Journal of the American Water Resources Association **43**:786-797.

Hankin, D. G., and G. H. Reeves. 1988. Use of visual methods for estimating fish abundance and habitat areas in small streams. Canadian Journal of Fisheries and Aquatic Sciences **45**:1-15.

Hanrahan, T. P., D. D. Dauble, and D. R. Geist. 2004. An estimate of chinook salmon (*Oncorhynchus tshawytscha*) spawning habitat and redd capacity upstream of a migration barrier in the upper Columbia River. Canadian Journal of Fisheries and Aquatic Sciences **61**:23-33.

Hayes, J. W., E. Goodwin, K. A. Shearer, J. Hay, and L. Kelly. 2016. Can Weighted Useable Area Predict Flow Requirements of Drift-Feeding Salmonids? Comparison with a Net Rate of Energy Intake Model Incorporating Drift–Flow Processes. Transactions of the American Fisheries Society **145**:589-609.

Hayes, J. W., N. F. Hughes, and L. H. Kelly. 2007. Process-based modelling of invertebrate drift transport, net energy intake and reach carrying capacity for drift-feeding salmonids. Ecological Modelling **207**:171-188.

Hegel, T. M., S. A. Cushman, J. Evans, and F. Huettmann. 2010. Current state of the art for statistical modelling of species distributions. Pages 273-311 Spatial complexity, informatics, and wildlife conservation. Springer.

Hendrix, N., E. Danner, C. M. Greene, H. Imaki, and S. T. Lindley. 2014. Life Cycle Modeling Framework for Sacramento River Winter-run Chinook Salmon. U. S. Dept. of Commerce, National Oceanic and Atmospheric Administration, National Marine Fisheries Service, Southwest Fisheries Science Center.

Hill, J., and G. D. Grossman. 1993. An energetic model of microhabitat use for rainbow trout and rosyside dace. Ecology **74**:685-698.

Hughes, N. F., and L. M. Dill. 1990. Position choice by drift-feeding salmonids: model and test for Arctic grayling (*Thymallus arcticus*) in subarctic mountain streams. Canadian Journal of Fisheries and Aquatic Sciences **47**:2039-2048.

Humphries, P., and K. O. Winemiller. 2009. Historical Impacts on River Fauna, Shifting Baselines, and Challenges for Restoration. Bioscience **59**:673-684.

Irvine, K. M., S. W. Miller, R. K. Al-Chokhachy, E. K. Archer, B. B. Roper, and J. L. Kershner. 2015. Empirical evaluation of the conceptual model underpinning a regional aquatic long-term monitoring program using causal modelling. Ecological Indicators **50**:8-23.

Isaak, D. J., and W. A. Hubert. 2001. A hypothesis about factors that affect maximum summer stream temperatures across montane landscapes. Journal of the American Water Resources Association **37**:351-366.

Isaak, D. J., C. H. Luce, B. E. Rieman, D. E. Nagel, E. E. Peterson, D. L. Horan, S. Parkes, and G. L. Chandler. 2010. Effects of climate change and wildfire on stream temperatures and salmonid thermal habitat in a mountain river network. Ecological Applications **20**:1350-1371.

Jackson, D. A., P. R. Peres-Neto, and J. D. Olden. 2001. What controls who is where in freshwater fish communities - the roles of biotic, abiotic, and spatial factors. Canadian Journal of Fisheries and Aquatic Sciences **58**:157-170.

Jang, J., and N. Gulley. 2014. Fuzzy Logic Toolbox: User Guide. Page 328. Mathworks, Natick, MA.

Jonasson, B., E. Sedell, S. K. Banks, A. B. Garner, C. Horn, K. L. Bliesner, J. W. Dowdy, F. W. Drake, S. D. Favrot, J. M. Hay, N. A. McConnell, J. P. Ophoff, B. C. Power, J. R. Ruzycki, and R. W. Carmichael. 2015. Investigations into the life history of naturally produced spring Chinook Salmon and summer steelhead in the Grande Ronde River Subbasin. Annual Report 2014, BPA Project # 1992-026-04. Oregon Department of Fish and Wildlife, La Grande, Oregon.

Kammel, L. E., G. B. Pasternack, D. A. Massa, and P. M. Bratovich. 2016. Near-census ecohydraulics bioverification of Oncorhynchus mykiss spawning microhabitat preferences. Journal of Ecohydraulics **1**:62-78.

Kampichler, C., R. Wieland, S. Calmé, H. Weissenberger, and S. Arriaga-Weiss. 2010. Classification in conservation biology: A comparison of five machine-learning methods. Ecological Informatics **5**:441-450.

Kareiva, P., M. Marvier, and M. McClure. 2000. Recovery and management options for spring/summer chinook salmon in the Columbia River basin. Science **290**:977-979.

Kawai, H., S. Nagayama, H. Urabe, T. Akasaka, and F. Nakamura. 2014. Combining energetic profitability and cover effects to evaluate salmonid habitat quality. Environmental Biology of Fishes **97**:575-586.

Keeley, E., and P. Slaney. 1996. Quantitative measures of rearing and spawning habitat characteristics for stream-dwelling salmonids: guidelines for habitat restoration. Watershed Restoration Program, Ministry of Environment, Lands and Parks.

Knudby, A., A. Brenning, and E. LeDrew. 2010. New approaches to modelling fish-habitat relationships. Ecological Modelling **221**:503-511.

Koenker, R., and G. Bassett Jr. 1978. Regression quantiles. Econometrica: journal of the Econometric Society:33-50.

Koenker, R., and K. Hallock. 2001. Quantile regression: An introduction. Journal of Economic Perspectives **15**:43-56.

Lefcheck, J. S. 2016. PIECEWISESEM: Piecewise structural equation modelling in R for ecology, evolution, and systematics. Methods in Ecology and Evolution **7**:573-579.

Lichatowich, J., L. Mobrand, and L. Lestelle. 1999. Depletion and extinction of Pacific salmon (*Oncorhynchus* spp.): A different perspective. Ices Journal of Marine Science **56**:467-472.

Liermann, M. C., R. Sharma, and C. K. Parken. 2010. Using accessible watershed size to predict management parameters for Chinook salmon, *Oncorhynchus tshawytscha*, populations with little or no spawner-recruit data: a Bayesian hierarchical modelling approach. Fisheries Management and Ecology **17**:40-51.

Lindeman, R. L. 1942. The trophic-dynamic aspect of ecology. Ecology **23**:399-418.

Maloney, K. O., and D. E. Weller. 2011. Anthropogenic disturbance and streams: land use and land-use change affect stream ecosystems via multiple pathways. Freshwater Biology **56**:611-626.

McCullough, D. A., S. M. White, C. Justice, M. Blanchard, R. Lessard, D. Kelsey, D. Graves, and J. Nowinski. 2015. Assessing the Status and Trends of Spring Chinook Habitat in the Upper Grande Ronde River and Catherine Creek. Annual Report to Bonneville Power Administration. Portland, OR: Columbia River Inter-Tribal Fish Commission.

Mcintire, C. D., and J. A. Colby. 1978. Hierarchical Model of Lotic Ecosystems. Ecological Monographs **48**:167-190.

McIntosh, B. A., J. R. Sedell, R. F. Thurow, S. E. Clarke, and G. L. Chandler. 2000. Historical changes in pool habitats in the Columbia River Basin. Ecological Applications **10**:1478-1496.

Meinshausen, N. 2006. Quantile regression forests. Journal of Machine Learning Research **7**:983-999.

Minns, C. K. 1997. Quantifying "no net loss" of productivity of fish habitats. Canadian Journal of Fisheries and Aquatic Sciences **54**:2463-2473.

Minns, C. K., R. G. Randall, K. E. Smokorowski, K. D. Clarke, A. Velez-Espino, R. S. Gregory, S. Courtenay, and P. LeBlanc. 2011. Direct and indirect estimates of the productive capacity of fish habitat under Canada's Policy for the Management of Fish Habitat: where have we been, where are we now, and where are we going? Canadian Journal of Fisheries and Aquatic Sciences **68**:2204-2227.

Mossop, B., and M. J. Bradford. 2006. Using thalweg profiling to assess and monitor juvenile salmon (*Oncorhynchus* spp.) habitat in small streams. Canadian Journal of Fisheries and Aquatic Sciences **63**:1515-1525.

Moussalli, E., and R. Hilborn. 1986. Optimal Stock Size and Harvest Rate in Multistage Life-History Models. Canadian Journal of Fisheries and Aquatic Sciences **43**:135-141.

Neuswanger, J. R., M. S. Wipfli, M. J. Evenson, N. F. Hughes, and A. E. Rosenberger. 2015. Low productivity of Chinook salmon strongly correlates with high summer stream discharge in two Alaskan rivers in the Yukon drainage. Canadian Journal of Fisheries and Aquatic Sciences:1-13.

Nislow, K. H., C. L. Folt, and D. L. Parrish. 1999. Favorable foraging locations for young atlantic salmon: application to habitat population restoration. Ecological Applications **9**:1085-1099.

Nislow, K. H., C. L. Folt, and D. L. Parrish. 2000. Spatially Explicit Bioenergetic Analysis of Habitat Quality for Age-0 Atlantic Salmon. Transactions of the American Fisheries Society **129**:1067–1081.

Odum, E. P., and G. W. Barrett. 2005. Fundamentals of Ecology, Fifth Ed. Brooks/Cole, Belmont, CA.

Olden, J. D., J. J. Lawler, and N. L. Poff. 2008. Machine learning methods without tears: a primer for ecologists. The Quarterly Review of Biology **83**:171-193.

Pauly, D. 1995. Anecdotes and the Shifting Base-Line Syndrome of Fisheries. Trends in Ecology & Evolution **10**:430-430.

Piccolo, J. J., B. M. Frank, and J. W. Hayes. 2014. Food and space revisited: The role of drift-feeding theory in predicting the distribution, growth, and abundance of stream salmonids. Environmental Biology of Fishes **97**:475-488.

Pinnegar, J. K., and G. H. Engelhard. 2008. The 'shifting baseline' phenomenon: a global perspective. Reviews in Fish Biology and Fisheries **18**:1-16.

Piper, R. G. 1982. Fish hatchery management. Department of the Interior, U.S. Fish and Wildlife Service.

Polis, G. A., M. E. Power, and G. R. Huxel. 2004. Food webs at the landscape level. Unversity of Chicago Press, Chicago, IL.

Power, M. E., and W. E. Dietrich. 2002. Food webs in river networks. Ecological Research **17**:451-471.

Power, M. E., A. Sun, G. Parker, W. E. Dietrich, and J. T. Wootton. 1995. Hydraulic Food-Chain Models. Bioscience **45**:159-167.

Prasad, A., L. Iverson, and A. Liaw. 2006. Newer classification and regression tree techniques: Bagging and random forests for ecological prediction. Ecosystems **9**:181-199.

Railsback, S. F., M. Gard, B. C. Harvey, J. L. White, and J. K. H. Zimmerman. 2013. Contrast of Degraded and Restored Stream Habitat Using an Individual-Based Salmon Model. North American Journal of Fisheries Management **33**:384-399.

Railsback, S. F., R. H. Lamberson, B. C. Harvey, and W. E. Duffy. 1999. Movement rules for individual-based models of stream fish. Ecological Modelling **123**:73-89.

Reeves, G. H., F. H. Everest, and T. E. Nickelson. 1989. Identification of physical habitats limiting the production of coho salmon in western Oregon and Washington. U.S. Forest Service General Technical Report PNW-245.

Ricker, W. 1975. Computation and interpretation of biological statistics of fish populations. . Bull. Fish. Res. Board Can.

Ricker, W. E. 1954. Stock and recruitment. Journal of the Fisheries Board of Canada **11**:559-623.

Rogers, L. A., and D. E. Schindler. 2008. Asynchrony in population dynamics of sockeye salmon in southwest Alaska. Oikos **117**:1578-1586.

Rosenfeld, J. 2003. Assessing the habitat requirements of stream fishes: An overview and evaluation of different approaches. Transactions of the American Fisheries Society **132**:953-968.

Rosenfeld, J., H. Beecher, and R. Ptolemy. 2016. Developing Bioenergetic-Based Habitat Suitability Curves for Instream Flow Models. North American Journal of Fisheries Management **36**:1205-1219.

Rosenfeld, J. S., N. Bouwes, C. E. Wall, and S. M. Naman. 2014. Successes, failures, and opportunities in the practical application of drift-foraging models. Environmental Biology of Fishes **97**:551-574.

Rosenfeld, J. S., T. Leiter, G. Lindner, and L. Rothman. 2005. Food abundance and fish density alters habitat selection, growth, and habitat suitability curves for juvenile coho salmon (*Oncorhynchus kisutch*). Can. J. Fish. Aquat. Sci **62**:1691-1701.

Sayre, N. F. 2008. The Genesis, History, and Limits of Carrying Capacity. Annals of the Association of American Geographers **98**:120-134.

Scheuerell, M. D., R. Hilborn, M. H. Ruckelshaus, K. K. Bartz, K. M. Lagueux, A. D. Haas, and K. Rawson. 2006. The Shiraz model: a tool for incorporating anthropogenic effects and fish-habitat relationships in conservation planning. Canadian Journal of Fisheries and Aquatic Sciences **63**:1596-1607.

Sexton, J., and P. Laake. 2009. Standard errors for bagged and random forest estimators. Computational Statistics \& Data Analysis **53**:801-811.

Shipley, B. 2002. Cause and Correlation in Biology: A User’s Guide to Path Analysis, Structural Equations and Causal Inference. 1st edition. Cambridge University Press, Cambridge, NY.

Singer, M. B., and T. Dunne. 2004. An empirical-stochastic, event-based program for simulating inflow from a tributary network: Framework and application to the Sacramento River basin, California. Water Resources Research **40**.

Souchon, Y., and H. Capra. 2004. Aquatic habitat modelling: biological validations of IFIM/Phabsim methodology and new perspectives. Hydroécol. Appl. **14**:9-25.

Thorson, J. T., M. D. Scheuerell, E. R. Buhle, and T. Copeland. 2014. Spatial variation buffers temporal fluctuations in early juvenile survival for an endangered Pacific salmon. Journal of Animal Ecology **83**:157-167.

Upper Columbia Salmon Recovery Board. 2007. Upper Columbia spring Chinook salmon and steelhead recovery plan.

Urabe, H., M. Nakajima, M. Torao, and T. Aoyama. 2010. Evaluation of Habitat Quality for Stream Salmonids Based on a Bioenergetics Model. Transactions of the American Fisheries Society **139**:1665-1676.

Valavanis, V. D., G. J. Pierce, A. F. Zuur, A. Palialexis, A. Saveliev, I. Katara, and J. Wang. 2008. Modelling of essential fish habitat based on remote sensing, spatial analysis and GIS. Hydrobiologia **612**:5-20.

Vannote, R. L., G. W. Minshall, K. W. Cummins, J. R. Sedell, and C. E. Cushing. 1980. River Continuum Concept. Canadian Journal of Fisheries and Aquatic Sciences **37**:130-137.

Wall, C. E., N. Bouwes, J. M. Wheaton, S. N. Bennett, W. C. Saunders, P. A. McHugh, and C. E. Jordan. 2016. Design and monitoring of woody structures and their benefits to juvenile steelhead (*Oncorhynchus mykiss*) using a net rate of energy intake model. Canadian Journal of Fisheries and Aquatic Sciences:1-12.

Wall, C. E., N. Bouwes, J. M. Wheaton, W. C. Saunders, and S. N. Bennett. 2015. Net rate of energy intake predicts reach-level steelhead (*Oncorhynchus mykiss*) densities in diverse basins from a large monitoring program. Canadian Journal of Fisheries and Aquatic Sciences.

Weber, N., N. Bouwes, and C. E. Jordan. 2014. Estimation of salmonid habitat growth potential through measurements of invertebrate food abundance and temperature. Canadian Journal of Fisheries and Aquatic Sciences **71**:1158-1170.

Wheaton, J. M., J. Brasington, S. E. Darby, J. Merz, G. B. Pasternack, D. Sear, and D. Vericat. 2010. Linking geomorphic changes to salmonid habitat at a scale relevant to fish. River Research and Applications **26**:469-486.

Woodward, G., and A. G. Hildrew. 2002. Food web structure in riverine landscapes. Freshwater Biology **47**:777-798.

Wu, A. D., and B. D. Zumbo. 2008. Understanding and using mediators and moderators. Social Indicators Research **87**:367.

Wurtsbaugh, W. A., N. A. Heredia, B. G. Laub, C. S. Meredith, H. E. Mohn, S. E. Null, D. A. Pluth, B. B. Roper, W. C. Saunders, D. K. Stevens, R. H. Walker, and K. Wheeler. 2014.

Approaches for studying fish production: Do river and lake researchers have different perspectives? Canadian Journal of Fisheries and Aquatic Sciences:1-12.

Yodzis, P., and S. Innes. 1992. Body Size and Consumer-Resource Dynamics. American Naturalist **139**:1151-1175.

Zadeh, L. A. 1965. Fuzzy sets. Information and control **8**:338-353.

Zou, S. M., and Y. S. Yu. 1994. A General Structural Equation Model for River Water-Quality Data. Journal of Hydrology **162**:197-209.

CHAPTER 2: HABITAT

2.b A habitat expansion approach to estimating parr rearing capacity of spring and summer Chinook in the Columbia River Basin

Morgan H. Bond (Ocean Associates, contracted to NOAA Fisheries, NWFSC, Seattle), Tyler G. Nodine (Ocean Associates, contracted to NOAA Fisheries, NWFSC, Seattle), Tim J. Beechie (NOAA Fisheries, NWFSC, Seattle), Rich Zabel (NOAA Fisheries, NWFSC, Seattle)

Introduction

Ecologists and fisheries resource managers have long recognized the value of diverse freshwater habitats for successive life stages of salmonids (Kiffney et al. 2006, Bisson et al. 2009). Not only are there ontogenetic shifts in habitat preference, but the relative value of those habitats changes with an individual's size, age and physiological state (Bisson et al. 1988, Rosenfeld and Boss 2001). Studies have begun to demonstrate the demographic benefits of increased stream complexity for juvenile salmonids with extensive stream rearing (e.g. coho salmon; *Oncorhynchus kisutch,* Chinook salmon; *O. tshawytscha*) (Morley et al. 2005, Rosenfeld et al. 2008, Bellmore et al. 2013), but evaluations of the potential benefits from large-scale restoration of freshwater habitats remain elusive (Wissmar and Bisson 2003).

Although stream complexity can take many forms, from small scales (e.g. streambed rugosity, large woody debris) to large (e.g. island braided channel networks), the complexity formed by the hydrology and geomorphology of the system will determine the large scale channel heterogeneity on which other attributes may further filter the rearing potential of a stream (e.g. primary productivity, predation, competition, etc.) (Beechie et al. 2006). Therefore, to determine the value of streams for rearing salmonids we can begin by estimating the propensity of streams to form anastomosing or braided channel networks from the hydrology and geomorphology of the system. For example, a highly confined channel with high slope may provide little refuge or foraging value for juvenile salmonids, while an equivalent length of island-braided channel may contain a relatively large area of rearing habitat (e.g. edge, pool).

Beechie and Imaki (2014) successfully modeled the presence (82% accuracy for qualitatively unmodified areas) of four different channel patterns: straight, meandering, island-braided, and braided (confined channels were assumed from confinement ratios and not modeled explicitly) for all Columbia River Basin (CRB) streams greater than 8 m bankfull width. Streams smaller than 8 m bankfull width are not expected to maintain multithread channels, and were excluded from their modeling (Hall et al. 2007). Beechie and Imaki (2014) provided evidence that the type of habitat available to fishes could be estimated from large-scale landscape data available throughout the CRB.

Although the estimation of channel forms in Beechie and Imaki (2014) validated the efficacy of predicting habitat types at large spatial scale and fine grain, to estimate the total habitat area and type available for salmonids a more detailed approach is required. The Beechie and Imaki approach was effective at predicting channel types in areas deemed to be largely free of anthropogenic disturbance that would restrict the channel to form side channels, primarily through confinement of the floodplain. However, throughout the CRB extensive development has modified the active channel widths, primarily through urban, agricultural, and road development (Figure 1). Therefore, to predict current side channel habitat and historical side channel potential, estimates of the current and historical floodplain width are needed.

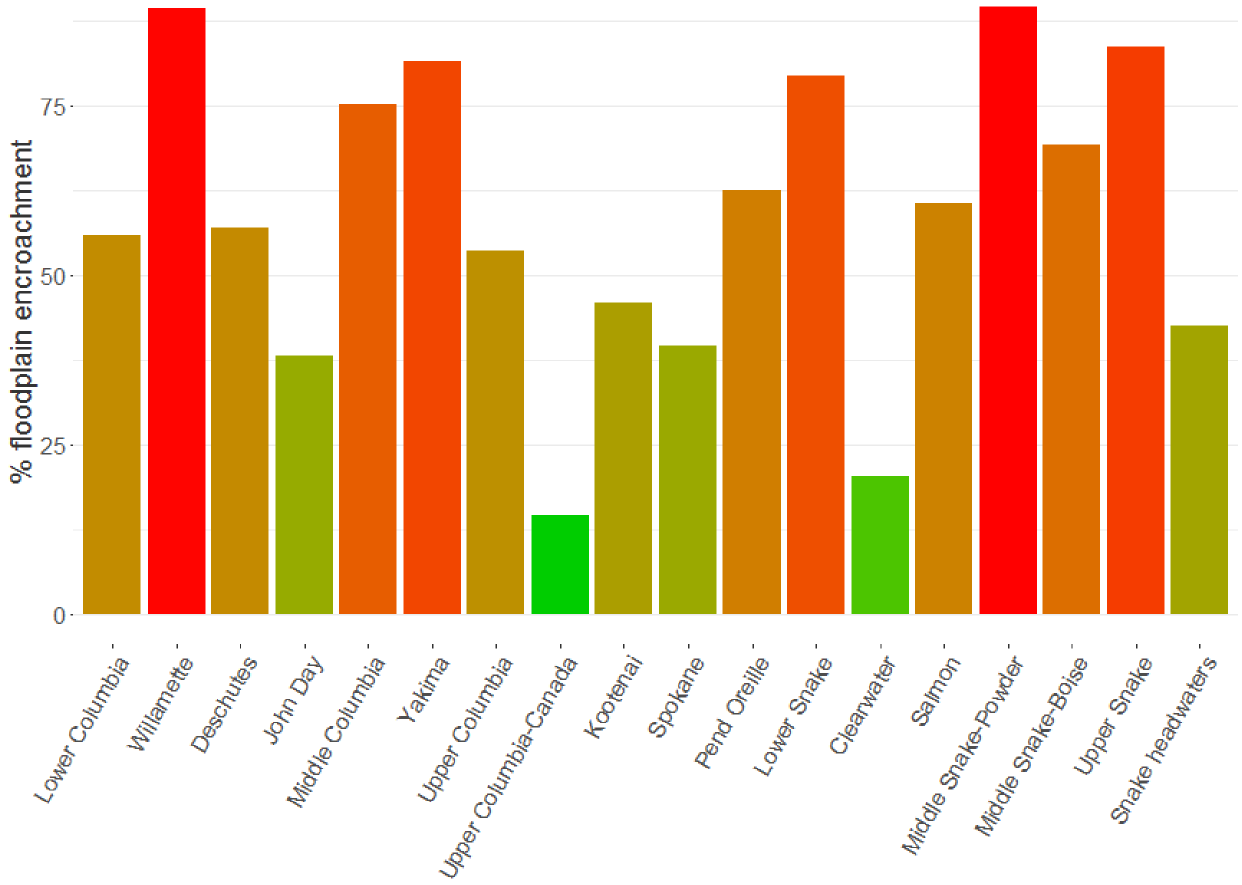

Figure 1. Average percentage width change from historical to a contemporary floodplain by sub-basin. Historical floodplain estimated by filling valley bottom to 6 m above lowest point in the digital elevation model. Contemporary floodplains are estimated by limiting the floodplain width to currently unmodified areas only, assuming anthropogenic development (crop land, range land, urban, roads) restricts the active channel and floodplain processes.

To make effective management recommendations about the relative benefit of various restoration scenarios that will affect stream habitats, each habitat type must be weighted appropriately for their value to the life stage of interest. Traditionally habitats are weighted by their capacity, or the maximum density of individuals that can be expected to reside in the habitat at that life stage. Therefore, habitats that support a disproportionate number of fish relative to their area are given a higher value than those rarely used. This forms the mechanism for identifying nursery habitats (Beck et al. 2001), and has been used in a number of studies to evaluate the restoration potential of salmonid habitats (Bartz et al. 2006, Beechie et al. 2012). The advantage of this approach, in addition to evaluating restoration scenarios, is the ability estimate the capacity for a life stage at different spatial scales by summing the individual capacities of each habitat component.

Recently, a large suite of machine learning tools have been developed to create powerful prediction models. Machine learning approaches (e.g. support vector machines, random forests, neural networks) are increasingly popular for prediction in ecological arenas because of their accuracy and ability to function with large datasets including nonlinearities and correlated variables (Olden et al. 2008). Random forests are one such ensemble classification or regression algorithm that is resistant to overfitting and deals well with unbalanced datasets by creating a suite of regression or classification tress, each with a random subset of predictors and data (Cutler et al. 2012). Here, we employ random forest models to predict habitat area for each 200 m stream segment throughout the CRB by including the variables included in the original Beechie and Imaki (2014) dataset as well as estimates of contemporary floodplain width, and historical and contemporary land cover/use. To estimate Chinook parr rearing capacity from estimates of habitat area three approaches of applying fish densities for each habitat at capacity were employed: 1. habitat specific densities of parr capacity from literature review, 2. Quantile random forest of observed parr densities and landscape characteristics from CRB rivers, 3. Capacity esitmates of Chinook parr from previous studies of mid-summer snorkel surveys in the Salmon River (Thorson et al. 2014).

Objectives

1. Estimate mainstem habitat area throughout the CRB.
2. Estimate contemporary and historical side channel area throughout the CRB.
3. Estimate the effects of floodplain reconnection scenarios (restore range land, crop land, and small roads) on side channel habitat.
4. Estimate current rearing capacity and the effects of restoration scenarios on rearing capacity for spring Chinook parr in currently accessible areas of the CRB.

Methods

Methods Overview

To estimate the parr rearing capacity of CRB tributaries we followed a habitat based approach employed in other watersheds in which geomorphic characteristics are used to make predictions of stream habitat area and condition (Bartz et al. 2006, Beechie et al. 2012). At its core, this approach uses attributes of geomorphology, geology, hydrology, and land use to estimate the discharge, gradient, sediment accumulation, sinuosity, and confinement of a stream, which are key drivers in determining channel planform (e.g. island-braided, meandering, etc.) and a stream's potential for providing quality fish habitat (Beechie et al. 2014).

We used these drivers and an associated geospatial stream network to estimate the areas of discrete habitat units meaningful for juvenile rearing within CRB tributaries. Subreach scale habitat units were selected based on available habitat specific fish densities and their ability to be accurately estimated at this spatial scale (Beechie et al. 2005). Within small streams (< 8 m wide) we estimated pool and riffle areas and for large streams (> 8 m wide) we estimated mainstem bank, bar and mid-channel areas as well as additional habitat area provided by side channels (Figure 2.). Due to the importance of side channels in providing high quality rearing habitat and their vulnerability to floodplain modification, we made additional estimates of side channel habitat area under historical conditions and two restoration scenarios that improve floodplain connectivity. After habitat unit areas were estimated, we identified reaches within our stream network accessible to spring run Chinook salmon and applied fish densities to each distinct habitat unit, which were then summed to make reach scale rearing capacities. We also leveraged our habitat predictions to make two alternate contemporary capacity estimates that utilize independent fish density data sources.

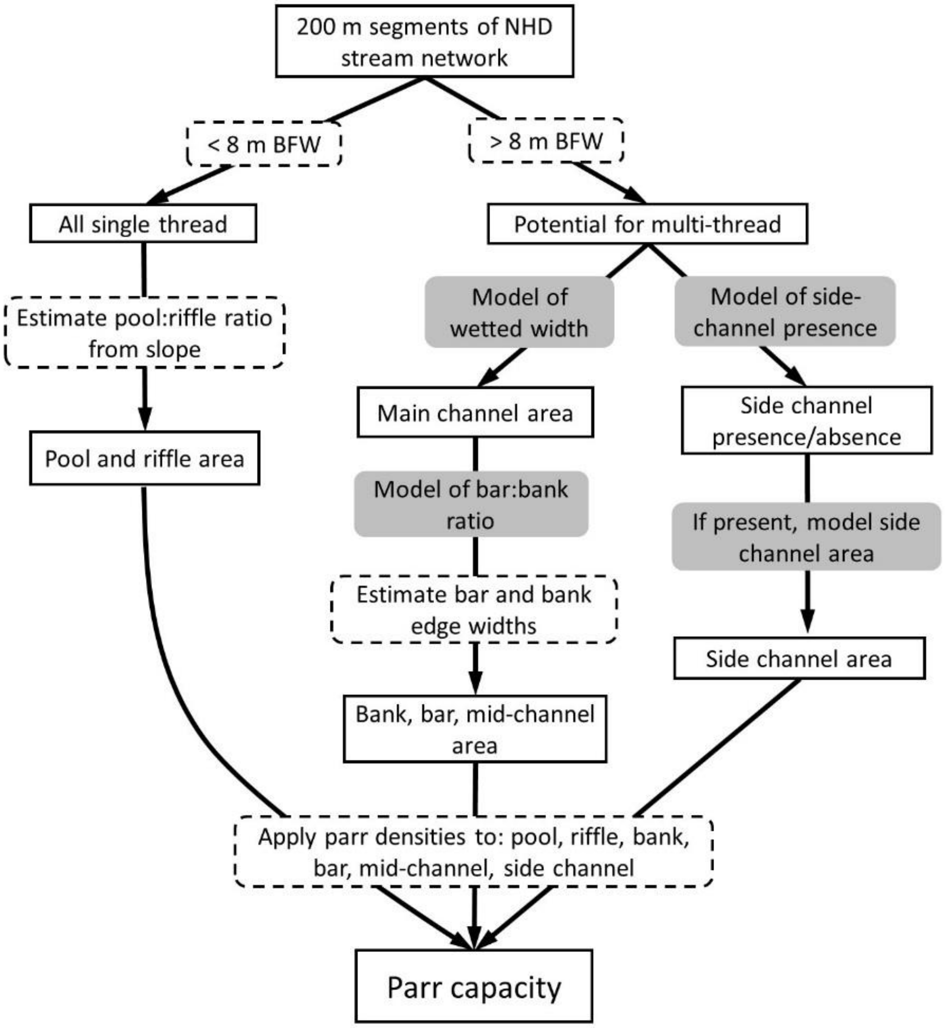

Figure 2. Flow chart of modeling process. Grey boxes indicate random forest models and dotted boxes indicate steps where we applied estimates to make decisions in branch direction or used established relationships to achieve outputs. All model outputs are in boxes with solid black lines.

Methods Part 1: Habitat Estimates

CRB stream network

For this analysis we used a stream network spanning the CRB and associated reach characteristics developed by Beechie and Imaki 2014. This stream layer consists of two merged hydrography datasets; the National Hydrography Dataset Plus (NHDplus, mapped at 1:100,000 scale) for U.S. streams and The Watershed Atlas (mapped at 1:50,000 scale) for Canadian streams. The stream network is broken into 200 m segments and reach attributes (habitat unit drivers) were calculated at this scale. Fish distribution data from the (StreamNet Project 2012) was joined to the stream layer and reaches were designated as being accessible or inaccessible to spring Chinook and whether they were utilized for rearing, migration or both. We split our stream network into reaches smaller than 8 m bankfull width (small streams) and streams larger than 8 m bankfull width (large streams) and used separate processes to estimate capacity for these two groups.

Small stream habitat

For streams smaller than 8 m bankfull width (BFW) we assume that all channels will be single thread as streams bellow this threshold are not expected to have sufficient discharge and sediment supply to maintain side channels (Hall et al. 2007)(Figure 3). In these small streams we account for heterogeneity in habitat value by estimating a pool to riffle ratio for each 200 m stream segment determined by slope (Beechie et al. 2001). This ratio is applied to the total channel area, the product of hydrography network derived reach lengths and estimated BFW, to calculate pool and riffle habitat unit areas.

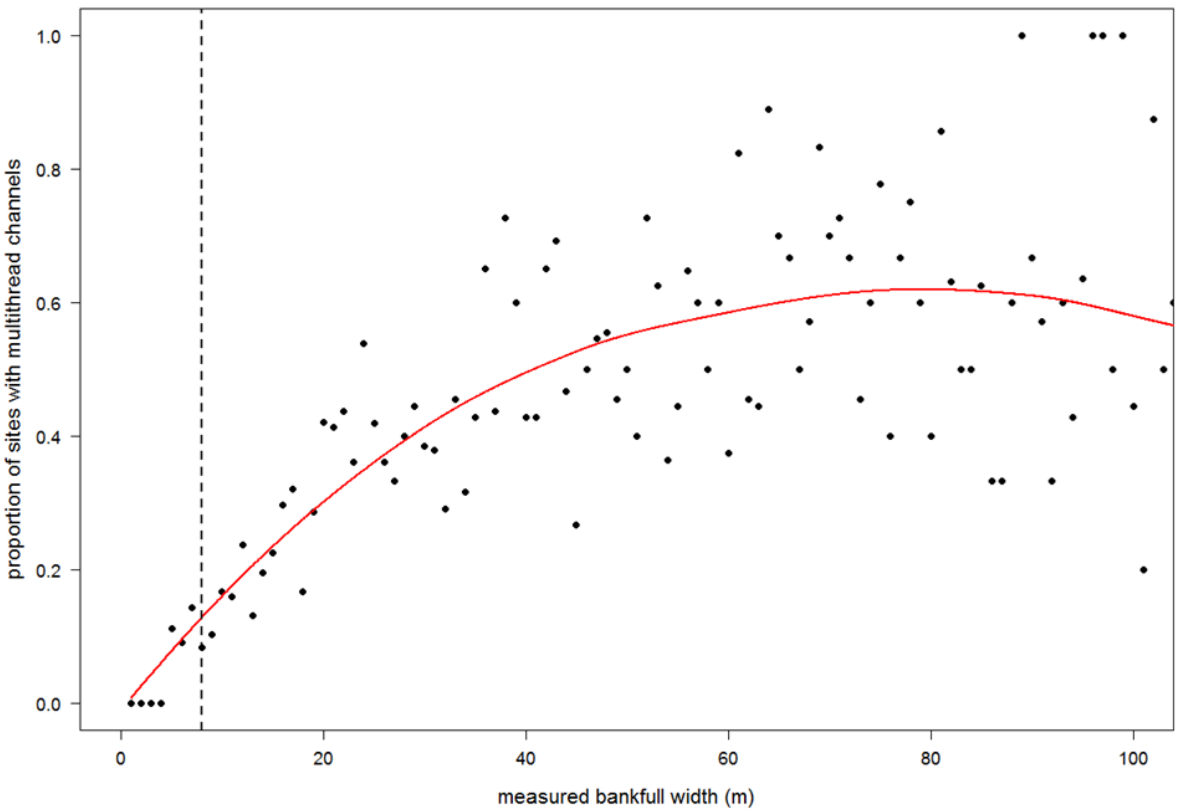

Figure 3. Proportion of sites that have any side channel habitat by the nearest integer bankfull width value. Red line is a loess smoother indicating the general increase in side channel with bankfull width. Dashed vertical line indicates the cutoff (8 m) used to separate sites included in the side channel model (> 8 m) and those assumed to be single thread channels (< 8 m).

Large stream habitat

For streams wider than 8 m BFW we developed a multi-step modeling process to capture habitat complexities provided by large and potentially multithreaded channel forms. To estimate mainstem habitat composition we first modeled mainstem wetted width and then broke it down into bank, bar, and mid-channel habitat units. Because many CRB streams display multithreaded morphologies where side channels contribute a large portion of high quality rearing habitat, estimates of side channel area were also necessary. To inform these habitat models we established a random spatially balanced sample population of stream reaches within the CRB and determined an appropriate approach for measuring habitat characteristics at sample reaches. After completing the sample measurements, we selected and developed predictor variables used to make habitat estimates across the basin.

I. Sample design

The study area used in the construction of our mainstem wetted width and side channel models included all rivers and streams over 8 m wide in the Columbia River Basin, which is comprised of 243,544 stream segments. Rather than restricting our study area to currently accessible streams, we included all reaches in the basin to encompass a wider range of potential stream conditions and channel morphologies. Although side channels are common in island-braided reaches many of the streams in the basin do not possess geomorphic characteristics necessary for multithreaded channel formation. As a result, our sampling size had to be large enough to capture an adequate number of sites where side channels were detected.

We used a Generalized Random Tessellation Stratified approach (GRTS, Kincaid 2016) to draw a spatially balanced sample of reaches throughout the Columbia River basin. We stratified our sample by land cover, channel type, and stream width resulting in 75 unique strata. Dominant land cover was assigned to each reach in our study area using a 250 m resolution continuous land cover dataset for North America (Commission for Environmental Cooperation, Land Cover 2010, Figure 4). We aggregated the dataset's land cover types into five classes (urban, cropland, grassland, shrubland, and forest) and calculated the dominant land cover class (class with highest frequency) that occurred in a 100 m radius of the midpoint of each stream segment. Using channel patterns predicted by Beechie and Imaki (2014) we also stratified by the following channel types: straight, meandering, island-braided, braided, and confined. Last, to ensure balanced representation of stream sizes in our sample we used estimated bank-full width to stratify by small (bfw < 20 m), medium (bfw 20-50 m) and large (bfw >50 m) streams (Table 1). We sampled 50 sites from all island-braided strata, where we expected to find the most side channel habitat, and for all other strata we sampled 25 sites or as many sites as were available for rare combinations, totaling a sample size of 2,093 reaches (Figure 5).

Table 1. Parameters governing the stratification of sites randomly chosen for satellite image analysis of channel habitat characteristics.

Sample Strata	
Land cover	urban
	cropland
	grassland
	shrubland
	forest
Channel type	straight
	meandering
	island-braided
	braided
	confined
Stream width	small < 20 m
	medium 20-50 m
	large > 50 m

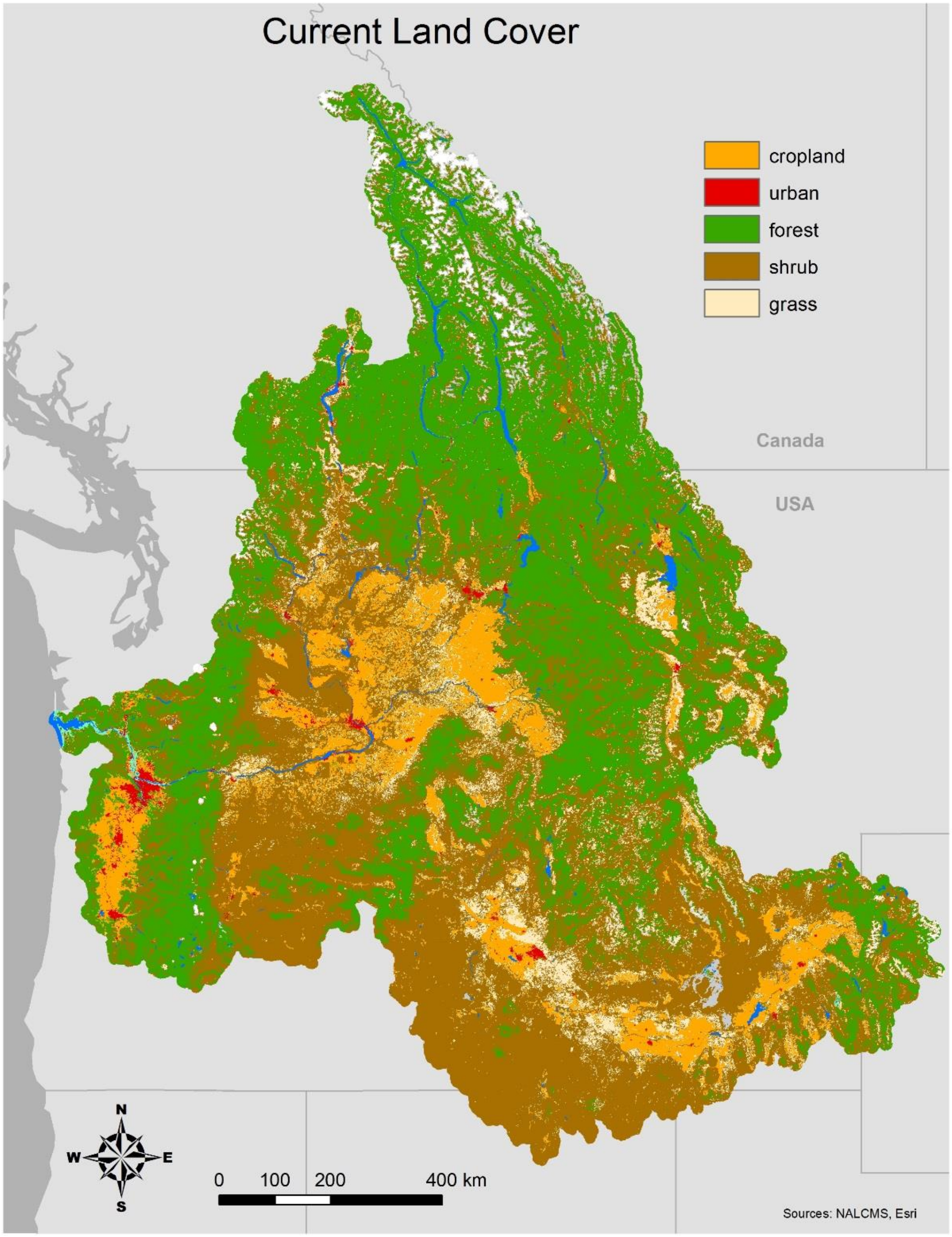

Figure 4. Contemporary land cover classes used in stratifying sample points throughout the CRB (Data from Commission for Environmental Cooperation, Land Cover 2010)

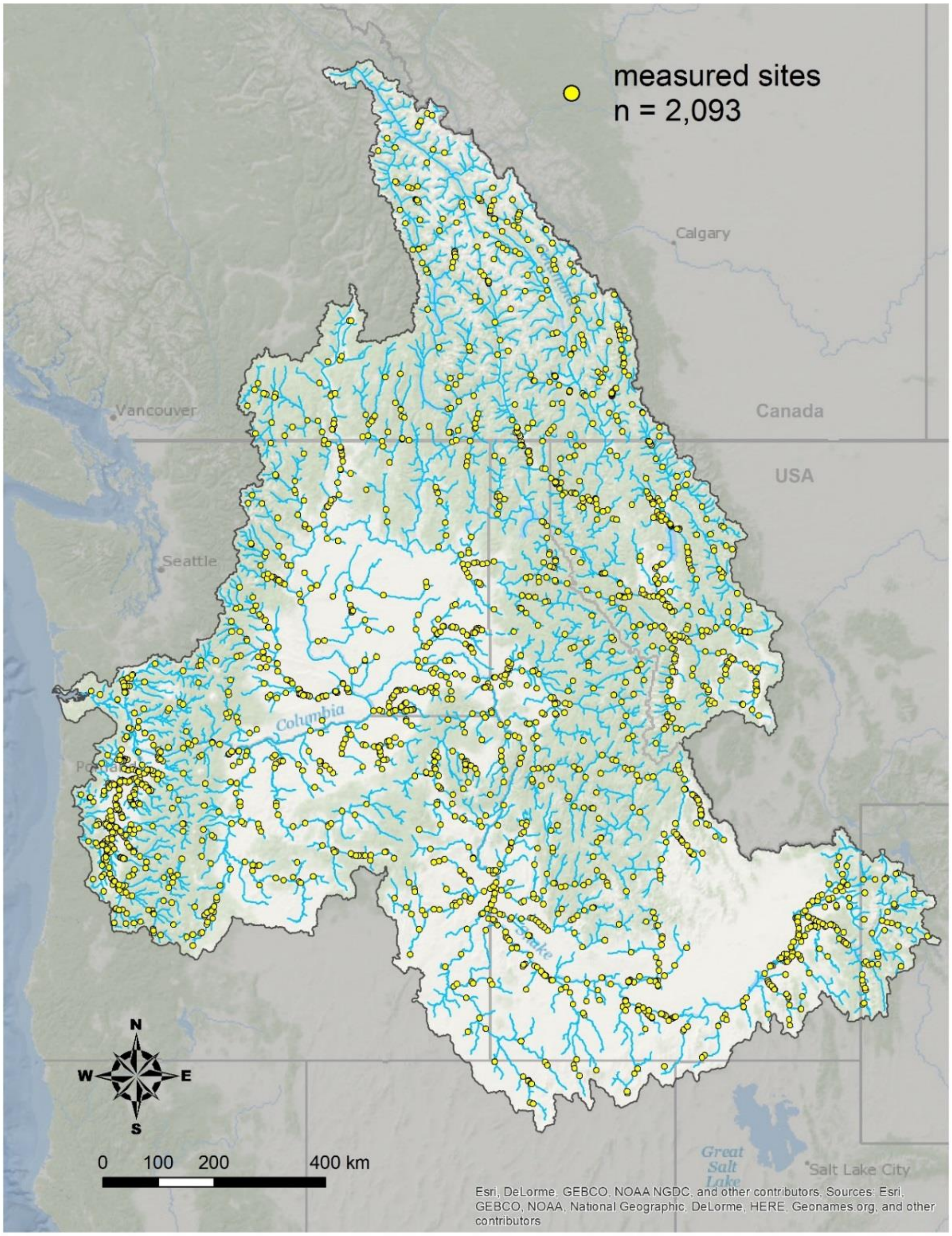

Figure 5. Sites randomly chosen with a stratified GRTS sample design. At each site satellite imagery was used to measure for stream size and side channel habitats.

II. Selection of transect measurement method

To construct a predictive model of habitat area we sought to measure main stem, off channel and side channel habitat at each of the 2093 selected stream segments. However, the time involved to fully digitize the area of all habitats within a reach would necessitate either a reduction in selected sites or the number of measurements per site. As an alternative to full digitization we sought to leverage the strong spatial autocorrelation in stream channels (i.e. The habitat of each length of stream is highly correlated with the adjacent length) by subsampling. To test this approach, we made 20 evenly spaced transects across 435 fully digitized (main channel, side channel, off channel) 200 m stream segments at 85 sites (1-22 segments per site) throughout the CRB (Figure 6). Transects were made perpendicular to the valley axis, and the widths of each habitat polygon where it intersected a transect were retained (Figure 5). We then varied the number of evenly spaced transects (1, 3, 5, 10, 20) to estimate how many transects per 200 m segment are required to detect the presence of side and off channel habitats. In addition, for each number of transects, we estimated the total side channel and off channel habitat in each stream segment with varying transect number, comparing estimates to actual habitat from digitized polygons.

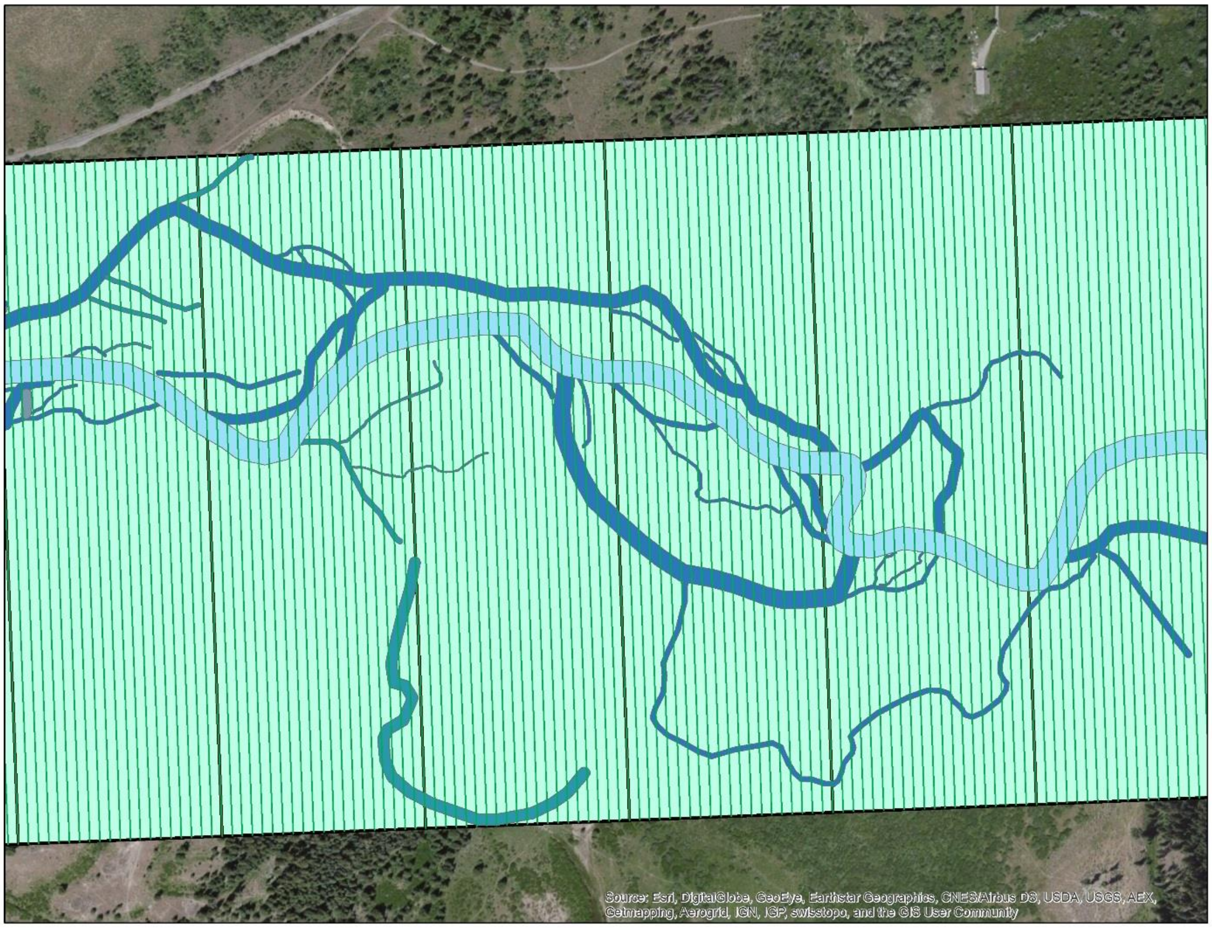
Source: Esri, DigitalGlobe, GeoEye, Earthstar Geographics, CNES/Airbus DS, USDA, USGS, AEX, Getmapping, Aerogrid, IGN, IGP, swisstopo, and the GIS User Community

Figure 6. Example site with polygons of each habitat type (main channel; dark blue, side channel; light blue, off channel; blue-green) digitized manually from satellite imagery. Heavy lines indicate 200 m segment breaks, while green lines indicate individual transects. Widths where transects cross habitat polygons were retained to determine the minimum number of transects required to characterize the habitat at each site.

We used two metrics to choose the number of transects required per stream segment based on a two-stage “hurdle model” approach to predicting off and side channel habitat. Because off and side channel habitats are relatively rare, we predict their presence first. The amount of habitat is then predicted separately for sites with side channels. Therefore we evaluated the detection of side channel and off channel habitat with varying transect number by comparing the side or off channel to main stem area ratio for all sites with a ratio greater than zero to the proportion of sites where side channel was detected (Figure 7). We found a dramatic increase in detection for both side and off channel habitats from one to three transects, with diminishing returns thereafter (Figure 7). For segments with low side to main stem ratios of 0.1, adding two transects to the single center transect increased the detection rate from 0.44 to 0.90. Similarly, off channel detection improved from 0.47 to 0.85. Adding additional transects beyond three only showed marked improvement at side or off to main stem ratios very close to zero. Likewise, we observed similar increases in the accuracy of extrapolating the total side and off channel area for 200 m segments from varying numbers of transects (Figure 8). We subtracted the estimated area from the actual area to demonstrate decrease in the number of extreme estimates with increasing number of transects. However, even a single transect provides an unbiased estimate with a mean difference of near zero. These metrics, combined with the additional time required to measure each additional transect, led us to measure three transects for each of the 2093 sites to build our predictive models.

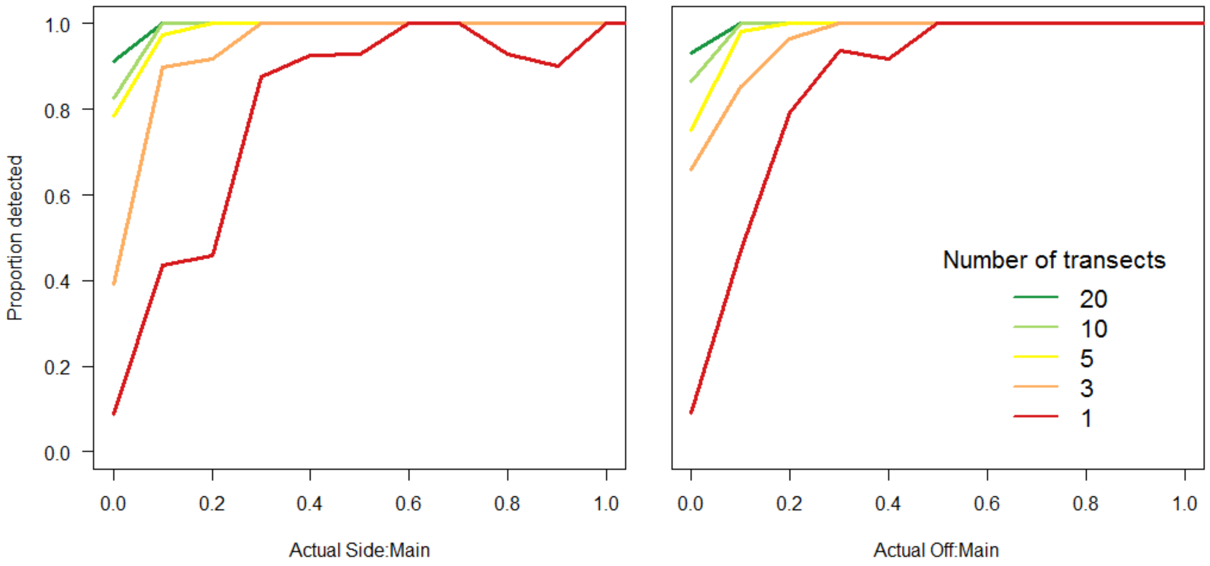

Figure 7. Proportion of sites where any side channel (left panel) or off channel (right panel) habitat was detected at 200 m stream segments with varying number of evenly spaced transects per segment. Side and off channel to main stem area ratios (side:main and off:main) exceeding 1 had a detection proportion of 1 for all numbers of transects.

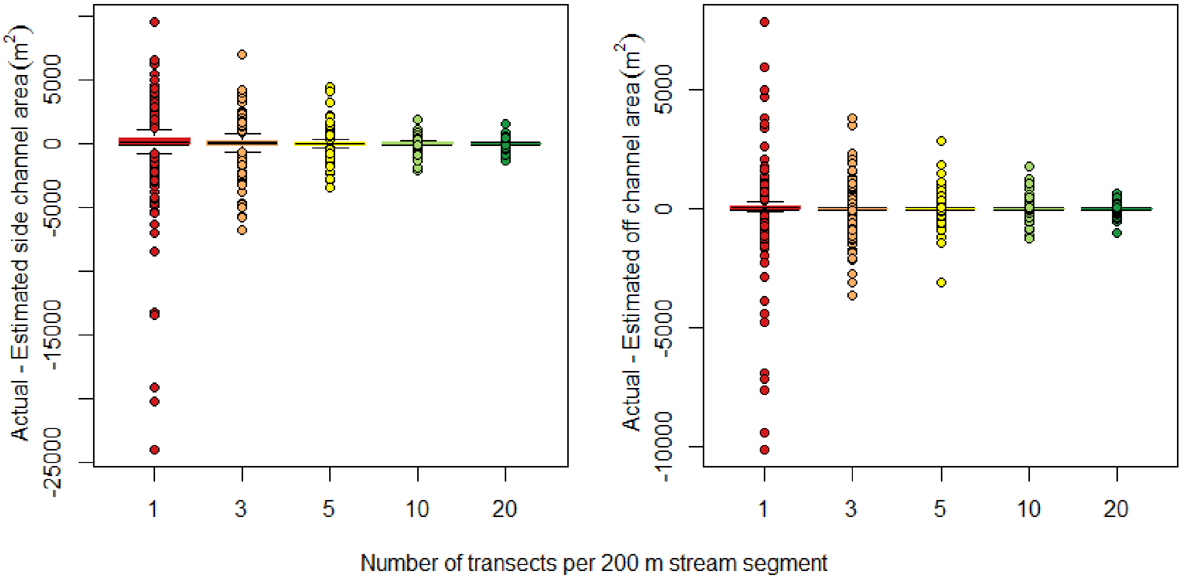

Figure 8. Boxplots of actual side channel (left) and off channel (right) area minus the estimated area by number of evenly spaced transects per 200 m stream segment. Although the number of outliers decreases with increasing transect number, the mean and median in all cases is near zero, as indicated by the small boxes (interquartile range) and whiskers (1.5 times interquartile range).

III. Measurement of response variables

We measured our habitat response variables using the highest quality aerial imagery available from Google and Bing. We used an imagery integration extension (Arc2Earth) to view this imagery in ArcMap 10.3 and digitize habitat characteristics. Satellite images used were primarily taken during summer months between June and August. Although flow conditions, and thus wetted area may vary among images, the relationship between main channel and side channel wetted area should be well maintained over the range of stream sizes and conditions evaluated. Few images during winter or fall flows were likely encountered, as satellite imagery requires clear sky conditions generally encountered in summer or early fall months in the Pacific Northwest. In addition, images with snowfall obscuring habitats were not used and alternative sites were selected from our random draw of sites.

At each sample site we measured wetted habitat features along three transects. Measurement transects were drawn perpendicular to valley axis with 100 m spacing. Our validation exercises showed that measuring habitat features at three transects at this spacing adequately characterized a 200 m reach. Transects spanned the width of the valley floor and wherever wetted habitat was crossed the width of the feature would be digitized and stored in a geodatabase with a common reach identifier.

Our primary response variables measured were side channel width and mainstem wetted width, but other habitat features were also digitized including bankfull width, braids, off-channels (sloughs and backwaters), and ditches as well as historic and contemporary floodplain widths. For our purposes we defined a side channel as an unmodified or minimally modified channel connected to the mainstem on two sides and separated from the mainstem by a vegetated island. This also included side channels that were disconnected from the main channel on one end due to flow levels when the imagery was taken. If the side channel was heavily altered or degraded from its natural state and not considered to be suitable salmonid habitat it was classified as a modified channel or ditch. Channels separated from the mainstem by an unvegetated gravel bar were also classified separately as braids. See table 2 for definitions of all our habitat metrics. All habitat feature widths were digitized along the measurement transect axis except for bankfull width, which was measured perpendicular to the direction of flow. Aside from the bankfull width metric which spanned the entire width of the main channel including unvegetated bars and islands, only wetted habitats were measured; if a transect crossed a dry side channel or slough the feature was not digitized. While side channel width and mainstem wetted width were our only measured response variable for this task, the additional habitat metrics were used to validate techniques employed to estimate predictor variables at all sites across the Columbia Basin.

Table 2. Measured variables with descriptions and standardized orientation of measurement.

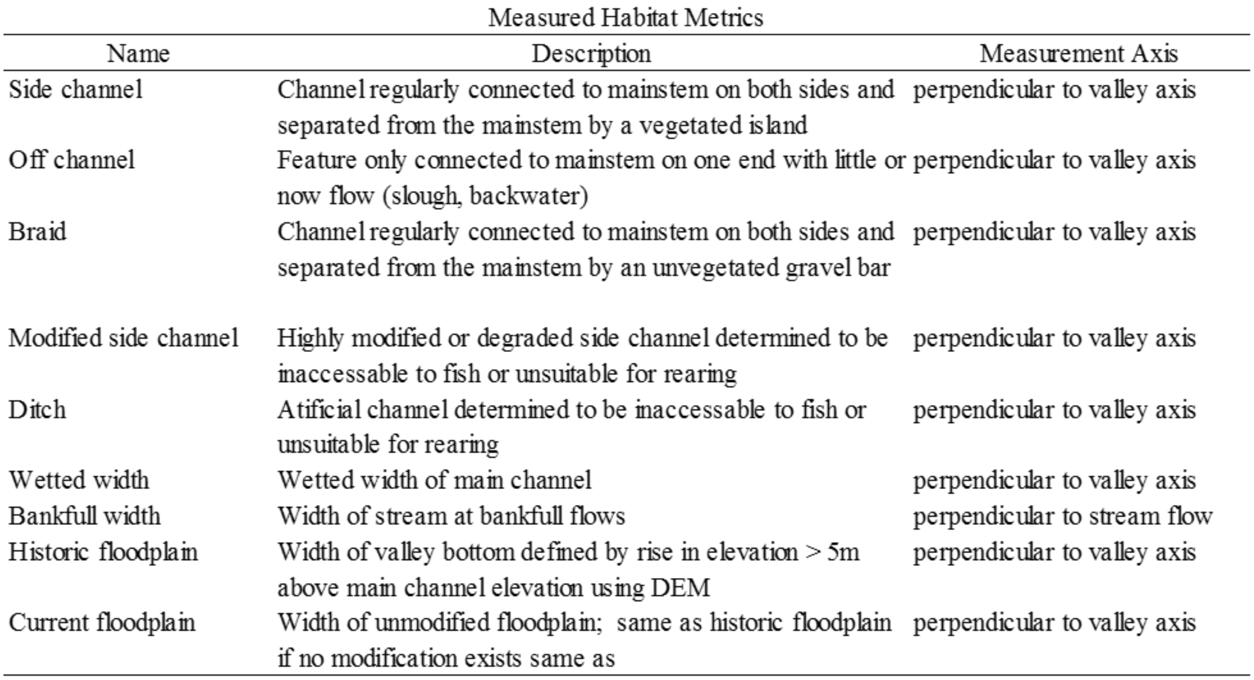
Measured Habitat Metrics

Name	Description	Measurement Axis
Side channel	Channel regularly connected to mainstem on both sides and separated from the mainstem by a vegetated island	perpendicular to valley axis
Off channel	Feature only connected to mainstem on one end with little or now flow (slough, backwater)	perpendicular to valley axis
Braid	Channel regularly connected to mainstem on both sides and separated from the mainstem by an unvegetated gravel bar	perpendicular to valley axis
Modified side channel	Highly modified or degraded side channel determined to be inaccessable to fish or unsuitable for rearing	perpendicular to valley axis
Ditch	Atificial channel determined to be inaccessable to fish or unsuitable for rearing	perpendicular to valley axis
Wetted width	Wetted width of main channel	perpendicular to valley axis
Bankfull width	Width of stream at bankfull flows	perpendicular to stream flow
Historic floodplain	Width of valley bottom defined by rise in elevation > 5m above main channel elevation using DEM	perpendicular to valley axis
Current floodplain	Width of unmodified floodplain; same as historic floodplain if no modification exists same as	perpendicular to valley axis

IV. Predictor variables

We estimated side channel and mainstem habitat for each reach in our stream network larger than 8 m BFW using geomorphic reach attributes calculated by Beechie and Imaki (2014) (Table 3) and additional metrics developed for this analysis. Variables developed by Beechie and Imaki (2014) include bankfull width, slope, elevation, discharge and sediment supply; all key drivers of channel pattern. Slopes and elevations were derived from a basin wide 10 m digital elevation model (DEM) that was created by merging U.S. (NED) and Canadian (CDED) elevation datasets. Bankfull width (BFW) and discharge were estimated based on DEM derived drainage area and mean annual precipitation models (PRISM, ClimateBC). We used two sediment supply surrogates that were derived from flow accumulation, fine sediment sources and relative slope. For more detail on the calculation of these reach attributes see Beechie and Imaki (2014).

We also developed floodplain width attributes calculated by generating transects perpendicular to the valley axis across the valley floor. We used valley floor polygons derived from a detrended DEM filled to 6m above main channel elevation (Beechie and Imaki 2014). In many streams however, floodplain width has effectively been reduced due to development and land modification, which can lead to a loss of channel complexity and restrict a streams' ability to migrate and form new multithreaded patterns. To make estimates of side channels as they currently exist on the landscape we estimated a contemporary floodplain variable. Using a 30 m resolution land cover datasets (Homer et al. 2015)(LU2010 Agriculture and Agri-Food Canada) we mapped floodplain modification and used these modified zones to truncate the original floodplain width assigned to each reach. We designated urban, agriculture, and rangeland classes as modified land. Ecoregion was assigned to reaches using EPA level III ecoregion classes.

To make historic side channel habitat predictions we substituted our current floodplain and land cover variables with estimated historic values. We calculated historic floodplain width from DEM derived valley floor polygons described above and ignored contemporary land use. We also estimated floodplain widths under two additional restoration scenarios where we assume floodplain reconnection could occur in currently modified areas. In the first scenario, we calculated floodplain width by removing rangeland and small road restrictions on the current floodplain width. In the second scenario, we assumed reclamation of rangeland, small roads, and cropland. We used these restored floodplain widths in our model runs to estimate side channel habitat area that could be gained under the above scenarios.

Table 3. Predictor variables and data sources used to predict the presence of side and off channel habitat throughout the CRB.

Predictor Variables	**Description**	**Data Source**
Bankfull width	Stream channel width at bankfull flows estimated from drainage area and mean annual precipitation upstream of each reach	Beechie and Imaki 2014
Discharge	2 year flood discharge estimated from drainage area and mean annual precipitation upstream of each reach	
Flow accumulation	Estimated from DEM derived drainage area. Flow accumulation weighted by precipitation and fine sediment source also included	
Slope	Reach slope estimated from digital elevation and hydrography models	
Elevation	Estimated from digital elevation and hydrography models	
Sinuosity	Shortest distance between reach endnodes divided by reach length	
Hydrologic Regime	Categorical variable indicating if reach belongs to a snow-melt dominated, rain dominated or transitional drainage	
Sediment supply	Sediment supply surrogates estimated from flow accumulation, fine sediment sources and relative slope	
Historic floodplain width	Valley bottom width estimated from DEM and hydrography models	
Current floodplain width	Width of currently unmodified floodplain estimated from DEM, hydrography models and land use data	Beechie and Imaki 2014; National Hydrography Dataset (NHD), https://nhd.usgs.gov/data.html; National Land Cover Database 2011 (NLCD 2011), http://www.mrlc.gov/nlcd2011.php; Agriculture and Agri-Food Canada Land Use 2010, http://www.agr.gc.ca/eng/?id=1343066456961
Restored floodplain width 1	Width of floodplain assuming reclamation of rangeland and small roads	
Restored floodplain width 2	Width of floodplain assuming reclamation of cropland, rangeland, and small roads	
Ecoregion	Level III EPA Ecoregions	EPA, https://www.epa.gov/eco-research/ecoregions

V. Side Channel area model construction

Following measurement of satellite imagery for side and off channel area, side channels were present in 35% of sites, while off channel habitats were found at 2% of sites. Low rates of the presence of any side or off channel habitat indicated a hurdle model approach may be the most effective at estimating their areas (Potts and Elith 2006). A hurdle model is used for count data where separate processes may govern the presence and magnitude of the response, and where the zeros cannot be effectively modeled with standard probability distributions (Martin et al. 2005). Therefore, the presence/absence is modeled first, and sites where the presence of habitat is predicted are placed into a second model to estimate the magnitude. Because our goal is to make accurate predictions of habitat area from the available data, rather than evaluate the statistical relationship of the factors governing or correlated with side channel habitat we elected to use random forest prediction models instead of more traditional statistical approaches like binomial/gamma hurdle models. Similar to classification and regression tree (CART) models, random forest models are powerful prediction algorithms that do not suffer from some of the limitations of more traditional statistical approaches. They adequately deal with very large datasets and can include many correlated predictors and, unlike CART, are resistant to overfitting by constructing thousands of shallow trees with a random subset of predictors, rather than a single large tree. In addition, random forest models perform equally well for both classification (presence or absence of habitat) and regression (habitat amount).

To construct predictive models we created a binary classification of side and off channel habitats, 0 where no habitat was present, and 1 where any side channel was measured. Therefore, the entire suite of 2093 sites were used to construct the classification model. We randomly selected 80% of sites to be included in training the model, with the remaining 20% reserved for testing model accuracy. To train the random forest model we included eight predictors: current floodplain width, historical floodplain width, discharge, average elevation, sinuosity, hydrologic regime and ecoregion (Figure 9). We constructed models with the randomForest and caret packages in the R statistical software platform version 3.2.3 (R Development Core Team 2011). During the training phase we used 10-fold cross-validation and tuned two parameters: the number of trees constructed, and the number of variables randomly drawn to include at each tree node. We used the kappa tuning metric, and evaluated the final model for balanced accuracy.

Our final model included 2000 trees and two variables at each node. A second regression random forest model was constructed with only the 874 sites that had side channels present, using the same suite of predictors: discharge, accumulated flow, estimated bankfull width, estimated bankfull depth, current floodplain width, sediment accumulation, and historical floodplain width (Figure 10). We used the same training procedure employed in the classification model but tuned the regression model by maximizing the receiver operating characteristic (ROC).

Once both models were sufficiently tuned, we used the classification model to predict the presence of side channel habitat for all CRB stream segments. Those sites that received a 1 during classification were then used to predict side channel area for each stream segment. To estimate historical side channel area or full floodplain restoration potential, we made new predictions with both models where floodplain width was updated to historical values. Similarly, we estimated side channel area under two restoration scenarios by using restored floodplain widths described above.

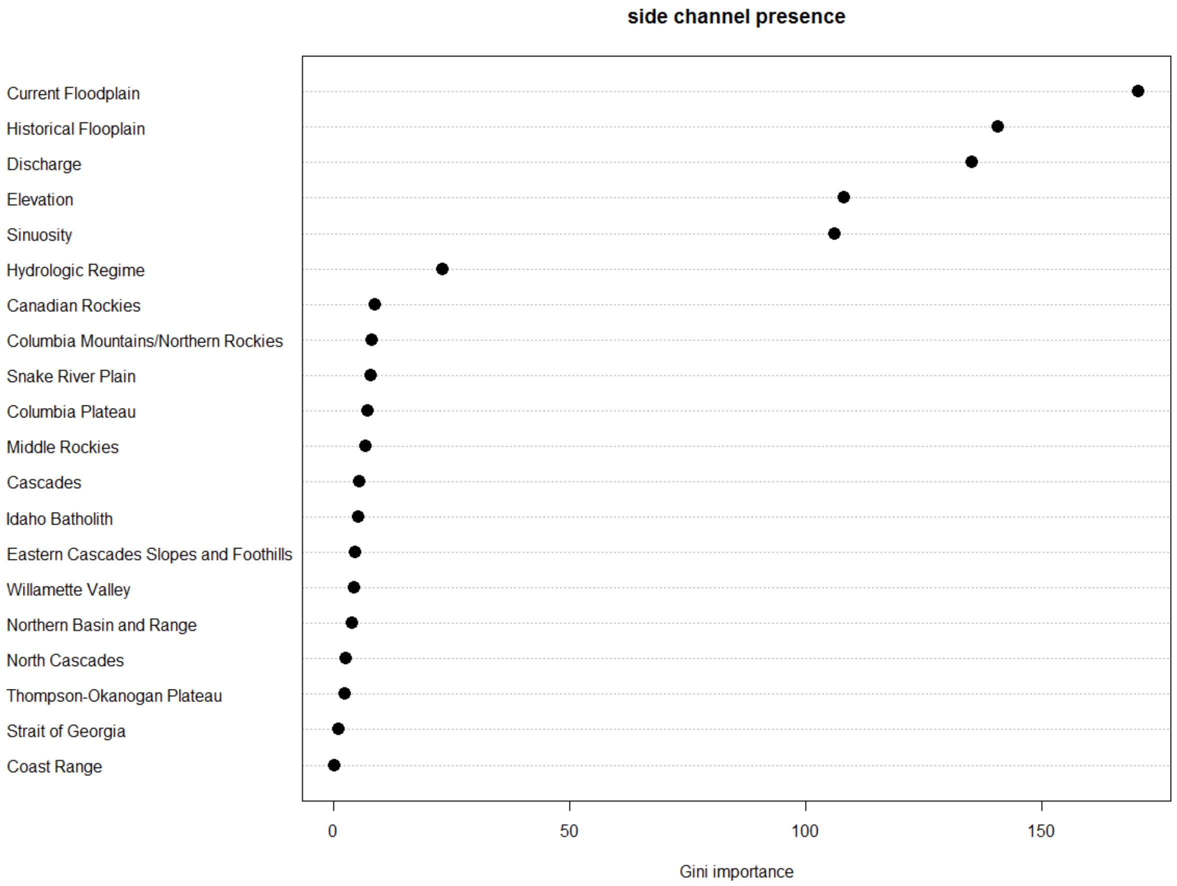

Figure 9. The importance of predictors in side channel presence. Gini importance indicates the average gain in purity for splits with each included variable.

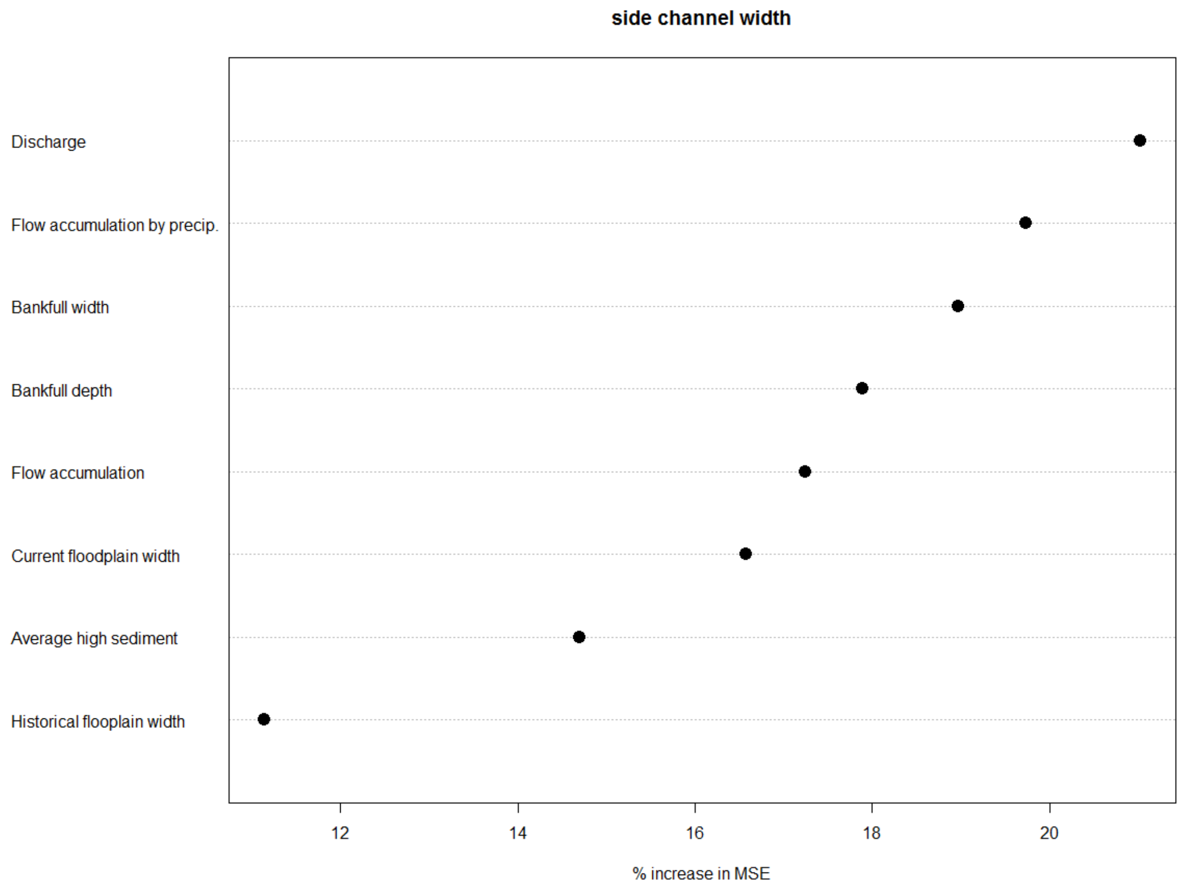

Figure 10. Importance of predictors by the percent increase in mean standard error in the random forest model predicting side channel amount (width).

VI. Mainstem habitats

To estimate mainstem habitat area, we modeled mainstem wetted widths using a random forest regression model with the same approach employed in side channel amount. The final tuned model included predictors: current floodplain width, sediment accumulation, discharge, bankfull width, bankfull depth, slope, sinuosity and elevation. Predicted wetted widths were then multiplied by stream segment length to estimate total wetted habitat area. To account for differences in juvenile salmonid capacity among mainstem stream habitats, we measured the bank to bar ratio of both banks for 1-5 km of stream at 70 sites throughout the CRB. We then used similar random forest procedures to the side channel model development to estimate the bank to bar ratio for each 200 m stream segment. The random forest regression model included slope, contemporary bankfull width, and sediment accumulation, and effectively predicted the bank to bar ratio for test sites (Fig 14). The bank to bar ratio was used to estimate the total stream bank length occupied by banks or bars. However, to estimate usable bank and bar area we used regressions of bar (Eq 1.) and bank (Eq 2.) width on total stream width developed from measurements of the Chehalis River in Washington State (Tim Beechie, unpublished data).

Eq 1. $Br_w = 0.0872 \times BFW + 2.114$

Eq 2. $Bk_w = 0.0837 \times BFW + 0.328$

Where Br_w is the bar width, Bk_w is the bank width, and BFW is the stream segment bankfull width. Estimated lengths and widths of banks and bars were then estimated for each stream segment. Mainstem habitat area not encompassed by bank and bar area was considered to be mid-channel area, which is not preferred habitat by salmon parr, and receives a unique density during fish capacity estimation.

Methods Part 2: Fish Capacity Estimation

To estimate capacity of each stream segment, we apply the maximum density we expect to observe in each habitat type. However, the data available for estimating the habitat capacity varies widely for spring Chinook. Therefore, we took three different approaches to estimating capacity form the available data;1) an expansion based on the finest level of habitat resolution estimated by our modeling approaches and a literature review of habitat specific fish densities, 2) a coarser expansion based on reach level habitat characteristics, total habitat area and a quantile regression of observed fish densities in the CRB, and 3) capacity estimated from mid-summer snorkel surveys in the Salmon River (Thorson et al. 2014).

The expansion approach applies expected fish capacity densities to each habitat area estimates for each stream segment. An extensive review of published and unpublished habitat specific capacities for both spring Chinook and steelhead young of the year (Beechie and Thompson, unpublished data, Table 4). These data are derived primarily from repeated beach seining or electrofishing specific habitat types over a range of conditions and spawner abundances, and the average maximum observed density is applied to each habitat type. Here, we used estimates for side channel, mainstem bank, mainstem bar, and mainstem mid-channel. Fish densities exist for finer levels of habitat distinction (e.g. mainstem backwaters, ponds, sloughs), than are currently estimated in the habitat modeling.

Table 4. Densities of Chinook parr used to estimate capacity with habitat expansion approach (From Beechie and Thompson unpublished review).

Habitat	Chinook parr · hectare^{-1}
main stem bank	8884
main stem bar	4720
main stem mid-channel	100
side channel	6000
small stream pool	452
small stream riffle	4

The quantile regression approach is similar to the expansion approach; applying fish densities to habitat area estimates. However, the fish density data available for this approach is density for entire stream reaches and is not separated by habitat type. Therefore, a single abundance and wetted area are used to calculate density. The Integrated Status and Effectiveness Monitoring Program (ISEMP) has been electrofishing stream reaches previously sampled by the Columbia River Habitat Monitoring Program (CHaMP) for several years. The ISEMP data have the advantage of being measured over a range of spawner abundances. However, the observed fish density at a given site may vary from zero to several fish per m^2 over the period of record. Therefore, a mean or median density may not accurately reflect capacity at the site level. To account for these differences we used quantile regression, which allows for the modeling of any percentile of fish density (Cade and Noon 2003). However as a predictive, rather than explanatory model, we chose to use quantile random forest procedures. We indexed the ISEMP sample densities to the sites used in our habitat model construction and used the same suite of habitat level predictors (i.e. we did not include ecoregion or land use) in creating a predictive model of fish capacity for both spring Chinook and steelhead. Quantile random forest models were created and tuned with the R package quantregForest using similar tuning procedures to the habitat estimation. After tuning, we predicted the 90th percentile fish density for each Willamette project stream segment, and multiplied those densities by sum of mainstem and side channel habitat for that reach.

Finally, we employed the spring Chinook capacity estimated from a hierarchical stock-recruit model of spawner and mid-summer parr densities in the Salmon River (Thorson et al. 2014).

Thorson et al. (2014) used decades of snorkel survey data to estimate an average capacity of 5200 parr · hectare^{-1}. To estimate capacity we multiplied the total habitat area (main stem bars, main stem banks, side channel) in hectares by 5200.

For each of the three expansion methods we sought to prevent the inclusion of habitats that are inaccessible, or unusable for rearing by spring or summer Chinook or steelhead. Therefore, the upstream and downstream extent of the network was limited by the stream sections listed as "spawning and rearing" or "migration and rearing" in the StreamNet spatial database (StreamNet Project 2012).

Results

Habitat area prediction

We estimated mainstem habitats with two models. The wetted width model performed well, with an $R^2 = 0.82$ (Figure 10). Similarly, bank to bar ratios were well estimated by the bank proportion random forest regression model ($R^2 = 0.68$, Figure 11.)

The random forest side channel classification model predicting the presence of any side channel had a balanced 74% accuracy, and there was little bias among false negative (23%) and false positive (28%) classification of side channel. Floodplain width was an important predictor in both side channel presence and side channel amount, although it was more influential in presence (Figures 8 and 9). Increasing floodplain width increased the presence and amount of side channel habitat, with the strongest effect at low width values (Figures 12 and 13). Both presence and magnitude models experienced a saturation of floodplain width near 2000 m (Figures 12 and 13). The side channel model contrasts starkly with the off channel model, which had no false negative detections, but a false positive rate of 18%. Therefore, we did not make predictions of off channel habitat, as it would likely drastically overestimate the amount of off channel habitat. The side channel area regression model had an R^2 of 0.52, and was only weakly biased low in its estimates of side channel area (Figure 14).

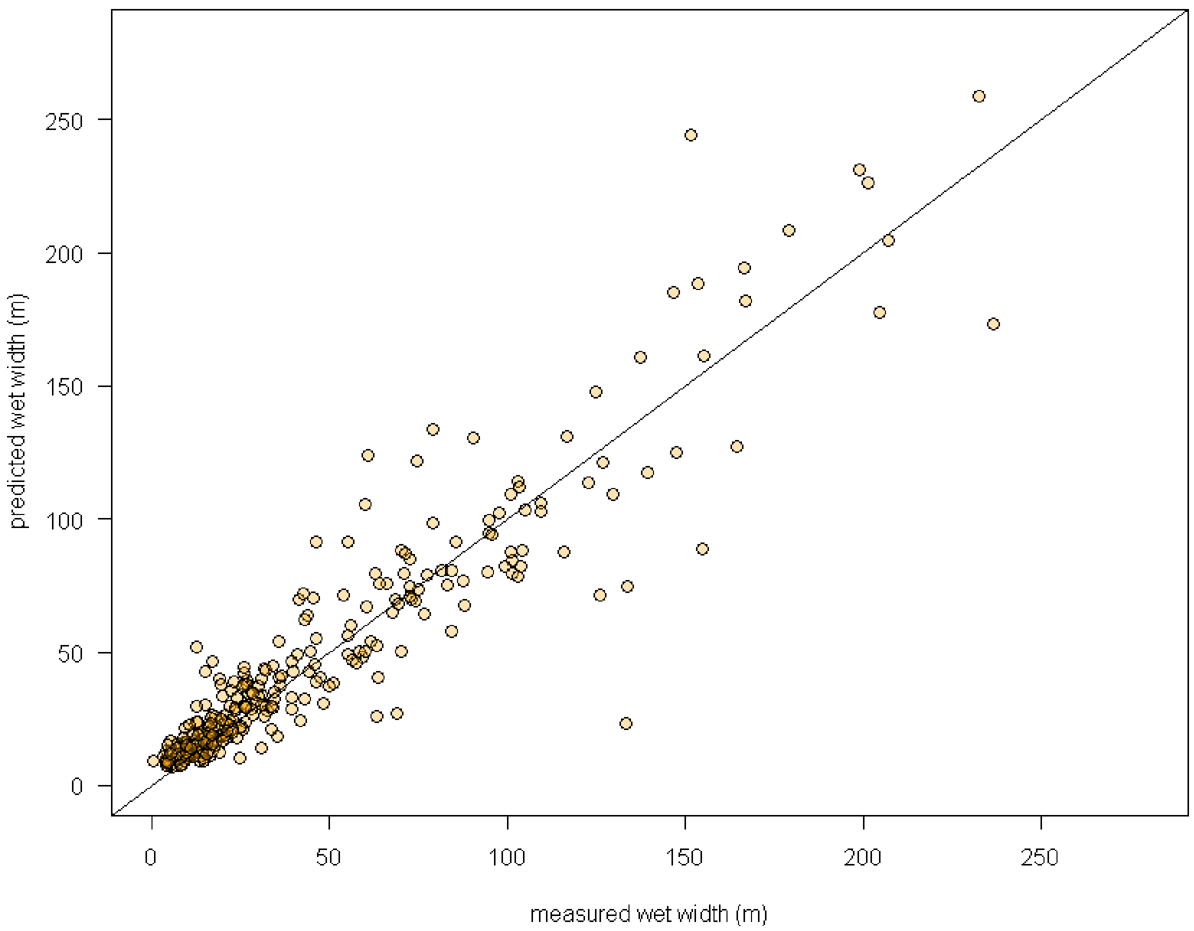

Figure 10. A comparison of measured wetted width (x –axis) and predicted wetted width (y-axis) from the random forest regression model for all sites measured with satellite imagery. Solid line indicates 1:1 correspondence between measurements and model output.

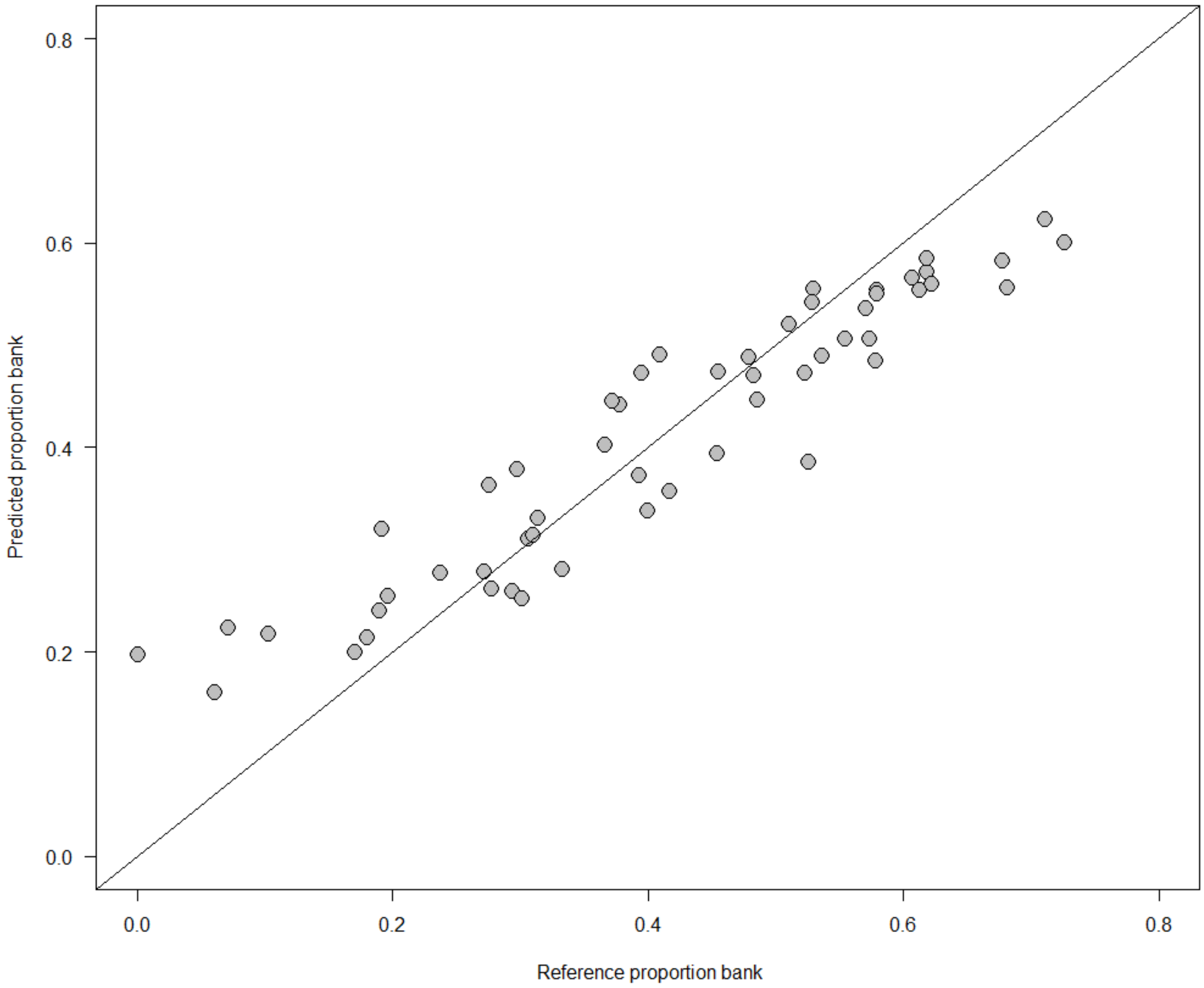

Figure 11. A comparison of measured bank proportions from satellite imagery (x-axis), and bank proportions predicted with random forest regression model.

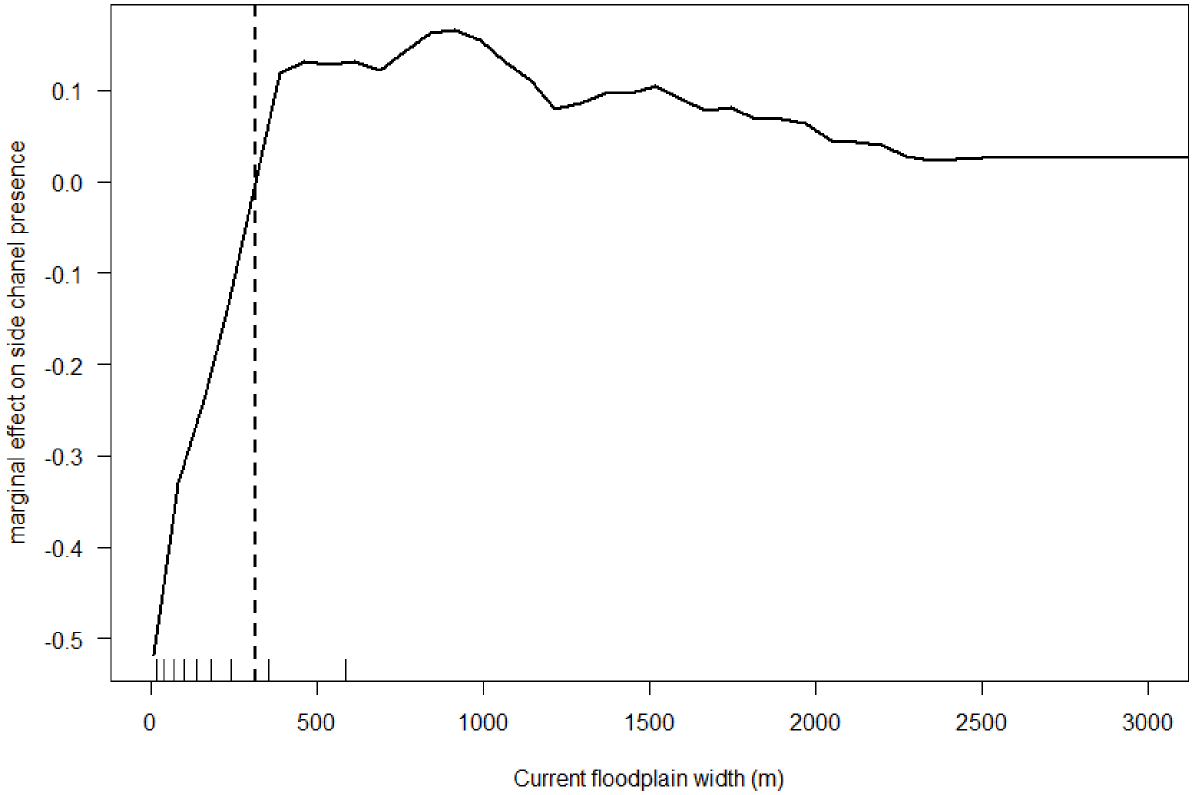

Figure 12. Vote influence of floodplain width on predictions of the presence of side channel habitat. Increasingly positive values of vote influence predict the presence of side channel habitat more strongly. Similarly, decreasing vote influence values indicate a stronger prediction of no side channel. Small ticks on the x-axis indicate deciles of floodplain width for all measured reaches. Vertical dashed line at a floodplain value of 315 m indicates the floodplain width where the marginal effect equals zero. Floodplains greater than 315 m are more likely to have side channel habitat, while those less than 315 m are less likely to have side channels. In very large floodplains (> ca. 2000 m) other processes dominate and the marginal effect returns to near zero.

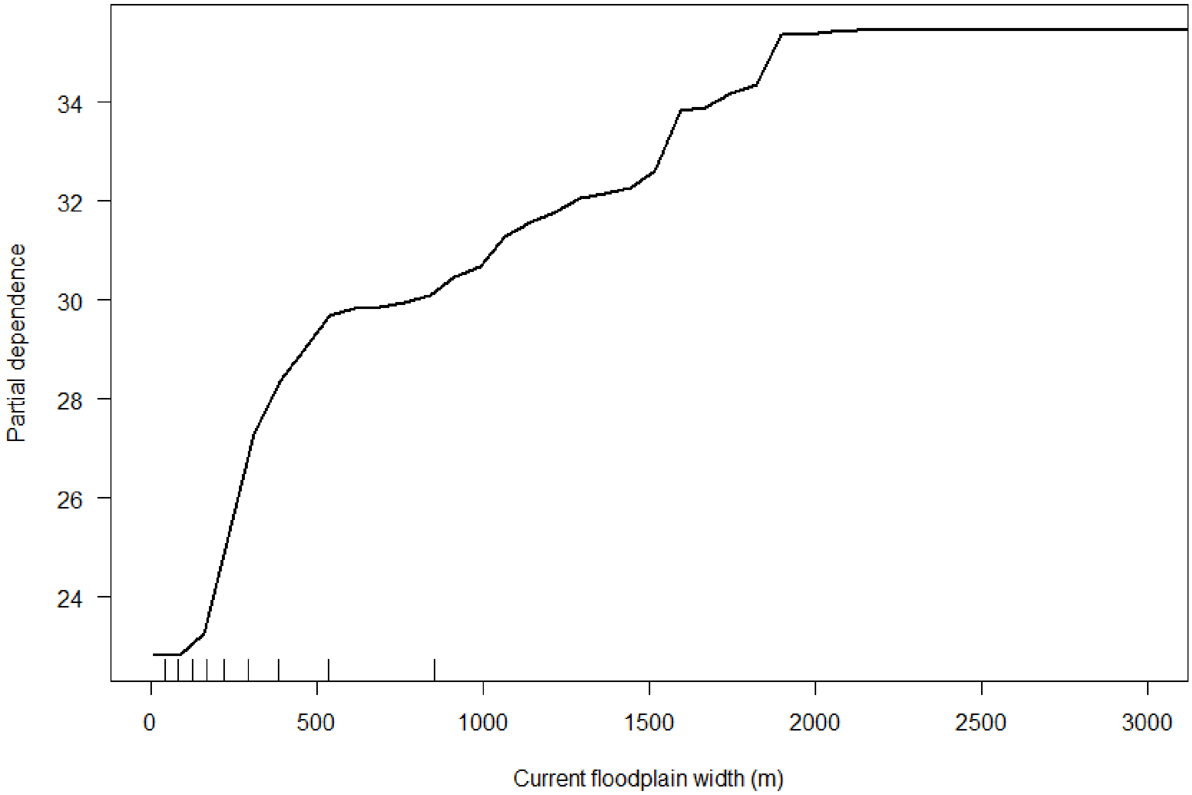

Figure 13. Partial dependence plot of the marginal effect of floodplain width on side channel width prediction. The influence of floodplain width becomes saturated at ca. 2000 m floodplain width. Small ticks on the x-axis indicate deciles of floodplain width for all measured stream segments.

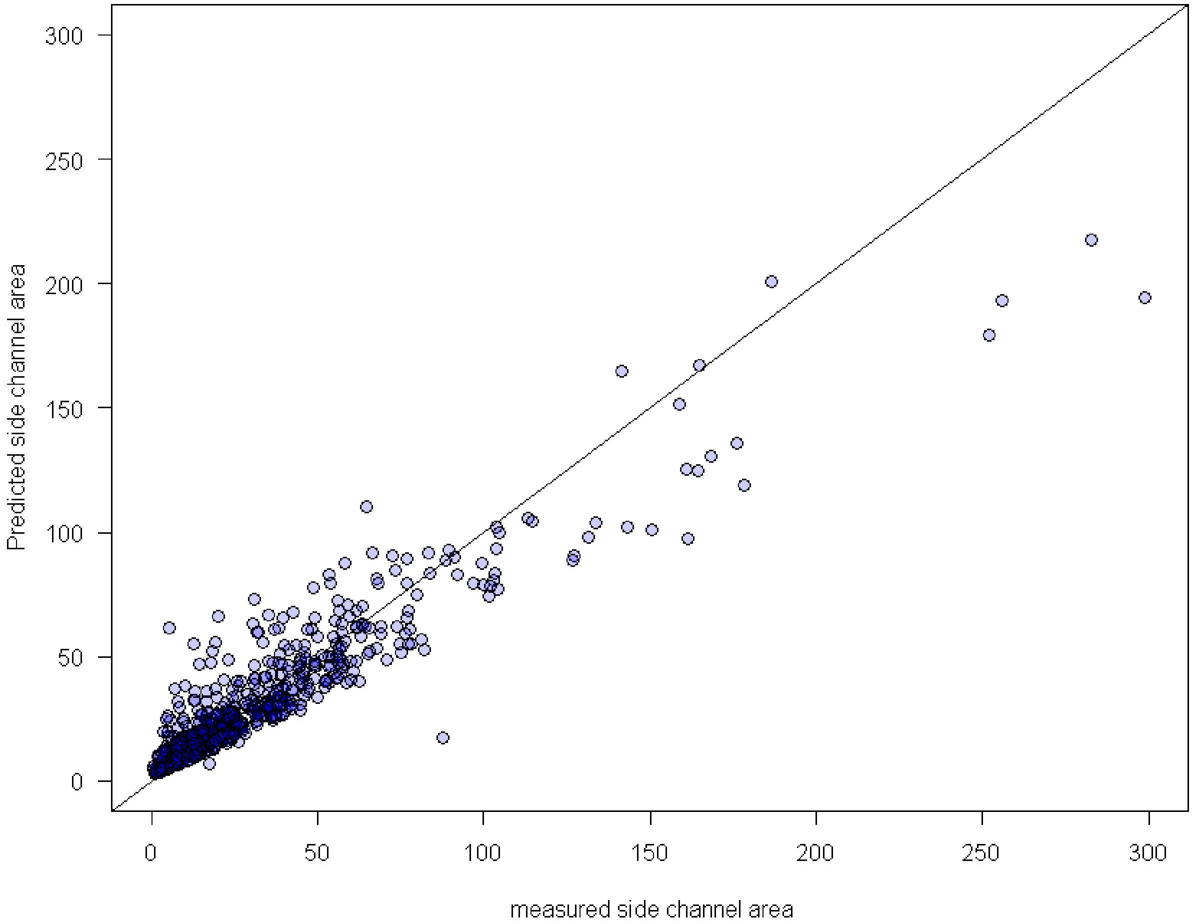

Figure 14. A comparison of measured side channel area (x –axis) and predicted side channel area (y-axis) from the random forest regression model for all side channel containing sites measured with satellite imagery. Solid line indicates 1:1 correspondence between measurements and model output.

Across all HUC-8 watersheds (US Geological Survey level 8 hydrologic unit) for spring Chinook (Table 5) we estimate approximately 52,852 hectares of contemporary wetted rearing habitat for spring and summer Chinook. For both Chinook run timings, contemporary side channel habitat comprises 13% of the total wetted habitat area. However, contemporary side channels comprise over 41% of the high value rearing habitat (i.e. side channels, mainstem banks and bars). Overall, historical estimates of side channel habitat were 34% greater than contemporary values, but varied widely by river, ranging from 0-435% change.

Fish capacity estimates

The three methods of assigning fish densities produced different capacity estimates in some HUC-8 watersheds, but similar estimates in others (Figure 15). Estimates of contemporary Chinook parr capacity using the habitat expansion method varied substantially among watersheds, and was 109.8 million across all watersheds (Table 5, Figure 16), with production from mainstem and side channel habitats varying among streams. As a percentage of total reach production, contemporary side channel habitat accounted for 37% of total capacity, although the percentage varied widely among watersheds, from 0-59% (Table 5, Figure 17). The quantile random forest method of assigning capacity to each stream segment predicted fewer fish in most watersheds, but many more at a few sites (e.g., Clearwater, HUC 1706030). Across all HUC-8 watersheds, the quantile regression method estimates a higher Chinook parr capacity than habitat expansion (120.9 million parr) (Table 5). Chinook parr capacity estimated from applying 5,200 fish per hectare to the total wetted area for each reach produced a lower total capacity than either expansion or quantile random forests (85.8 million parr across all watersheds).

Historical estimates of spring Chinook parr capacity across the Columbia basin were 13% higher than contemporary estimates (Table 5, Figure 18). To estimate potential changes in Chinook parr capacity due to restoration, we used two scenarios of floodplain reconnection. First we increased the current floodplain width to include rangelands (i.e., we estimate side channel areas as if all rangelands were converted to natural landcover), which increased CRB-wide capacity by 7.6% over the contemporary estimate (Figure 198). However, in some watersheds with large amounts of rangeland on the floodplain, the restoration scenario produced parr capacity increases of 25% or more. In the second scenario, restoring both rangeland and cropland areas produced only a slightly larger increase in capacity (8.6% over contemporary estimates), and there were relatively few additional watersheds with increases of 25% or more (Figure 20).

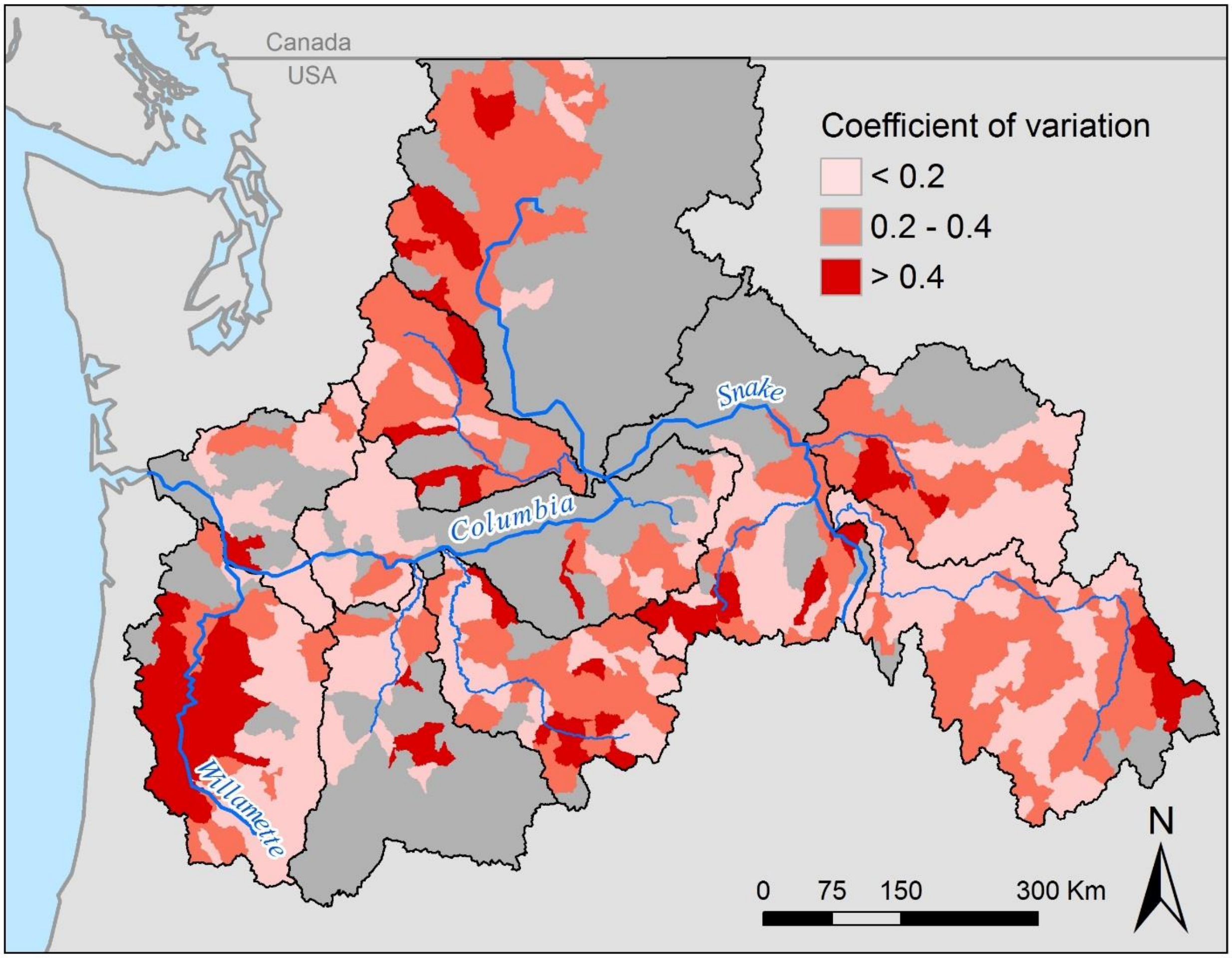

Figure 15. The coefficient of variation for spring/summer Chinook parr capacity estimates at HUC-10 watershed boundary spatial scale. Estimates were made with habitat expansion, quantile random forests, and applying 5200 parr per hectare of estimated Chinook rearing area.

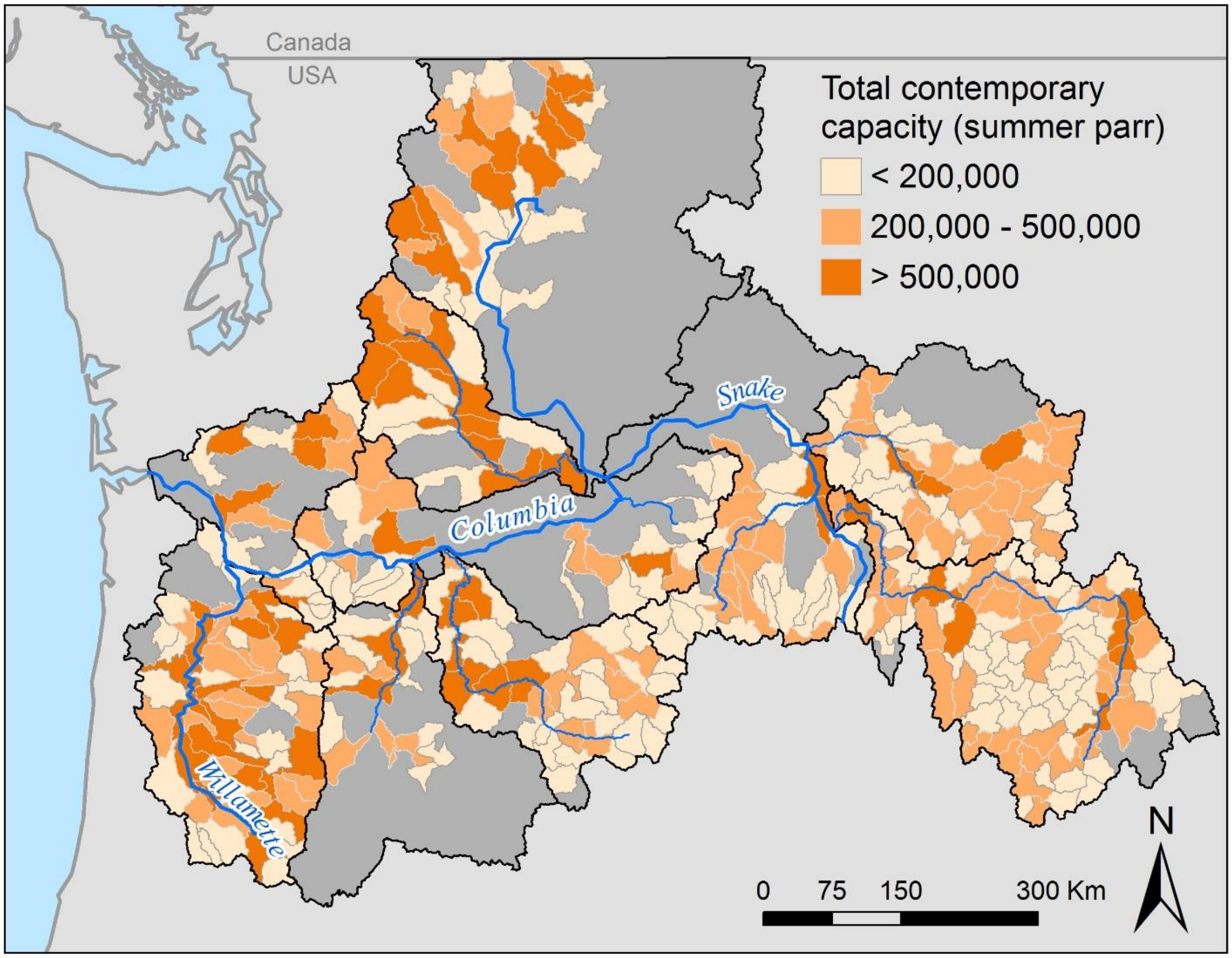

Figure 16. Contemporary summer parr rearing capacity of Spring Chinook within the domain currently accessible to anadromous fishes as determined by the habitat expansion approach of estimating main stem and side channel habitat and assigning fish densities to each habitat at the 200 m stream segment scale. For graphical purposes, estimates are aggregated at the HUC-10 watershed boundary spatial scale.

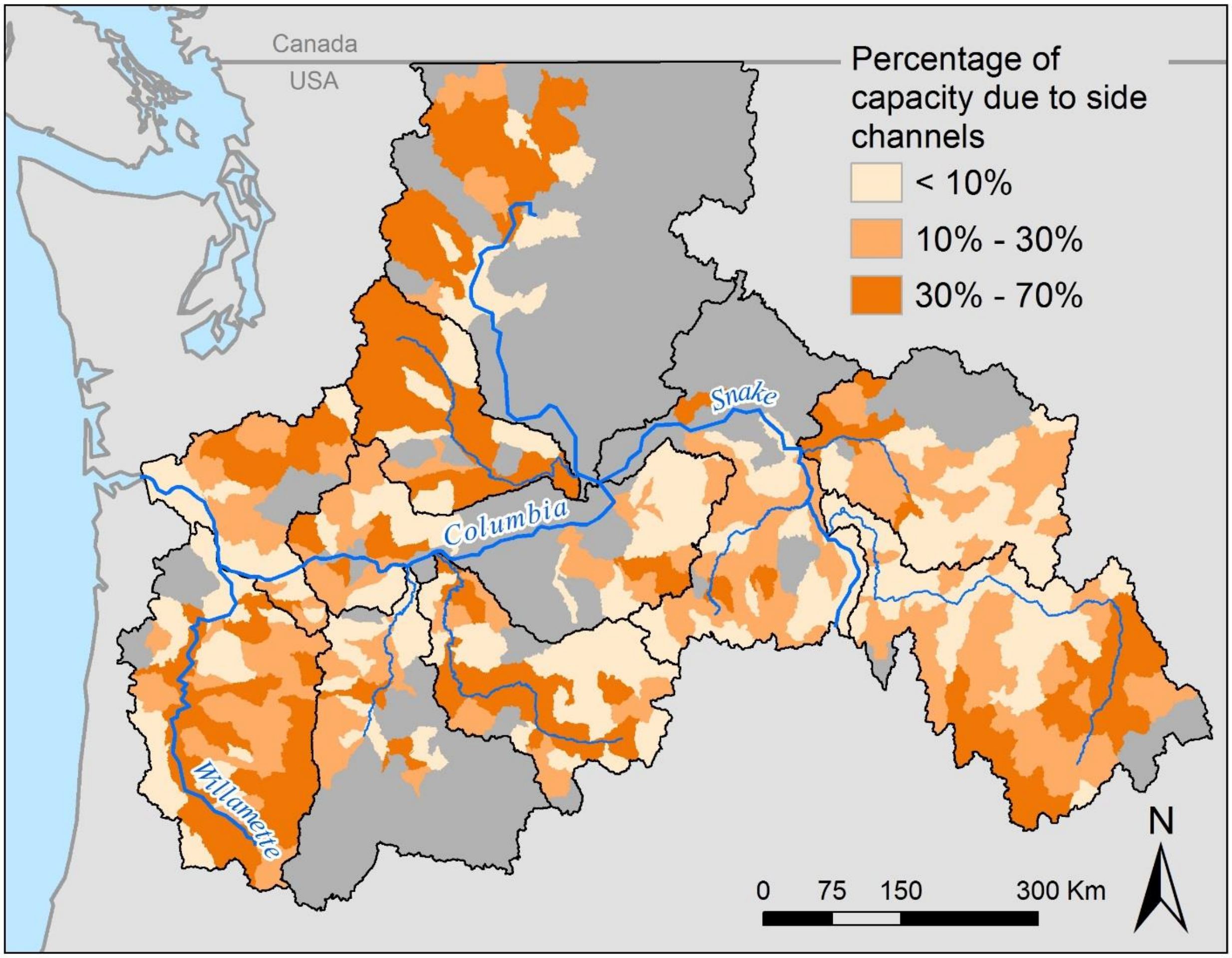

Figure 17. Contemporary percentage of total estimated spring Chinook parr rearing capacity attributed to side channel habitat. Estimates were made with the habitat expansion approach and aggregated at the HUC-10 watershed spatial scale.

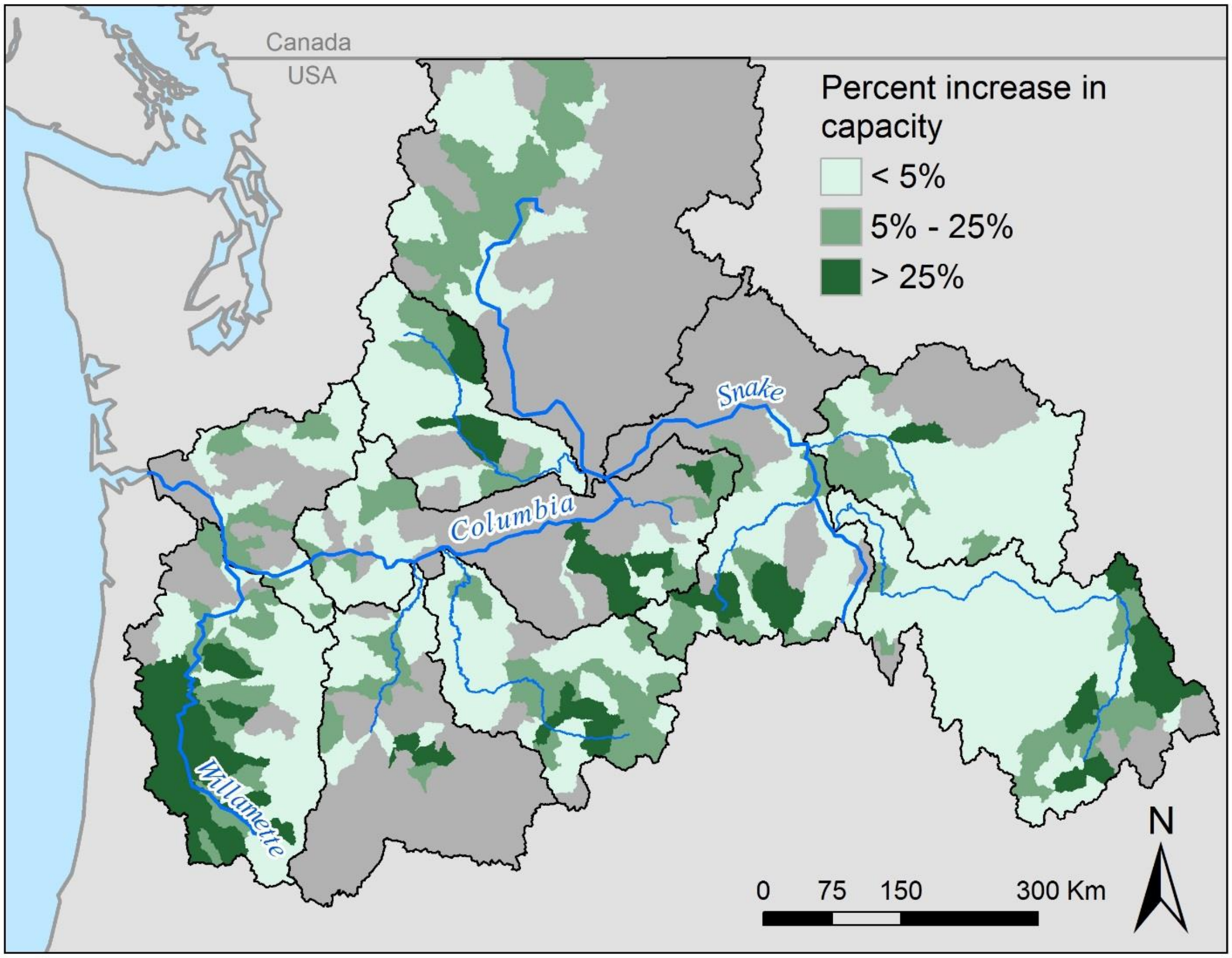

Figure 18**. Historical condition**: Estimated increase in spring Chinook parr capacity from contemporary conditions resulting from side channel creation in floodplains reconnected through stream restoration to historical width as determined by the valley bottom filled to a depth of 6 m. In addition to range and croplands, this scenario restores areas currently limited by urbanization and large roads**.** Estimates were made with the habitat expansion approach and aggregated at the HUC-10 watershed spatial scale.

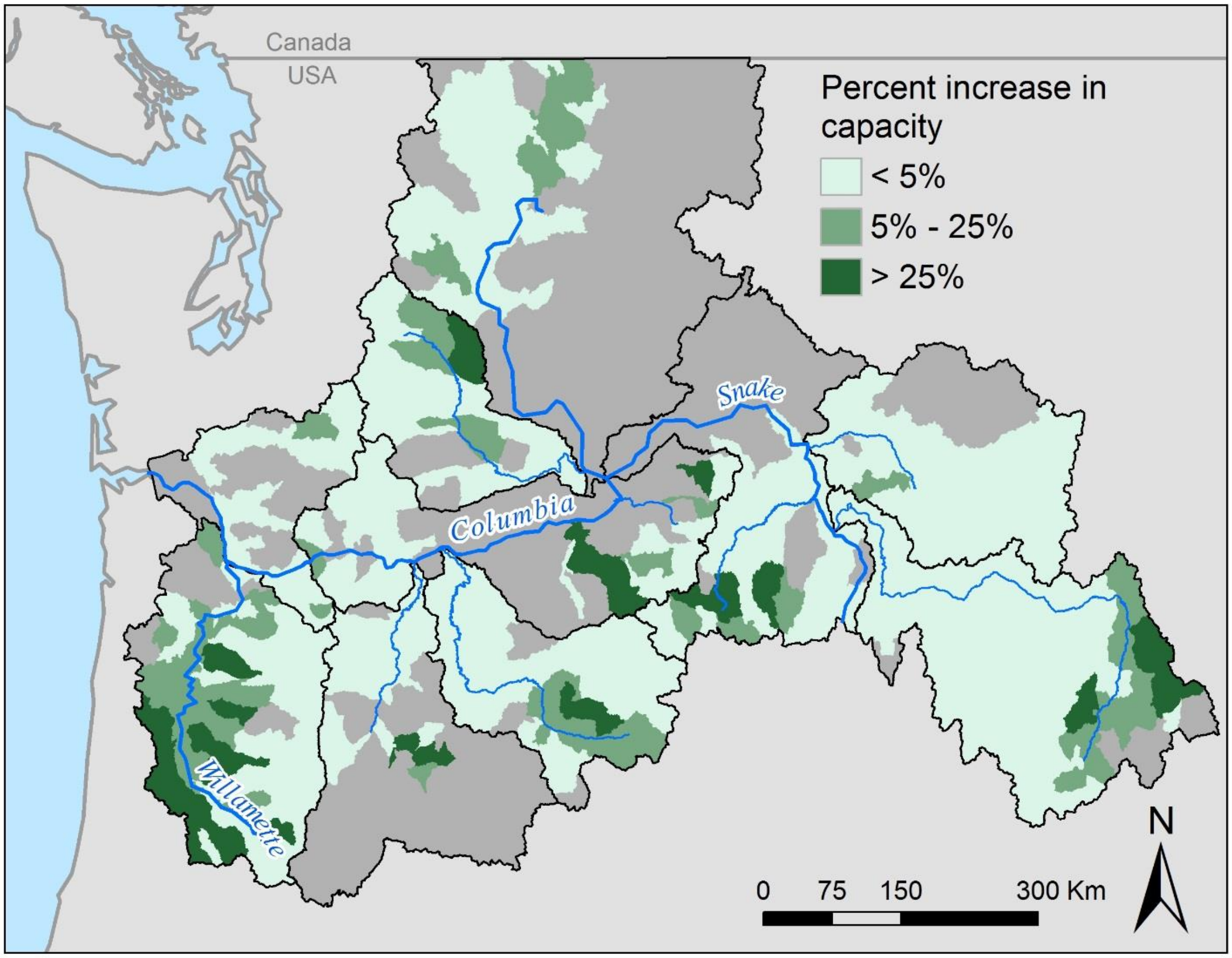

Figure 19. **Rangeland restoration**: Estimated increase in spring Chinook parr capacity from contemporary conditions resulting from side channel creation in floodplains reconnected through stream restoration in rangeland. Additionally, we assume restoration of habitat currently impeded by small private roads. Estimates were made with the habitat expansion approach and aggregated at the HUC-10 watershed spatial scale.

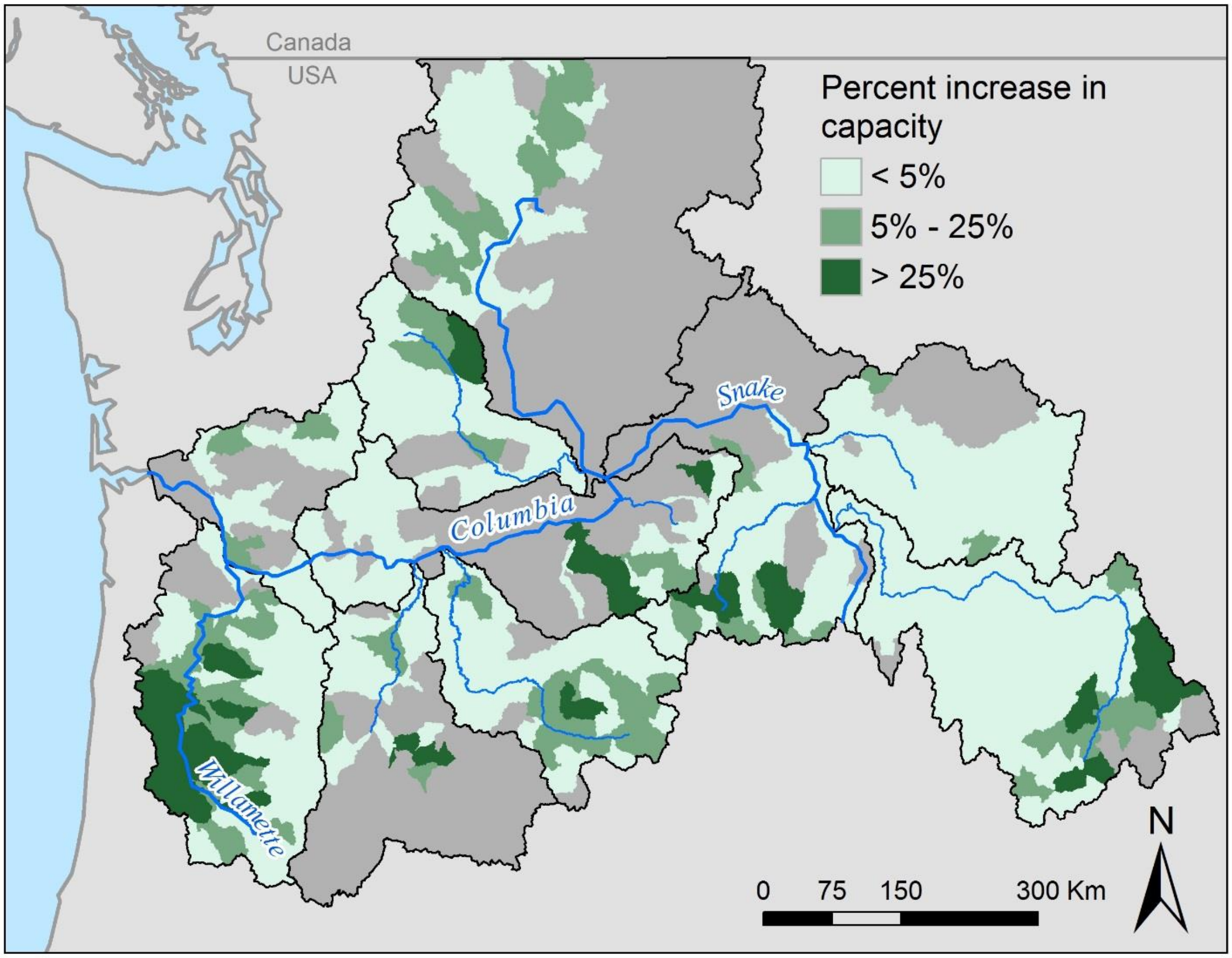

Figure 20**. Rangeland and cropland restoration**: Estimated increase in spring Chinook parr capacity from contemporary conditions resulting from side channel creation in floodplains reconnected through stream restoration in rangeland and cropland. Additionally, we assume restoration of habitat currently impeded by small private roads. Estimates were made with the habitat expansion approach and aggregated at the HUC-10 watershed spatial scale.

Table 5. Spring and summer Chinook parr summer rearing capacity by HUC-8 sub-basin. Main stem indicates the expansion method sum of bank, bar, and mid-channel capacity. Contemporary and historical side channel indicate the expansion method estimate for current and full floodplain reconnection respectively. Expansion total is the sum of main stem and contemporary side channel estimates. QRF total indicates estimates from quantile random forest (90th percentile) of ISEMP fish survey data and total habitat area. Both historical and contemporary estimates are limited to the currently accessible habitats defined as rearing habitat by StreamNet.

HUC-8	Name	Mainstem	Contemporary side channel	Historical side channel	> 8m BFW Expansion total	> 8m BFW QRF total	> 8m BFW 5200/ hectare	< 8m BFW total
17020005	Chief Joseph	6,020	3,327	4,109	9,348	4,969	7,753	169
17020006	Okanogan	1,870,864	1,990,837	2,591,994	3,861,701	5,028,897	3,029,114	-
17020007	Similkameen	175,554	208,705	252,712	384,258	174,519	309,575	-
17020008	Methow	1,844,013	1,356,729	1,510,509	3,200,742	1,444,670	2,607,603	21,557
17020009	Lake Chelan	15,849	6,092	11,406	21,941	10,157	17,430	-
17020010	Upper Columbia-Entiat	282,497	166,744	234,201	449,241	142,817	364,158	9,498
17020011	Wenatchee	1,641,537	1,227,573	1,585,610	2,869,110	1,218,187	2,299,398	40,374
17020012	Moses Coulee	3,196	-	-	3,196	2,576	2,652	-
17030001	Upper Yakima	1,800,801	1,698,267	2,077,083	3,499,068	1,801,625	2,817,275	37,807
17030002	Naches	705,590	635,650	695,451	1,341,240	737,197	1,084,655	40,522
17030003	Lower Yakima, Washington	2,543,289	3,534,895	3,914,090	6,078,184	6,807,410	4,935,626	50,341
17060101	Hells Canyon	37,792	-	-	37,792	31,256	28,104	40,291
17060102	Imnaha	782,669	102,757	115,285	885,426	513,132	687,420	62,733
17060103	Lower Snake-Asotin	1,744,703	399,915	471,839	2,144,618	2,815,432	1,562,290	16,696
17060104	Upper Grande Ronde	1,187,687	316,190	1,443,877	1,503,877	2,176,811	1,160,457	86,611
17060105	Wallowa	1,011,256	251,142	549,775	1,262,398	1,153,676	966,512	35,964
17060106	Lower Grande Ronde	778,464	98,725	96,725	877,189	633,121	657,119	70,300
17060107	Lower Snake-Tucannon	211,863	37,506	54,425	249,368	236,333	192,086	8,420
17060201	Upper Salmon	2,091,593	968,630	1,418,538	3,060,223	3,118,350	2,402,031	572,012
17060202	Pahsimeroi	156,652	192,846	226,614	349,497	184,292	289,469	-
17060203	Middle Salmon-Panther	2,065,635	1,435,910	1,647,985	3,501,545	4,302,807	2,732,895	209,370
17060204	Lemhi	378,964	191,343	725,637	570,307	156,898	458,452	43,315
17060205	Upper Middle Fork Salmon	988,871	527,325	545,309	1,516,197	1,742,764	1,209,109	380,324
17060206	Lower Middle Fork Salmon	1,273,261	118,845	124,908	1,392,105	1,735,069	1,014,904	268,377
17060207	Middle Salmon-Chamberlain	2,273,860	51,704	51,704	2,325,564	2,228,930	1,654,933	194,336
17060208	South Fork Salmon	1,440,726	238,943	252,282	1,679,670	2,044,231	1,263,941	253,775
17060209	Lower Salmon	2,716,293	132,656	188,187	2,848,949	2,594,527	2,070,358	81,506
17060210	Little Salmon	401,449	59,964	72,772	461,413	543,339	354,089	33,937
17060301	Upper Selway	919,134	106,914	106,865	1,026,048	819,270	765,741	190,910
17060302	Lower Selway	1,199,377	75,209	63,528	1,274,586	801,184	944,119	98,923
17060303	Lochsa	1,584,042	177,109	211,966	1,761,151	1,591,429	1,304,017	165,793
17060304	Middle Fork Clearwater	657,954	226,683	153,983	884,637	376,147	684,528	56,743
17060305	South Fork Clearwater	1,084,190	156,383	203,401	1,240,573	858,797	927,369	254,070
17060306	Clearwater	2,217,489	560,702	672,080	2,778,192	1,486,872	2,146,813	277,559
17060308	Lower North Fork Clearwater	31,171	15,029	16,286	46,199	21,859	36,123	-
17070102	Walla Walla	313,123	28,909	125,773	342,033	364,072	274,270	21,345
17070103	Umatilla	891,865	552,762	1,356,644	1,444,628	1,203,297	1,159,626	38,983
17070105	Middle Columbia-Hood	661,764	402,549	432,048	1,064,312	918,031	839,490	106,043
17070106	Klickitat	929,418	554,051	620,610	1,483,469	1,460,173	1,158,633	7,745
17070201	Upper John Day	848,766	580,470	834,230	1,429,236	1,930,852	1,176,785	32,296
17070202	North Fork John Day	1,175,717	259,474	355,880	1,435,191	1,560,261	1,097,226	88,239
17070203	Middle Fork John Day	432,823	116,174	152,663	548,997	245,816	436,931	94,416
17070204	Lower John Day	2,919,820	2,032,601	2,208,101	4,952,420	4,815,557	3,870,168	45
17070301	Upper Deschutes	343,889	62,192	87,508	406,081	458,014	317,094	2,739
17070305	Lower Crooked	499,692	105,642	454,922	605,335	800,183	461,405	-
17070306	Lower Deschutes	2,519,498	683,927	911,747	3,203,425	2,537,810	2,456,100	14,817
17070307	Trout	663	871	1,233	1,534	494	1,286	-
17080001	Lower Columbia-Sandy	865,675	401,395	446,205	1,267,070	1,103,586	977,073	33,101
17080002	Lewis	210,898	75,033	114,189	285,931	319,336	218,374	28,771
17080003	Lower Columbia-Clatskanie	394,918	111,639	127,199	506,556	497,068	373,926	43,193
17080004	Upper Cowlitz	960,651	1,013,984	1,153,777	1,974,635	1,792,603	1,574,004	10,663
17080005	Lower Cowlitz	632,219	346,058	514,364	978,276	1,177,151	743,042	33,168
17090001	Middle Fork Willamette	1,527,465	1,557,756	1,777,566	3,085,220	3,009,425	2,470,267	131,771
17090002	Coast Fork Willamette	430,144	283,296	724,829	713,440	1,245,196	557,368	2,310
17090003	Upper Willamette	3,223,180	4,176,266	7,041,368	7,399,446	16,479,084	5,894,195	41,321
17090004	Mckenzie	2,148,831	3,059,165	3,461,332	5,207,995	5,443,837	4,199,754	127,283
17090005	North Santiam	1,570,824	1,928,816	2,318,093	3,499,640	4,922,581	2,801,469	47,428
17090006	South Santiam	1,373,490	1,039,429	1,520,966	2,412,919	4,017,124	1,907,205	26,642
17090007	Middle Willamette	2,882,041	2,826,205	3,954,036	5,708,246	9,112,475	4,480,042	65,055
17090008	Yamhill	567,837	46,950	10,547	614,787	923,017	426,453	21,309
17090009	Molalla-Pudding	1,280,949	390,182	594,002	1,671,132	2,532,000	1,273,057	31,219
17090011	Clackamas	1,338,408	747,720	843,307	2,086,128	2,477,358	1,611,201	21,188
17090012	Lower Willamette	39,637	1,848	6,037	41,485	41,686	29,328	23,475

Discussion

Mainstem habitat

Our estimates of bankfull width for main stem channels were in general larger than those estimated by Beechie and Imaki (2014). However, we have not yet validated the precision of our satellite imagery based measurements with field measurements. On the other hand, bank and bar widths, where edge velocity and depth is in the preferred region for Chinook, are driven largely by the intercept from equations 1 and 2. Therefore, misidentification of bankfull width has a larger effect on the mid-channel area, which we assume is largely unused by Chinook in streams greater than 8 m bankfull width. Although our model of the ratio of banks and bars for edge habitat performs well in areas with little bank modification, we currently do not model either other edge habitats or the likely change in edge habitat with different land use or riparian condition. For example many areas may have hydromodified banks with lower capacity for juvenile salmonids. Similarly, main stem backwaters may have a high capacity and contribute disproportionately to capacity. Future model development should include main stem habitat characterization at our random selection of sites to better assess current condition and changes to edge habitat with varying land use practices. In addition, we cannot assess edge widths from satellite imagery so our current estimates rely heavily on regressions of bar and bank width from measurements in the Chehalis River basin. Although there are likely many similaries between the banks and bar forming processes in the Chehalis and CRB, an emphasis should be placed on measuring bar and bank widths at various location in the CRB where flow and sediment dynamics may differ from the more coastal, low elevation floodplain of the Chehalis R. Additionally, our model does not address other mainstem habitat forms such as hydromodified banks and backwaters; which have been shown to decrease and increase rearing capacity, respectively. Hydromodified banks in particular may be prominent in areas below impoundments or with substantial urban development and road density, and have the potential to substantially decrease rearing capacity.

Side channel habitat

Side channels are known to be prominent rearing habitats for young of the year salmonids (Morley et al. 2005, Bellmore et al. 2013). Our model of side channel area was developed with stratified randomly chosen sites throughout the Columbia River basin, including areas not currently or historically occupied by salmon. Our sampling design helps to ensure that both modified and unmodified stream segments with similar underlying landform characteristics (e.g. slope, historical floodplain width) were represented in model development. This representation should allow more accurate estimation of the historical state of the side channel in currently modified areas. In our final predictive model floodplain width was the most important variable in predicting side channel presence. Ecoregion was included, but was less important, lending credence to making training measurements throughout the CRB. Surprisingly, land cover type immediately adjacent to the site did not improve model accuracy. Our side channel models were constructed with estimates of floodplain width that best matched measured active channel widths for each site; historical floodplain restricted by urban, rangeland and cropland land classes. Partial dependence plots of floodplain widths on side channel presence and amount both indicated a saturating effect of floodplain at a width of ca. 2000 m. More prominently for restoration actions of floodplain, the steep slope at the origin of the partial dependence plots indicates that even moderate increases in useable floodplain width can greatly increase the presence and width of side channel habitats. To make specific estimates of the likely gains in side channel habitat with large scale floodplain reconnection, we supplied our models with floodplain widths that reclaim rangeland, or rangeland and cropland. Historical estimates assume a completely unrestricted floodplain. On a basinwide scale, most gains in side channel area were made with a rangeland restoration scenario, with inclusion of cropland adding a small amount to the total. From a restoration perspective, this may be encouraging as restoration of the rangeland floodplain may be more feasible than with cropland. By comparison, floodplain reconnection in urbanized areas (including impervious roads) has little effect on overall capacity.

Despite much discussion in the published literature about the value of side channel habitats for juvenile salmon rearing, the vast majority of the parr density data in side channels is from studies of coho salmon, while relatively little side channel-specific density data exist for Chinook. However, what little data are available appear to support the higher rearing densities for Chinook, and is supported by the similar values for habitat expansion and quantile regression in smaller streams.

Our estimates of capacity from habitat expansion and quantile regression are similar in many reaches for Chinook salmon, providing a useful corroboration from two different approaches and fish density data sources. Unlike habitat expansion, the quantile regression approach estimates an average capacity for all wetted areas of a stream segment (side and mainstem combined). Quantile regression random forest estimates from ISEMP stream survey data of primarily spring-run Chinook were used to make summer Chinook parr estimates, and were in lower at most sites, and quite a bit higher at a few sites. In particular, large streams where much of the habitat is allocated to low value mid-channel habitat in the expansion model, is estimated at a single value across its width in the quantile regression model, leading to higher estimates in large streams, as large streams are not included in the ISEMP stream survey.

Much of the data informing the habitat expansion estimates is derived from surveys in north Cascade Puget Sound rivers (e.g. Skagit R.), where Chinook densities may differ from areas of the upper and mid-Columbia where much of the CHaMP and ISEMP monitoring is conducted. Although local data are nearly always preferred to remove the confounding watershed level effects (e.g. primary productivity, temperature, predation, etc.), Chinook in some CRB watersheds may be far enough below capacity that even local sampling may not detect evidence of density dependence or capacity.

Future directions

A thorough body of work has related presence of wood in streams to habitat quality for salmonids (Montgomery et al. 2003). Recently, it has been demonstrated that much of the benefit of wood in streams for salmonids comes through the creation of pool and side channel habitat (Beechie and Sibley 1997). Additional information about the riparian buffer width and canopy height would provide useful metrics of both the delivery of large wood to the stream, as well as the cooling shade effect of the riparian canopy. Therefore, an estimate of wood in streams would likely increase the accuracy of side channel estimation as well as fish capacity. New spatially continuous models of tree stand height, species composition, and canopy cover provided useful shade covariates in stream temperature estimation (Isaak 2016), and may prove useful in estimating the contribution of wood delivery to stream segments. Beechie and Imaki (2014) speculated that estimates of large wood may have greatly improved the channel type estimation model that forms much of the foundation of our current side channel estimation.

In addition to large wood inputs, there are undoubtedly other aspects of stream habitat loss that are not estimable at this spatial scale. For example, over-widening in areas with heavy grazing pressure and a history of flashboard dams have degraded habitats in ways that are not accounted for in our current model. Additionally, a historical legacy that has fundamentally altered the stream morphology would not be well predicted by our model (e.g. Mining tailings in Yankee Fork, Salmon River, or Volcanic runoff in the Toutle R.). Current remote sensing techniques that rely on satellite imagery are often too coarse to estimate finescale features. In addition, headwater tributaries are largely heavily forested. Although these forests and riparian zones may signal intact stream channels and healthy fish habitat, these areas cannot be verified from satellite imagery and would require local stream surveys to measure channel forms. Fortunately, many headwater streams are estimated to be <8 m bankfull width and are not expected to have persistent side channel habitat.

Our estimates demonstrate only modest losses in habitat area, and hence capacity, from historical to current estimates. Although in many places floodplains are greatly restricted from their historical state, truncation of the floodplain does not necessarily translate into large losses of side channels. The active channel width (i.e. the region of the floodplain in each stream segment currently used for channel forming processes) is a better indicator of potential side channel habitat, but cannot be readily estimated with the current resolution digital elevation model available for the CRB. Although higher resolution Light Detection and Ranging (LiDAR) techniques increase the elevation detail, use of LiDAR derived elevations has a tendency to overestimate inundated areas. However, LiDAR may be useful for defining active channel widths with better accuracy than flooding the relatively coarse scale (10 m) digital elevation model, but LiDAR coverage throughout the CRB is patchy. Therefore, additional information from ground based surveys like the Columbia Habitat Monitoring Program (CHaMP) may provide the best validation of estimates, where they are available.

Finally, further salmon capacity estimation work from habitat area should include aspects of water quality. In particular, temperature has important implications for all life stages of salmonids, from mortality of migrating adults, to embryo development rates and mortality, and life history determination, habitat occupancy, and growth of juveniles. Current and future summer temperatures can now be modeled for the entire CRB (Isaak 2016), and future work should move from the base capacity as determined by wetted habitat area to capacity limitations based on extreme environmental conditions like high summer temperature, or low overwinter temperatures, both of which may be limiting for salmon growth and survival .

References

Bartz, K. K., K. M. Lagueux, M. D. Scheuerell, T. Beechie, A. D. Haas, and M. H. Ruckelshaus. 2006. Translating restoration scenarios into habitat conditions: an initial step in evaluating recovery strategies for Chinook salmon (Oncorhynchus tshawytscha). Canadian Journal of Fisheries and Aquatic Sciences **63**:1578-1595.

Beck, M. W., K. L. Heck, Jr., K. W. Able, D. L. Childers, D. B. Eggleston, B. M. Gillanders, B. Halpern, C. G. Hays, K. Hoshino, T. J. Minello, R. J. Orth, P. F. Sheridan, and M. P. Weinstein. 2001. The identification, conservation, and management of estuarine and marine nurseries for fish and invertebrates. Bioscience **51**:633-641.

Beechie, T., and H. Imaki. 2014. Predicting natural channel patterns based on landscape and geomorphic controls in the Columbia River basin, USA. Water Resources Research **50**:39-57.

Beechie, T., G. Pess, and H. Imaki. 2012. Estimated changes to Chinook salmon (*Oncorhynchus tshawytscha*) and steelhead (*Oncorhynchus mykiss*) habitat carrying capacity from rehabilitation actions for the Trinity River, North Fork Trinity to Lewiston Dam.

Beechie, T. J., B. D. Collins, and G. R. Pess. 2001. Holocene and recent geomorphic processes, land use, and salmonid habitat in two north Puget Sound river basins. Geomorphic processes and riverine habitat, Water Science and Application **4**:37-54.

Beechie, T. J., M. Liermann, M. M. Pollock, S. Baker, and J. Davies. 2006. Channel pattern and river-floodplain dynamics in forested mountain river systems. Geomorphology **78**:124-141.

Beechie, T. J., and T. H. Sibley. 1997. Relationships between channel characteristics, woody debris, and fish habitat in northwestern Washington streams. Transactions of the American Fisheries Society **126**:217-229.

Bellmore, J. R., C. V. Baxter, K. Martens, and P. J. Connolly. 2013. The floodplain food web mosaic: a study of its importance to salmon and steelhead with implications for their recovery. Ecological Applications **23**:189-207.

Bisson, P. A., J. B. Dunham, and G. H. Reeves. 2009. Freshwater Ecosystems and Resilience of Pacific Salmon: Habitat Management Based on Natural Variability. Ecology and Society **14**.

Bisson, P. A., K. Sullivan, and J. L. Nielsen. 1988. Channel hydraulics, habitat use and body form of juvenile coho salmon, steelhead and cutthroat trout in streams. Transactions of the American Fisheries Society **117**:262-273.

Cade, B. S., and B. R. Noon. 2003. A gentle introduction to quantile regression for ecologists. Frontiers in Ecology and the Environment **1**:412-420.

Cutler, A., D. R. Cutler, and J. R. Stevens. 2012. Random Forests. Ensemble Machine Learning: Methods and Applications:157-175.

Hall, J. E., D. M. Holzer, and T. J. Beechie. 2007. Predicting river floodplain and lateral channel migration for salmon habitat conservation. Journal of the American Water Resources Association **43**:786-797.

Homer, C. G., J. A. Dewitz, L. Yang, S. Jin, P. Danielson, G. Xian, J. Coulston, N. D. Herold, J. Wickham, and K. Megown. 2015. Completion of the 2011 National Land Cover Database for the conterminous United States-Representing a decade of land cover change information. Photogrammetric Engineering and Remote Sensing **81**:345-354.

Isaak, D. J. W., Seth J.; Peterson, Erin E.; Ver Hoef, Jay M.; Hostetler, Steven W.; Luce, Charlie H.; Dunham, Jason B.; Kershner, Jeffrey L.; Roper, Brett B.; Nagel, David E.; Chandler, Gwynne L.; Wollrab, Sherry P.; Parkes, Sharon L.; Horan, Dona L. 2016. NorWeST modeled summer stream temperature scenarios for the western U.S.*in* Forest Service Research Data Archive, editor., Fort Collins, CO.

Kiffney, P. M., C. M. Greene, J. E. Hall, and J. R. Davies. 2006. Tributary streams create spatial discontinuities in habitat, biological productivity, and diversity in mainstem rivers. Canadian Journal of Fisheries and Aquatic Sciences **63**:2518-2530.

Martin, T. G., B. A. Wintle, J. R. Rhodes, P. M. Kuhnert, S. A. Field, S. J. Low-Choy, A. J. Tyre, and H. P. Possingham. 2005. Zero tolerance ecology: improving ecological inference by modelling the source of zero observations. Ecology Letters **8**:1235-1246.

Montgomery, D. R., B. D. Collins, J. M. Buffington, and T. B. Abbe. 2003. Geomorphic effects of wood in rivers. Ecology and Management of Wood in World Rivers **37**:21-47.

Morley, S. A., P. S. Garcia, T. R. Bennett, and P. Roni. 2005. Juvenile salmonid (Oncorhynchus spp.) use of constructed and natural side channels in Pacific Northwest rivers. Canadian Journal of Fisheries and Aquatic Sciences **62**:2811-2821.

Olden, Julian D., Joshua J. Lawler, and N. L. Poff. 2008. Machine Learning Methods Without Tears: A Primer for Ecologists. The Quarterly Review of Biology **83**:171-193.

Potts, J. M., and J. Elith. 2006. Comparing species abundance models. Ecological Modelling **199**:153-163.

R Development Core Team. 2011. R: A language and environment for statistical computing. R foundation for Statistical Computing, Vienna, Austria.

Rosenfeld, J. S., and S. Boss. 2001. Fitness consequences of habitat use for juvenile cutthroat trout: energetic costs and benefits in pools and riffles. Canadian Journal of Fisheries and Aquatic Sciences **58**:585-593.

Rosenfeld, J. S., E. Raeburn, P. C. Carrier, and R. Johnson. 2008. Effects of side channel structure on productivity of floodplain habitats for juvenile coho salmon. North American Journal of Fisheries Management **28**:1108-1119.

StreamNet Project. 2012. StreamNet Generalized Fish Distribution, Fall Chinook ftp://ftp.streamnet.org/pub/streamnet/gisdata/map_data_biological/StreamNet_FishDist_July2010.zip.

Thorson, J. T., M. D. Scheuerell, E. R. Buhle, and T. Copeland. 2014. Spatial variation buffers temporal fluctuations in early juvenile survival for an endangered Pacific salmon. Journal of Animal Ecology **83**:157-167.

Wissmar, R. C., and P. A. Bisson, editors. 2003. Strategies for restoring river ecosystems: sources of variability and uncertainty in natural and managed systems. American Fisheries Society, Bethesda, Maryland.

CHAPTER 2: HABITAT

2.c: Modeling juvenile Chinook production in 22 Columbia River stream locations

Martin Liermann (NOAA Fisheries, NWFSC, Seattle), Morgan H. Bond (Ocean Associates, contracted to NOAA Fisheries, NWFSC, Seattle)

Introduction

Understanding juvenile survival and capacity is important

Freshwater habitat condition is one of the factors affecting the recovery and maintenance of Chinook salmon populations in Columbia River (citation). Habitat restoration is therefore one of the tools being used in restoration efforts (Roni et al. 2002). While much work has been done to better understand the effects of habitat conditions on Chinook salmon freshwater population dynamics, this work has tended to occur in relatively small geographic areas (Cederholm et al. 1997, Roni et al. 2002), has focused on small scale habitat fish relationships and often focuses on a single point in time (e.g., summer density when data collection is feasible) (Roni and Quinn 2001). It is therefore difficult to know if these relationships are generalizable across broader regions, and if results demonstrated at small temporal and spatial scales, scale up to encompass the aggregate population dynamics as these fish grow, experience mortality and move though the freshwater habitat (Reeves et al. 1989).

Challenges of using data aggregated to the basin scale

However, there are also many challenges to using fish data that aggregates these factors over time and space (for example screw trap data or total estimated spawners). Due to resources necessary to collect this type of data and the fact that the number of basins declines with increasing scale, the sample size tends to be small limiting the number of fish habitat relationships that can be effectively explored. For example, Harrel (2015) recommends the number of predictor variables considered be limited to N/10 or less (where N is the sample size) when developing predictive models. Due to the complex suite of life history strategies that Chinook salmon exhibit, the habitat variables that are most important may vary from year to year and location to location. Further, a single metric of capacity that is comparable across regions may be difficult to achieve when alternative life histories predominate among watersheds or populations. Therefore, most capacity work focuses on a life stage that is common to most (e.g. summer parr) (Justice et al. 2017) or all populations (e.g. smolts, or smolt equivalents) (Walters et al. 2013). Finally, historic patterns of development have tended to correlate with habitat characteristics. For example, lower elevation reaches with broad floodplains are more likely to be developed than those that are higher elevation and confined (This report, Chapter 2.b). This confounds the relationship between factors that define a sites potential and land use making it difficult to disentangle the relative impacts of the two factors (Lucero et al. 2011).

Possible solutions

There are a number of approaches for dealing with situations where there are large numbers of potential predictor variables and a paucity of data (e.g. see chapter 4 of Harrell 2015). The set of potential predictor variables can be reduced before including the y variable by excluding variables based on expert knowledge and the correlation structure, or a small number of new composite variables can be constructed (e.g. Principle Components Analysis). Alternatively approaches such as LASSO regression, random forests, and model averaging include automated dimension reduction. Ultimately, without constraining the set of potential hypotheses though expert knowledge (assumptions), the results will almost certainly be vague, supporting many different potential mechanisms.

Our approach

Previous efforts to model whole watershed capacity from spawner-recruit data have focused on including watershed size as a covariate (Parken et al. 2006, Liermann et al. 2010) to allow predictions for areas without fish abundance estimates. Although watershed area is positively correlated with habitat area, other landscape and climactic features will mediate the amount and quality of habitat available for stream fishes within a watershed. Fortunately, stream network and landscape attributes have been developed for the entire Columbia River basin (Hall et al. 2007, Beechie and Imaki 2014) and can be aggregated at spatial scales that correspond with estimates of fish production. The habitat expansion approach has been used to estimate Chinook parr capacity by summing total estimates of main stem and side channel habitat area from habitat models, and applying capacity densities of fish to those areas (This report, Chapter 2.b). The habitat expansion capacity forms an index of habitat area weighted by the capacity of each habitat type for juvenile Chinook. For example, two watersheds with a similar watershed area may have different geomorphology and precipitation resulting in different useable habitat area and capacity despite their similar area. In this context, the habitat expansion based capacity may prove a more useful predictor of rearing capacity than watershed area. Here we use screw trap data from 22 basins across the Columbia River basin (CRB) to investigate the utility of using a habitat based metric of Chinook parr capacity (This report, Chapter 2.b) to explain patterns in juvenile production. Here, all of the potential habitat metrics have been condensed into this single metric of capacity before the modeling process. Instead of focusing on which components of the physical habitat are important we explore how this capacity metric performs and illustrate how the metric in combination with the fish data can be used to make predictions about juvenile population dynamics across the different basins. Through this modeling we can account for density dependence, incorporate different life-history strategies, and estimate aggregate survival over most of the freshwater residence.

Methods

Rotary screw trap data

We compiled annual abundance estimates of redds and offspring fall migrant parr (± SE) and spring smolts (± SE) from 22 sites throughout the CRB (Figure 1). These data were collected by ODFW, WDFW, IFG, the Nez Perce Tribe, Shoshone-Bannock Tribe and represent 435 trap-years of monitoring effort. All included juvenile abundance estimates were collected with rotary screw traps (Volkhardt et al. 2007). Abundance was estimated from raw catch data by correcting for changes in trap efficiency with a series of mark-and-recapture trials, where marked groups of fish were released above the traps and recaptured in the days following release. The trapping period was basin specific but depending on both the estimated timing of out-migration, and the feasibility of trap operation given the in-river conditions. Similarly, the years of trap operation varied among locations, but there is broad overlap in trap operation among sites from 1993-2014. Redd counts were estimated from extrapolation of foot or boat surveys in index reaches, or in some cases from a weir where total estimates of fish passing the weir were used to estimate redds

Study area

For each trap site, we used a habitat expansion approach to estimate summer parr rearing capacity (This report, Chapter 2.b) for all areas upstream of the trap that are considered accessible to and used for rearing by spring or summer run Chinook salmon via the StreamNet spatial database (StreamNet Data 2012, Figure 1.). For each 200 m segment of stream in the trapping region, we estimated the amount of side channel, bank, bar, and mid-channel habitat. Maximum rearing densities were applied to each habitat area, and were summed for all stream segments to produce an index of parr capacity for each trap region (This report, Chapter 2.b).

PIT tagging data for survival to dam

A subset of the fish captured at 20 of the traps were tagged using passive integrated transponder (PIT) tags (Prentice et al. 1990a, Prentice et al. 1990b). A subset of these fish were then detected at antenna arrays downstream at the first major dam with PIT tag detection in juvenile passage facilities (Axel et al. 2005). For approximately 76% of the years and traps, estimates of uncertainty were also available either as a standard error or confidence interval. To accommodate the observation component of our model we used these values along with the estimates to derive log-normal observation distributions. That is, we found log-normal parameters that came closest to explaining the estimate along with standard error or confidence interval. In cases where uncertainty was not describe for an estimate, we used the average estimated standard deviation from other years for that population. If no, estimates of uncertainty were available for a population we used the average estimate of standard deviation across all populations.

The statistical models

We constructed two separate models, a parr capacity model describing the population dyanmics from spanwer to migration past the screw traps and a trap to dam survival model which describes the survival of fish PIT tagged at the traps to the first major downstream dam.

Modeling juvenile out-migrants

Population dynamics from spawner to juvenile out-migrant is modeled using a state space model. This type of model includes a process model which describes the underlying population dynamics and an observation model which relates the observed data to the predictions made in the process model.

The process model

Parr are modeled as a function of spawners. Here we use the hockey stick model.

$$parrPred_{i,y} = f(spawners_{y,i}, prod_i, capacity_i) = min(prod_i spawners_{i,y}, capacity_i)$$

We then add process error to account for year to year variability in recruitment.

$$parr_{i,y} \sim lognormal(parrPred_{i,y}, parrSD_i)$$

Because we do not observe parr, $parr_{i,y}$ is a latent variable, or parameter, that the model estimates.

Population specific productivity and and capacity are modeled hierarchically. That is, they are allowed to be differ across population but are assumed to come from a common distribuiton.

$$log(prod_i) \sim normal(prodMu, prodSD)$$

For the capacity paramters, the population specific means are assumed to follow a log-log relationship with the habitat based capacity estimate (Bond et al. chapter 2 b), $capHab_i$,

$$log(capacity_i) \sim normal(capMu + capSlope * capHab_i, capSD)$$

Note that $capHab_i$ is centered so that the intercept of the relation is the mean, $capMu$.

The proportion of parr that migrate out of the basin before the winter is modeled as:

$$parrOut_{i,y} = parr_{i,y} pOut_{i,y}$$

where $pOut_{i,y}$ is modeled using the logistic normal distribution. Year and population specific temperatures $temp_{i,y}$ and population specific basin areas $capHab_i$ are included as predictor variables.

$$logit(pOut_{i,y}) \sim normal(pOutMuPop_i + pOutMuYr_y + tempSlope * temp_{i,y}, pOutSD)$$

$$pOutMuPop_i \sim normal(pOutMu + pOutSlope * capHab_i, pOutPopSD)$$

$$pOutMuYr_y \sim normal(0, pOutYrSD)$$

Finally, the fish that overwinter are subjected to a constant over winter mortality and then all the remaining fish are assumed to migrate out. And the number that migrate out the following spring is:

$$smoltOut_{i,y} = parr_{i,y}(1 - pOut_{i,y}) * winterSurv$$

Winter survival is assumed constant because productivity, pOut, and over winter survival cannot all be identified with spawner and trap data.

We also included simple models of temperature and spawners to allow for missing years. Spawners was modeled as:

$$log(spawners_{i,y})$$
$$\sim normal(spawnersMu + capHab_i + spawnersMuPop_i$$
$$+ spawnersMuYr_y, spawnersSD)$$

Where $spawnersMuPop_i$ and $spawnersMuYr_y$ are assumed to be normally distributed.

Temperature is modeled as:

$$temp_{i,y} \sim normal(tempMuPop_Effect_i + tempMuYr_y, tempSD)$$

Where $tempMuPop_i$ and $tempMuYr_y$ are assumed to be normally distributed.

Observation model

Observed out-migrants in the fall and spring are modeled using a log normal distribution.

$$log(parrOutObs_{i,y}) \sim normal(parrOut_{i,y}, parrOutObsSD_{i,y})$$

$$log(smoltOutObs_{i,y}) \sim normal(smoltOut_{i,y}, smoltOutObsSD_{i,y})$$

Notice that $parrOutObsSD_{i,y}$ and $smoltOutObsSD_{i,y}$ are assumed known (not estimated by the model).

Observed spawners are also modeled using the log normal distribution, where the standard deviation is fixed at 0.15.

$$log(spawnersObs_{i,y}) \sim normal(spawners_{i,y}, spawnersObsSD)$$

Temperature is assumed to be measured with negligible observation error so an observation error model is not included.

Modeling Survival from trap to dam

Parr and smolt survival from the traps to the first dam encountered was estimated by PIT tagging fish captured in the traps. We treated the survival estimates along with standard errors or confidence intervals as data and modeled the underlying survival process using logistic normal distributions.

Process model

Predicted survival of parr and smolt to the dams included grand means as well as population and year effects.

$$logit(parrSurv_{i,y}) \sim normal(parrMu + parrMuPop_i + parrMuYr_y, parrSD)$$

$$logit(smoltSurv_{i,y}) \sim normal(smoltMu + smoltMuPop_i + smoltMuYr_y, smoltSD)$$

The population effects $parrMuPop_i$ and $smoltMuPop_i$ were modeled hierarchically and assumed to follow normal distributions.

$$parrMuPop_i \sim normal(0, parrMuPopSD)$$

$$smoltMuPop_i \sim normal(0, smoltMuPopSD)$$

The year effects were modeled as centered random walks.

$$parrMuYrRW_y \sim normal(parrMuYrRW_{y-1}, parrMuYrSD)$$

$$parrMuYr = parrMuYrRW/mean(parrMuYrRW)$$

$$smoltMuYrRW_y \sim normal(smoltMuYrRW_{y-1}, smoltMuYrSD)$$

$$smoltMuYr = smoltMuYrRW/mean(smoltMuYrRW)$$

Observation model

observation error in the logit survivals is assumed to follow a normal distribution.

$$logit(parrSurvObs_{i,y}) \sim normal(logit(parrSurv_{i,y}), parrSurvSD_{i,y})$$

$$logit(smoltSurvObs_{i,y}) \sim normal(logit(smoltSurv_{i,y}), smoltSurvSD_{i,y})$$

Results

Predicting parr and smolt out-migrants

The parr habitat capacity index (This report, Chapter 2.b) explained about half of the variability in estimated capacity (posterior median = 0.49, 95% CI = 0.12-0.69) (Figure 2, left panel). The posterior median for the slope of the relationship is 0.73 with very high probability that the slope is positive (Figure 3, upper panel). When the slope is less than one, the relationship is non-linear with less predicted capacity per unit of habitat index as the habitat unit index increases. However, the posterior does no exclude the possibility that the slope is 1. To further explore this possibility we also fit the model with the slope fixed to one (figure 2, panel 3). In this case the model appeared to fit comparably with slightly over 50% of the variability explained (posterior median = 0.55, 95% CI = 0.17-0.72). Notice that capacity is also estimated, so these values are not comparable in the same way as a standard regression. When the slope is fixed at one the relationship is simply capacity=a×capHab$_i$. The posterior median for a was, 0.113 (95% CI = 0.003-0.187). The parr habitat index was better at explaining patterns in estimated parr capacity than basin area (figure 2, panels 1 and 2). Basin area explained about 1/5th of the variability (posterior median = 0.21 95% CI = -0.18 0.53). Individual fits of the model to the relationship between spawners and smolt out-migrants varied across populations (figure 4). For some populations the capacity was relatively constrained by the data while for other locations estimates of capacity was very uncertain.

The estimated proportion of parr that left the basin in the fall, pOut varied between populations, ranging from less than 5% for the Methow River to close to 75% for Marsh Creek (figure 5, panel 1). The parr habitat index explained about 40% of this variability, with larger basins tending to have fewer fall out-migrants. The results were comparable with or without setting the slope between capacity and the parr habitat index to 1 (figure 5, panel 3). However, basin area explained less than 15% of the variability in pOut (figure 5, panel 2). There was a slight negative relationship between year and basin specific summer temperature and pOut (figure 3, bottom panel). That is, basins with colder temperatures were predicted to have more fall out-migrants.

Predicting survival

Trap to dam survival was not consistently available across traps and years (figures 6 and 7). However, there were apparent patterns across year and site. Average survival of parr from the trap to the first dam tended to range from 20% to 40%, while smolt to dam survival tended to fall between 40% and 70%. There were common temporal patterns in trap to dam survival across the populations especially for parr (see the year factor panel in figures 6 and 7). The ratio of parr survival to smolt survival may serve as a very approximate estimate of over-winter survival (figure 8). This also varied across population and years but tended to average around 50%.

Discussion

The parr habitat index proved useful in explaining between basin differences in estimated capacity. The parr habitat index performed substanially better than basin area, explaining more than twice as much of the variability in estimated capacity. While the posterior distribution for the slope parameter in the log-log relationship was centered below one (median = 0.79), a value of one was plausible which would simplify the relationship to $capacity = a \times capHab_i$ where $a = 0.11$ (posterior median). While the parr habitat index was based on observed densities of fish, there are a number of reasons this value may be less than 1. For example, we define parr as the number of parr immediately before out-migration in the fall. Parr densities, on the other hand, are often measured earlier in the summer. In addition, the densities used in the habitat index were based on work in the Skagit River, much of which is in relatively good condition and differs substantially from the east side basins in the study. Other possible explanations include hatchery effects, clumpy distributions of spawners creating small scale density dependence (Walters et al. 2013). This relationship between capacity and the parr habitat index can be used to predict juvenile production in other basins without smolt traps. Since the index can also be calculated based on a hypothetical restored basin, where human impacts are removed, restoration effect sizes can be expressed in terms of predicted increases in parr capacity (or juvenile production at full seeding).

The proportion of parr that migrated out of the basin in fall tended to be higher for basins with smaller parr habitat indices. There are a number of plausible explanations for this pattern. If fish tend to move a fixed distance downstream, then a higher proportion will tend to leave a smaller basin. Smaller basins will also be less likely to have larger substrate that has been shown to be a preferred over-winter habitat for juvenile chinook. Smaller basins tend to be at higher elevation and colder in the winter, providing another potential mechanism. We added temperature to our model of $pOut$ but the temperatures that were available were summer temperatures, which may not correlate well with winter temperatures. In addition, because basin size and temperature are correlated, this will make estimating the two coefficients difficult. We found some weak evidence for a positive effect of temperature on $pOut$ but this is an area that will need additional work. Predicting the proportion of fish that leave at different life history stages provides information to managers on the degree to which over-winter habitat is important. Predictions can also be used to identify populations with anomalous migration patterns which may indicate restoration potential. Because $pOut$ is linked to the parr habitat index and temperature, estimates of $pOut$ can be made for populations without fish data.

To estimate the effective freshwater productivity of individual basins requires estimates of survival during the remainder of freshwater residence. The differences in trap to dam survival between populations for both parr and smolt migrants suggests that the larger geographic context is important. Next steps in this research include integrating the basin specific spawner to parr productivies with $pOut$, trap to dam survivals and dam to Bonneville survivals to construct basin specific estimates of productivity that integrate over the entire period of juvenile freshwater residence. This can then be used to help prioritize basins for restoration. Those basins that appear to be limited by capacity and not productivity (due to lower downstream survival) would tend to be better candidates for parr habitat restoration.

Acknowledgements

A project of this scope could not have been completed without the efforts of the agencies, tribes and countless individuals that have operated screw trap to enumerate juvenile salmonids throughout the CRB. In particular, we would like to thank: IDFG; Tim Copeland and Bruce

Barnett, WDFW; Jeremy Cram, Andrew Murdock, David Grundy, Michael Gallinat, Alex Repp, ODFW; Rich Carmichael, Brian Jonasson, Ian Tattam, Robert Reagan, Josh Hanson, Tim Hoffnagle, USFWS; Tom Desgroseillier, Nez Perce Tribe; Devin Olsen, Shoshone Bannock Tribes, BioAnalysts, Inc; Tracy Hillman. In addition, we received helpful advice and comments from NWFSC scientists: Damon Holzer, Tom Cooney, Jim Myers, Jeff Jorgensen, Michael Beakes, Corey Phillis, Kevin See. This work was funded in part from BPA: 1989-098-00, 1997-015-01.

References

Axel, G. A., E. F. Prentice, and B. P. Sandford. 2005. PIT-tag detection system for large-diameter juvenile fish bypass pipes at Columbia River basin hydroelectric dams. North American Journal of Fisheries Management 25:646-651.

Beechie, T., and H. Imaki. 2014. Predicting natural channel patterns based on landscape and geomorphic controls in the Columbia River basin, USA. Water Resources Research 50:39-57.

Cederholm, C. J., R. E. Bilby, P. A. Bisson, T. W. Bumstead, B. R. Fransen, W. J. Scarlett, and J. W. Ward. 1997. Response of juvenile coho salmon and steelhead to placement of large woody debris in a coastal Washington stream. North American Journal of Fisheries Management [N. AM. J. FISH. MANAGE.]. Vol. 17:no. 4.

Data, S. G. 2012. PNW Spring chinook salmon distribution referenced to StreamNet's hydrography (MSHv3.1). URL: http://www.streamnet.org/data/interactive-maps-and-gis-data.

Hall, J. E., D. M. Holzer, and T. J. Beechie. 2007. Predicting river floodplain and lateral channel migration for salmon habitat conservation. Journal of the American Water Resources Association 43:786-797.

Harrell, F. 2015. Regression modeling strategies: With applications to linear models, logistic and ordinal regression, and survival analysis. Springer.

Justice, C., S. M. White, D. A. McCullough, D. S. Graves, and M. R. Blanchard. 2017. Can stream and riparian restoration offset climate change impacts to salmon populations? Journal of Environmental Management 188:212-227.

Liermann, M. C., R. Sharma, and C. K. Parken. 2010. Using accessible watershed size to predict management parameters for Chinook salmon, Oncorhynchus tshawytscha, populations with little or no spawner-recruit data: a Bayesian hierarchical modelling approach. Fisheries Management and Ecology 17:40-51.

Lucero, Y., E. A. Steel, K. M. Burnett, and K. Christiansen. 2011. Untangling human development and natural gradients: Implications of underlying correlation structure for linking landscapes and riverine ecosystems. River Systems 19(3):207–224.

Parken, C., R. McNicol, and J. Irvine. 2006. Habitat-based methods to estimate escapement goals for data limited Chinook salmon stocks in British Columbia, 2004 Nanaimo, British Columbia.

Prentice, E. F., T. A. Flagg, and C. S. McCutcheon. 1990a. Feasibility of using implantable passive integrated transponder (PIT) tags in salmonids. Pages 317-322 in N. C. Parker, A. E. Giorgi, R. C. Heidinger, J. Jester, D. B., E. D. Prince, and G. A. Winans, editors. American Fisheries Society Symposium, Bethesda, Maryland.

Prentice, E. F., T. A. Flagg, C. S. McCutcheon, and D. F. Brastow. 1990b. PIT-tag monitoring systems for hydroelectric dams and fish hatcheries. Pages 323-334 in N. C. Parker, A. E. Giorgi, R. C. Heidinger, J. Jester, D. B., E. D. Prince, and G. A. Winans, editors. American Fisheries Society Symposium, Bethesda, Maryland.

Reeves, G. H., F. H. Everest, and T. E. Nickelson. 1989. Identification of physical habitats limiting the production of coho salmon in western Oregon and Washington. U.S. Forest Service General Technical Report PNW-245.

Roni, P., T. J. Beechie, R. E. Bilby, F. E. Leonetti, M. M. Pollock, and G. R. Pess. 2002. A review of stream restoration techniques and a hierarchical strategy for prioritizing restoration in Pacific northwest watersheds. North American Journal of Fisheries Management 22:1-20.

Roni, P., and T. P. Quinn. 2001. Effects of wood placement on movements of trout and juvenile coho salmon in natural and artificial stream channels. Transactions of the American Fisheries Society 130:675-685.

Volkhardt, G. C., S. L. Johnson, B. A. Miller, T. E. Nickelson, and D. E. Seiler. 2007. Rotary screw traps and inclined plane screen traps:235–266. American Fisheries Society, Bethesda, Maryland.

Walters, A. W., T. Copeland, and D. A. Venditti. 2013. The density dilemma: limitations on juvenile production in threatened salmon populations. Ecology of Freshwater Fish 22:508-519.

Figures

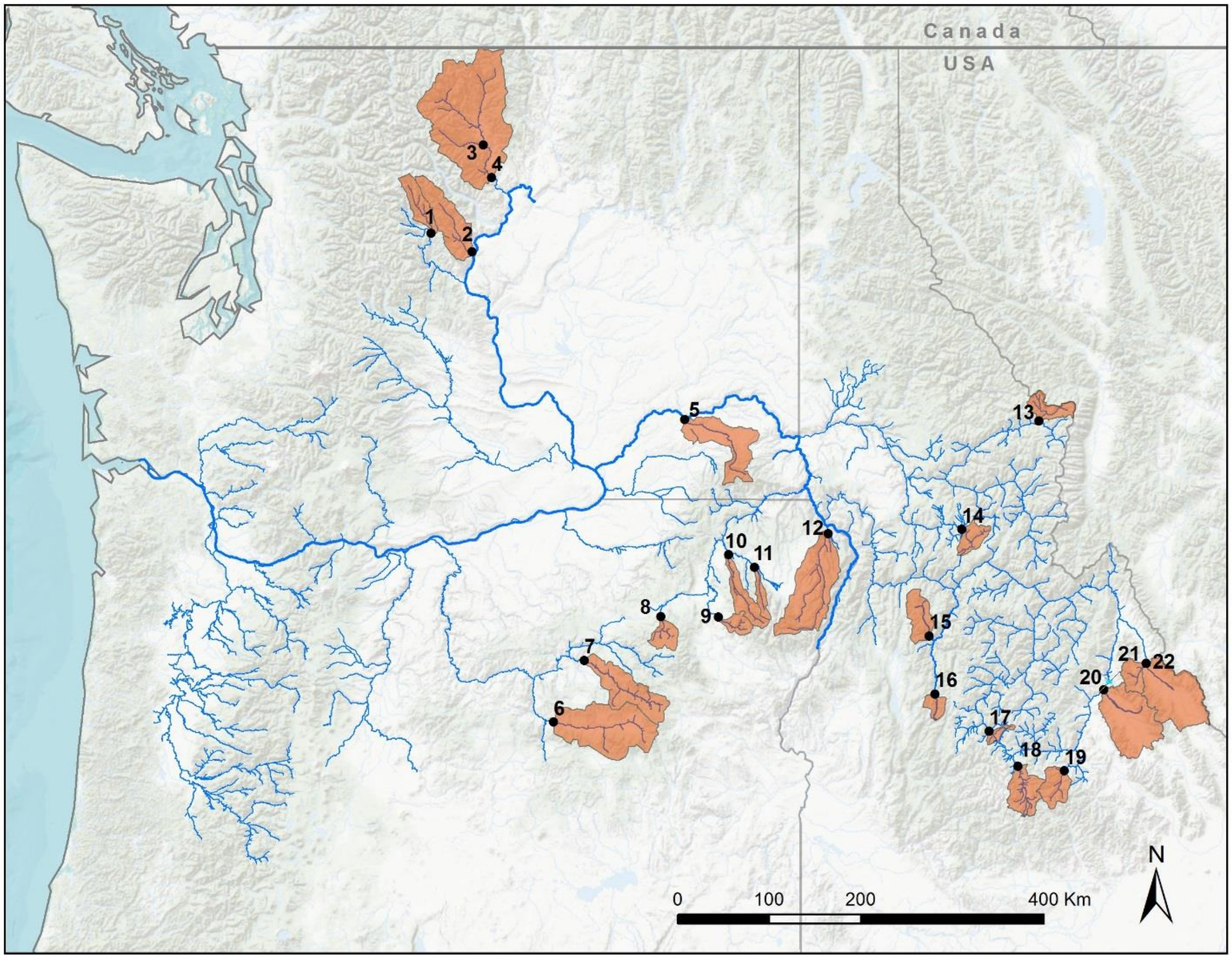

Figure 1. Included locations in the CRB with rotary screw trap (points) abundance data for spring-run Chinook fall migrant parr and spring smolts. Orange regions indicate the watershed area upstream of the trap that was included in habitat expansion estimates of summer parr capacity. 1. Chiwawa River, 2. Entiat R., 3. Twisp R., 4. Methow R., 5. Toucannon R., 6. Upper mainstem John Day R., 7. Middle Fork John Day R., 8. Upper Grande Ronde R., 9. Catherine Creek, 10. Minam R., 11. Lostine R., 12. Imnaha R., 13. Crooked Fork Creek, 14. Red R., 15. Secesh R., 16. South Fork Salmon R., 17. Mash Creek, 18. Upper Salmon R., 19. East Fork Salmon R., 20. Pahsimeroi R., 21. Hayden Creek, 22. Upper Lemhi R.

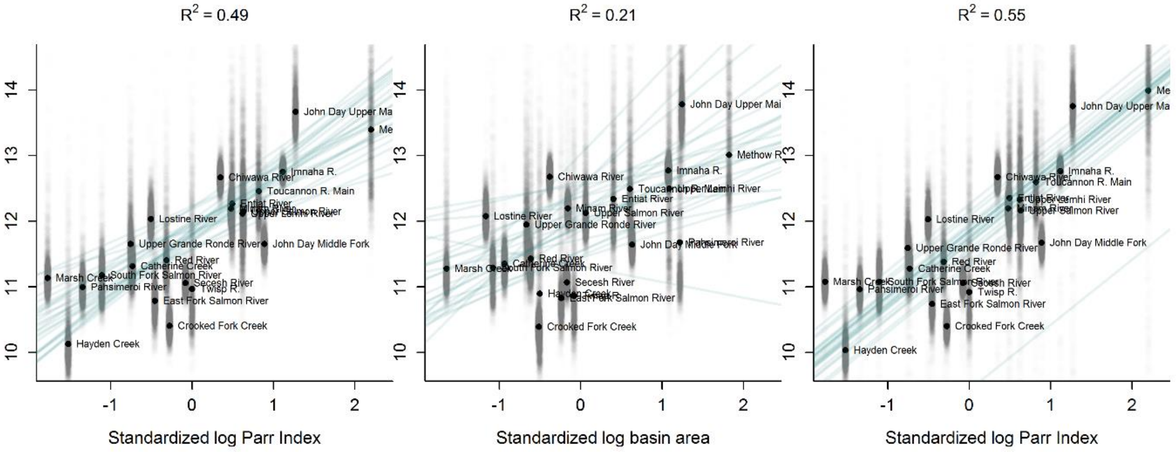

Figure 2. The relationship between metrics of habitat capacity (x-axis) and model estimated capacity (y-axis). The left panel represents the base model run where a log-log relationship is assumed between the parr habitat index and estimated capacity. In the middle panel, the same model is run, but log basin area is substituted for the parr index. In the right panel, the base model is run, but the slope is constrained to be 1.

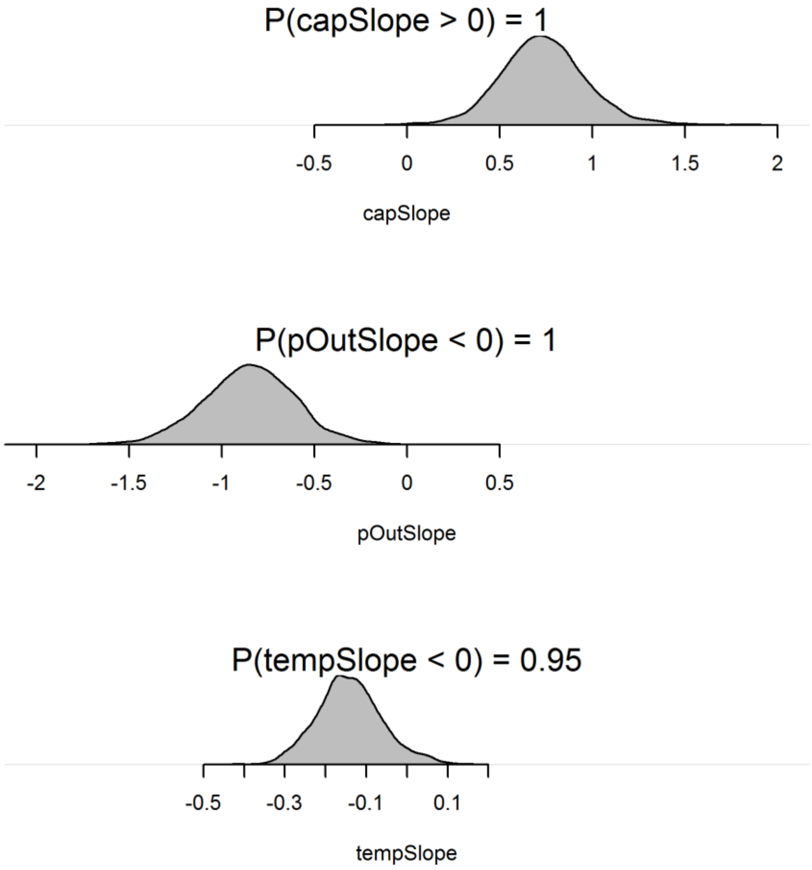

Figure 3. The posterior distributions for the slopes between estimated capacity and the parr habitat index (upper panel), pOut and the parr capacity index, and pOut and summer temperature. The probability that the values are above or below zero is included above each plot. The three densities are plotted such that the magnitudes are relative to the standard deviation of the x-variable. This means that magnitude (distance above or below 0) is a rough metric of parameter importance.

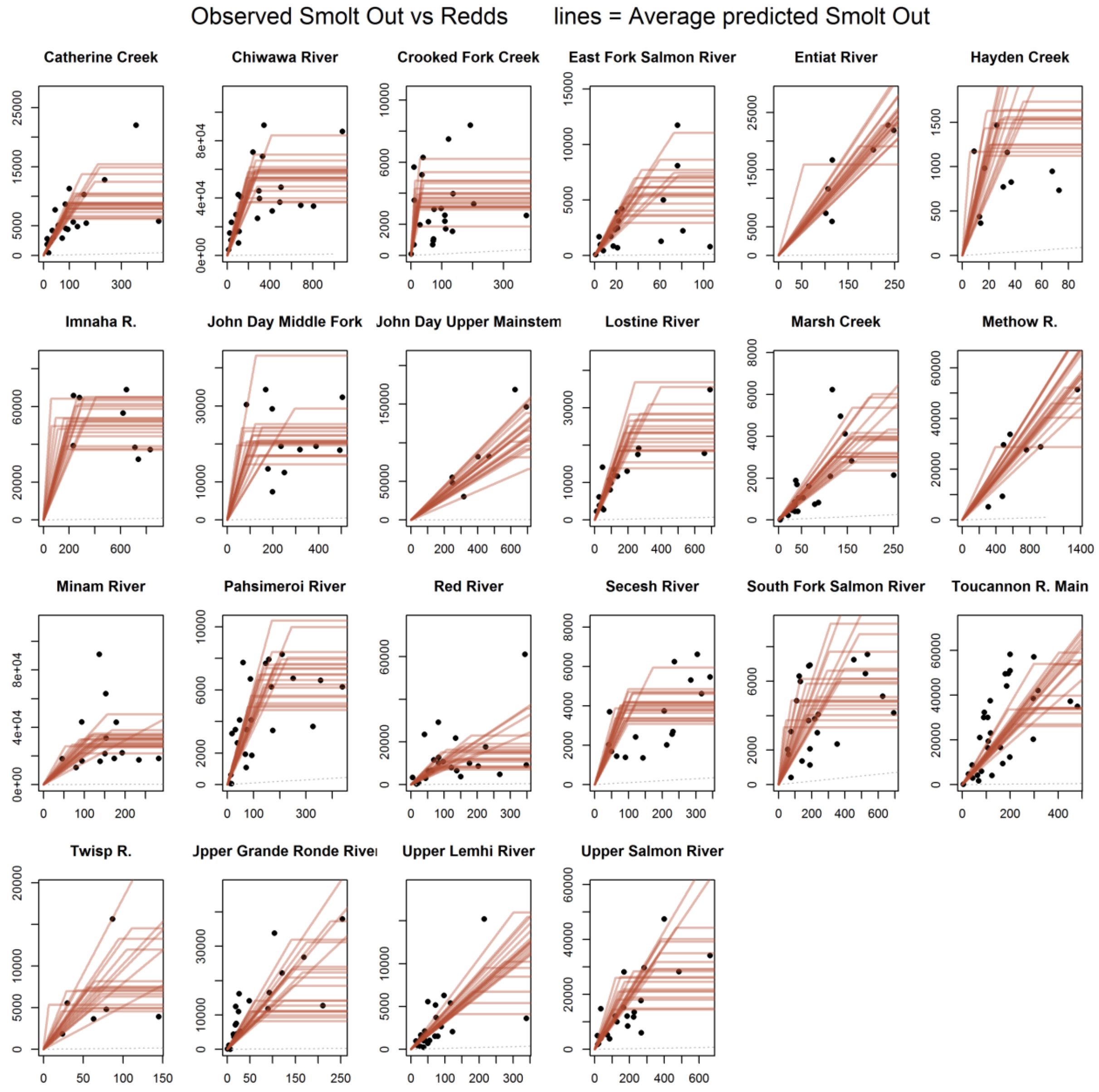

Figure 4. Spawners (x-axis) plotted against smolt out-migrants (y-axis). The red lines represent plausible relationships based on 20 random draws from the posterior distribution.

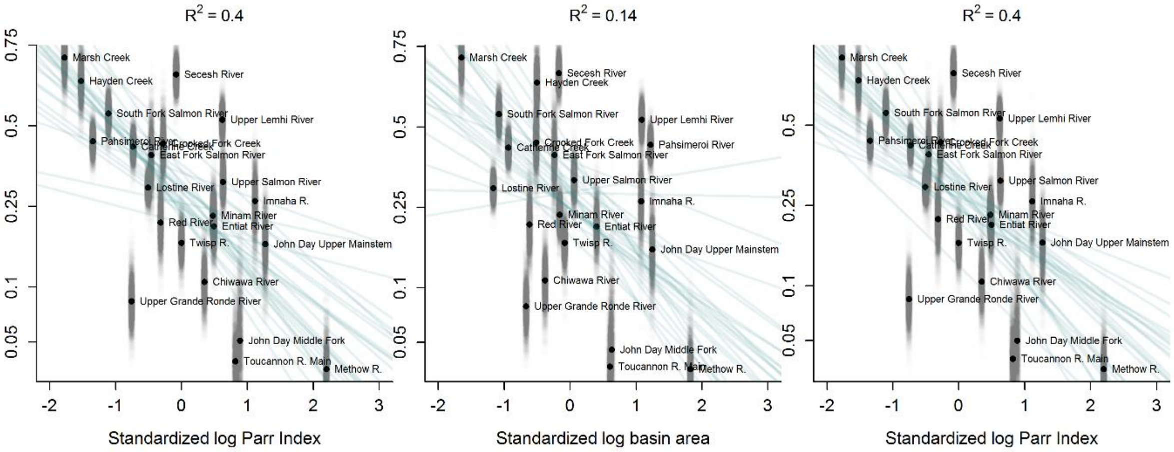

Figure 5. The relationship between metrics of habitat capacity (x-axis) and model proportion of parr that migrate out of the basin in the fall, pOut, (y-axis). The left panel represents the base model run where a log-log relationship is assumed between the parr habitat index and estimated pOut. In the middle panel, the same model is run, but log basin area is substituted for the parr index. In the right panel, the base model is run, but the relationship between the parr habitat index and estimated capacity is assumed to have a slope of 1.

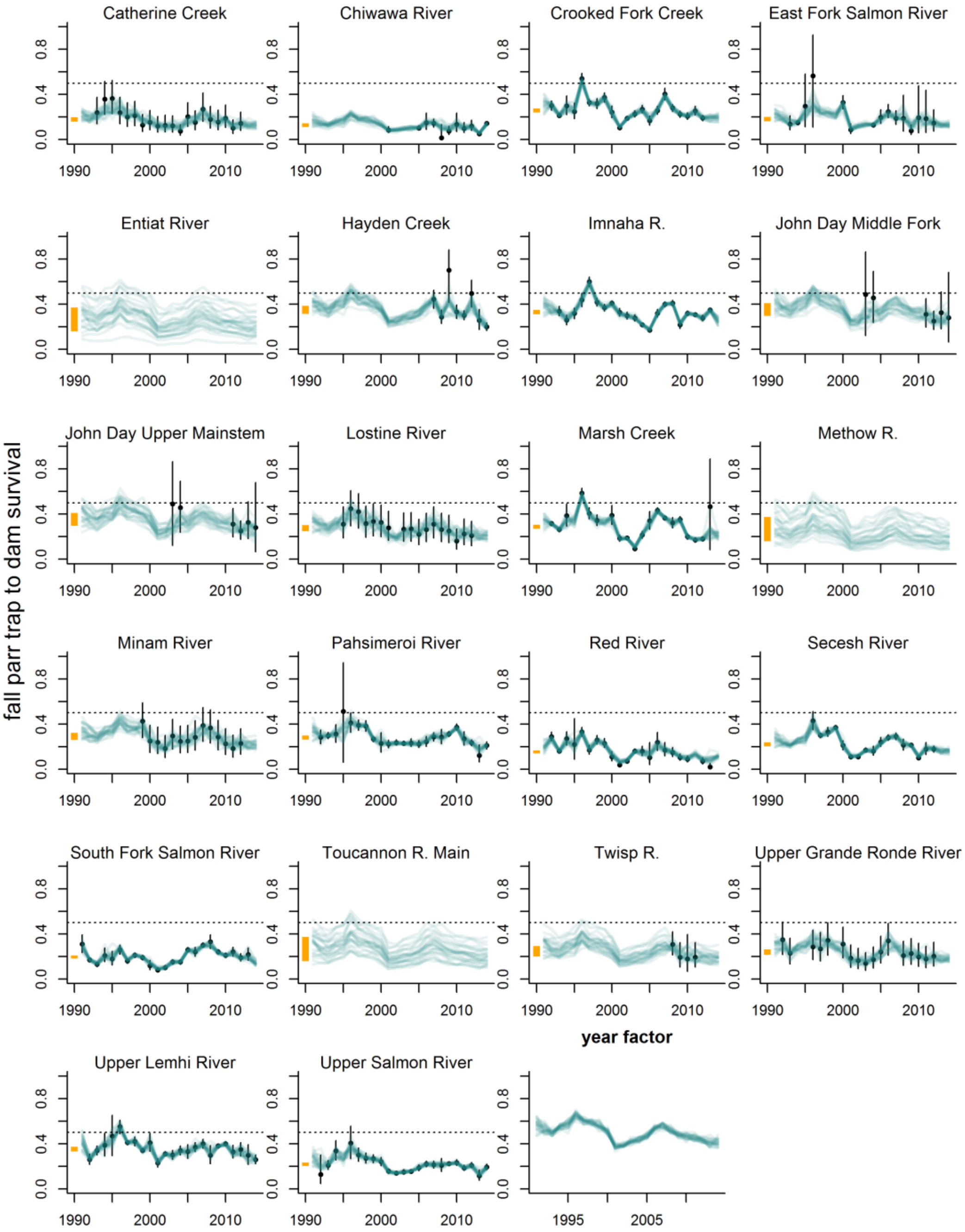

Figure 6. Parr survival from the smolt trap to the first downstream dam based on PIT tags. The points represent the estimate, the vertical black bars are 80% confidence intervals, and the green bars are plausible year and basin specific model fits based on 20 random samples from the posterior distribution. The vertical orange bars represent the 80% credible interval for population specific average survival.

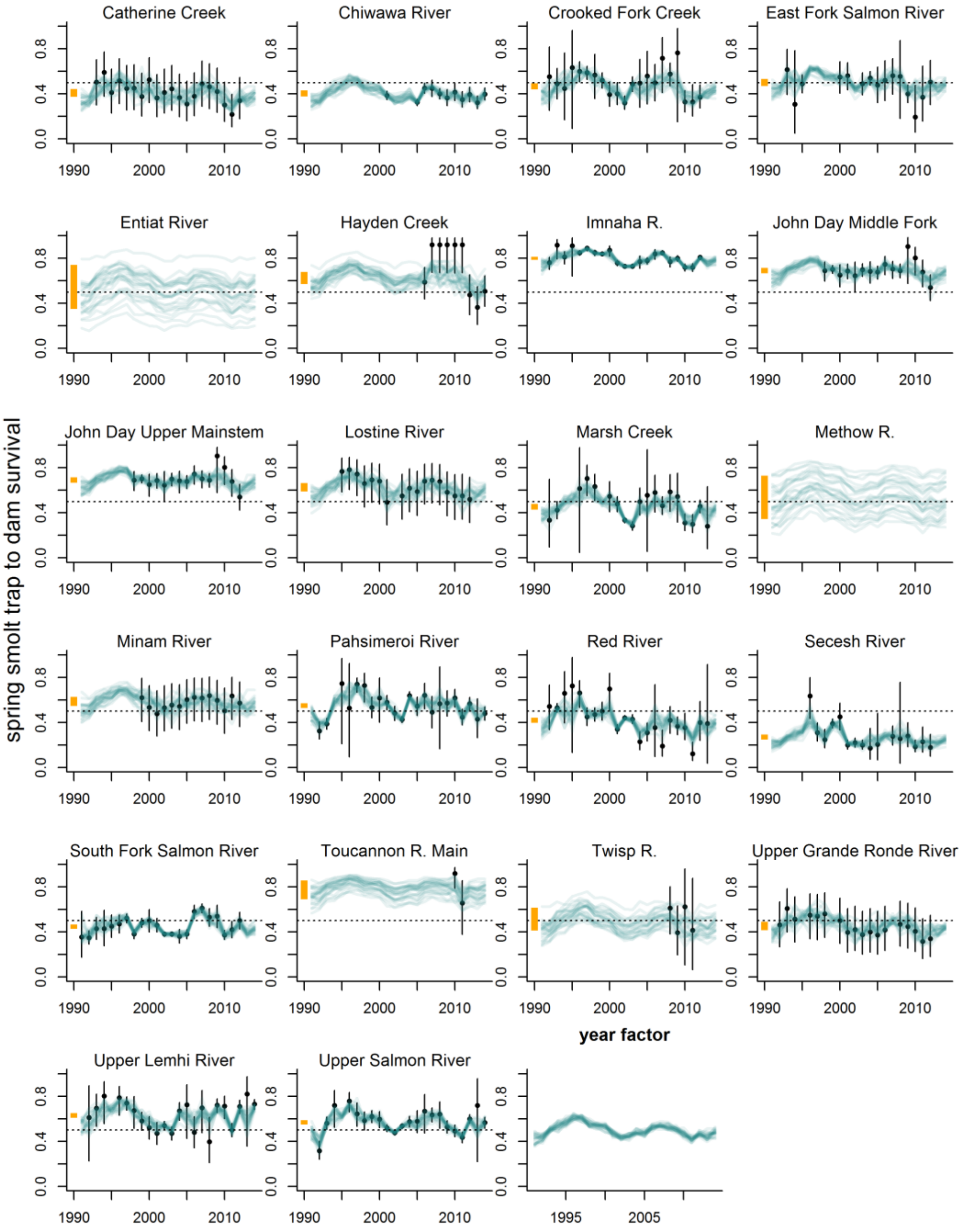

Figure 7. Smolt survival from the smolt trap to the first downstream dam based on PIT tags. The points represent the estimate, the vertical black bars are 80% confidence intervals, and the green bars are plausible year and basin specific model fits based on 20 random samples from the posterior distribution. The vertical orange bars represent the 80% credible interval for population specific average survival.

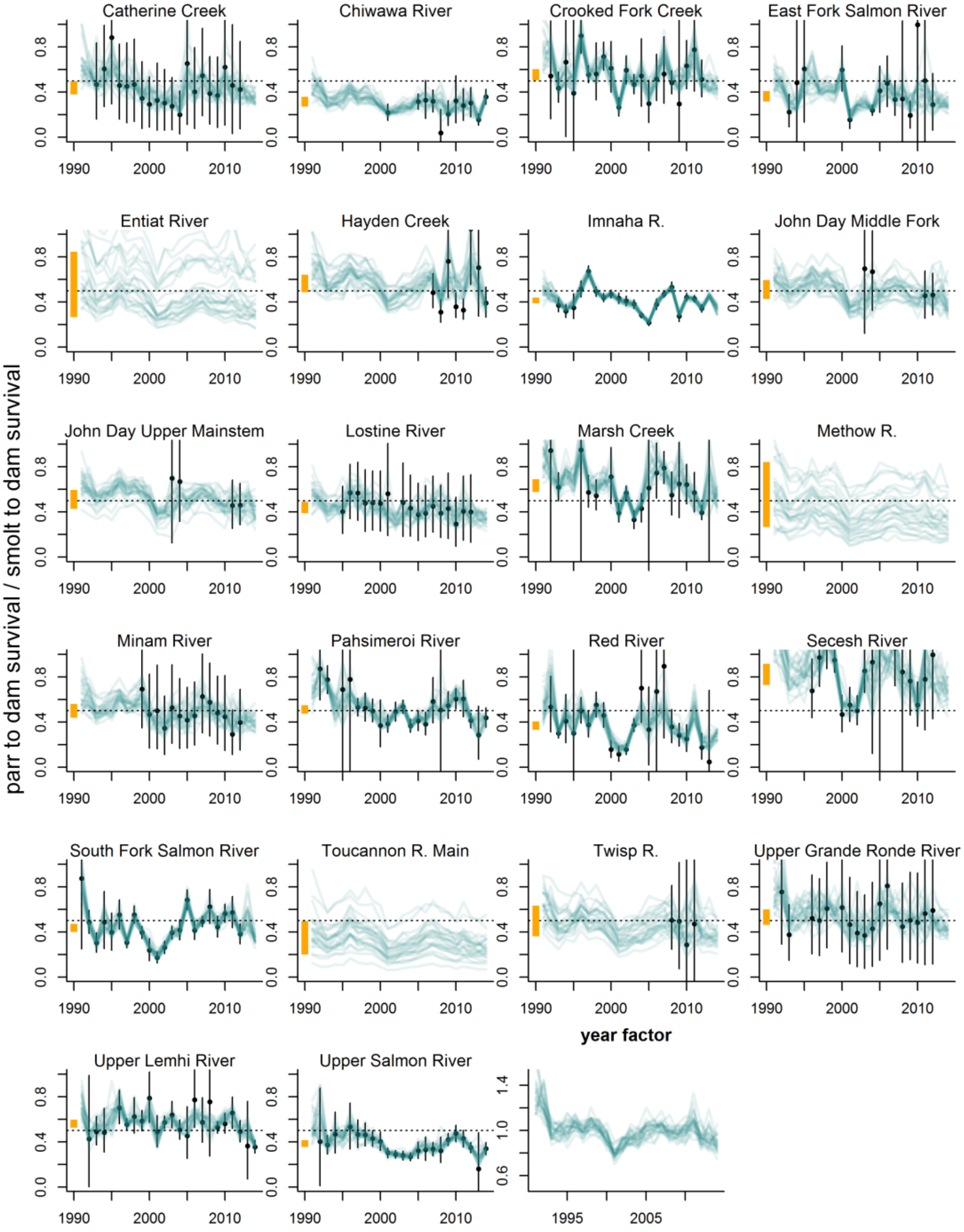

Figure 8. The ration of parr survival to smolt survival from the smolt trap to the first downstream dam based on PIT tags. The points represent the estimate, the vertical black bars are 80% confidence intervals, and the green bars are plausible year and basin specific model fits based on 20 random samples from the posterior distribution. The vertical orange bars represent the 80% credible interval for population specific average survival.

CHAPTER 2: HABITAT

2.d Movement & Survival based on Mark-Recapture data

W. Carl Saunders (Department of Watershed Sciences, and Eco Logical Research), Kevin See (QCI), Shubha Pandit (Terraqua), Eric Buhle (QCI), Nicolaas Bouwes (Eco Logical Research), Pamela Nelle (Terraqua), Tom Degroseiller (USFWS), Keith VanDenBroek (Terraqua), Chris Jordan (NOAA-NMFS-NWFSC)

Introduction

Despite a rich history of life-cycle model (LCM) applications to salmon recovery-related questions (see Good et al. 2007 for a recent review), previous attempts to link habitat restoration scenarios impacting freshwater life stages with future population performance have met with limited success. For example, studies have modelled population responses to hypothetical survival increases assumed to be achievable through habitat restoration, but without explicit consideration of current conditions or restoration feasibility (e.g., Kareiva et al. 2000). More recent assessments have integrated habitat–survival relationships and basin-specific habitat condition into modelling (e.g., McHugh et al. 2004, Scheuerell et al. 2006, Honea et al. 2009), assessed restoration potential based on relationships between watershed condition and in-stream habitat metrics (e.g., Sharma et al. 2005, Bartz et al. 2006, Jorgensen et al. 2009), or increased the spatial resolution of LCMs (Scheuerell et al. 2006). However, parameterization of freshwater productivity parameters for the majority of density-dependent LCM applications are derived from stage-specific abundance data (e.g., out migrating smolts and adult returns or redd counts), which fail to differentiate among juvenile life stages, lack the spatial resolution necessary to inform most restoration actions, and often require relatively large data sets for accurate parameter estimation. While the realism of LCMs has thus improved greatly, these tools continue to inform restoration practice at a coarse level and in the absence of mechanistic insight on fish–habitat associations.

Although restoration comes in many forms, the general goal of most projects is to increase the quality or quantity of habitats that are believed to limit particular life stages and overall population abundance (Barnas et al. 2015). Accordingly, there is a need for modelling approaches that can accurately depict complex life histories and simultaneously maximize the realism of species–environment relationships for life stages targeted by management and restoration. To assess the long-term population-level benefits of specific restoration alternatives using a life-cycle modelling approach, candidate restoration projects must be translated into an expected fish response (Honea et al. 2009). While it has proven difficult to estimate the impacts of habitat restoration on tradition measures of productivity (i.e., smolts per spawner) used for LCM applications, advances in fish marking and resighting technology have led to a significant increase in the number of fish that can be marked and an increased ability to estimate population parameters, such as life-stage specific survival (Skalski et al. 1998, Al-Chokhachy et al. 2009). This is particularly evident in the Columbia River basin, where over 35 million Pacific salmon *Oncorhynchus spp*. and steelhead *O. mykiss* were tagged with PIT tags between 1987 and 2016.

Mark-recapture data provide an alternative means to estimate stage-specific probabilities of survival and movement of juvenile salmonids, which can be collected at the reach scale and over moderate timescales. For example, the Cormack-Jolly-Seber (CJS, Cormack 1964) model has been used to provide estimates of apparent survival for smolts traveling throughout the mainstem Columbia River. However, unlike in the mainstem Columbia River where fish behavior is relatively consistent (all fish are moving in one direction over a relatively short period), the complex life histories and long periods of juvenile rearing in tributary habitats results in biased estimates of survival from the CJS model (Barbour et al. 2013, Conner et al. 2015). To account for complex life histories, high rates of movement among rearing habitats, and use of diverse resighting technologies (i.e., physical capture methods as well as mobile and passive data collection from PIT tags), managers and researchers have used the Barker Model (Horton and Letcher 2008, Conner et al. 2015) and the Multi-State Model (Horton et al. 2011) to analyze mark-recapture data. Thus, approaches that integrate LCMs with the ability to estimate survival and movement probability directly from fish tagging data at spatial scale at which restoration is often implemented, may provide an effective means to prioritize among potential restoration actions.

Our objectives are to demonstrate how mark-recapture data can be used to 1) estimate time and stage-specific survival for juvenile anadromous salmonids, 2) estimate movement probabilities among the spatially linked sub-populations, and 3) describe relationships between these demographic rates and habitat quality.

In this chapter, we

1) Outline how mark-recapture data can be integrating into LCMs to inform habitat restoration planning,
2) Provide examples of how estimates of survival and movement probabilities can be used to increase the realism of LCM applications, and
3) Outline approaches to account for density-dependence in survival and movement probabilities.

However, we do not attempt provide a census of mark-recapture sampling or analysis across the Columbia River Basin, but rather outline how tagging data can be used to address restoration applications and identify critical uncertainties regarding the estimation of demographic rates and their integration into LCMs.

Linking population demographics to fish habitats

The estimation of capacity and productivity parameters from population-scale abundance data limits the potential to develop mechanistic means to model the outcome of restoration actions or correctly account for the extent and spatial location of restoration actions. While indexes of adult abundance can be obtained for varying spatial extents through redd surveys, estimates of smolt abundance are often limited to the watershed scale owing to logistical constraints of operating small traps. Therefore, empirical estimates of productivity (i.e., smolts per spawner) derived from these data integrate the entire range of habitat conditions present within a watershed, but cannot be explicitly linked to habitat quality at any given location within the watershed. In contrast, Mark-recapture data on individually tagged fish can be used to estimate reach specific survival estimates as well as the probability of individual fish moving between sampled reaches, depending on sampling intensities. Furthermore, both environmental (e.g., metrics of habitat quality) and individual covariates (e.g., fish size or age) can be used to model specific linkages between demographic rates and habitat quality. For example, Bouwes et al. (2016) estimated that survival of juvenile steelhead (*O. mykiss)* in stream reaches where restoration was conducted to encourage beaver dam development and increase retention of these dams increased by 52%, relative to stream reaches characterized by entrenched channels. Similarly, Letcher and Horton (2008) demonstrated the mark-recapture data can be used to estimate size-dependent, seasonal survival rates for Atlantic salmon *(Salmo salar)*. Thus, by collecting data at the scale of stream reaches, mark-recapture data can be used to explicitly link demographic rates for juvenile salmonids to habitat conditions the spatial scale that is consistent with that at which restoration actions are often implemented.

However, owing to differences in the way mark-recapture data are collected, there is not a single approach to estimate demographic rates. Nor is there a single approach by which to integrate these estimates into LCM applications. A common approach to collecting mark-recapture data on juvenile anadromous salmonids in tributary habitats is to conduct seasonal, or annual, sampling to physically collect fish (typically over a relatively short period of time), where any previously unobserved individuals are tagged and those previously captured are noted as recaptured individuals. This type of sampling yields discrete mark-recapture data, and can be analyzed under a wide variety of model frameworks (e.g., CJS, Barker, Multistate). In contrast, many watersheds throughout the Columbia River basin are equipped with passive antenna arrays to detect fish previously implanted with PIT tags. In such systems, individuals can be detected at any time they swim over and antenna array and detections typically are not constrained to short "sampling" periods. This type of data are considered continuous, and can only be jointly analyzed with discrete data using a limited number of model frameworks (i.e., the Barker model).

Barker Model applications (juvenile survival example)

In constructing lifecycle model for steelhead in the Middle Fork of the John Day River, we sought to assess the potential benefits of two commonly pursued restoration approaches; one that aims to enhance rearing capacity and survival for juveniles by providing cooler summer temperatures, and another that aims to increase juvenile carrying capacity through increased structural/hydraulic complexity of select reaches (McHugh et al. 2017). The LCM itself is a basin- and species-specific (i.e., steelhead) adaptation of the model of Sharma et al. (2005), a stage-structured, stochastic salmonid population model (Chapter 9d). This LCM propagates steelhead cohorts through their life history according to a sequence of density-dependent Beverton-Holt 'spawner' (Ni) and 'recruit' (Ni+1) relationships (Beverton and Holt 1957, Moussalli and Hilborn 1986), with stage-specific capacity (ci) and productivity (pi, maximum recruits per spawner) parameters determining realized survival across life stage transitions. To parameterize this lifecycle model we estimated stage specific survival probabilities for juvenile steelhead from mark-recapture data collected from both physical fish collections as well as continuous fish detections at passive PIT tag arrays, and then determined the productivity (pi) parameters that corresponded to these values to produce the time series of realized survival estimates similar to those estimated from mark-recapture data (see below).

To jointly analyze the discrete and continuous mark-recapture data, we used the Barker model (Barker 1997, Barker and White 1999), which results more precise and typically less bias estimates of survival than the CJS model (Conner et al. 2015). We used data from approximately 7000 individually tagged juvenile steelhead, sampled during 2007-2013. We estimated survival separately for fish 60-100 mm total length (TL, age-0 parr) and fish greater than 100 mm TL (age-1 to age-3 pre-smolts, Figure 5.a.1) (see McHugh et al. 2017 for complete description of model parameterization). In ongoing work, survival of age-0 parr is also being modeled as a function of fish length at the time of initial tagging (Figure 5.a.2). The stage-specific parameterization of the LCM for the Middle Fork John Day hottest to specifically evaluate the potential impacts of habitat restoration actions targeting water temperature reduction (e.g., vegetation plantings additional water allocation) as well as construction of large Woody structures in tributary and mainstem habitats (results summarized in Chapter 9.d, see McHugh et al. 2017 for details). Further, in ongoing work the incorporation of size specific survival for age-0 parr allows us to model survival throughout the watershed is a function of water temperature and prey availability using a bioenergetics model (Hanson et al. 1997, Hartman and Kitchell 2008).

To parameterize the LCM for the Middle Fork John Day, we pooled mark-recapture data across the watershed. However, one of the strengths of using mark-recapture data is that one can obtain reach-specific estimates of survival model sub-populations with different survival rates resulting from variation in habitat quality throughout a watershed or to account for different management actions. For example, development of a LCM for spring Chinook (*O. tshawytscha*) in the Entiat River watershed is focused on modeling sub-populations in five geomorphically distinct reaches of the watershed (Figure 5.a.3). We PIT-tag juvenile Chinook during annual mark-recapture sampling events in the summer and winter. Additional recapture data are generated at a rotary screw trap operated March – November at the mouth of the Entiat River. Year-round resight data are generated through six permanent instream PIT-tag detection arrays installed at the upper and lower boundaries of each geomorphic reach, temporary arrays operated intermittently within several minor tributaries and important off-channel habitats, and from detections/recaptures within the Columbia River hydroelectric system.

We have taken a similar approach to jointly analyzing discrete (i.e., physical fish capture) and continuous (passive PIT tag relocation) data to obtain seasonal estimates of apparent survival (owing to relatively low detection of fish leaving the study area) within each of the five geomorphic regions (Figure 5.a.4). Using these reach-specific estimates of survival, we are able to evaluate the population consequences of restoration actions in a LCM framework, while accounting for sub-population dynamics that are typically not captured in LCMs where watershed productivity is estimated from stage-specific abundance data.

Multi-State Model applications (fish movement example)

Salmonids exhibit a remarkable phenotypic plasticity in migratory life histories and juveniles may spend several months to years in the freshwater tributary environment before emigrating from the natal stream to the ocean. Fry dispersal and emigration are not passive responses (e.g., Bradford and Taylor 1997), and the timing of emigration varies among species (Friesen et al. 2007), populations (Tucker et al. 2009), and geographic locations (McMichael et al. 2010) and has an impact on the overall population life cycle. For example, fish size at emigration has a significant impact on the number of returning adults because smaller size at emigration is often associated with a low probability of estuary and ocean survival (Sogard 1997, Zabel and Williams 2002). Movement data within and out of a watershed are an important component of any assessment of a fish population's recovery potential and can help to prioritize restoration activities in a watershed: the estimation of movement between different spatial scales can be used in a LCM to predict stage-specific (e.g., fry, parr, smolt) abundances in different habitats within the natal area, allowing us to identify which areas should be prioritized for restoration. Multistate capture-mark-recapture models are commonly used to estimate movement probabilities among discrete geographic units or states (Blums et al. 2003, Martin et al. 2007, Horton et al. 2011). Here we describe an approach to estimate movement probabilities using a multistate model that is an extension of the Cormack-Jolly-Seber (CJS, Cormack 1964, Jolly 1965, Seber 1965) live recapture model extended to multiple areas or states. However, one drawback to using the multistate modes is that all data much be transformed into discrete data.

We used data from 5,420 spring Chinook, PIT-tagged during 2010-2013, to estimate movement probabilities among six states (geomorphicly distinct valley segments, VS1a, VS1b, VS2, VS3, Mad, Outside), 46% of which were marked and released population in VS1a, 29% in VS3, 14% in VS2, 6% in the Mad River, and 5% in VS1b (Figure 5.a.3). Preliminary results indicate that movement probabilities for juvenile spring Chinook differed by valley segment and through time. There was no evidence of upstream movement, but downstream movement probabilities segments ranged from 1 to 73%. The greatest downstream movement probability occurred between summer and winter (over-winter) for fish leaving the watershed from VS1a (0.73 ± 0.10 (SE)), indicating that fish tagged in VS1 had a very high probability of emigrating out of the Entiat as sub-yearlings. Fish tagged in VS2 and VS3 had the lowest probability of moving during the over-winter period. However, this is not unexpected since valley segments 2 and 3 offer the better habitat than VS1, with a lower gradient, multi-thread channel, more pools and wood, and greater access to the floodplain and off-channel habitat.

These estimates of movement among geomorphically distinct regions of the Entiat River, in conjunction with region-specific survival estimates (see above), form the basis for developing a LCM that accounts for both the highly mobile nature of spring Chinook in the Entiat River and region-specific survival rates, that are likely driven by habitat conditions within the distinct valley segments. We hypothesize that restoration actions targeted at improving habitat in VS2 and VS3 would further reduce over-winter movement out of these areas, retaining more fish in higher quality habitat to emigrate as yearlings, and therefore experience higher estuary and ocean survival rates. However, we acknowledge that responses to habitat improvement reflected in reduced emigration rates out of VS2 and VS3, may be limited by density dependence observed as a negative impact on fish growth. We can test these hypotheses with the LCM using the movement probabilities among valley segments and changes in habitat quantity and quality due to restoration to evaluate the effect on the life history patterns of juvenile spring Chinook.

Accounting for density-dependence

One potential drawback to parameterizing stage-specific Beverton-Holt (B-H) productivity (pi) parameters using mark-recapture data is that field sampling is usually conducted under conditions that are neither at carrying capacity or completely free of density dependence. Therefore, because the realized survival during stage-to-stage transitions in the LCM framework outlined above is governed by B-H density-dependent (D-D) dynamics, empirical estimates of survival (Si, from mark-recapture data) need to be re-scaled into a B-H productivity equivalent (pi, which represents maximum survival at low abundance). This is typically the case for juveniles (parr, presmolts), as these stages 1) provide the greatest opportunity for informing LCM structure with mark-recapture data, and 2) are frequently modeled with D-D present.

One basic approach to determing B-H productivity equivalents from mark-recapture derived estimates of realized survival can be built upon the following assumptions:

Stage-to-stage transitions occur according to the B-H model, i.e.,:

$$N_{i+1} = \frac{N_i}{\frac{1}{p_i} + \frac{1}{c_i} N_i} \qquad (1)$$

within which pi is the theoretical maximum survival at low abundance (i.e., as abundance approaches zero) and ci is the population’s carrying capacity for stage i (e.g., i = parr and i+1 = age-1 presmolts, Middle Fork John Day steelhead example above).

Realized survival (Si), estimated through mark-recapture sampling, attempts to estimate the following:

$$S_i = \frac{N_{i+1}}{N_i} \qquad (2)$$

However, if density dependence is assumed to be negligible for a given stage, carrying capacity (ci) becomes infinite and equation 1 reduces to:

$$N_{i+1} = N_i p_i \qquad (3)$$

and thus the pi input can be taken as equivalent to realized survival (i.e., Si = Ni+1 /Ni).

In contrast, if one can reasonably assume that sampling estimates of Si were derived from years during which surveyed habitats were fully seeded (i.e., at or near capacity), then equation 1 reduces to:

$$N_{i+1} = \frac{N_i}{\frac{1}{p_i}+1} \qquad (4)$$

which, via substitution and algebraic rearrangement, suggests pi can be approximated from sampling estimates of Si via the following:

$$p_i = \frac{1}{\frac{1}{S_i}-1} \qquad (5)$$

Finally, if it is unclear how abundance during the years for which Si was estimated relate to the carrying capacity for that life stage, one could modify equation 5 for beliefs/assumptions about abundance actually being at x % of capacity and compute pi as:

$$p_i = \frac{1}{\frac{1}{S_i}-x} \qquad (6)$$

Equations 3, 5 and 6 can be graphical depiction, for varying levels of x, using a carrying capacity of 100K and the base stage-specific survival estimate of 0.49 (Figure 5.a.5).

Given the synopsis above and the patterns shown in Figure 5.a.5, it is clear that some adjustment of Si is likely to be necessary for many natural populations. However, because implementation of juvenile capacity limitation in steelhead LCM calculations is complicated by the presence of multiple competing 'presmolt' ages, there isn't a straightforward analytical approach to solve this impasse. For this reason, we numeric solved for a pi value that yield realized survival estimates (calculated from LCM output) that were similar to those estimated from mark-recapture data. For example, in the Middle Fork John Day application outline above it appears that modifying the Si input according to x = 0.25 (i.e., ~ assumes mark-recap sites were seeded at ~25% of the theoretical maximum capacity during sampling years) results in a time series of realized survivals that mirror the observed Si (Figure 5.a.6).

This exercise illustrates that it is indeed feasible to calibrate the B-H pi parameter (the model input) so that population dynamics are consistent with the sampling data used to guide overall model parameterization. Further, it is clear that doing nothing will result in realized survivals that are biased low relative to sampling data.

In circumstances where there are fewer "competing" juvenile life stages simultaneously occupying the available habitat being modeled in a LCM (e.g., many Chinook populations), a more rigorous approach can be taken to solve for stage-specific productivity parameters using a combination of survival estimates derived from mark-recapture data and stage-specific abundance data. For example, In the Lemhi watershed, spring/summer Chinook parr are tagged throughout the watershed in late summer, and we are interested in estimating their survival as smolts to Lower Granite Dam (LGD) the following spring. For a species such as Chinook, with directed juvenile movement downstream, the primary detection sites are at several paired rotary screw traps and PIT antennas, both within the Lemhi watershed and at the mouth of the Lemhi. In addition, PIT tags are detected at LGD. However, not all Chinook overwinter in the same location, so it is necessary to differentiate overwinter survival in the upper and lower areas of the watershed, as well as in the mainstem Salmon River. To do so, we used the TribPit software (Buchanan et al. 2015), to take advantage of all the within-watershed detections. It provides estimates of the joint probabilities of survival and movement for various spatial areas across two time-periods so that survival during fall or spring migrations within a short time window can be differentiated from over-winter survival during a longer time window within the same spatial area. The various movement/survival probabilities can be combined into a single estimate of survival to LGD for a particular cohort or brood year.

Subsequently, we used a Bayesian state-space framework to construct an integrated population model (Kéry and Schaub 2012) to estimate productivity parameters for spawner-to-parr and parr-to-smolt transitions from survival estimates from seven brood years and estimates of spawner and parr abundances, and associated uncertainty, gathered during the same time period. To improve productivity parameter estimates, we also incorporated estimates of parr capacity generated by quantile regression forests (QRF), and the assumption that smolt capacity within the Lemhi would be less than or equal to parr capacity. Through this process, we can account for both the potential influence of density dependence on realized survival rates as well as observation error in the field data (Figure 5.a.7).

Summary

Extensive fish sampling programs conducted over the last couple of decades have increased our ability to mark and relocated tagged fish across a wide range of field conditions. Indeed, sampling technologies exist to collect mark-recapture data on many of the freshwater rearing lifestages of anadromous salmonids that inhabit both large river systems as well as remote tributaries. Including these data in life cycle modeling programs is likely to increase the realism of stage-specific LCM as mark-recapture data can be used to estimate spatially explicit survival rates. Further, by modeling reach-level survival with environmental and individual covariates we can test mechanistic hypotheses about factors driving survival rate under varying habitat conditions, and explicitly at locations were restoration actions have occurred, or are planned. Finally, the extent of mark-recapture data necessary to produce accurate and precise estimates of survival, in many systems, is logistically feasible to collect. Ultimately, mark-recapture data can be used to augment the typical abundance monitoring conducted at the watershed-scale to specifically allow managers to asked questions about the population level responses of specific restoration plans. However, although mark-recapture data provide a promising means to life cycle modeling efforts, there are limits to the extent mark-recapture data are likely to be appropriate or necessary in the diversity of LCM applications across the Columbia River Basin (see for example Integrated Population Models Buhle et al Chapter 7.

Future research needs

1) Barker model
    a. Extent to which we will be able to obtain survival estimates for species that demonstrate a high degree of movement throughout their life history (e.g., Chinook)
2) Multistate model
    a. Degree to which using continuous data in a discrete model framework biases survival and transition probabilities
    b. It is still unclear what sampling intensity is needed under typical capture and resighting success to produce accurate and precise estimates.
3) General mark-recapture concerns
    a. How to appropriately deal with long time series of mark-recapture data in which fish that have relatively short life expectancies are no longer in the population, but remain in the mark-recapture data set
    b. Shed tags are likely to cause and increasing issue as more programs conduct mobile surveying. Ample evidence for this from the Asotin.
    c. Currently many monitoring programs are limited by the size of fish that they can tag.
        i. Many Chinook populations are already moving at high rates by the time they reach a tagable size
        ii. Furthermore, the fry life stage is likely a critical life stage for density dependence drivers of population dynamics (this is one reason that abundance monitoring data is necessary to constrain survival estimates in LCM applications.)

References

Al-Chokhachy, R., P. Budy, and M. Conner. 2009. Detecting declines in the abundance of a bull trout (*Salvelinus confluentus*) population: understanding the accuracy, precision, and costs of our efforts. Canadian Journal of Fisheries and Aquatic Sciences **66**:649-658.

Barbour, A. B., J. M. Ponciano, and K. Lorenzen. 2013. Apparent survival estimation from continuous mark-recapture/resighting data. Methods in Ecology and Evolution **4**:846-853.

Barnas, K. A., S. L. Katz, D. E. Hamm, M. C. Diaz, and C. E. Jordan. 2015. Is habitat restoration targeting relevant ecological needs for endangered species? Using Pacific salmon as a case study. Ecosphere **6**:1-42.

Bartz, K. K., K. M. Lagueux, M. D. Scheuerell, T. Beechie, A. D. Haas, and M. H. Ruckelshaus. 2006. Translating restoration scenarios into habitat conditions: an initial step in evaluating recovery strategies for Chinook salmon (Oncorhynchus tshawytscha). Canadian Journal of Fisheries and Aquatic Sciences **63**:1578-1595.

Beverton, R., and S. Holt. 1957. On the dynamics of exploited fish populations. Fisheries Investigation Series 2, volume 19, UK Ministry of Agriculture. Fisheries, and Food, London, UK.

Blums, P., J. D. Nichols, J. E. Hines, M. S. Lindberg, and A. Mednis. 2003. Estimating natal dispersal movement rates of female European ducks with multistate modelling. Journal of Animal Ecology **72**:1027-1042.

Bouwes, N., N. Weber, C. E. Jordan, W. C. Saunders, I. A. Tattam, C. Volk, J. M. Wheaton, and M. M. Pollock. 2016. Ecosystem experiment reveals benefits of natural and simulated beaver dams to a threatened population of steelhead (Oncorhynchus mykiss). Scientific Reports **6**.

Bradford, M. J., and G. C. Taylor. 1997. Individual variation in dispersal behaviour of newly emerged chinook salmon (Oncorhynchus tshawytscha) from the Upper Fraser River, British Columbia. Canadian Journal of Fisheries and Aquatic Sciences **54**:1585-1592.

Buchanan, R. A., J. R. Skalski, G. Mackey, C. Snow, and A. R. Murdoch. 2015. Estimating cohort survival through tributaries for salmonid populations with variable ages at migration. North American Journal of Fisheries Management **35**:958-973.

Conner, M. M., W. C. Saunders, N. Bouwes, and C. Jordan. 2015. Evaluating impacts using a BACI design, ratios, and a Bayesian approach with a focus on restoration. Environmental Monitoring and Assessment **188**:555.

Cormack, R. 1964. Estimates of survival from the sighting of marked animals. Biometrika **51**:429-438.

Friesen, T. A., J. S. Vile, and A. L. Pribyl. 2007. Outmigration of juvenile Chinook salmon in the lower Willamette River, Oregon. Northwest Science **81**:173-190.

Good, T. P., T. J. Beechie, P. McElhany, M. M. McClure, and M. H. Ruckelshaus. 2007. Recovery planning for Endangered Species Act-listed Pacific salmon: using science to inform goals and strategies. Fisheries **32**:426-440.

Hanson, P. C., T. B. Johnson, D. E. Schindler, and J. F. Kitchell. 1997. Fish Bioenergetics 3.0. Techinical Report WIS-CU-T-97-01, University of Wisconsin Sea Grant Institute, Madison.

Hartman, K. J., and J. F. Kitchell. 2008. Bioenergetics modeling: progress since the 1992 symposium. Transactions of the American Fisheries Society **137**:216-223.

Honea, J. M., J. C. Jorgensen, M. M. McClure, T. D. Cooney, K. Engie, D. M. Holzer, and R. Hilborn. 2009. Evaluating habitat effects on population status: influence of habitat restoration on spring-run Chinook salmon. Freshwater Biology **54**:1576-1592.

Horton, G. E., and B. H. Letcher. 2008. Movement patterns and study area boundaries: influences on survival estimation in capture–mark–recapture studies. OIKOS **117**:1131-1142.

Horton, G. E., B. H. Letcher, and W. L. Kendall. 2011. A multistate capture–recapture modeling strategy to separate true survival from permanent emigration for a passive integrated transponder tagged population of stream fish. Transactions of the American Fisheries Society **140**:320-333.

Jolly, G. M. 1965. Explicit estimates from capture-recapture data with both death and immigration-stochastic model. Biometrika **52**:225-247.

Jorgensen, J. C., J. M. Honea, M. M. McClure, T. D. Cooney, K. Engie, and D. M. Holzer. 2009. Linking landscape-level change to habitat quality: an evaluation of restoration actions on the freshwater habitat of spring-run Chinook salmon. Freshwater Biology **54**:1560-1575.

Kareiva, P., M. Marvier, and M. McClure. 2000. Recovery and management options for spring/summer chinook salmon in the Columbia River Basin. Science **290**:977-979.

Kéry, M., and M. Schaub. 2012. Bayesian population analysis using WinBUGS: a hierarchical perspective. Academic Press.

Letcher, B. H., and G. E. Horton. 2008. Seasonal variation in size-dependent survival of juvenile Atlantic salmon (Salmo salar): performance of multistate capture–mark–recapture models. Canadian Journal of Fisheries and Aquatic Sciences **65**:1649-1666.

Martin, T. G., I. Chadès, P. Arcese, P. P. Marra, H. P. Possingham, and D. R. Norris. 2007. Optimal conservation of migratory species. PLoS One **2**:e751.

McHugh, P., P. Budy, and H. Schaller. 2004. A model-based assessment of the potential response of Snake River spring–summer Chinook salmon to habitat improvements. Transactions of the American Fisheries Society **133**:622-638.

McHugh, P. A., W. C. Saunders, N. Bouwes, C. E. Wall, S. Bangen, J. M. Wheaton, M. Nahorniak, J. R. Ruzycki, I. A. Tattam, and C. E. Jordan. 2017. Linking models across scales to assess the viability and restoration potential of a threatened population of steelhead (Oncorhynchus mykiss) in the Middle Fork John Day River, Oregon, USA. Ecological Modelling **355**:24-38.

McMichael, G. A., M. B. Eppard, T. J. Carlson, J. A. Carter, B. D. Ebberts, R. S. Brown, M. Weiland, G. R. Ploskey, R. A. Harnish, and Z. D. Deng. 2010. The juvenile salmon acoustic telemetry system: a new tool. Fisheries **35**:9-22.

Moussalli, E., and R. Hilborn. 1986. Optimal stock size and harvest rate in multistage life history models. Canadian Journal of Fisheries and Aquatic Sciences **43**:135-141.

Scheuerell, M. D., R. Hilborn, M. H. Ruckelshaus, K. K. Bartz, K. M. Lagueux, A. D. Haas, and K. Rawson. 2006. The Shiraz model: a tool for incorporating anthropogenic effects and fish–habitat relationships in conservation planning. Canadian Journal of Fisheries and Aquatic Sciences **63**:1596-1607.

Seber, G. A. 1965. A note on the multiple-recapture census. Biometrika **52**:249-259.

Sharma, R., A. B. Cooper, and R. Hilborn. 2005. A quantitative framework for the analysis of habitat and hatchery practices on Pacific salmon. Ecological Modelling **183**:231-250.

Skalski, J. R., S. G. Smith, R. N. Iwamoto, J. G. Williams, and A. Hoffmann. 1998. Use of passive integrated transponder tags to estimate survival of migrant juvenile salmonids in the Snake and Columbia rivers. Canadian Journal of Fisheries and Aquatic Sciences **55**:1484-1493.

Sogard, S. M. 1997. Size-selective mortality in the juvenile stage of teleost fishes: a review. Bulletin of Marine Science **60**:1129-1157.

Tucker, S., M. Trudel, D. W. Welch, J. Candy, J. Morris, M. Thiess, C. Wallace, D. J. Teel, W. Crawford, and E. Farley Jr. 2009. Seasonal stock-specific migrations of juvenile sockeye salmon along the west coast of North America: implications for growth. Transactions of the American Fisheries Society **138**:1458-1480.

Zabel, R. W., and J. G. Williams. 2002. Selective mortality in Chinook salmon: what is the role of human disturbance? Ecological Applications **12**:173-183.

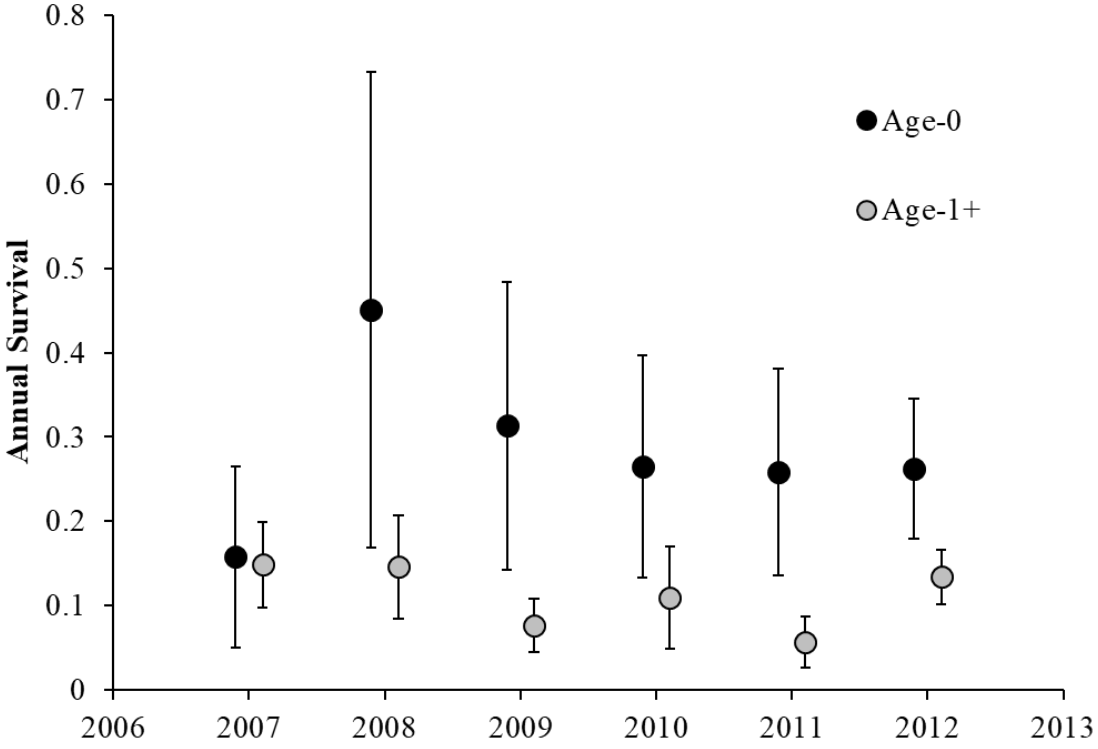

Figure 5.a.1 – Estimates of annual survival for Age-0 parr (black circles) and Age-1+ pre-smolts (gray circles) steelhead estimated using the Barker model to analyze mark-recapture data originating from both physical fish capture events (discrete capture data) and passive PIT tag detections (continuous capture data). Survival estimates were used to parameterize a stage-specific lifecycle model for steelhead in the Middle Fork John Day River. Error bars show 95% confidence intervals

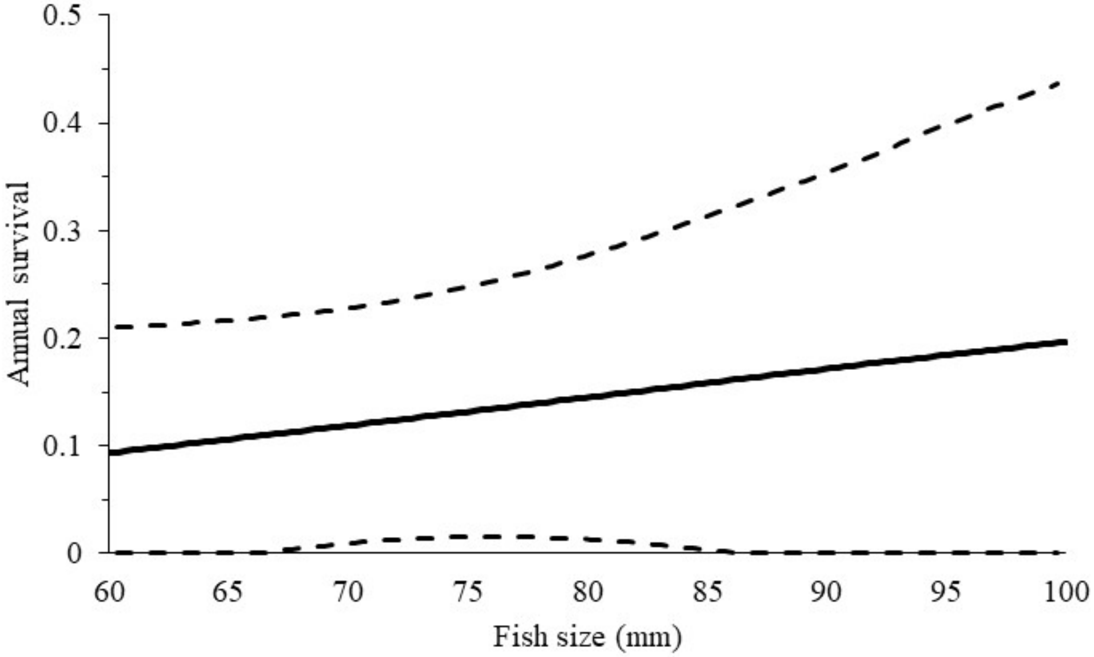

Figure 5.a.2 – Estimates of annual survival for Age-0 parr steelhead estimated using the Barker model to analyze mark-recapture data originating from both physical fish capture events (discrete capture data) and passive PIT tag detections (continuous capture data). Survival estimates were used to parameterize a stage-specific lifecycle model for steelhead in the Middle Fork John Day River.

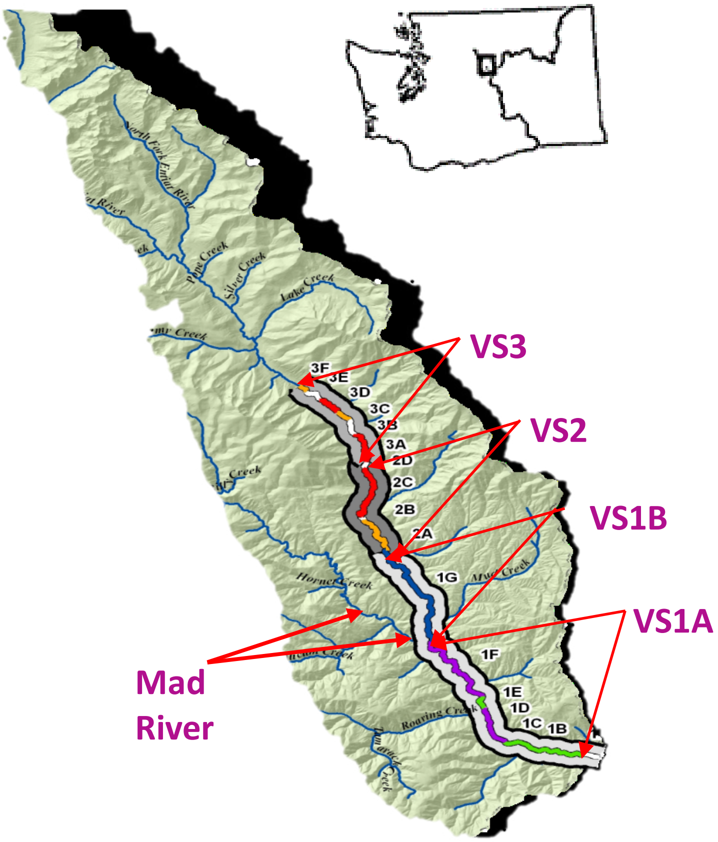

Figure 5.a.3 – Location and extent of the geomorphically distinct valley segments and the Mad River, the major tributary to the Entiat River, in the Entiat Intensively Monitored Watershed.

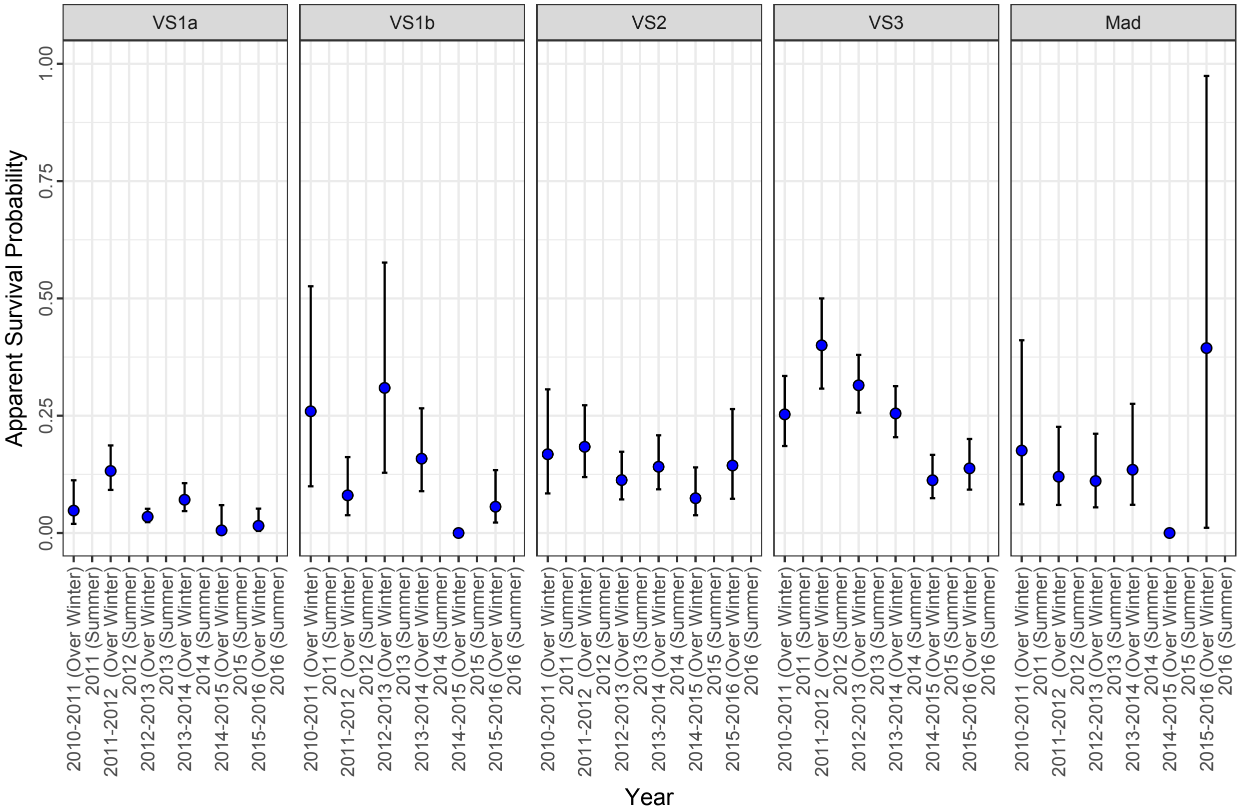

Figure 5.a.4 – Apparent over winter and summer survival probability and 95% confidence intervals for juvenile spring Chinook salmon by valley segment within the Entiat and Mad River sub-basin.

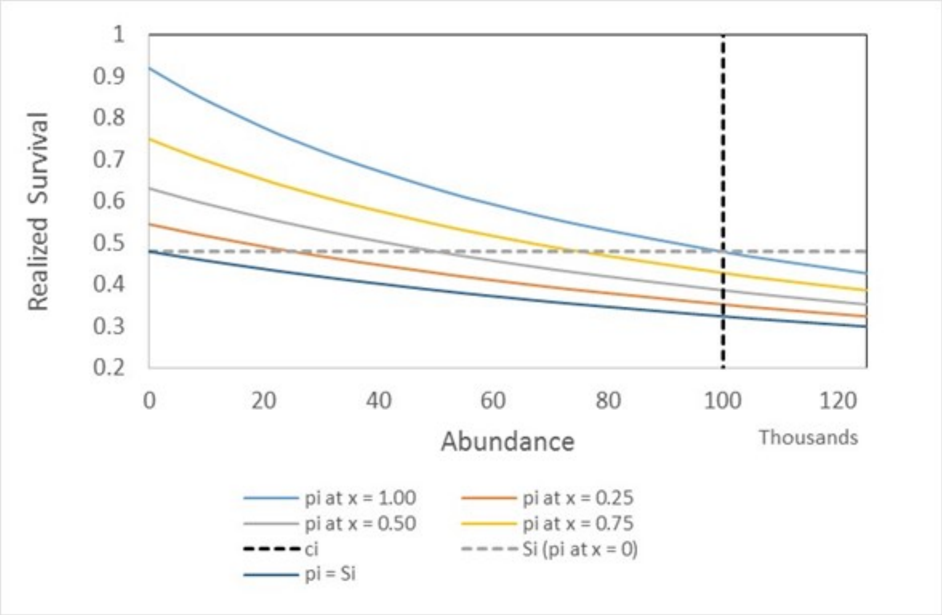

Figure 5.a.5 – The realized survival (Si calc = Ni+1 /Ni) computed from a Beverton-Holt equation at varying levels of abundance, given (1) a capacity (ci) input of 100K (vertical dashed line) and (2) with pi (colored lines) approximated from a sampling estimate (horizontal dashed gray line) given different assumptions (colored lines) about where true population abundance was (i.e., relative to true carrying capacity) at the time mark-recap sampling occurred. Note that the lowest curve is what happens if Si is assumed to be synonymous with. At the other extreme, the pi estimate approximated according to equation 5 produces realized survivals approaching observed survival only when abundance nears capacity. Note also that the flat dashed line is both a horizontal reference for the sampling Si value and what happens when capacity is infinitely large (i.e., equation 3 or x = 0).

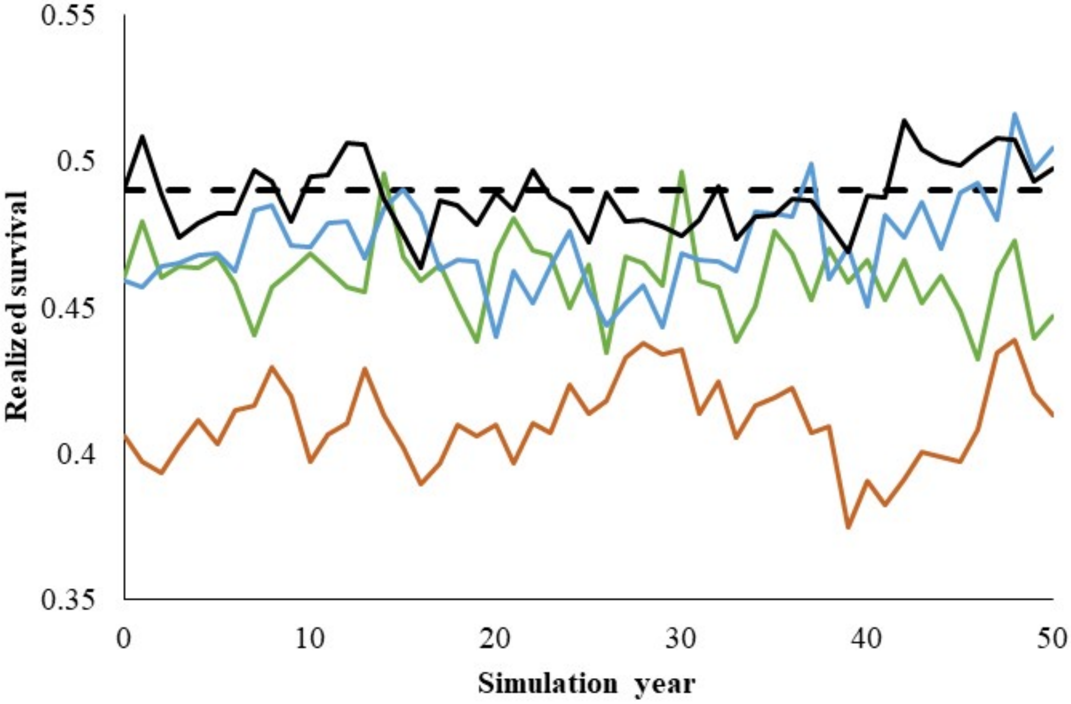

Figure 5.a.6 – Average realized juvenile survival generated through 200 simulations under different Si-to-pi adjustment conditions. Note that the **black** line, x = 0.5 for all juvenile life stages, tracks about the sampling estimate (black dashed line) used in the original draft LCM parameterization. Also, treating Si and pi as though they're one in the same (lowermost **orange**) results in simulations within which realized survival is consistently below the field sampling estimate. Note that simulation year omits a 50-year burn in period. For the **blue** line, x = 0.75 for Age-0 parr and x = 1.0 for Age-1+ pre-smolts. For the **green** line, x = 0.25 for all juvenile life stages.

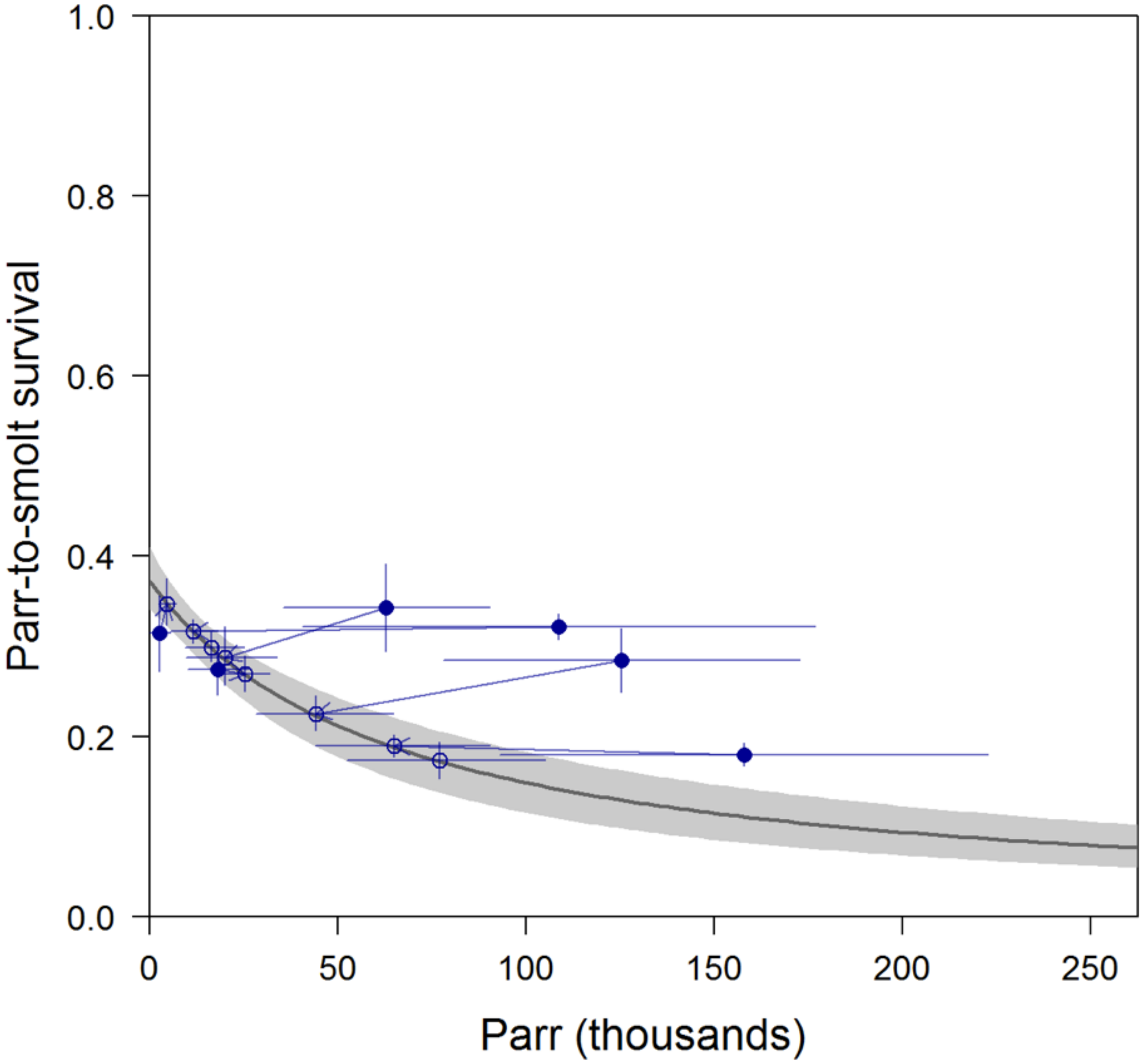

Figure 5.a.7 – Results of Bayesian state-space model used to estimate parr-to-smolt productivity. Data are shown as filled circles, with approximate 95% confidence intervals based on the observation error variances. Arrows connect each observation to the corresponding estimated "true" value (open circle), shown with 95% posterior credible intervals. Because there is no process error, the true values lie along the fitted curve (posterior mean, with gray envelope showing the 95% credible interval of the function).

Section 2e: Habitat Actions and Chinook parr-adult survival

Charlie Paulsen, Paulsen Environmental Research, Ltd.

Tim Fisher, Fisher Fisheries, Ltd.

Abstract

In previous publications using PIT-tagged Chinook salmon parr (*Oncorhynchus tshawytscha*), we demonstrated that age 0 parr rearing in selected Snake River basin streams that received a large number of habitat restoration actions had higher parr–smolt (age 1) survival than juveniles rearing in streams with relatively few actions. In this analysis, we update the previous work, and demonstrate how juvenile parr–to–adult (ages 2+)) and smolt-to-adult survival was higher for juveniles from streams with more habitat actions versus those with fewer actions. Using log-linear regression models with over 1.14 million tagged parr, the number of habitat actions was associated with significant increases in survival. Furthermore, these increases were sufficiently large to potentially be of importance to the co-managers of these stocks. Past habitat actions likely substantially increased survival, and there may be real potential for carrying out additional actions that might benefit many of these populations. While we could not demonstrate mechanistic relationships between habitat actions and survival, we discovered that higher numbers of actions were associated with larger parr at age, which in turn were associated with higher survival rates.

Introduction

Snake River spring-summer-run Chinook were listed under the Endangered Species Act (ESA) by the U.S. National Oceanic and Atmospheric Administration's National Marine Fisheries Service (NOAA Fisheries 1992). They have since been the focus of both ESA related litigation and numerous management actions designed to increase their survival and abundance (e.g., National Wildlife Federation v. National Marine Fisheries Service 2005; Bonneville Power Administration (BPA 2016). In the most recent biological opinion (BiOp - a proposed management plan under the ESA) on the U.S. federal Columbia River power system (FCRPS; NOAA Fisheries 2013), NOAA Fisheries relied in part on improvements in freshwater habitat in spawning and rearing tributaries to help improve Chinook populations that spawn in tributaries of the Snake River. They related habitat restoration or remediation actions (“actions”) to changes in survival using expert opinion, since directed, empirical studies regarding the effects of habitat restoration on the survival of interior Columbia River stocks had never been carried out.

Since 2004 over $1.75 billion has been expended by BPA alone on fish habitat restoration and protection in the Columbia River basin (all species combined; BPA 2016.). Barnas et al. (2015) state that “[t]he Pacific Northwest now contains one of the highest densities of freshwater restoration projects in the U.S., and is essentially the largest freshwater restoration effort ever undertaken on behalf of an endangered species with billions of dollars spent to date.” The Oregon Watershed Enhancement Board spent over $3 million in 2014 and 2015 in the Columbia basin (OWEB 2016). NOAA Fisheries’ Pacific Coastal Salmon Recovery Fund has spent $355 million from 2002-2013, much of it in the Columbia basin (NOAA Fisheries 2014).

The BiOp places substantial reliance on improvements in habitat quality/quantity to increase survival rates for ESA-listed populations. Due to the paucity of empirical field studies of the survival effects of habitat generally - and habitat improvement actions in particular - on anadromous salmonid survival, the plans rely on expert panels of knowledgeable specialists to infer how habitat actions will change habitat quality. Past work (Paulsen and Fisher 2001; 2005) made an initial attempt at relating survival to habitat actions for spring-summer Chinook, but much remains to be done in this area. As Liermann and Roni (2008) noted, "[a]lthough vast amounts of money are spent on watershed restoration in the Pacific Northwest, there is very little direct evidence linking restoration actions with increases in salmonid population abundance or production."   Barnas et al. (2015) state: "To obtain reliable inferences of management action effectiveness on the scale of a salmon population would require either data that does not currently exist over that scale, including restoration project success criteria, habitat monitoring, and spatially explicit habitat assessments, or application to a species with smaller spatial scales."

Promising intensively monitored watershed studies (IMW's; PNAMP 2016) are underway to help inform the expert panels and related regional decision-making processes, but definitive results from these studies are several years out. Furthermore, at present it is unclear how one would generalize from the six or so IMW's to the other listed populations of stream-type (spring-summer) Chinook and steelhead in the interior Columbia. The Columbia Habitat Monitoring Program (CHaMP 2014), initiated in 2011 in nine watersheds, is collecting information on habitat characteristics thought to be important to anadromous salmon survival in tributaries. For instance in one CHaMP monitored watershed (Weber et al. 2015) presented promising results of a study relating beaver dam habitat restoration to juvenile steelhead *O. mykiss* survival.

While many lab and spawning channel studies relate survival to water temperature, fine sediments, and other characteristics, to date there have been few attempts to relate field based measurements of habitat attributes to measures of wild salmonid survival (Crozier and Zabel 2006), the common currency in BiOp life cycle analyses (Liermann and Roni et al. 2008). Roni et al. (2014) updated and classified their prior work and found 409 studies that could have a bearing on predicting salmonid quantities as a function of habitat restoration, very few of which were undertaken in the Columbia River basin. Of those, only 19 related habitat actions to survival of salmonids, and only one (Paulsen and Fisher 2005) was located in the Columbia basin. In fact, only within the past few years have there been any widespread efforts to evaluate their effectiveness in remediating the habitat degradation they were intended to improve (Roni et al. 2013).

In light of this, the present analysis attempts to examine the relationship (if any) between putatively beneficial habitat actions and fish survival. It updates our 2005 analysis referenced above, and extends it from parr-smolt survival to adulthood (fish returning to Lower Granite dam as one-ocean jacks or 2+ ocean adults).

The methods used here are broadly similar to those employed before when we investigated relationships between land use/cover and parr-to-smolt survival (Paulsen and Fisher 2001), and looking at habitat actions versus parr-smolt survival (Paulsen and Fisher 2005). The major difference, beyond updating the data we employ, is the focus on long-term survival from age-0 parr to age 2+ jack and adult returns, in addition to from survival to age-1 smolts. Previous work (Paulsen and Fisher; unpublished) indicated that parr survival did not appear to be density dependent. Therefore we do not use indexes of parent spawner abundance herein (e.g., density of redds in spawning stream reaches).

Parr data

Over two million wild spring-summer Chinook parr (tagged between June and December, inclusive) have been released in tributaries in the lower Snake (Columbia Basin PIT Tag Information System (PTAGIS); PSMFC 2016). Of these, we use just over 1.1 million tagged from 1992-2013, with known size at tagging. We selected 27 spring-summer Chinook populations that had sufficient numbers of parr tagged between 1992-2013 to support the analysis. The spawning and rearing locations for each of the 27 populations are shown in Figure 1. All fish were measured for length at tagging, and released into their natal watersheds from June through December. Size at tagging/release was between 55 and 115 mm. Figure 2 displays the number of parr tagged by year, while Table 1 shows how parr are distributed among Chinook populations.

Figure 1. Snake River spring-summer Chinook populations examined in the analysis.

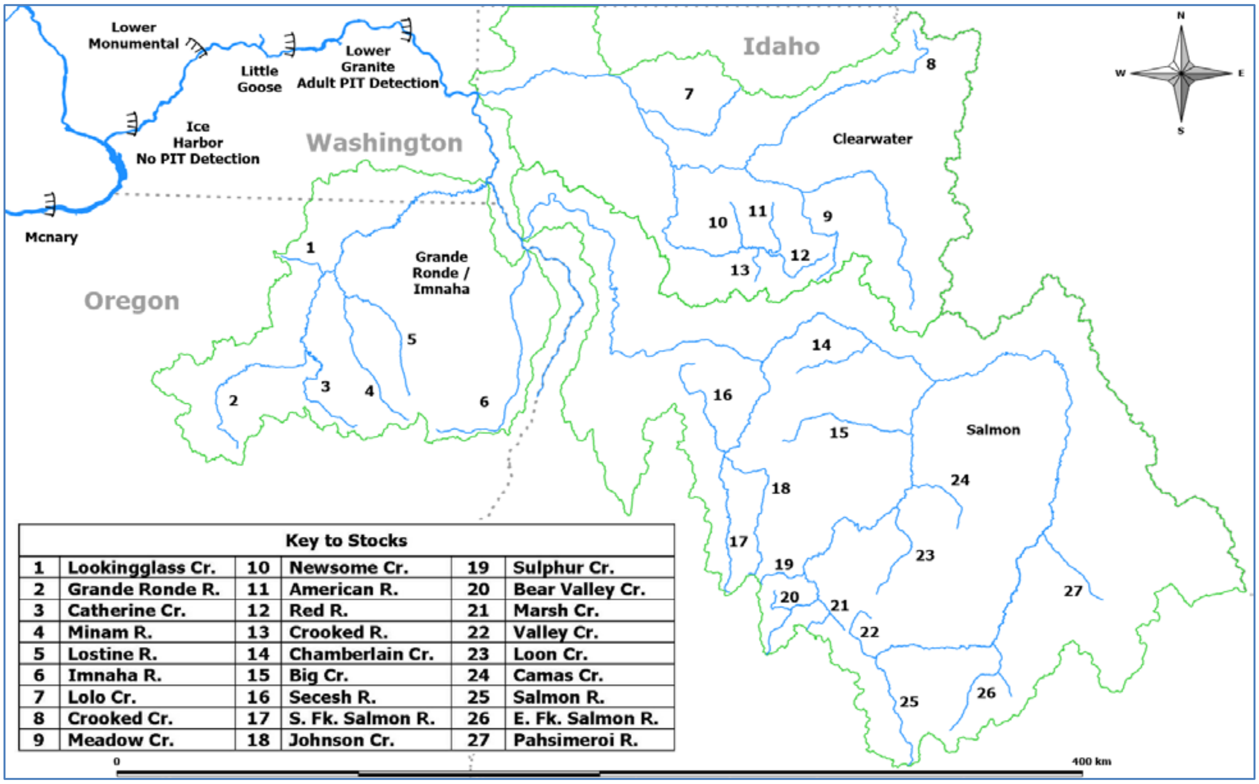

Figure 2. Number of parr PIT tagged by year of tagging for all populations.

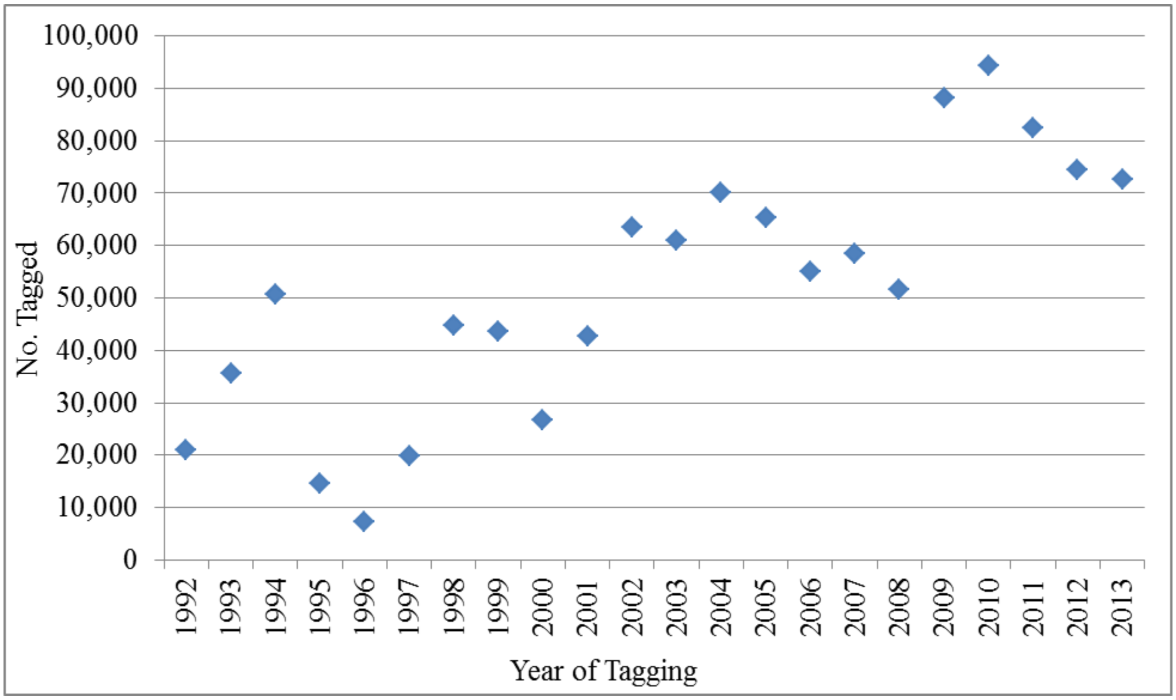

Table 1. Number of tagged parr used in the analysis for each population.

Population	Number Tagged
American River	13,730
Bear Valley Creek	23,501
Big Creek	59,199
Camas Creek	10,278
Catherine Creek	37,364
Chamberlain Creek	14,258
Crooked Creek	40,534
Crooked River	10,885
East Fork Salmon River	11,696
Grande Ronde River	22,058
Imnaha River	114,010
Johnson Creek	85,349
Lolo Creek	26,534
Lookingglass Creek	30,445
Loon Creek	11,521
Lostine River	37,019
Marsh Creek	115,733
Meadow Creek	15,930
Minam River	31,534
Newsome Creek	28,165
Pahsimeroi River	43,340
Red River	30,827
South Fork Salmon River	117,406
Salmon River	70,757
Secesh River	94,273
Sulphur Creek	9,948
Valley Creek	37,071
Total	1,143,365

Habitat Actions

Actions taken to improve or restore anadromous fish habitat are defined as the cumulative number of completed projects “habitat actions” for each population and year. The actions were carried out over a span of about 30 years by various federal, state, and tribal government agencies, as well as private and other public entities. The sources of habitat actions were primarily federal agencies and federal and state sponsored watershed groups (BPA 2016); Grande Ronde Model Watershed Program 2016; Northwest Power and Conservation Council 2006, USDA Agriculture extension service, US Bureau of Land Management, US Forest Service, and state government entities (e.g., Oregon Watershed Enhancement Board 2016); The Conservation Registry 2016). See Fisher (2007) for an earlier detailed accounting of these actions in the subbasins of interest.

We used our judgment to narrow the list of actions to those which would most likely affect the survival of juvenile Chinook. These were generally targeted at five commonly perceived problem areas: restoration of riparian areas and streambanks; controlling livestock grazing and access; improvement of instream rearing habitat; improvement of stream passage conditions or expanding access for parr and/or smolts; increasing instream water flow; and abatement of sources of water quality degradation such as sediment and nonpoint pollution sources. In calculating the number of actions, we assumed that any action, once taken, would be effective from the year in which it was implemented through the end of 2013. There are of course exceptions to this assumption (e.g., riparian plantings) but for consistency and due to the fact that many projects involved multiple types of restoration, all projects were treated identically.

We used all actions that were undertaken in years prior to and including 2013 that we could document and locate with reasonable accuracy on a map. Note that the cumulative total habitat actions for tagging year 1992 include all actions we could locate that took place prior to and during 1992 (the earliest project we could locate occurred in 1950). We defined a habitat action as the suite of individual actions—initiated in the same year and 6th field HUC—under an implementing agency's "project" (i.e., the agency identified the actions as one project). Under this simple definition, an action can consist of more than one activity – instream work, riparian work, etc. – that was carried out in the same HUC/year. We included only those actions that took place upstream of the downstream-most PIT tagging site in each population , and were located within buffers around stream reaches likely to be used by Chinook (Streamnet 2012 spatial dataset; Figure 3). We then used 6th field HUCs from the National Hydrologic Dataset (US Geological Survey 2011) to split habitat actions that were represented by lines or areas by HUC. See Figure 4 for an example of the methodology for selecting habitat actions for inclusion in the analysis.

Figure 3. Example of spawning and rearing stream reaches, 6th field HUCs, and habitat action buffers for the upper Grande Ronde River population. Buffers were placed along stream reaches identified as spawning and/or juvenile rearing areas and up to 10 km upstream of these reaches. Tributaries with no identified Chinook use were excluded.

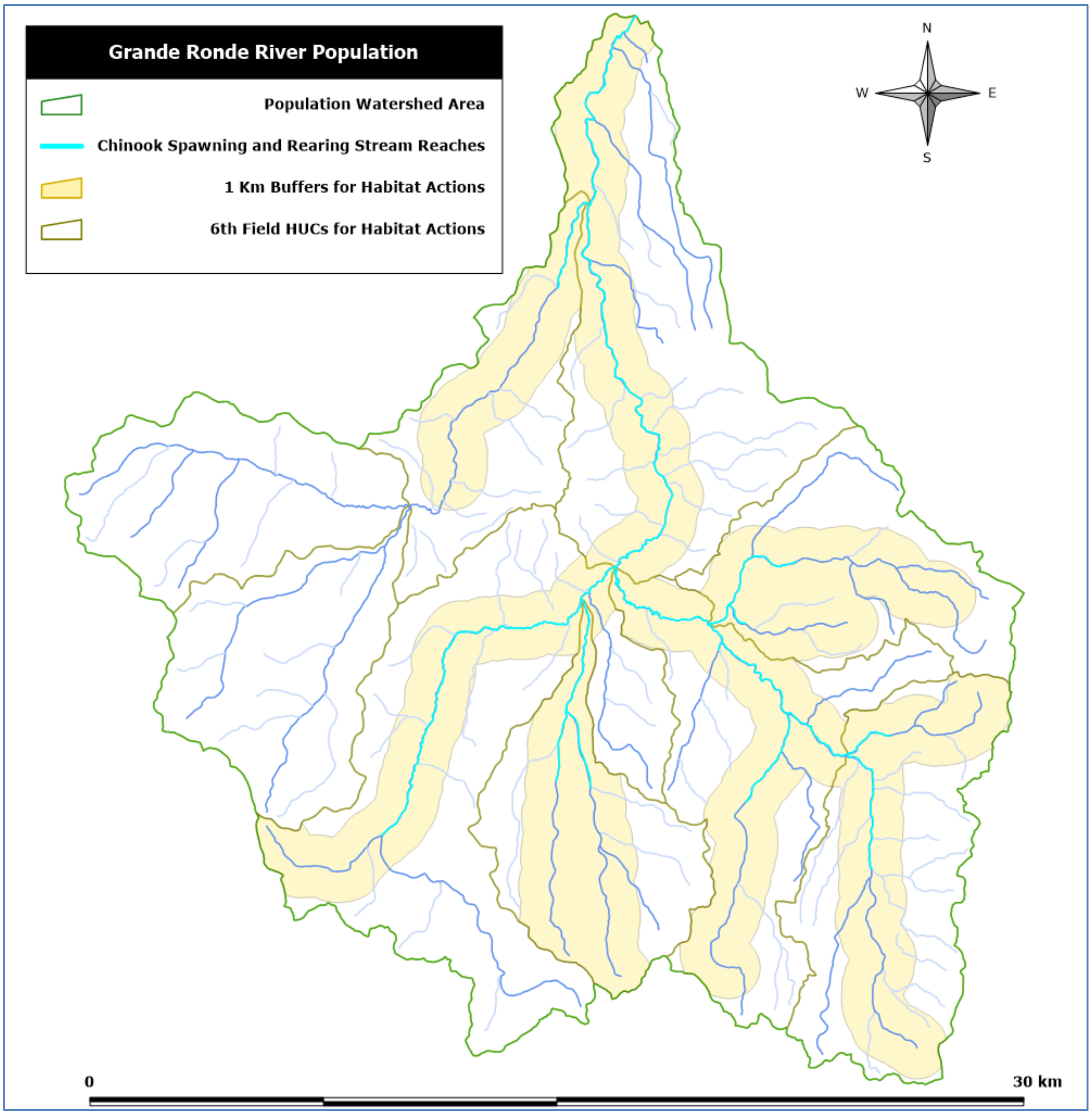

Figure 4. Example of habitat actions for a portion of the upper Grande Ronde River population. An action was defined as a suite of activities undertaken under one “project” in one 6th field HUC in one year. Actions were split by 6th field HUC and the 1 km buffers. Only actions inside buffers were used in the analysis.

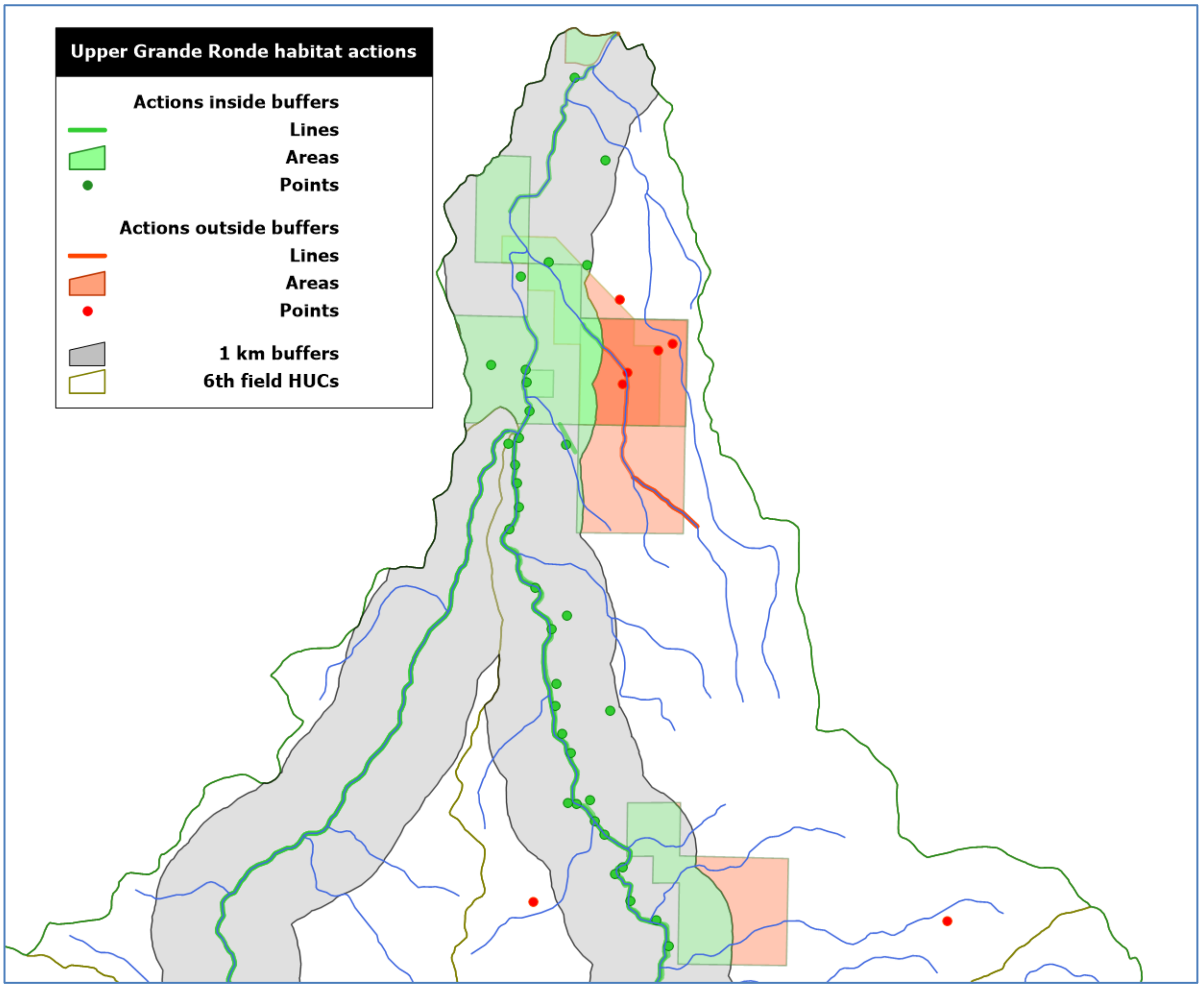

We specifically excluded those actions which took place in areas in the watershed that were far removed from these reaches or were unlikely to benefit survival in the short term (e.g., remotely located roads, tributaries not used by Chinook, timber stands, agricultural fields, and livestock grazing leases; Figure 4). The initial (1992) and cumulative (2013) number of actions shown in Table 2 of course varies among stocks and over time, with a minimum of zero and a maximum of 110 actions.

As we noted in the 2005 paper, this very simple approach, where a “project” is defined as all actions taking place in a given reach and year, ignores the intensity of restoration efforts. It is not what we would have chosen given better data on the actions themselves and on pre-action habitat conditions, but unfortunately these data are not available, especially for projects undertaken early in the time series.

Unlike our previous analyses, the Lemhi River population was considered but rejected from the populations in this analysis. The Lemhi has a cumulative 244 habitat actions through 2013, over twice the second highest population. Many recent actions have focused on reconnecting blocked tributaries to the mainstem Lemhi River (primarily for adult steelhead access); Chinook may only receive marginal benefit due to the small size of tributaries and relatively steep channel gradients. Furthermore, we believe that the Chinook accessible stream reaches may be “saturated” with habitat improvements, at least for summer rearing habitat, and that recent projects may have had increasingly diminishing returns.

Table 2. Habitat restoration actions as of 1992 and 2013 by population. Note that the Lemhi River population was not used in the analysis.

Population	Cumulative no. of actions in 1992	Cumulative no. of actions in 2013
American River	6	21
Bear Valley Creek	6	21
Big Creek	1	7
Camas Creek	2	14
Catherine Creek	3	90
Chamberlain Creek	0	3
Crooked Creek	6	15
Crooked River	4	21
East Fork Salmon River	8	99
Grande Ronde River	14	70
Imnaha River	9	97
Johnson Creek	5	26
Lemhi River	*6*	*244*
Lolo Creek	11	58
Lookingglass Creek	0	9
Loon Creek	0	1
Lostine River	4	43
Marsh Creek	4	16
Meadow Creek	0	1
Minam River	0	5
Newsome Creek	2	14
Pahsimeroi River	1	70
Red River	9	35
South Fork Salmon River	25	92
Salmon River	17	110
Secesh River	1	30
Sulphur Creek	0	0
Valley Creek	9	60

Methods

As noted in the introduction, there are very few previous studies that have traced any relationship between fish survival or fitness and habitat actions. In a previous version of this work, we employed a method know as smoothing splines (Wood 2003) that is very flexible, especially when treating each tagged parr as an individual observation. However, concerns regarding pseudo-replication were raised by reviewers, so we have now reverted to much simpler log-linear models. We investigated three life stages: parr-to-smolt, parr-to-adult, and smolt-to-adult. The models for all three are similar:

$$Ln(S_{i,t}) = b_0 + Y_t + P_i + \omega M_t + \varsigma H_{i,t} + \sigma A_{i,t} + \lambda L_{i,t}$$

$Ln(S_{i,t})$ denotes a survival rate for population *i*, in year *t*. b_0 is the intercept term, while the Y_t terms (one for each year) are year "effect" dummy, index or class variables common across all fish tagged in a given year. The P_i terms are class or index variables for each population. M_t denotes the calendar month of tagging, with an estimated coefficient ω. $H_{i,t}$ are our estimates of habitat actions for each population and year, with estimated coefficient ς . $L_{i,t}$ denotes length at tagging ,(mm) while λ is the estimated coefficient for same.

We applied the parr-to-smolt and smolt-to-adult models to release groups (from a given population and year) to those having at least 100 tagged parr. Because parr-to-adult survival is quite low (about 0.2%) we confined this model to release groups of at least 500 fish. Despite these constraints, about a third of the parr-adult and smolt-adult groups had no adult returns.

Removing them from the samples would clearly bias survival rates upwards, so we added 0.1 to all adult return counts for every group.

In our earlier work on this topic, we developed a suite of models (e.g. 18 models were used in Paulsen and Fisher 2005) and used AICc weights to select the best models. In the current analysis, we instead used year and population index variables and a single model for each life stage. We did this for simplicity, to focus on habitat actions, and to reduce confounding with land use patterns. Habitat actions are undertaken primarily in areas with substantial anthropogenic disturbance, as opposed to wilderness areas. In addition, as funding for habitat remediation has increased over time, we suspect that most areas that are thought to require habitat improvements have seen at least some attention. The population and year index variables allow for a very flexible approach to accounting for background differences in survival while minimizing confounding with the variables of interest.

Results

Table 3 displays univariate statistics for the variables of interest. Survival from parr tagging to smolt at Lower Granite averages about 20%, while survival from tagging back to Lower Granite Dam as jacks or adults is only about 0.2%. Smolt-to-adult survival is higher, of course, averaging about 1%. Mean length at tagging is about 74 mm, while the number of habitat actions ranges from zero to 110. The number of year/stock groups decreases as one moves from parr-smolt survival to parr-adult and smolt-adult survival, since the minimum number of fish in the various groups increases (from 100 for parr-smolt to 500 for parr-adult), and the number of smolts detected at the Snake dams is roughly an order of magnitude smaller than the number of parr tagged.

Table 3. Univariate statistics for three groupings used in the analysis (parr-to-smolt, parr-to-adult, and smolt-to-adult survival).

3a. Parr to smolt (N tag groups = 493, N tagged fish = 1,143,365).

Variable	Minimum	Mean	Maximum
Ln(Survival, parr to LGR)	-3.24	-1.46	-0.35
Year of tagging	1992.00	2004.05	2013.00
Mean month of tagging	6.07	9.07	11.34
Mean length at tagging, mm	60.25	76.45	104.00
Number of habitat actions	0.00	30.39	110.00

3b. Parr to adult (N tag groups = 430, N tagged fish = 1,121,723).

Variable	Minimum	Mean	Maximum
Ln(Parr-adult survival)	-10.75	-7.24	-4.03
Year of tagging	1992.00	2003.22	2013.00
Mean Length at Tagging, mm	60.25	74.23	102.10
Number of habitat actions	0.00	25.33	110.00

3c. Smolt to adult (N tag groups = 365, N tagged fish = 160,329).

Variable	Minimum	Mean	Maximum
Ln(smolt-adult survival)	-9.43	-5.46	-2.93
Year of tagging	1992.00	2003.12	2013.00
Mean Length at Tagging, mm	62.36	77.64	101.40
Number of habitat actions	0.00	26.41	110.00

Table 4 shows the correlations among the variables we employed (month of tagging was not important for the parr-to-adult and smolt-to-adult models). Length at tagging is positively correlated ($p < 10\%$) with survival for the parr-smolt and parr-adult samples, but not for smolt-adult survival, perhaps because the bypass systems at the Snake dams select for smaller fish (Hostetter et al. 2015). The number of habitat actions is positively correlated with length at tagging for all three samples, and with the two samples that track fish to jack/adult returns at Lower Granite Dam.

Table 4. Correlations for three fish groupings. Bold numbers are significant at α = 0.10.

4a. Parr-to-smolt survival.

Variable	Ln (parr to LGR survival)	Year of tagging	Mean month of tagging	Mean length at tagging, mm	No. of habitat actions
Ln(Survival, parr to LGR)	**1.00**	**-0.18**	**0.37**	**0.64**	-0.06
Year of tagging	**-0.18**	**1.00**	-0.07	-0.24	**0.37**
Mean month of tagging	**0.37**	**-0.07**	**1.00**	0.39	**0.24**
Mean length at tagging, mm	**0.64**	**-0.24**	0.39	**1.00**	**0.10**
Number of habitat actions	-0.06	**0.37**	**0.24**	**0.10**	**1.00**

4b. Parr-to-adult survival.

Variable	Ln (Parr-adult survival)	Year of tagging	Mean length at tagging, mm	No. of habitat actions
Ln(Parr-adult survival)	**1.00**	**0.20**	**0.25**	**0.18**
Year of tagging	**0.20**	**1.00**	-0.08	**0.37**
Mean length at tagging, mm	**0.25**	-0.08	**1.00**	**0.19**
Number of habitat actions	**0.18**	**0.37**	**0.19**	**1.00**

4c. Smolt-to-adult survival.

Variable	Ln (smolt-adult survival)	Year of tagging	Mean length at tagging, mm	No. of habitat actions
Ln(smolt-adult survival)	1	**0.22**	0.04	**0.22**
Year of tagging	**0.22**	1.00	**-0.12**	**0.37**
Mean length at tagging, mm	0.04	**-0.12**	1.00	**0.16**
Number of habitat actions	**0.22**	**0.37**	**0.16**	1.00

Table 5 displays the models' coefficients for month, length, and number of actions, as well as goodness-of-fit measures. While month of tagging was not important, length and number of actions were positive and significant at 10% for all three models. R-squares and adjusted r-squares display reasonably tight fits to the data (the year and stock effects were significant in all models). Focusing on the coefficients for habitat actions, we were surprised to see that the coefficient for the parr-to-smolt model, at 0.0019, was indistinguishable from the estimated value from Paulsen and Fisher (2005), 0.002. As with the earlier result, the implication is that for a stock having 100 habitat actions, parr-smolt survival would increase by about 21% (exp(100 * 0.0019)), compared to populations with no actions, all else equal.

Table 5. Estimated coefficients from regression models.

5a. Parr-to-smolt survival.

Variable	Estimated Coefficient	Standard Error	P value	R-square	Adjusted R-square
Mean month of tagging	-0.0136	0.0221	0.72	0.80	0.78
Mean length at tagging	0.0278	0.0028	0.0001		
No. of habitat actions	0.0019	0.0009	0.03		

5b. Parr-to-adult survival.

Variable	Estimated Coefficient	Standard Error	P value	R-square	Adjusted R-square
Mean length at tagging	0.0422	0.0125	0.0007	0.67	0.63
No. of habitat actions	0.0085	0.0046	0.0634		

5c. Smolt-to-adult survival.

Variable	Estimated Coefficient	Standard Error	P value	R-square	Adjusted R-square
Mean length at tagging	0.0438	0.0128	0.0006	0.61	0.55
No. of habitat actions	0.0096	0.005	0.0543		

The parr-to-adult model’s action coefficient, at 0.0085, is both substantially larger and somewhat less precisely estimated. Taking the point estimate at face value, it implies that a population with 100 actions would experience a 230% increase in parr-to-adult survival (exp(100*0.0085)). This raises an obvious question: assuming that both the parr-to-smolt and smolt-to-adult results are a reasonable approximation of reality, why should the increase in survival to adult be ten times greater than the increase in parr-to-smolt survival?   Absent direct estimates of survival in the estuary and ocean, we can only offer informed speculation. As seen in Table 4, for all three samples an increase in habitat actions is associated with an increase in parr size at tagging. We know from other research (Muir et al. 2006) that larger smolts are more likely to return as adults, in part because they are less susceptible to predation. If areas with more actions can grow parr faster than those with fewer actions, it may be that those parr, in addition to surviving at higher rates to the smolt stage, may be less likely to be preyed upon in the estuary and ocean.

The smolt-to-adult results (Table 5c) are very similar to the parr-to-adult results just described. The difference, of course, is that we know that the smolt sample was alive at the time of detection at the Snake dams. The tradeoff is the much smaller sample size. As with the parr-to-adult results, these indicate a larger effect of habitat actions in a later life stage.

As a back-check on the statistical results, we show how actual parr-to-adult survival rates, not predictions, changed over time for six stocks (Figure 5): the three with the lowest number of actions, and the three with the highest number. As one can see, from 1992 to about 2005, the two stock groups had similar parr-adult survival, but from 2007 to 2013 the high-action group survived at roughly double the rate of the low-action group. While one should not read too much into this simple display of data   it does suggest that the actual data – no modeling involved – supports our overall conclusions. One additional point may be noteworthy: the three populations with the fewest actions are all in designated wilderness areas, while those with the highest number of actions are in areas with high land-use impacts.

Figure 5. Actual parr-adult survival for 3 stocks with lowest number of actions (Sulphur Creek, Meadow Creek, and Loon Creek) and 3 stocks with highest number of actions (Imnaha River, East Fork Salmon River, and Salmon River). Years with no tagging have no observations.

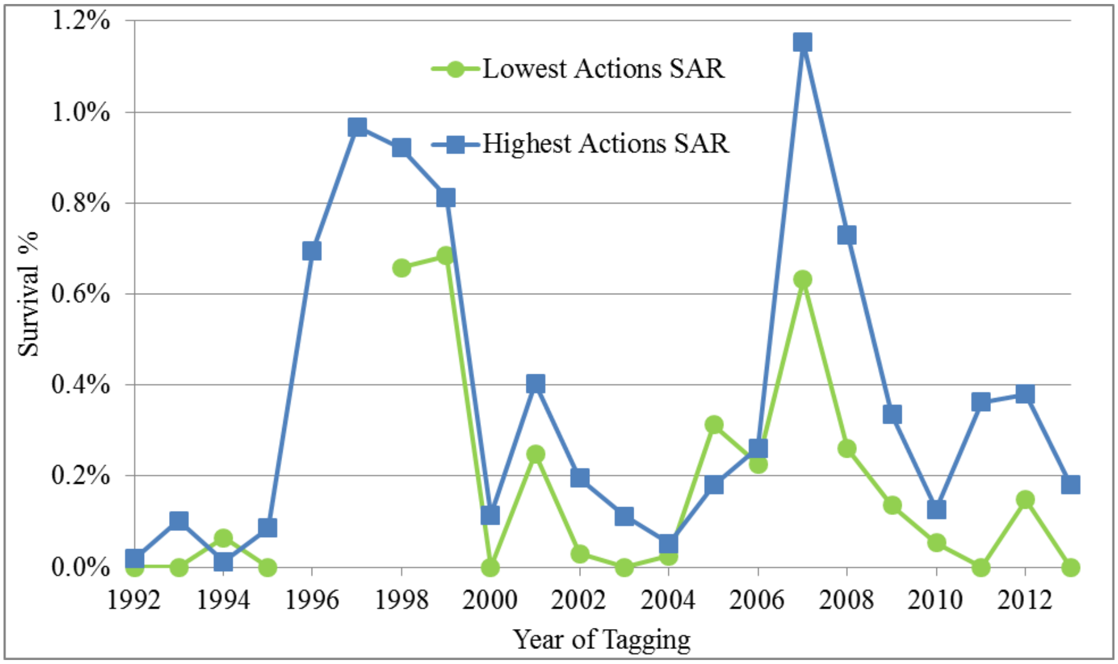

Discussion

The results described here should be encouraging for fisheries managers and funding agencies, which have heretofore relied on the expert judgment of specialists. It appears that, for the populations we analyzed, habitat actions may truly increase parr-adult survival. There also appears to be a crude but plausible mechanism for the results: more actions are associated with greater size at age, and hence higher survival to adult.

These results should be interpreted with caution, as the data are obviously not derived from randomized experiments. The habitat actions were undertaken as opportunities in the spawning and rearing streams of these stocks arose over more than two decades, and the location, relative extent, and type of action are dependent on the judgment of numerous specialists. At the time the actions were undertaken, there were no parallel plans to evaluate their effects on salmonid survival. In fact, only within the past few years has there been any widespread efforts to evaluate their effectiveness in remediating the habitat degradation they were intended to improve. While it would be useful to have estimates of habitat quality pre- and post-actions, the necessary data simply do not exist. Programmatic monitoring of habitat actions has yet to be implemented at a basin-wide scale, and has only recently been proposed (Roni et al. 2013). Habitat actions cannot be emplaced everywhere these stocks spawn, especially in designated wilderness areas, which comprise approximately one fifth of the drainage area surrounding spawning and rearing areas. In addition, as with the Lemhi, some subbasins may already have had most or all of the beneficial actions that they can usefully support, short of major changes in land use. Finally, of course, correlation should not be confused with causation, and it is possible, albeit improbable, that the results are due to simple random variation.

Since stocks with many actions seem to have higher juvenile survival than those with few, one may wonder if this is reflected in adult measures of stock performance (e.g., adult recruits per spawner, R/S). We have investigated this informally (Paulsen and Fisher, unpublished), and could find little or no trace of habitat action influence on adult population trends or R/S. We suspect that a combination of density dependence, imprecise estimates of adult age-at-return, and imprecise expansion from redds to spawners, may contribute to our inability to detect similar associations using adult data. The apparent importance of density dependence for adult R/S models suggests that future actions might be aimed at increasing the capacity of existing habitat and, where feasible, opening new habitat via barrier removal or tributary reconnections, as in the Lemhi.

The combined results of this analysis and that in Paulsen and Fisher 2005 may also be useful in designing the IMWs noted previously. There is a reasonable certainty that large numbers of habitat actions result in both higher parr-adult survival, and furthermore the magnitude of these survival changes is estimable. The survival changes estimated in Paulsen and Fisher 2005 were about a 20% increase in parr-to-smolt survival for stocks that received a large number of habitat actions as compared to stocks that did not receive any actions. The projected changes in survival suggest that as one moves from zero actions to the maximum of 110 in this sample, survival to adult roughly doubles. We suspect, but cannot prove, that the much larger increase in survival to adulthood is associated with the production of larger parr, and hence larger smolts, which likely survive at higher rates during outmigration through the dams, reservoirs, and in the early marine environment. In addition, even though we have excluded the Lemhi from the current analysis, the average number of habitat actions in these data is about 33 (Table 2), almost double that of the actions in Paulsen and Fisher (2005), which used data to 2002.

Close monitoring of parr-adult survival for treated watersheds, and tagging sufficient parr to detect changes in marine survival that may be caused by habitat improvements, may be warranted if the results of this analysis generalize to other locations and species. We suggest two potential geographic extensions, to the Upper Columbia and John Day Basins, both of which have extensive habitat actions and juvenile salmonid tagging programs.

Potential application of these results into life cycle models (LCMs) can be viewed as a two-part question. First, for population that have had large numbers of past actions, the regression models predict that parr-smolt and smolt-adult survival has increased over time as actions were implemented. This would likely need to be accounted for in calibrating LCMs to estimates of past years' spawning escapement, juvenile production, and life stage survival rates. If an LCM is employed to predict future population viability for a stock that is scheduled to have additional future habitat actions, one could use the results to adjust projected life stage survival rates, and incorporate the changes into predictions of spawner abundance, extinction probabilities, etc.

In conclusion, there was a strong association between survival and the number and type of habitat actions undertaken for these stocks. This result is both useful in and of itself, and for those who may be planning small scale experimental treatment and control studies. Furthermore, examination of the results strongly suggests not only that habitat actions really do "keep on giving" after parr emigrate from their natal streams, but also that studies which focus solely on the smaller-scale effects of habitat restoration on freshwater rearing may overlook an important benefit of investments in the restoration of anadromous salmon freshwater habitats.

References

Barnas, K. A., S. L. Katz, D. E. Hamm, M. C. Diaz, and C. E. Jordan. 2015. Is habitat restoration targeting relevant ecological needs for endangered species? Using Pacific Salmon as a case study. Ecosphere 6(7):110. Available: http://dx.doi.org/10.1890/ES14-00466.1.

Bonneville Power Administration. 2016. BPA Fish and Wildlife Program Fund Summary Available: https://www.cbfish.org/Fund.mvc/Summary/1.

Columbia Habitat Monitoring Program (CHaMP). 2014. Combined Annual Technical Report for the Integrated Status and Effectiveness Monitoring Program and the Columbia Habitat Monitoring Program. Available: https://www.champmonitoring.org/Program/Details/1#tab-overview.

Crozier, L., and R.W. Zabel. 2006. Climate impacts at multiple scales: evidence for differential population responses in juvenile Chinook salmon. Journal of Animal Ecology 75: 1100–1109. Available: http://onlinelibrary.wiley.com/doi/10.1111/j.1365-2656.2006.01130.x/full.

Fisher, T. R. 2007. Mapping of Anadromous Fish-Related Habitat Projects and Long-Term Monitoring Efforts in Selected Columbia River Subbasins. Report to US DOE Bonneville Power Administration Division of Fish and Wildlife Policy and Planning Branch, Portland,
Oregon. Available: http://www.cbfwa.org/csmep/web/content.cfm?ContextID=20.

Grande Ronde Model Watershed Program. 2016. Project Database. Available: http://grmw.org/projectdb.

Hostetter, N. J., A. F. Evans, F. J. Loge, R. R. O'Connor, B. M. Cramer, D. Fryer and K. Collis. 2015. The Influence of Individual Fish Characteristics on Survival and Detection: Similarities across Two Salmonid Species. North American Journal of Fisheries Management 35: 1034-1045.

Liermann, M., and P. Roni. 2008. More sites or more years? Optimal study design for monitoring fish response to watershed restoration. North American Journal of Fisheries Management 28: 935-943. Available: http://www.fishsciences.net/reports/NAJFM_u-d_6-28/NAJFM_28_p935-43_More_sites.pdf.

Muir, W. D., D. M. Marsh, B. P. Sanford, S. G. S. G. Smith, and J. G. Williams. 2006. Post-Hydropower System Delayed Mortality of Transported Snake River Stream-Type Chinook Salmon: Unraveling the Mystery. Transactions of the American Fisheries Society 135: 1523–1534.

National Oceanic and Atmospheric Administration (NOAA) Fisheries. 1992. Endangered and Threatened Species; Threatened Status for Snake River spring-summer Chinook Salmon, Threatened Status for Snake River Fall Chinook Salmon. 57 FR 14653. Available: http://www.westcoast.fisheries.noaa.gov/publications/frn/1992/57fr14653.pdf.

NOAA Fisheries. 2013. Endangered Species Act Section 7(a)(2) Biological Opinion Supplemental Consultation on Remand for Operation of the Federal Columbia River Power System. Available: http://www.westcoast.fisheries.noaa.gov/publications/hydropower/fcrps/2013_draft_fcrps_biological_opinion_090913.pdf.

NOAA Fisheries. 2014. Pacific Coastal Salmon Recovery Fund FY 2000–2013 2014 Report to Congress. Accessible: http://www.westcoast.fisheries.noaa.gov/publications/recovery_planning/salmon_steelhead/pcsrf/pacific_coastal_salmon_recovery_fund_2014_report_to_congress.pdf.

National Wildlife Federation v. National Marine Fisheries Service 422 F.3d 782 (9th Cir. 2005). Summary at http://elawreview.org/case-summaries/national-wildlife-federation-v-national-marine-fisheries-service/.

Northwest Power and Conservation Council. 2006. Subbasin Planning. Available: http://www.nwcouncil.org/fw/subbasinplanning/Default.htm.

Oregon Watershed Enhancement Board (OWEB). 2016. Investments by Reporting Basin in the 2013-2015 Biennium. Accessible: http://www.arcgis.com/home/webmap/viewer.html.

Pacific Northwest Aquatic Monitoring Partnership (PNAMP). 2016. Intensively Monitored Watersheds. Available: http://www.pnamp.org/imw/home.

Pacific States Marine Fisheries Commission. 2016. Columbia Basin PIT Tag Information System (PTAGIS). Available: http://www.ptagis.org/.

Paulsen, C. M., and T. R. Fisher. 2001. Statistical relationship between parr-to-smolt survival of Snake River spring/summer chinook salmon and indices of land use. Transactions of the American Fisheries Society 130**:** 347-358. Available: http://www.fishsciences.net/reports/Transactions/Tr_130_p347-58_Statistical_relationship_between_parr-to-smolt.pdf.

Paulsen, C. M., and T. R. Fisher. 2005. Do Habitat Actions Affect Juvenile Survival? An Information-Theoretic Approach Applied to Endangered Snake River Chinook Salmon. Transactions of the American Fisheries Society 134:68-85. http://www.fishsciences.net/reports/Transactions/Tr_134_p68-85_Do_habitat_actions_affect_juv_survival.pdf.

Roni, P., R. Scranton, and J. O’Neal. 2013. Action Effectiveness Monitoring of Tributary Habitat Improvement: a Programmatic Approach for the Columbia Basin Fish and Wildlife

Program. Available: http://www.pnamp.org/sites/default/files/ae_monitoring_programmatic_plan_final_i.pdf.

Roni, P., G. R. Pess, T. J. Beechie, and K. M. Hanson. 2014. Fish-Habitat Relationships and the Effectiveness of Habitat Restoration. NOAA Technical Memorandum NMFS-NWFSC-127. Available: https://www.nwfsc.noaa.gov/assets/25/7422_08122014_141405_FishHabRelationshipsTM127WebFinal.pdf.

Streamnet. 2012. PNW Spring chinook salmon distribution (GIS dataset). Available: http://www.streamnet.org.

The Conservation Registry. 2016. Available: http://www.conservationregistry.org/.

US Geological Survey (USGS). 2011. National Hydrography Dataset. Available: http://nhd.usgs.gov/data.html.

Weber, N., C. Jordan, N. Bouwes, and G. Walthen. 2015. Partnering with Beavers to Recover Incised Streams - 5 Years after Restoration on the Bridge Creek Intensively Monitored Watershed. American Fisheries Society 2015 National Meeting, Portland, OR. Available: https://www.researchgate.net/publication/281119557_Partnering_with_Beavers_to_Recover_Incised_Streams_-_5_Years_after_Restoration_on_the_Bridge_Creek_Intensively_Monitored_Watershed.

Wood, S. N. 2003. Thin plate regression splines. Journal of the Royal Statistical Society: Series B (Statistical Methodology) 65: 95-114.

CHAPTER 3: ESTUARY/OCEAN SURVIVAL

3.a Ocean Survival

Brian J. Burke (NOAA Fisheries, NWFSC), Lisa Crozier (NOAA Fisheries, NWFSC), Jeff Jorgensen (NOAA Fisheries, NWFSC), Tom Cooney (NOAA Fisheries, NWFSC), and Rich Zabel (NOAA Fisheries, NWFSC)

Intro to using PIT data (including what we used before)

Relative to the freshwater life stage, modeling the ocean life stage has received less attention in many salmon life cycle models. This chapter describes an effort to put a bit more focus on this important life stage by first assembling a dataset that specifically addresses marine survival. We also chose to completely revise the analytical approach, taking advantage of recent data sources that were not available during earlier efforts. Much of the initial efforts to revise our approach involved evaluations and data explorations that won't be directly useful in LCMs, but rather helped us make important choices on which data sets to include or exclude. Data, methods, and model results described here are therefore preliminary and, to a limited extent, still in flux.

Switching from SAR to PIT tag data

In previous efforts (Zabel et al. 2013), the ocean component of the life cycle was evaluated using SAR data as the response variable, a value which was often calculated from juvenile counts at Lower Granite Dam and resulting adult counts at Lower Granite Dam. In these models, SAR had to be adjusted to account for downstream and upstream in-river survival and age composition, each of which has uncertainty associated with them that was difficult to transfer to the adjusted SAR values. Therefore, resulting estimates of ocean survival were often artificially correlated with in-river survival. This approach was taken out of necessity, as no other data were available to directly represent the ocean component of salmon life cycle.

More recently, the time series of ocean survival based on PIT tag data is long enough that we can more directly and more accurately model this component of the salmonid life cycle. Rather than estimating SAR from Lower Granite Dam back to Lower Granite Dam (and then backing out in-river survival), we can isolate fish detected at Bonneville Dam as juveniles and estimate their survival back to Bonneville Dam. Therefore, no in-river survival adjustments are necessary and resulting estimates of ocean survival are independent of estimates of downstream and upstream in-river survival.

Data sources

PIT-tag data were assembled by Columbia Basin Research (CBR) via PTAGIS for outmigration years 2000 through 2013. These data go through a rigorous set of algorithms to determine whether data are from juveniles or adults and from transported or in-river migrants. Additionally, data files include 1) last detection date at Bonneville Dam as juveniles, 2) rear type (hatchery or wild), and 3) whether fish survived back to the river. For survivors, the file also includes the number of years fish spent in the ocean and the date and location of the first adult detection at one of the mainstem Columbia River dams. Updates to these files will be posted each year on the CBR website (http://www.cbr.washington.edu/).

We obtained covariate data from a variety of sources (Table 1). Variables represent large-scale oceanographic patterns as well as regional and local physical and biological metrics. Although not all variables will have a direct mechanistic relationship with salmon survival, these variables occupy many locations along the continuum of being easily accessible vs. being mechanistic.

Table 1. Covariate data and sources.

Variable	Description	Years Available	URL / Source
CRflow.spr **CRflow.sum**	[A]Seasonal Columbia River flow as measured near Bonneville Dam	1978-present	http://waterservices.usgs.gov/rest/DV-Service.html
CRtemp.spr **CRtemp.sum**	[A]Seasonal Columbia River temperatures at Bonneville Dam	1997-present	http://waterservices.usgs.gov/rest/DV-Service.html
cui.win **cui.spr** **cui.sum** **cui.aut**	[B]Seasonal coastal upwelling index	1946-present	http://www.pfeg.noaa.gov/products/PFELData/upwell/monthly/upanoms.mon
mei.win **mei.spr** **mei.sum** **mei.aut**	[B]Seasonal Multivariate ENSO Index	1950-present	http://www.esrl.noaa.gov/psd/enso/mei/table.html
npgo.win **npgo.spr** **npgo.sum** **npgo.aut**	[B]Seasonal North Pacific Gyre Oscillation	1950-present	http://www.o3d.org/npgo/npgo.php
npi.win **npi.spr** **npi.sum** **npi.aut**	[B]Seasonal North Pacific Index (index of Aleutian Low Pressure)	1899-present	https://climatedataguide.ucar.edu/sites/default/files/npindex_monthly.txt
oni.win **oni.spr** **oni.sum** **oni.aut**	[B]Seasonal Oceanic Niño Index	1950-present	http://www.cpc.ncep.noaa.gov/products/analysis_monitoring/ensostuff/ensoyears.shtml
pdo.win **pdo.spr** **pdo.sum** **pdo.aut**	[B]Seasonal Pacific Decadal Oscillation	1900-present	http://jisao.washington.edu/pdo/PDO.latest
sst.win **sst.spr** **sst.sum** **sst.aut**	[B]Seasonal coastal sea surface temperature, averaged over buoys (LAPW1, 46211, 46041, 46029, 46050)	1991-present	http://www.ndbc.noaa.gov/maps/nw_straits_sound_hist.shtml
ersst.DJF (win) **ersst.MAM (spr)** **ersst.JJA (sum)** **ersst.SON (aut)**	[B]Extended reconstructed seasonal sea surface temperature, Washington coast	1854-present	https://www.ncdc.noaa.gov/data-access/marineocean-data/extended-reconstructed-sea-surface-temperature-ersst-v3b accessed via http://cci-reanalyzer.org/Reanalysis_monthly/tseries.php (using E1: 237.1335, E2: 233.9523, N: 48.50611, S: 46.05009)
sstarc.win **sstarc.spr** **sstarc.sum** **sstarc.aut**	[B]Seasonal sea surface temperature from Johnstone and Mantua (2014)	1900-2016	http://www.ndbc.noaa.gov/maps/nw_straits_sound_hist.shtml
transport.win **transport.spr** **transport.sum**	[B]Seasonal Sverdrup transport, positive values indicate northward transport	1967-present	http://upwell.pfeg.noaa.gov/products/PFEL/modeled/indices/transports/transports.html

transport.aut			
UppTempWin[C]	Mean temperature in the upper 20m at station NH05 from Nov-May	1998-present	www.nwfsc.noaa.gov/oceanconditions
UppTempSum[C]	Mean temperature in the upper 20m at station NH05 from May-Sep	1998-present	www.nwfsc.noaa.gov/oceanconditions
DeepTemp[C]	Mean temperature at 50m at station NH05 from May-Sep	1998-present	www.nwfsc.noaa.gov/oceanconditions
DeepSalinity[C]	Mean salinity at 50m at station NH05 from May-Sep	1998-present	www.nwfsc.noaa.gov/oceanconditions
CopRichness[C]	Copepod species richness at station NH05	1998-present	www.nwfsc.noaa.gov/oceanconditions
NCopBiomass[C]	Biomass of northern species of copepods at station NH05	1998-present	www.nwfsc.noaa.gov/oceanconditions
SCopBiomass[C]	Biomass of southern species of copepods at station NH05	1998-present	www.nwfsc.noaa.gov/oceanconditions
BioTrans[C]	Biomass of southern species of copepods at station NH05	1998-present	www.nwfsc.noaa.gov/oceanconditions
IchthyoBio[C]	Biomass of ichthyoplankton collected across the Newport Hydrographic Line (Jan-Mar)	1998-present	www.nwfsc.noaa.gov/oceanconditions
IchthyoComp[C]	Species composition of ichthyoplankton collected across the Newport Hydrographic Line (Jan-Mar)	1998-present	www.nwfsc.noaa.gov/oceanconditions
PC1	First Principal Component of NWFSC variables	1998-present	www.nwfsc.noaa.gov/oceanconditions
IGF	Insulin-like Growth Factor 1	1998-present	Brian Beckman, pers. comm.
CRflow7 **CRtemp7** **SST7** **CUI7**	Derived variables. Computed for each fish individually as the mean value of each variable over a 7 day period starting the day the fish passed Bonneville Dam	NA	See above

A Seasonal Indices represent the average of daily values, spr=Mar-May, sum=Jun-Aug
B Seasonal Indices represent the average of daily values, win=Dec-Feb, spr=Mar-May, sum=Jun-Aug, aut=Sep-Nov
C NWFSC sampling, summarized in PC1 and PC2

Sample sizes

The vast majority of PIT tagged fish in the last 20 years were from the Snake River Basin (>75%). As we develop these new methods for representing the ocean phase of the salmonid life cycle, we chose to focus on Snake River spring/summer Chinook because of their importance to the region, the advanced stage of the existing life cycle model for this group, and the large data set available. Once the main methods are worked out, we will expand the modeling effort to other stocks (e.g. Upper Columbia River spring Chinook).

An average of 82.5 thousand PIT tagged juvenile Snake River spring/summer Chinook were detected each year passing Bonneville Dam from 2000 through 2013. However, less than 3% of these fish were wild fish migrating in-river, the target group for our life cycle modeling efforts. The vast majority of PIT tagged Snake River Chinook were transported hatchery fish (Figure 1). Below, we evaluate whether we can include hatchery fish or transported fish in the model to increase sample size, with some sort of offset to account for differences among groups. From these data explorations, we concluded that using only the wild, in-river fish would be the most appropriate data set, despite the much lower sample size. This resulted in a total of 25,167 fish over 14 years.

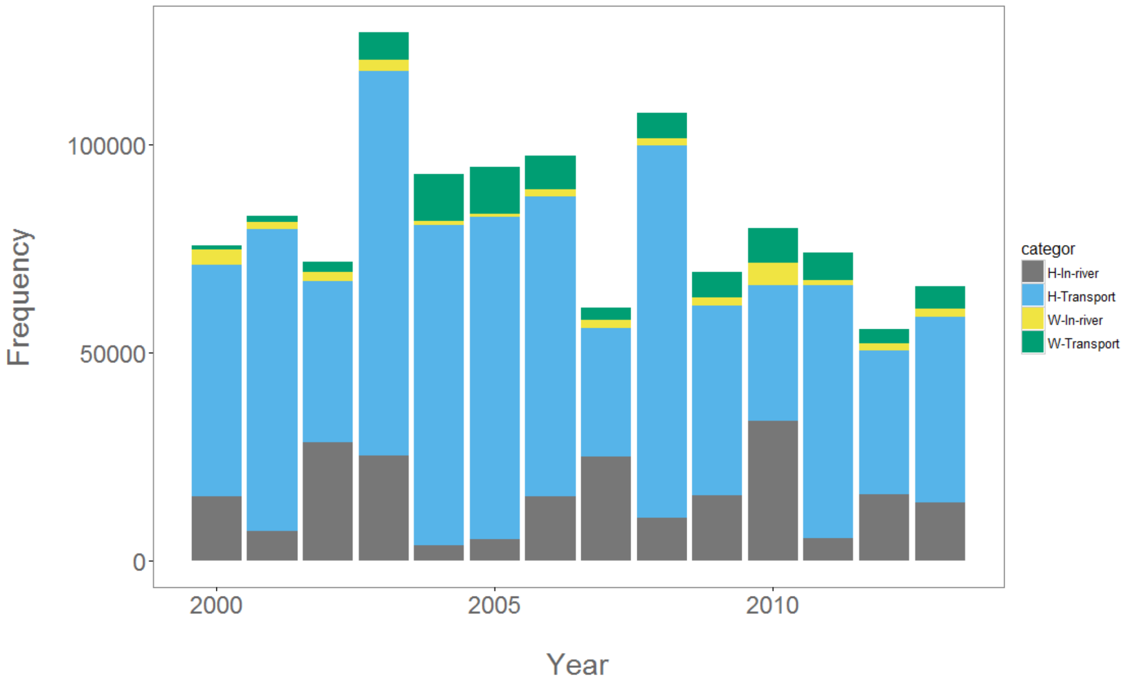

Figure 1. Frequency of PIT tagged fish per year, by rear type and migration route.

Hatchery fish

Given that over 90% of the PIT tagged juveniles detected at Bonneville Dam are hatchery fish, it would be worth including them in any analysis – if they survive at similar rates and respond to the environment similarly to wild fish. Unfortunately, a simple comparison between hatchery and wild fish survival (for in-river fish only) shows that wild fish can survive at rates anywhere from 0.5 to 2.5 times those of hatchery fish (Figure 2). The interannual variability in this relationship makes it difficult to account for it in models without adding a lot of model complexity.

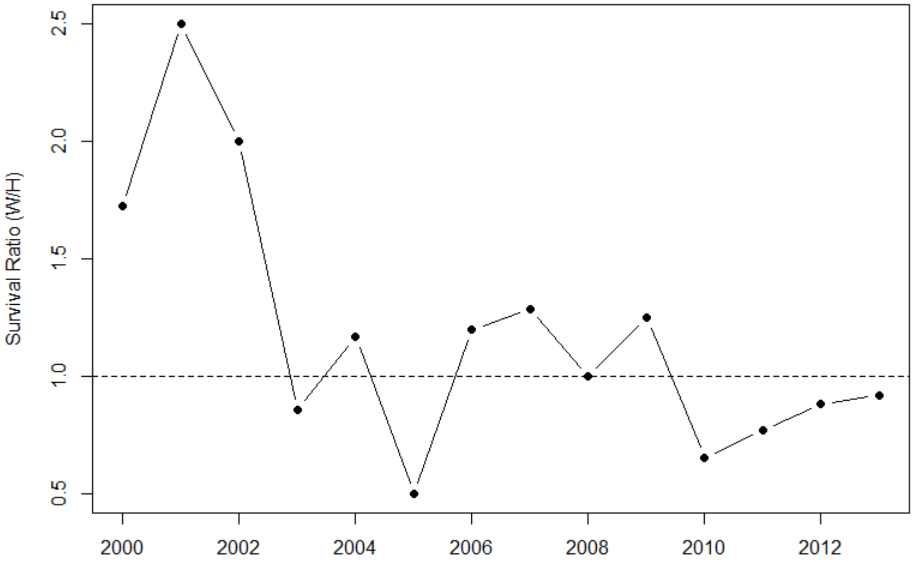

Figure 2. Survival ratio between wild and hatchery fish (values above 1 indicate wild fish survived at higher rates). Data for in-river fish only.

Another complication that comes with including hatchery fish in an analysis is the presence of minijacks. These are fish that migrate to the ocean (or, at least below Bonneville Dam), but migrate back upstream later that same year (as opposed to jacks, which spend one winter in the ocean). For the most part, wild fish do not exhibit this strategy, partly because maturation rates are determined by size and growth rate and wild fish are smaller than hatchery fish when entering the ocean.

When estimating and modeling ocean survival, we can either include minijacks or not. If we exclude them (delete the known minijacks, which are all survivors, from the data set), the presence of fish in a data set that would have been minijacks, but died prior to returning to the river will be lumped in with the rest of the mortalities (i.e., jacks and adults) and included in the denominator of survival rates, biasing the ocean survival rate downward. If we include minijacks, we can account for these fish with an additional parameter (representing the portion of the entire first ocean year survival that is experienced during the first couple months), but this would have to be assumed, as there are no data to fit against. Moreover, modeling the minijack response to ocean conditions can be difficult, because they experience such a short period in the ocean.

Transported fish

Similar to hatchery fish, if transported fish have a constant survival relationship with in-river fish, we can include them in the analysis, accounting for them with a model offset. The ratio of transport to in-river survival has been studied extensively (Anderson et al. 2012). As found in other analyses, this ratio is not constant in these data (Figure 3) and complicate the addition of transported fish into ocean survival models.

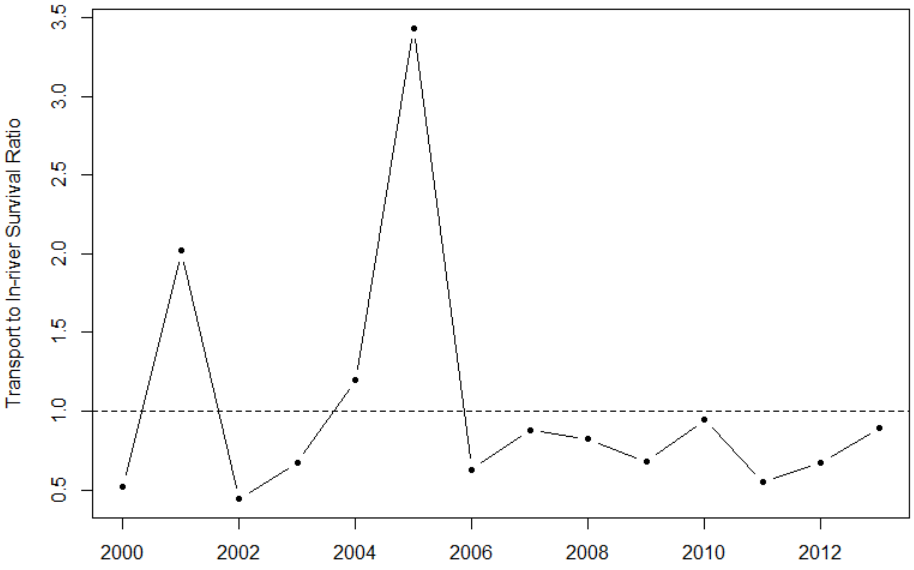

Figure 3. Survival ratio between transported and in-river fish (wild fish only).

Model structure

Using PIT tag data allows the use of individual fish in our analysis. For each fish detected at Bonneville Dam as a juvenile, we know the date it passed Bonneville Dam, the environmental conditions at that time, and whether it returned to the dam as an adult; detection efficiency in the adult ladders averages 98.7%, with a minimum of 95.2% in 2005, (Crozier et al. 2016).

We used a logistic regression model to determine the effect of environmental covariates on the probability an individual would survive (binomial response). As previous work has shown the importance of migration timing (Scheuerell et al. 2009, Holsman et al. 2012), we included Julian date at Bonneville Dam as a covariate. Moreover, the importance of timing can shift from year to year. We therefore allowed the effect of Julian date in the model to vary among years by treating it as a random effect (each year's coefficient is assumed to come from a common normal distribution of potential coefficient values).

Based on some support for a nonlinear effect of date, we tested a quadratic Julian date term. As the random component of mixed-effects models must be specified prior to model selection on the fixed effects (Zuur et al. 2009), we initially compared models with a linear random effect of date to models with a quadratic random effect. Over several model designs, the linear random effect of Julian date was better supported by the data. However, during initial model selection exercises, the squared term for Julian date was supported in the fixed-effects component of the model. Therefore, we chose a null model with a quadratic effect in the fixed-effects term and a linear effect in the random effects term:

$$logit(survival) \sim 1 + julian + julian^2 + (1 + julian \mid year).$$

A model with this structure would allow the effect of Julian date to be quadratic, with each year having a slightly different shape (Figure 4).

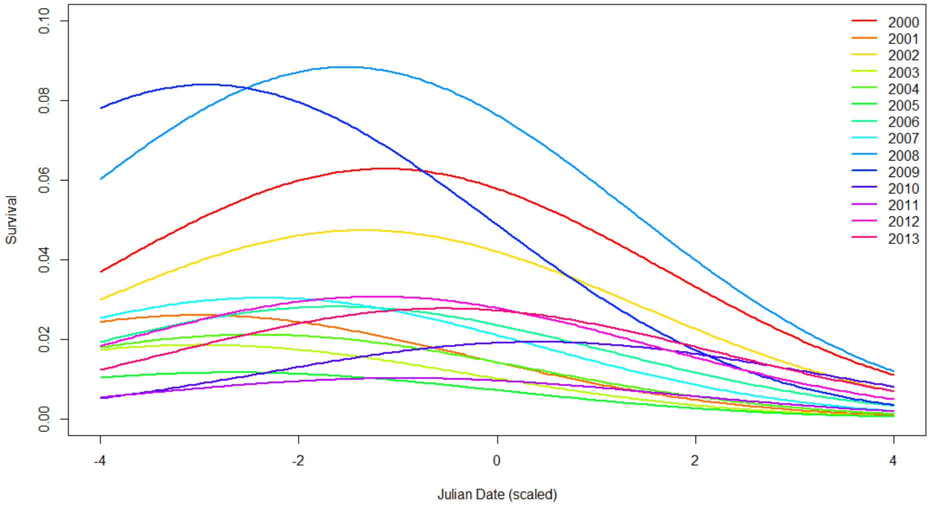

Figure 4. Effect of Julian date in the null model.

Other covariates were entered into competing models and we compared all subsets of covariates from Table 1, with a maximum of two parameters (in addition to the Julian date parameters) in any one model. Due to the large number of competing models, we refined the list of potential covariates by comparing univariate models to the null model. Only variables that resulted in at least a decrease of one AICc unit from the null model were considered for further analyses (Figure 5).

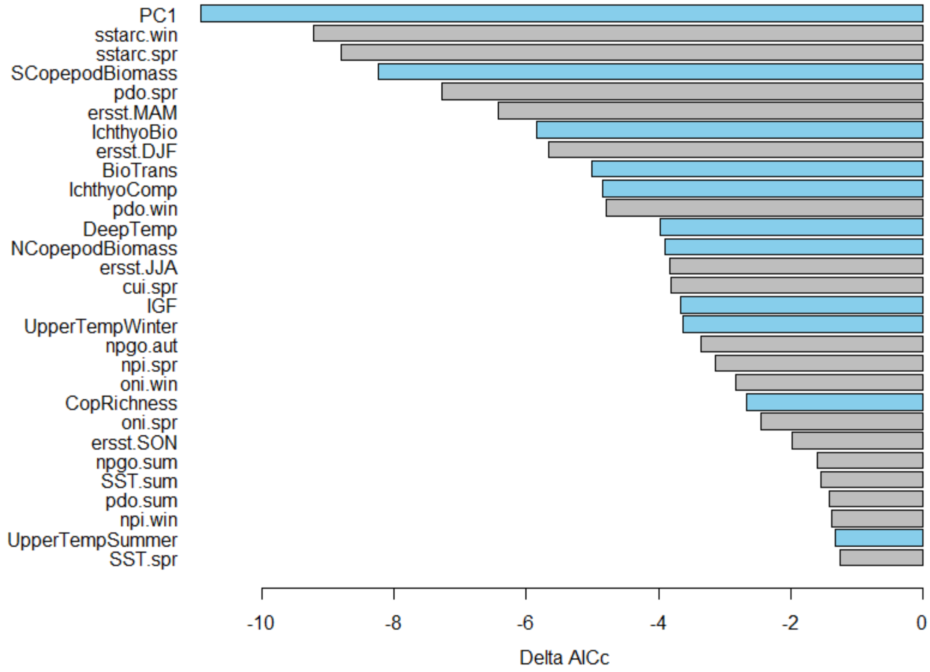

Figure 5. Univariate model comparison used as an initial covariate filter. Variables that did not improve the AICc by more than one unit over the null model are not shown and were not included in further analyses. Blue bars represent data coming from the NWFSC stoplight chart (www.nwfsc.noaa.gov/oceanconditions).

Many of the covariates tested have a substantial level of cross-correlation (Figure 6). We therefore excluded any two variables with an absolute value of the correlation coefficient greater than 0.7 from being in the same model.

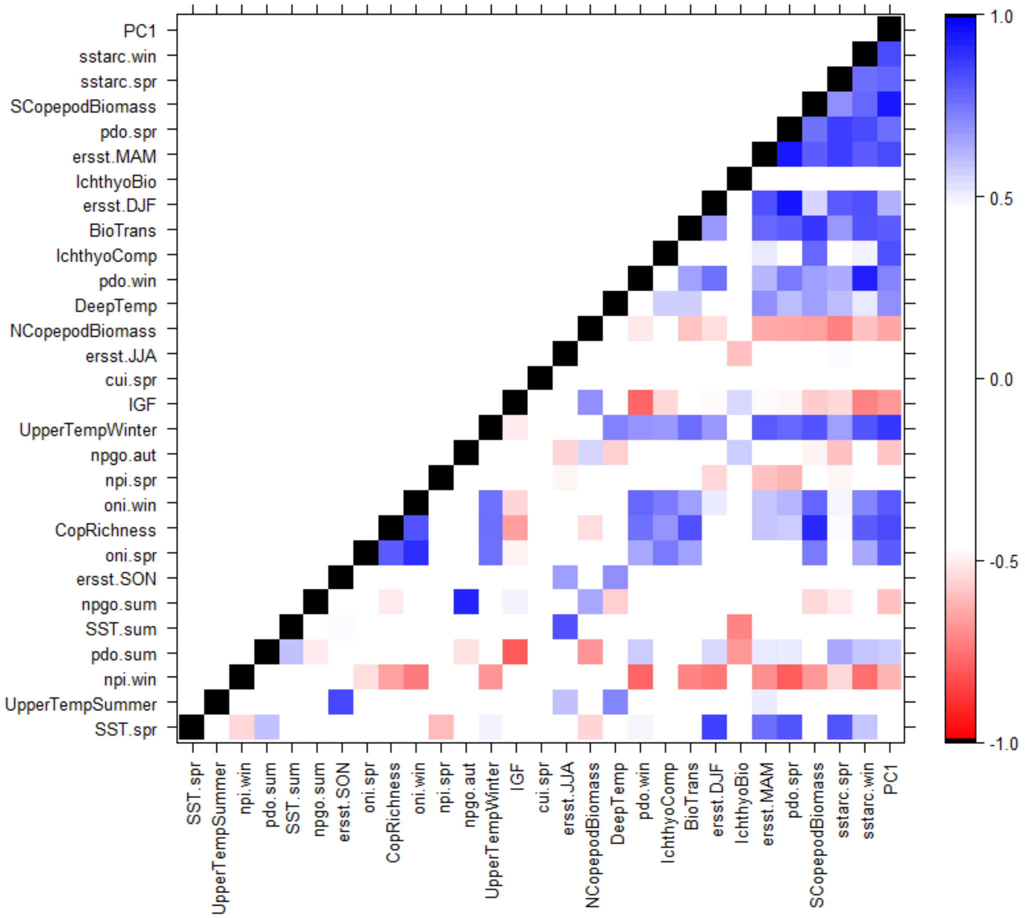

Figure 6. Correlation matrix (Pearson's correlation coefficient) among potential covariates.

Results for Snake data

Based on univariate models (the null model containing Julian date plus one other variable), 29 variables resulted in an improvement in the AICc of at least one unit over the null model (Figure 5). Eleven of the top univariate models represented a variable from the NWFSC stoplight chart (www.nwfsc.noaa.gov/oceanconditions), including the top univariate model.

We performed model selection across 358 models with a maximum of two additional variables to the null model. Although several potential covariates showed support from the data, the first principal component of the NWFSC stoplight chart had the highest mean importance, followed closely by sea surface temperature 'arc' in winter, winter ichthyoplankton biomass, and coastal upwelling in spring (Figure 7).

The best model included coastal upwelling in spring and the NWFSC stoplight chart PC1 (Table 2). This model fit the survival data quite well (Figure 8) and had relatively stable parameter estimates (Figure 9). Similarly good fits were obtained from many of the top models (Figure 10).

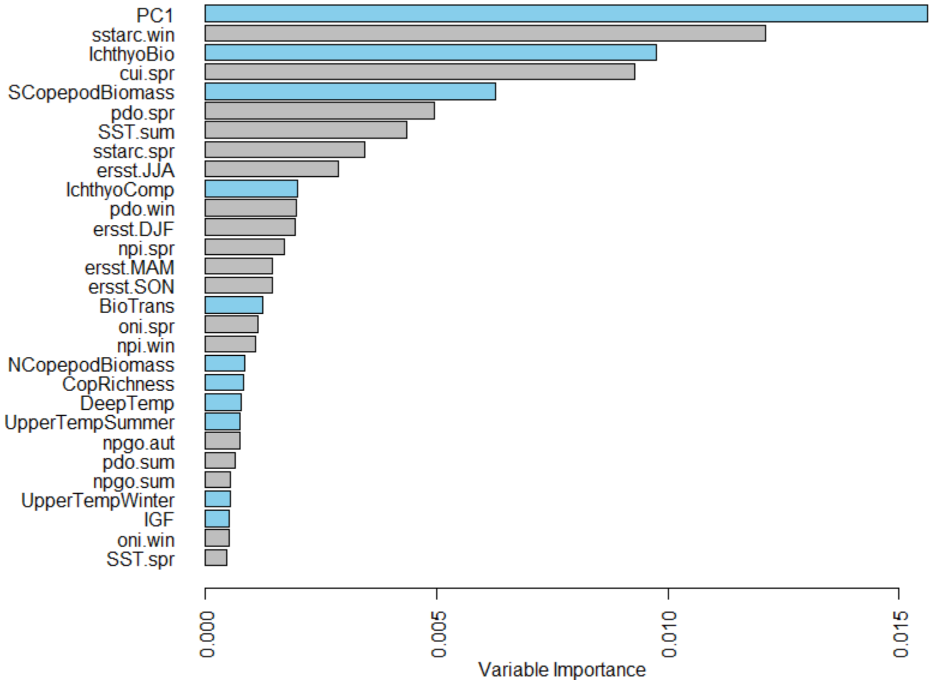

Figure 7. Mean variable importance scores (sum of the AICc weight of models containing this variable divided by the number of models containing the variable).

Table 2. Model selection table and standardized coefficients (only showing the top 6 models).

Model	Intercept	julian	julian^2	cui spr	ersst JJA	ichthyo bio	PC1	pdo spr	S. cop. bio.	SST sum	SSTarc win	df	AICc	Delta AICc	weight
1	-3.8	-0.28	-0.07	0.34			-0.61					8	5495.72	0	0.38
2	-3.8	-0.22	-0.08							-0.36	-0.59	8	5496.58	0.87	0.25
3	-3.78	-0.25	-0.07			0.44		-0.44				8	5497.36	1.64	0.17
4	-3.79	-0.25	-0.08			0.4			-0.52			8	5498.03	2.31	0.12
5	-3.78	-0.23	-0.07			0.34					-0.47	8	5498.58	2.87	0.09
6	-3.8	-0.24	-0.07		-0.31						-0.52	8	5498.93	3.21	0.07

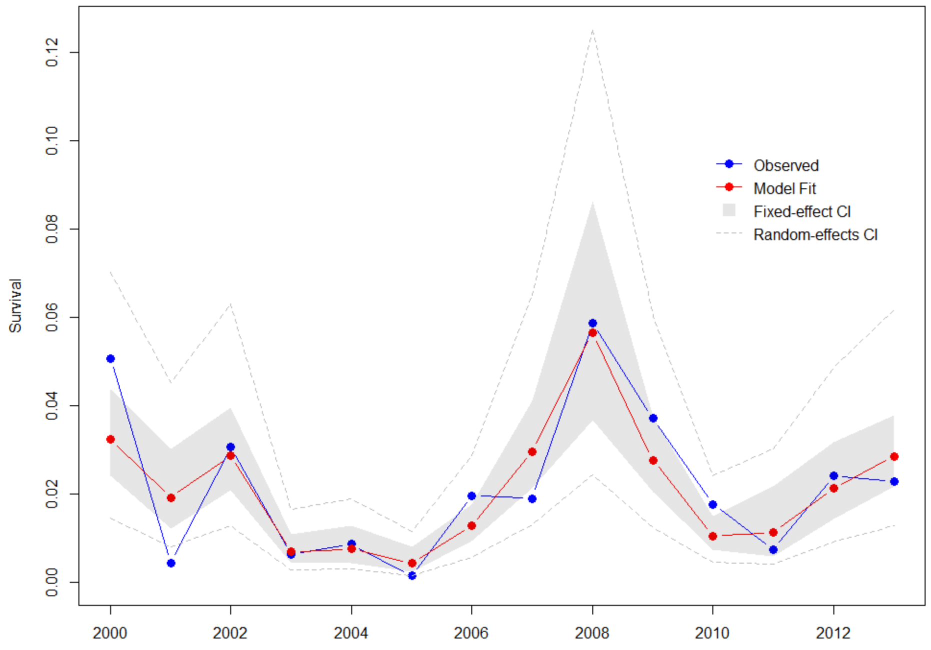

Figure 8. Observed survival and model fit from the best model.

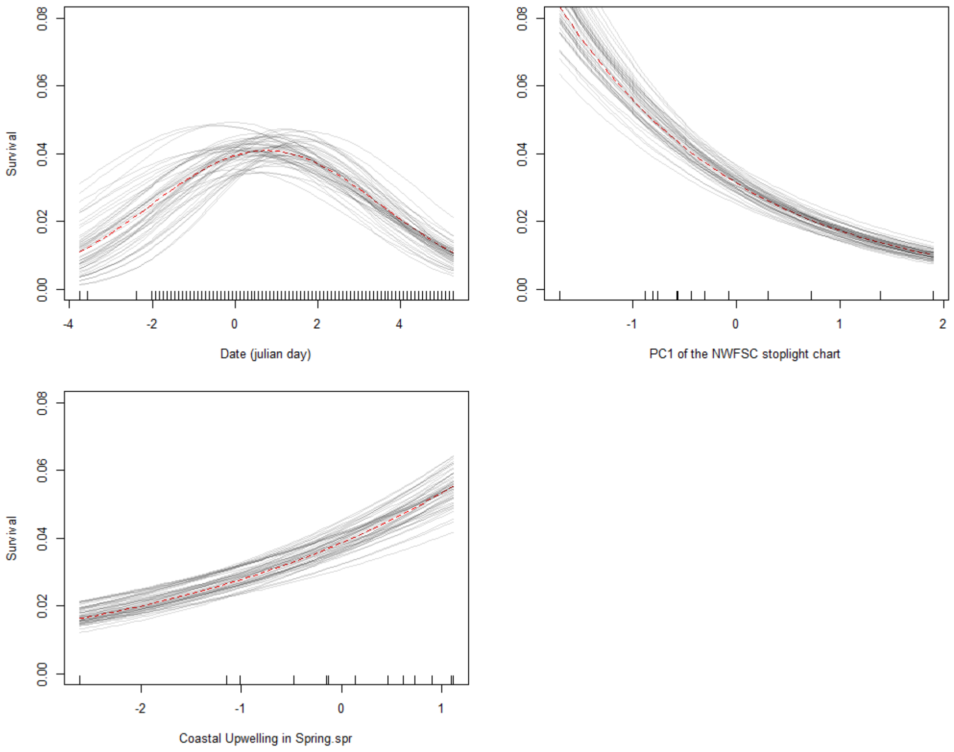

Figure 9. Cross validation to estimate the sensitivity of parameter estimates to the source data. We ran 50 iterations of k-fold cross validation where k=10.

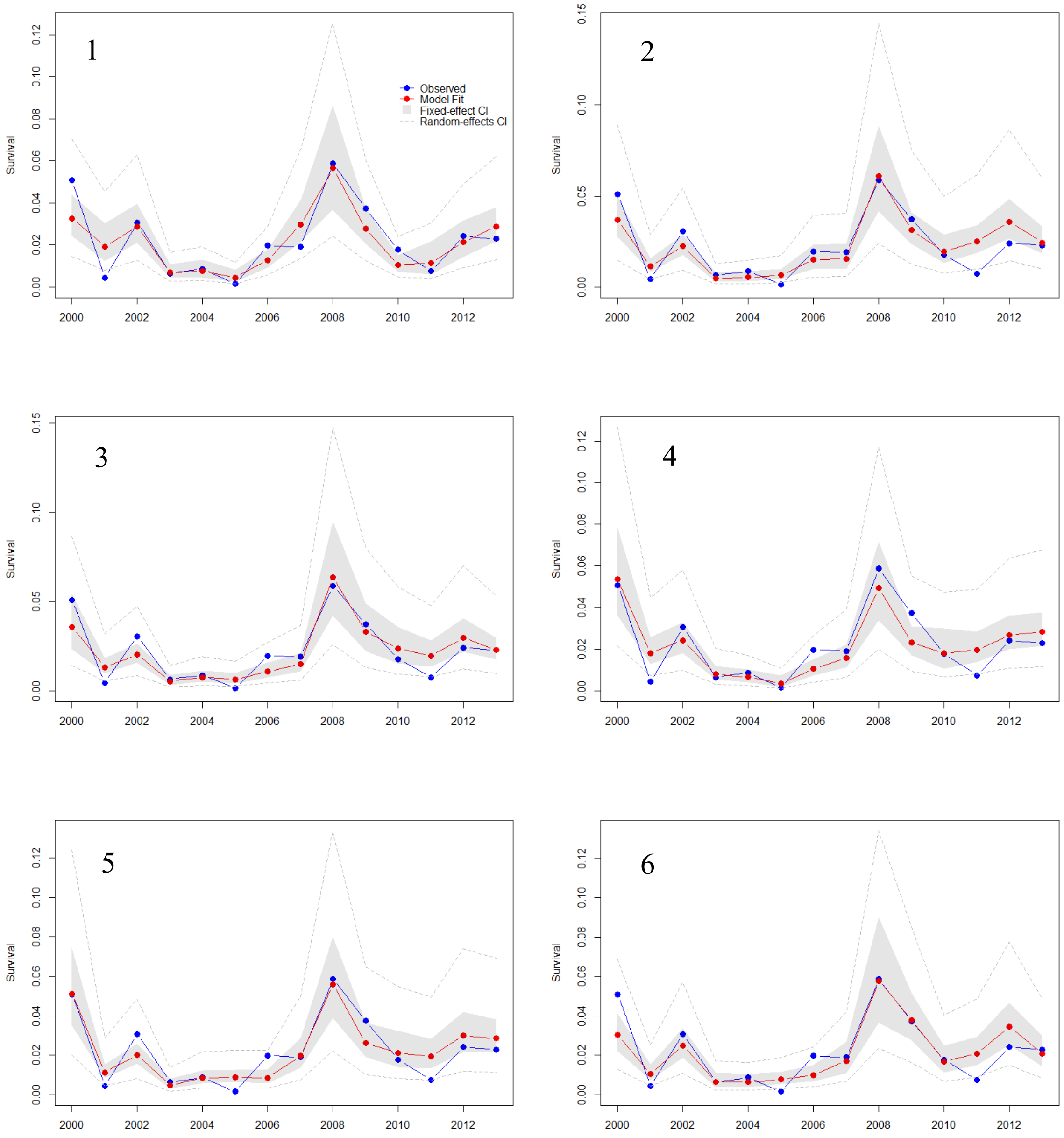

Figure 10. Model fit from the top 6 models.

Interestingly, a disproportionate share of the model support went to models that contained both a winter variable (before salmon out-migrated) and a spring or summer variable. Excluding some of the stoplight chart variables, many of which extend into the autumn, there were 66 models that had both a winter variable and a spring/summer variable, making up slightly less than 19% of the models. However, these models held over 31% of the AICc weight. This suggests that salmon survival is a complex result of environmental conditions across multiple seasons. Note, the top model does not technically qualify as having one winter and one spring or summer variable because PC1 extends across seasons and therefore was not included in this little analysis. However, it also supports (inherently) the idea of including information from multiple seasons.

Complications

Switching to PIT tag data comes with some complexities and new limitations. First, we can only use data from populations that have been PIT tagged in sufficient numbers. Many populations in the Snake River Basin have been PIT tagged since the late 1990s, but this is less true for the Upper Columbia River. Additionally, the various subbasins will have different amount of tagging effort, so distinct populations may be suboptimally weighted in the data set.
Second, the length of the time series is much shorter for PIT tag data than it is for SAR estimates. The main adult PIT tag detectors at Bonneville Dam were installed in 1998 and did not cover all adult routes until 2002 (http://www.ptagis.org/sites/mrr-site-metadata). For analyses here, we started all time series of PIT tag data in outmigration year 2000 (most Chinook return after 2 ocean years, which would be 2002). Using only cohorts that have completely returned to the river by 2016, this leaves 2000 to 2013, or 14 years of data. This is a relatively short period compared to the 35 years used in the previous analysis for Snake River Chinook (Zabel et al. 2013).

Discussion and future efforts

Even with the reduced sample size when excluding hatchery and transported fish, we were able to effectively model recent ocean survival of Snake River spring and summer Chinook salmon. Several of the competing models produced good fits and environmental data from multiple sources contributed significantly to these results. Given the early stage of these efforts, we are encouraged by results to date.

Additional populations

As we develop these methods further, we will be applying them to a second data set, in this case from the Upper Columbia River. A well-developed life cycle model for the Wenatchee Basin is currently being revised (see Chapter 9). Although smaller than the Snake River data set, this data set contains PIT tag data for about 67 thousand spring Chinook salmon over 14 years and should allow us to refine the ocean component of this life cycle model. The approach taken will be similar to one described here, though customization will result in some details differing.

Age structure

Faster-growing fish tend to return at younger ages, which is even evident in these PIT tag data (Figure 11). Smaller fish may spend more time in the ocean to increase size and gain mass for spawning, which can influence their survival. Therefore, age structure and ocean survival are explicitly intertwined. Age structure varies among years (Figure 12), although fish spending two years in the ocean dominate in almost every year.

A model structure that either predicts age structure as well as survival, or accounts for age structure while predicting survival would be a large improvement over the current method (see Chapter 7). However, due to their inter-dependent nature, it is very difficult to model age structure and survival together.

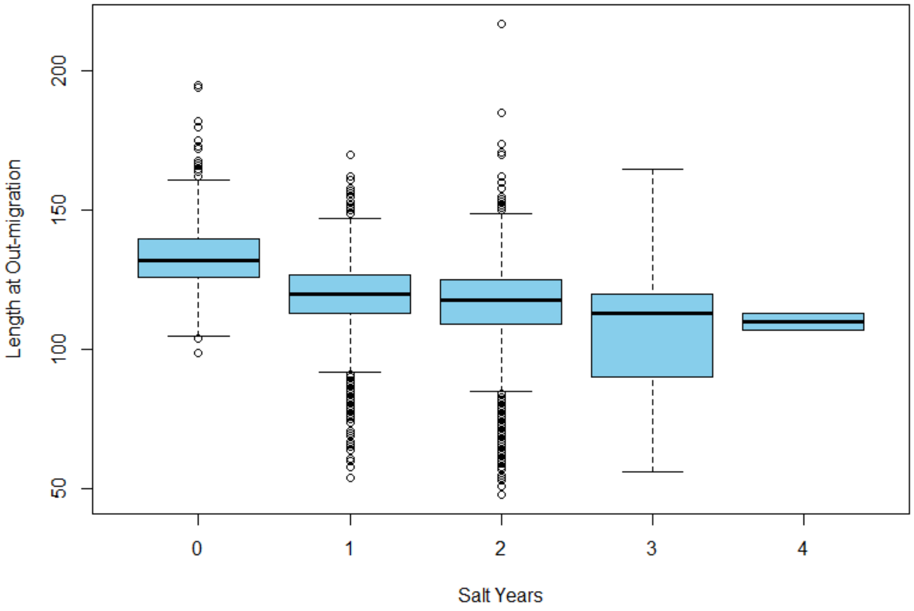

Figure 11. Juvenile salmon size distribution for fish returning after different number of years in the ocean (salt years).

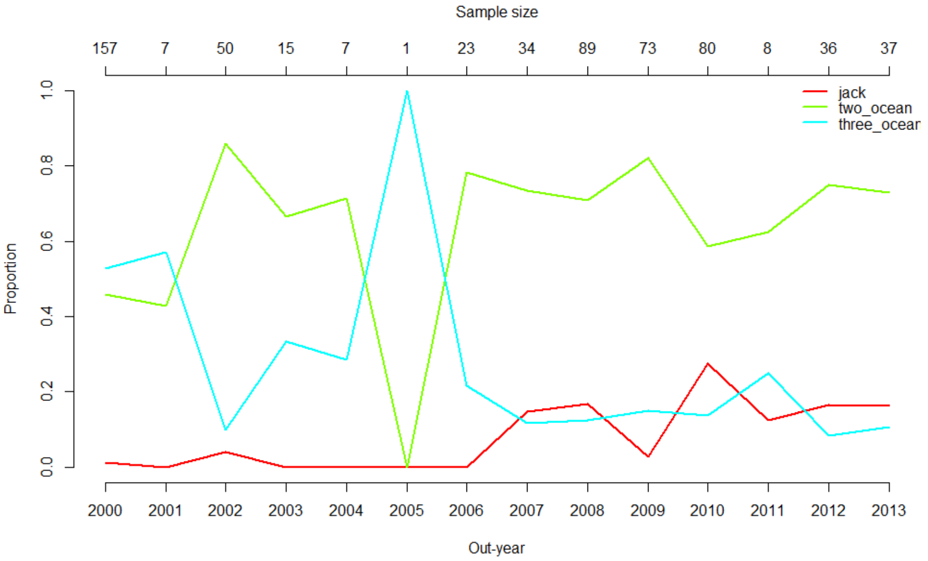

Figure 12. Age distribution for wild, in-river spring Chinook salmon. Sample size shown at the top.

Scenarios

One of the goals of LCMs is to have a quantitative tool to explore the effect of future climate change scenarios as well as potential management decisions. There are several ways to implement the evaluation of future scenarios. For example, a simple method would be to subsample observed survival rates, replicating a series of low (but observed) survival years to represent poor future ocean conditions or a series of high survival years to represent good ocean conditions. By skipping the environmental drivers, this method becomes easily implemented, but perhaps not very useful mechanistically.

More complex methods would involve using fitted models like those described here to forecast survival under estimated future climate scenarios. This approach depends on having future scenarios of the particular covariates that were important in the survival model (coastal upwelling and PC1 in this case). In this latter mode, the design of the model can have a large effect on how scenarios are created. For example, the effect of Julian date varied each year (by the design of the model). As scenarios are developed, we could subsample (with replacement) observed years, such that the effect of Julian date is pulled directly from one of the 14 years modeled, or we could create new year types, based on model-averaged coefficients. The impact of these decisions on model results are unknown and will have to be evaluated.

References

Anderson, J., K. Ham, and J. Gosselin. 2012. Snake River Basin Differential Delayed Mortality Synthesis. Battelle, Pacific Northwest Division, Richland, WA.

Crozier, L., E. Dorfmeier, T. Marsh, B. Sandford, and D. Widener. 2016. Refining our understanding of early and late migration of adult Upper Columbia spring and Snake River spring/summer Chinook salmon: passage timing, travel time, fallback and survival. Fish Ecology Division, Northwest Fisheries Science Center, National Marine Fisheries Service Seattle, WA.

Holsman, K. K., M. D. Scheuerell, E. Buhle, and R. Emmett. 2012. Interacting Effects of Translocation, Artificial Propagation, and Environmental Conditions on the Marine Survival of Chinook Salmon from the Columbia River, Washington, U.S.A. Conservation biology : the journal of the Society for Conservation Biology **26**:912-922.

Johnstone, J. A., and N. J. Mantua. 2014. Atmospheric controls on northeast Pacific temperature variability and change, 1900–2012. Proceedings of the National Academy of Sciences.

Scheuerell, M. D., R. W. Zabel, and B. P. Sandford. 2009. Relating juvenile migration timing and survival to adulthood in two species of threatened Pacific salmon (Oncorhynchus spp.). Journal of Applied Ecology **46**:983-990.

Zabel, R., et, and al. 2013. Life-Cycle models of salmonid populations in the interior Columbia River Basin. NWFSC, NOAA Fisheries, Seattle, WA 98112.

Zuur, A. F., E. N. Ieno, N. J. Walker, A. A. Saveliev, and G. M. Smith. 2009. Mixed effects models and extensions in ecology with R. Springer.

CHAPTER 4: HYDRO MODELING

4.a Integrated Population Model of the Grande Ronde Basin

Robert B Lessard (Columbia River Inter-Tribal Fish Commission)

Introduction

This analysis focuses on spring/summer Chinook salmon in the Grande Ronde basin. The Snake River spring/summer chinook ESU contains several major population aggregates in Idaho, Washington and Oregon. The Grande Ronde/Imnaha Major Population Group (MPG) consists of several populations migrating into the Snake river. The Upper Grande Ronde (GR), Catherine Creek (CC), Lostine/Wallowa (LOS), Minam (MIN), Wenaha (WEN), and Imnaha (IMN) are six populations making up the MPG, and are the focus of this analysis. The populations occupy a range of habitats of varying complexities and human land use, and vary in terms of their population sizes and productivities. Watersheds vary from highly disturbed to being predominantly contained in wilderness areas. Considerable habitat restoration efforts are under way in the more disturbed watersheds, and many have active hatchery supplementation programs.

This life cycle modeling analysis is aimed at providing perspective and guidance to restoration planning. Populations examined in this analysis all have unique challenges in freshwater, and yet all populations share common juvenile migration and ocean survival conditions. Recovery planning at the MPG scale can’t necessarily meet the unique needs of each population, but planning objectives can be sensitive to the unique responses that each population may have to broad scale recovery actions. In particular, hydro passage actions aimed at increasing mainstem juvenile survival needs to account for the relative responses of individual watersheds, and the differing potential for habitats to support additional spawners. By accounting for the individual freshwater production dynamics of each population, and examining how each population responds to mainstem hydro actions, planners can gauge the relative benefits of all types of recovery actions, and also gauge what levels of habitat actions need to be implemented to support recovery actions implemented via hydro operations.

By accounting for variability both in freshwater dynamics as well as in mainstem and ocean dynamics, a complete life cycle analysis can provide a probabilistic sense of recovery goals. Ocean survival probabilities have been associated with indices of ocean conditions such as the Pacific Decadal Oscillation (PDO) (Mantua et al., 1997), upwelling indices indicative of primary production, and sea surface temperature (Petrosky and Schaller 2010). Additionally, evidence has emerged that environmental conditions in the river affect the physical condition of out-migrating fish, and influence the rate of mortality after the fish enter the ocean (Petrosky et al. 2001; Budy et al. 2002). Petrosky and Schaller (2010) showed that early ocean survival varied with PDO, upwelling, and a variable describing juvenile interaction with powerhouses. The study found that the sum of the spill-adjusted powerhouse contact values (NPH) was negatively correlated with survival below BON and during the first year in the ocean.

In this analysis, survival is partitioned through the hydrosystem into transported and untransported life histories. Survival differences both during these two routes of passage, as well as survival differences that occur upon ocean entry are accounted for. The analysis is aimed at providing a quantitative assessment of the relative life cycle production benefits of improving survival conditions in the spawning and rearing versus improving survival conditions during juvenile outmigration through the mainstem. It applies population specific in-river harvest using US v OR Technical Advisory Committee (TAC) estimates of Zone 6 and commercial harvest, and includes brood stock removals and upstream conversion rates. The analysis provides a comparison of the potential benefits of managing freshwater spawning and rearing habitat for increased productivity and capacity, versus the potential benefit of managing the hydrosystem, and evaluates long-term projected return abundances. It uses estimated productivity and capacity rates in freshwater, and predicts the magnitudes of the effects of hydrosystem and environmental conditions on in-river route of passage and ocean survivals. To represent future unobserved environmental conditions, simulated time series of in-river and ocean variables are used that are either drawn randomly from historical values, or simulated to represent conditions similar to historical or expected future conditions.

Data

There are three types of data used in this analysis: 1. forcing variables used to predict survival (environmental and anthropogenic data), 2. empirical abundances (juvenile and adult) used for comparison with predicted abundances, and 3. survival rates used to compare to the predicted trends in survival.

The Northwest Fisheries Science Center of the National Marine Fisheries Service (NMFS) publishes salmon population summaries annually (SPS[1]). These summaries include annual estimates of the number of spawners, the age compositions of spawners, the proportion of hatchery fish on spawning grounds, and harvest rates. The annual record can be used to account for the number of fish of each age from each spawning year (or brood year) that later return to spawn, including those that were caught in fisheries or collected for hatchery brood stock. The full account of this is called a brood table and is used in this analysis for each of the six listed populations of the MPG. The time period was selected such that all populations were monitored and environmental data were available. Thus, early years where not all populations were monitored were not included. Adult returns were available up until 2013, meaning that three year old returns from brood year 2010 were accounted for, along with four year old returns from 2009, and five year olds from 2008. This results in a multi-population brood table spanning the brood years 1964 to 2008, where 2008 is the most recent brood year where all ages of adults have been observed on spawning grounds. Conversion rates, Zone 6 harvest estimates, and commercial harvest estimates from TAC Biological Assessment Tables were used to reconstruct the number of adults that would have been present at the mouth of the Columbia, based on the number that were observed on the spawning grounds. Those numbers are used to compare to the predicted returns to the mouth. Tributary harvest rates and collection for brood stock, which are also used in this back-calculation, were obtained from ODFW population reconstruction tables.

One facet of this analysis is focussed on the effects of environmental conditions in the

---

[1] https://www.webapps.nwfsc.noaa.gov/apex/f?p=261:home:0

Columbia River during smolt outmigration, and environmental conditions in the ocean when smolts enter their ocean residency stage. A powerhouse contact rate was derived from PIT tag data (PITPH) to predict in-river and ocean survival (Appendix J, McCann et al., 2015). The PITPH index uses the PIT tag detection rate and an estimated fish guidance efficiency to estimate the fraction of fish passing through the powerhouse (bypass and turbine routes combined). This is predicated on the fact that the actual number passing through the powerhouse is the number of bypass detections divided by the guidance efficiency. PITPH implicitly captures traditional spill and surface passage. The index is the sum of the fractions passing through the powerhouses of all projects combined.

An index of water travel time (WTT) was used to predict in-river survival. WTT was obtained by dividing the total volume of reservoirs by the flow rate, with adjustments in McNary pool to account for Columbia River versus Snake River flows (Tuomikosky et al., 2012). To predict the fraction of juveniles that are transported, an index (PTRANS) is used that was reported in the 2014 CSS annual report. For early ocean survival, the PDO in May and the upwelling index (UPW) in April are used, and additionally, a mechanism is implemented by which the ocean survival of in-river migrants is also affected by PITPH. The time series of environmental conditions is shown in Figure 1. PITPH appears to generally reflect the number of powerhouses in place and the proportion of total flow that has occurred as spill at each project over the time series. This time series encompasses a period of time when several changes took place in the hydrosystem. Fewer powerhouses were operational in the hydrosystem until the mid 1970's, so PITPH was lower. The transmission capabilities were limited prior to the construction of the DC and AC Intertie transmission lines, which resulted in a considerable amount of uncontrolled spill. As a consequence of this construction, the occurrence of uncontrolled spill declined. Full transportation as a mitigation measure was implemented for several years and no spill occurred at the transport projects. In addition, several planned spill programs were in place, including the Spill Memorandum of Agreement prior to the 1992 Biological Opinion. Subsequent increases in spill levels occurred through the series of Biological Opinions until the 2008 Biological Opinion.

The most significant changes in spill came after 2005, when a court opinion granted the summer spill portion of the National Wildlife Federation's request for injunctive relief to provide spill to gas cap limits at Lower Granite, Little Goose, Lower Monumental, and McNary dams.

Juvenile data (Favrot 2012[2]) are available for four of the six populations in the MPG: Catherine Creek, the Grande Ronde River, the Lostine/Wallowa and the Minam river. Data are not available for each year for each population, but the range was between 1992 to 2009, and some missing years are excluded from model fitting procedures.

SAR and in-river survival rates S_R were obtained from PIT tag data for migration years 1994 to 2012. Prior to 1992, SARs were obtained by dividing the returns to the mouth of the Columbia River by number of smolts at the upper dam (Petrosky and Schaller, 2010). For 1980 and prior migration years, data from Williams et al. (2001) were used for in-river survival rates. 1981-1984 in-river survival rates are from Marmorek and Peters (1998). Yearly variance estimates for SARs ($\sigma^2_{SAR,y}$) were derived by assuming a normal distribution in bootstrapped estimates and using the 90% confidence numbers to calculate a variance based on the upper and lower 90% values being at the value of the bootstrapped SAR $\pm 1.645\sigma_{SAR,y}$. Yearly variance estimates $\sigma^2_{S_{R,y}}$ for in-river survival were derived the same way.

Methods

Using maximum likelihood estimation, parameter estimates are obtained that best fit trends in abundance and survival. Additionally, the result of statistical fitting is used as the basis for predicting abundance trends under alternative potential changes to both tributary and mainstem survival. An Alternative Treatment Evaluation (ATE) is used to compare the potential relative benefit of a level of improvement to juvenile passage survival to a level of improvement in freshwater spawning and rearing productivity. The ATE method factors the uncertainty in parameter estimates into predictions, and therefore predicts the range of possible outcomes from each alternative treatment level.

---

[2] https://pisces.bpa.gov/release/documents/documentviewer.aspx?doc=P128637

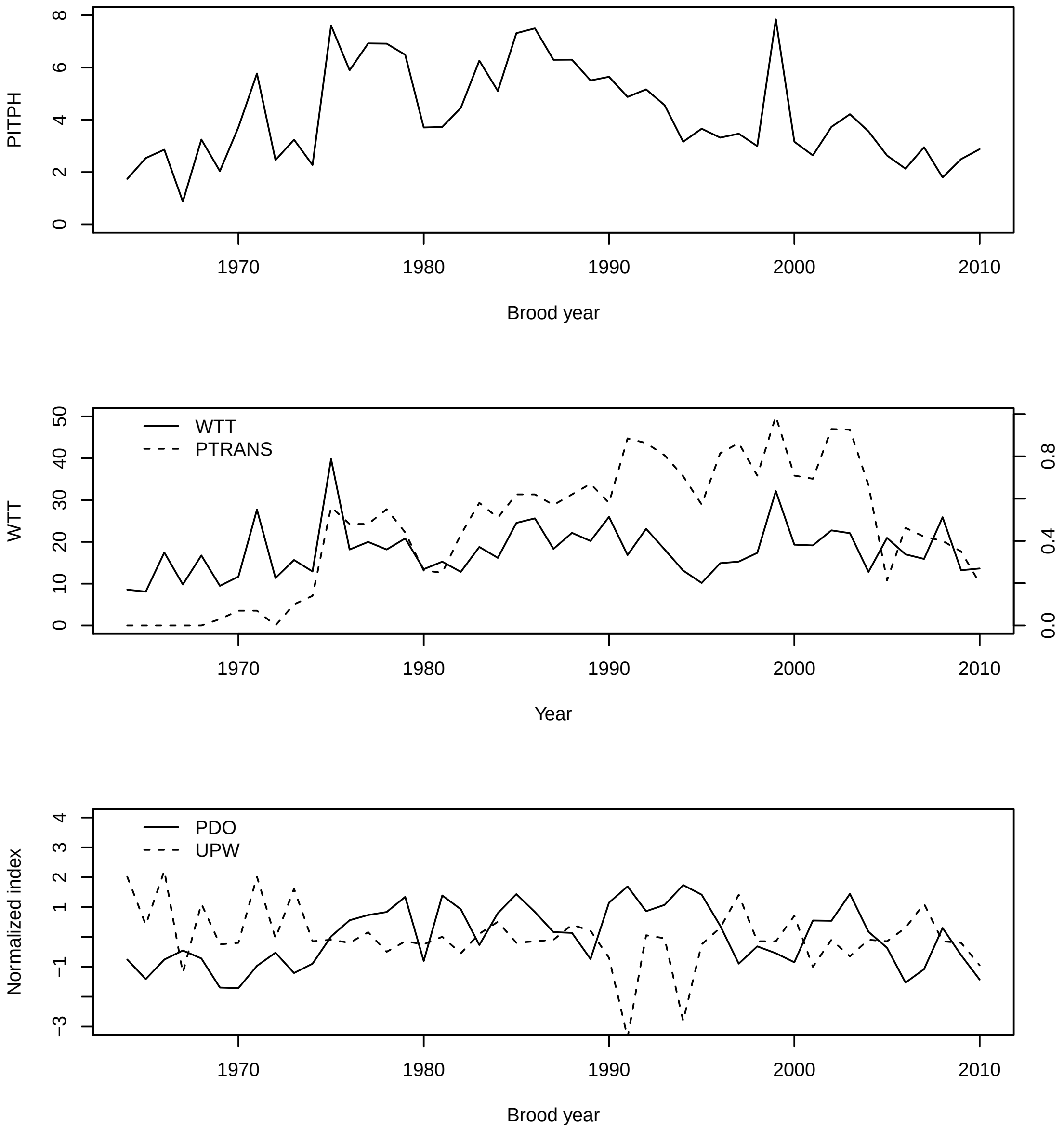

Figure 1: PITPH (upper panel) WTT and Transport (middle panel) and ocean environmental conditions (lower panel) used in model predictions.

Models

Typically, freshwater salmonid production is described in terms of spawners, eggs, fry, parr and smolts. Ricker (1954) and Beverton and Holt (1957) provided fundamentals useful in establishing spawner/recruit relationships. Both assume density dependence, and both are valid to describe survival between life history stages. The Beverton-Holt (BH) stock recruitment relationship is a somewhat more generic representation of density dependent survival, simply because it does not assume overcompensation, which is not realistic at every stage, nor even for spawner to smolt survival at low densities. Aa BH function was used to characterize survival between stages, though density dependence is only modeled at the smolt production stage, not in the mainstem, nor ocean stages.

Figure 2 shows the correlations between log of recruits per spawner for each population in the MPG. We see that recruits per spawner are correlated among populations, and nearly as correlated to the environmental indices, indicating that a large portion of the variability can be explained from the mainstem outward. The correlations should be expected to have some noise due to fluctuations caused by any density dependence in the tributaries, but correlation with the indices provides a basis for building a common relationship. At the very least, it is known that populations spawn and rear as juveniles in distinctly different spatial areas, then migrate to the ocean using the same pathway. The potential effect of distinct migration timing is not considered. Freshwater smolt production of distinct populations is predicted and merged together into a single migration unit, sharing common outmigration dynamics and a combined in-river/first year ocean survival, before maturing on a common maturation schedule and returning to spawn after 1, 2, or 3 winters in the ocean (see Figure 3). Migration through the mainstem explicitly distinguishes between transported and in-river juveniles migrating through the hydrosystem. This distinction is clearly formulated in the model description (Equations (9)-(11)), where it can be seen that each population has a transported and an in-river survival probability, and once the fish enter the ocean, the transported and in-river fish have different survival probabilities.

Figure 2: Correlation plots of log(R/S) of each population with PDO, UPW, PITPH, WTT, and PTRANS. Brood years 1964-2008 are included.

To estimate parameters, brood years 1964-2008 of observed spawners are used to predict age class returns from each brood year, and the predicted returns from observed data are compared to observed returns. The statistical estimation assumes that the age of returns are measured without error, and differences between observations and predictions are the result of errors in prediction, known as a process error model (Quinn and Deriso, 1999). The model was fit to empirical juvenile abundance data, adult abundance data, empirical in-river survival, and empirical SARs. Smolts were predicted from the combined natural and hatchery spawners on the spawning grounds, but the returning adults were compared to natural returns only, meaning that hatchery fish on the spawning ground contribute to production and their offspring are counted as natural production. The model fitting was performed using maximum likelihood estimation (MLE) techniques. Markov Chain Monte Carlo simulations (a Bayesian technique) was used to explore variability in parameter estimates.

Equations (1) - (8) describe the life cycle from spawners to adults for a single brood year. Upper case letters are state variables of predicted (indicated by ˆ) or observed life history stages. Lower case letters and Greek symbols are either estimated parameters, fixed parameters, or derived parameters. Table 1 describes each parameter and variable in the model, and whether it's estimated, fixed, derived, or predicted. Smolts in brood year t from population p are predicted from spawners as

$$\hat{M}_{p,t+2} = \frac{a_p S_{p,t}}{1 + a_p S_{p,t}/b_p} \tag{1}$$

where a_p is the productivity for population p. Adults in the ocean following one winter in the ocean are predicted by the relationship

$$\hat{O}_{1,p,t+3} = \overbrace{\tau_{t+2} \underbrace{0.98}_{Barge} \underbrace{s_{T,t+2}}_{Ocean} \hat{M}_{p,t+2}}^{Transported} + \overbrace{(1 - \tau_{t+2}) \underbrace{s_{R,t+2}}_{River} \underbrace{s_{H,t+2}}_{Ocean} \hat{M}_{p,t+2}}^{Inriver} \tag{2}$$

where τ_t is the proportion of juveniles transported estimated from PIT tag data. Transported fish are assumed to have transportation survival probability of 98%. $s_{T,t}$ is the survival in year t of

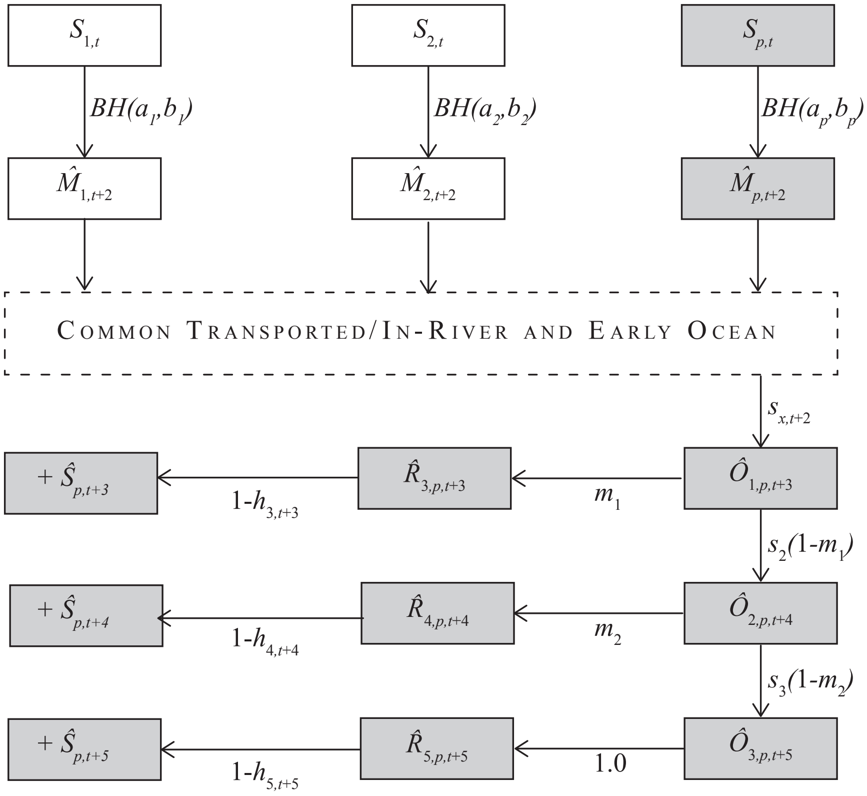

Figure 3: Diagram of the structure of the multiple population life cycle model. Shaded boxes indicate the trajectory of a single population. Before entering the common mainstem and early ocean phases, all parameters are unique to spawning populations. Afterwards, all populations share the same parameters. Spawners, smolts, ocean abundances, and returns are all indexed to brood year and population. Survival between the smolt stage and the end of the first year in the ocean ($\hat{S}_{x,t+2}$, where x denotes either transported (T) or in-river migrants (H)) is predicted differently for transported and in-river fish (Equations (9)-(11)). The + symbol before $\hat{S}_{p,t+a}$ indicates that unfished returns of age a are being added to the total number of spawners in year $t+a$.

Table 1: Description of variables and parameters used in Equations (1) to (12). All variables are time-indexed to brood year t. Parameters and variables indexed by population p have dimension 6. Parameters estimated directly are indicated. Parameters derived from auxiliary data and estimated parameters indicate equation of origin.

Variable	Parameter	Description (year t, population p)	Value
$\hat{M}_{p,t+2}$		Brood year t Smolts	Equation (1)[1]
$\hat{O}_{1,p,t+3}$		Brood year t first year ocean resident	Equation (2)
$\hat{R}_{3,p,t+3}$		Brood year t 1-salt returns	Equation (3)[1]
$\hat{O}_{2,p,t+4}$		Brood year t second year ocean residents	Equation (4)
$\hat{R}_{4,p,t+4}$		Brood year t 2-salt returns	Equation (5)[1]
$\hat{O}_{3,p,t+5}$		Brood year t third year ocean residents	Equation (6)
$\hat{R}_{5,p,t+5}$		Brood year t 3-salt returns	Equation (7)[1]
$\bar{R}_{p,j,i}$		Mean recruitment for spill scenario j, MCMC iteration i	Calculated
$\hat{S}_{p,t}$		Brood year t spawners	Equation (8)[1]
$S\hat{A}R_t$		Brood year t SAR	Equation (12)[1]
	$h_{p,t}$	Harvest rate for population p year t	Derived[2]
	a_p	Spawner to smolt productivity for population p	Estimated
	b_p	Spawner to smolt capacity for population p	Estimated
	$s_{R,t}$	Survival of in-river migrants from LGR to BON	Equation (9)
	$s_{H,t}$	Early ocean survival of in-river migrants	Equation (10)
	$s_{T,t}$	Early ocean survival of transported fish	Equation (11)
	τ_t	Proportion of fish transported	CSS estimate[3]
	s_2	Survival through second ocean winter	0.6[4]
	s_3	Survival through third ocean winter	0.7[4]
	m_1	Maturation rate after first ocean winter	0.02[4]
	m_2	Maturation rate after second ocean winter	Estimated
	δ_R	$s_{R,t}$ In-river logistic intercept	Estimated
	δ_{PH}	$s_{R,t}$ In-river logistic PITPH coefficient	Estimated
	δ_{WTT}	$s_{R,t}$ In-river logistic WTT coefficient	Estimated
	γ_H	$s_{H,t}$ Early ocean logistic in-river intercept	Estimated
	γ_T	$s_{T,t}$ Early ocean logistic transport intercept	Estimated
	γ_{PDO}	$s_{1,t}$ Early ocean logistic PDO coefficient	Estimated
	γ_{UPW}	$s_{1,t}$ Early ocean logistic UPW coefficient	Estimated
	γ_{PH}	$s_{1,t}$ Early ocean logistic PITPH coefficient	Estimated

[1] Observed quantities (without ˆ) also represented for these variables.

[2] https://www.webapps.nwfsc.noaa.gov/apex/f?p=261:home:0

[3] CSS 2013 annual report.

[4] Fixed value.

ocean entry from the tailrace of Bonneville dam for transported juveniles. $s_{R,t}$ is the in-river survival in year t of non-transported fish. $s_{H,t}$ is the survival in year t of ocean entry from the tailrace of Bonneville dam for in-river migrants. The number of 1-salt fish (three years old) that mature and migrate to spawn is given by

$$\hat{R}_{3,p,t+3} = m_1 \hat{O}_{1,p,t+3} \tag{3}$$

where m_1 is the maturation rate of 1-salt fish. The predicted abundance of 2-salt fish after the second year in the ocean is

$$\hat{O}_{2,p,t+4} = s_2(1 - m_1)\hat{O}_{1,p,t+3} \tag{4}$$

where s_2 is the survival probability in the second year. The number of maturing 2-salt fish (four years old) that return to spawn is

$$\hat{R}_{4,p,t+4} = m_2 \hat{O}_{2,p,t+4} \tag{5}$$

where m_2 is the maturation rate of 2-salt fish. The predicted abundance of 3-salt fish after the third year in the ocean is

$$\hat{O}_{3,p,t+5} = s_3(1 - m_2)\hat{O}_{2,p,t+4} \tag{6}$$

All fish are assumed to return after the third winter (five years old) in the ocean, i.e,

$$\hat{R}_{5,p,t+5} = \hat{O}_{3,p,t+5} \tag{7}$$

The number of spawners is the sum of the run of each age class of fish not harvested, where there is a harvest rate $h_{p,t}$ for each population p and each year t.

$$\hat{S}_{p,t} = \hat{R}_{3,p,t}(1 - h_{p,t+3}) + \hat{R}_{4,p,t}(1 - h_{p,t+4}) + \hat{R}_{5,p,t}(1 - h_{5,t+5}) \tag{8}$$

The model predicts three survival probabilities through the hydrosystem until the end of the first year in the ocean: 1. the in-river survival probability $S_{R,t}$, 2. the first year ocean survival probability of in-river migrating fish that are exposed to conditions in the hydrosystem $S_{H,t}$, and 3. the first year ocean survival probability of transported fish $S_{T,t}$. The predicted SAR is calculated from smolts and adult returns not harvested.

$$
\begin{aligned}
logit(s_{R,t}) &= \delta_R + \delta_{PH} PITPH_t + \delta_{WTT} WTT_t && (9)\\
logit(s_{H,t}) &= \gamma_H + \gamma_{PDO} PDO_t + \gamma_{UPW} UPW_t + \gamma_{PH} PITPH_t && (10)\\
logit(s_{T,t}) &= \gamma_T + \gamma_{PDO} PDO_t + \gamma_{UPW} UPW_t && (11)\\
SAR_t &= \frac{\hat{R}_{3,p,t+3} + \hat{R}_{4,p,t+4} + \hat{R}_{5,p,t+5}}{\hat{M}_{p,t+2}} && (12)
\end{aligned}
$$

Survivals are linear in logit space, with intercepts δ_R, γ_H, and γ_T. $\delta_{PH,WTT}$ and $\gamma_{PH,PDO,UPW}$ are slope coefficients that predict the magnitude of influence of environmental factors. PITPH is implemented in such a way as to allow the parameter estimation to predict if it is significant in both in-river and early ocean survivals. The logit transform is used here because it allows the search algorithm in the statistical fitting procedure to choose values of the δs and γs in the range $(-\infty, \infty)$ without causing the survival estimate to leave the range (0,1).

Model fitting

Parameters are estimated by comparing the predicted to observed smolt and adult abundances, as well as comparing predicted to observed in-river survival and overall SARs. The abundance comparisons include comparing the total returning adult fish of each age $R_{a,t}$ to the returns of each age in the NMFS population summary data, and comparing the predicted smolts to observed smolts. The returns at age for each year in the NMFS data are obtained by adding the spawners of a given age to the catch and hatchery broodstock collection, if any. The parameter estimates are obtained by minimizing the negative log-likelihoods of the following Equations:

$$\mathscr{L}_{R_{p,a}}\left(R_{a,t}|\Theta_p\right) = \prod_{t=1}^{n} \frac{1}{\sigma_{R_{p,a}}\sqrt{2\pi}} \exp\left[-\frac{\left(log(R_{p,a,t}) - log(\hat{R}_{p,a,t})\right)^2}{2\sigma^2_{R_{p,a}}}\right] \quad (13)$$

where Θ_p is the set of parameters a_p and b_p for p=1...6, m_1, and m_2, and also the δs and γs that predict survivals in Equations (9)-(11). $\sigma^2_{R_{p,a}}$ is the process error variance of the prediction of returning spawners at age. The likelihood term for smolts (Equation (14)) uses the same form, but uses observed and predicted juvenile numbers for the populations that had juvenile surveys and is given by

$$\mathscr{L}_{M_p}\left(M_{p,t}|\Theta_p\right) = \prod_{t=1}^{n} \frac{1}{\sigma_{M_p}\sqrt{2\pi}} \exp\left[-\frac{\left(log(M_{p,t}) - log(\hat{M}_{p,t})\right)^2}{2\sigma^2_{M_p}}\right] \tag{14}$$

Predicted returns at age and smolt data are treated as having unknown σ^2_R. The negative log-likelihood is minimized while substituting the maximum likelihood estimate for σ^2_R into the likelihood equations. The substitution of this nuisance parameter with its MLE reduces the number of parameters that need to be estimated. This is done for both process and observation error assumptions. The MLE for $\hat{\sigma}^2_R$ is given by

$$\hat{\sigma}^2_{R_{p,a}} = \sum_t \frac{(log(R_{a,p,t}) - log(\hat{R}_{a,p,t}))^2}{n} \tag{15}$$

The same assumption was made for juvenile data, so $\hat{\sigma}^2_{M_p}$ is estimated using a similar substitution. The empirical in-river survival probability estimates (S_R) and the SAR are also included in likelihoods. The in-river survival likelihood is given by

$$\mathscr{L}_{s_R}\left(s_{R,t}|\Theta_R\right) = \prod_{t=1}^{T_R} \frac{1}{\sigma_{s_{R,t}}\sqrt{2\pi}} \exp\left[-\frac{(log(s_{R,t}) - log(\hat{s}_{R,t}))^2}{2\sigma^2_{s_{R,t}}}\right] \tag{16}$$

where the $\sigma_{s_{R,t}}$ come from the CSS 2013 annual report, and result in an inverse variance weighting of the in-river survival estimates for this likelihood term. The likelihood for the SAR is given by

$$\mathscr{L}_{SAR}\left(SAR_t|\Theta_{SAR}\right) = \prod_{t=1}^{T_{SAR}} \frac{1}{\sigma_{SAR}\sqrt{2\pi}} \exp\left[-\frac{\left(log(SAR_t) - log(S\hat{A}R_t)\right)^2}{2\sigma^2_{SAR}}\right] \tag{17}$$

where σ_{SAR} is treated the same way as in the abundance likelihoods, with the estimate of the standard deviation being substituted into the likelihood.

The likelihoods and the life cycle model were coded and implemented using the AD Model Builder optimization software (ADMB, free to download at www.admb-project.org). The package is designed for large scale non-linear optimization problems and is commonly used in fisheries stock assessments. The best fit to the data was obtained by minimizing the sum of all the negative logarithms of the likelihoods, which is equivalent to maximizing the product of the likelihoods. Rather than report the values of the maximum likelihood parameter estimates, the range of variability in parameter estimates is reported by performing Markov Chain Monte Carlo (MCMC) simulations using a Metropolis Hastings algorithm native to the ADMB package. The MCMC simulations produce samples of the posterior probability densities of each parameter. A chain of 1,000,000 samples was simulated after a burn-in period of 100,000 samples. An uninformative prior distribution for each parameter was assumed, so the limits of the range of the sampling distributions are bounded, but the shape of the distribution is predicted by the data. Sampling from the chain of parameter estimates obtained from the MCMC simulations, frequency histograms were produced that show the shapes of the distributions of parameter estimates. Whereas the maximum likelihood estimation provides estimates of each parameter at the mode, and an estimate of the variance in each parameter evaluated near the mode, the posterior densities reflect the frequency with which given parameter values are chosen at random and found to explain the data better than alternative random choices (the essence of MCMC simulation). Posterior distributions are presented in lieu of point estimates because this provides a better sense of how well the model was able to fit all abundance and survival data sources, and gives a relative sense of how well the data might have been explained by parameter values higher and lower than the most probable combination of parameters.

Prospective simulation

Parameters determine survival rates in relation to environmental conditions, as well as how recruitment differs among populations because of estimated productivities and capacities. We can use estimated parameter values to simulate projected future population trends by initializing the model with recent spawning abundances. Once the model predicts the adult returns, it can propagate population trends multiple generations into the future without the need for additional empirical spawning abundances. We can use the projected population trends as the basis for evaluating the relative benefits of alternative spill scenarios. Further, we can project the population trend response to these spill scenarios across ranges of potential changes to freshwater habitat conditions, and therefore the effect habitat restoration could have on freshwater productivity and capacity. Further still, by looking at the predicted response across ranges of variability in parameter estimates, we can examine the variability in the population trend response to spill and habitat restoration.

The life cycle model is used to predict the long-term effects of four experimental spill alternatives on population recovery. The experimental spill levels are defined in terms of the limits of total dissolved gas (TDG) produced at each project.

BiOp Maintain spill levels according to the regulations consistent with the current Biological Opinion.

115%/120% Increase spill up to limits of 120% TDG in the tailraces and 115% TDG in the forebay.

120% Increase spill up to a limit of 120% TDG in tailraces and forebays.

125% Increase spill up to a limit of 125% TDG in tailraces and forebays.

The actual spill percentage or volume to produce specified TDG levels depends on flows at each project (Appendix J, McCann et al., 2015). Since the goal of evaluating different spill scenarios is to evaluate the effect of spill on PITPH, each experimental level is evaluated at three flow levels (high, average, and low flow), which produces a total of twelve spill scenarios. Each scenario predicts a different value of PITPH, which was evaluated with spill caps applied to the hourly flow data at all eight projects from April 1 through August 31. Flow levels were used from

Table 2: PITPH and WTT values used for each spill and flow level.

Scenario	Spill level	Flow[1]	PITPH	WTT (days)
1	BIOP	High	2.99	13
2	BIOP	Average	3.06	16
3	BIOP	Low	1.95	26
4	115%/120%	High	2.37	13
5	115%/120%	Average	2.16	16
6	115%/120%	Low	0.87	26
7	120%	High	2.12	13
8	120%	Average	1.88	16
9	120%	Low	0.80	26
10	125%	High	1.01	13
11	125%	Average	0.44	16
12	125%	Low	0.28	26

[1] Flow were assumed to correspond to observed years
High=2011, Average=2009, Low=2010

specific years as surrogates for high, average, and low years. 2011 is used to represent a typical high flow year, 2009 to represent an average year, and 2010 to represent a low flow year. These three years represent a range of flow conditions relative to the historic data (1929 to 2012). The three years also represent operations that reflect the most recent configuration and operation of the FCRPS. While 2010 was not a low flow year when the whole spring and summer period is considered, the flows that took place during the spring period being modeled were considerably less than other years. Historical water transit times were used from 2011, 2009, and 2010 for the high, average, and low flow scenarios. The resulting values are in Table 2. Since the future projections lack the historical record of environmental conditions that existed during the statistical model fitting, time series of environmental variables need to be provided as model inputs. These inputs include: a powerhouse passage index, water travel time, PDO, upwelling, harvest rates, proportion transported, and conversion rates. Transport was set at 20% for all future years to reflect the declining rate of transport in recent years. The rest of the variables are described below.

PITPH The prospective simulations use powerhouse passage index values predicted for each of the twelve spill scenarios. PITPH values were produced using an estimate obtained from a statistical fitting of passage rates at known spill levels and known flow levels. Historical passage rates derived from PIT tag data were compared to flow and spill data to estimate the effectiveness of spill levels across a range of flow levels for each project. The cumulative powerhouse passage rate was obtained by summing the project rates. A powerhouse passage index specific to a combination of spill alternatives and flows was used for all future years, e.g., a BiOp spill at low flow would yield a value of PITPH, which would be assumed every year into the future. The methods to obtain these values are discussed in Appendix J of the CSS 2015 Annual Report.

WTT Water transit times were used from 2011, 2009, and 2010 to represent WTT in high flow, average flow, and low flow.

PDO The Pacific Decadal Oscillation is a statistical calculation of oceanographic conditions that does not have a mechanism for prospective prediction, but the historical record can be described as a temporally autocorrelated time series. In order to simulate future population trends in relation to the PDO effect that was estimate in the statistical fitting, something other than an average value needs to be used, otherwise none of the inter-annual variability in its effect on ocean survival will be simulated. To produce a "PDO-like" time series it should be noted that the PDO is normalized and roughly generates decadal cycles, but the predominant factor relevant to producing simulated future time series is that it vary from year to year, reach similar peaks and valleys to a historical record, and sustain increases and decreases predominantly for about 5 years before reversing direction. Ultimately, a simulated PDO need only produce a cyclical trend similar in frequency and magnitude to the PDO. A PDO time series was generated by creating a time series of random draws from a normal distribution $\epsilon_t \sim N(0,1)$. An AR(1) autocorrelation sequence was then generate, setting $\text{PDO}_1 = \epsilon_1$, and $\text{PDO}_t = 0.5\text{PDO}_{t-1}+0.7\epsilon_t$ for $t \in (2,n)$. The simulated PDO index was then normalized to ensure the range of values was on the same scale as the empirical PDO.

UPW The upwelling index has no cyclical trend, nor is it correlated with the PDO, nor does it have a discernible temporal trend. To generate a future time series, the historical time series was sampled at random.

Harvest Historical harvest rates of Snake River Spring Chinook have varied from as high as 70% in the late 1960's to under 10% in recent years. Those ranges of total exploitation rates are a combination of sequential harvests in commercial and sport sectors in the lower Columbia, Zone 6 harvest, tributary harvests, and brood stock removal. Regulations at current return abundances call for lower river and Zone 6 rates not to exceed 17%. Since the purpose is to simulate population recovery potential, return abundances can be expected to increase if management scenarios are effective. Harvest rates were therefore modeled to increase as return abundances increase. The harvest rate was modeled to increase asymptotically to 40%, and to reach 20% at an aggregate run abundance of 5000 for all populations.

Conversion Rate Conversion rates represent adult losses net of harvest, e.g., a conversion rate of 0.5 means that 2 adults would need to return to the mouth of the Columbia so that 1 adult could make it to the spawning ground. Those losses represent all factors not related to harvest, including predation loss, pre-spawn mortality, adult passage related mortality, and other causes. In recent years, conversion rates have been fairly high, and historically they were comparatively low because less passage infrastructure was in place. In an attempt to capture the variability, but contain the rate in the range of values of recent years where passage infrastructure is more representative of future conversion rates, random values were drawn from the most recent 20 years of conversions rates, which produced simulated future time series of conversion rates in the range of 60% to nearly 100%.

Each prospective simulation draws upon several things: 1. the underlying parameters that predict survival in relation to environmental conditions, 2. the projected environmental conditions, and 3. the alterations to underlying conditions that make up the basis for an alternative management scenario. In the hydrosystem, those are the four spill alternatives evaluated at three flow levels. In freshwater, the alterations are presumed levels of productivity or capacity that could be achieved via habitat improvements. Prospective simulations can capture all combinations of these alterations to the full life cycle, and represent the predicted outcomes in terms of the predicted uncertainty that arises from the underlying uncertainty in parameter estimates.

Alternative Treatment Evaluation

The MCMC simulations build a sequence of vectors of parameter values by generating values at random, and accepting or rejecting randomly generated vectors in proportion to the relative likelihoods of predicting empirical data. The sequence building proposes a potential improvement to the fit with a randomly generate alternative parameter vector. The proposed new vector is accepted or rejected based on relative likelihoods. Eventually, a sequence of a desired number of samples is produced, which contains many combinations of parameters. The more likely combinations appear in the chain more frequently than the less likely ones, so if we draw randomly from the posterior chain thousands of times, we tend to draw the more likely ones more often. With each draw, we can produce a simulated population trend that is different from another draw. We can simulate thousands of different population predictions, and the predictions themselves take on distributions. As a result, we can simulate a population trend where the conditions can be the same as historical conditions, i.e., same environmental and anthropogenic conditions, or we can simulate a trend where we manipulate key underlying aspects of the system to mimic a scenario or question of interest. The result of simulating contrasting scenarios provides a sense of how much change to overall system behavior can be expected from relative changes to underlying conditions. Those can either be natural biotic (change in food or competitors), natural abiotic (changes to climate and the environment), or anthropogenic (changes in exploitation or hydrosystem operations).

Posterior densities were used as a basis for simulating ranges of possible population trends when alternative spill levels are assumed under the three flow levels. The Alternative Treatment Evaluation (ATE) uses a 10,000 samples of parameter values drawn from the MCMC posterior chain to simulate future population trends until 2050. It initializes population projections with empirical spawners from 2010-2014 and parameters from a posterior sample, and uses simulated conditions in future years (PITPH, WTT, PDO, UPW, TRANS, commercial and Zone 6 harvest, and upstream migration survival) to predict subsequent spawners of each age in years 2015-2050. Predicted returning spawners in each year after the first complete brood year returns in 2015 are used to predict successive generations, meaning the model spawns new generations from predicted returns and does not require empirical spawners past 2014.

For the ATE analysis, two questions were posed: 1. What is the potential for changes to spawning and rearing productivity to increase long-term adult return abundance?, and 2. What is the potential for changes to hydrosystem operations to increase average long-term adult return abundance and SARs? To address these questions, prospective population trends were simulated, and average long-term return abundances and SARs were examined. Population trends were simulated 10,000 times by drawing parameter values randomly from the posterior chain saved from the MCMC simulations. 10,000 simulated population trends were produced for each of the twelve spill scenarios, which produces 10,000 population trends for each population, and therefore an average return abundance for each of the six population for each of the twelve scenarios. Comparing relative return abundance averages provides an indication of the relative benefits of the spill scenarios to each of the populations. Simulations were projected for 35 years and the last 10 years of complete brood returns were used to evaluate performance. Averages are reported over the period 2036 to 2045.

The potential for the relative benefits of spill scenarios to differ among populations was also examined. To examine the effect of different spill levels, average long-term abundances were simulated and the average recruitment abundance and SARs from each population were calculated. The following logic was used:

1. Start with scenario $j = 1$
2. Get PITPH$_j$ and WTT$_j$ for scenario j from Table 2

3. Set PITPH$_t$ = PITPH$_j$ for all years t
4. Set WTT$_t$ = WTT$_j$ for all years t
5. Draw a set of parameters Θ_i from the posterior chain
6. Simulate population trends from initial spawning abundances and calculate $\bar{R}_{p,j,i}$ for each population p, where $\bar{R}_{p,j,i}$ is the average recruitment to the spawning ground indexed by brood year, and averaged over the last ten years simulated.
7. Calculate $S\bar{A}R_{p,j,i}$ for each population p, where $S\bar{A}R_{p,j,i}$ is the average SAR in the last ten years simulated.
8. Return to step 5 until i = 10,000 draws of Θ_i
9. Return to step 1 and set j = j + 1 until the 12^{th} scenario
10. Use the 6 x 12 x 10,000 $\bar{R}_{p,j,i}$ and $S\bar{A}R_{p,j,i}$ arrays to show the quantile ranges of predicted average abundance and SARs from 2036 to 2045 for each population p of each spill scenario j.

To examine the potential effect of changes in productivity, $\bar{R}_{p,j,i}$ was simulated at four different spill levels across a productivity range of 50-250 smolts per spawner. Simulations were evaluated at average flow conditions only. Similar predictions at high or low flows would be relative to $\bar{R}_{p,j,i}$s evaluated at the MLE of productivity (i.e., $\bar{R}_{p,j,i}$ would be higher for low flows and lower for high flows). The following steps describes the procedure:

1. Get PITPH$_j$ and WTT$_j$ for scenario j = 2 from Table 2
2. Set PITPH$_t$ = PITPH$_j$ for all years t
3. Set WTT$_t$ = WTT$_j$ for all years t
4. Set a_p = 50 for each of the 6 population productivities and replace the value drawn from the chain with a_p.
5. Draw a set of parameters Θ_i from the posterior chain.
6. Simulate population trends from initial spawning abundances and calculate $\bar{R}_{p,j,i}$ for each population p, where $\bar{R}_{p,j,i}$ is the average recruitment to the spawning ground indexed by

brood year, and averaged over the last ten years simulated, where i is the iteration, and j is the level of a_p.

7. Go back to step 5 and repeat for 10,000 draws of Θ_i.
8. Go back to step 4 using a_p+10 until all 21 values the range $a_p \in$ [50-250] have been simulated.
9. Return to step 1 and set j equal to scenarios 5, 8, and 11
10. Use the 6 x 21 x 10,000 $\bar{R}_{p,j,i}$ array to show the quantile range of predicted average abundance from 2036 to 2045 for each population p of each level j.

To examine the potential effect of changes in capacity, a capacity range of 5000-50000 smolts was used, and $\bar{R}_{p,j,i}$ was simulated at four different spill levels evaluated at average flow conditions. The following steps describes the procedure:

1. Get PITPH$_j$ and WTT$_j$ for scenario j = 2 from Table 2
2. Set PITPH$_t$ = PITPH$_j$ for all years t
3. Set WTT$_t$ = WTT$_j$ for all years t
4. Set b_p = 5000 for each of the 6 population productivities and replace the value drawn from the chain with b_p.
5. Draw a set of parameters Θ_i from the posterior chain.
6. Simulate population trends from initial spawning abundances and calculate $\bar{R}_{p,j,i}$ for each population p, where $\bar{R}_{p,j,i}$ is the average recruitment to the spawning ground indexed by brood year, and averaged over the last ten years simulated, where i is the iteration, and j is the level of a_p.
7. Go back to step 5 using b_p+5000 until all 10 values the range $b_p \in$ [5000-50000] have been simulated.
8. Go back to step 4 and repeat for 10,000 draws of Θ_i.
9. Return to step 1 and set j equal to scenarios 5, 8, and 11
10. Use the 6 x 21 x 10,000 $\bar{R}_{p,j,i}$ array to show the quantile range of predicted average

abundance from 2036 to 2045 for each population p of each level j.

Results

The model was fit to juvenile abundance data, adult abundance data, and in-river survival and SARs using likelihood Equations (13)-(17). Every possible model combination was examined by including or excluding PITPH and WTT for predicting S_R with PITPH and WTT, and for predicting S_H and S_T with PDO, UPW, and PITPH (only S_H). Using AIC values to evaluate the top fitting model, the best fit occurred when PITPH and WTT were both included in the prediction of S_R, when PDO, UPW, and PITPH were included in the prediction of S_H, and when PDO and UPW were included in the prediction of S_T. This implies that the overall SAR has an in-river survival component that is affected by PITPH as well as an ocean survival that is affected by PITPH, i.e., hydrosystem effects predict variability in early ocean survival (a.k.a: delayed mortality). The top model was greater than 4 AIC units better fitting than the second best model, and was used as the basis for doing MCMC simulations and performing the ATE analysis.

Rather than present the point estimates of each variable, the posterior distributions are presented from samples of the MCMC chain (see Figure 4). The histograms show the relative frequency of parameter values when 1,000 samples are drawn at random from an MCMC simulation chain of one million estimates after a burn-in of one hundred thousand samples. Means and standard deviations are shown above each histogram. The MCMC plots illustrate the relative certainty in parameter estimates. The narrower the range of predicted values, the more informative the data were to explaining that parameter. In general, parameter estimation was bounded to restrict the search algorithm to look within biologically plausible ranges. In the case of productivity parameters like the Imnaha and Minam productivities, the estimates indicate that productivities might be higher than the allowed range, but the productivity was bounded to search between about 20 and 1000 smolts per spawner (actually, between 3 and 7 in log-space), which should be broad enough to fit any spawner to smolt relationship (approximately 0.4-40% egg to smolt survival). Possible explanations for this are under reported spawners, strong hatchery influence on spawning grounds, or over reported smolt abundance, all of which would elevate apparent smolts per spawner.

Figure 5 shows the correlations between environmental indices and predicted survival. It can be seen that the predicted $s_{R,t}$ is most related to PITPH (a negative relationship). There are strong correlations between PITPH and both $s_{R,t}$ and $s_{H,t}$. $s_{T,t}$ shows a very strong correlation with PDO and also with UPW – stronger than the correlation between $s_{H,t}$ and UPW.

By separating hydro passage into transported and in-river migrants, it is possible to further examine the effect of transportation. Predicted $S_{H,t}$ and $S_{T,t}$ are shown in Figure 6, and $S_{T,t}$ is consistently predicted to be lower than $S_{H,t}$. The predicted survival of in-river migrants are shown along with empirical data as well. The predicted SAR in Figure 6 is higher than the empirical SAR derived from the aggregate of the Snake River PIT tag data, possibly indicating that the Grande Ronde / Imnaha populations survive better than the Snake aggregate, but alternatively, this could be compensation for the fact that the predicted in-river survival is lower than the empirical trend in recent years. Figure 5 indicates that lower early ocean survival of transported fish may be attributable to the PDO, which is seen to have a higher correlation with $S_{T,t}$ than with $S_{H,t}$. The upwelling index is also only somewhat correlated with $S_{T,t}$, not with $S_{H,t}$. These two correlations suggest that transported fish are more sensitive to ocean conditions than in-river migrants, but the in-river migrants are modeled to be sensitive to PITPH, whereas transported fish are only modeled to be sensitive to PDO and UPW.

The model fitting results are shown in Figures 7 and 8. Since all populations are forced to follow the same mainstem and ocean dynamics, yet do not experience the same FSR dynamics, it should not be expected that all models fit their respective abundance data in the same way. CC and GR predicted recruits are negatively biased in the first half of of the time series. The remaining populations do not appear to have the same negative temporal bias in the same early time period, and overall the IMN, LOS, MIN, and WEN predicted population trends are consistent with empirical observations, i.e., a declining trend from the late 1960's until around

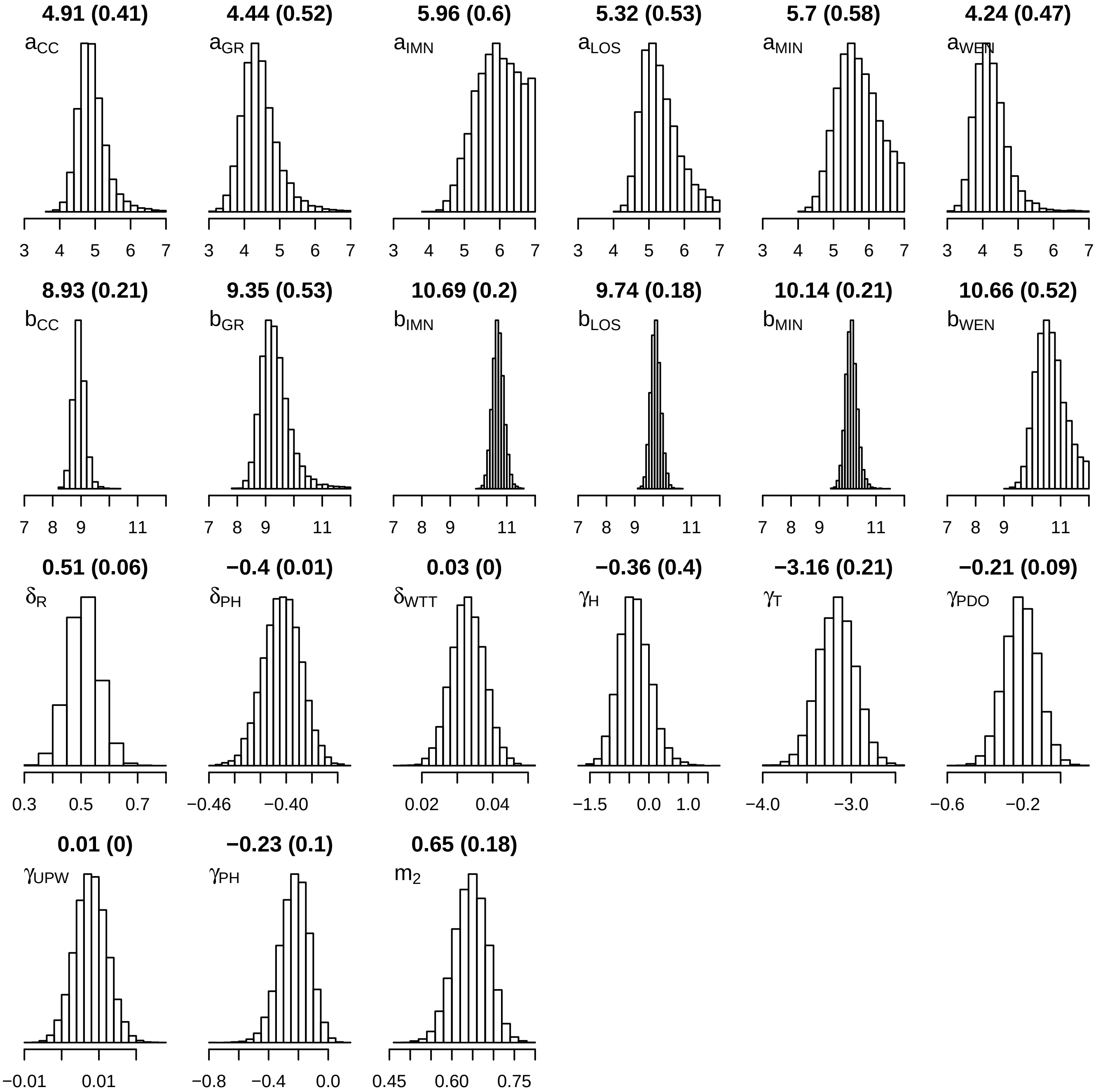

Figure 4: Posterior estimates of the model parameters for the model. Each histogram shows frequency of samples from parameter values coming from a Markov chain of length 1,000,000, sampled 10,000 times. Estimated means (and standard deviations) for each posterior sample appear at the top of each histogram. The top row contains the log productivities for CC, GR, IMN, LOS, MIN and WEN respectively. The second row contains log capacities for the same populations. The remaining posterior panels are labeled with corresponding symbols.

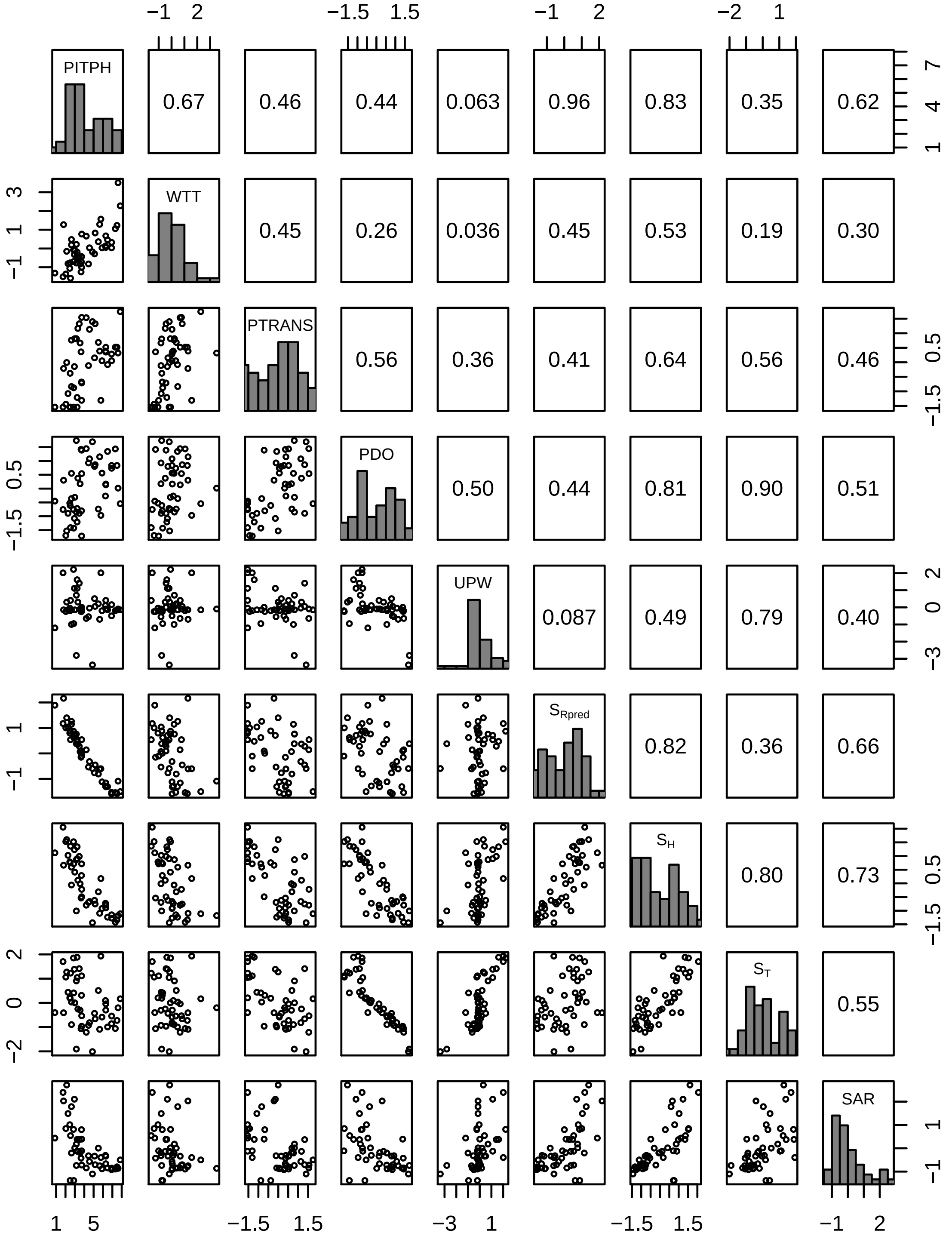

Figure 5: Correlations between estimated in-river, transported, and early ocean survival, and environmental indices. The lower diagonal shows the scatter plots between variables. The upper diagonal shows the correlation coefficients.

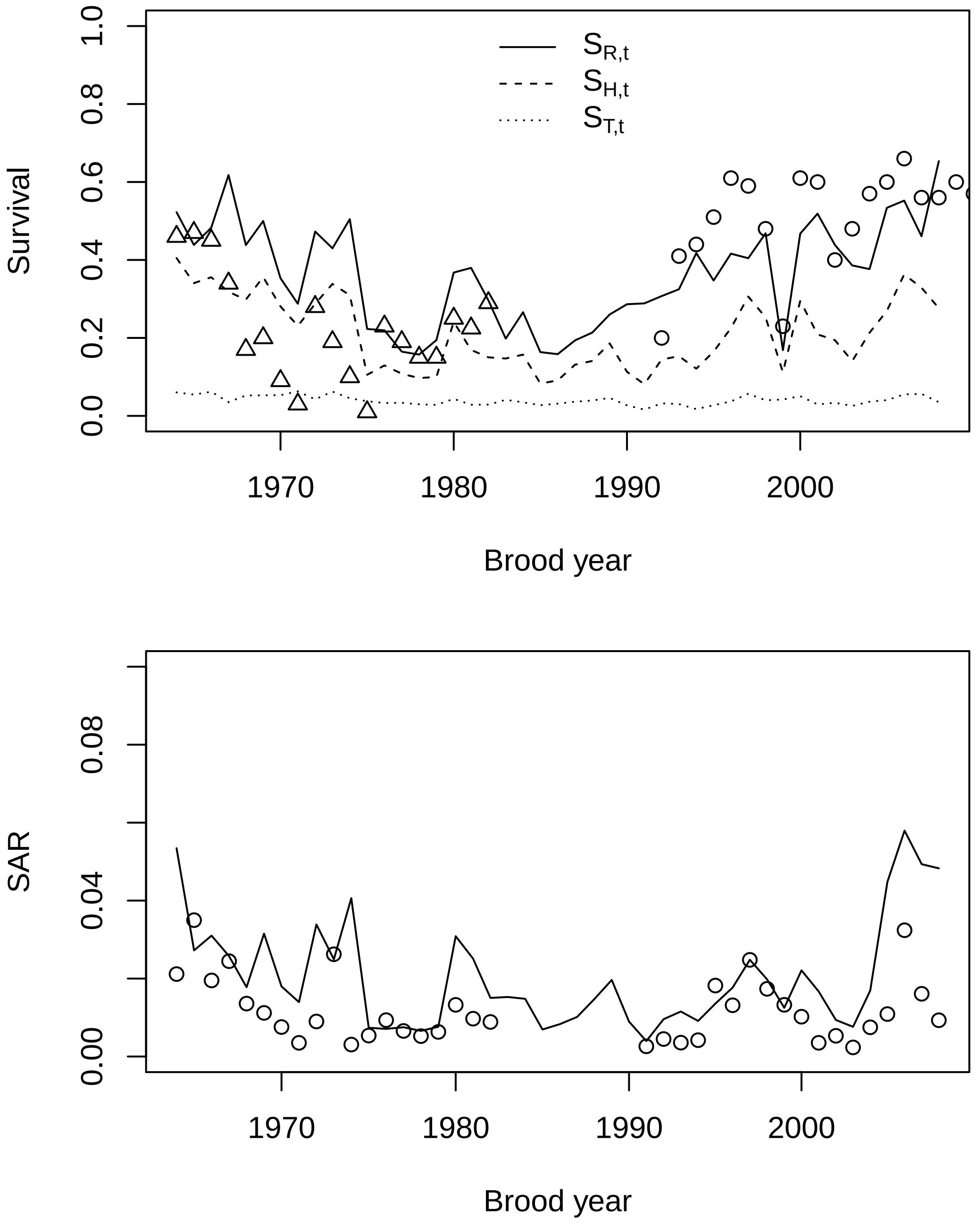

Figure 6: Upper panel shows observed in-river survival (circles) and predicted in-river survival S_R, early ocean survival for in-river S_H migrants, and early ocean survival for transported fish S_T. Circles show the PIT tag derived estimates of in-river survival. Triangles show the pre 1985 migration year in-river survival rates from Williams et al. (2001) and Marmorek and Peters (1998). Lower panel shows observed (circles) and predicted SAR (line).

1990, then an increase. The smolts per spawner fit (Figure 8) shows density dependence in all four populations for which smolt data were available.

Figure 9 shows the relative performance of the twelve spill scenarios across all six populations. The three assumed flow levels are represented in clusters of three (high, average, and low flow) in each four of the BiOp, 115%/120%, 120%, and 125% spill levels. The general pattern is that increasing the spill level produces an increase in the total average number of returning spawners, but within each spill level, the low flow scenario produces more returns than the high and average flow conditions. This is a product of the fact that the spill is more effective at lower flow, i.e., when spilling to the same TDG target, a smaller fraction of fish will go through the powerhouse in low flow years because of increased spill efficiency. The shaded boxes represent the 25% to 50% quartiles of average adult return abundances ($\bar{R}$) from a sample of 10,000 simulations drawing parameters from the joint posterior distribution of parameters. The whiskers extend the range to the outer 10% and 90%. Variation in simulated outcomes comes from the variability in parameter estimates, as well as the variability in the simulated PDO. The Upper Grande Ronde and Wenaha show the most variability in $\bar{R}$, likely owing to the fact that the combined uncertainty in productivity and capacity yielded more uncertainty in simulated outcomes.

Figure 10 shows the predicted average SARs for all six populations to LGR. The average SARs are not adjusted for harvest, meaning that the rate assumes adult returns to LGR after harvest and adult interdam losses. The SARs reflect the simulated harvest where the harvest rate increases asymptotically to a maximum of 40%, attaining a rate of 20% at 5000 total Grand Ronde / Imnaha returns to the mouth. The SAR can be viewed as more of a smolt to Spawner ratio, because it also captures what would otherwise have been considered tributary harvest and broodstock removals. As with the $\bar{R}$ shown in Figure 9, spilling to high TDG levels increases SARs, and all spill levels show the highest SAR at the lowest flow. At most spill levels, there is a greater than two fold increase in the SAR at low versus high flows. Across spill levels, there is approximately a two fold increase in the SAR when increasing TDG cap level from BiOp levels

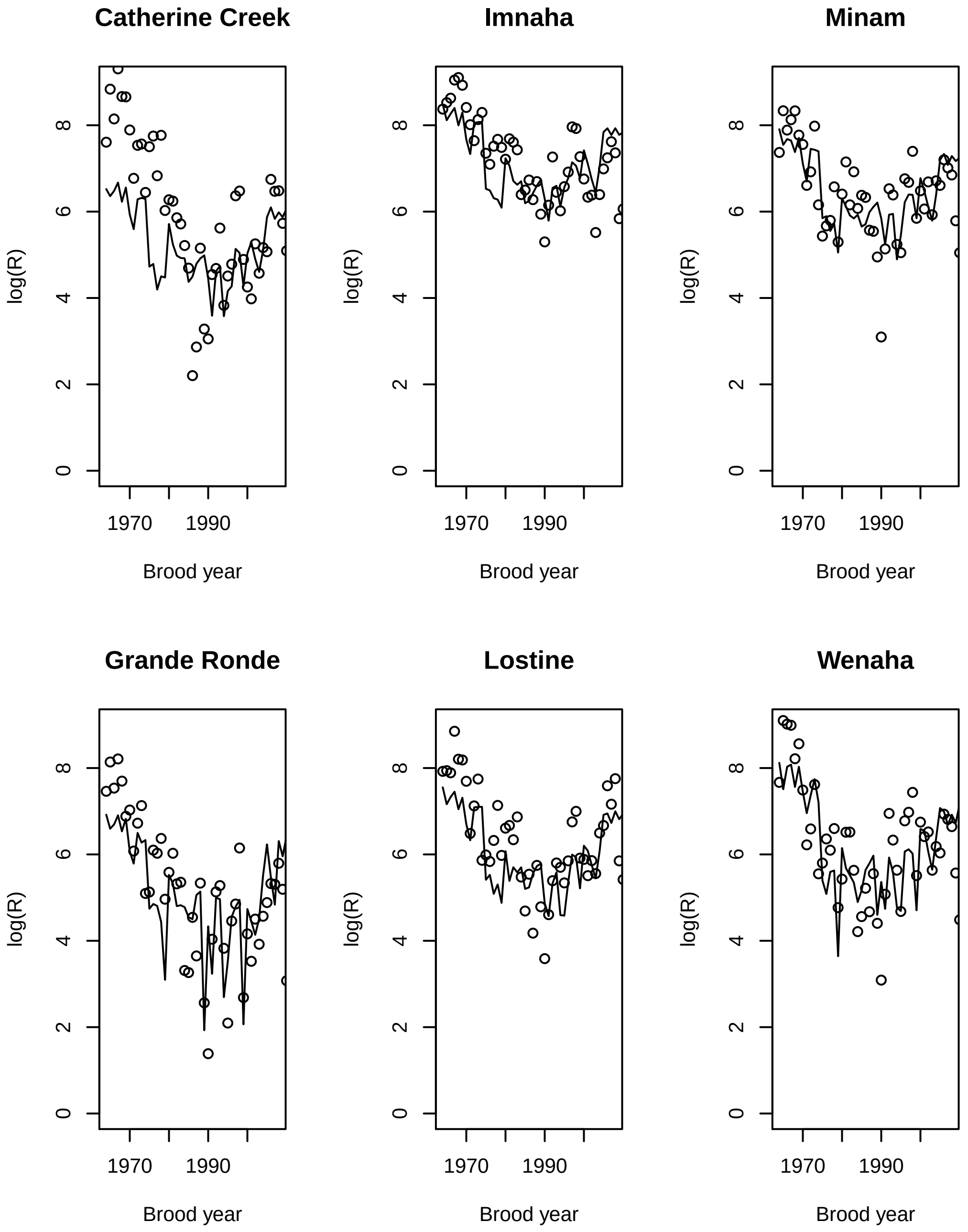

Figure 7: Observed (circles) and the predicted (line) recruits for each brood year.

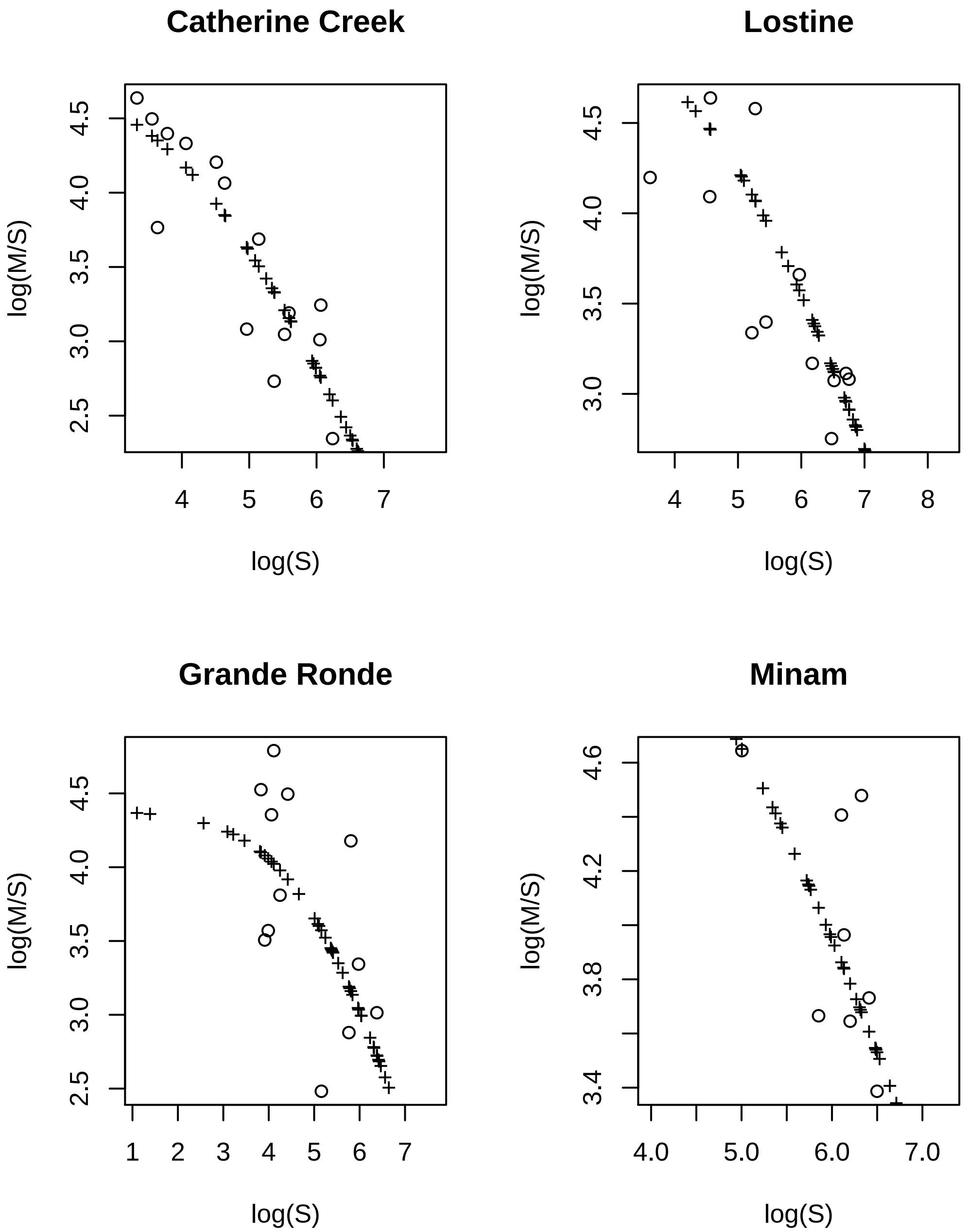

Figure 8: Observed (circles) and the predicted (plus symbols) smolts per spawner vs spawners.

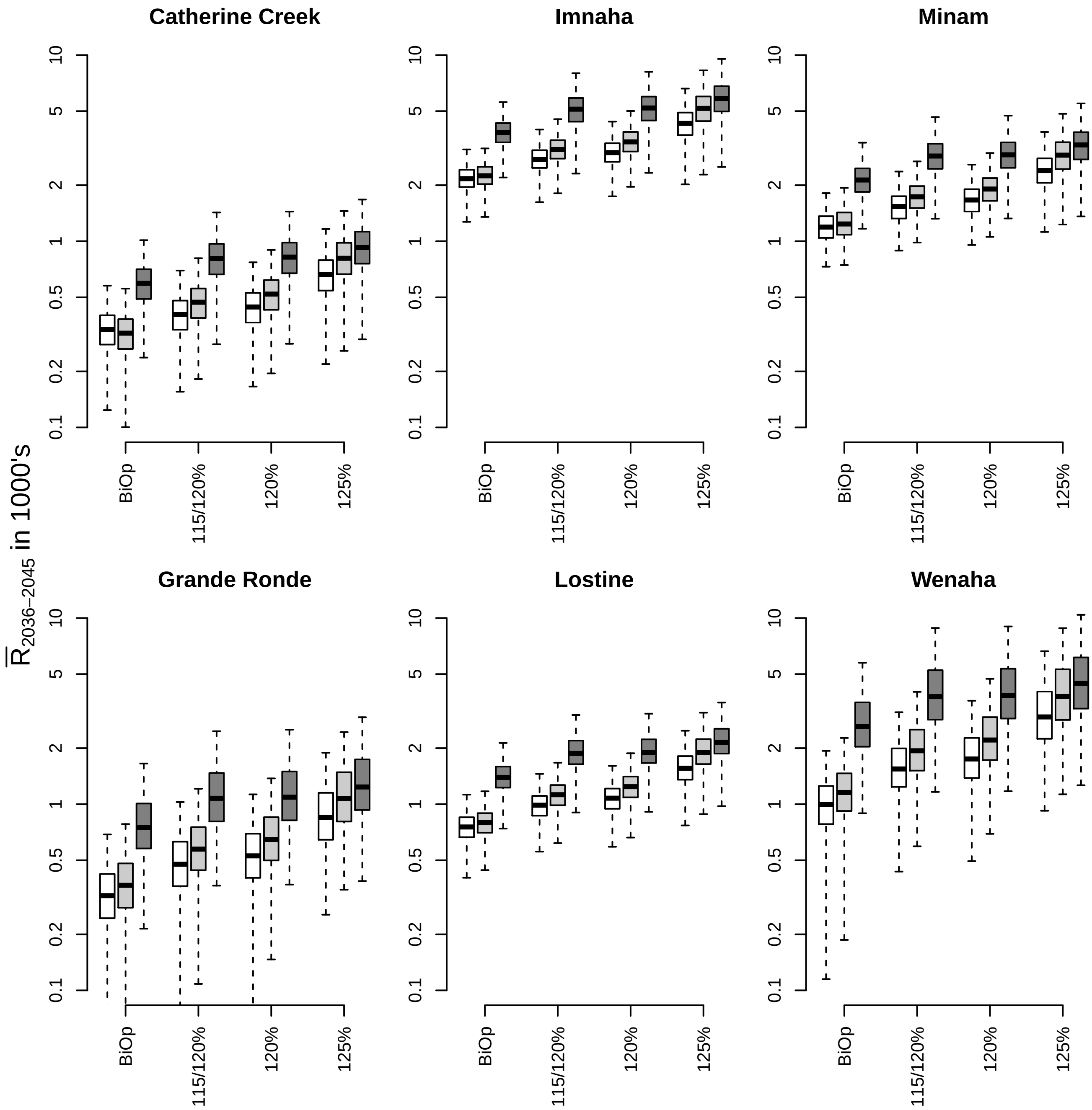

Figure 9: Sensitivity analysis of predicted long-term average predicted average abundance between 2036 and 2045 ($\bar{R}$ in log scale) at all combinations of spill levels and flow levels. Each cluster of three bars represent high flow (white boxes), average flow (light grey boxes), and low flow (dark grey boxes). Boxes represent the 25%-75% quartiles. Whisker represent the outer 10% and 90%. Median values are shown with dark horizontal lines inside boxes.

to the 125% level. Interestingly, there is an apparent net decrease in the SAR for the Catherine Creek population at BiOp level spills when the assumed flow levels decrease from high to average flows. This is only evident in the Catherine Creek population. The most likely explanation for this is that Catherine Creek is the population with the lowest capacity, and thus is limited in total production, which can interact with harvest rates in a depensatory way because of the way the simulated harvest rates increase as the total MPG returns increase. At the lower total life cycle productivities implicit in lower spill rates, the effect is that slightly higher in-river juvenile migration survival increase total MPG returns enough to drive the harvest rate up, and the Catherine Creek population suffers the consequence of being the weaker stock in a mixed stock complex. The effect is present, but less noticeable in the returns (see Figure 9). Figure 11 shows that the SARs at the mouth of the Columbia are the same for all populations, confirming that harvest is the cause.

Relative performances of spill scenarios can also be evaluated using the ratio of the median of long-term average return abundances to the BiOp level spill prediction at each flow level. Figure 12 shows the median $\bar{R}$ (of the 10,000 predicted $\bar{R}$s) at a given spill level for each flow level compare to the median BiOp level spill for the same flow level. There is nearly a 50% gain from BiOp to 115%/120% for all flow levels, but only high and average flows show noticeable gains in the transition from 120% spill to 125% spill. The ratio of the medians is shown without uncertainty to make the trend in the ratios more apparent. The same trend can be seen when the ratio of each independent simulation is shown with associated uncertainty (see Figure 13). This perspective only illustrates what performance would look like if spill were increased relative to BiOp at a given flow, and only if spill levels were sustained every year, and flows remained at the same level every year. Looking at ratios of median $\bar{R}$s for each flow level relative to high flows at BiOp, the importance of flow levels is more apparent. Figure 14 shows the ratio of the median predicted $\bar{R}$ at each spill scenario at a flow level to median predicted $\bar{R}$ atBiOp spill and high flow. The flow level alone explains about a 100% improvement or more at a BiOp level spill when comparing low to high flow. The highest incremental gains come at average

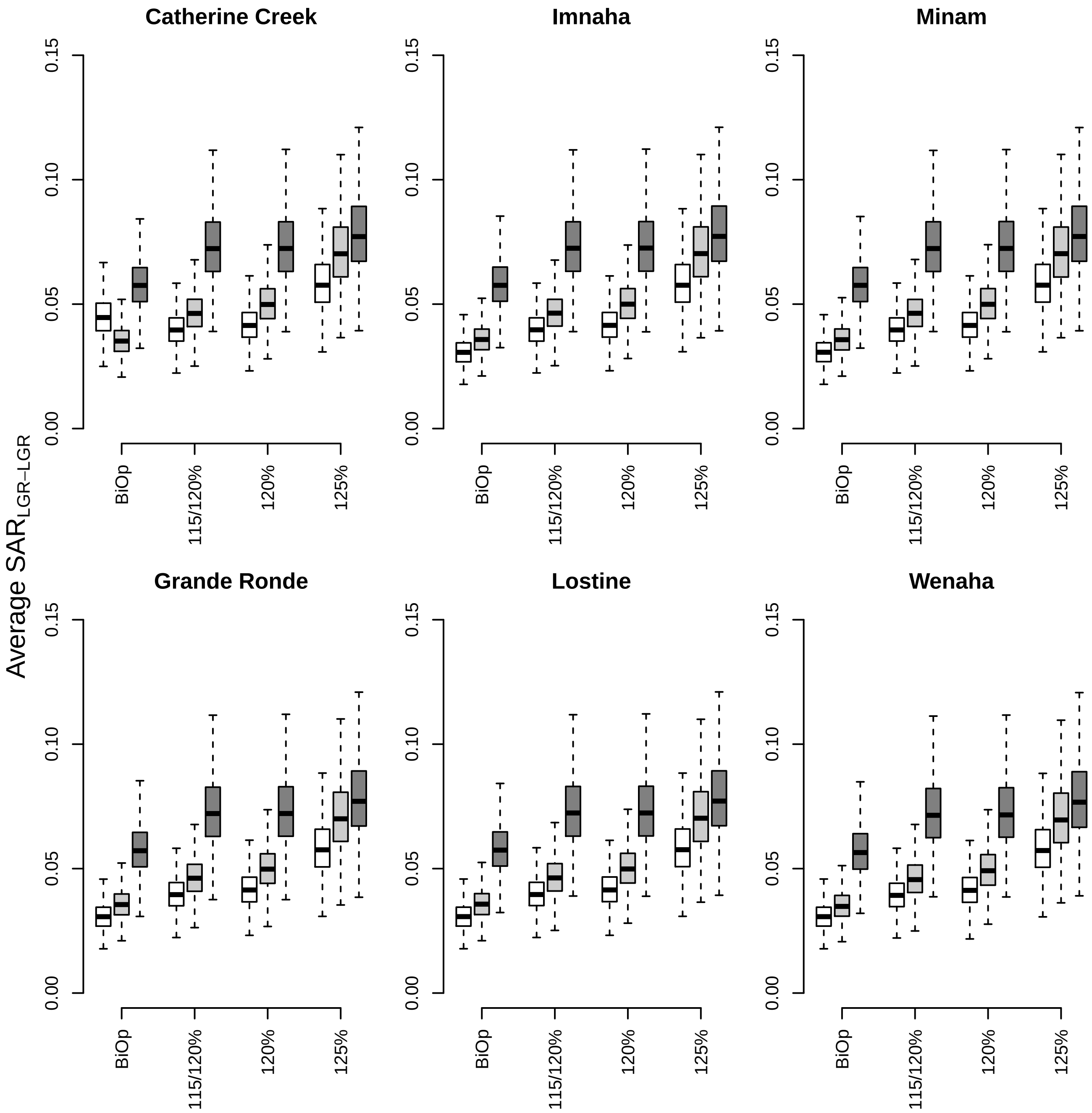

Figure 10: Sensitivity analysis of predicted long-term average SAR at LGR between 2036 and 2045 at all combinations of spill levels and flow levels. Each cluster of three bars represent high flow (white boxes), average flow (light grey boxes), and low flow (dark grey boxes). Boxes represent the 25%-75% quartiles. Whisker represent the outer 10% and 90%. Median values are shown with dark horizontal lines inside boxes.

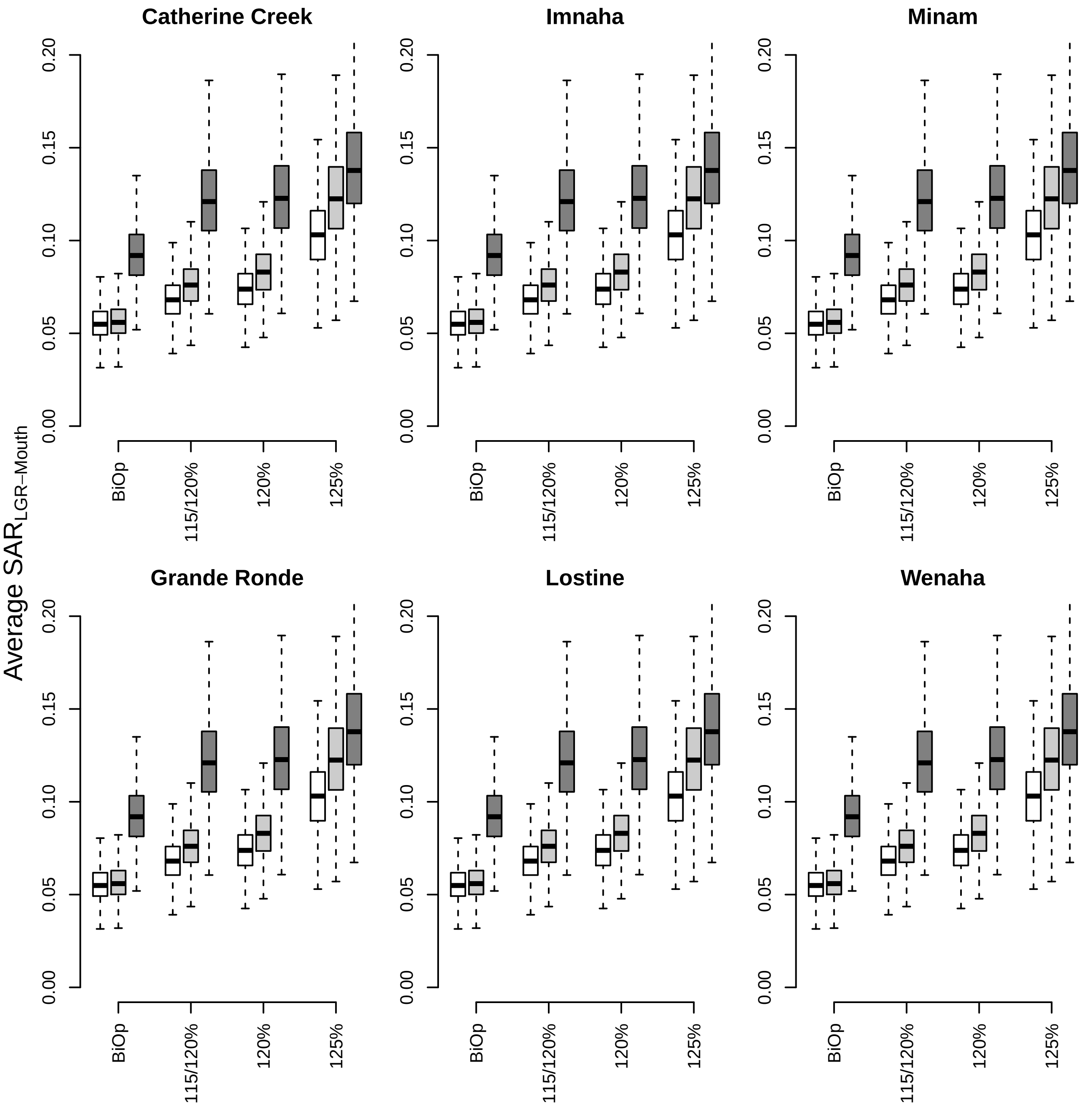

Figure 11: Sensitivity analysis of predicted long-term average SAR to the mouth of the Columbia River between 2036 and 2045 at all combinations of spill levels and flow levels. Each cluster of three bars represent high flow (white boxes), average flow (light grey boxes), and low flow (dark grey boxes). Boxes represent the 25%-75% quartiles. Whisker represent the outer 10% and 90%. Median values are shown with dark horizontal lines inside boxes.

and high flows when spill is increased to 125%, but it can be seen that relative to low flow BiOp spill, average and low flows show higher relative gains.

Figure 15 shows the effect of spilling, but evaluated across a range of productivities for each population. Each line represents one of the four spill levels evaluated at average flows for each of the spill levels (BiOp, 115%/120%, 120%, and 125%). The lines represent the median predicted $\bar{R}$ from 10,000 simulations. The figure is intended to demonstrate the relative change in $\bar{R}$ across a range of productivities at four spill scenarios. Uncertainty around each line cannot be shown without obfuscating the contrast among spill scenarios, but can be inferred from Figure 9, where the variability at the estimated productivity is shown for each spill scenario at average flow. The grey shaded area in Figure 15 corresponds to the 25%-75% quartile range of uncertainty in the productivity estimate, so improvements to productivity would fall to the right of the shaded area. The general pattern is that larger gains from increased spill are realized by populations that have high capacity (Imnaha and Wenaha), and that the gain is greater still if the productivity is high (Imnaha).

In all six population, there is a predicted increase in $\bar{R}$ if productivity is increased, but unless capacity is relatively high, the gains are not very significant. The Imnaha, Minam, and Wenaha have the highest capacities, and therefore predict larger gains in average abundance from increases in productivity. There are no cases where increasing freshwater productivity has more influence on $\bar{R}$ than increasing spill levels.

Figure 16 shows the effect of spilling, but evaluated across a range of capacities for each population. Like the productivity comparisons, the lines represent the median predicted $\bar{R}$ from 10,000 simulations at four spill scenarios. At the levels of SARs simulated, freshwater productivity does little to limit $\bar{R}$ when population trends are projected across a range of capacities. This is because as long as average SARs are sufficient to return enough adults to replace the number of parents that produced those smolts, the only thing limiting population increase is capacity. The shaded areas represent the 25%-75% quartile range of estimated value of

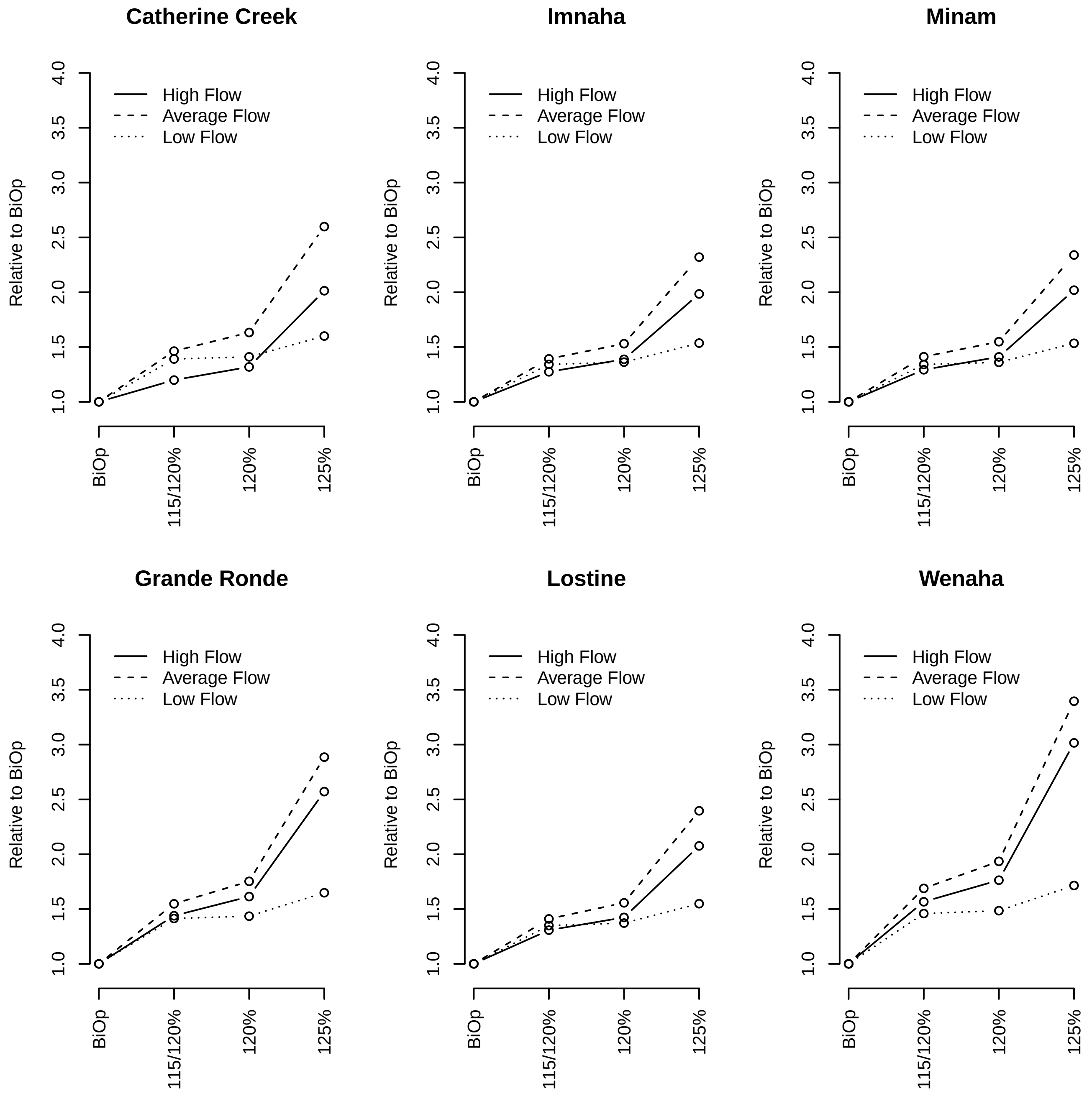

Figure 12: Sensitivity analysis of predicted long-term average return abundance between 2036 and 2045 at each flow level when compared to BiOp spill at each flow level.

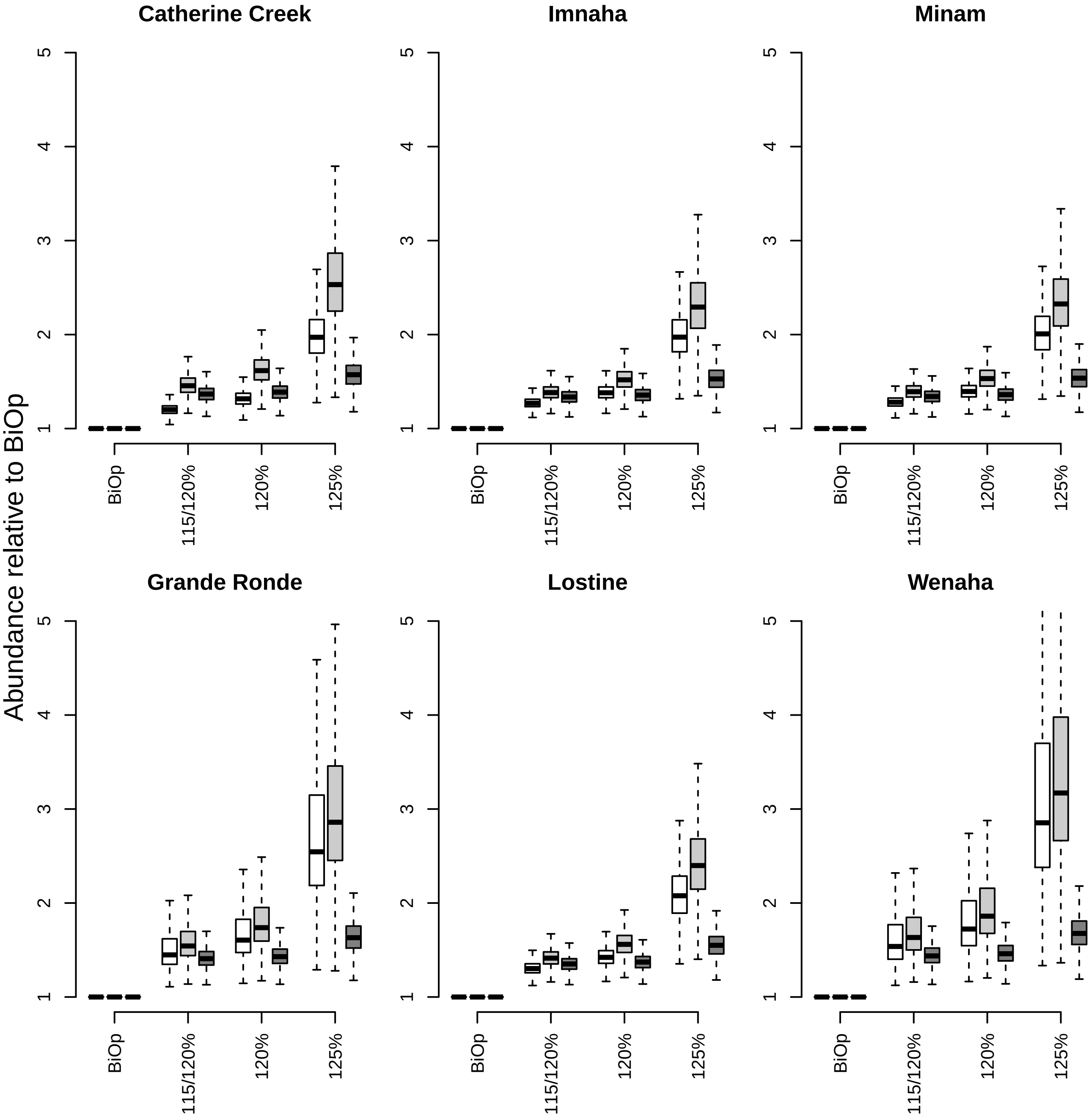

Figure 13: Comparison of the ratio of simulated long-term average return abundance between 2036 and 2045 at each flow level when compared to BiOp spill at each flow level. Each cluster of three bars represent high flow (white boxes), average flow (light grey boxes), and low flow (dark grey boxes) ratios of predicted average abundances to BiOp level spills for that flow level. Boxes represent the 25%-75% quartiles. Whisker represent the outer 10% and 90%. Median ratio values are shown with dark horizontal lines inside boxes.

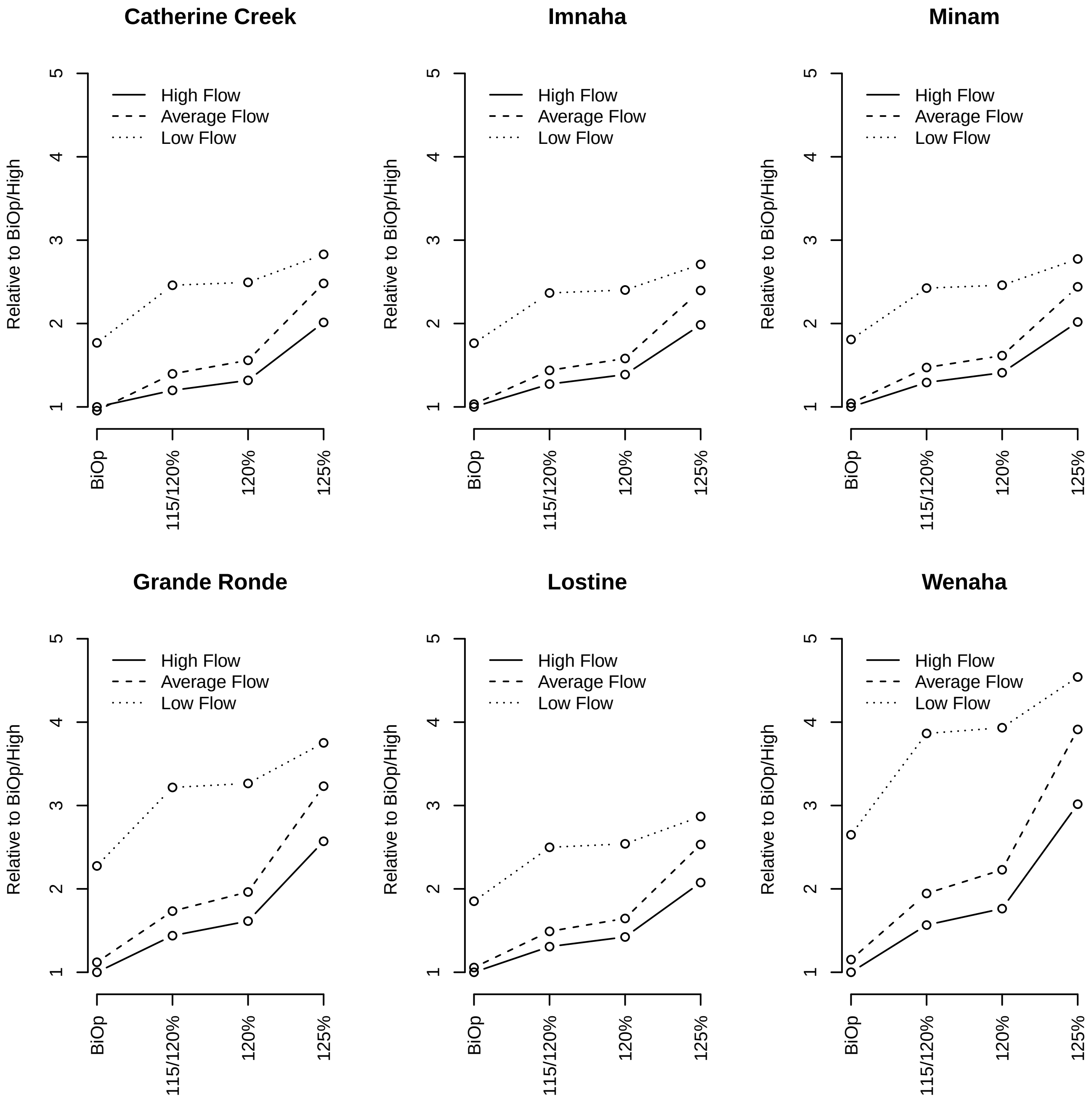

Figure 14: Sensitivity analysis of predicted long-term average return abundance between 2036 and 2045 at each flow level when compared to BiOp spill at a high flow level.

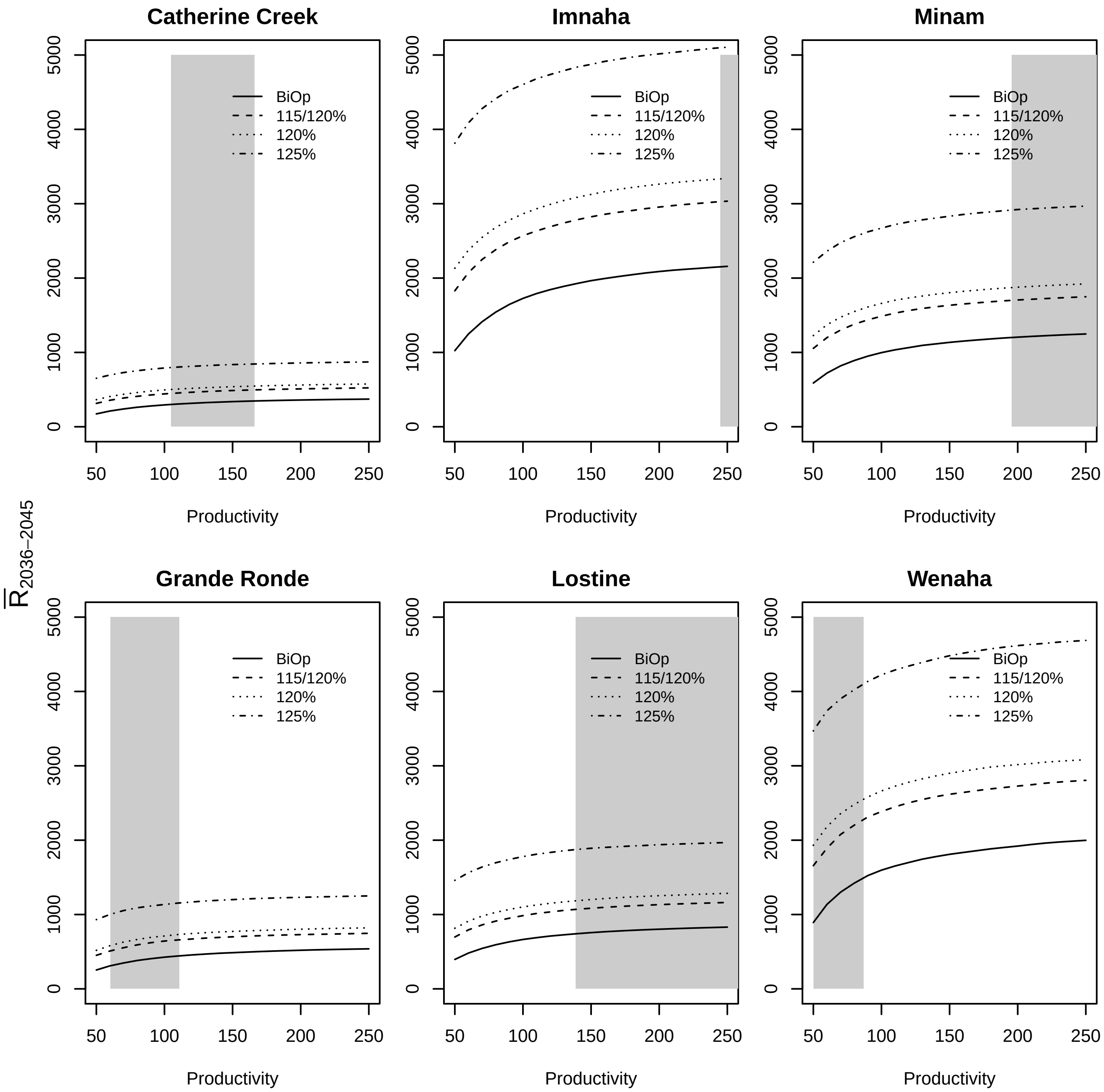

Figure 15: Sensitivity analysis of predicted long-term average return abundance between 2036 and 2045 when tributary productivities span the range from 50 to 250 smolts per spawner. The lines are the median ($\bar{R}$) predicted average return abundance at four spill levels evaluated at average flows. Grey shaded areas denote the estimated range of variability in the productivity parameters evaluated from posterior distributions.

the capacity estimated from the posterior chain of parameter estimates which, if no action were taken, is the level of benefit expected from increasing spill.

Discussion

The predicted benefits of spill levels across high, average, and low flows were examined, and it was shown that predicted SARs and long-term average return abundances respond positively to increased spill. It was also shown that the most significant benefits to SARs occur at the highest TDG limit spill levels, at the lowest flow levels. It was also shown that low flows are predicted to contribute more significantly to increases in SARs at BiOp level spills than at higher levels of spill. However, at higher assumed flow levels, the life cycle model predicted that the highest TDG limit spill level (125% TDG) produced a larger incremental benefit to SARs than the transition upward from the lower spill levels.

The MCMC posteriors show the range of variability in the δ_{PH} parameter estimate to be very narrow with estimates of approximately δ_{PH} = -0.4 and $\hat{\sigma}_{\delta_{PH}}$ = 0.01. To put that in context, the estimated in-river survival at average levels of PITPH and WTT is estimated to be around 0.37 with δ_R = 0.51. That would be the estimated survival at average historical levels of PITPH and WTT, meaning that it is not the highest survival possible with PITPH and WTT at their most favorable values. If we consider values of PITPH of 3 and 0.3, representing high and low spill scenario values, then the in-river survival is predicted to increase from 0.42 to 0.70 at average WTT values (by adding -0.4 times a difference of PITPH = -2.7 to the logistic term in Equation (9)). This implies that PITPH is capable of explaining shift in in-river survival of about 0.28 across the range of spill scenario PITPH values. There is slightly more variation in the estimate of γ_H ($\hat{\sigma}_{\gamma_H}$ = 0.22), but the effect is similar to how PITPH affects early ocean survival of in-river migrants. The model predicts that at average PDO and UPW conditions, PITPH can explain an increase in first year ocean survival.

The relative benefits of changes to freshwater production parameters and changes to hydrosystem operations were presented. Simulations showed that the relative average return

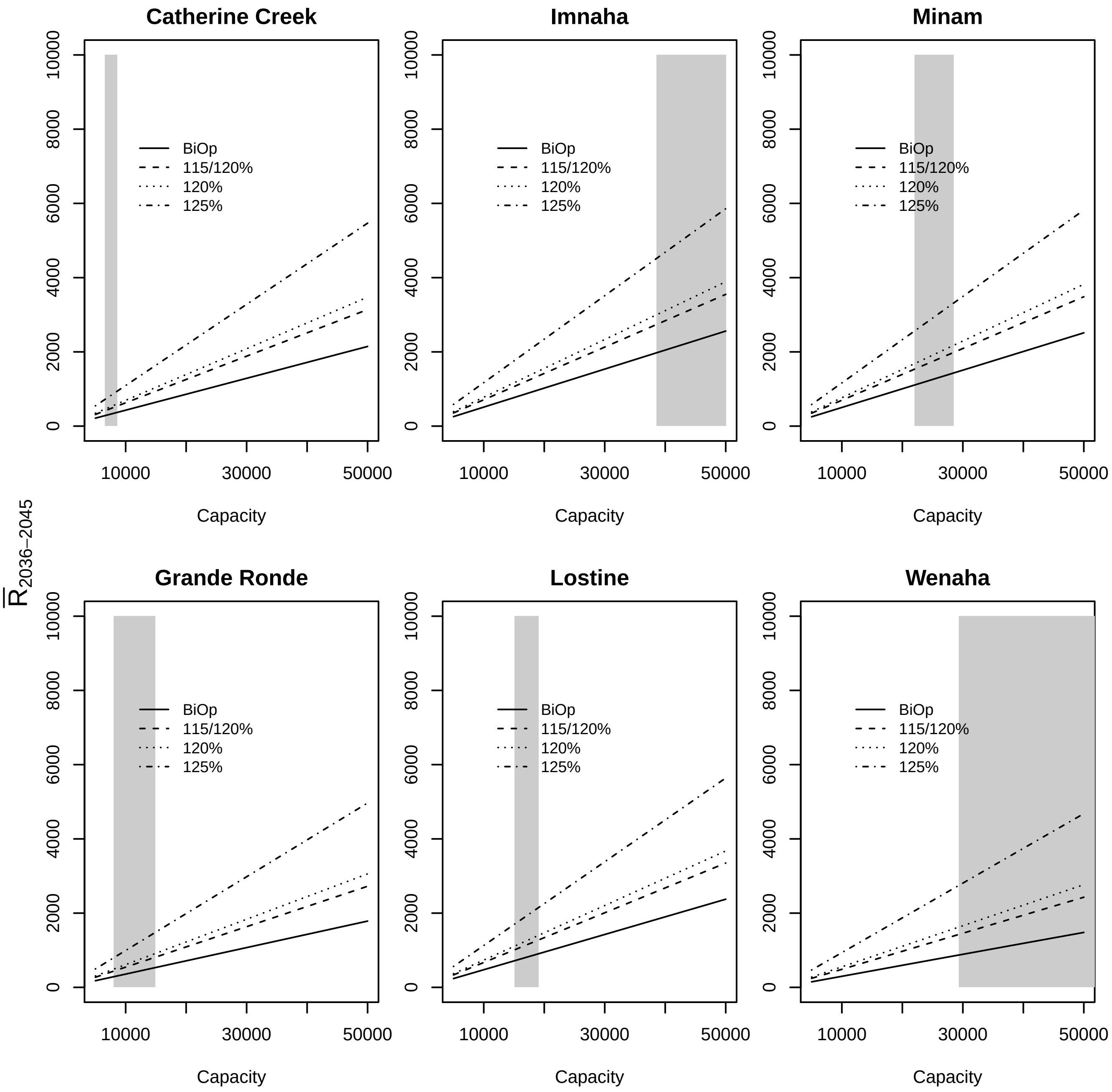

Figure 16: Sensitivity analysis of predicted long-term average abundance between 2036 and 2045 ($\bar{R}$) when tributary capacities span the range from 5000 to 50000 smolts. The lines are the median ($\bar{R}$) predicted return average abundance at four spill levels evaluated at average flows. Grey shaded areas denote the estimated range of variability in the capacity parameters evaluated from posterior distributions.

abundance (see Figure 9) benefits are predominantly limited by capacity. The range of benefit from additional spill was a two to three fold increase in average return abundance evaluated at average flow levels, with the most extreme case being a 4.3 fold increase in average return abundance from a BiOp spill level at high flows compared to a 125% TDG spill level at low flows in the Wenaha (which has the highest estimated capacity). Looking more closely at how increased spill interacts with changes to productivity and capacity, it was predicted that most of the potential gains from productivity came from populations that have low productivities and high capacities (see Figures 15 and 16), and the benefits came from increasing productivity up to 150 smolts per spawner, but not much beyond that unless the capacity was exceptionally high.

Increasing spill levels provides a benefit regardless of the productivity or capacity. Looking at the potential benefits of increasing capacity at different spill levels, the contrast across populations is not as strong. This is because the benefit of increasing in-river survival of juvenile migrants is more significant than the differences in freshwater productivities. From these results it seems apparent that benefits obtained from increases to productivities are ultimately bounded by capacities, as are the benefit obtainable from increased spill, but with the distinction that the increased average abundances predicted from increasing productivities by 50 smolts per spawner are less than the benefit of going from a BiOp spill scenario to the next higher TDG level spill. It should be noted that there is a more significant relative improvement in long-term average abundance going from a BiOp to 115%/120% level of spill than the next increase to 120% TDG.

The analysis shows that there are predicted benefits from increasing spill levels at all levels of flow, but most significantly at low flows, which is when spill efficiency is highest. Those benefits not only exceed the benefits of habitat actions aimed at productivity increases, but they are more immediately implementable. Ultimately, habitat actions are required to bring population abundances back to historical levels, but increased spill scenarios provide a timely means of increasing SARs and abundances. Looking at the results on a case by case basis for each population, it should be noted that there are some obvious contrasts. The Imnaha and Minam both have good productivities and capacities, but being partially in Wilderness Areas, are not likely recipients of any habitat actions . The Upper Grande Ronde and Catherine Creek, on the other hand, have very low estimated capacities, and the Upper Grande Ronde has a very low productivity. Both of these could benefit from habitat improvements, but private land ownership within the drainages impedes and delays habitat restoration action on significant portions of the drainages, making it difficult to effect change with the speed and intensity required. On the other hand increased spill levels could have immediate benefit, and this analysis predicts that increasing from BiOp to 115%/120% levels could lead to about a 50% increase in return abundances, and spill to a 125% TDG level could lead to about a three fold increase at current productivity and capacity levels. It seems on first glance at the predicted sensitivity to productivity increases that changes are ineffectual relative to increased spill levels, but this view does not account for the natural outcome that increasing productivity inherently involves improving areas that currently have very low productivity, and by doing so opens up new areas for spawning and rearing. Adding areas of improved productivity reduces the burden on other areas to support production, which has the effect of increasing capacity simultaneously. In short, capacity increases are implicit in actions to increase productivity.

It has been shown that increases in $\bar{R}$ can be effected by three different means, and that the relative gains from productivity improvements can be dependent on capacity limits in freshwater spawning and rearing. Increasing spill levels can increase predicted median $\bar{R}$ by up to 4.3 fold if capacity is high enough, and generally by 2 fold or more, depending on flow levels. Because the magnitude of the performance gain at low flows is highest going from BiOp to 115%/120%, it seems an obvious minimum operation alternative to spill at 115%/120% at low flows. The performance gains in the next transition to 120% are not predicted to be as high, i.e., an apparent diminishing return. The final transition to 125% TDG level spill predicts a more significant gain in predicted median $\bar{R}$ than the previous increment. At average and high flows, the relative increases in $\bar{R}$ are gradual and consistent, without the diminishing returns seen at lower flows. Figure 9 and 10 show these gradual and diminishing returns of performance across spill scenarios.

It is noted that predicted average SARs are higher (in the range of 0.02-0.06) than empirically observed SARs (less than 0.005 to about 0.03 in recent years since court mandated spills), but it should be emphasized that the analysis is intended to gauge relative expected increases in SARs, not predict absolute SARs. The higher estimate is consistent with the positive bias seen in the comparison of predicted and empirical SARs. The reasons for the bias are unclear at the current stage of the analysis. It could be because too much weight is being given to fitting older SARs and in-river survivals, or it could be because the SARs are derived from the entire Snake River aggregate and are being compared to predicted SARs based on predicted returns of populations in the Grande Ronde / Imnaha MPG. Fitting to abundance data may actually predict higher SARs than the Snake River aggregate SAR, or alternatively, the abundance data may contain a bias that predicts a higher SAR. A 20% transportation rate was also assumed for simulation purposes, which is lower than the average of 37% transportation between 2007 and 2012 migration years. Since transported fish are predicted to survive in the ocean at a lower rate than in-river migrants, the simulation analysis should be expected to predict higher overall SARs than if the transportation rate was higher.

Focussing not on the absolute magnitude of the SARs, but rather on the relative predicted change in SARs with increased spill, the predicted increase from the 0.02-0.06 range at BiOp spill to the 0.06-0.08 range at 125% spill can be interpreted by the change in PITPH. The 125% scenario represents PITPH values of 0.28-1.01 across all flows, as opposed to the range of 1.95-3.06 at BiOp spill. These numbers can be compared to the SARs of John Day Chinook, which experience five less powerhouses than Snake River Chinook. John Day SARs are in the 0.02-0.08 range. PITPH averages about 2.7 across all flow levels in the BiOp scenario for Snake River Chinook crossing 8 dams. If John Day Chinook cross only 3 dams, then the PITPH should be in the vicinity of a 3/8th fraction of PITPH, which is 1.00. The 120% scenario is the closest to having an average PITPH of 1.00 across all flow levels, and its predicted SARs are similar to those of the John Day.

$\bar{R}$ was predicted across a range of assumed fixed freshwater productivity levels and capacity levels that differed from the estimated values of the parameters. $\bar{R}$ was also predicted across a range of fixed alternative hydrosystem operational levels. The predicted $\bar{R}$s show the relative predicted outcome under those fixed conditions and provides an indication of the relative behavior of the populations. This oversimplifies operational and biological realities, but nonetheless provides a perspective of the relative benefits that can be expected. The comparative benefits from tributary actions assumed that productivity and capacity would immediately take on fixed values reflecting improved conditions. This means that when we look at the predicted value of $\bar{R}$ at 150 smolts per spawner, we are assuming that demographic rates applied immediately from 2010 on onward, however it's important to keep in mind that any treatment intended to effect an increase in productivity or capacity would involve a lag time before reaching the target rate. For comparative purposes it's still meaningful to see the relative gain across a range of productivities, but in reality it can take a long time for any changes to habitat to translate to increases in productivity. The same goes for capacity. Furthermore, just like freshwater conditions won't remain static, it clearly can't be the case that flows will always be one of the three levels examined. Notwithstanding the limitation of the static assumptions in the model predictions, presenting the relative outcomes still gives us a sense of how much life cycle survival can improve when year to year variability in flow and operational conditions occur. What has been shown is that an increase in $\bar{R}$ is predicted to occur if spill is increased, and that the relative increase depends on the flow and the spill scenario. While flows will vary from year to year, the results show that there is a measurable predicted increase in $\bar{R}$ with increased spill, and the increase is relative to flow.

Results indicate that abundance can increase as a result of alternative treatments. A target $\bar{R}$ can be achieved by means of selecting a target productivity, capacity, or alternative spill level. In either of the three cases, there may be implementation issues or time lag issues. Despite any caveats to the limitations in attaining productivity or capacity improvements however, it must be noted that action both in freshwater and in the hydrosystem is likely to be most effective, and gains obtained from reducing PITPH via increased spill serve as a buffer for potential implementation lags in productivity and capacity treatments. Ultimately, where habitat improvements are needed, they provide the highest long-term abundance gains, particularly where capacity is increased, but the immediate benefits of increasing spill are evident and should be considered vital to recovering abundances.

Conclusions

The results presented in this analysis demonstrate the relative sensitivity of long-term return abundance to changes in freshwater production parameters and hydrosystem operations. Relying on the empirical estimates of life cycle model parameters, and particularly the finding that a PIT tag based indicator of powerhouse passage is a significant determinant of in-river survival and early ocean survival, it was demonstrated that alternative spill scenarios can have varying degrees of influence on population recovery, depending on the productivities and capacities of the populations. It was found that populations with low capacities (eg: Catherine Creek, Upper Grande Ronde, and to a lesser extent the Lostine) don't realize as much benefit from increasing freshwater productivity as population with higher capacities, but it is expected that habitat improvements aimed at increasing productivity would benefit capacity as well, so the actual gains need to account for the dual benefit of habitat improvements.

This analysis predicted that average return abundances and SARs increase with higher spill. The results are preliminary in the sense that the simulated future conditions are speculative and have a strong influence on predicted survival. The predicted outcomes represent approximations of the relative magnitude of increased survival and return abundance that are predicted relative to spill levels. The results are presented as contrasts under different fixed flow conditions, which can be used to provide guidance in the application of spill at relative approximate flow levels. It was shown that at low flows, substantial gains in performance are predicted to occur if spill levels are increased from BiOp levels to the 115%/120% TDG levels. Approximately a 50% increase in average return abundances was predicted. 125% spill levels in years of high flows predicted greater than two fold increases in return abundances, with some population receiving greater benefits from higher spills because of their high freshwater spawning and rearing capacities. This analysis predicts that higher SARs and long-term abundance increases can be achieved by increasing spill levels, and that the benefits of spill are sensitive to flows. The immediate benefits of increased flow levels, combined with the long-term benefits of habitat actions predict potential recovery of populations to up to three fold increases in abundance above levels predicted by BiOp level spill.

Literature cited

Beverton, R. J. H. and Holt, S. J. 1957. On the Dynamics of Exploited Fish Populations. Caldwell, NJ: Blackburn Press.

Budy, P., G.P. Thiede, N. Bouwes, C.E. Petrosky, and H. Schaller. 2002. Evidence linking delayed mortality of Snake River salmon to their earlier hydrosystem experience. North American Journal of Fisheries Management 22: 35-51.

Mantua, N.J., Hare, S.R., Zhang, Y., Wallace, J.M. & Francis, R.C. 1997. A Pacific decadal climate oscillation with impacts on salmon. Bulletin of the American Meteorological Society 78: 1069–1079.

Marmorek, D.R., C.N. Peters and I. Parnell (eds.). 1998. PATH final report for fiscal year 1998. Compiled and edited by ESSA Technologies, Ltd., Vancouver, B.C. Available from Bonneville Power Administration, Portland, Oregon (http://www.efw.bpa.gov/Environment/PATH/reports/ISRP1999CD/PATH\%20Reports/WOE_Report/).

McCann, J., B. Chockley, E. Cooper, H. Schaller, S. Haeseker, R. Lessard, C. Petrosky, E. Tinus, E. Van Dyke and R. Ehlke. 2015. Comparative Survival Study (CSS) of PIT tagged Spring/Summer Chinook and Summer Steelhead. 2015 Annual Report. Project No. 199602000. http://fpc.org/documents/CSS/CSS_2105AnnualReport.pdf (November 2015).

Petrosky, C.E., and H.A. Schaller. 2010. Influence of river conditions during seaward migration and ocean conditions on survival rates of Snake River Chinook salmon and steelhead. Ecology of Freshwater Fish 19(4): 520–536.

Petrosky, C.E., H.A. Schaller, and P. Budy. 2001. Productivity and survival rate trends in the freshwater spawning and rearing stage of Snake River Chinook salmon (Oncorhynchus tshawytscha). Canadian Journal of Fisheries and Aquatic Sciences 58: 1196–1207.

Ricker, W. E. 1975. Computation and interpretation of biological statistics of fish populations. Fisheries Research Board of Canada Bulletin 19.

Tuomikoski, J., J. McCann, T. Berggren, H. Schaller, P. Wilson, S. Haeseker, J. Fryer, C. Petrosky, E. Tinus, T. Dalton, and R. Elke. 2012. Comparative Survival Study (CSS) of PIT-tagged Spring/Summer Chinook and Summer Steelhead, 2012 Annual Report.Project No. 199602000. http://www.fpc.org/documents/CSS/2012 CSS Annual Report-Final.pdf

Williams, J.G., S.G. Smith, R.W. Zabel, W.D. Muir, M.D. Scheuerell, B.D. Sandford, D.M. Marsh, R.A. McNatt, and S. Achord. 2005. Effects of the Federal Columbia River Power System on salmonid populations. NOAA Technical Memorandum NMFS-NWFSC-63. (http://www.nwfsc.noaa.gov).

4b. The COMPASS Model for Assessing Juvenile Salmon Passage through the Hydropower Systems on the Snake and Columbia Rivers

James R. Faulkner, Daniel L. Widener, and Richard W. Zabel

Introduction

The Comprehensive Passage (COMPASS) Model was developed as a tool for investigating the passage experience of migrating juvenile salmon and steelhead under various environmental conditions and management scenarios (Zabel et al. 2008, COMPASS 2008). COMPASS was reviewed by the ISAB in 2008 and has been used to inform a variety of management decisions concerning juvenile salmon since then.

COMPASS contains physical descriptions of the Snake and Columbia Rivers and their main tributaries, which include spatial representations with widths, depths, and elevations to allow volume and velocity calculations. The hydroelectric dams in the system are also represented and algorithms are used to route flow through the set of passage routes unique to the configurations at each dam. This allows dam operations such as spill and surface collector operation to be accounted for on daily or finer time steps.

Flow is input at the river headwaters or at the dams, either as measured observations or as predictions from hydrological models. Other possible environmental inputs include temperature, turbidity, and dissolved gas. COMPASS can also take spill proportions as inputs and can take surface weir volumes and operation schedules. Schedules and rates of smolt transportation on barges are also taken as inputs for operation of collector dams.

COMPASS contains a set of biological models we developed for arrival timing at the head of the hydropower system, reservoir travel time, reservoir and dam survival, and dam passage routing for various species. These models were all fitted to observed data and are functions of the set of variables describing environmental conditions and dam operations that are available to COMPASS. When combined together, these sub-models allow predictions of the passage experience of population releases through the system to Bonneville Dam tailrace. We can then use predicted arrival distributions at Bonneville Dam as inputs into models for smolt-to-adult returns (SAR).

Here we demonstrate the use of the model on a set of simulated data representing five different management scenarios. These scenarios represent different sets of rules for the operation of hydroelectric dams which are meant to improve conditions for fish passage. We present COMPASS model results for these scenarios. We also briefly describe some of the updates that have been done to COMPASS since 2008.

Methods

Model Updates

Since the most recent documentation of COMPASS (Zabel et al. 2008; COMPASS 2008), we have made several updates to the sub-models and to the general functionality of the COMPASS. The following is a brief list of changes:

- Updated the data used to calibrate the travel time and reservoir survival components of the model to 1998-2015.

- Updated the data for the dam passage routing models (spill efficiency and fish guidance efficiency) to 1998-2013. Also made changes to passage models to better account for observation uncertainty.
- Updated estimates of route-specific survival for dams on the Snake and lower Columbia Rivers. These estimates come from experiments on fish implanted with radio tags or acoustic tags.
- Changed the structure of the reservoir survival models. We use a hierarchical modeling format where random effects for the true unknown survival probabilities follow beta distributions, and the observed survival (Cormack-Jolly-Seber estimates) follow log-normal distributions conditional on the latent random survival effects. This structure allows a more accurate decomposition of the uncertainty.
- Added component to the reservoir survival models that allows predator density and smolt density to affect survival through a functional response.
- Updated models that predict dissolved gas supersaturation based on flow, spill, temperature. This allows us to produce estimates of exposure to supersaturation and even related mortality.
- Added models for dam passage for the dams on the Upper Columbia River. These including route specific survival and functions for passage route probabilities. We also have travel time and survival models for fish originating in the Upper Columbia.
- Added more time steps to the reservoir passage model (up to 16 per day) to allow more accurate travel time calculations.

Prospective Modeling

Five management scenarios were investigated. The first scenario, labeled as the Base scenario, represents the current configurations and operations of the dams, including timing of transportation. Three scenarios, labeled Opt1, Opt2, and Opt3, represent minor adjustments to the operations of the Base scenario, including slightly higher levels of spill in Opt2 and Opt3. The final scenario, labeled ORPIv2, has the same dam configurations and transport rules, but has higher levels of spill throughout the migration season. This was generated by increasing the allowed spill caps at all the dams.

The Bonneville Power Administration (BPA) generated the scenarios using their hydrological model, HYDSIM. This model accurately accounts for power generation and spill and associated hydrology in the hydropower system and outputs daily predictions of flow, spill, and reservoir elevation associated with each dam. This was done for a set of 80 water years representing headwater inputs for the years 1929-2008. These water inputs are applied to the operation rules determined by each scenario by HYDSIM. We used the daily flow, spill, and reservoir elevation values predicted by the HYDSIM model for the 80 water years for each scenario as inputs to COMPASS.

We constructed average population arrival distributions at Lower Granite Dam for the combined population run at large (combined hatchery and wild, tagged and untagged) based on historical data. We used relationships from regression models of median arrival date on median April-June flow to shift the average population distribution in response to predicted flows. This allowed arrival timing at Lower Granite Dam to vary with water year as a function of flow. These predicted population distributions were used as release profiles in COMPASS, where each water year had the same number of fish released.

We ran the COMPASS model for each of the 80 water years for each scenario. We produced separate results for Snake River spring-summer Chinook and steelhead. We collected several summary measures of passage experience for each year, including in-river survival from Lower Granite Dam to Bonneville Dam, proportion of fish transported, average travel time between Lower Granite Dam and Bonneville Dam, and SAR for combined transported and in-river migrants.

Results

Here we present results from prospective model runs for all five scenarios (Tables 1, 2). In general, differences between scenarios for the various COMPASS output statistics were smaller than the year-to-year variability within scenarios.

For Snake River spring-summer Chinook salmon, the Opt1 scenario was almost indistinguishable from the baseline scenario in all COMPASS output statistics. The Opt2 and Opt3 scenarios showed small changes from the baseline; both scenarios have slight improvements in in-river survival (Figure 1), small decreases to travel time (Figure 2), and a small increase in SAR over the baseline (Figure 3); however, the two scenarios are difficult to distinguish from each other. The ORPIv2 scenario shows larger differences from the baseline than the Opt2 or Opt3 scenario for all COMPASS output statistics, but the difference in in-river survival is still small (Figure 1). The ORPIv2 scenario does have a noticeable decrease in travel time compared to the baseline, and a corresponding increase in overall SAR (Figures 2, 3). The scenarios with increased levels of spill (Op1, Op2, ORPIv2) showed steadily decreasing numbers of fish transported (Table 1).

Patterns in COMPASS predictions for Snake River steelhead resembled those seen for Chinook. Once again, all other scenarios showed small increases in survival and small decreases to travel time relative to the Base scenario; however, the Opt1 scenario was so close that it cannot be considered significantly different (Figures 4, 5). The Opt2 and Opt3 scenarios are fairly close to each other, but the Opt3 scenario has a slightly lower SAR than the Opt2 scenario, despite having slightly shorter travel times (Figures 5, 6). This is likely due to differences in the survival rates of later migrating fish, since despite the shorter travel times, the Opt3 scenario has a slightly later mean arrival date at Bonneville than the Opt2 scenario (Table 2). Later arriving fish have a lower SAR, so if more late in-river migrants survive to Bonneville, the mean SAR will decrease. This can be unintuitive, since the total number of fish surviving to adulthood will still be increasing due to the improved in-river survival rate. A similar pattern appears to be occurring for the ORPIv2 scenario; the ORPIv2 scenario has lower transport SAR and inriver SAR than several of the other scenarios, but it has the highest overall SAR (Table 2). This results from the low proportion of fish transported in ORPIv2, since our models of SAR predict that in-river migrants have higher SAR than transported fish that arrive at Bonneville on the same date. We must stress that the reason some of these unintuitive patterns are arising in the COMPASS outputs is because the differences in survival, travel time, and SAR are quite small.

The most significant impact these scenarios appear to be having is in the proportion of fish destined for transportation.

Table 1. Mean COMPASS statistics predicted for Snake River spring Chinook salmon for the five management scenarios. PDT = Proportion of fish destined for transport.

Scenario	**Mean Survival**	**Mean Arrival at BON**	**Mean Overall SAR**	**Inriver SAR**	**Transported SAR**	**PDT**
Base	0.5500	135.36	0.01195633	0.01739869	0.00713516	0.401
Opt1	0.5514	135.15	0.01191687	0.01745339	0.00714477	0.407
Opt2	0.5615	134.91	0.01231473	0.01748916	0.00712973	0.375
Opt3	0.5593	135.68	0.01256217	0.01743250	0.00704118	0.345
ORPIv2	0.5624	135.48	0.01284946	0.01730052	0.00707142	0.315

Table 2. Mean COMPASS statistics predicted for Snake River steelhead for the five management scenarios. PDT = Proportion of fish destined for transport.

Scenario	**Mean Survival**	**Mean Arrival at BON**	**Mean Overall SAR**	**Inriver SAR**	**Transported SAR**	**PDT**
Base	0.4325	134.13	0.01701985	0.02073902	0.01522759	0.494
Opt1	0.4331	133.96	0.01701391	0.02076847	0.01525240	0.501
Opt2	0.4410	134.27	0.01714402	0.02072272	0.01521292	0.469
Opt3	0.4385	135.22	0.01711942	0.02071713	0.01488289	0.434
ORPIv2	0.4405	135.14	0.01731227	0.02052812	0.01505192	0.408

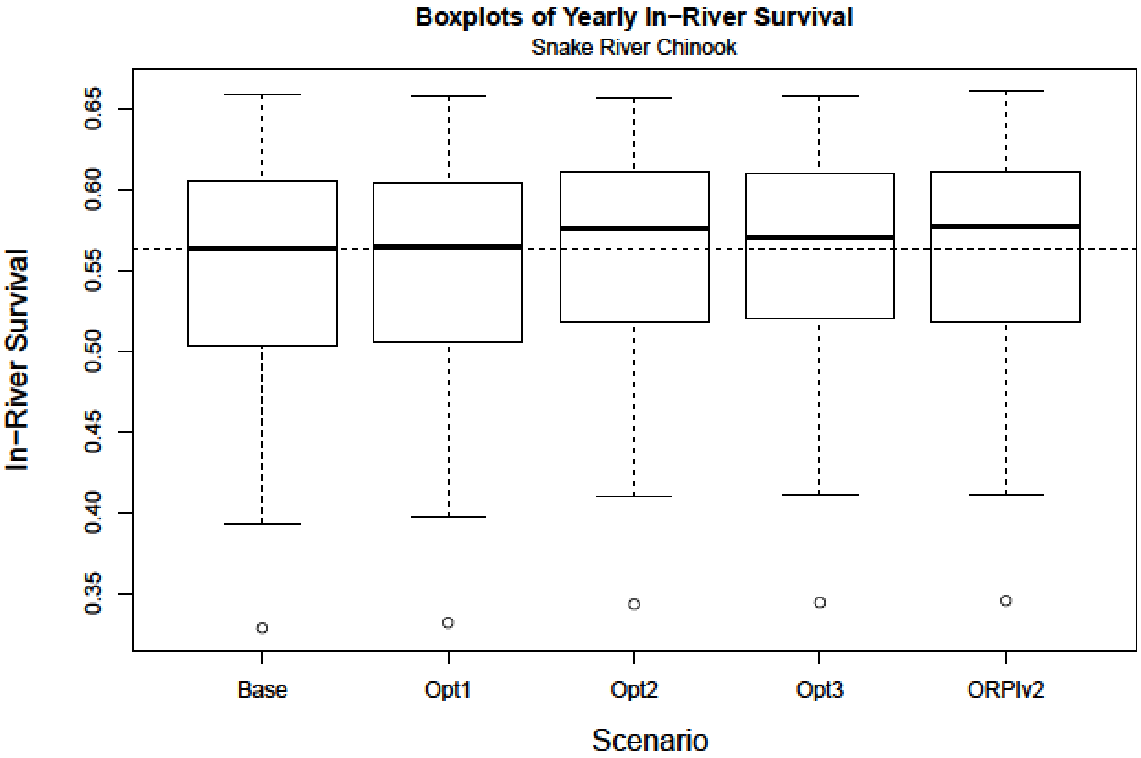

Figure 1. Boxplots of COMPASS predicted in-river survival for Snake River spring Chinook salmon by management scenario.

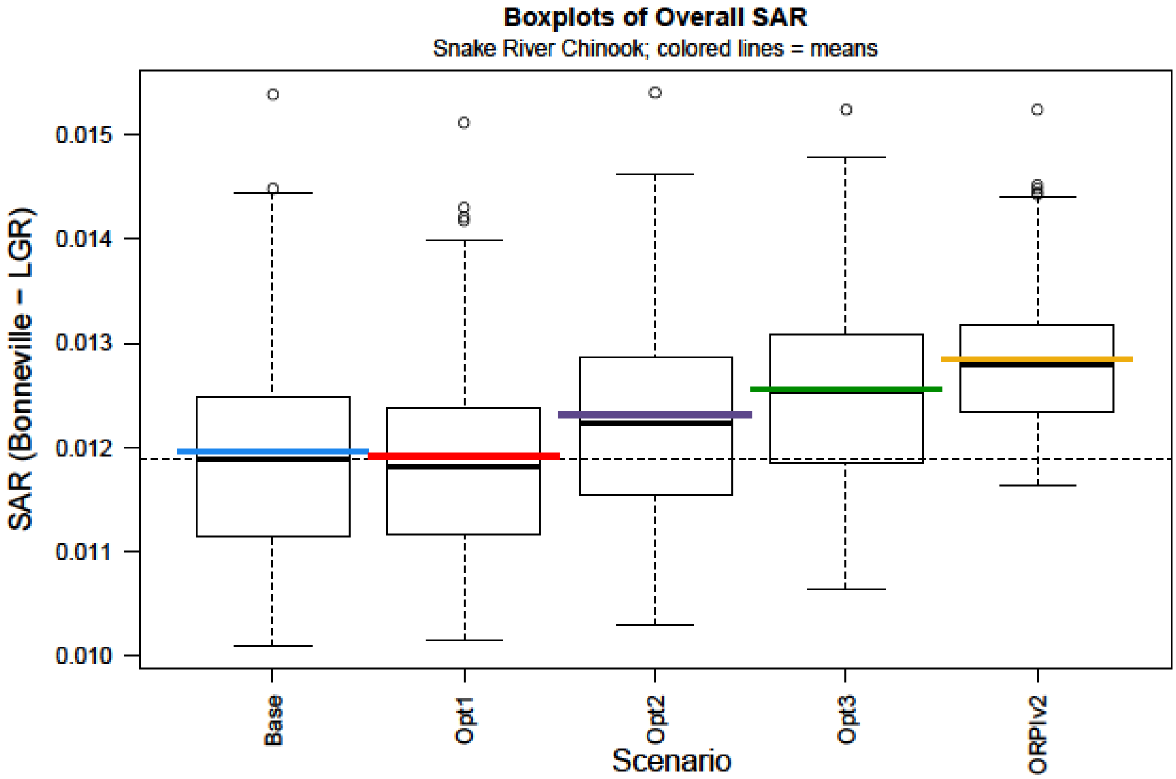

Figure 2. Boxplots of COMPASS predicted SAR (in-river and transported fish combined) for Snake River spring Chinook salmon by management scenario. Means are presented with colored lines and medians with black lines.

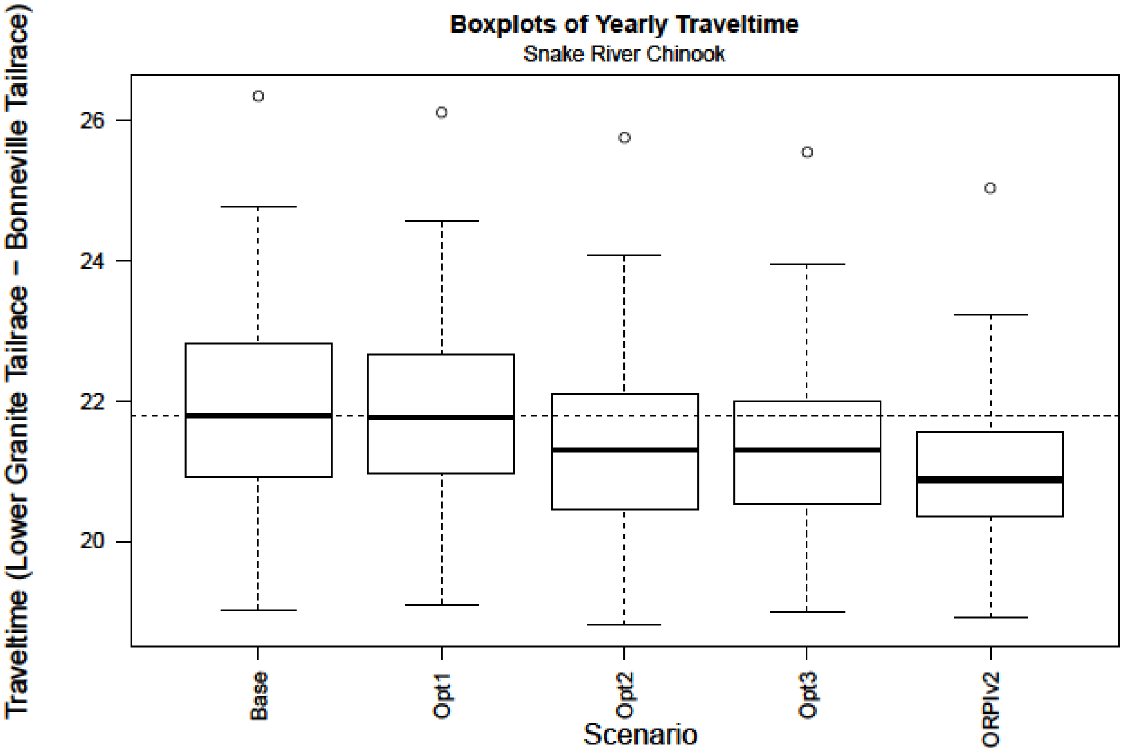

Figure 3. Boxplots of COMPASS predicted in-river travel time for Snake River spring Chinook salmon by management scenario.

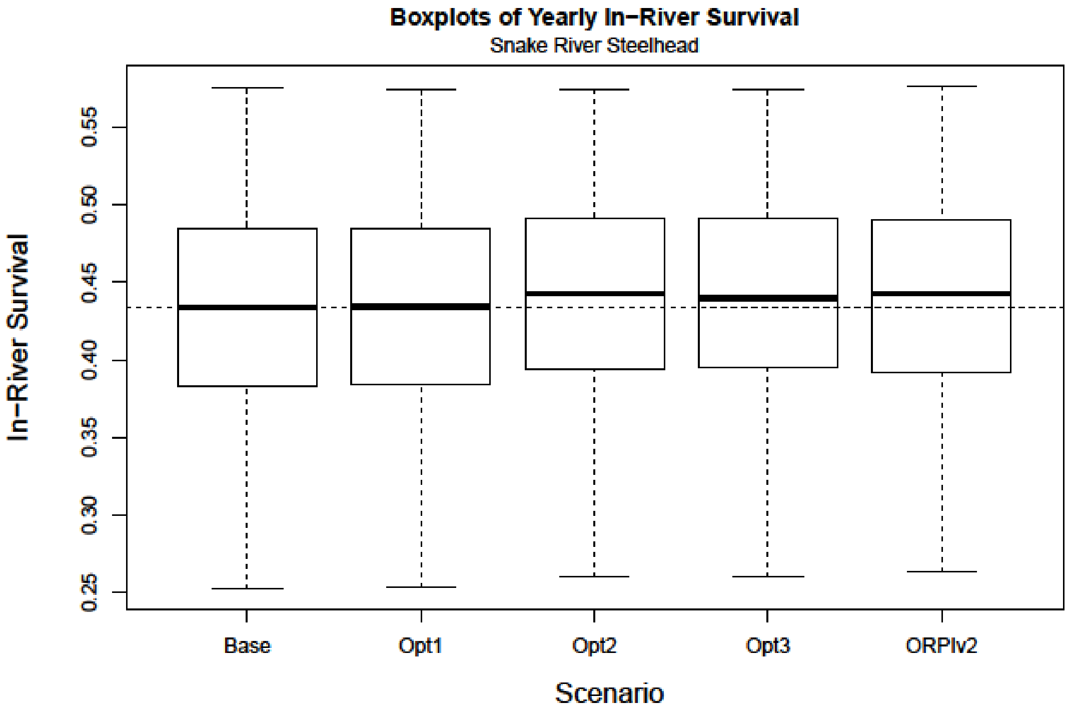

Figure 4. Boxplots of COMPASS predicted in-river survival for Snake River steelhead by management scenario.

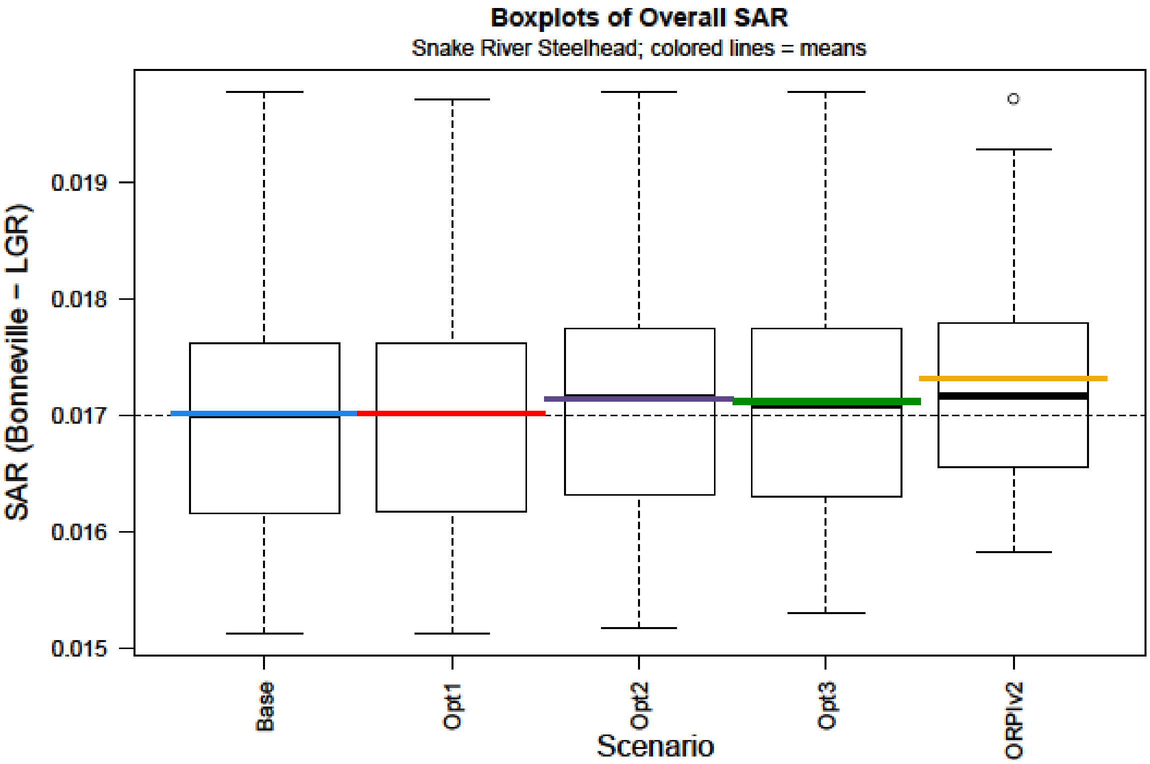

Figure 5. Boxplots of COMPASS predicted SAR (in-river and transported fish combined) for Snake River steelhead by management scenario. Means are presented with colored lines and medians with black lines.

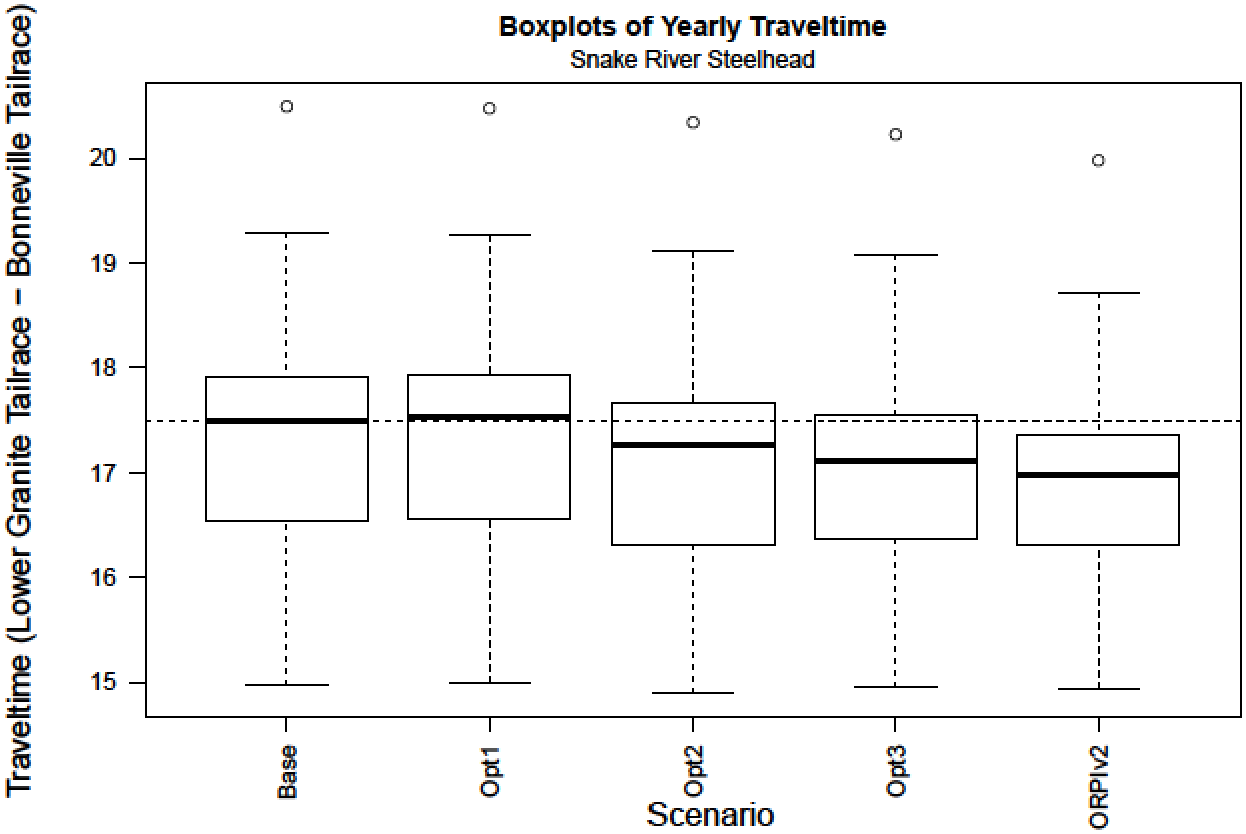

Figure 6. Boxplots of COMPASS predicted in-river travel time for Snake River steelhead by management scenario.

Discussion

The results from the management scenarios show that the scenarios with increased spill had small effects on in-river survival. The increased spill resulted in shorter predicted travel times and smaller predicted proportions of fish transported. Faster travel times will get fish to the estuary sooner. There is an optimal time window for arrival at the estuary, with too early or late arrivals resulting in lower SAR's. The SAR relationships differ for transported and in-river fish, so the amount and timing of transportation will affect overall combined SAR's.

One may question whether the small change in predicted responses for the ORPIv2 scenario with significantly increased spill relative to those from the Base scenario representing current conditions suggest that COMPASS is not accurately predicting the effects of spill on survival and SAR. Our response is that the predictive models we use are fit to data, and large effects of spill were not supported by those data. We account for direct mortality due to spill and other passage routes at the dams. The passage route probabilities are dynamic and depend on spill, flow, and other inputs. Therefore, spill affects passage routing, and that in combination with route-specific mortality rates determines overall dam survival. During the calibration (model fitting) and model selection for our reservoir survival models, we allowed a variable to enter the models that measured the proportion of fish in a reservoir that passed through a spill or surface passage route at the previous dam. This variable was not retained in the best models selected by our model selection process, and typically was not a significant predictor of survival. A similar variable was used in our travel time models to account for delay at a dam on the downstream end of a reservoir. This variable was selected by many of our travel time models, and therefore spill and surface passage have an effect on travel times in the model. Those travel times directly affect reservoir survival and indirectly affect SAR through arrival times at Bonneville Dam. Therefore, spill affects survival directly at dams and indirectly affects survival and SAR through travel times.

We did not attempt to account for the negative effects of increased spill related to increased production of saturated gas and possible trauma induced by passage through highly turbulent spillways. Spill level and pattern can also create eddies in the tailraces of some dams depending on flow and turbine operations. Fish trapped in eddies are more vulnerable to predation and are subject to longer travel times. Such conditions are not modeled in COMPASS and effects on survival are not explicitly accounted for.

References

Comprehensive Passage (COMPASS) Model – version 1.1. 2008. Review draft. Available online at: http://www.cbr.washington.edu/sites/default/files/manuals/COMPASS_manual_april_2008.pdf

Zabel, R. W., J. R. Faulkner, S. G. Smith, J. J. Anderson, C. Van Holmes, N. Beer, S. Iltis, J. Krinke, G. Fredricks, B. Bellerud, J. Sweet, and A. Giorgi. 2008. Comprehensive passage (COMPASS) model: a model of downstream migration and survival of juvenile salmonids through a hydropower system. Hydrobiologia 609:289-300.

Modeling Arrival Distributions of Populations of Juvenile Snake River Spring-Summer Chinook and Steelhead at Lower Granite Dam and Effects of Arrival Timing on Predicted Survival and Population Experiences

James R. Faulkner, Daniel L. Widener, and Richard W. Zabel
Fish Ecology Division, Northwest Fisheries Science Center, Seattle, WA

Introduction

The migration timing of juvenile salmonids determines the conditions they will experience within their migration corridor as well as conditions they will encounter when they enter the estuary and ocean. These conditions determine their probability of survival and determine the resources they will encounter in their search for continued growth. Accurate prediction of migration timing and arrival distributions of populations at key points in their migration corridor is therefore a critical component in life cycle models used for predicting population trends and assessing management scenarios.

We focus on the timing of individuals arriving at Lower Granite Dam (LGD), which is the first dam on the lower Snake River encountered by juvenile migrants. This location also acts as an entry point into the Federal Columbia River Power System (FCRPS), which is composed of a series of dams and reservoirs on the lower Snake and Columbia Rivers, is closely monitored, and benefits from a set of detailed ecological models developed to describe the process of smolt migration through the system (Zabel et al. 2008). Arrival timing at LGD is determined by both the timing of initiation of migration and the subsequent time it takes to travel to LGD.

Many biological and environmental factors can influence the initiation of migration for juvenile salmon.

The main biological factor is the timing of smoltification, which coincides with the readiness to migrate. Smoltification depends on fish size, photoperiod, and temperature (Johnsson and Clarke 1988; Beckman et al. 1998; McCormick et al. 2000). Fish size is determined by growth as parr, which is dependent on temperature, photoperiod, competition, and food availability (McCormick et al. 1998). Once a fish has started smoltification and is becoming behaviorally ready to migrate, release factors that may trigger migration include photoperiod, temperature, flow, turbidity, and social cues (Bjornn 1971; Hansen and Jonsson 1985; Jonsson 1991; Sykes et al. 2009).

Migration is not always initiated from natal streams, since many individuals may begin to move downstream as parr. Shrimpton et al. (2014) found evidence for extensive downstream movements in Chinook prior to smoltification and actual migration based on stream chemistry signatures in otoliths. These pre-smolt downstream movements could be due to a variety of factors present in natal streams, including inadequate habitat for overwintering, unsuitable stream temperatures, limited food availability, and high population densities (Bjornn 1971; Cunjak 1996). Pre-smolt movements could also be involuntary and due to heavy precipitation or flow events that wash individuals downstream. The pre- and early stages of migration likely consist of a slow and iterative process of moving downstream and holding over until smoltification begins and stream conditions are right for starting migration (Steel et al. 2001).

Travel time of migrating spring-summer Chinook and steelhead has been shown to be associated with distance traveled, water velocity, temperature, degree of smoltification, and fish size (Zabel et al. 1998; Smith et al. 2002; Zabel 2002; Zabel et al. 2008). Smaller fish and those just starting smoltification will likely move slower by staying out of the main channel. Chinook tend to travel slower earlier in the migration season and then speed up as the season progresses (Zabel et al. 1998).

We currently do not have sufficient data to explicitly separate the time of initiation of migration and the travel time to LGD for individual fish. We only have data on the arrival timing of individual fish at LGD, which is a function of initiation of migration and travel time. However, the factors that determine arrival timing at LGD should be a combination of the factors that determine initiation of migration and travel time. Achord et al. (2007) analyzed arrival timing at LGD for spring-summer Chinook from the Salmon River basin and found that average temperatures in the spring and previous autumn and average streamflow in March best explained median arrival times. Higher temperatures and higher flows resulted in earlier arrival times. Autumn temperature could affect growth and pre-smolt movements downstream, and spring flow and temperatures could affect both initiation of migration and travel time.

Given the complex processes that produce arrival distributions, it is not surprising that these distributions exhibit a variety of complex characteristics, including multiple modes, sharp spikes, and long tails, and that the shape, location, and spread of these distributions can vary across populations and years. We needed a modeling method that would capture these complex distributional forms and be based on inputs that could be used in prospective modeling exercises. We developed a method based on a combination of quantile regression and nonparametric smoothing that predicts continuous probability distributions for arrival times based on a set of predictor variables. We fit the models to arrival times for populations of spring-summer

Chinook and steelhead from the Snake and Salmon River basins. We then use those models to predict arrival distributions under prospective scenarios and summarize the resulting population-specific experiences in the hydropower system and subsequent adult returns.

Methods

PIT Tag Data

The observational data we used to fit our models of arrival timing were the detection times at LGD for fish implanted with passive integrated transponder (PIT) tags. For our models, we used PIT-tagged fish from Endangered Species Act (ESA) listed populations of spring Chinook salmon and steelhead trout in the Snake River basin (NMFS 2016). There are a total of 31 ESA-listed populations of spring Chinook above LGD; these populations are grouped into five different Major Population Groups (MPGs): Lower Snake, Grande Ronde/Imnaha, South Fork Salmon, Middle Fork Salmon, and Upper Salmon. Due to the small amount of data available in some of the ESA-defined MPGs, we decided to group the Lower Snake and Imnaha/Grande Ronde MPGs and the South and Middle Fork Salmon MPGs for model fitting (Table 1). Not all of the ESA-listed populations of Snake River steelhead directly correspond to those for spring Chinook, but to simplify our modeling we used the same set of population designations and groupings for steelhead.

A number of researchers and organizations have PIT tagged wild fish from these populations on a regular basis, starting from the early 1990s (e.g., Achord et al. 2007). All PIT tag mark and observation data collected within the wider Columbia River basin is stored in the PTAGIS database operated by the Pacific States Marine Fisheries Commission (PSMFC 1996-present).

We queried the PTAGIS database to select all available mark and observation data of wild fish from the ESA-listed populations in the Snake River basin.

Table 1. A list of all ESA-listed populations above LGD and their associated MPG, organized by the groupings we used to fit our arrival models.

ESA MPG	ESA Populations by Model Group
	Grande Ronde/Imnaha
Lower Snake	Asotin River
Grande Ronde/Imnaha	Big Sheep Creek, Imnaha River, Grande Ronde River, Wenha River, Catherine Creek, Lostine River, Minam River, Lookingglass Creek
	Lower Salmon
South Fork Salmon	East Fork South Fork Salmon, Little Salmon River, South Fork Salmon, Secesh River
Middle Fork Salmon	Bear Valley Creek, Big Creek, Camas Creek, Chamberlain Creek, Loon Creek, Marsh Creek, Sulfur Creek, Middle Fork Salmon Below Indian Creek, Middle Fork Salmon Above Indian Creek
	Upper Salmon
Upper Salmon	Pahsimeroi River, Lemhi River, Salmon River Below Redfish Lake, Salmon River Above Redfish Lake, Valley Creek, Yankee Fork, East Fork Salmon River, North Fork Salmon River, Panther Creek

For the collection of mark data, we obtained from the PTAGIS database the locations of every mark/release site in one of the Salmon, Imnaha, or Grande Ronde River hydrologic units. We then assigned every smolt trap or general riverine mark/release site in each hydrologic unit to a specific ESA-listed population, as long as the site was on the main river assigned to the population, or a tributary (Appendix Table 1).

After assigning PTAGIS mark/release sites to each ESU population, we then queried the PTAGIS database, selecting the records of all juvenile Chinook and steelhead released at the selected mark/release sites and also detected as a juvenile at LGD. For Chinook salmon, we selected the records of fish with wild or unknown rearing types, and spring, summer, or unknown run types. For steelhead, we selected the records of fish with wild or unknown rearing types and all run types. We used the first detection time at LGD in the fish's migration year, and ignored any later detections. The resulting data covers the years 1990-2015, with more fish tagged in later years (Table 2).

Table 2. Populations of Chinook and steelhead with numbers of fish with PIT-tag detections at LGD across all years with data. Populations are ordered by MPG. Years in which data were available varied by population, and only populations with 50 or more total detections were used in model fitting.

Population	Code	Years	Chinook	Steelhead
Asotin River	ASO	2005-2015	20	7,946
Big Sheep Creek	BSC	-	0	0
Imnaha River	IMN	1990-2015	46,842	31,870
Grande Ronde River	GRN	1993-2015	21,054	9,110
Wenha River	WEN	-	0	0
Catherine Creek	CAT	1991-2015	3,930	1,735
Lostine River	LOS	1990-2015	6,914	1,873
Minam River	MIN	1993-2015	4,837	1,415
Lookingglass Creek	LGC	1994-2015	3,076	2,312
Bear Valley Creek	BVC	1990-2015	3,065	88
Big Creek	BIG	1990-2015	7,436	1,946
Camas Creek	CAM	1993-2015	726	693
Chamberlain Creek	CHA	1992-2015	853	1,810
Loon Creek	LOO	1993-2015	1,047	67
Marsh Creek	MAR	1990-2015	12,818	801
Sulfur Creek	SUL	1990-2015	761	89
Middle Fork Salmon, below Indian Creek	BIC	-	0	0
Middle Fork Salmon, above Indian Creek	AIC	-	0	0
East Fork South Fork Salmon	ESF	1993-2015	14,928	3,012
Little Salmon River	LIT	1998-2014	121	1,242
South Fork Salmon	SFS	1991-2015	13,448	2,612
Secesh River	SEC	1990-2015	14,248	1,851

Pahsimeroi River	PAH	1993-2015	9,776	1,292
Lemhi River	LEM	1992-2015	12,322	2,902
Salmon River, below Redfish Lake	SBR	-	0	0
Salmon River, above Redfish Lake	SAR	1990-2015	10,467	704
Valley Creek	VAL	1990-2015	1,629	25
Yankee Fork	YNK	1995-2015	721	115
East Fork Salmon River	EFS	1991-2015	2,559	69
North Fork Salmon River	NFS	1993-1995	92	0
Panther Creek	PAN	-	0	0

Flow and Temperature Data

We decided to confine our predictor variable set to only those environmental covariates that would be available in a prospective modeling framework; considering this limitation, we used flow and temperature in the reservoir of Lower Granite Dam as our chief predictors of arrival timing at LGD.

We acquired raw flow data by downloading the flow records for Lower Granite Dam, 1989-2016, from the DART website (Columbia River DART 2017). For temperature data, we downloaded the 1989-2016 records of the WQM temperature reading at Lower Granite Dam, also from the DART website. For both datasets, any gaps in the time series were filled via linear interpolation; however, for the time period relevant to our analysis (January-June), gaps were infrequent and rarely longer than a few days.

We created monthly statistics for January through June from these data time series for use as our predictor variables. From the flow dataset, for each month we estimated mean flow, the Julian date of maximum flow, and the Julian date of the largest daily change in flow. This resulted in a total of 18 monthly flow predictor variables. The monthly mean flow variables were highly correlated, so we used principle components analysis (PCA; Hotelling 1933; Joliffe 2002) to find a set of linear combinations of the monthly mean flows that were uncorrelated but still captured the variation in the data. The resulting six PC's were used as predictor variables in place of the mean flows.

We also created monthly statistics for January through June from the temperature dataset. We calculated monthly mean temperature and the range in temperature for each month, resulting in 12 monthly temperature predictors. The monthly mean temperature predictors were highly correlated, so we used PCA to calculate six PC's to be used as predictors in place of the monthly means. Monthly temperature range was not highly correlated among months so was not transformed. We also estimated the mean temperature in the previous autumn for each year by averaging October through December temperatures, for a total of 13 temperature predictors.

Prospective Environmental Data

For prospective modeling of arrival timing at LGD, we used a management scenario produced by the Bonneville Power Administration (BPA)'s HYDSIM model, referred to as the "Base" scenario. This scenario replicates current management operations and imposes them on 80 historical water years from 1929 through 2008. We used the loadings and centers generated from the PCA's of flow and temperature to produce the 18 flow and 13 temperature predictors for each year in the 80-year Base scenario.

Retrospective Modelling

We used a combination of quantile regression (Koenker and Basset, 1978; Koenker 2005; Cade and Noon, 2003) and nonparametric smoothing splines (Green and Silverman 1994; Hastie et al. 2009) to generate probability distributions for arrival times at LGD. A quantile is the value of a random variable associated with a particular value of its cumulative probability distribution. For example, in terms of arrival time distributions, the 0.05 quantile represents the time on which 5% of the population has arrived, and the 0.95 quantile represents the time when 95% has arrived. The median of a distribution is the 0.5 quantile. Quantile regression is a method used to model associations between specific quantiles and a set of predictor variables.

We used quantile regression to relate environmental factors and population indicators to arrival times.

For any quantile $\tau \in (0,1)$, the quantity $\widehat{\boldsymbol{\beta}}(\tau)$ is the vector of regression parameters that solves

$$\widehat{\boldsymbol{\beta}}(\tau) = \text{argmin}_{\boldsymbol{\beta}\in\mathbb{R}^p} \sum_{i=1}^{n} \rho_\tau \left(y_i - \boldsymbol{x}_i'\boldsymbol{\beta}\right)$$

where $\rho_\tau(u) = u\big(\tau - I(u < 0)\big)$ and $I(\cdot)$ denotes the indicator function. This minimization is performed with linear programming optimization methods. We used the rq function in the quantreg package in R to fit the quantile regression models. Models were fit separately for each population group, where population groups were as described previously in the Data section. Further details of the variable selection are described below.

We fit multiple quantiles simultaneously. Due to restrictions of the fitting routine, this meant that each quantile model shared the same set of predictor variables. However, the estimated parameters differed across the quantile models. This resulted in reduced flexibility in the possible sets of individual quantile models, but greatly reduced the model space we needed to explore.

The quantile regression models provided a set of predicted times of arrival corresponding to the set of quantiles specified by the models. Due to the time scale of the covariate measures (one observation per covariate per population per year), each population had a set of predicted quantiles for each year for which there were data. These quantiles provide a partial representation of the entire arrival distribution for a population in a year. For an example of a quantile regression fit to our data using a single predictor, see Figure 1.

To fill in the entire continuous set of quantiles, we fit smoothing splines to the predictions from the quantile regression models. Smoothing splines are a nonparametric regression method that fits a smooth curve to a set of data points. Smoothing splines were fit to logit-transformed cumulative probabilities corresponding to the model-predicted quantiles for each population in each year. The logit transformation constrained the predicted cumulative probabilities to the (0,1) interval. The number of *degrees of freedom* of a smoothing spline represents the effective number of parameters used to fit the smoothing spline. The maximum degrees of freedom is the number of observations in the data (assuming no replicate points). Fewer degrees of freedom results in more smoothing and the maximum degrees of freedom will result in interpolation. We tested a range of degrees of freedom for each smoothing spline model. The number of knots for each model were equal to the number of data points. The smoothing spline fits resulted in predictive models for a continuous set of cumulative proportions. The first derivative of these models for cumulative probabilities provide an approximate probability density function for the arrival distribution of a population under a set of input conditions.

We note that smaller degrees of freedom of the smoothing splines, relative to the number of possible degrees of freedom, result in more smoothing, which means the predicted curves would lie further from the data points (model predicted cumulative probabilities) than models with higher degrees of freedom. Therefore, higher degrees of freedom are actually better for our purposes since we would like the spline predictions to be as close to the quantile model predictions as possible.

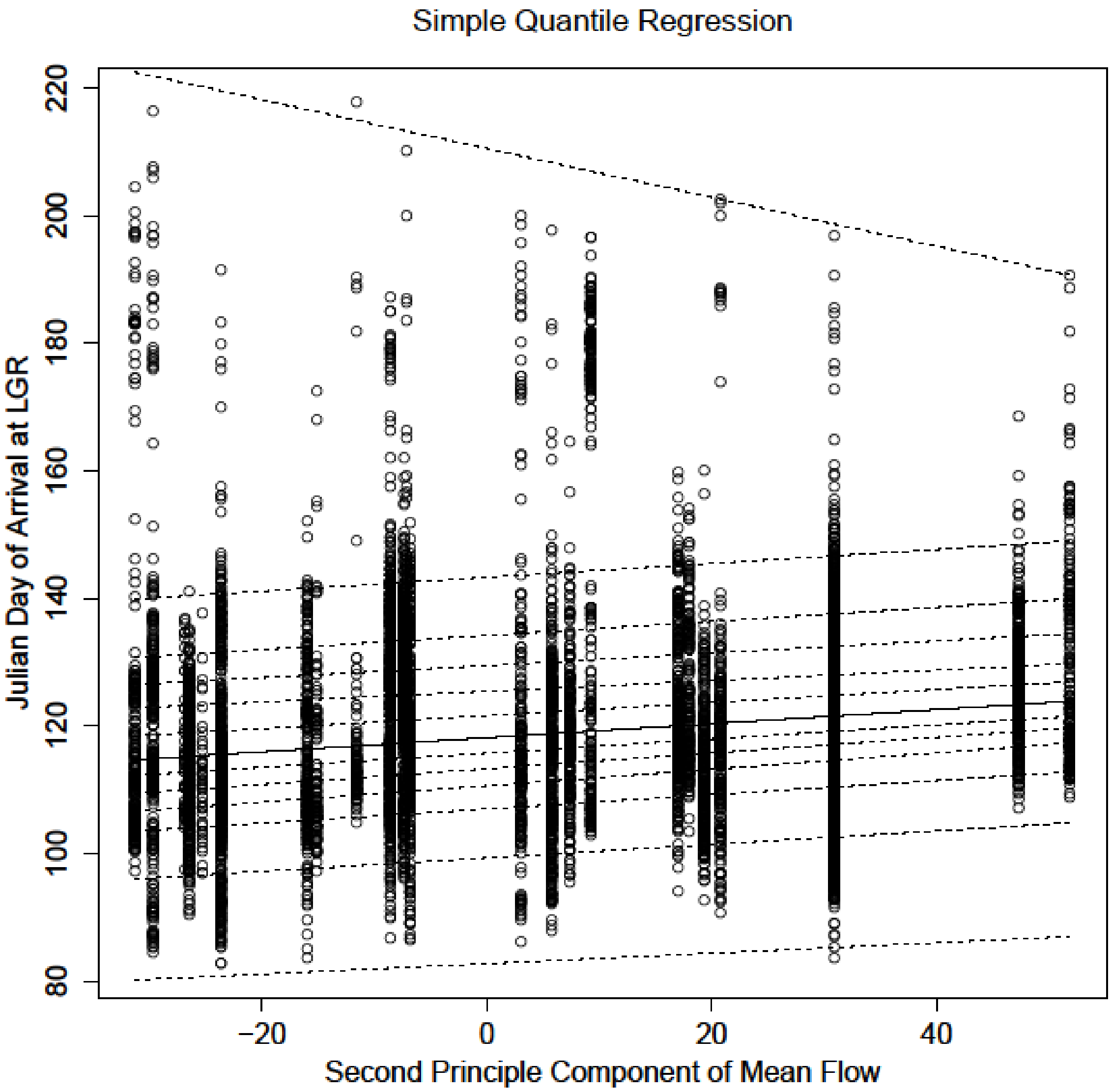

Figure 1. Example of a simple quantile regression fit to our arrival time data, using only a single environmental predictor; in this case, the second principle component of monthly mean flow. 13 quantiles were fit, ranging from the 0.0001 quantile to the 0.9999 quantile. The median quantile is shown as a solid line.

The resulting predicted probability density functions could then be used to calculate the likelihood of the observed arrival times under the model and estimated parameters. The likelihoods were therefore based on the combined quantile regression and smoothing spline model predictions and used all of the individual arrival time data. The likelihood for the estimated model parameters, $\widehat{\boldsymbol{\theta}}$, given the arrival time of fish *i* in population *j* in year *k* was calculated as

$$\mathcal{L}\left(\widehat{\boldsymbol{\theta}}\middle|t_{ijk}\right) = \hat{f}_{jk}(t_{ijk}|\widehat{\boldsymbol{\theta}})$$

where $\hat{f}_{jk}(\cdot\ |\boldsymbol{\theta})$ is the estimated probability density function for the arrival times of fish in population *j* in year *k*, conditional on the estimated model parameters. The likelihood for the entire set of data given the estimated parameters was then the product of the individual likelihood components:

$$\mathcal{L}\left(\widehat{\boldsymbol{\theta}}\middle|\boldsymbol{t}\right) = \prod_{i,j,k} \hat{f}_{jk}(t_{ijk}|\widehat{\boldsymbol{\theta}})$$

We calculated likelihoods on the log scale to avoid numerical issues. We then used the resulting log-likelihood values to calculate Akaike Information Criteria (AIC) values for each model. The number of parameters in each model was equal to the number of parameters in the quantile regression model multiplied by the number of quantiles plus the number of degrees of freedom used in the smoothing spline. The appropriate number of parameters for the smoothing spline component would be the number of spline degrees of freedom times the number of populations and years for each population. However, we did not realize this in time for the writing of this document, but will apply that method going forward.

We fit models for 13, 15, 17, 19, 21 quantiles. For each set of quantiles, the 0.0001, .05, 0.5, 0.95, and 0.9999 quantiles were always included, and the remaining quantiles were equally spaced between the .05 quantile and median, and 0.95 quantile and median. This arrangement was chosen to allow consistency in how the tails were modeled across quantile sets. For each number of quantiles, we performed a forward variable selection procedure based on the AIC values calculated from the model likelihoods described above. At each step, a single new predictor variable was selected from the set of remaining variables and added to the current best model, the quantile regression models were fit, smoothing splines were fit to the predicted cumulative probabilities for each population and year, and AIC was calculated. We fit a series of separate smoothing splines with different degrees of freedom, where degrees of freedom ranged between 2 and one less than the number of quantiles in a model. For each level of degrees of freedom we calculated the resulting AIC and kept the spline model that resulted in the lowest AIC. All of the remaining variables were tested one at a time in this manner and the new model that resulted in the largest reduction in AIC was retained as the new best model. This process was repeated until the addition of new variables no longer resulted in a reduction in AIC. The model selection process was therefore targeting the best combination of predictor variables, number of quantiles, and level of smoothing of the quantiles in terms of AIC. The forward selection procedure was chosen to reduce the model space and avoid fitting all possible combinations of predictor variables.

Cumulative probability distributions are strictly non-decreasing functions. The smoothing spline fits to the cumulative probabilities predicted by the quantile regression models did not always result in strictly non-decreasing functions. The first derivatives of sections of decreasing cumulative functions are therefore negative, which corresponds to a negative probability density in that segment. When this occurred, we set the probability density to zero and scaled the remaining density so that it would integrate to 1. Sections of decreasing functions were infrequent and usually short in length so discontinuities in the predicted arrival densities were small.

The quantile regression models were not strictly constrained to maintain order of quantiles for all predictions. Therefore, some quantiles could be predicted close enough that their order would switch. If this occurred, we simply sorted the predicted quantiles to maintain the proper ordering. This did not occur very often with our models, and when it did the predicted quantiles were close together so that the re-ordering had little effect on model results.

We note that within-season variation in detection probabilities at LGD could affect the shape of arrival distributions, since only detected fish are included in the samples. We found that detection probabilities had more variability between years than within years, and annual variation will not adversely affect the quantile estimation. We assumed the within-season variation in detection probabilities was not large enough to affect the parameter estimation or model performance. We will investigate how to include detection probability in future models.

Prospective Modelling

The COMPASS model is used to assess various aspects of the passage experience of migrating juvenile salmon through the hydropower system on the Snake and Columbia Rivers under different management scenarios (Zabel et al 2008). The Bonneville Power Administration (BPA) generates hydrological data for a set of 80 water years under different scenarios using their HYDSIM hydrological model. The HYDSIM model outputs daily predictions for flow, reservoir elevation, and spill at all dams in the system for each water year. Those predictions are input into the COMPASS model along with predictions of water temperature to generate predictions of passage experience for a particular population for each water year. Differences in the population release distributions will result in different exposures to changing river conditions, different exposures to transportation, and different timing at the estuary. Each of these components will contribute to different model predicitions.

We used our fitted models of arrival timing at LGD with the flow and temperature predictors we generated from the 80 water years of the “Base” BPA scenario to generate unique arrival distributions for each fish population and year. Some of these predicted distributions had very early or very late tails; in these cases we truncated the predicted distributions at day 60 and day 200 and rebalanced them to sum to 1. We then ran COMPASS on the 80 water years using these arrival distributions as the release distributions at LGD. The aspects of passage experience that we summarize here are survival of fish migrating in river (not transported), proportion of fish transported, travel time from Lower Granite Dam to Bonneville Dam, and smolt-to-adult return (SAR) from Bonneville Dam as juveniles to Lower Granite Dam as adults.

Results

Retrospective Modelling

Many of the models selected by AIC resulted in larger numbers of quantiles and larger degrees of freedom of the smoothing splines. We were concerned that the complexity of these models could result in spurious predictions and excessively complex distribution shapes. The penalties for numbers of parameters in the AIC calculations did not seem sufficient to overcome this apparent overfitting of the data. We therefore decided to use models with only 13 quantiles for all models in an effort to minimize excess complexity yet still maintain enough flexibility to capture various distribution shapes. Thus, all results shown here and in the prospective modeling are for models with 13 quantiles.

Several of the populations had no or very few tagged fish, and we were unable to fit arrival models for them. These included the Asotin, Big Sheep Creek, Wenha, Panther Creek, Salmon below Redfish Lake, and both mainstem Middle Fork Salmon populations of spring Chinook, and the Big Sheep Creek, Wenha, North Fork Salmon, Panther Creek, Salmon below Redfish Lake, and both mainstem Middle Fork Salmon populations of steelhead. The Pahsimeroi River population of spring Chinook displayed a unique pattern in its arrival data, with large peaks in arrival in late June and July in many years. These peaks are much later than any other population in the dataset, and could indicate large numbers of summer Chinook in that population. Our COMPASS models of survival and migration timing are only fitted to data within the spring migration period and are thus not valid for later-migrating summer Chinook, so we decided to exclude the Pahsimeroi population of Chinook from our arrival model fitting and prospective analysis.

The best-fitting 13 quantile models were complex, with the simplest model having 13 predictors, and the most complex having 23. The smoothing splines were typically fitted with at least two to three degrees of freedom fewer than the number of quantiles, resulting in a fair amount of smoothing (Table 3).

The best-fitting 13 quantile models are able to capture a variety of shapes in observed arrival distributions, including fairly normal distributions and distributions with more than one distinct mode (Figures 2, 3). However, multimodal distributions where the individual modes are less distinct tend to be fitted with less fidelity to each individual peak (Figure 4).

Table 3. Predictor variables selected by the best 13-quantile models by AIC for each species and population grouping. DF = Degrees of Freedom.

Species and *MPG*	**Selected Predictors**	**Spline DF**
Chinook *Imnaha/Grande Ronde*	January, March, April, June Date of Maximum Daily Change in Flow; January, March, April Date of Peak Flow; 1st, 2nd, 3rd, 4th, 5th Principle Components of Monthly Flow; January, April, June Temperature Range; 1st, 3rd, 4th, 6th Principle Components of Monthly Temperature, Autumn Temperature	11
Chinook *Lower Salmon*	January, February, March, April, May, June Date of Maximum Daily Change in Flow; March, April, May, June Date of Peak Flow; 2nd, 3rd, 4th, 5th, 6th Principle Components of Monthly Flow; January, February, May, June Temperature Range; 1st, 2nd, 4th, 5th Principle Components of Monthly Temperature	9
Chinook *Upper Salmon*	March, April, May Date of Maximum Daily Change in Flow; March, April, May, June Date of Peak Flow; 1st, 3rd, 4th, 5th, 6th Principle Components of Monthly Flow; April, May Temperature Range; 2nd, 3rd, 4th, 5th, 6th Principle Components of Monthly Temperature	9
Steelhead *Imnaha/Grande Ronde*	February, March, April, May Date of Maximum Daily Change in Flow; January, February, April, May, June Date of Peak Flow; 1st, 3rd, 4th Principle Components of Monthly Flow; January, March, May Temperature Range; 1st, 2nd Principle Components of Monthly Temperature	11
Steelhead *Lower Salmon*	February, March, April, June Date of Maximum Daily Change in Flow; February, May, June Date of Peak Flow; 1st, 6th Principle Components of Monthly Flow; January, March, April, May Temperature Range; 3rd, 4th Principle Components of Monthly Temperature	7
Steelhead *Upper Salmon*	February, March Date of Maximum Daily Change in Flow; January, March, May, June Date of Peak Flow; 3rd, 5th Principle Components of Monthly Flow; February, March, April Temperature Range; 1st, 4th Principle Components of Monthly Temperature	8

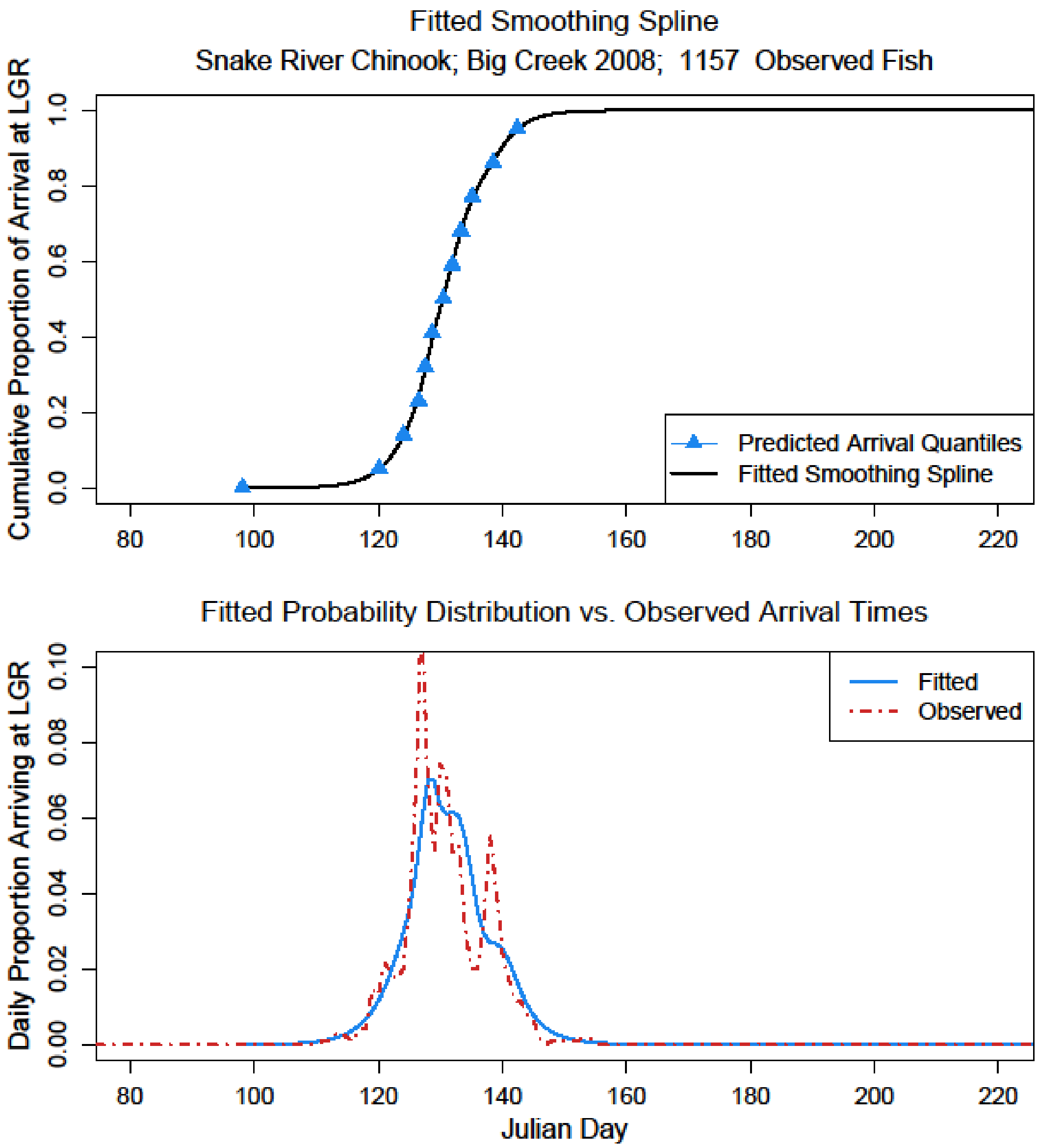

Figure 2. The top panel shows the predicted cumulative proportions and associated quantiles with the fitted smoothing spline (using the AIC-selected best degrees of freedom) for the Big Creek population of Chinook in 2008. The bottom panel shows the resulting probability distribution (first derivative of fitted cumulative distribution) with observed arrivals of Big Creek Chinook in 2008. Note that the maximum quantile was outside the range of the plotting window and is not shown.

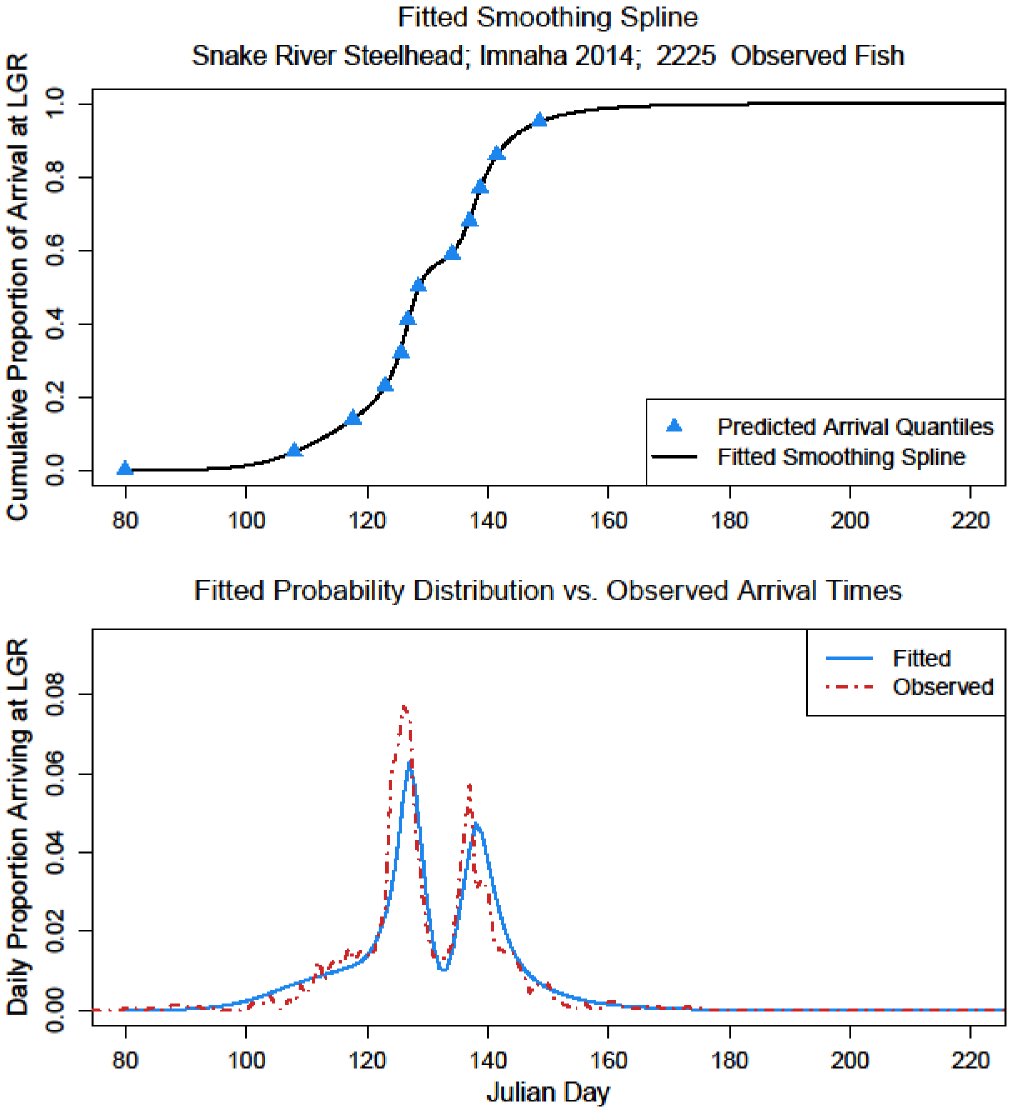

Figure 3. The top panel shows the predicted cumulative proportions and associated quantiles with the fitted smoothing spline (using the AIC-selected best degrees of freedom) for the Imnaha population of steelhead in 2014. The bottom panel shows the resulting probability distribution (first derivative of fitted cumulative distribution) with observed arrivals of Imnaha steelhead in 2014. Note that the maximum quantile was outside the range of the plotting window and is not shown.

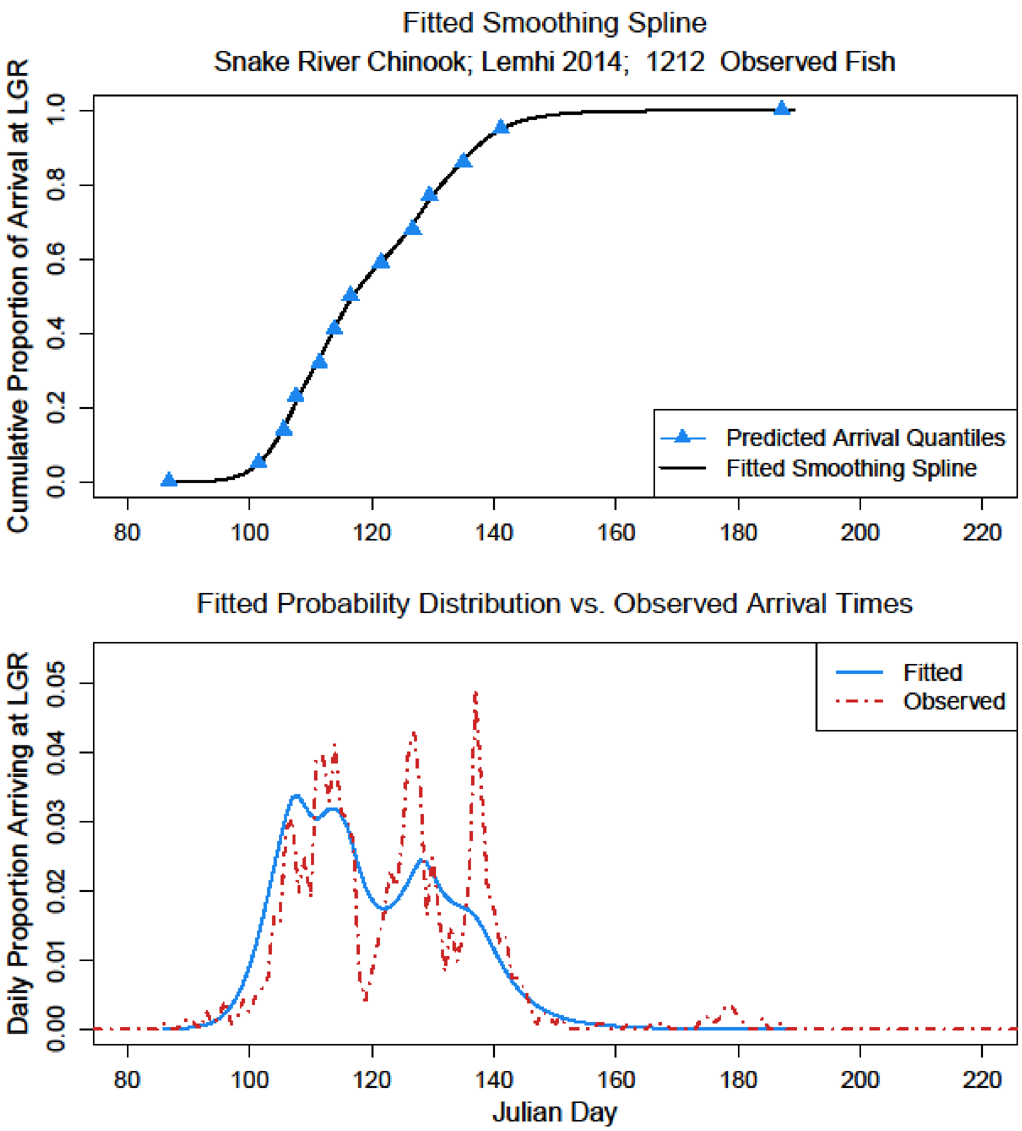

Figure 4. The top panel shows the 13 predicted cumulative proportions and associated quantiles with the fitted smoothing spline (using the AIC-selected best degrees of freedom) for the Lemhi population of Chinook in 2014. The bottom panel shows the resulting probability distribution (first derivative of fitted cumulative distribution) with observed arrivals of Lemhi Chinook in 2014.

Prospective Arrival Modelling

Arrival distributions predicted from the 80 water years of the “Base” scenario tended to show some consistent differences between population groupings, as would be expected due to the fact that different population groupings use different predictive models. However, within population groupings some populations were also significantly different from others in the same group, while other population groupings have fairly consistent predictions for all populations in the group.

For Snake River Chinook salmon (Figures 5, 6), the Lower Salmon population group had the earliest predicted arrival timings, and predicted arrival was similar for almost all populations in the group. The Upper Salmon population group tended to have slightly later predicted arrival, but populations within the group showed significant differences from each other, with the East Fork Salmon and Lemhi populations arriving no later than the Lower Salmon populations, and the Yankee Fork population arriving much later. The Imnaha/Grande Ronde population group had later predicted arrival times than the Salmon population groups, but less year-to-year variability within arrival timing. The Catherine Creek population stands out from the others, and is predicted to be the latest arriving population of spring Chinook in our dataset.

Snake River steelhead (Figures 7, 8) showed similar patterns in predicted arrival timing to Chinook salmon. The Lower Salmon population group had the earliest predicted arrival timings, and predicted arrival was very similar for all populations in the group. Both the Upper Salmon and Grande Ronde/Imnaha population groups had later predicted arrival times than the Lower Salmon Group, but unlike Chinook salmon, for steelhead the Upper Salmon population group had slightly later predicted arrival than the Grande Ronde/Imnaha population group, and populations within those groupings were similar to each other in predicted arrival timing.

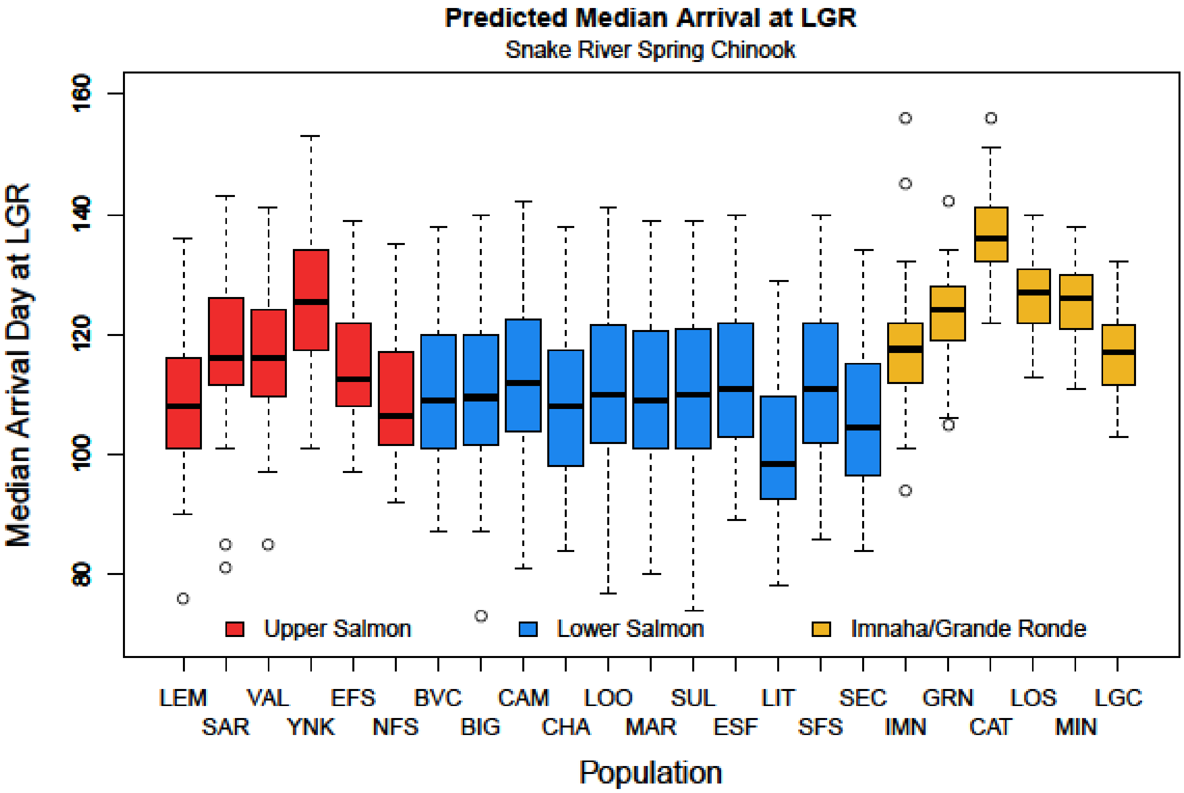

Figure 5. Boxplots of median predicted arrival timing for the 80 water years of the "Base" scenario, for all populations of spring Chinook salmon. The different population groups are broken out by color. Population abbreviation codes are in Table 2.

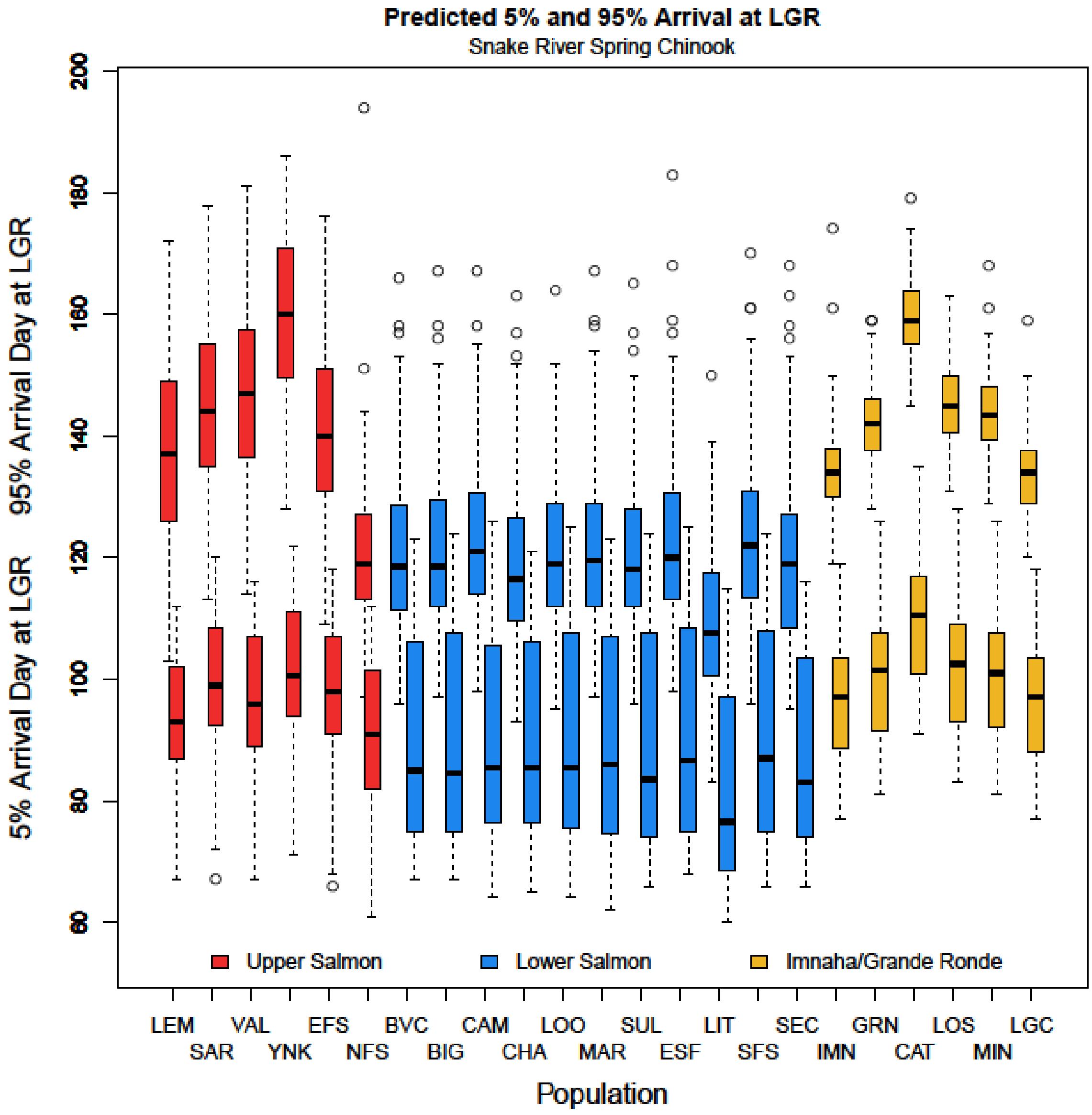

Figure 6. Boxplots of the 5% and 95% predicted arrival quantiles for the 80 water years of the "Base" scenario, for all populations of spring Chinook salmon. The different population groups are broken out by color. Population abbreviation codes are in Table 2.

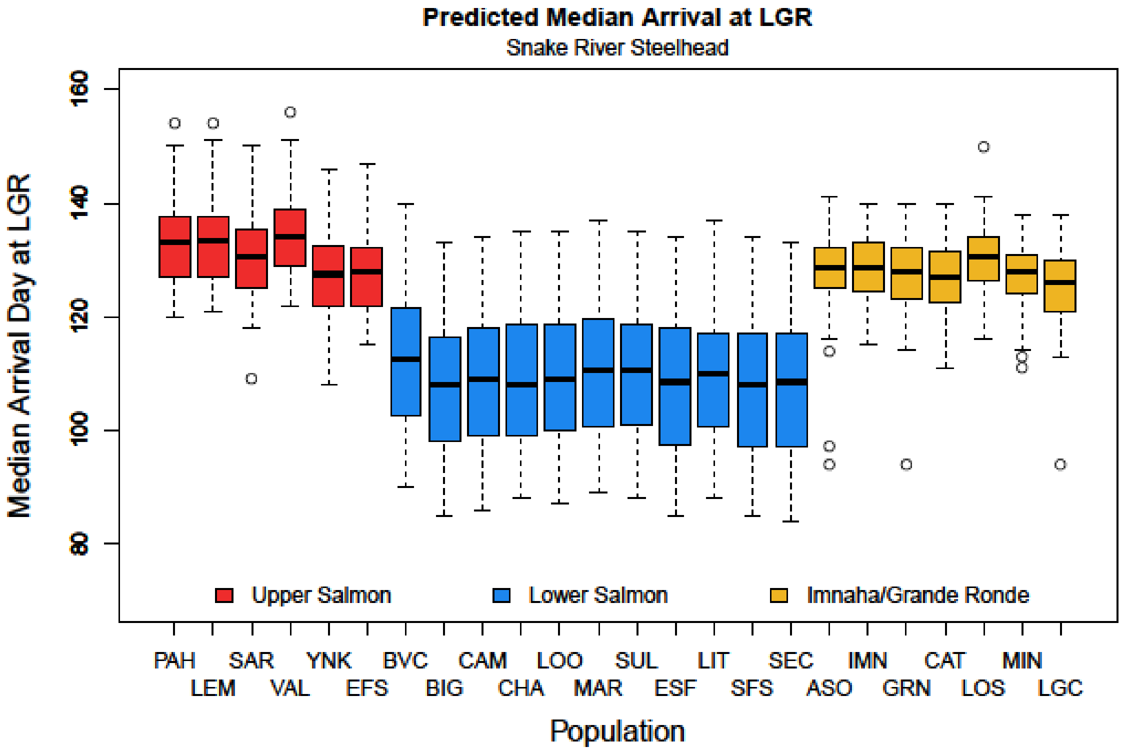

Figure 7. Boxplots of median predicted arrival for the 80 water years of the "Base" scenario for all populations of Snake River steelhead. The different population groups are broken out by color. Population abbreviation codes are in Table 2.

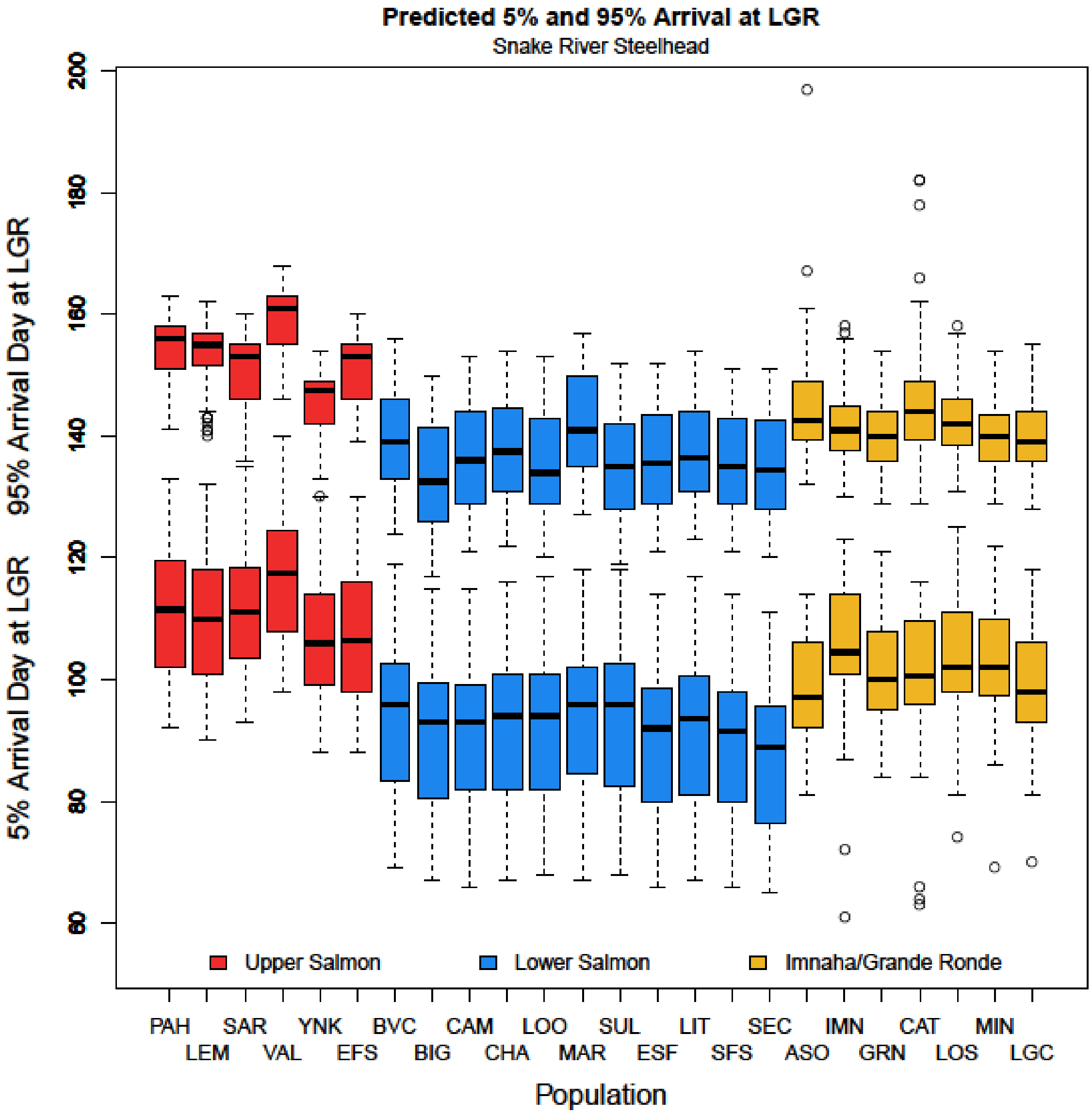

Figure 8. Boxplots of the 5% and 95% predicted arrival quantiles for the 80 water years of the “Base” scenario, for all populations of Snake River steelhead. The different population groups are broken out by color. Population abbreviation codes are in Table 2.

Prospective COMPASS Runs

The COMPASS outputs produced by running the “Base” scenario with the different sets of release distributions predicted by our arrival models show significant differences between populations for some statistics, but small differences for others. For Snake River spring Chinook salmon, most populations show only small differences in COMPASS predicted in-river survival (Figure 9). The only populations that significantly stand out from the others are Yankee Fork, from the Upper Salmon group, and Catherine Creek, from the Grande Ronde/Imnaha population group. These two populations had lower in-river survival than the rest. It is worth noting that these two populations are predicted to be the latest arriving at LGD.

The differences between spring Chinook populations are more noticeable in COMPASS predicted SAR and proportion destined for transport (Figures 10, 11). Both of the later-migrating population groups (Upper Salmon and Grande Ronde/Imnaha) had significantly lower predicted SARs and larger proportions destined for transport than the Lower Salmon population group, and there were large within-group differences as well. The Little Salmon River population, which had slightly earlier predicted arrival than the other Lower Salmon populations, had higher predicted SARs, and very low proportion destined for transport.

The Snake River steelhead populations we modeled showed only small differences in COMPASS predicted in-river survival. Those populations within the same population group were very similar to each other, but the Upper Salmon and Grande Ronde/Imnaha groups had slightly lower survival than the Lower Salmon group (Figure 12). COMPASS predicted SAR and proportion destined for transport showed similar patterns, though the magnitude of the differences was larger than for in-river survival (Figures 13, 14).

In general, across both species and all population groups, the populations with later predicted arrival timing at LGR had lower COMPASS predicted survival, lower SAR, and larger proportions destined for transport.

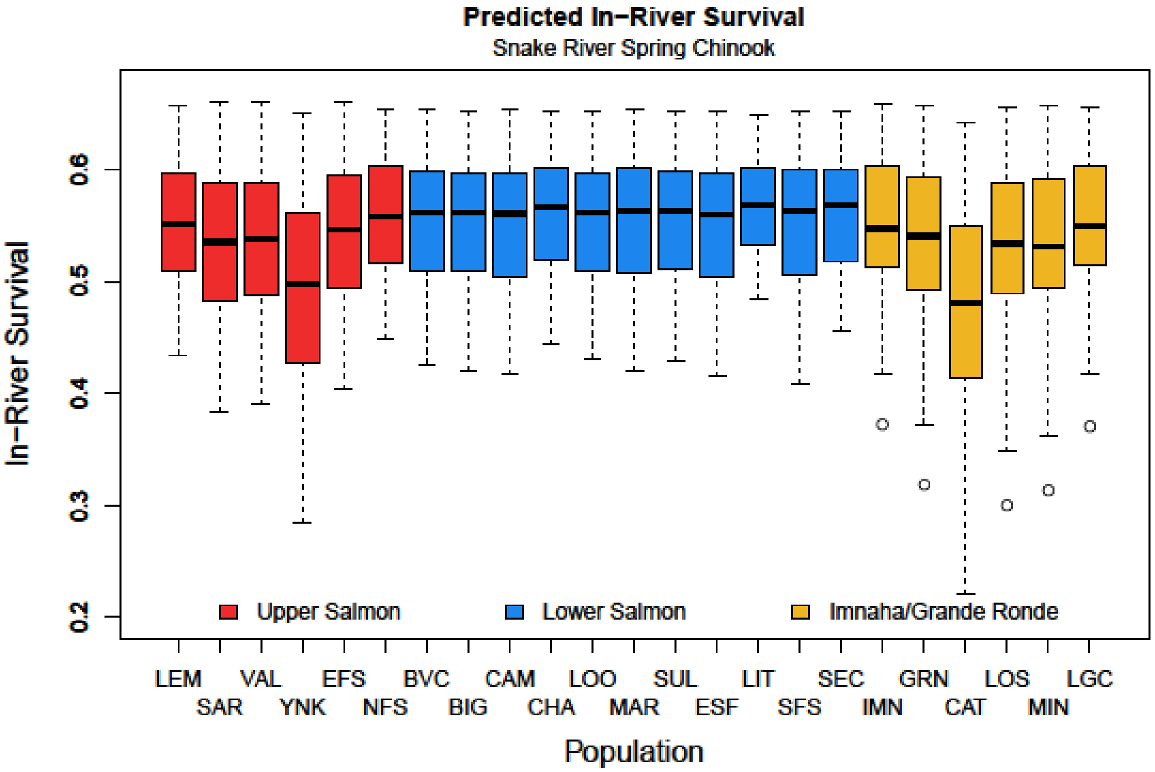

Figure 9. Boxplots of in-river survival (Lower Granite Dam to Bonneville Dam) predicted by COMPASS for the 80 water years of the “Base” scenario for all populations of Snake River spring Chinook salmon. Population groups are denoted by color; see Table 2 for population abbreviations.

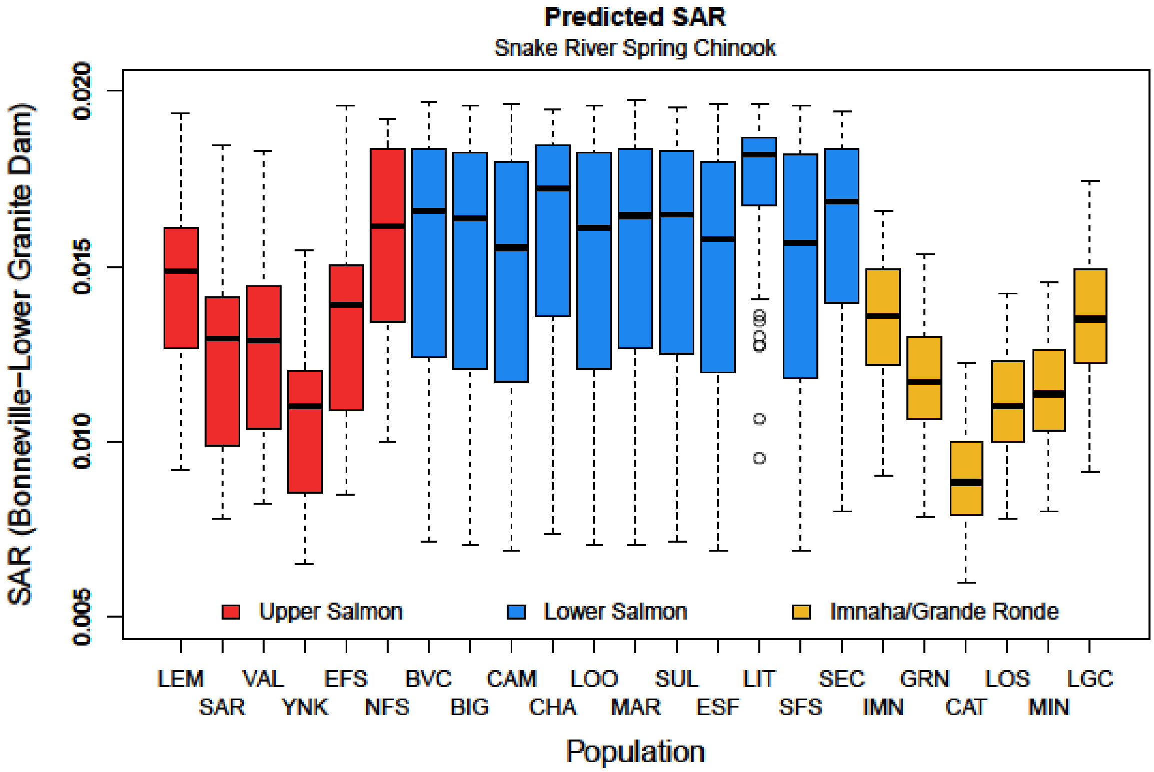

Figure 10. Boxplots of SAR predicted by COMPASS for the 80 water years of the "Base" scenario for all populations of Snake River spring Chinook salmon. Population groups are denoted by color; see Table 2 for population abbreviations.

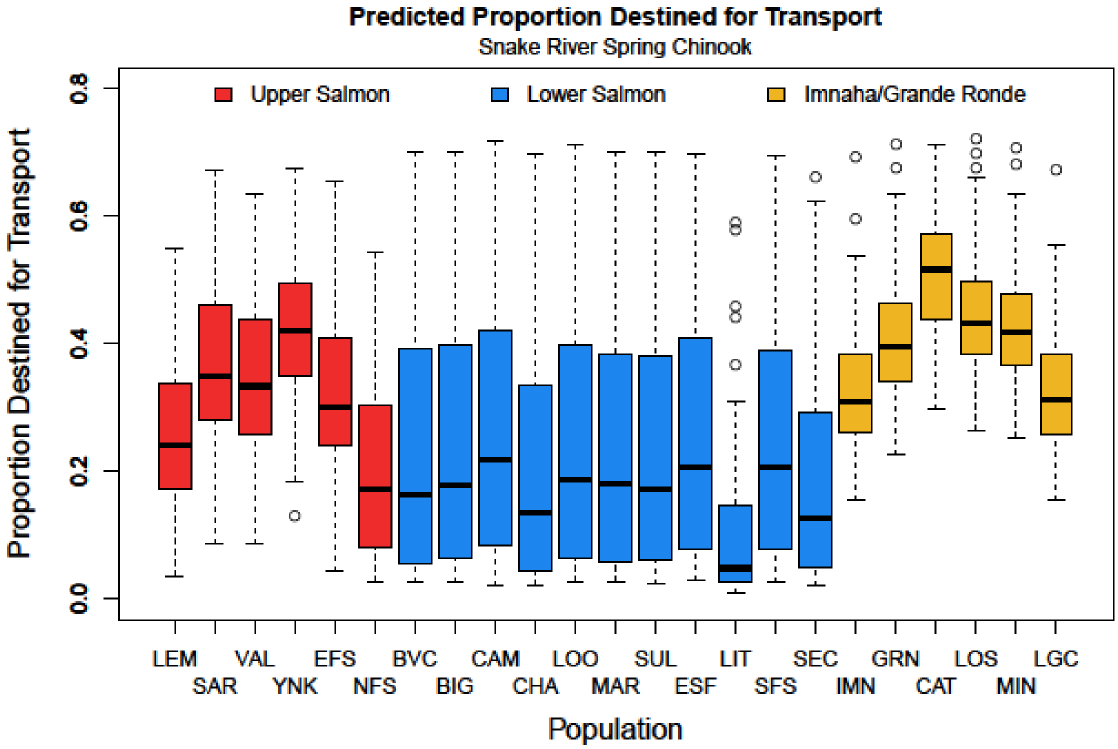

Figure 11. Boxplots of proportion destined for transport (the proportion of the population that would be transported if survival were 100%) predicted by COMPASS for the 80 water years of the "Base" scenario for all populations of Snake River spring Chinook salmon. Population groups are denoted by color; see Table 2 for population abbreviations.

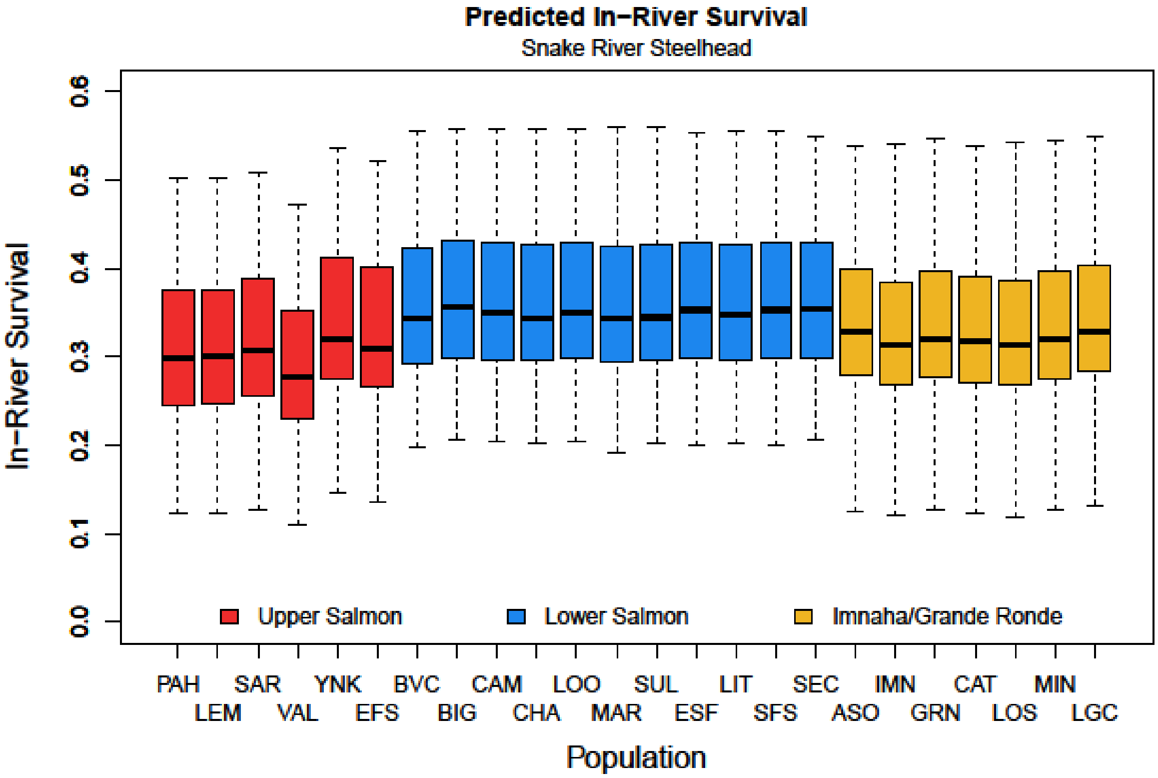

Figure 12. Boxplots of in-river survival (Lower Granite Dam to Bonneville Dam) predicted by COMPASS for the 80 water years of the "Base" scenario for all populations of Snake River steelhead. Population groups are denoted by color; see Table 2 for population abbreviations.

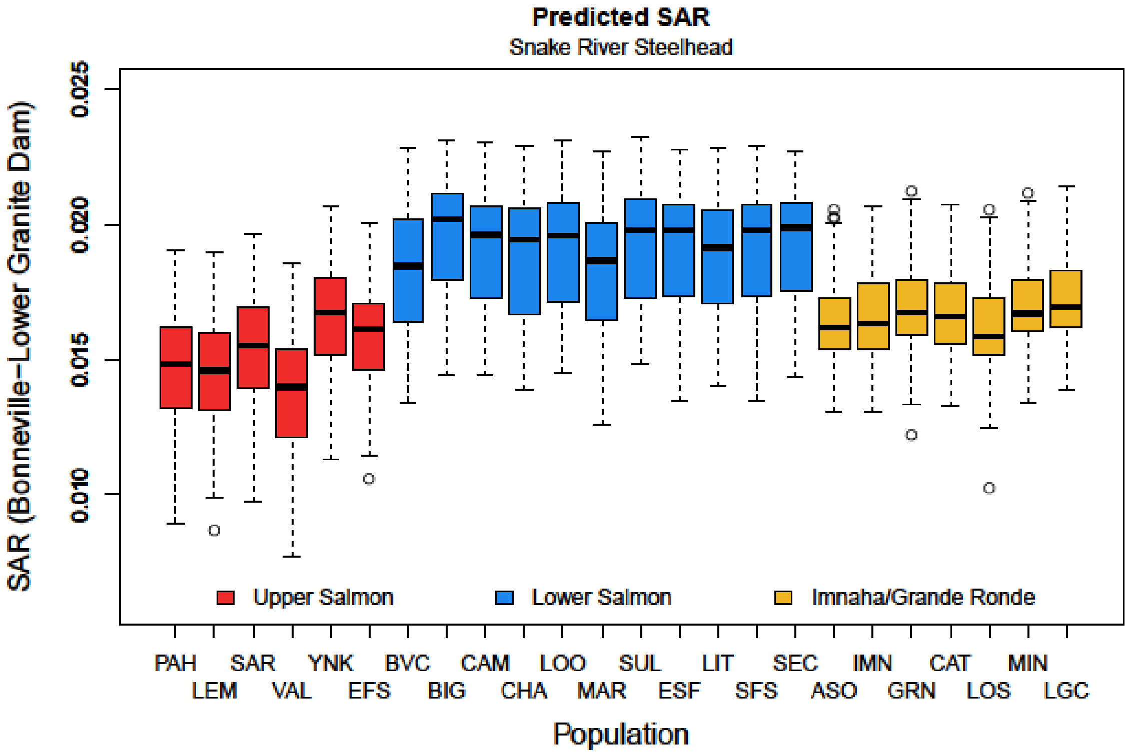

Figure 13. Boxplots of SAR predicted by COMPASS for the 80 water years of the “Base” scenario for all populations of Snake River steelhead. Population groups are denoted by color; see Table 2 for population abbreviations.

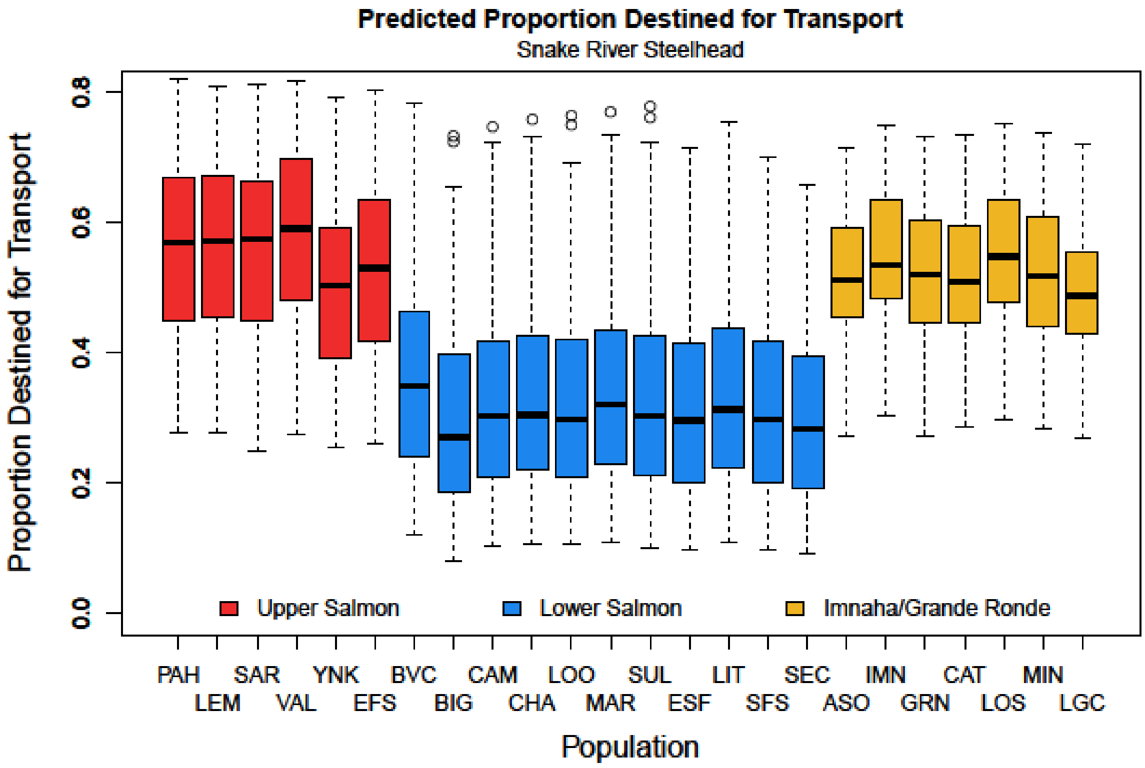

Figure 14. Boxplots of proportion destined for transport (the proportion of the population that would be transported if survival were 100%) predicted by COMPASS for the 80 water years of the "Base" scenario for all populations of Snake River steelhead. Population groups are denoted by color; see Table 2 for population abbreviations.

Discussion

We present a new method for predicting distributions of arrival times of migrating juvenile salmon at Lower Granite Dam. This method is flexible enough to capture the complex structure in arrival distributions, which can include multiple modes, spikes, and long tails, yet also has the ability to produce smooth distributions with simple features and single modes. The models are built on a set of predictor variables that can be used in prospective models used to assess the subsequent survival and passage experience of migrating smolts below Lower Granite Dam. Accurate predictions of arrival distributions will allow for more accurate predictions produced by the subsequent predictive models that use arrival distributions as inputs.

The results from the prospective modelling exercises show that variation in arrival timing can result in different experiences of populations both in the hydropower system and after exiting the hydropower system. Later arriving populations tended to have lower SAR's and higher proportions transported. In-river survival was less affected by arrival timing, but later arriving populations tended to have lower survival. We do not have sufficient PIT tag data to fit separate travel time, survival, or SAR models for the different population groups. However, it is clear that we can capture some of the variation in conditions experienced by these populations with our models of arrival timing.

The models selected by AIC in the retrospective modeling tended to have large numbers of quantiles (17-21). We decided to limit the number of quantiles to 13 to guard against overfitting and spurious predictions. The penalties for numbers of parameters in the AIC calculations were apparently not adequate to guard against overfitting. This could be improved in at least two ways. The first would be to more appropriately account for the total number of parameters associated with the smoothing spline models. This could be done by multiplying the degrees of freedom of a single smoothing spline by the total number of populations and years, which is an improvement over just using the degrees of freedom of a single spline model. This would result in models with more quantiles having larger penalties. A second improvement would be to somehow account for the quality of fit of each individual quantile model at the level of the individual quantile model fits before the spline and full likelihood calculations. It could be that some quantiles are actually not well described by a set of shared predictor variables, but the resulting full likelihood and AIC still select for that set of predictors as a whole. A solution may be to allow separate predictor variables for each quantile and find the best combination of individual quantile models based on a minimum combined AIC of the quantile models.

We wanted to control the spline fits of the cumulative probabilities such that the predicted probabilities would go through zero and one at the minimum and maximum quantiles, respectively. We fit the 0.0001 and 0.9999 quantiles and used those to anchor the cumulative probabilities. We later discovered that the predicted values for these extreme quantiles can be sensitive to the data and might produce predicted distributions with unusually long tails. This is not a big concern due to the small proportion of the populations represented by the tails of the distributions. However, we plan to adapt the method used to smooth the cumulative probabilities so that we can fit less extreme end quantiles and still retain the necessary resulting distributional properties.

The models described here perform well but could be improved upon to allow a more mechanistic representation of the processes driving arrival timing. Our models are based on environmental variables summarized at a monthly level. The model predictions could likely be improved if daily measurements of environmental variables could be included in the models. Our current methods do not easily allow for such daily data. Our methods also require a two-step model fitting process that involves many model components. This makes the resulting models cumbersome and could possibly lead to overfitting if care is not taken in the model selection process. The two-step method also does not adequately account for uncertainty in the joint model predictions. A different modeling approach based on methods developed for time-to-event data or counting processes may allow a simpler model representation that better captures the underlying processes involved and associated prediction uncertainty while also allowing predictor variables measured on a finer time scale. We intend to develop such models in the future as well as develop models that more explicitly account for the migration process from rearing sites to Lower Granite Dam.

References

Achord, S., R. W. Zabel, and B. P. Sandford. 2007. Migration timing, growth, and estimated parr-to-smolt survival rates of wild Snake River spring-summer Chinook salmon from the Salmon River basin, Idaho, to the lower Snake River. Transactions of the American Fisheries Society 136:142-154.

Beckman, B. R., D. A. Larsen, S. Moriyama, B. Lee-Pawlak, W. W. Dickhoff. 1998. Insulin-like growth factor-I and environmental modulation of growth during smoltification of spring chinook salmon (*Oncorhynchus tshawytscha*). General and Comparative Endocrinology 109:325-335.

Bjornn, T. C. 1971. Trout and salmon movements in two Idaho streams as related to temperature, food, stream flow, cover, and population density. Transactions of the American Fisheries Society 100:423-438.

Cade, B. S., and B. R. Noon. 2003. A gentle introduction to quantile regression for ecologists. Frontiers in Ecology and the Environment 1:412-420.

Columbia River DART (Data Access in Real Time). 2017. Columbia Basin Research, School of Aquatic & Fisheries Sciences, University of Washington, Seattle, Washington. Available: www.cbr.washington.edu/dart/dart.html.

Cunjak, R. A. 1996. Winter habitat of selected stream fishes and potential impacts from land-use activity. Canadian Journal of Fisheries and Aquatic Sciences 53:267-282.

Green, P. J., and B. W. Silverman. 1994. Nonparametric regression and generalized linear models: a roughness penalty approach. CRC press.

Hansen, L. P., and B. Jonsson. 1985. Downstream migration of hatchery-reared smolts of Atlantic salmon (*Salmo salar* L.) in the River Imsa. Aquaculture 45:237-248.

Hastie, T., R. Tibshirani, and J. Friedman. 2009. The elements of statistical learning: data mining, inference, and prediction. Second Edition. Springer.

Hotelling, H. 1933. Analysis of a complex of statistical variables into principal components. Journal of Educational Psychology 24:498-520.

Johnsson, J., and W. C. Clarke. 1988. Development of seawater adaptation in juvenile steelhead trout and domesticated rainbow trout – effects of size, temperature, and photoperiod. Aquaculture 71:247-263.

Joliffe, I. 2002. Principal component analysis. John Wiley and Sons.

Jonsson, N. 1991. Influence of water flow, water temperature, and light on fish migration in rivers. Nordic Journal of Freshwater Research 66:20-35.

Koenker, R., and G. W. Bassett. 1978. Regression quantiles. Econometrica 46:33-50.

Koenker, R. 2005. Quantile regression. Econometrics Society Monograph 38. Cambridge University Press.

McCormick, S. D., L. P. Hansen, T. P. Quinn, and R. L. Saunders. 1998. Movement, migration, and smolting of Atlantic salmon (*Salmo salar*). Canadian Journal of Fisheries and Aquatic Sciences 55:77-92.

McCormick, S. D., S. Moriyama, and B. T. Bjornsson. 2000. Low temperature limits photoperiod control of smolting Atlantic salmon through endocrine mechanisms. American Journal of Physiology Regulatory, Integrative, and Comparative Physiology 278:R1352-R1361.

NMFS (National Marine Fisheries Service). 2016. 2016 5-year review: summary and evaluation of Snake River sockeye, Snake River spring-summer Chinook, Snake River fall-run Chinook, and Snake River basin steelhead. National Marine Fisheries Service, West Coast Region, Portland, OR.

PSMFC (Pacific States Marine Fisheries Commission). 1996 present. PIT tag information system. Interactive database maintained by the Pacific States Marine Fisheries Commission, Portland, Oregon. Available: www.ptagis.org.

Shrimpton, J. M., K. D. Warren, N. L. Todd, C. J. McRae, G. J. Glova, K. H. Telmer, and A. D. Clarke. 2014. Freshwater movement patterns by juvenile Pacific salmon *Oncorhynchus* spp. Before they migrate to the ocean: Oh the places you'll go! Journal of Fish Biology 85:987-1004.

Smith, S. G., W. D. Muir, J. G. Williams, and J. R. Skalski. 2002. Factors associated with travel time and survival of migrant yearling Chinook salmon and steelhead in the lower Snake River. North American Journal of Fisheries Management 22:385-405.

Steel, E. A., P. Guttorp, J. J. Anderson, and D. C. Caccia. 2001. Modeling juvenile salmon migration using a simple Markov chain. Journal of Agricultural, Biological, and Environmental Statistics 6:80-88.

Sykes, G. E., C. J. Johnson, and J. M. Shrimpton. 2009. Temperature and flow effects on migration timing of Chinook salmon smolts. Transactions of the American Fisheries Society 138:1252-1265.

Zabel, R. W., J. J. Anderson, and P. A. Shaw. 1998. A multiple-reach model describing the migratory behavior of Snake River yearling Chinook salmon (Oncorhynchus tshawytscha). Canadian Journal of Fisheries and Aquatic Sciences 55:658-667.

Zabel, R. W. 2002. Using "travel time" data to characterize the behavior of migrating animals. The American Naturalist 159:372-387.

Zabel, R. W., J. R. Faulkner, S. G. Smith, J. J. Anderson, C. Van Holmes, N. Beer, S. Iltis, J. Krinke, G. Fredricks, B. Bellerud, J. Sweet, and A. Giorgi. Comprehensive passage (COMPASS) model: a model of downstream migration and survival of juvenile salmonids through a hydropower system. Hydrobiologia 609:289-300.

Appendix 1

Appendix Table 1. A complete list of all ESA-listed populations (separated into major population group) within the Snake River basin, and the PTAGIS mark/release sites we assigned to each population.

Population	PTAGIS Mark/Release Sites
	Lower Snake
Asotin River	ASOTIC, ASOTNF, ASOTSF, GEORGC, CHARLC
	Grande Ronde/Imnaha
Big Sheep Creek	BSHEEC, LSHEEC, LICK2C, SALTC, CANALC, REDMOC, MCCULC
Imnaha River	IMNAHW, IMNTRP, IMNAHR, GUMBTC, HORS3C, MAHOGC
Grande Ronde River	GRNTRP, GRANDR, GRAND1, GRAND2, GRANDW, GRANDP, JOSEPC
Wenha River	WENR, WENRNF, WENRSF
Catherine Creek	CATHEC, CATHEP, CATHEW, CATCMF, CATCNF, CATCSF, LCATHC
Lostine River	LOSTIR, LOSTIW, BCANF, WALLOR
Minam River	MINAMR
Lookingglass Creek	LOOKGC
	Middle Fork Salmon
Bear Valley Creek	BEARVC, ELKC, CAPEHC
Big Creek	BIG2C, CROO2C, BRAMYC, BEAV4C, SMITHC, LOGANC, CAVEC, CABINC, BUCK2C, RUSHC, RUSHWF, MONUMC, SNOSLC, MONCWF
Camas Creek	CAMASC, YELLJC
Chamberlain Creek	CHAMBC, CHAMWF, FLOSSC, MOOSEC, SALR2
Loon Creek	LOONC
Marsh Creek	MARSHC, MARTRP, MARTR2, KNAPPC
Sulfur Creek	SULFUC, BOUNDC, DAGGEC
Middle Fork Salmon, Below Indian Creek	SALMF1, WILSOC, SHEPC
Middle Fork Salmon, Above Indian Creek	SALMF2, INDIAC, PISTOC, RAPR, FALLC
	South Fork Salmon
East Fork South Fork Salmon	SAEFSF, JOHTRP, SUGARC, JOHNSC, BURNLC
Little Salmon River	LSALR, BOUL2C, HARDC, HAZARC, RAPIDR, RAPIWF, RPDTRP
South Fork Salmon	SALRSF, LSFTRP, SFSRKT, ELK2C, GOATC, BEAR4C, SFSTRP, KNOXB, SALSFW, RICEC, FITSUC

Secesh River	SECESR, SECTRP, ALEXC, FLATC, GROUSC, LICKC, LAKEC, PHOEBC, PIAHC, RUBYC, SUMITC, ZENAC, ZENAWF

Appendix Table 1. Continued.

Population	**PTAGIS Mark/Release Sites**
	Upper Salmon
Pahsimeroi River	PAHTRP, PAHSIW, PAHSIR
Lemhi River	LEMHIW, LEMHIR, 18MILC, AGNCYC, BASINC, BASN2C, BIG8MC, BIGB2C, BIGSPC, BOHANC, BOHEFC, BTIMBC, BUCK4C, CANY2C, CRUIKS, DEERC, FLUMEC, HAWLYC, HAYDEF, HAYDNC, HAYNSC, KENYC, LEEC, LIT8MC, LLSPRC, LTIMBC, MCDEVC, MILL5C, PATTEC, PRATTC, QKASPC, RESVRC, TEXASC, TRAILC, WILDCC, WIMPYC, WITHGC, WRIGTC, YRIANC
Salmon River, Below Redfish Lake	RLCTRP, REDFLC, SALR3, SALR4, SLAT2C, SQAW2C, CHALLC, CROOC, BASN3C, IRONC, SQUAWP
Salmon River, Above Redfish Lake	SAWTRP, GOLDC, WILLIC, FISHEC, CHAMPC, 4JULYC, POLEC, FRENCC, SMILEC, BEAVEC, ALTULC, YELLLC, VATC, PETTLC, HELLRC, HUCKLC, DECKEC
Valley Creek	VALEYC, STANLC, ELK3C
Yankee Fork	YANKFK, YANKWF
East Fork Salmon River	SALEFT, SALEFW, HERDC, SALREF
North Fork Salmon River	SALRNF, CARMEC, TOWERC, 4JUL2C
Panther Creek	PANTHC, MUSCRC, MOYERC

CHAPTER 5: TOXICS AS AN OBSTACLE TO SALMON RECOVERY IN THE COLUMBIA RIVER BASIN

This document has not undergone internal review by the Northwest Fisheries Science Center. The views expressed are those of the authors and not necessarily of NOAA Fisheries

Jessica I. Lundin (NOAA), Lyndal L. Johnson (NOAA), Julann Spromberg (NOAA), Cathy Laetz (NOAA), David Baldwin (NOAA), and Nathaniel L. Scholz (NOAA)

5.a Introduction

This chapter explores the role of toxic chemicals as limiting factors for the conservation and recovery of Pacific salmon and steelhead in the Columbia River Basin (CRB). The goal is not a comprehensive overview of contaminants in salmon habitats, inclusive of surface waters, sediments, and food webs. Rather, the sections that follow are case examples of how different human land uses, past and present, influence the chemical characteristics of freshwater and estuarine habitats. In areas where toxics and salmon co-occur, there is often a high likelihood of biological degradation in the forms of impaired salmon health, reduced prey abundance, or both. However, the relative benefits of improving habitat quality by preventing or remediating pollution – as a means to recover threatened and endangered salmonid populations – are not well understood. Consequently, priorities for new scientific research and assessment are identified, to reduce resource management uncertainty.

The first section (5.b) addresses modern (or current use) pesticides. Pesticides encompass an extraordinarily large and diverse ensemble of chemicals that are specifically intended to kill or otherwise control birds (avicides), fish (piscicides), small mammals (rodenticides), insects (insecticides), plants (herbicides), fungi (fungicides), and many other biological organisms. They are widely used throughout the CRB on forested lands, rangelands, agricultural crops, transportation corridors, and commercial and residential properties. They are also commonly detected in salmon habitats. However, exposure conditions for salmon and their macroinvertebrate prey are highly variable in space and time. The section addresses novel approaches for identifying areas of high exposure vulnerability, as a basis for prioritizing local actions to improve water quality in salmon-supporting habitats.

The second section (5.c) briefly reviews the current state of the science on exposures to legacy or persistent organic pollutants (POPs), primarily through the diet of juvenile salmon. Certain of these POPs, including DDTs and polychlorinated biphenyls (PCBs), were in societal use until the 1970s but have since been banned because of their persistent and bioaccumulative properties and their toxicity to fish and wildlife. Others, including brominated flame retardants (PBDEs), are a consequence of modern uses. Exposure to POPs is an inescapable fact for all salmon in the CRB, even those populations that spawn and rear in relatively pristine inland watersheds. This is due, in part, to the fact that all juvenile salmon migrate through the Columbia River Estuary, relying on estuarine food webs contaminated with POPs from historical industrial activities and current point and non-point source pollution. The section reviews monitoring data for POPs in the diets and tissues of juvenile salmon – primarily from the lower Columbia and Willamette Rivers – in the context of known toxicity thresholds for reduced growth, disease susceptibility, and other processes that determine juvenile salmon survival.

The third section (5.d) is a discussion of wastewater and risks to salmon, including an introduction to chemicals of emerging concern (CECs). These are contaminants that are relatively new to salmon habitats in the CRB, and are often poorly studied. They originate primarily from direct municipal or industrial discharges, and they include such things as pharmaceuticals, plasticizers, and many other compounds. Certain CECs are specifically designed to alter the physiology of vertebrates, including antidepressants and estrogenic compounds (e.g., birth control pills). They are not removed by conventional sewage treatment, and therefore have the potential to impact the physiology of salmon, including the nervous system (behavior) and reproductive biology. For most CECs, however, the environmental health consequences for salmon are almost completely unknown. As an initial step towards reducing this uncertainty, the section suggests targeted monitoring to more accurately profile CEC exposures in juvenile salmon.

The final section (5.e) evaluates the population-scale benefits of restoring chemical habitat quality by removing legacy pollution. The long-term goal is to develop a modeling framework that allows a direct comparison of different restoration actions in terms of salmon recovery – i.e., increases to the abundance and intrinsic growth of wild populations.   To date, the importance of habitat for salmon in the CRB has primarily focused on physical processes. If toxics reduction strategies are to become a larger part of salmon recovery efforts, new tools will be needed to scale improvements to the health and survival of individual salmon. This will support future decision making in terms of cost-benefit tradeoffs for restoration projects that focus on water and sediment quality.

The chapter contains several overarching themes. The first is that a large diversity of common environmental contaminants have been directly shown to impair a range of physiological and behavioral attributes that are essential for salmon behavior, growth, reproduction, and survival. Thus, the management question is not whether toxics are limiting salmon recovery in the CRB, but rather by how much and where. The second theme is chemical habitat complexity. For salmonids, exposure to complex chemical mixtures is the norm and not the exception. This may range from a dozen pesticides in agricultural watersheds to hundreds of contaminants in urban runoff. In general, mixture toxicity is not well understood. Third, the sections emphasize the importance of biological scaling. Thanks in part to the Clean Water Act, outright fish kills in the CRB attributable to pollution are rare. Therefore, most forms toxicity are sublethal and delayed in time. This requires empirical connections between suborganismal physiological processes (e.g., endocrine disruption), reductions in the lifetime reproductive success of individual salmon, and changes at the population scale. Fourth, non-chemical habitat stressors can influence the relative impacts of contaminants on salmon. These include, for example, warmer stream temperatures and exposures to pathogens among salmon with weakened immune systems. Fifth, there are no aquatic life criteria or similar guidelines for the vast majority of potentially toxic chemicals in salmon habitats. This is particularly true of the CECs, but also most pesticides and many contaminants in urban runoff. The final theme reflects the current reality – i.e., environmental health science for salmon (ecotoxicology) is not keeping pace with existing and emerging data gaps. Nevertheless, targeted research and monitoring in recent decades has been informative, and can be used as a basis for evaluating the effectiveness of future habitat improvement efforts that reduce or remove toxics.

5.b Spatial vulnerability analysis for pesticides in the Columbia River Basin

Background

Current-use pesticides represent a large and important class of chemical contaminants in aquatic environments. These chemicals are applied to agricultural, commercial, residential, and urban landscapes for controlling undesirable biological organisms. They move from use sites by spray drift, surface runoff, irrigation return flows, and other transport processes to aquatic environments that provide habitat for threatened and endangered fish species. For example, extensive monitoring by the U.S. Geological Survey's National Water Quality Assessment (NAWQA) Program has shown that more than fifty different pesticides and pesticide breakdown products occur in the surface waters of several large western basins, including the Yakima River Basin (see the USGS Pesticide National Synthesis Project at http://water.usgs.gov/nawqa/pnsp/). Notably, one or more pesticides were detected in 98% of surface water samples from streams throughout the Yakima River Basin in 1999 and 2000 (Fuhrer et al. 2004).

Pesticides found in these freshwater habitats can adversely affect fish physiology, behavior, growth, reproduction, and survival. The degree to which a specific pesticide poses a risk to Endangered Species Act (ESA)-listed fish in the CRB depends on the toxicity of the pesticide, the physiology of the organism, and the environmental concentrations. Thousands of different pesticides are currently registered for use on lands throughout the Columbia River Basin. Permitted chemicals include insecticides such as chlorpyrifos and permethrin to control insect pests; herbicides such as glyphosate and atrazine to control weeds and moss; and fungicides like pyraclostrobin and captan used to kill various strains of mold and fungus. The current use of organophosphate (OP) insecticides is common. The OPs comprise a highly toxic group of chemicals that have been manufactured since the 1950s and predominantly used in agriculture. Recent work has focused on the OP chlorpyrifos, one of the most commonly detected OPs in NAWQA basins throughout the United States (Hamilton et al. 2004). Chlorpyrifos significantly inhibits the enzyme acetylcholinesterase (AChE) in the nervous system and muscle of juvenile salmon (Sandahl et al. 2005; Sandahl and Jenkins 2002) at concentrations below 0.5 µg/L, or part per billion. These exposure levels are within the range of chlorpyrifos detections in salmon habitats (Werner et al. 2000; Dubrovsky 1998). Sublethal inhibition of AChE activity correlates closely to reductions in both swimming behavior and feeding rate (Sandahl et al. 2005). These studies collectively show that low-level, environmentally realistic chlorpyrifos exposures are sufficient to inhibit brain AChE activity and reduce feeding behavior. One consequence of reduced swimming and feeding is a reduction in food uptake and somatic growth of juvenile salmon rearing in freshwater stream systems. While the response of salmon to chlorpyrifos has been well studied, other ESA-listed species in the CRB, such as green sturgeon and eulachon, have comparatively much less data describing the consequences of pesticide exposure.

Insecticides such as chlorpyrifos may not only affect a salmon’s ability to feed but also kill much of their prey thereby limiting somatic growth (Macneale et al. 2010; Naiman et al. 2012; Anderson et al. 2006; Gilliom 2007). For some insecticides, reductions in prey alone are sufficient to reduce salmon productivity. The potential impact depends on the frequency and duration of the exposure concentration, as well as the dynamics of the prey community (Macneale et al. 2014). In Chinook, reductions in the somatic growth rate of fry and smolts lead to an increase in size-dependent mortality (Healey 1982; West and Larkin 1987). In an analysis of over 50,000 tagged fish, Zabel and Achord (Zabel and Achord 2004) observed strong size-dependent survival for juvenile Chinook during their outmigration. Smaller salmon are more susceptible to predation during their first year in the marine environment (Healey 1982; Beamish and Mahnken 2001; Holtby et al. 1990). Therefore, pesticide exposures that reduce salmon growth may reduce individual survival and, by extension, the recovery potential for ESA-listed populations (Baldwin et al. 2009). In contrast to the OPs, data on the toxicity of other pesticides to ESA-listed fish are typically quite limited, but food web effects are anticipated to result from the action of these biocides (Naiman et al. 2012; Macneale et al. 2014).

Another important factor when considering toxicity is exposure to pesticide mixtures. Given the many different land types within the CRB and the large number of pesticides registered for use, there is a strong likelihood that aquatic species will be exposed to complex pesticide mixtures. This is supported by monitoring data that routinely detected numerous pesticide chemicals in any one given sample (WSDA 2014; Gilliom 2007). For example, greater than 90% of water samples from urban, agricultural and mixed use areas nationwide contained more than one pesticide (Gilliom 2007). The risk posed by mixtures is important to consider because exposure to complex mixtures can cause greater toxicity than that produced from a single pesticide [e.g. (Laetz et al. 2009) for five specific OPs in salmon; (Cedergreen 2014) for a comprehensive review of numerous pesticides and species].

Challenges in defining the pesticide exposure conditions for salmon and their prey

Depending on product formulation, hundreds of different pesticide active ingredients are presently permitted for use throughout the Columbia River Basin. Ambient surface water monitoring [e.g. (WSDA 2014)] has provided snapshot exposure information about what pesticides reach aquatic habitats, but this has generally been limited to one-time sampling events in limited geographic areas. While pesticide product labels define allowable use (i.e., location, timing, and duration), actual use remains a significant information gap. Many of these chemicals are eventually conveyed to aquatic habitats via spray drift, runoff, and other transport processes. However, the occurrence and persistence of pesticides in proximity to ESA-listed species are highly variable in space and time, and therefore poorly understood. This is due, in part, to a general lack of use reporting and site-specific monitoring.

Periodically, the USDA NASS (National Agricultural Statistics Survey) conducts surveys of chemical uses on select agricultural crops and locations. In 2015, for example, the NASS surveyed chemical uses on apples in Washington state. The application of 149 different chemicals, including insecticides, fungicides, and herbicides, was reported for this single crop (https://quickstats.nass.usda.gov). Table 5.b.1 contains a partial list of chemicals and the pounds applied in 2015. Some additional data (e.g., acres treated and application rates) are also available from the NASS. Of note, this type of survey data is often not available for minor agricultural crops or any non-agricultural uses. Survey data can be useful to represent pesticide use. However, using survey data to quantify specific usage locations, rates, frequencies, and timing (time of day, seasonal, etc.) over a large area such as the CRB is problematic because of inconsistencies in the voluntary reporting of usage specifics. Additionally, pesticides are labelled for application in the context of a large number of different land uses. Several major examples are listed in Table 5.b.2. The uncertainty surrounding actual use is propagated into uncertain environmental exposure concentrations, limiting their utility in determining any resulting potential adverse biological effects on ESA-listed species within the CRB.

At more local scales (e.g. individual fields or reaches) and for specific pesticides, more information may be available regarding potential pesticide use and less uncertainty may exist. In these instances, fate and transport models (e.g., Environmental Protection Agency (EPA)'s Pesticide Water Calculator; available from https://www.epa.gov/pesticide-science-and-assessing-pesticide-risks/models-pesticide-risk-assessment#aquatic) exist that can be used to estimate environmental concentrations in aquatic habitats that are proximal to pesticide use. This modeling incorporates available information such as the physio-chemical properties of the pesticide (e.g., aquatic hydrolysis half-life), the application site (e.g., soil type of the field), the application itself (e.g., rate and method), and the aquatic habitat (e.g., water volume and flow). These provide a better estimate of pesticide exposures in habitats near use sites than ambient monitoring since it will reflect the specific site and application, rather than a chance grab sample that may miss important pulses in pesticide exposures. However, these modelled environmental concentrations are also limited in their utility since they represent exposures that could happen at a local scale (e.g. a water body at the edge of a specific field) assuming that an application occurs. For example, not all potential use sites for a pesticide within a watershed will have applications occur. For any given pesticide, the combination of ambient monitoring data and modeled environmental concentrations provide a range of potential exposures that ESA-listed fish in a watershed may experience.

Land cover as a proxy for pesticide exposure

For reasons discussed above (e.g. the large number of possible pesticides and wide range of potential environmental concentrations), the uncertain nature of pesticide exposures in aquatic systems in space and time means that it is currently not possible to precisely characterize exposure conditions over very large scales such as the CRB. However, land cover and land use can serve as proxies for identifying hotspot areas that are likely to increase exposure vulnerability. For example, it is likely that watersheds having a greater spatial overlap with potential pesticide use sites also have greater pesticide loading. Additionally, watershed-scale assessments of potential pesticide loading can be combined with important species-specific life-history information to inform exposure vulnerability. ESA-listed fish in the CRB are migratory and individuals of many species travel through the same corridor such as the Lower Columbia River. Also, specific resting, rearing, and spawning areas may be important habitat to life stages critical to the productivity of the species.

Current-use pesticide applications are allowed on a variety of land types throughout the CRB (see Table 5.b.2 for examples). These include agricultural lands, managed forests, transmission line and road rights-of-way, and developed lands. Figure 5.b.1 shows classifications of land types in the CRB from the USGS 2011 National Land Cover Database. Pesticide labels define the parameters of allowed applications to both agricultural and non-agricultural uses. Labels for some pesticides, such as chlorpyrifos, include uses for mosquito control or ant/termite control (‘wide area’) that do not restrict where application can occur. Other labels specify use on a specific set of crops (e.g. apples, lettuce, hay) or locations (e.g. rights of ways, building foundations). Most of the different land cover classifications within the CRB seen in Figure 5.b.1 (highlighting the portion that is range for NMFS ESA-listed fish, hereafter referred to as CRB ESA range) represent potential use sites for pesticides. The numerous use sites are often grouped into categories. For example, cultivated land is composed of many field crops (e.g., potatoes, mint, onions, cucumbers, etc. can be grouped as vegetables and ground fruits). Table 5.b.2 shows the list of use categories developed by the EPA, USFWS, and NMFS for nationwide pesticide assessments.

EPA has developed maps of these use categories using sources such as the USGS National Land Cover Database and the USDA Cropland Data Layer. Figure 5.b.2 maps the extent of two specific use categories (i.e., managed forest and pasture) within the CRB ESA range. The percent of the area of each watershed (12-digit hydrologic unit; HUC12) that overlaps a specific use is denoted by color. As can be seen by comparing the two maps, different portions of the CRB ESA range differ in the amount of overlap with the two uses. Table 5.b.2 summarizes the extent of overlap for different use categories across the entire CRB ESA range. Managed forests, for example, represent 25.56% of the entire area. A large portion of the CRB ESA range, therefore, is a potential location for pesticide use associated with this use category. As can be seen in Figure 5.b.2, however, a specific use category (e.g., pasture) will be higher in specific locations of the area and lower in others. Additionally, areas with high overlap with one use (e.g. managed forests) may have low overlap with other use categories (e.g., pasture in Figure 5.b.2). Of note, two use categories (mosquito control and wide area) can lead to pesticide applications anywhere in the CRB ESA range (i.e. have 100% overlap in Table 5.b.2).

To assess the spatial extent of all potential uses, the individual use categories were aggregated by simple summation of the percent overlaps in each watershed. The resulting map is seen in Figure 5.b.3. It is important to note that this aggregate index value does not have any meaning in an absolute sense, and it cannot be used as a risk index to calculate a potential response (e.g. mortality) to pesticides by ESA-listed fish in a specific watershed. Rather, the aggregate index allows for comparison of the overall potential for pesticide influence between different watersheds of the CRB. Additionally, areas with high aggregate indexes can be distinguished based on which uses are present (e.g. the three watersheds highlighted in Figure 5.b.3).

Data gaps and uncertainties

The collective use of pesticides across the CRB has a high potential for limiting the productivity of ESA-listed fish in the CRB. However, at this time it is not feasible to assess the impacts of pesticide use in detail or to provide a specific magnitude of an adverse population-level effect. There are numerous data gaps that, independently and collectively, are too great for any quantitative measure of overall risk to ESA-listed fish. Examples include the long and changing list of possible pesticides, the lack of detailed information on their use, the limited data on the toxicity of pesticides to ESA-listed fish, and the limited data on the possible mixtures that may be present in the CRB.

Recommended actions

There are numerous areas within the CRB where ongoing pesticide use is likely to degrade water quality to the extent that it impairs the health of ESA-listed fish or the integrity of freshwater macroinvertebrate prey communities. We have listed below a few recommended steps to identify where pesticide mitigation measures might most effectively improve habitat conditions, thereby contributing positively to species recovery.

- Map potential use sites throughout the CRB to prioritize watersheds that may be more vulnerable to pesticide exposure and effects. These watersheds could then be the focus for further data collection efforts, such as pesticide use surveys, ambient monitoring studies, or targeted monitoring studies to measure pesticide concentrations during and following specific pesticide applications.

- Support targeted mitigation measures such as vegetated buffers, no-spray buffers, and irrigation practices to reduce pesticide loading into watersheds identified as vulnerable. The types of uses leading to a higher priority index would be essential to inform which type of mitigation efforts would be most appropriate for that area. Many of the available mitigation measures, such as vegetated buffers, are not pesticide specific and would be effective for many different types of pesticides and application methods.
- Develop a prioritized list of pesticides using existing monitoring data, survey data, and model-derived estimated environmental concentrations. Available toxicity data could further prioritize pesticides to those that are highly toxic to fish and invertebrates.
- Perform toxicity tests to inform our understanding of potential adverse effects to ESA-listed fish, focusing on data-poor species such as green sturgeon and eulachon.

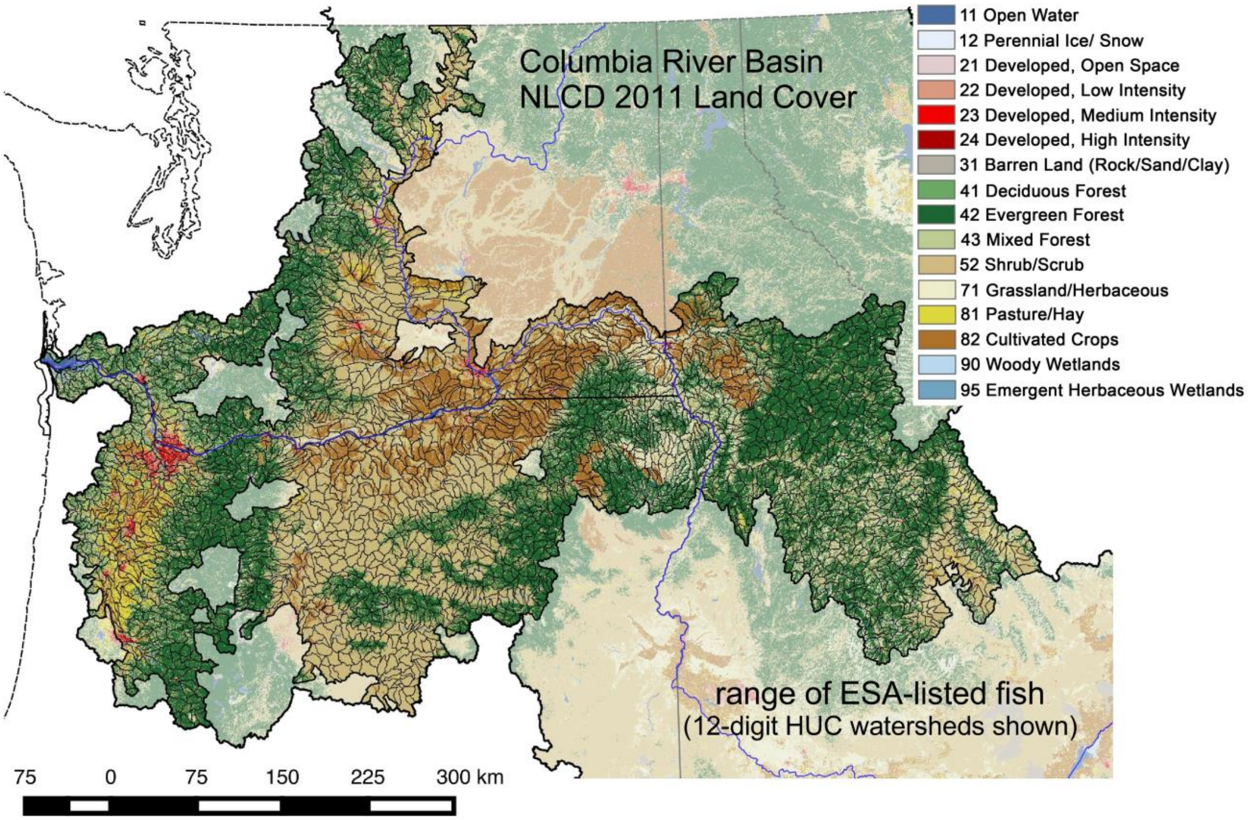

Figure 5.b.1. Map of land types within the CRB highlighting the range of NMFS ESA-listed fish. Watershed boundaries based on 12-digit hydrologic units (HUCs) are denoted within the ESA-range.

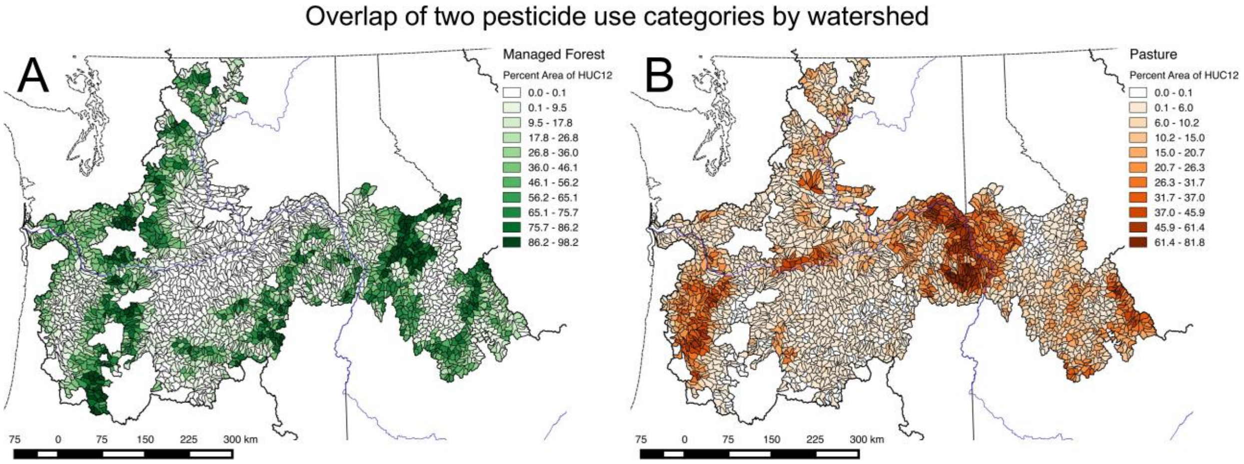

Figure 5.b.2. Maps showing the percent of the area of each watershed that consists of either A) managed forest or B) pasture. Both represent use categories of potential pesticide applications.

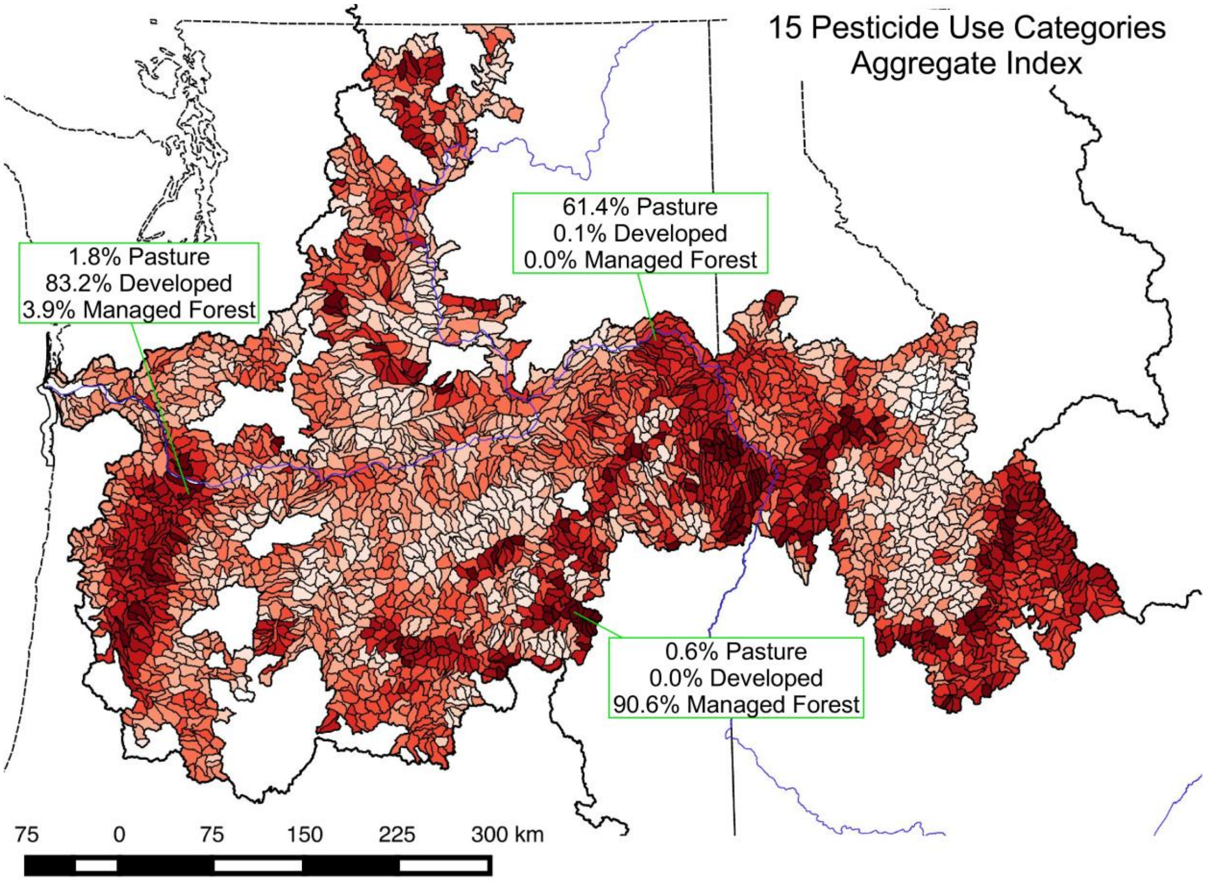

Figure 5.b.3. Map showing the aggregated index of 15 different use categories to identify areas of expected pesticide influence. Data from three of the use categories are shown for three watersheds to highlight similar aggregate indexes for different reasons.

Table 5.b.1 Reported chemical uses on apples in Washington State in 2015. Data from surveys conducted by the USDA's National Agricultural Statistics Survey. A total of 149 chemicals were reported. Minor uses (<1% of total) and those with data withheld are not listed.

Insecticides	**Pounds**	**% of Total**
Kaolin	558,200	49%
Petroleum distillate	175,200	15%
Chlorpyrifos	136,400	12%
Carbaryl	129,900	11%
Phosmet	38,700	3%
Diazinon	19,200	2%
Chlorantraniliprole	11,600	1%
Acetamiprid	9,400	1%
Methoxyfenozide	9,000	1%
Fenbutatin-oxide	7,700	1%
Spirotetramat	6,700	1%
Imidacloprid	6,200	1%
Total	*1,137,900*	*100%*
Fungicides		
Calcium polysulfide	1,607,800	61%
Sulfur	704,400	27%
Mancozeb	61,500	2%
Copper oxide	52,500	2%
Copper hydroxide	48,600	2%
Triflumizole	24,400	1%
Total	*2,645,600*	*100%*
Herbicides		
Glyphosate iso. Salt	55,300	42%
Paraquat	24,200	18%
Glufosinate-ammonium	10,800	8%
Pendimethalin	7,800	6%
Oryzalin	5,400	4%
Oxyfluorfen	4,600	4%
2,4-d, dimeth. Salt	3,400	3%
Glyphosate amm. Salt	2,800	2%
Glyphosate	2,200	2%
Simazine	800	1%
Rimsulfuron	700	1%
Total	*131,100*	*100%*
Other		
Mineral oil	4,148,400	97%
Ethephon	27,700	1%
Total	*4,296,100*	*100%*

Table 5.b.2. Pesticide use categories and the percent of that land type within the range of Columbia River Basin NMFS ESA listed species.

Use Category	**Median Percent Area of CRB ESA range** Across 6 years of crop data
Mosquito Control	100
Wide Area Use	100
Rangeland	33.57
Managed Forests	25.56
Pasture	10.39
Right of Way	5.02
Wheat	3.67
Other Crops	3.07
Developed	1.72
Cull Piles[1]	1.67
Open Space Developed	1.62
Vegetables and Ground Fruit	0.90
Orchards and Vineyards	0.87
Corn	0.28
Other Grains	0.26
Christmas Trees	0.17
Other Row Crops	0.06

[1] Non-harvested areas associated with Orchards

5.c Impacts of persistent organic pollutants (POPs) on ESA-listed fish

Background

Persistent organic pollutants (POPs) are ubiquitous environmental contaminants that are not readily degraded in the environment and can biomagnify in aquatic and marine food webs (Johnson et al. 2014; Jones and de Voogt 1999; Mackay and Fraser 2000; Safe 1994). They include a wide range of legacy contaminants [e.g., PCBs, and organochlorine (OC) pesticides including DDTs, chlordanes, and hexachlorobenzene (HCB)], as well as some chemicals of emerging concern [e.g., polybrominated diphenyl ethers (PBDEs), perfluorinated compounds]. These compounds are lipophilic and can be found in relatively high concentrations in tissues of aquatic organisms, including fish and marine mammals. Many of these chemicals were or are used as industrial compounds (e.g., PCBs, PBDEs) or pesticides (e.g., dieldrin, DDT). Other classes of POPs [e.g., polychlorinated dibenzofurans (PCDFs) and polychlorinated dibenzodioxins (PCDDs)] can be produced during natural disasters (e.g., forest fires, volcanic eruptions) or as by-products during wood pulp processing, the synthesis of chlorinated chemicals, or as a result of incineration of chlorine-containing compounds. Although many POPs have been banned for production and use in North America, they are still commonly detected in environmental samples and to affect the health of humans, fish, and wildlife. Notably, several classes of POPs, including PCBs, DDTs, and PBDEs, have been identified as contaminants of concern in the Columbia River Basin specifically because of their widespread distribution in the region (U.S. EPA 2009).

The toxicity of POPs is well-documented [e.g., (Bols et al. 2001; Boas et al. 2006; Johnson et al. 2014)]. Some classes of POPs (e.g., DDTs, PCBs, PCDDs) have long been recognized as reproductive and developmental toxicants in fish and wildlife (Tyler et al. 1998). PCBs and PBDEs are also known to disrupt thyroid function, with associated impacts on early development, metabolism, and growth. Recent studies have shown that various legacy POPs can alter the immune system of fish as well as their susceptibility to disease. Several classes of POPs contribute to toxicopathic liver disease, especially PCBs and dioxins, and are associated with the development of neoplasms in fish (Myers and Fournie 2002; Myers et al. 2003, Vethaak et al. 2009). Studies also show that body lipid content can influence toxicity because POPs tend to be lipophilic and are sequestered in fat stores (Lassiter and Hallam 1990). When lipid stores are depleted, more of the contaminants are mobilized and available to exert harmful effects on other tissues, increasing the risk of toxic injury.

NOAA scientists have estimated critical lipid-normalized body residues for the toxic effects of several classes of POPs in salmonids and other fish, based on laboratory exposure studies. Toxicological studies on juvenile salmonids, examining effects ranging from enzyme induction to mortality, have indicated an adverse health effects threshold for PCBs (namely, Aroclors) of 2400 ng/g lipid (Meador et al. 2002). Although a specific effect threshold for DDTs in juvenile salmon has not been developed, one study determined that a concentration above 600 ng/g wet weight (Beckvar et al. 2005), or 6000 ng/g lipid (Johnson et al. 2007), may cause adverse effects in a variety of fish including salmonids. Body concentrations of PBDEs associated with injury were estimated from studies by Arkoosh et al. [(Arkoosh et al. 2010; Arkoosh et al. 2015; Arkoosh et al. 2013); see also (O’Neill et al. 2015)], which demonstrated altered immune function and thyroid hormone levels, as well as increased disease susceptibility in juvenile salmon exposed to PBDEs in the diet. In these studies, body PBDE concentrations in the 470 to 2500 ng/g lipid range were associated with increased disease susceptibility, while those in the 1500 to 2500 ng/ g lipid range were associated with thyroid hormone alterations.

POPs concentrations in ESA-listed species and risks to fish health

An increasing body of work has emphasized the risks to outmigrating salmon posed by POPs consistently detected in the river water, sediments, and salmon tissues in the Columbia River. Monitoring studies have examined the uptake of selected POPs in spring Chinook salmon as they outmigrate from Snake River hatcheries to John Day or Bonneville Dam (Arkoosh et al. 2011) and in Chinook salmon in the lower Columbia River and estuary (LCREP 2007; Johnson et al. 2013; Johnson et al. 2007; Sloan et al. 2010). In these studies, PCBs, PBDEs, and DDTs and other OC pesticides (e.g., chlordanes and HCB) were detected in the bodies of Chinook salmon from multiple stocks (Fig. 5.c.1 and 5.c.2).

Exposure to POPs is clearly a potential threat to Chinook salmon from the Lower Columbia and Upper Willamette ESUs (Table 5.c.1). Almost 400 composite samples have been analyzed from Lower Columbia River Chinook salmon from sites between Bonneville Dam and the estuary mouth (LCREP 2007; Johnson et al. 2013). Body concentrations of PCBs in samples from this ESU were above the toxicity threshold in 13% of samples, while concentrations of PBDEs were above the effects threshold for immune dysfunction in 47% of samples, and above the threshold for effect on thyroid function in 9% of samples. In Upper Willamette Spring Chinook salmon, extremely high concentrations of PCBs and DDTs (10,000 to 15,000 ng/g lipid) were observed in fish collected within the Portland Harbor Superfund site, though concentrations are lower in the smaller number of samples collected in the lower reaches of the river. Some Snake River fall Chinook have also been collected as part of Lower Columbia River sampling, with PCB concentrations up to 2600 ng/g lipid, DDT concentrations up to 1700 ng/g lipid, and PBDE concentrations up to 580 ng/g lipid. In 5% of 19 samples analyzed, PCB concentrations were above the effect threshold, and in 11% of the samples, PBDE concentrations were in the range where effect on immune function may occur.

The Lower Columbia Estuary studies also show that POPs concentrations are relatively low from fish collected in the Columbia Gorge, reach peak levels in the Portland/Vancouver area, and then show moderate declines downstream but remain higher than levels measured in fish collected in the Gorge (Fig. 5.c.2). Moreover, for the stocks collected in both areas (Lower Columbia River Chinook, Snake River fall Chinook) concentrations of PCBs, DDTs, and PBDEs are all lower in fish collected in the Gorge compared to those collected from sites in or downstream of the Portland/Vancouver area (Fig. 5.c.3). These findings highlight the importance of the urban and industrial Portland/Vancouver area as a source of contaminant exposure for outmigrant juvenile salmon.

Less information is available on Interior Columbia River spring Chinook stocks. Only seven samples of Middle and Upper Columbia River Spring Chinook have been analyzed, five from the Columbia Gorge and two from the mouth of the estuary. POPs concentrations in the Gorge samples were quite low, with no samples having POP concentrations above critical body residues associated with toxicity. The two samples of Middle and Upper Columbia River Spring Chinook smolts collected in the mouth of the estuary had lower lipid levels than the Gorge fish (0.8% vs. 4.8%) and higher mean lipid-adjusted concentrations of DDTs (4000 vs. 210 ng/g lipid), PCBs (1700 vs. 430 ng/g lipid) and PBDEs (140 vs. 23 lipid for PBDEs).

Our data on Snake River spring Chinook come primarily from a study by Arkoosh et al (Arkoosh et al. 2011), in which POPs concentrations were measured in juvenile Snake River

Spring Chinook collected from hatcheries on the Snake and Clearwater Rivers, and during downstream migration at Lower Granite, McNary, John Day, and Bonneville Dams. DDTs, PCBs, and PBDEs were detected in the fish at the hatcheries, and lipid-adjusted concentrations of these contaminants continued to increase with outmigration to reach maximum levels at the terminal dams. These increases were due in part to lipid depletion, as lipid content declined from 5-7% in hatchery samples to 0.3 to 1.8% at John Day and Bonneville Dams. However there also appeared to be some accumulation of DDTs and PBDEs during outmigration, as wet weight concentrations of these contaminants also increased. Depending on the year sampled, mean concentrations of PBDEs at the terminal dams ranged from 160 to 2100 ng/g lipid, DDT concentrations ranged from 730 to 8700 ng/g lipid, and PCB concentrations ranged from 440 to 3100 ng/g lipid. In addition to these fish, some Snake River spring Chinook smolts were collected at the estuary mouth (Johnson et al. 2013). The lipid content of these fish was quite low (0.8%), and POPs concentrations were comparable to those measured in Snake River Spring Chinook (Arkoosh et al. 2011). Though the data are limited, they suggest that Interior Columbia Chinook salmon, as well as Lower Columbia and Willamette River stocks, are accumulating POPs during outmigration, and that lipid depletion as a result of migration stress and smoltification may exacerbate their risk of toxic injury. However, much is still uncertain about how POPs may be affecting the survival and recovery of listed fish species in the Columbia Basin.

Key data gaps and challenges

Several data gaps constrain our ability to assess the risks that POPs exposure poses for ESA-listed fish in the Columbia Basin. First, we have only limited exposure data for several critical stocks and species. As noted above, POPs exposure levels are not well described for interior Columbia Basin spring and fall Chinook, and almost no data are available on any stocks of coho, chum, sockeye, or steelhead.

Moreover, our information is also geographically limited, and consists mostly of data on juvenile Chinook salmon collected in the Lower Columbia River and Estuary. With the exception of the data collected by Arkoosh et al. (Arkoosh et al. 2011) on hatchery origin Spring Chinook salmon, we have very little information on POPs concentrations in fish collected from critical habitats in the Upper and Middle Columbia or Snake Rivers. Thus, we know little about POP accumulation at early stages of rearing and migration in these regions. This is a concern because high concentrations of DDTs, PCBs, dioxins, and OC pesticides have been reported in resident fish in some portions of the Upper and Middle Columbia and Lower Snake River that serve as critical habitat for Interior Columbia stocks (Hinck et al. 2006; Seiders et al. 2015; Seiders et al. 2012).

Additionally, we lack data for critical life stages of listed species and stocks. The majority of our POPs data are from outmigrant juvenile salmon parr and smolts. While these life stages are considered especially vulnerable and have a large impact on population growth rates (Spromberg and Johnson 2008; Spromberg and Meador 2005), there is also potential exposure to POPs in eggs, larvae, and alevins, as well as adults. In the late 1990s, the EPA detected various classes of POPs, including DDTs and other organochlorine pesticides, PCBs, and dioxins in bodies and eggs of adult spring and fall Chinook salmon, coho salmon, and steelhead from the multiple sites in the Middle and Upper Columbia River and its tributaries (U.S. EPA 2002). This study was focused on human health effects from fish consumption, and did not address toxicity to fish, though concentrations were generally less than those thought to cause injury.

In addition to salmonids, NOAA Fisheries has designated Columbia River eulachon as a threated species (Gustafson et al. 2010; NMFS 2016) and green sturgeon within the Columbia River as a species of concern (NMFS 2015; BRT 2005; Doukakis 2014). While poor water quality and pollution have been identified as factors that could to threaten the survival and recovery of these species, very little information is available on their POPs concentrations. In the late 1990s, the EPA detected PCBs and DDTs in the 20-50 ng/g ww range in eulachon collected between RM 39 and 41 in the Columbia River (U.S. EPA 2002). Given the high lipid content (14%) of these fish, these levels would be below critical body concentrations, though the number of samples is very small. As for green sturgeon, designated critical habitat ranges from the mouth of the Lower Columbia River Estuary to RM 45, so they could be exposed to contaminants present in the lower reaches of the estuary. However, no data on body concentrations of POPs in green sturgeon are available. Elevated levels of POPs, as well as reproductive alterations, have been documented in white sturgeon (Feist et al. 2005; U.S. EPA 2002), but at sites in the Middle Columbia River, where green sturgeon do not occur.

Finally, in addition to the contaminants discussed above, there are other pollutants of concern in the Snake and Columbia Rivers with potential effects on salmon (U.S. EPA 2009). These include combustion byproducts such as dioxin and “contaminants of emerging concern” such as pharmaceuticals and personal care products, some of which may bioaccumulate in tissues (Morace 2012; Meador et al. 2016). Additional information, including toxicity evaluations and geographically targeted studies on these contaminants, is needed to evaluate their potential risk to listed fish in the Snake and Columbia Rivers. Additional refinement of tissue effects thresholds for PCBs, DDTs, and PBDEs may also be needed to incorporate more recent information and to accommodate important life stages in addition to juveniles. For example, as

Beckvar and colleagues note (Beckvar et al. 2005), the DDT threshold estimate relies heavily on effects associated with mortality, and thus may not be completely protective for significant sublethal effects and delayed mortality juvenile salmon.

Recommended actions

To address these issues we recommend the following areas where new scientific information could most effectively influence ongoing efforts to recover salmon exposed to POPs:

- Conduct targeted monitoring for vulnerable fish species to address data gaps specific to contaminant exposure and accumulation for major classes of POPs. This would include targeted monitoring in geographic areas where little information is available for listed species, as well as where other data suggest risks for POPs exposure. The Upper Columbia Basin is one example of an area where this is needed, because of the widespread DDT and PCB contamination indicated by monitoring of resident fish. Much of this work could be carried out in collaboration with ongoing studies that collect juvenile salmon for other purposes. Studies are also needed on critical life stages where data are not available, such as eggs and larvae, and in some cases, adults. Sufficient information should also be collected to characterize POPs uptake in sockeye, chum, and coho salmon and steelhead, as well as other species of concern such as eulachon and green sturgeon and other species of concern.
- Incorporate POPs impacts into ongoing efforts to restore and improve habitats. When actions are undertaken to restore access to previously unutilized habitat, it is important to avoid unintentionally exposing fish to POPs or other contaminants. To prevent this, localized monitoring may be needed to collect baseline data in some

areas where habitat restoration is planned and/or ongoing. In addition to identifying areas where habitat restoration effects could be affected by toxic contaminants, there is a need to incorporate pollution reduction and mitigation techniques into restoration projects when toxics may be a concern, and to conduct effectiveness monitoring for toxics at such sites to ensure these efforts are working. For POPs, this might include stormwater filtration, riparian buffers, improving soil conservation practices [see (U.S. EPA 2009)].

- Conduct research needed to develop and refine toxicity evaluations for POPs, including bioaccumulative contaminants of emerging concern, to ensure that sensitive life stages and species are adequately protected.

Table 5.c.1. Mean (SD) contaminant concentrations and ranges in ng/g wet wt and ng/g lipid for juvenile Chinook salmon from Columbia and Snake River ESUs collected in the Lower Columbia River, and the percentages of samples above estimated critical body residues for toxic effects for PCBs, DDTs, and PBDEs. For PCBs, this value is 2400 ng/g lipid (Meador et al. 2002); for DDTs, it is 6000 ng/g lipid (Beckvar et al. 2005), as adjusted for lipid content in (Johnson et al. 2007). For PBDEs, values for disease resistance (470 ng/g lipid) and thyroid hormone alteration (1500-2500 ng/g lipid) are included, based on studies by Arkoosh et al. (Arkoosh et al. 2013; Arkoosh et al. 2010; Arkoosh et al. 2015). Contaminants and lipids were measured in composite samples containing 2-5 salmon bodies each (stomach contents removed).

Stock/ESU	**Total PCBs[1]**	**ΣDDTs[2]**	**ΣPBDEs[3]**
Lower Columbia (n=339)			
Mean ± SD wet wt (ng/g)	25 ± 33 ng/g ww (339)	18 ± 13 (339)	11 ± 14 (339)
Range wet wt	4.1 – 570 ng/g ww	3.6 - 78	0.1 = 93
Mean ± SD lipid wt (ng/lipid)	1600 ± 2100	1100 ± 750 (339)	670 ± 850
Range lipid wt	190 – 31000	140 - 6000	4 - 7400
% above CBR	13%	0.3%	47%[4] and 9%[5]
UpperWillamette (n=12)			
Mean ± SD wet wt (ng/g)	25 ± 14 (12)	14 ± 7 (12)	8.1 ± 8.7 (12)
Range wet wt	4.5 - 56	4.7 - 29	0 - 23
Mean ± SD lipid wt (ng/lipid)	1300 ± 820	720 ± 460	390 ± 370
Range lipid wt	108 – 2500	140 - 1600	0 - 890
% above CBR	8%	0%	33% and 0%
Snake River spring (n=6)			
Mean ± SD wet wt (ng/g)	11 ± 2 (6)	26 ± 8 (6)	3.1 ± 0.9 (6)
Range wet wt	8.6 - 12	17 - 36	2.0 – 3.9
Mean ± SD lipid wt (ng/lipid)	1500 ± 680	3500 ± 1400	430 ± 230
Range lipid wt	690 - 2700	2000 - 5000	220 – 850
% above CBR	17%	0%	33% and 0%
Snake River fall (n=19)			
Mean ± SD wet wt (ng/g)	18 ± 13 (19)	13 ± 6 (19)	3.9 ± 3.3 (19)
Range wet wt	6.6 - 55	6.1 - 26	0.8 - 11
Mean ± SD lipid wt (ng/lipid)	840 ± 800	640 ± 530	210 ± 210
Range lipid wt	110 - 2600	110 - 1700	15 – 580
% above CBR	5%	0%	11% and 0%
Upper Col spring (n=7)			
Mean ± SD wet wt (ng/g)	12 ± 3 (7)	11 ± 8 (7)	2.2 ± 2.9 (7)
Range wet wt	8.2 -16	4.1 - 23	0.4 – 8.4
Mean ± SD lipid wt (ng/lipid)	800 ± 950	1300 ± 2300	240 ± 360
Range lipid wt	130 – 2800	46 - 6400	4 - 860
% above CBR	14%	14%	29% and 0%
Upper Col Fall (n=50)			
Mean ± SD wet wt (ng/g)	24 ± 17 (50)	17 ± 8 (50)	5.6 ± 3.8 (50)
Range wet wt	1.4 - 110	3.3 - 39	1.1 - 20
Mean ± SD lipid wt (ng/lipid)	1600 ± 1400	1100 ± 560	360 ± 230
Range lipid wt	36 - 9600	84 – 2400	17 - 990
% above CBR	10%	0%	26% and 0%

[1] Total PCBs reported as ∑17PCBs*2 [PCBs 18, 28, 44, 52, 95, 101(90), 105, 118, 128, 138 (163,164), 153 (132), 170, 180, 187 (159,182), 195, 206, 209]

[2] ∑DDTs reported as ∑6DDTs (p,p'-DDD, p,p'-DDE, p,p'-DDT, o,p'-DDD, o,p'-DDE, o,p'-DDT)

[3] ∑PBDEs reported as ∑7BDEs (BDEs 28, 47, 49, 66, 85, 99, 100)

[4] disease resistance

[5] thyroid hormone alteration

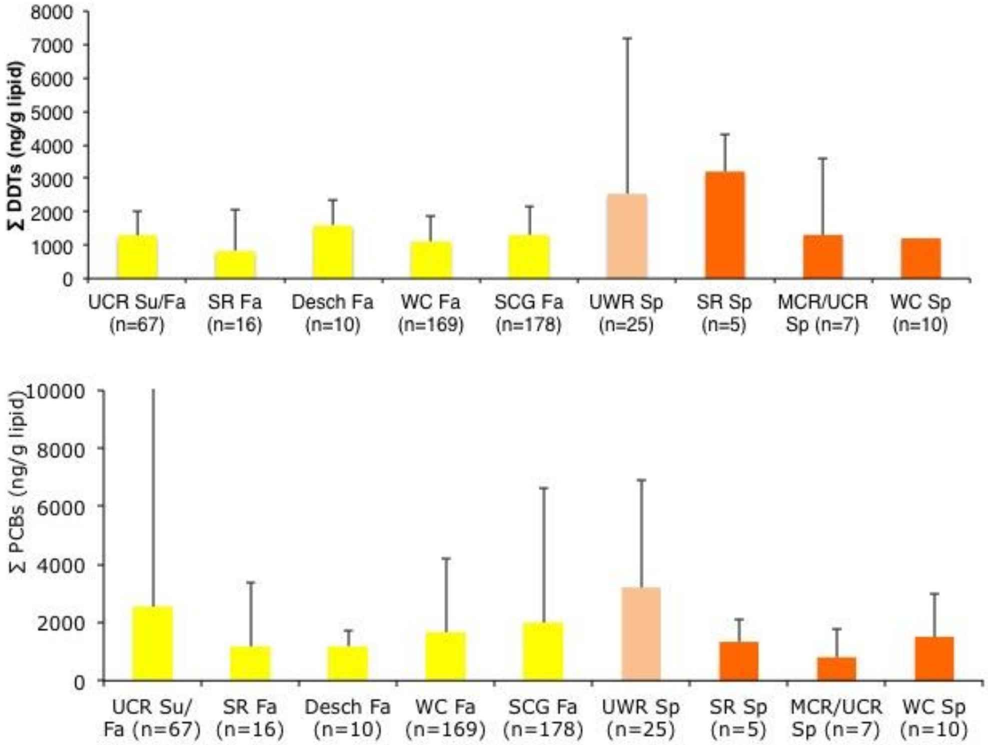

Fig. 5.c.1. Concentrations of DDTs and PCBs in Columbia River Chinook salmon stocks (Johnson et al. 2007; Johnson et al. 2013) PCBs reported as ∑17PCBs*2 [PCBs 18, 28, 44, 52, 95, 101(90), 105, 118, 128, 138 (163,164), 153 (132), 170, 180, 187 (159,182), 195, 206, 209] and DDTs reported as ∑3DDTs (p,p’-DDD, p,p’-DDE, p,p’-DDT)

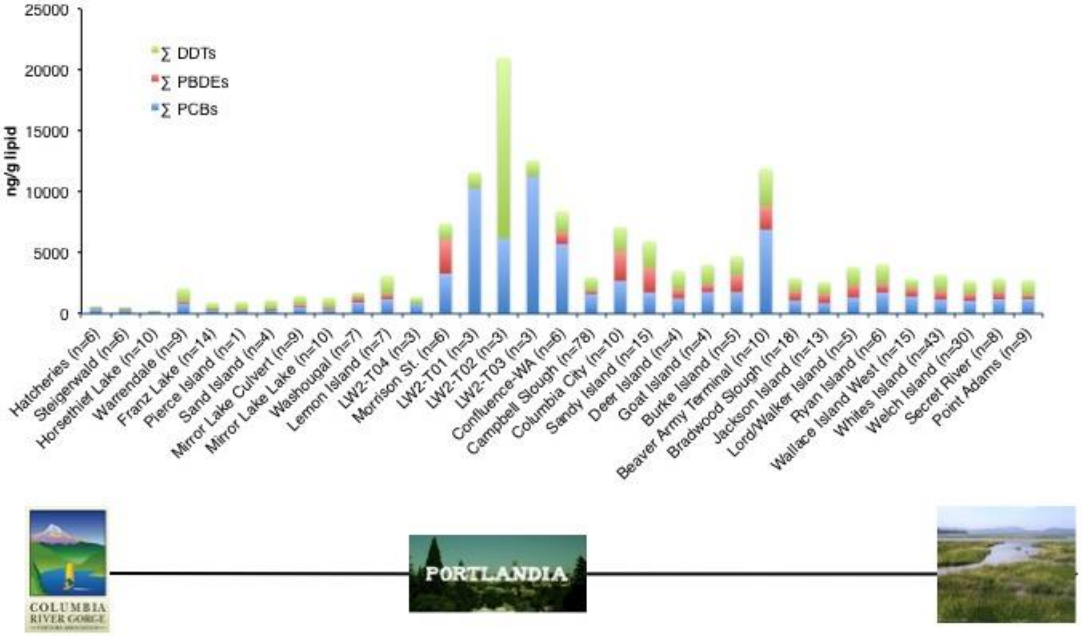

Fig. 5.c.2. Concentrations of DDTs, PBDEs, and PCBs in juvenile Chinook salmon from Lower Columbia River sites. PCBs reported as ∑17PCBs*2 [PCBs 18, 28, 44, 52, 95, 101(90), 105, 118, 128, 138 (163,164), 153 (132), 170, 180, 187 (159,182), 195, 206, 209. DDTs reported as ∑6DDTs (p,p’-DDD, p,p’-DDE, p,p’-DDT, o,p’-DDD, o,p’-DDE, o,p’-DDT; PBDEs reported as ∑7BDEs (BDEs 28, 47, 49, 66, 85, 99, 100)

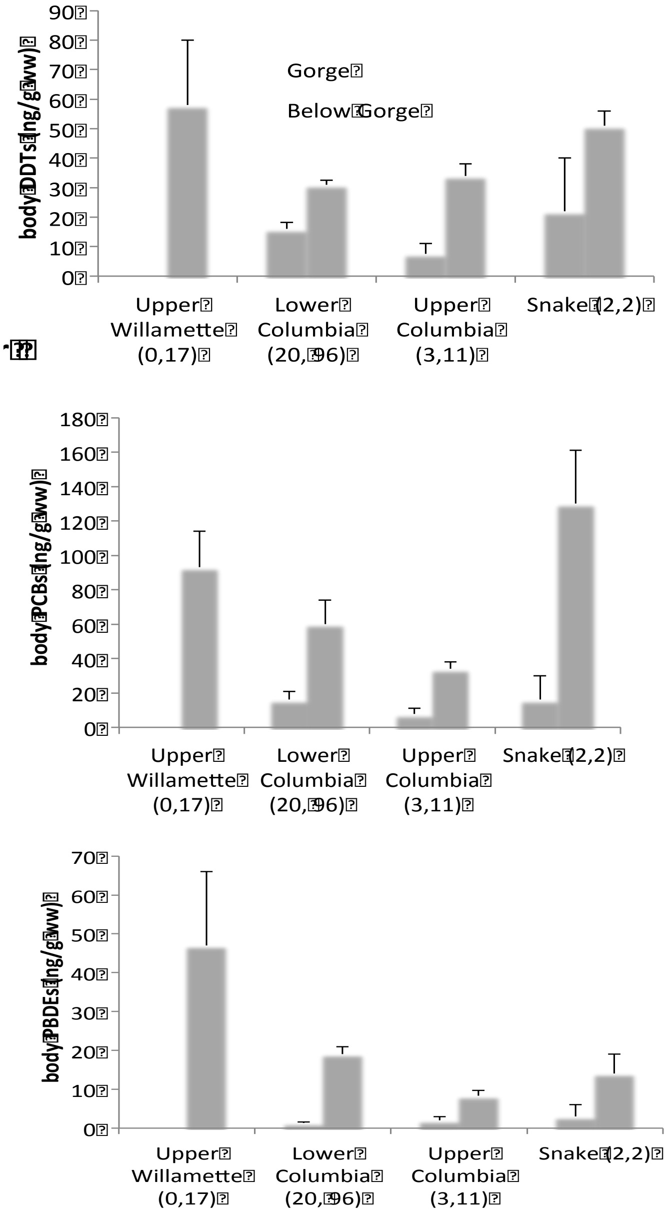

Fig. 5.c.3. Concentrations of PCBS, DDTs, and PBDEs in Juvenile Chinook salmon from Columbia River stocks from sites in the Columbia Gorge and below the Columbia Gorge (modified from Johnson et al. 2013). PCBs reported as ∑17PCBs*2 [PCBs 18, 28, 44, 52, 95, 101(90), 105, 118, 128, 138 (163,164), 153 (132), 170, 180, 187 (159,182), 195, 206, 209. DDTs reported as ∑6DDTs (p,p’-DDD, p,p’-DDE, p,p’-DDT, o,p’-DDD, o,p’-DDE, o,p’-DDT; PBDEs reported as ∑7BDEs (BDEs 28, 47, 49, 66, 85, 99, 100)

5.d Wastewater pollution and chemicals of emerging concern: risks to salmon

Background

Wastewater pollution is a growing concern for aquatic habitat quality throughout the Pacific Northwest. Wastewater can be point-source discharge from publicly owned water treatment facilities (municipal), or industrial discharge, that is regulated by permit. Current wastewater effluent criteria for contaminants in surface waters (i.e., aquatic life criteria) are established thresholds for the protection of aquatic life based on water quality standards developed and revised by the U.S. EPA to accurately reflect the latest scientific knowledge as mandated in the Clean Water Act (CWA) of 1972. A limited number of individual chemical compounds are covered; these include conventional pollutants (e.g., pH, biochemical oxygen demand, etc), priority pollutants, and non-conventional pollutants. In the U.S., the EPA mandates that permitted effluent meet water quality standards for the protection of aquatic life, but there are exceptions, including: (1) water quality standards are lacking for nearly all chemicals of emerging concern (CECs), including pharmaceuticals and personal care products (e.g., estrogenic chemicals, microplastics in toothpaste and skin care products), therefore these are not monitored; and (2) discharged compounds can be above established thresholds for the protection of aquatic life in permitted mixing zones. This section describes a screening-level assessment focused on wastewater effluent with a specific focus on salmon health, survival, and lifetime reproductive success. The goal is to better understand the extent to which wastewater may be a limiting factor for salmon recovery.

Effluents contain unregulated and/or unmonitored compounds

Over 85,000 synthetic chemicals are approved for widespread use in the U.S., with approximately 600 new chemicals approved by the U.S. EPA each year (Trasande 2016; U.S. EPA 2017). The overall number of chemicals in modern societal use that have established aquatic life criteria is small. Many of these compounds are not routinely monitored in the environment, are not removed by conventional sewage treatment, and in many cases toxicity is not known. Considerable attention in aquatic and conservation sciences has been generated for CECs (OW/ORD 2008). This term encompasses pollutants that are not currently included in conventional water quality or effluent monitoring programs. Common modern pollutants with potential biologic effects in salmonids include: pharmaceuticals and personal care products, including human prescribed drugs (e.g., metformin) and bactericides (e.g. triclosan); persistent organic pollutants, including PBDEs and perfluorinated compounds; and endocrine disrupting chemicals, including 17a-ethynylestradiol (synthetic estrogen), 18b-trenbolone (anabolic steroid), and alkylphenols (Morace 2012; Meador 2016; Phillips 2012). These compounds may impact the nervous system (through enzyme inhibition), reproductive function (due to estrogenic compounds and endocrine disruption), growth, metabolism, immune function, among other endpoints. Current-use pesticides, as described in Section 5.b, are broadly used throughout the Columbia River Basin with well-established adverse effects related to fish physiology, behavior, growth, reproduction, and survival. However, commonly used pesticides such as malathion and chloripyrifos are not routinely monitored in wastewater, even though they have established aquatic life criteria. Nanomaterials such as carbon nanotubules, silver, and titanium dioxide are also of concern particular in that little is known about their environmental or physiological fate or effects.

Aquatic life criteria may not be adequately protective of salmonids

The U.S. EPA aquatic life criteria are designed to protect a range of species and taxa, including representative fish, amphibians, and aquatic invertebrates with impacts ranging from mortality, to growth and reproduction (US EPA 1985). While data on a salmonid fish must be included in criteria development, this does not ensure that the criteria are always protective of especially sensitive threatened and endangered salmon species. The protection afforded by the ESA, on the other hand, is more focused and include activities that would harass or harm protected individuals, interfere with breeding and behavioral activities, or degrade critical habitat. This distinction is exemplified by a recent characterization of aquatic life criteria for select pollutants (ammonia, arsenic, cadmium, copper, cyanide, mercury, and selenium) as not protective for ESA-listed salmonid species (i.e., jeopardy status) [Biological Opinions on Water Quality Criteria for toxic pollutants in Oregon and Idaho prepared by the National Marine Fisheries Service in accordance with section 7(a)(2) of the Endangered Species Act (NMFS 2014, 2012)].

The current definition of acute effects for U.S. EPA aquatic life criteria focuses on direct mortality (e.g., LC50) without inclusion of sublethal impacts, which may underestimate the extent of toxicity for ESA-listed species. This is especially important when it is considered that some of these exposures and sublethal effects may have serious long-term consequences that would not be observed in the relatively short-term toxicity tests on which the aquatic life criteria are generally based. For example, reduced growth is a common sublethal endpoint; the etiology ranges from pollutants affecting behavior (neurotoxicants, e.g., copper, diazinon), nutrient assimilation (e.g., copper), ion imbalance (e.g., cadmium), compromised swimming performance (e.g., cyanide), among others. Reduced growth has been related to decreased 1st-year survival and associated population abundance estimates (Zabel and Achord 2004; Spromberg and Meador 2005), including decreased 1st-year survival from reduced growth specifically attributed to copper exposure (Mebane and Arthaud 2010). Other sublethal endpoints, such as compromised immune function and impaired reproductive capabilities, among others, have been related to delayed mortality (Arkoosh et al. 1998; Arkoosh et al. 2001) and may also be linked to population-level effects (Spromberg and Meador 2005).

Lastly, while aquatic life criteria are intended to protect aquatic species for the harmful effects of a single pollutant, discharged effluents are almost always complex mixtures of chemicals with different toxicological properties. The aquatic life criteria do not account for the potential interaction of chemicals in mixtures, including synergistic effects (Laetz et al. 2009), or for interactions between chemical and non-chemical stressors.

Mixing zones: permitted exceedance of aquatic life criteria

A mixing zone, defined as space in the receiving water where water quality criteria can be exceeded, may be authorized by each individual state if a pollutant will not meet water quality criteria after application of technology-based methods of control, prevention, and treatment. Mixing zones are commonly found throughout the Columbia River Basin, and are likely encountered by salmonids. The Columbia and Snake River salmon traverse up to 900 river miles across 3 U.S. states (WA, OR, and ID); many wastewater outfalls and permitted mixing zones overlap within this and other salmon habitat and migration corridors (U.S. EPA 2009). Mixing zones, by WA, OR, and ID state criteria, are not allowed to overlap, but the criteria for a multi-state consideration of several mixing zones within the same waterbody is not clear. The cumulative effect of multiple mixing zones would increase the overall exposure time to pollutants, thereby increasing the likelihood of health risks associated with these exposures.

Current mixing zone regulations in the Columbia River Basin

The U.S. EPA acknowledges elevated concentrations of pollutants could adversely affect the productivity of a waterbody and may result in unanticipated ecologic consequences (US EPA 1994). As such, the U.S. EPA provides specific suggestions for state mixing zone policies. The EPA suggests mixing zone policies should ensure pollutant concentrations within a mixing zone are not lethal to aquatic organisms or pose significant risks to human health, and bioaccumulative, pathogenic, or carcinogenic pollutants should not be allowed. Further, mixing zones should not negatively impact critical habitat for ESA-listed species, areas with sensitive biota, shellfish beds, fisheries, drinking water sources, or recreational areas. Lastly, mixing zones should not overlap, and the cumulative effect of multiple mixing zones within the same waterbody (e.g., Columbia River Basin) should be considered. Mixing zone guidelines specific to salmon and ESA-listed species were reviewed for Washington, Oregon, and Idaho, the U.S. states that include the Columbia River Basin and major tributaries (namely, the Snake River).

In the state of Idaho, mixing zones within areas that would interfere with spawning or rearing habitat are given special consideration to ensure pollutants do not have the potential to interfere with habitat used by endangered or threatened species or species of concern, including Chinook salmon (ID DEQ 2016). The state of Idaho requires a zone of passage for salmonids with a low threshold concentrations of pollutants observed to elicit avoidance responses in salmonids that would interfere with migration [namely: cadmium, chromium, copper, lead, mercury, nickel, and zinc at levels up to 20-times lower than the U.S. EPA recommended freshwater acute aquatic life criteria], as well as an evaluation of channel morphology to ensure the mixing zone does not overlap with areas of a stream that are capable of supporting aquatic life passage.

The Oregon Department of Environmental Quality mixing zone guidelines: (1) require critical resource areas are not impaired; (2) prevent shore and bottom-hugging mixing zones; and (3) outline temperature thermal plume limitations to protect salmon spawning areas (OR DEQ 2012). Oregon general guidelines include avoiding the overlap of mixing zones, and maintaining a zone of passage defined as 75% of the cross-sectional area or volume of flow of a stream or estuary. Additionally, field assessments are recommended when a mixing zone "encroaches on spawning or unique habitat of threatened or endangered species."

Washington state Department of Ecology mixing zone guidelines were also reviewed (WA ECY 2015). Salmon spawning, rearing, and migration are acknowledged under Aquatic Life Uses, and have criteria for temperature, dissolved oxygen, turbidity, total dissolved gas, and pH, but not priority or non-conventional pollutants. Endangered species protection and zone of passage considerations were not evaluated in these guidelines.

Salmonid life history is an important determinant of exposure and susceptibility to toxic chemicals

Salmonids exhibit important differences in susceptibility to chemical contaminants at different life stages (juveniles, spawners, etc.); as such, salmonid life history is an important determinant of chemical exposure and toxicity. Salmonid life-histories, including rearing and outmigration duration, vary by species. For example, chum and pink outmigrate to estuaries within days of hatching, whereas stream-type chinook and coho rear in freshwater streams for up to two years, depending on the population, before outmigrating (Quinn 2005). This extended residency in freshwater habitats, particularly during a critical time of growth and development, make juvenile chinook salmon particularly vulnerable to the effects of contaminants. Juveniles that rest and feed in contaminated areas increase their direct exposure time to contaminated water and increase their likelihood of consuming contaminated small invertebrates such as insects and crustaceans. The juvenile salmon diet is a well-established exposure route for arsenic, copper, mercury, selenium, and other pollutants in habitats receiving wastewater discharges. Aquatic life criteria, established to be protective of aquatic species, defines exposure limitations as 1-hour for acute criteria (based average concentration over a 1-hour residence time), and 4-days for chronic criteria. However, during their up to 2-year outmigration to the ocean (Quinn 2005), juvenile chinook salmon may exceed this exposure time.

Recommended actions

We recommend the following areas where new scientific information could most effectively support ongoing efforts to more accurately profile wastewater exposures and associated risks to salmonid species in a migratory corridor where multiple outfalls are present.

- Focused monitoring is recommended along the Columbia and Snake Rivers either through the direct sampling of salmonids, a surrogate species, or using passive samplers. Sampling site selection should be controlled for location of wastewater outfalls, depth of water, flow intensity, among other considerations that may affect residency time (i.e., exposure time) of juvenile fish. Genetic confirmation of stock is recommended to match temporal sampling along the corridor by population. This is of particular importance when considering the effect of exposure to multiple outfalls and mixing zones within a migratory corridor. The wastewater exposure should focus on pollutants common in mixing zones with known risks for salmon (e.g., ammonia, arsenic, cadmium, copper, cyanide, mercury, and selenium) to more accurately profile exposure to multiple mixing zones during passage through the Columbia River Basin, contaminants of emerging concern (currently not regulated or monitored), and current use pesticides (not routinely monitored).

- Characterization of the impact of toxic exposure in juvenile salmonids through the measurement of physiologic endpoints is recommended. Suggested markers include indicators of endocrine disruption, metabolism effects, decreased growth, immune dysfunction, enzyme inhibition, among others.

5.e Population-scale benefits of reducing toxics across the Columbia River Basin for ESA-listed

Background

The effect of contaminants on fish and associated consequences on distribution and abundance is an important knowledge gap in salmon productivity and recovery. A proper understanding of the relative influences of chemical, physical, and biological habitat characteristics on salmon fitness would allow a for direct comparison of different restoration actions and be informative for salmon recovery management and planning efforts. This would be particularly important in support of resource allocation for future restoration projects that focus of water and sediment quality. The integration of toxic impacts into a population-level assessment provides a structure to assess scenarios of remediation and removal of toxic insult on population sustainability and recovery. A rigorous and balanced evaluation would require a population with ample demographic data, along with physical and biological habitat characteristic information and measured toxicant concentrations in tissue samples. Such data are available for the lower Willamette River, which serves as an example of how life-cycle modeling can incorporate the impact of chemical habitat factors on salmon populations across the broad geographic landscape of the Columbia River Basin.

Influence of chemical habitat on salmon survival

The toxicity and broad environmental distribution of legacy pollutants is well-documented, as outlined in Section 5.c. These compounds (e.g., PCBs, DDTs, and PBDEs) are reproductive, immune, and developmental toxicants in fish and wildlife, as well as endocrine disruptors with noted effects specific to thyroid hormone. High environmental concentrations of common legacy pollutants (DDTs and PCBs) cause acute mortality (Beckvar et al. 2005; Meador et al. 2002). Research studies assessing lower concentrations of these compounds in salmonid species have demonstrated delayed mortality (i.e., sublethal effects) through compromised immune response in the presence of a pathogen (Arkoosh et al. 1998; Arkoosh et al. 2001) and decreased growth leading to a diminished probability of ocean survival (Casillas et al. 1998; Varanasi et al. 1993; Zabel and Achord 2004). Further, a study of smolt to adult return rates (SAR) for 230 million hatchery-reared Chinook released between 1972-2008 in Puget Sound revealed the estimated mean survival for juvenile Chinook migrating out through contaminated estuaries was 45% lower than for fish outmigrating through non-contaminated estuaries (SAR values 0.48% versus 0.87%, $p < 0.0001$) (Meador 2014). Chinook salmon from the Lower Columbia, Upper Willamette River, Snake River, and Upper Columbia River ESUs are clearly at risk based on demonstrated tissue concentrations of POPs and the associated percentage of samples above estimated critical body resides for toxic effects (PCBs, range across all site samples: 5-17%; DDTs, 0-14%; and PBDEs, 11-47%) (Table 5.c.1).

Translating toxic exposure to population-level effects

Demographic models provide the opportunity to demonstrate potential population-level effects related to age-stage specific modifications, including acute and delayed mortality events associated with exposures to contaminants. Sublethal endpoints in individuals have previously been translated to population effects in juvenile Chinook salmon, specifically decreased first year survival, with endpoints including compromised immune function and decreased reproductive success attributable to legacy contaminants (Spromberg and Meador 2005), as well as with reduced growth attributable to copper exposure (Mebane and Arthaud 2010). However, these examples used simplified, theoretical models. Looking forward, a modeling framework that incorporates demographic and life-history diversity data, as well as physical, biologic, and chemical habitat characteristic information, specific to an endangered or threatened population would refine the ability of these model to inform restoration actions specific and unique to different salmon populations.

Example: Portland Harbor

Portland Harbor was added to the Comprehensive Environmental Response, Compensation, and Liability Act (CERCLA) National Priorities List (i.e., Superfund site) by the U.S. EPA in 2000 due to extensive legacy pollution. This area of the lower Willamette River, just north of Portland, Oregon, has served as a commercial shipping port and working waterfront for more than a century. Priority contaminants of concern include PCBs and DDTs, among others. Previous field collections of juvenile Chinook salmon at multiple sites throughout, and downstream of, Portland Harbor provided estimates of contaminant exposures (LWG 2006; Johnson 2013; LCREP 2007). These contaminant exposures were reviewed against controlled laboratory studies to estimate aggregate losses of outmigrating juvenile Chinook, considering reduced growth and immune dysfunction as endpoints (Johnson 2014).

The potential population-scale benefit of improving chemical habitat conditions, through remediation efforts and subsequent increases in survival and productivity of juvenile Chinook, was estimated using a life-cycle model of Upper Willamette River Chinook developed at NOAA Fisheries (Zabel 2015). The model's established physical parameters were modified and extended using empirical data for chemical habitat impacts, particularly relating established adverse impacts of priority contaminants in Portland Harbor to the survival of subyearlings. Initial modelling results suggest a substantial increase in the abundance of spawners on the ESU scale with pollution mitigation efforts. This merger of empirical contaminant and associated adverse effects data with an existing life-cycle model allowed for the direct comparison of chemical habitat as a limited factor for salmon recovery relative to more conventional physical and biological factors.

Population-level effects of remediation throughout the Columbia River Basin: Key data gaps and challenges

Extensions of the population-level model described above can be applied to other salmonid populations in the Columbia and Snake River Basins. This can serve to evaluate impacts of toxics, track the effectiveness of ecosystem recovery efforts, and scale improvements to the health and survival of individual salmon populations. Essential to this effort is the availability of demographic and life-history data on ESA-listed populations, along with chemical, physical, and biological habitat information to explain current habitat restoration effort limitations and effectiveness. A series of population models have already been created through the life-cycle modeling workgroup efforts; these models span the Columbia and Snake River Basins. The data gap of greatest need will be toxics information on fish species that is specific to populations and ESUs, particularly for the Middle- to Upper- Columbia. Legacy toxics have been measured along the Columbia and Snake River corridors and tributaries, with much higher sample frequency of fish from the Lower Columbia River compared to the sampling areas further up river (Table 5.c.1).

Recommended actions

To address these issues we recommend the following areas where new scientific information could most effectively support ongoing efforts to evaluate population-level effects of chemical habitats along the Columbia and Snake Rivers:

- Conduct targeted monitoring for vulnerable fish species to address data gaps specific to contaminant exposure and accumulation for major classes of POPs, as outlined in the recommended actions for Sections 5.c., as well as for contaminants of emerging concern and current-use pesticides.
- Perform controlled laboratory experiments, such as a diet study with individual compounds within a range of environmentally relevant doses, including legacy compounds, contaminants of emerging concern, current-use pesticides, and complex mixtures to more accurately assess concentrations associated with critical health endpoints such as immune impairment and decreased growth. The resulting scientific data would provide environmentally relevant dose-response data specific to adverse endpoints that could be applied to population-models throughout the entire Columbia and Snake River Basins, as well as in other management areas with modern levels of contaminants.

5.f Conclusions

A large variety of environmental contaminants are present throughout the Columbia River Basin in habitats critical to threatened and endangered salmon. This chapter highlights three specific classes of compounds that are of particular concern in the region: current use pesticides, persistent organic pollutants, and wastewater and stormwater contaminants. These chemicals are known to impair salmon behavior, growth, reproduction, and survival, so, as stated in the Introduction to this chapter, the management question is not so much whether toxics are limiting salmon recovery in the CRB, but rather by how much and where.

This chapter highlights a variety of actions that are needed to meet the challenge of understanding how much and where toxic contaminants are limiting salmon recovery in the CRB, and which stocks and species are most vulnerable to their effects. First, it will be important to conduct targeted monitoring for vulnerable fish species to address data gaps specific to contaminant exposure and accumulation. For example, sufficient information should be collected to characterize POPs uptake in Interior Columbia Chinook salmon stocks, as well as sockeye, chum, and coho salmon, steelhead, and other species of concern such as eulachon and green sturgeon. Similarly, watersheds that are most vulnerable to current use pesticide exposure can be prioritized for targeted monitoring studies that measure pesticide concentrations during and following specific pesticide applications. Especially for contaminants of emerging concern, such as pharmaceuticals and personal care products in wastewater, research may be needed to develop toxicity evaluations for sensitive life stages and species. Contaminant exposure and effects data can then be incorporated into stock specific population models, as was illustrated in the example with Willamette River spring Chinook in Section 5e, so we can better understand the impacts of toxicants on stock productivity, and the extent to which contaminant remediation can contribute to stock recovery.

Equally important is the need to incorporate toxicant impacts into ongoing efforts to restore and improve habitats. Localized monitoring may be needed to collect baseline data in some areas where habitat restoration is planned and/or ongoing. Pollution reduction and mitigation techniques that can improve habitat conditions should also be incorporated into restoration projects where toxic contaminants are a concern. These measures include vegetated buffers, spray buffers, and irrigation and soil conservation practices which reduce pesticide loading into aquatic habitats, as well as stormwater filtration and incorporation of green infrastructure to reduce inputs of stormwater contaminants. To date, habitat restoration efforts in the CRB have focused largely on physical habitat, neglecting the important role toxic contaminants can play in degrading habitat essential to ESA-listed species. The inclusion of toxics into basin-wide planning and restoration efforts is an important step towards improving salmon productivity as well as overall habitat conditions for aquatic species throughout the Columbia River Basin.

References

Anderson, Brian S, Bryn M Phillips, John W Hunt, Karen Worcester, Mary Adams, Nancy Kapellas, and Ron S Tjeerdema. 2006. 'Evidence of pesticide impacts in the Santa Maria River watershed, California, USA', *Environmental Toxicology and Chemistry*, 25: 1160-70.

Arkoosh, M. , J. Dietrich, G. M. Ylitalo, L. J. Johnson, and S. M. O'Neill. 2013. 'Polybrominated biphenyl ethers (PBDEs) and Chinook salmon health. U.S. Department of Commerce. National Oceanic and Atmospheric Association, National Marine Fisheries Service, Northwest Fisheries Science Center, Newport, Oregon. 49 pp. plus Appendices.'.

Arkoosh, Mary R, Deborah Boylen, Joseph Dietrich, Bernadita F Anulacion, Claudia F Bravo, Lyndal L Johnson, Frank J Loge, and Tracy K Collier. 2010. 'Disease susceptibility of salmon exposed to polybrominated diphenyl ethers (PBDEs)', *Aquatic toxicology*, 98: 51-59.

Arkoosh, Mary R, Ed Casillas, Paul Huffman, Ethan Clemons, Joy Evered, John E Stein, and Usha Varanasi. 1998. 'Increased susceptibility of juvenile chinook salmon from a contaminated estuary to Vibrio anguillarum', *Transactions of the American Fisheries Society*, 127: 360-74.

Arkoosh, Mary R, Ethan Clemons, Paul Huffman, Anna N Kagley, Edmundo Casillas, Nick Adams, Herb R Sanborn, Tracy K Collier, and John E Stein. 2001. 'Increased susceptibility of juvenile chinook salmon to vibriosis after exposure to chlorinated and aromatic compounds found in contaminated urban estuaries', *Journal of Aquatic Animal Health*, 13: 257-68.

Arkoosh, Mary R, Stacy Strickland, Ahna Van Gaest, Gina M Ylitalo, Lyndal Johnson, Gladys K Yanagida, Tracy K Collier, and Joseph P Dietrich. 2011. 'Trends in organic pollutants and lipids in juvenile Snake River spring Chinook salmon with different outmigrating histories through the Lower Snake and Middle Columbia Rivers', *Science of the Total Environment*, 409: 5086-100.

Arkoosh, Mary R, Ahna L Van Gaest, Stacy A Strickland, Greg P Hutchinson, Alex B Krupkin, and Joseph P Dietrich. 2015. 'Dietary exposure to individual polybrominated diphenyl ether congeners BDE-47 and BDE-99 alters innate immunity and disease susceptibility in juvenile Chinook salmon', *Environmental science & technology*, 49: 6974-81.

Baldwin, David H, Julann A Spromberg, Tracy K Collier, and Nathaniel L Scholz. 2009. 'A fish of many scales: extrapolating sublethal pesticide exposures to the productivity of wild salmon populations', *Ecological Applications*, 19: 2004-15.

Beamish, Richard J, and Conrad Mahnken. 2001. 'A critical size and period hypothesis to explain natural regulation of salmon abundance and the linkage to climate and climate change', *Progress in Oceanography*, 49: 423-37.

Beckvar, Nancy, Tom M Dillon, and Lorraine B Read. 2005. 'Approaches for linking whole-body fish tissue residues of mercury or DDT to biological effects thresholds', *Environmental Toxicology and Chemistry*, 24: 2094-105.

Boas, Malene, Ulla Feldt-Rasmussen, Niels E Skakkebæk, and Katharina M Main. 2006. 'Environmental chemicals and thyroid function', *European Journal of Endocrinology*, 154: 599-611.

Bols, Niels C, John L Brubacher, Rosemarie C Ganassin, and Lucila EJ Lee. 2001. 'Ecotoxicology and innate immunity in fish', *Developmental & Comparative Immunology*, 25: 853-73.

BRT. 2005. 'Biological Review Team. Green Sturgeon (Acipenser medirostris) Status Review Update Biological Review Team. NOAA, National Marine Fisheries Service, Southwest Fisheries Science Center, Santa Cruz, CA. 31 p. '.

Cedergreen, Nina. 2014. 'Quantifying synergy: a systematic review of mixture toxicity studies within environmental toxicology', *PLoS One*, 9: e96580.

Doukakis, P. 2014. 'Informal status review for the Northern Distinct Population Segment of the North American green sturgeon (Acipenser medirostris). Protected Resources Division, West Coast Region, NOAA Fisheries. 26 p. '.

Dubrovsky, Neil M. 1998. *Water Quality in the San Joaquin-Tulare Basins, California, 1992-95* (US Geological Survey).

Feist, Grant W, Molly AH Webb, Deke T Gundersen, Eugene P Foster, Carl B Schreck, Alec G Maule, and Martin S Fitzpatrick. 2005. 'Evidence of detrimental effects of environmental contaminants on growth and reproductive physiology of white sturgeon in impounded areas of the Columbia River', *Environmental Health Perspectives*: 1675-82.

Fuhrer, GJ, JL Morace, HM Johnson, JF Rinella, JC Ebbert, SS Embrey, IR Waite, KD Carpenter, DR Wise, and CA Hughes. 2004. 'Water quality in the Yakima River Basin, Washington, 1999–2000: US Geological Survey Circular 1237', *US Geological Survey, Reston, VA*.

Gilliom, Robert J. 2007. 'Pesticides in US streams and groundwater', *Environmental Science and Technology*, 41: 3408-14.

Gustafson, R. G., M. J. Ford, D. Teel, and Drake. J. S. 2010. 'Status review of eulachon (Thaleichthys pacificus) in Washington, Oregon, and California. US Department of Commerce, NOAA Technical Memorandum NMFS-NWFSC-105. '.

Hamilton, Pixie A, Timothy Lee Miller, and Donna N Myers. 2004. *Water quality in the nation's streams and aquifers: overview of selected findings, 1991-2001* (US Geological Survey).

Healey, MC. 1982. 'Timing and relative intensity of size-selective mortality of juvenile chum salmon (Oncorhynchus keta) during early sea life', *Canadian Journal of Fisheries and Aquatic Sciences*, 39: 952-57.

Hinck, Jo Ellen, Christopher J Schmitt, Vicki S Blazer, Nancy D Denslow, Timothy M Bartish, Patrick J Anderson, James J Coyle, Gail M Dethloff, and Donald E Tillitt. 2006. 'Environmental contaminants and biomarker responses in fish from the Columbia River and its tributaries: Spatial and temporal trends', *Science of the Total Environment*, 366: 549-78.

Holtby, L Blair, Bruce C Andersen, and Ronald K Kadowaki. 1990. 'Importance of smolt size and early ocean growth to interannual variability in marine survival of coho salmon (Oncorhynchus kisutch)', *Canadian Journal of Fisheries and Aquatic Sciences*, 47: 2181-94.

ID DEQ. 2016. 'Idaho (ID) Department of Environmental Quality (DEQ), Idaho Mixing Zone Implementation Guidance'.

Johnson, L. L., B. F. Anulacion, M. R. Arkoosh, D. G. Burrows, D. A. da Silva, J. P. Dietrich, M. S. Myers, J. A. Spromberg, and G. M. Ylitalo. 2014. 'Effects of legacy persistent organic pollutants (POPs) in fish.' in K. B. Tierney (ed.), *Organic Chemical Toxicology of Fishes* (Elsevier: London).

Johnson, Lyndal, Bernadita Anulacion, Mary Arkoosh, O Paul Olson, Catherine Sloan, Sean Y Sol, Julann Spromberg, David J Teel, Gladys Yanagida, and Gina Ylitalo. 2013. 'Persistent organic pollutants in juvenile Chinook salmon in the Columbia River basin: implications for stock recovery', *Transactions of the American Fisheries Society*, 142: 21-40.

Johnson, Lyndal L, Gina M Ylitalo, Catherine A Sloan, Bernadita F Anulacion, Anna N Kagley, Mary R Arkoosh, Tricia A Lundrigan, Kim Larson, Mark Siipola, and Tracy K Collier. 2007. 'Persistent organic pollutants in outmigrant juvenile chinook salmon from the Lower Columbia Estuary, USA', *Science of the Total Environment*, 374: 342-66.

Jones, K. C., and P. de Voogt. 1999. 'Persistent organic pollutants (POPs): state of the science', *Environmental Pollution*, **100**: 209-21.

Laetz, Cathy A, David H Baldwin, Tracy K Collier, Vincent Hebert, John D Stark, and Nathaniel L Scholz. 2009. 'The synergistic toxicity of pesticide mixtures: implications for risk assessment and the conservation of endangered Pacific salmon', *Environmental Health Perspectives*, 117: 348-53.

Lassiter, Ray R, and Thomas G Hallam. 1990. 'Survival of the fattest: implications for acute effects of lipophilic chemicals on aquatic populations', *Environmental Toxicology and Chemistry*, 9: 585-95.

LCREP. 2007. 'Lower Columbia River Estuary Partnership. Lower Columbia River and Estuary Ecosystem Monitoring: Water Quality and Salmon Sampling Report. Lower Columbia River Estuary Partnership, Portland, OR. 70 pp.'.

Mackay, D., and A. Fraser. 2000. 'Bioaccumulation of persistent organic chemicals: mechanisms and models', *Environmental Pollution*, **110**: 375-91.

Macneale, Kate H, Peter M Kiffney, and Nathaniel L Scholz. 2010. 'Pesticides, aquatic food webs, and the conservation of Pacific salmon', *Frontiers in Ecology and the Environment*, 8: 475-82.

Macneale, Kate H, Julann A Spromberg, David H Baldwin, and Nathaniel L Scholz. 2014. 'A Modeled comparison of direct and food web-mediated impacts of common pesticides on Pacific salmon', *PLoS One*, 9: e92436.

Meador, James. 2014. 'Do chemically contaminated river estuaries in Puget Sound (WA, USA) affect the survival rate of hatchery-reared Chinook salmon?'.

Meador, James P, Tracy K Collier, and John E Stein. 2002. 'Use of tissue and sediment-based threshold concentrations of polychlorinated biphenyls (PCBs) to protect juvenile salmonids listed under the US Endangered Species Act', *Aquatic Conservation: Marine and Freshwater Ecosystems*, 12: 493-516.

Meador, James P, Andrew Yeh, Graham Young, and Evan P Gallagher. 2016. 'Contaminants of emerging concern in a large temperate estuary', *Environmental Pollution*, 213: 254-67.

Mebane, Christopher A, and David L Arthaud. 2010. 'Extrapolating growth reductions in fish to changes in population extinction risks: copper and Chinook salmon', *Human and Ecological Risk Assessment*, 16: 1026-65.

Morace, Jennifer L. 2012. *Reconnaissance of contaminants in selected wastewater-treatment-plant effluent and stormwater runoff entering the Columbia River, Columbia River Basin, Washington and Oregon, 2008-10* (US Department of the Interior, US Geological Survey).

Naiman, Robert J, J Richard Alldredge, David A Beauchamp, Peter A Bisson, James Congleton, Charles J Henny, Nancy Huntly, Roland Lamberson, Colin Levings, and Erik N Merrill.

2012. 'Developing a broader scientific foundation for river restoration: Columbia River food webs', *Proceedings of the National Academy of Sciences*, 109: 21201-07.

NMFS. 2012. "National Marine Fisheries Service. Jeopardy and Destruction or Adverse Modification of Critical Habitat. Endangered Species Act Biological Opinion for Environmental Protection Agency’s Proposed Approval of Certain Oregon Administrative Rules Related to Revised Water Quality Criteria for Toxic Pollutants. NMFS Consultation Number: 2008/00148. Federal Action Agency: U.S. Environmental Protection Agency. https://www.oregon.gov/deq/RulesandRegulations/Documents/OregonToxics-BiOp.pdf." In.

NMFS. 2014. 'National Marine Fisheries Service. Endangered Species Act Section 7(a)(2) Biological Opinion and Magnuson-Stevens Fishery Conservation and Management Act Essential Fish Habitat (EFH) Consultation Idaho Water Quality Standards for Toxic Substances. NMFS Consultation Number: 2000-1484. Action Agency: United States Environmental Protection Agency. http://www.deq.idaho.gov/media/1117928/triennial-review-noaa-toxics-biological-opinion-0514.pdf'.

NMFS. 2015. 'National Marine Fisheries Service. Southern Distinct Population Segment of the North American Green Sturgeon (Acipenser medirostris) 5-Year Review: Summary and Evaluation. National Marine Fisheries Service West Coast Region Long Beach, CA. 42 p. '.

NMFS. 2016. 'National Marine Fisheries Service. Status Review Update of Eulachon (Thaleichthys pacificus) Listed under the Endangered Species Act: Southern Distinct Population Segment. National Marine Fisheries Service West Coast Region, Portland, OR. 50 p.'.

O’Neill, Sandra M, Andrea J Carey, Jennifer A Lanksbury, Laurie A Niewolny, Gina Ylitalo, Lyndal Johnson, and James E West. 2015. 'Toxic contaminants in juvenile Chinook salmon (Oncorhynchus tshawytscha) migrating through estuary, nearshore and offshore habitats of Puget Sound'.

OR DEQ. 2012. 'Oregon (OR) Department of Environmental Quality (DEQ), Regulatory Mixing Zone Internal Management Directive. DEQ Publication Number 07-WQ-012, Revision 2.0.'.

OW/ORD. 2008. "Office of Water/Office of Research and Development, Emerging Contaminants Workgroup. WHITE PAPER AQUATIC LIFE CRITERIA FOR CONTAMINANTS OF EMERGING CONCERN. PART I GENERAL CHALLENGES AND RECOMMENDATIONS. https://www.epa.gov/sites/production/files/2015-08/documents/white_paper_aquatic_life_criteria_for_contaminants_of_emerging_concern_part_i_general_challenges_and_recommendations_1.pdf." In.

Quinn, T. P. 2005. *The Behavior and Ecology of Pacific Salmon and Trout -- 1st ed.* (Univeristy of Washington Press).

Safe, Stephen H. 1994. 'Polychlorinated biphenyls (PCBs): environmental impact, biochemical and toxic responses, and implications for risk assessment', *Critical reviews in toxicology*, 24: 87-149.

Sandahl, Jason F, David H Baldwin, Jeffrey J Jenkins, and Nathaniel L Scholz. 2005. 'Comparative thresholds for acetylcholinesterase inhibition and behavioral impairment in coho salmon exposed to chlorpyrifos', *Environmental Toxicology and Chemistry*, 24: 136-45.

Sandahl, Jason F, and Jeffrey J Jenkins. 2002. 'Pacific steelhead (Oncorhynchus mykiss) exposed to chlorpyrifos: benchmark concentration estimates for acetylcholinesterase inhibition', *Environmental Toxicology and Chemistry*, 21: 2452-58.

Seiders, K., C. Deligeannis, and M. Friese. 2012. 'Washington State Toxics Monitoring Program: Freshwater Fish Tissue Component, 2010. Publication No. 12-03-023. Washington Department of Ecology, Olympia, WA '.

Seiders, K., C. Deligeannis, M. McCall, and P. Sandvik. 2015. 'Freshwater Fish Contaminant Monitoring Program Annual Report for 2013. Washington Department of Ecology Publication No. 15-03-016. Washington Department of Ecology, Olympia, WA '.

Sloan, Catherine A, Bernadita F Anulacion, Jennie L Bolton, Daryle Boyd, O Paul Olson, Sean Y Sol, Gina M Ylitalo, and Lyndal L Johnson. 2010. 'Polybrominated diphenyl ethers in outmigrant juvenile Chinook salmon from the lower Columbia River and Estuary and Puget Sound, Washington', *Arch Environ Contam Toxicol*, 58: 403-14.

Spromberg, J. A. , and L. L. Johnson. 2008. 'Potential effects of freshwater and estuarine contaminant exposure on Lower Columbia River Chinook salmon (Oncorhynchus tshawytscha) populations. .' in H. R. Akcakaya, J.D. Stark and T. S. Bridges (eds.), *Demographic toxicity methods in ecological risk assessment.* (Oxford University Press: Oxford, United Kingdom).

Spromberg, Julann A, and James P Meador. 2005. 'Relating results of chronic toxicity responses to population-level effects: Modeling effects on wild chinook salmon populations', *Integrated Environmental Assessment and Management*, 1: 9-21.

Trasande, Leonardo. 2016. 'Updating the toxic substances control act to protect human health', *Jama*, 315: 1565-66.

Tyler, C. R., S. Jobling, and J. P. Sumpter. 1998. 'Endocrine disruption in wildlife: a critical review of the evidence', *Crit Rev Toxicol*, 28: 319-61.

U.S. EPA. 2002. 'United States Environmental Protection Agency. Columbia River Basin Fish Contaminant Survey 1996-1998. EPA 910-R-02-006. '.

U.S. EPA. 2009. 'U.S. Environmental Protection Agency, Columbia River basin—State of the river report for toxics: U.S. Environmental Protection Agency, EPA 910–R–08–004, accessed March 1, 2017, https://permanent.access.gpo.gov/LPS113319/LPS113319/yosemite.epa.gov/r10/ECOCOMM.NSF/Columbia/SoRR/$FILE/SORR-columbia-09-Full.pdf.'.

U.S. EPA. 2017. 'U.S. EPA, Toxic Substance Control Act. https://www.epa.gov/reviewing-new-chemicals-under-toxic-substances-control-act-tsca Accessed Feb 23, 2017.'.

US EPA. 1985. "Guidelines for Deriving Numerical National Water Quality Criteria for the Protection Of Aquatic Organisms and Their Uses. PB85-227049. https://www.epa.gov/sites/production/files/2016-02/documents/guidelines-water-quality-criteria.pdf." In, edited by Environmental Research Laboratories. Duluth Office of Research and Development, Minnesota; Narragansett, Rhode Island; Corvallis, Oregon.

US EPA. 1994. 'US Environmental Protection Agency's Water Quality Standards Handbook. https://www.epa.gov/wqs-tech/water-quality-standards-handbook. Accessed December 22, 2016.'.

WA ECY. 2015. 'State of Washington (WA) Department of Ecology (ECY). Water Quality Program Permit Writer's Manual. Publication no. 92-109. https://fortress.wa.gov/ecy/publications/documents/92109.pdf'.

Werner, Ingeborg, Linda A Deanovic, Valerie Connor, Victor de Vlaming, Howard C Bailey, and David E Hinton. 2000. 'Insecticide-caused toxicity to Ceriodaphnia dubia (CLADOCERA) in the Sacramento–San Joaquin River delta, California, USA', *Environmental Toxicology and Chemistry*, 19: 215-27.

West, Cameron J, and PA Larkin. 1987. 'Evidence for size-selective mortality of juvenile sockeye salmon (Oncorhynchus nerka) in Babine Lake, British Columbia', *Canadian Journal of Fisheries and Aquatic Sciences*, 44: 712-21.

WSDA. 2014. 'Washington State Department of Agriculture. Surface water monitoring program for pesticides in salmonid-bearing streams, 2013 data summary. AGR PUB 103-411(N/8/14). 120pp.'.

Zabel, Richard W, and Stephen Achord. 2004. 'Relating size of juveniles to survival within and among populations of Chinook salmon', *Ecology*, 85: 795-806.

Chapter 6: ECOLOGICAL INTERACTIONS

6.a Population-specific migration timing affects en route survival of adult Chinook salmon through the Lower Columbia River

Mark H. Sorel (Ocean Associates Inc. *contracted to* NMFS, Northwest Fisheries Science Center), A. Michelle Wargo Rub (NMFS, Northwest Fisheries Science Center), and Richard W. Zabel (NMFS, Northwest Fisheries Science Center)

Introduction

Spring-summer Chinook salmon (*Oncorhynchus tshawytscha*) in the Columbia and Snake Rivers are composed of multiple populations with unique migration timings that affect en route mortality rates of adults migrating upstream (Keefer et al. 2004, Crozier et al. 2008, Keefer et al. 2012, Rub et al. in prep.). They comprise two evolutionarily significant units (ESUs) listed as threatened under the Endangered Species Act (ESA) due to reductions in their abundance and productivity as a result of large-scale hydropower development, habitat degradation, harvest, and hatchery supplementation to provide harvesting opportunities (Matthews and Waples 1991, National Research Council 1996). Mature adults migrate from their adult rearing grounds in the North Pacific Ocean to the Columbia River, and then hundreds of kilometers upstream to their spawning grounds. The salinity gradient experienced upon river entry is physiologically stressful, and they are vulnerable to predation and harvest due to their concentration in the estuary at predictable times each year (Clarke 1995, Wright et al. 2007).

A recent study by Rub et al. (in prep.) found that the survival of returning adults transiting from the Columbia River mouth near Astoria (RKm 44) to Bonneville Dam fish ladders (RKm 233) was remarkably low and decreased substantially between 2010 and 2015. Survival was lowest for fish that arrived earlier in the season, suggesting that stressors and threats within the estuary differentially affected populations with different migration timings. These survival patterns coincided with the interannual trend and seasonality of the presence of

California sea lions (*Zalophus californianus*), which suggested that predation mortality had a significant effect on adult spring-summer Chinook salmon survival (Brown and Wright in prep, Rub et al. in prep.) Decreased estuarine survival represents an emerging threat and additional insult to which depressed populations may not be resilient. However, different populations appear to have variable survival through the Lower Columbia River due to their migration timing, suggesting that there is a gradient of risk (Keefer et al. 2012).

The Upper Columbia and Snake River ESUs are composed of multiple major population groups (MPGs) composed of individual populations, each with unique migration timings. Migration timing is a heritable behavior that has evolved in response to optimal migration conditions, enabling spawning in locations and at times that maximize reproductive success and survival of offspring (Healey et al. 1991, Quinn et al. 2002, Waples et al. 2004, Crozier et al. 2008). It has also been influenced by hatchery supplementation using broodstock from out-of-basin stocks in some populations (Keefer et al. 2004). Migration timing shifts subtly from year to year in response to environmental conditions within the marine and riverine environments, but chronology of populations returning to the river is conserved across years (Keefer et al. 2008, Anderson and Beer 2009). Populations are categorized into spring or summer runs based on their migration timing, spawning location, and genetics (Matthews and Waples 1991). In general, spring-run populations begin their spawning migrations earlier than summer-run populations, which appears to subject them to lower survival through the Lower Columbia River (Rub et al. in prep.) Given the threatened and endangered status of these populations, this increased estuarial mortality could significantly affect the viability of these populations.

The goal of this analysis was to estimate the survival rates of adult Chinook salmon populations from the mouth of the Columbia River to Bonneville Dam as a function of their migration timing, for implementation in life-cycle models. Extensive data on the migration timing of Chinook salmon in the Columbia and Snake River basins are available due to large-scale tagging of juvenile parr with passive integrated transponder (PIT) tags and the presence of high-efficiency tag detectors within adult fish ladders at Bonneville Dam. We used these data and a recent study of survival through the Columbia River estuary to characterize how migration timing influenced the exposure of different populations to an emerging and temporally variable threat within their migration corridor. We calculated the proportional decline in survival during a recent period of heightened California sea lion presence (2013–2015) relative to a baseline period (1998–2012), to simulate the decrease in survival with life-cycle models that already incorporate historical baseline survival rates in parameters for marine life stages.

Methods

We predicted average population- and year-specific survival rates of adult Chinook salmon between the Columbia River delta (near Astoria, Oregon) and Bonneville Dam fish ladders from 1998 to 2015, and calculated ratios of average survival between the recent period of increased California sea lion presence (2013–2015) and the historical baseline period (1998–2012). We predicted daily survival rates between 20 March and 14 June of 1998–2015 based on environmental and ecological variables that were correlated with survival in 2010-2015. We developed a model of annual population-specific migration timing in these years and applied it to model-predicted daily survival rates to estimate population-specific annual survival rates. We bootstrapped the data to sample the uncertainty in both models.

Mark-recapture survival model

Survival rates of adult spring-summer Chinook salmon from the Columbia River delta to Bonneville Dam were estimated with a mark-recapture study by Rub et al. (in prep.), who captured fish near the river's mouth, east of Astoria at RKm 44, and implanted them with PIT tags (Supplementary Table 1). They used genetic stock identification to isolate fish originating from and presumably returning to habitats upstream of the dam (Teel et al. 2009). Tagged fish originating from populations upstream of Bonneville Dam were interrogated for the presence of tags at the adult fish ladders in the dam (RKm 234). Assuming 100% detection efficiency at Bonneville Dam, we used detections to indicate survival (Rub et al. in prep.).

We used a logistic regression model to estimate survival rates from the Columbia River mouth to Bonneville Dam (s), and excluded fish that were ≤ 55 cm (Jacks) because they aren't generally considered in population viability analyses (Zabel et al. 2006) (Supplementary Table 2). The independent variables were the log-transformed 7-day running mean number of California sea lions hauled out near Astoria and water temperatures in the lower Columbia River on the date of tagging, as well as the presence of an adipose fin-clip. We failed to reject the null hypothesis that this model did not fit the data based on a Hosmer-Lemeshow goodness-of-fit test with 10 groups conducted with the *ResourceSelection* package in the statistical software program R ($\hat{C}$ = 6.951, df = 8, p = 0.542; R Core Team 2015 , Lele et al. 2016).

We predicted survival for unclipped fish in 1998 and 2000–2015 based on time series of the independent variables in the survival model. Sea lion counts in Astoria were provide by the Oregon Department of Fish and Wildlife (Brown and Wright in prep), and we filled short gaps in the record by linear interpolation. Historical water temperatures were obtained from the Columbia River DART (1993) website. We predicted survival rates for unclipped fish because we were interested in the survival of wild populations.

We were ultimately interested in quantifying how survival rates had changed due to the recent increase in pinniped presence, because life-cycle model parameters already incorporate baseline levels of adult estuarine mortality. Therefore, we examined ratios of survival rates between a baseline period of 1998–2012 and the 2013–2015 interval when sea lion presence was highest. By examining ratios, we eliminated bias in survival estimates from handling and tagging effects, which were presumably equal in all years. The exception would be if handling effects had a significant interaction with pinniped presence, which Rub et al. (in prep.) did not believe to be the case. Ashbrook et al. (2009) estimated that post-release survival of Chinook salmon captured in tangle nets in the lower Columbia River to Bonneville Dam was approximately 87.2% in the absence of pinniped predation, suggesting that our predicted survival rates were roughly 12.8% lower than that of untagged fish.

Migration-timing models

Given the variability in survival among cohorts of fish that entered the estuary on different days, we accounted for the arrival timing of different ESA-listed populations into the estuary near Astoria to calculate their annual population-specific survival rates. To estimate the population- and year-specific arrival timing of adult Chinook salmon in the Lower Columbia River, we fit a model of Bonneville Dam passage timing based on detections of fish that had been marked with PIT tags as juveniles in their natal habitats and were therefore identifiable to population of origin. We subtracted predictions of the number of days between when fish were tagged in Astoria and when they passed Bonneville Dam from a travel-time model to estimate their arrival timing in Astoria.

We fit the passage-timing model at Bonneville based on PIT-tag detections from 2001 through 2016, when there were between 130 and 899 detections per year that fit our criteria (Supplementary Table 3). Detections were queried from the PIT Tag Information System database (PTAGIS 2016), and we assigned fish to populations based on their tagging location as juveniles (Supplementary Table 4). We restricted our analysis to wild ESA-listed populations within the Upper Columbia River spring and Snake River spring-summer Chinook salmon ESUs with > 90 total adult detections. We only used fish released in known locations within the natal habitat of a single population in the analysis. Populations were designated as spring- or summer-run based on previous work examining their life histories and genetics (Matthews and Waples 1991, PTAGIS 2016). Summer-run Chinook from the Upper Columbia River are not part of that ESU and were therefore not included in the analysis. Jacks were also excluded from the analysis because they are mostly males that contribute less than older fish to population viability (Zabel et al. 2006).

The population-specific distributions of detection dates in Bonneville Dam fish ladders appeared to be log-normally distributed based on visual examination. To develop lognormal passage-timing distributions for each population and year, we fit a generalized linear model of the mean log-transformed Julian date of arrival for each population and adult-return year, where both year and population were categorical fixed effects. In addition to the mean arrival date for each population and year, we were interested in the variances of arrival dates, which characterized the shapes of arrival-timing distributions. Due to small sample sizes for some populations in some years (Supplementary Table 3), we assumed constant year effects across populations and constant variances within populations across years. Thus, we assumed that each population had an inherent spread of passage dates, which shifted forward or backward by the same amount as all other populations in a given year. Model fitting was conducted with the *gls* function in the ‘nmle’ package in R (Pinheiro et al. 2015). We also fit models where year effects were unique for each ESU, MPG, population, or run type to see if there was increased support for any of these models.

We fit a similar model that predicted year effects based on environmental variables in order to predict historical run timing in years with insufficient numbers of PIT-tag detections. We based the candidate environmental variables on a set used by Keefer et al. (2008), who established relationships between migration timing and riverine, oceanic, and climatic factors. We tested the North Pacific Index (NPI; Climate Analysis Section et al. 1994) for December–March, and the Pacific Decadal Oscillation (PDO; Mantua and Hare) for January–April. We also tested the monthly averages of the following climatic and riverine variables for February–April: air temperature (C°) at Portland International Airport (~RKm 175; National Weather Service Forecast Office), surface water temperature (C°) above Bonneville Dam (Columbia River DART 1993), and discharge (m^3/s) at Bonneville Dam (Columbia River DART 1993).

We used the *dredge* function in the ‘MuMIn’ package in R (Barton 2016) to fit models with different combinations of environmental variables and ranked them based on Akaike Information Criterion (AIC). We restricted the number of environmental variables allowed in the model to three because adding more variables required significantly more computing time and provided minimal improvements in model fit. The best model selected by backward stepwise regression contained 14 environmental variables and was clearly “overfit” as shown by its unrealistic predictions of passage timing outside the range of years in the data set. Although so called “data dredging” has the potential to produce models based on spurious relationships (Burnham and Anderson 2002), our set of candidate variables were strategically chosen because they are understood to impact the distribution of salmon in the ocean, their initiation of migration, and their travel times through lower river (Keefer et al. 2008). Therefore, we believe that the relationships identified through our model-selection procedure represented a reasonable model for predicting migration timing for three years prior to the start of our data set of PIT-tag detections. To predict the proportion of each population arriving at the dam on each date in each year, we used the *dlnorm* function in R to obtain densities of lognormal distributions defined by the means and standard deviations estimated by the model (Figure 1 & 2).

We modeled survival as a function of tag date, which corresponded with river-entry date near Astoria; so, we needed to estimate the timing of fish entering the river as a function of their timing passing Bonneville Dam. To do so, we developed a model of the number of days between tagging near Astoria and passing Bonneville Dam, hereafter referred to as travel time (Supplementary Figure 1). We normalized observed travel times with a log transformation and regressed them against environmental variables. To model seasonality and interannual variability in travel time, we employed the same candidate environmental variables as used above for modeling arrival timing at the dam. In addition, we included water temperature, discharge, and spill at the dam over 15, 20, and 25 days following river-entry of each fish. We used the 'dredge' function to select the best model based on AIC. We restricted the number of explanatory variables to two because adding more variables produced overfitting, as evidenced by unrealistic predictions of travel times where data were unavailable.

We fit lognormal distributions of population- and year-specific arrival timing in the river near Astoria based on modeled Bonneville Dam passage timing and predicted travel-times (Figure 1). We used the 'predict' function in R to estimate the mean and 95% prediction interval of travel times for each cohort of fish that entered the river on a Julian date (c) and year (y), and divided half of the prediction interval by 1.96 to define the standard deviation of lognormal distributions of travel times for each cohort. We used the 'dlnorm' function in R to predict the proportions of each cohort that passed Bonneville Dam on each subsequent date (b) based on densities of the lognormal travel-time distributions. In order to predict Bonneville-passage-timing distributions from river-entry-timing distributions, the proportions of each cohort that arrived at Bonneville on each date were weighted by the proportion of the population (*i*) in each cohort, and summed across cohorts for each Bonneville-passage date (equation 1).

$$p_{i,b,y} = \sum_{c=1}^{b} p_{b,c,y} * p_{i,c,y} \ . \qquad (1)$$

We used the *mle* function in the 'stats4' package to fit river-entry-timing distributions to the predicted Bonneville-passage-timing distributions from the model described above (Figure 1).

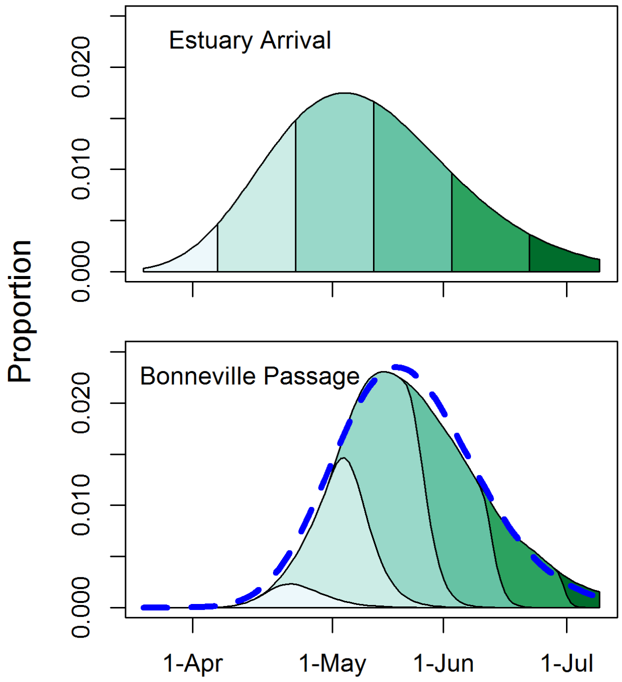

Figure 1. Green-shaded areas represent modeled estuary-entry (top panel) and resulting Bonneville-passage timing (bottom panel) based on the travel-time model, for the Wenatchee River Population in 2014. We fit these to the estimated Bonneville-passage timing (blue-dashed line) that was modeled based on PIT-tag detections. The different-colored areas represent quantiles of the run, designed to show how we used the travel-time model to estimate Bonneville-passage-timing distributions based on estuary-entry-timing distributions.

Population- and year-specific survival

To estimate population (P)- and year (y)-specific survival rates (S), we took an average of modeled cohort (c)-specific survival rates, weighted by the modeled proportions of each population in each cohort (Equation 2). We restricted the range of possible river-entry cohorts to be between 20 March and 14 June, the range of Julian dates in which Rub et al. (in prep.) measured survival in the mark-recapture study. We added the proportions of each population that were predicted to enter the river before or after this interval to the first and last days of the interval. The average proportion of the run that passed Bonneville before 20 March across all populations and years was 2.3 % (range = 0.0–21.6%), and 8.0% after 14 June (range = 0.0–39.4%).

$$S_{P,y} = \sum_{c=79}^{165} p_{\mathrm{P,y,c}} * S_{c,y} \ . \tag{2}$$

We characterized model uncertainty and generated distributions of population- and year-specific survivals by bootstrapping the data sets of arrival timing at Bonneville Dam and survival 1,000 times. For each iteration, the models were refit to random samples of the original data sets, drawn with replacement, of the same size of the original data sets.

Results

Population- and year-specific migration timing

All coefficients for populations and years were highly significant ($p < 0.001$) in the model of Bonneville-passage timing. Visual examination of model fits suggested that the model accurately described Bonneville-passage timing (Figure 2). Models that included unique year effects for individual ESUs, MPGs, populations, or runs received significantly less support based on AIC than the model with common year effects across all populations, indicating that interannual shifts in migration timing were similar across populations (Supplementary Table 5).

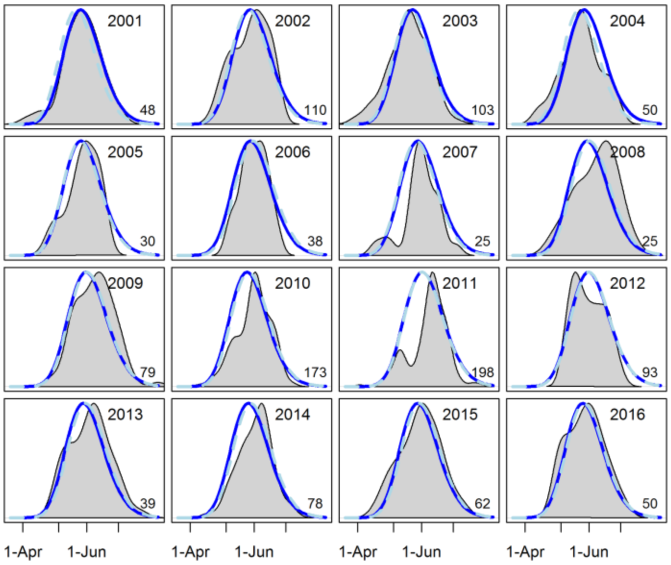

Figure 2. Kernel density distributions of adult Chinook salmon detection dates in Bonneville Dam fish ladders (grey shaded area), for the Imnaha River population in 2001–2016. Numbers of detections are shown in the lower right corner of each panel. The dark-blue solid lines represent lognormal distributions fit to detections of fish from multiple different populations, where each population has a constant variance across years, and the mean passage date of all population shifts forward or backwards by the same amount in a given year. The light-blue dashed lines represent distributions from a similar model where we predicted the annual shifts in passage timing based on environmental variables.

The highest-ranked environmental model of arrival timing at Bonneville Dam contained the variables January PDO, March NPI, and February discharge (Supplementary Table 6). Despite the higher AIC of the environmental model (-8,461) than the model with coefficients for each individual year (-8,496), both models produced very similar predictions based on visual examination (Figure 2). We used the environmental-variable model to generate distributions of passage timing at Bonneville Dam in the remainder of our analysis, because it could be used to predict historical arrival timing in the years 1998 and 2000. There were insufficient numbers of adult Chinook detections to characterize migration timing in these years, but there were records of California sea lion counts and water temperatures with which to predict historical survival rates. The earliest predicted passage timing at Bonneville Dam between 1998 and 2016 occurred in the year 2003 and was approximately ten days earlier than the latest, which occurred in 2000 (Figure 3).

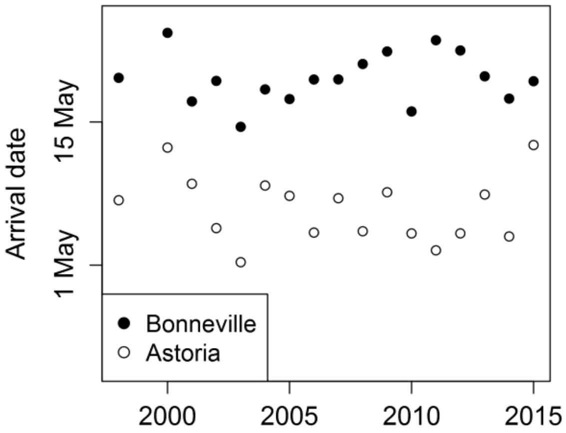

Figure 3. Model-predicted average arrival date for all populations combined in the river mouth near Astoria and date of passage at Bonneville Dam.

There was considerable variability among populations in passage timing at Bonneville Dam, including within individual MPGs (Figure 4). For example, the Upper Grande Ronde (above the Wallowa River) and Catherine Creek populations, both within the Grande Ronde MPG, migrated earlier than the Lostine River population, also in the Grande Ronde MPG. Across all populations examined, there did not appear to be distinct early- and late-arriving groups, but rather a continuum of run timings. Furthermore, some spring-run populations, such as the Lostine River, had relatively late arrival timings that were closer to summer-run populations. However, summer-run populations did have considerably later migration timings than spring-run populations on average.

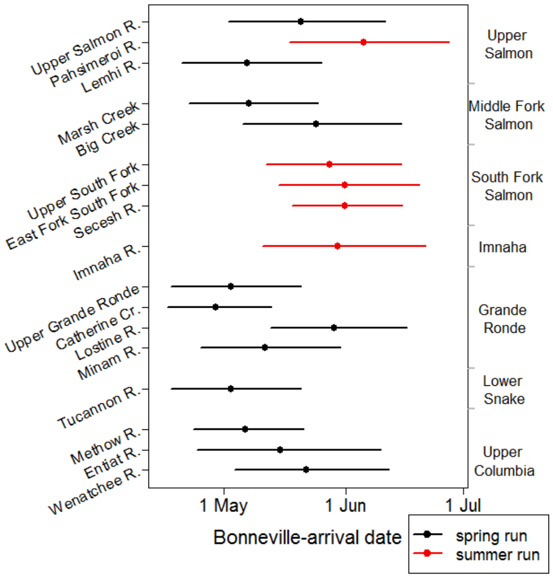

Figure 4. Average mean passage date (points) at Bonneville Dam for wild spring and summer Chinook salmon populations in 1998–2015. The lines represent the ranges of dates in which we predict that 75 % of each population would pass Bonneville Dam in this hypothetical average year. There was considerable variation across populations, and earlier-migrating populations had lower survival than later-migrating populations.

Travel times between the river mouth and Bonneville Dam decreased from an average of 30–40 days at the beginning of the mark-recapture study in late March to 5–10 days in mid-June (Supplementary Figure 1). The best model of travel times contained terms for average discharge over 20 days following river entry, and average water temperature over 25 days following river entry (Supplementary Table 7). Outflow had a positive relationship with travel times while temperature had a negative relationship with travel times. The modeled average travel times and prediction intervals appeared to fit the observed data well (Supplementary Figure 1).

Due to the interannual viability in travel times, annual arrival dates at Bonneville were only moderately correlated with modeled river-entry dates at Astoria across the years 1998–2015 (Pearson correlation = 0.254; Figure 3). The average annual travel time across years was 12.7 days and ranged from a maximum of 20.5 days in 2011 to a minimum of 6.2 days in 2015. The year with the earliest average river-entry was 2003, and the latest average river-entry occurred in 2015 (11.5 days later than 2003). The river-entry timing distributions interacted with cohort-specific survival rates to drive population- and year-specific survival rates in our model (Supplementary Figure 2).

Survival to passing Bonneville Dam

Timing of river entry had a strong effect on population-specific survival rates, especially in 2013-2015, when survival was very low in the early part of the season (Figure 5). The earliest-arriving of the spring-run populations examined—Lemhi River, Marsh Creek, Upper Grande Ronde, Catherine Creek, Tucannon River, and Methow River—had somewhat lower survival rates than other populations in 2010–2012, when annual medians ranged from 69% to 81%, and much lower survival rates in 2013–2014, which had a 50–70% range in annual median survivals. Populations with intermediate run timing such as the Upper Salmon River, Big Creek, Minam River, Entiat River, and Wenatchee River had experienced survival that was somewhat lower in 2013–2015, with annual medians of 67–85%, than 2010–2012's 79% to 88% range. Late-arriving populations—Pahsimeroi River, Upper South Fork Salmon River, East Fork South Fork Salmon River, Secesh River, Imnaha River, and Lostine River—most of which are considered summer-run, had the highest survival rates with the least interannual variability. Unlike early-arriving populations, these fish had similar survival rates in 2010–2012, with annual medians ranging from 84% to 92%, and 2013–2014 (83–92%). While the effects of handling and tagging biased these survival estimates low, they represent the trends in survival among years and populations with different migration timing.

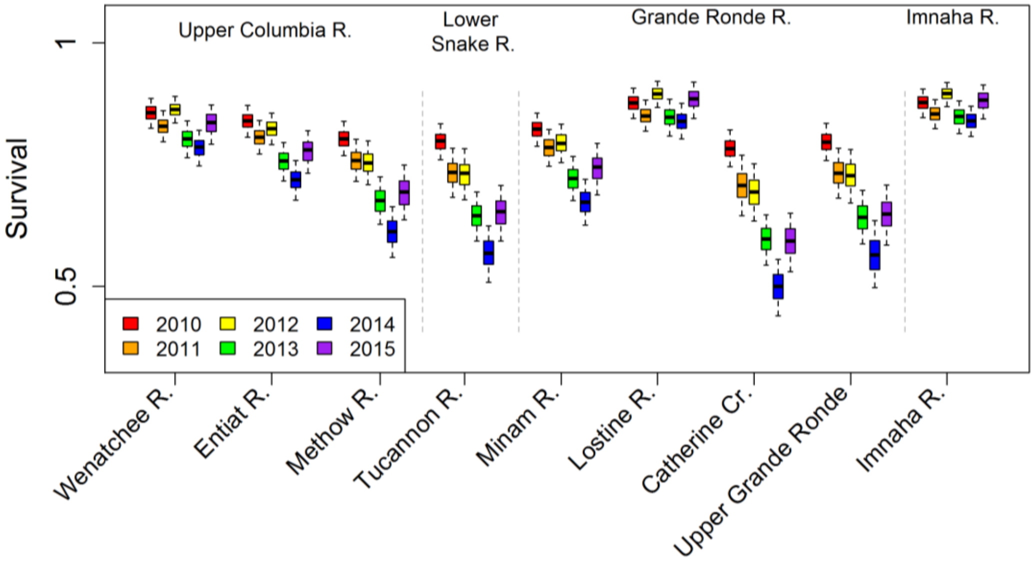

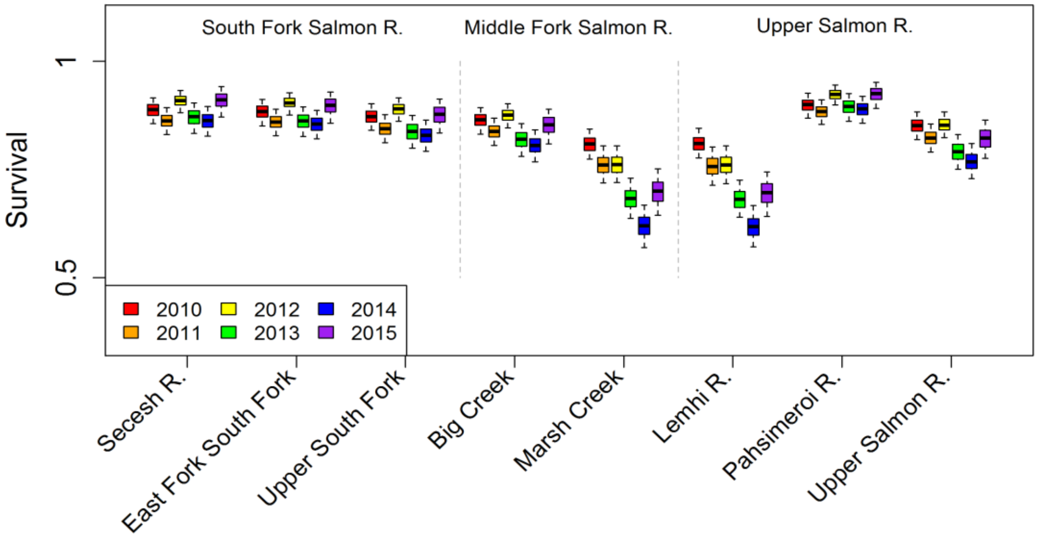

Figure 5. Modeled population- and year-specific survival rates of adult spring Chinook salmon during their migration from the mouth of the Columbia River (near Astoria, OR) to Bonneville Dam from 2010 to 2015. The centerline of each box represents the median survival estimate, the range of each box represents the interquartile range, and whiskers reach the 5th and 95th percentiles. These survival estimates are likely biased low by approximately 13% due to tagging and handling effects in the mark-recapture study.

Average population-specific survival exhibited significant interannual variability between 1998 and 2015, but survival was consistently higher from 1998 through 2012 than during the 2013–2015 period (Figure 6). Predicted survival rates were slightly lower in 2002 and 2003 than the other years between 1998 and 2012, because fish arrived early and California sea lion presence was somewhat elevated. Average survival of the early-migrating populations was 22% lower in the 2013–2015 period than during the 1998–2012 baseline period. Average survival of the populations with intermediate migration timing was 11% lower, and survival of the late-migrating populations decreased by only 6% coinciding with the increase in sea lion presence in 2013-2015 relative to the baseline period.

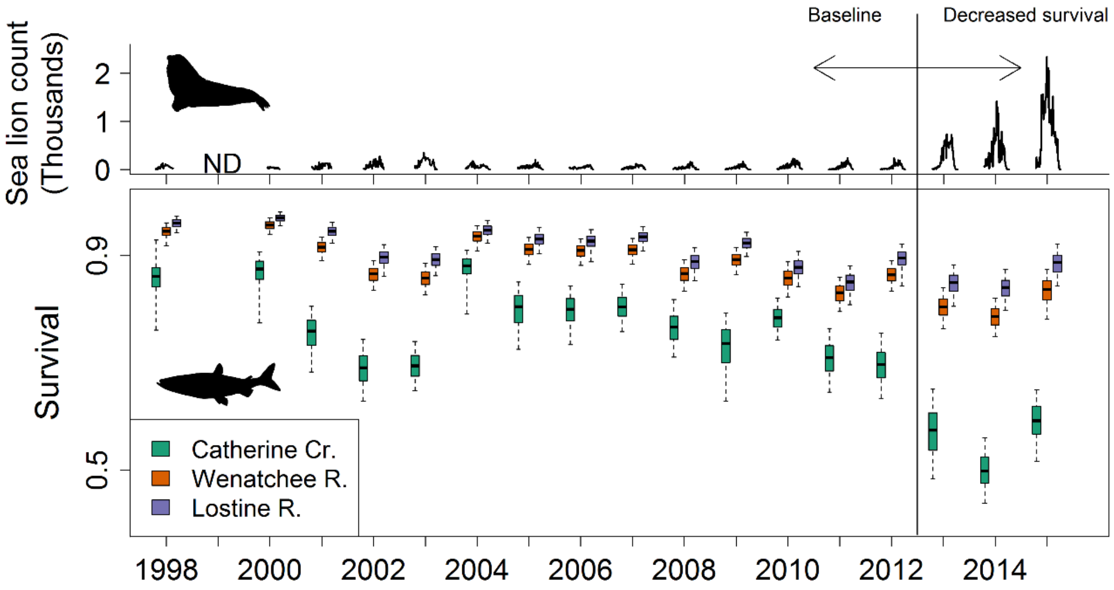

Figure 6. Top Panel: Daily counts of California sea lions hauled out at the East Moring Basin in Astoria from 1 January to 30 June of 1998–2015. Sea lion counts were unavailable for 1999. Bottom Panel: Predicted population- and year-specific survival rates of adult spring-summer Chinook salmon during their upstream migration from the mouth of the Columbia River (near Astoria) to Bonneville Dam passage. The boxplots represent medians, interquartile ranges, and 5th and 95th percentiles of confidence intervals. These survival estimates are likely biased low by approximately 13% due to tagging and handling effects in the mark-recapture study, but show the degree that survival decreased in 2013–2015 relative to historical baseline period.

Discussion

The coincident increase in California sea lion presence and decrease in salmon survival suggests that predation by pinnipeds significantly influenced salmon survival, which presents a management dilemma because both groups of animals are protected by Federal statutes. The overall decrease in survival through the Lower Columbia River in late March through April of 2013–2015 strongly affected the survival rates of earlier-migrating spring-run Chinook salmon populations, whereas it had much less of an effect on later-migrating populations. Our analysis suggests that survival rates of early migrating fish decreased by 22%, which would significantly affect population viability if sustained. This decrement can be applied in life-cycle models to simulate the effects that recent conditions would have on the viability of individual populations if sustained.

The positive relationship between survival probabilities and water temperatures on the day that a fish was tagged may have been the result of multiple seasonal factors, as temperature had a Pearson correlation coefficient of 0.84 with Julian day of tagging. Chinook salmon exhibited faster swimming speeds and shorter travel times at the warmer temperatures experiences later in the season, which reduced their overall time of exposure through the study area and may have helped them avoid pinniped attacks (Salinger and Anderson 2006, Rub et al. in prep.). In addition, California sea lion behavior may have changed throughout the season, with the animals that preyed most heavily on salmon migrating to the breeding grounds in Southern California earliest (Wright et al. 2010). Predation by other pinniped species like Steller sea lions also likely contributed to mortality rates and may have varied throughout the season. Based on catch data, fishery removals comprised a negligible portion of total mortality for natural-origin fish, but likely explained the lower survival rates for adipose fin-clipped fish for which there is a selective fishery (Rub et al. in prep).

The interannual variation in arrival timing at Bonneville dam was correlated with winter and early-spring oceanic and riverine conditions prior to the peak migration of spring-summer Chinook. However, January PDO and February discharge were significantly correlated with river temperatures and discharge during the peak migration, making it difficult to infer the drivers of migration timing (Keefer et al. 2008, Anderson and Beer 2009).

Water temperature and discharge in the lower river appeared to drive interannual variability in travel times, which significantly affected our estimates of survival by influencing river-entry timing predictions. Due to the variability in travel time between years, passage timing at Bonneville Dam was not always a good predictor of arrival timing in the river mouth. It appears that cooler water may have slowed down migration in some years; however, cooler river temperatures upstream of the study reach are beneficial for subsequent en route survival (Crozier et al. 2016).

In the Columbia River, average survival of natural-origin Chinook salmon populations through the 236 km of river between Bonneville Dam and McNary Dam ranged between 77% and 97% from 2004 to 2015 (Crozier et al. 2016). Late-migrating populations exhibited lower survival over this period, presumably due in part to warmer water temperatures and potentially from post-release mortality in the fishery that occurs after 15 June. This suggests that there were survival advantages to late migration from the river mouth to Bonneville Dam, whereas there were advantages to early migration from Bonneville Dam to McNary Dam

To project more accurately the potential future impact of mortality incurred between the river mouth and Bonneville Dam on population viability, we need a better understanding of the underlying mortality mechanisms including predation by pinnipeds. Additionally, there is a need to evaluate the effects of conditions in the lower river on subsequent survival through the remainder of their migration and on reproductive success (Naughton et al. 2011). Potential causes of increased mortality include compounding effects of pinniped predation, disease, thermal stress, inadequate energy reserves, fisheries, and other factors (Cooke et al. 2006, Farrell et al. 2008, Miller et al. 2011, Keefer et al. 2012). The coincident increase in California sea lion presence and decrease in estuarine survival implicates them in the observed mortality, and warrants further investigation and potentially management action. The presence of pinnipeds in the Columbia River Estuary in the future will likely have a significant effect on the viability of salmon populations, so managers should consider the drivers of their seasonal abundance (Schakner et al. 2016).

Life-cycle models that incorporate demographic rates at multiple life stages will be valuable for evaluating the effect of en route mortality on population dynamics (Kareiva et al. 2000, Zabel et al. 2006). Life-cycle models can estimate the impacts of the recent declines in survival during 2013-2015 on population viability by applying our estimates to marine life stages, which already incorporate historical baseline levels of estuarine survival. Detailed viability analyses will be especially important when evaluating management actions because one Federally protected species poses a threat to another Federally protected species (Redpath et al. 2013).

Migrations in general, and especially reproductive migrations, represent inherently stressful events in animals’ life histories. Migratory populations often travel long distances during which they are vulnerable to predators, disease, starvation, and adverse weather (Cooke et al. 2006); anthropogenic habitat modifications and climate change are likely to alter conditions experienced along migration corridors (Marra et al. 2005, Crozier et al. 2008, Mysterud 2013). We must consider these factors in order to conserve highly migratory populations, especially when they are already depressed due to insults to their primary habitats. Mortality during migrations appears to have significant effects on the viability of certain populations, and we must monitor and potentially mitigate for it to prevent extinctions. In this instance, early migrating populations are at the highest risk from mortality mechanisms during their upstream migration through the estuary as adults.

References

Anderson, J. J., and W. N. Beer. 2009. Oceanic, riverine, and genetic influences on spring chinook salmon migration timing. Ecological Applications **19**:1989-2003.

Ashbrook, C., J. Dixon, D. Griffith, K. Hassel, C. Peery*, and E. Schwartz. 2009. Evaluate Live Capture Selective Harvest Methods: 2003.*in* D. o. F. a. Wildlife and B. P. Administration, editors.

Barton, K. 2016. Multi-Model Inference.

Brown, R. F., and B. E. Wright. in prep. California sea lion counts at the East Morning Basin, Astoria, 1998-2015.

Burnham, K. P., and D. R. Anderson. 2002. Model selection and multimodel inference: a practical information-theoretic approach. Springer Science & Business Media.

Clarke, W. 1995. Osmoregulation. Physiological ecology of Pacific salmon:317-377.

Climate Analysis Section, National Center for Atmospheric Research, K. E. Trenberth, and J. W. Hurrell. 1994. NP Index Data Boulder, USA.

Columbia River DART. 1993. Columbia Basin Research, School of Aquatic and Fishery Sciences, University of Washington, Seattle.

Cooke, S. J., S. G. Hinch, G. T. Crossin, D. A. Patterson, K. K. English, M. C. Healey, J. M. Shrimpton, G. Van Der Kraak, and A. P. Farrell. 2006. Mechanistic basis of individual mortality in Pacific salmon during spawning migrations. Ecology **87**:1575-1586.

Crozier, L. G., E. Dorfmeier, T. Marsh, B. P. Sandford, and D. Widener. 2016. Upstream passage and survival of adult spring and spring/summer Chinook in the Columbia River Basin. National Marine Fisheries Service.

Crozier, L. G., A. Hendry, P. W. Lawson, T. Quinn, N. Mantua, J. Battin, R. Shaw, and R. Huey. 2008. Potential responses to climate change in organisms with complex life histories: evolution and plasticity in Pacific salmon. Evolutionary Applications **1**:252-270.

Farrell, A., S. Hinch, S. Cooke, D. Patterson, G. Crossin, M. Lapointe, and M. Mathes. 2008. Pacific salmon in hot water: applying aerobic scope models and biotelemetry to predict the success of spawning migrations. Physiological and Biochemical Zoology **81**:697-709.

Healey, M., C. Groot, and L. Margolis. 1991. Life history of chinook salmon (Oncorhynchus tshawytscha). Pacific salmon life histories:311-394.

Kareiva, P., M. Marvier, and M. McClure. 2000. Recovery and management options for spring/summer chinook salmon in the Columbia River Basin. science **290**:977-979.

Keefer, M. L., C. A. Peery, and C. C. Caudill. 2008. Migration timing of Columbia River spring Chinook salmon: effects of temperature, river discharge, and ocean environment. Transactions of the American Fisheries Society **137**:1120-1133.

Keefer, M. L., C. A. Peery, M. A. Jepson, K. R. Tolotti, T. C. Bjornn, and L. C. Stuehrenberg. 2004. Stock-Specific Migration Timing of Adult Spring–Summer Chinook Salmon in the Columbia River Basin. North American Journal of Fisheries Management **24**:1145-1162.

Keefer, M. L., R. J. Stansell, S. C. Tackley, W. T. Nagy, K. M. Gibbons, C. A. Peery, and C. C. Caudill. 2012. Use of Radiotelemetry and Direct Observations to Evaluate Sea Lion Predation on Adult Pacific Salmonids at Bonneville Dam. Transactions of the American Fisheries Society **141**:1236-1251.

Lele, S. R., J. L. Keim, and P. Solymos. 2016. ResourceSelection: Resource Selection (Probability) Functions for Use-Availability Data.

Mantua, N., and S. Hare. PDO Index Monthly Values: January 1900-present. Obtained with permission from the University of Washington's Joint Institute for the Study of the Atmosphere and Oceans (http://research.jisao.washington.edu/).

Marra, P. P., C. M. Francis, R. S. Mulvihill, and F. R. Moore. 2005. The influence of climate on the timing and rate of spring bird migration. Oecologia **142**:307-315.

Matthews, G. M., and R. S. Waples. 1991. Status review for Snake River spring and summer Chinook salmon. National Marine Fisheries Service, Northwest Fisheries Center, Coastal Zone and Estuarine Studies Division.

Miller, K. M., S. Li, K. H. Kaukinen, N. Ginther, E. Hammill, J. M. Curtis, D. A. Patterson, T. Sierocinski, L. Donnison, and P. Pavlidis. 2011. Genomic signatures predict migration and spawning failure in wild Canadian salmon. science **331**:214-217.

Mysterud, A. 2013. Ungulate migration, plant phenology, and large carnivores: The times they are a-changin'. Ecology **94**:1257-1261.

National Research Council. 1996. Upstream: salmon and society in the Pacific Northwest. Washington, DC: National Academy Press.

National Weather Service Forecast Office. Daily Temperatures: Portland (1940-2015, text file). Portland, Oregon.

Naughton, G. P., M. L. Keefer, T. S. Clabough, M. A. Jepson, S. R. Lee, C. A. Peery, C. C. Caudill, and M. Bradford. 2011. Influence of pinniped-caused injuries on the survival of adult Chinook salmon (Oncorhynchus tshawytscha) and steelhead trout (Oncorhynchus mykiss) in the Columbia River basin. Canadian Journal of Fisheries and Aquatic Sciences **68**:1615-1624.

Pinheiro, J., D. Bates, S. DebRoy, D. Sarkar, and R. C. Team. 2015. nlme: Linear and Nonlinear Mixed Effects Models_. R package version 3.1-121. <URL: http://CRAN.R-project.org/package=nlme>.

PTAGIS. 2016. "Columbia Basin PIT Tag Information System." Retrieved Nov 1, 2015.

Quinn, T. P., J. A. Peterson, V. F. Gallucci, W. K. Hershberger, and E. L. Brannon. 2002. Artificial selection and environmental change: countervailing factors affecting the timing of spawning by coho and chinook salmon. Transactions of the American Fisheries Society **131**:591-598.

R Core Team. 2017. R: A language and environment for statistical computing. R Foundation for Statistical Computing, R Foundation for Statistical Computing, Vienna, Austria.

Redpath, S. M., J. Young, A. Evely, W. M. Adams, W. J. Sutherland, A. Whitehouse, A. Amar, R. A. Lambert, J. D. Linnell, and A. Watt. 2013. Understanding and managing conservation conflicts. Trends in Ecology & Evolution **28**:100-109.

Rub, A. M. W., D. Huff, B. P. Sandford, M. H. Sorel, and R. W. Zabel. in prep. Interannual variation in survival of endangered salmon through the Columbia River Estuary.

Salinger, D. H., and J. J. Anderson. 2006. Effects of water temperature and flow on adult salmon migration swim speed and delay. Transactions of the American Fisheries Society **135**:188-199.

Schakner, Z. A., M. G. Buhnerkempe, M. J. Tennis, R. J. Stansell, B. K. van der Leeuw, J. O. Lloyd-Smith, and D. T. Blumstein. 2016. Epidemiological models to control the spread of information in marine mammals. Page 20162037 *in* Proc. R. Soc. B. The Royal Society.

Teel, D. J., C. Baker, D. R. Kuligowski, T. A. Friesen, and B. Shields. 2009. Genetic stock composition of subyearling Chinook salmon in seasonal floodplain wetlands of the lower Willamette River, Oregon. Transactions of the American Fisheries Society **138**:211-217.

Waples, R. S., D. J. Teel, J. M. Myers, and A. R. Marshall. 2004. Life-history Divergence in Chinook salmon: historic contingency and parallel evolution. Evolution **58**:386-403.

Wright, B. E., S. D. Riemer, R. F. Brown, A. M. Ougzin, and K. A. Bucklin. 2007. Assessment of harbor seal predation on adult salmonids in a Pacific Northwest estuary. Ecological Applications **17**:338-351.

Wright, B. E., M. J. Tennis, and R. F. Brown. 2010. Movements of Male California Sea Lions Captured in the Columbia River. Northwest Science **84**:60-72.

Zabel, R. W., M. D. Scheuerell, M. M. McClure, and J. G. Williams. 2006. The interplay between climate variability and density dependence in the population viability of Chinook salmon. Conservation Biology **20**:190-200.

Supplementary Tables

Supplementary Table 1. Annual sample sizes of adipose-fin clipped and unclipped (presumed natural origin) Chinook salmon tagged in the Columbia River Estuary in 2010–2015.

	Natural origin	Clipped	Total
2010	17	154	171
2011	94	278	374
2012	96	273	372
2013	21	48	72
2014	77	211	288
2015	39	132	171
Total	343	1,096	1,439

Supplementary Table 2. Coefficients for model of adult Chinook salmon survival on the logit scale, from the Columbia River mouth near Astoria to Bonneville Dam fish ladders. *CSL* = the 7-day running-mean count of California sea lions hauled out in Astoria on the date of tagging; *Temp* = water temperature measured at Warrenton, OR, on the date of tagging; and *clip* = presence of adipose-fin clip.

	Estimate	Std. Error	z-value	Pr(>|z|)
Intercept	1.41574	0.45136	3.137	0.00171
ln(CSL)	-0.55258	0.05696	-9.702	<2.00E-16
Temp	0.26858	0.03788	7.091	1.34E-12
Clip	-0.37617	0.14096	-2.669	0.00762

Supplementary Table 3. Sample sizes of adult Chinook salmon that were PIT tagged as juvenile in their natal basin and subsequently detected as adults at Bonneville Dam, by population and year of detection.

	2001	2002	2003	2004	2005	2006	2007	2008	2009	2010	2011	2012	2013	2014	2015	2016	Total
Big Creek	2	1	3	3	2	0	0	1	21	76	76	35	29	23	26	17	315
Catherine Creek	1	3	7	4	2	3	2	6	6	9	23	13	13	8	5	6	112
East Fork South Fork Salmon	25	29	40	31	6	8	11	39	15	37	39	35	27	30	13	8	393
Entiat River	0	0	0	0	2	4	6	8	9	77	78	53	31	42	52	47	409
Imnaha River	48	110	103	50	30	38	25	25	79	173	198	93	39	78	62	50	1208
Lemhi River	8	9	11	6	2	3	4	6	27	35	40	15	35	53	67	28	349
Lostine River	7	14	15	10	4	5	5	9	14	17	35	15	11	19	22	13	216
Marsh Creek	1	12	14	9	3	0	1	1	17	69	55	27	29	33	26	16	314
Methow River	0	0	0	0	0	0	1	3	8	30	23	6	7	17	20	19	134
Minam River	1	2	6	5	2	2	2	4	9	28	14	9	3	20	11	7	125
Pahsimeroi River	6	6	3	1	0	4	3	5	7	14	11	6	17	19	20	4	126
Secesh River	9	22	33	13	3	2	4	15	69	128	68	36	42	34	25	11	515
Tucannon River	2	0	0	1	2	0	0	1	10	31	29	7	15	18	32	10	158
Upper Grande Ronde	1	3	5	0	4	5	2	7	4	16	7	6	12	9	8	3	93
Upper Salmon River	3	5	9	13	8	10	9	21	14	26	27	25	23	22	28	14	257
Upper South Fork Salmon	16	25	56	4	2	4	3	7	21	22	43	56	26	22	11	6	324
Wenatchee River	0	0	0	0	5	3	1	23	35	100	133	78	36	44	63	49	570
Total	130	241	305	150	77	91	79	181	365	888	899	515	395	491	491	308	

Supplementary Table 4. List of release sites for PIT-tagged fish included in each population. Only release sites located within the natal habitat of a single population were included in the data set.

ESU	MPG	Run	Population	Release Site	Latitude	Longitude
Snake	Grande Ronde / Imnaha	Spring	Catherine Creek	Catherine Creek	45.20966612	-117.8878496
			Upper Grande Ronde	Grande Ronde River - Wallowa River to headwaters (km 131–325)	45.3256363	-117.9205262
			Lostine River	Lostine River	45.37281443	-117.4235889
			Minam River	Minam River	45.33887738	-117.6001786
		Summer	Imnaha River	Imnaha River	45.39694069	-116.7918754
				Imnaha River Weir	45.19427639	-116.8686635
				Imnaha Trap	45.7637	-116.7:2148
	Lower Snake	Spring	Tucannon River	Tucannon River	46.39571678	-117.7112008
	Middle Fork Salmon	Spring	Big Creek	Big Creek, Middle Fork Salmon River	45.15775882	-115.12014
			Marsh Creek	Capehorn Creek	44.35682643	-115.2196822
				Lower Marsh Creek Trap at RKm 8	44.4084466	-115.1816474
				Marsh Creek	44.39025653	-115.1632599
				Marsh Creek Trap	44.39383164	-115.1673549
	South Fork Salmon	Summer	East Fork South Fork Salmon	Johnson Creek	44.73392789	-115.5486019
				Johnson Creek Trap	44.91761448	-115.4833437
			Secesh River	Lake Creek	45.32905869	-115.9492036
				Secesh River	45.15195322	-115.796847
				Secesh River Screw Trap	45.05943169	-115.7566901
				Summit Creek, Secesh River Basin	45.20762581	-115.9454983
			Upper South Fork Salmon River	Knox Bridge, South Fork Salmon River	44.65551546	-115.7023954
				Lower South Fork Salmon River Trap at RKm 61	45.01468201	-115.715024
				SF Salmon River Trap (Archaic, replaced with SALRSF or KNOXB)	44.65551546	-115.7023954
	Upper Salmon	Spring	Lemhi River	Big Springs Creek, Lemhi River Basin	44.70845448	-113.4056972
				Hayden Creek, Lemhi River Basin	44.75276564	-113.7129834
				Lemhi River	44.9105456	-113.6250366
				Lemhi River Weir	44.86596003	-113.624721
		Summer	Pahsimeroi River	Pahsimeroi River Trap	44.684528	-114.040438
Upper Columbia	Entiat	Spring	Entiat River	Entiat River	47.91097008	-120.4903306
				Mad River (Entiat River watershed)	47.82092948	-120.5161779
	Methow	Spring	Methow River	Chewuch River	48.75050678	-120.1371161
				Methow River	48.35359525	-120.1092355
				Methow Smolt Trap at McFarland Creek Road Bridge	48.15108488	-120.0565842
				Twisp River	48.35388354	-120.3650912
	Wenatchee	Spring	Wenatchee River	Chiwawa River	47.9506332	-120.7768394
				Chiwawa River Trap, 0.5 km below CHIP acclimation pond	47.78812112	-120.6511455

	Lower Wenatchee trap, 2.8 km below Mission Creek	47.51193198	-120.4482675
	Nason Creek (tributary to Wenatchee River)	47.7819426	-120.8776371
	Peshastin River	47.45684205	-120.6588198
	Upper Wenatchee smolt trap just below Lake Wenatchee	47.80976111	-120.7156389
	Upper Wenatchee trap, 4 km above Chiwawa River	47.79787109	-120.6661512
	Wenatchee River	47.58484333	-120.6773509
	Wenatchee River trap at West Monitor Bridge	47.5007	-120.4257
	White River, Wenatchee River Basin	47.92390792	-120.9041708

Supplementary Table 5. AIC values for models of log-transformed detection date at Bonneville Dam for PIT-tagged adult spring-summer Chinook salmon from the Upper Columbia River and Snake River ESUs. In all models, we assumed that variances were constant across years within populations. Pop = population (based on tagging location of juveniles); Yr = year; MPG = major population group; Run = spring or summer run; and ESU = endangered species unit.

Model	# Parameters	AIC	Δ AIC
Pop + Yr	33	-8,495	0
Pop + Yr + Yr x Run	49	-8,319	176
Pop + Yr + Yr x ESU	44	-8,282	213
Pop + Yr + Yr x MPG	121	-8,277	218
Pop + Yr + Yr x Pop	255	-8,168	327

Supplementary Table 6. Coefficients for environmental variables used to predict annual shifts in model of adult Chinook salmon passage timing at Bonneville Dam. Variables were monthly averages of the Pacific Decadal Oscillation in January, Discharge at Bonneville Dam in February, and the North Pacific Index in March.

	Estimate	Std. Error	z-value	Pr(>|z|)
Jan PDO	-0.01345	0.00128	-10.49	0
Feb Discharge	0.00033	4.1E-05	8.104	0
Mar NPI	0.00134	0.00062	2.174	0.0298

Supplementary Table 7. Coefficient estimates for a model of log-transformed travel times between Astoria and Bonneville Dam. *Outflow 20* is the average outflow at Bonneville Dam over 20 days following tag date; and *Temp 25* is average temperature at Bonneville Dam over 25 days following tagging.

	Estimate	Std. Error	t value	Pr(>|t|)
Intercept	4.432514	0.07776	57	<2e-16
Outflow 20	0.001435	0.000133	10.78	<2e-16
Temp 25	-0.17501	0.006039	-28.98	<2e-16

Supplementary Figures

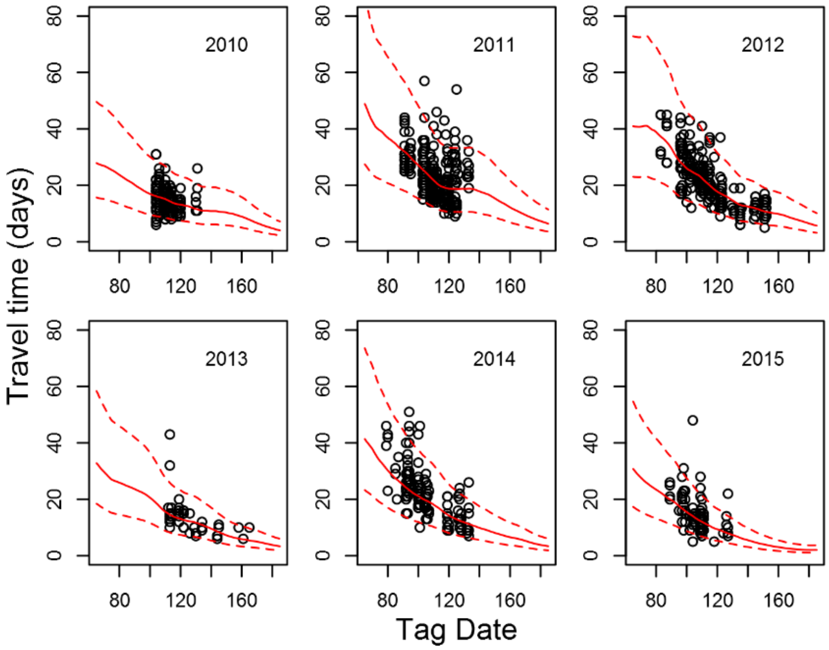

Supplementary Figure 1. Observed travel times of PIT-tagged fish between Astoria and Bonneville Dam (points) and modeled average travel times and 95% prediction intervals (red lines). We modeled travel times as a function of water temperature and outflow at Bonneville Dam.

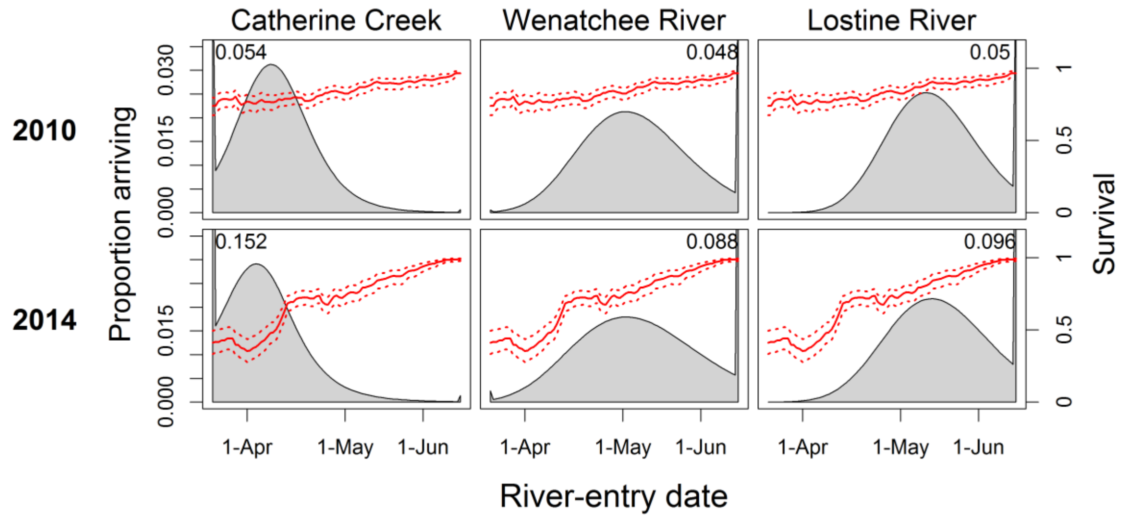

Supplementary Figure 2. Modeled year-specific river-entry timing distributions of three spring Chinook salmon populations (shaded gray areas, left y-axis). The numbers in the upper corners of the panels represent the proportions of the populations assumed to arrive on and before the first date of the interval or on and after the last date, when they are above the range of the y-axis. Solid red lines represent model-predicted survival for cohorts of fish entering the river on each date, based on the mark-recapture study conducted by Rub et al. (in prep), and dashed-red lines represent 95% confidence intervals around these estimates. We weighted cohort-specific survival rates by the proportions of each population in each cohort in order to estimate population-specific annual survival rates.

Chapter 6B: Avian predation management effects

Charlie Paulsen, Paulsen Environmental Research

Introduction

In the Columbia basin, avian predation on outmigrating salmonid smolts has been extensively investigated since the 1990’s, when terns and cormorants began nesting in large numbers on Rice Island and elsewhere in the Columbia estuary (e.g., Evans et al 2012). More recently, USACE and BPA have funded efforts to control the size of nesting colonies and move them toward the lower end of the estuary in an effort to reduce consumption of Chinook and steelhead smolts (Evans et al 2016). In this chapter, we highlight recent estimates of the effects of reducing nesting habitat on East Sand Island, a major breeding ground for both terns and cormorants, and review past efforts at assessing the compensatory effects of the predator control efforts.

Figure 6B.1 shows the study area, with East Sand Island at the extreme left. Figure 6B.2 shows the East Sand Island (ESI) nesting areas and how management actions have constricted them over time. Table 6B.1 displays the estimated effects of ESI nesting restrictions. The predation rates are based on a Bayesian estimate that combines PIT tag detections on the island, detection rates for the tags, and deposition rates (Evans et al 2016).

Figure 6B.1. Study Area

Figure 6B.2. ESI Action area

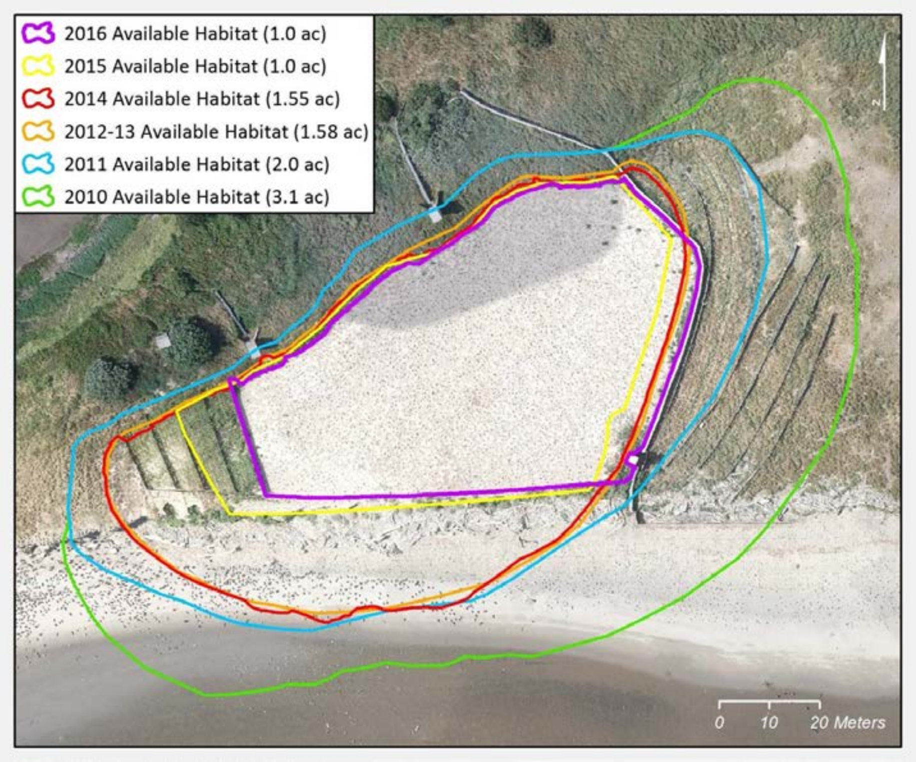

Table 6B.1 Average annual predation rates (95% credible intervals) by Caspian terns nesting on East Sand Island prior to and following periods of management. Salmonid populations (ESU/DPS) with runs of spring (Sp), summer (Su), and fall (Fall) fish were evaluated, where applicable. Asterisks denote differences that were statistically significant. From Evans et al. 2016.

ESU/DPS	Pre-management (2000-2010)	Post-Management (2011-2015)
Snake River Sockeye (1)	1.5% (0.9-2.2)	1.6% (1.2-2.2)
Snake River Yearling Chinook	4.8% (4.3-5.4)	1.7% (1.4-2.1)*
Upper Columbia River Spring Chinook	3.9% (3.4-4.6)	1.4% (1.1-1.9)*
Snake River Fall Chinook	2.5% (2.2-3.0)	0.9% (0.7-1.2)*
Upper Columbia River Spring Chinook (2)	2.5% (1.9-3.3)	0.9% (0.6-1.3)*
Snake River Steelhead	22.2% (20.3-24.8)	10.7% (9.2-12.8)*
Upper Columbia River Steelhead	17.2% (15.7-19.3)	9.9% (8.5-12.0)*
Middle Columbia River Steelhead (3)	14.9% (13.1-17.6)	9.3% (7.7-11.4)*

[1] *Predation rate estimates were not available in 2000-2008*

[2] *Predation rate estimates were not available in 2000-2006*

[3] *Predation rate estimates were not available in 2000, 2002-2006*

Compensatory effects

As noted by the ISAB in their review of predator management efforts (ISAB 2016) predators may not select their prey randomly from the target population: smaller, less healthy smolts may be preferred by avian predators because they are easier to detect or catch. For example, Hostetter et al (2012) note that “recoveries of PIT tags on a downstream colony of Caspian terns … indicated that steelhead susceptibility to Caspian tern predation increased significantly with decreases in steelhead external condition." On the other hand, they also state that "[s]usceptibility to Caspian tern predation also increased with increasing steelhead fork length up to 202 mm but then decreased for longer steelhead." So, on the one hand, predation was higher for fish in worse condition, but terns actively selected for larger fish up to a size limit, and it seems reasonable to assume that larger smolts would be more likely to survive and return as adult spawners.

There are methods available to test whether or not compensatory mortality is occurring in a population. Haeseker (2015) employed one from Burnham and Anderson (1984), and was unable to detect any effect of the predator management program. He concluded that the effects must therefore be compensatory. However, as Burnham and Anderson note in their paper, the method requires that other sources of mortality are roughly constant over time. While this requirement was met for their data on duck and goose mortality, it is clear from figures 6B.3 and 6B.4 that Snake River steelhead survival rates vary by a factor of about 20 for wild steelhead, from a low of about 0.1% in 2004 to a high of over 1.6% in 1999. Similarly high variability is apparent for hatchery steelhead as well. Clearly, Burnham and Anderson's constant-mortality assumption is not met. Furthermore, the high interannual variability likely precludes any possibility of detecting the relatively modest changes in mortality rates (about 11% post-action vs. 22% pre-action for the Snake ESU, Table 1), even assuming no compensatory effects whatsoever.

Figure 6B.3. Wild Snake Steelhead SARs, inriver-migrating transport study fish tagged at Lower Granite Dam.

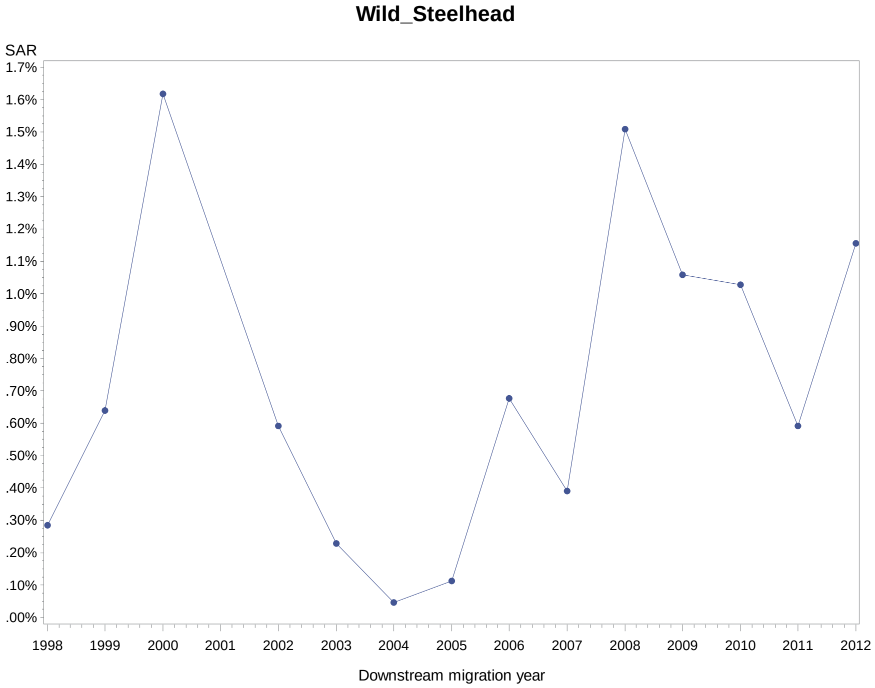

Figure 6B.4. Hatchery Snake steelhead SARs, inriver-migrating transport study fish tagged at Lower Granite Dam.

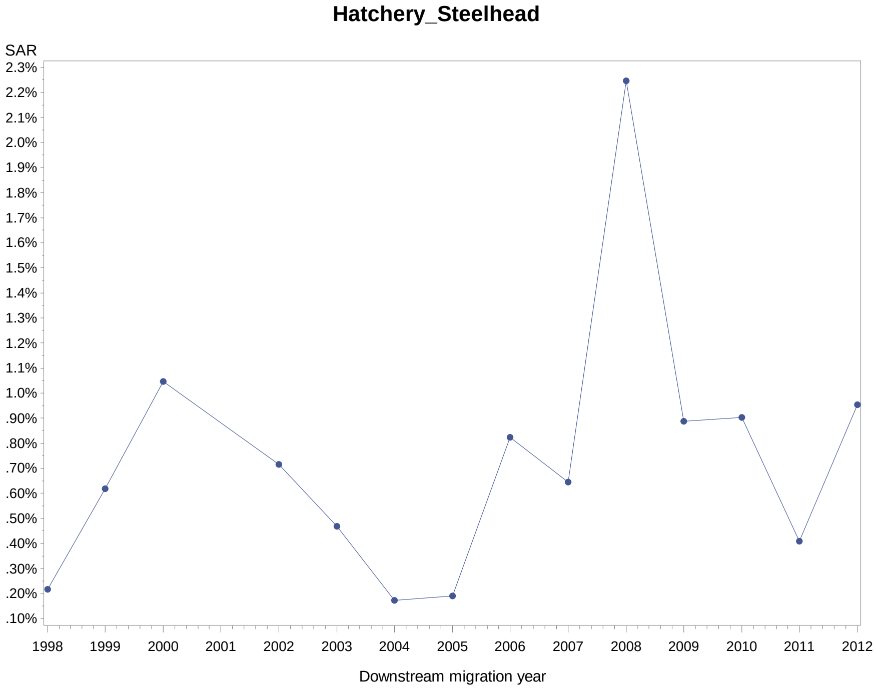

Discussion

It is clear that detecting short-term, localized effects of predator management actions (e.g., Table 6B.1) is more straightforward than detecting effects on returning adults. The very high variations in smolt-to-adult survival rates will make detection of longer-term effects difficult at best, and they may simply be impossible, even in a system as heavily monitored as the Columbia. This is so even in the absence of compensatory effects, where a 10% increase in estuary survival translates directly to a 10% increase in adult returns.

We also suspect that upriver populations might well show a greater response to predator management, since bird predation occurs throughout the migration corridor. but analyses like those we have incorporated for East Sand Island are still in progress (Allen Evans, pers. comm.).

References

Burnham, K.P., Anderson D.R. 1984. Tests of compensatory vs. additive hypotheses of mortality in mallards. Ecology 65:105-112

Evans, A.F., N.J. Hostetter, K. Collis, D.D. Roby, D.E. Lyons, B.P. Sandford, R.D. Ledgerwood, and S. Sebring. 2012. A system-wide evaluation of avian predation on juvenile salmonid in the Columbia River Basin based on recoveries of passive integrated transponder tags. Transactions of the American Fisheries Society 141: 975-989.

Evans, A.F, Q. Payton, B.M. Cramer, K. Collis, D.E. Lyons, and P. J. Loschl. 2016. Predation Impacts on Juvenile Salmonids by Double-crested Cormorants and Caspian Terns Nesting on East Sand Island in the Columbia River Estuary. Final technical report submitted to the U.S. Army Corps of Engineers in partial fulfillment of Contract No. W912EF-14-D-0004, Task Order No. 0004.

Haeseker, S. 2015. Tests of whether double-crested cormorants are an additive versus compensatory source of mortality for Snake River steelhead (USFWS draft memo).

Hostetter, N.J., A.F. Evans, D.D. Roby, and K. Collis. 2012. Susceptibility of juvenile steelhead to avian predation: the influence of individual fish characteristics and river conditions. Transactions of the American Fisheries Society 141: 1586-1599

ISAB 2016. ISAB Predation Metrics Report: Developing and Assessing Standardized Metrics to Measure the Effects of Predation on Columbia River Basin Salmon and Steelhead.

CHAPTER 6: ECOLOGICAL INTERACTIONS

6.c Incorporating food web dynamics into life cycle modeling

Joseph R. Benjamin (U.S. Geological Survey, Forest and Rangeland Ecosystem Science Center), J. Ryan Bellmore (U.S. Forest Service, Pacific Northwest Research Station), Emily Whitney (University of Alaska Southeast), and Jason Dunham (U.S. Geological Survey, Forest and Rangeland Ecosystem Science Center)

Understanding the mechanisms that fuel freshwater fish production will require expanding models beyond direct relationships between physical habitat and fish, to include the complex biotic interactions that can mediate fish response to physical habitat (Wipfli and Baxter 2011). There are now numerous examples where changes in nutrient availability and/or food webs (without any significant changes in physical habitat) have led to either serious environmental issues (e.g., Ellis et al. 2011), or improved freshwater conditions (see Carpenter et al. 1995). More recently, there has also been a challenge by the Columbia River Independent Scientific Advisory Board to incorporate food web dynamics into freshwater models of fish production (NPCC 2011, Naiman et al. 2012). Understanding how freshwater systems might respond to management strategies and environmental change will require holistic approaches that link the physical and biotic compartments of ecosystems in a manner that allows researchers to simulate how different scenarios impact the flows of energy that fuel anadromous salmonid production.

We have created a general food web model (Benjamin and Bellmore 2016; Bellmore et al. 2017) that is currently being applied to the Methow River, a major tributary to the upper Columbia River and the focus of a host of restoration efforts intended to improve habitat for Pacific salmon, steelhead, and other species. This model was created to provide an understanding of the biotic and abiotic mechanisms that underpin the freshwater productivity of anadromous fishes and evaluate potential impacts of management actions and environmental changes on freshwater productivity. In previous analyses, we showed this model can reproduce the general trophic dynamics observed in the Methow River. Although the initial versions of this model did not have an explicit linkage to the life-cycles of anadromous fishes, it provides the basis for exploring how the structure and dynamics of river food webs influences salmon and steelhead populations. Here, we describe a linkage of the food web model with a basic life cycle model for spring Chinook salmon (*Oncorhynchus tshawytscha*).

Model description

Study area

Modeling efforts have been focused in the Methow River, a fifth order tributary of the Columbia River in north-central Washington. We used this watershed because: 1) the Bureau of Reclamation is pursuing a suite of restoration actions; 2) environmental data needed to parameterize the model are available (see Benjamin and Bellmore 2016; Bellmore et al. 2017); and 3) empirical food web data existed to compare with model simulations (Bellmore et al. 2013; Zuckerman 2015). For the purposes of the model effort described below, we used input parameters for an average 1 km reach where spring Chinook salmon spawn and rear.

The Aquatic Trophic Productivity model

The Aquatic Trophic Productivity (ATP) model has been described in detail elsewhere, including a comprehensive list of parameter values, sensitivity analyses, coding, and comparisons to empirical data (Benjamin and Bellmore 2016; Bellmore et al. 2017). Below we provide a general description.

The ATP model is a dynamic food-web simulation model, whereby the capacity of stream and river ecosystems to sustain fish is explicitly tied to transfers of organic matter between different components of a simplified river food web (Figure 1). This model mechanistically links the dynamics of the food-web and the resultant performance of different web members to (1) the physical and hydraulic conditions of the stream, (2) the structure and composition of the adjacent riparian zone, and (3) marine nutrient subsidies delivered by adult salmon. The modeling framework assumes that the general dynamics of river food webs can be predicted if the dynamics of these three environmental factors are known. Following this assumption, the model can be used to explore how environmental changes wrought by restoration might affect the overall dynamics of the food web and the performance of specific web members.

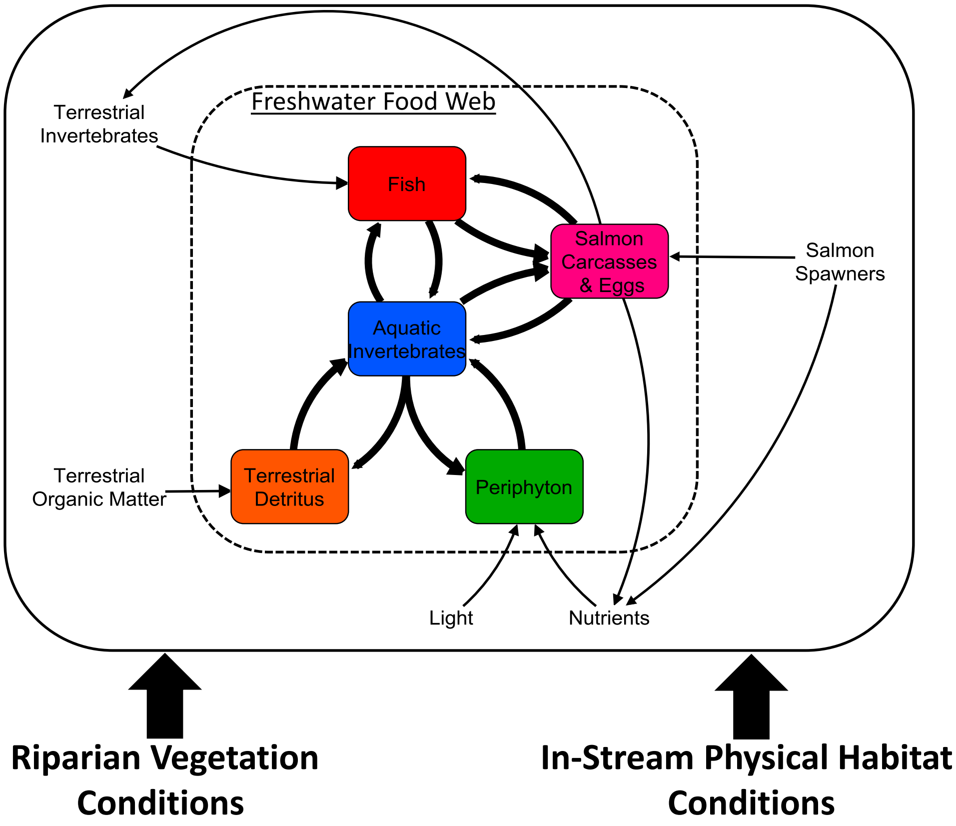

Figure 1. Conceptual diagram showing Aquatic Trophic Productivity model, illustrating biomass stocks of organisms and organic matter (rectangular boxes), consumer-resource interactions (thick arrows), inputs of energy, nutrients and organic matter from outside the system (thin arrows), and explicit linkages to in-stream physical habitat and adjacent riparian vegetation.

The food web component of the model contains four biomass stocks or state variables: (1) periphyton, (2) terrestrially derived organic matter, (3) aquatic invertebrates, and (4) fish (Figure 1). The fish stock includes a target fish stock to represent juvenile spring Chinook salmon and steelhead, and a non-target fish stock, which represents the rest of the fish in the community that may compete with the target fish (e.g., coho salmon, whitefish, sculpin) or prey upon target fish (e.g, bull trout). In the model, periphyton and terrestrial detritus are consumed by aquatic invertebrates, and aquatic invertebrates are consumed by fish (both target and non-target stocks). The dynamics of each biomass are governed by a series of mass balance equations (Table 1). Biomass increases if the processes that contribute to biomass gains (such as, consumption and energy assimilation, upstream/lateral inputs, production) outweigh the processes that contribute to biomass losses (such as, predation, downstream export, respiration). Energy and materials enter the modeled reach from external locations that include: (1) light, which provide the energy for photosynthesis; (2) nutrients and organic material from upstream reaches, which provide resources necessary for periphyton production; (3) lateral inputs from the riparian zone, which provide detrital organic matter (leaf litter) and direct food resources (terrestrial invertebrates) for fish; and (4), returning adult salmon, which represent a source of marine carbon and nutrients that are incorporated into the food web via nutrient uptake by periphyton and direct consumption of carcass material by fish and invertebrates.

The physical, chemical, and environmental conditions of the reach drive the dynamics represented in the food web. For example temperature strongly affects bioenergetics (e.g., consumption, respiration, and decay) and ultimately the accumulation of biomass of each trophic stock. Channel discharge, size, and substrate composition affect the scour and downstream export of periphyton and invertebrates via friction velocity and shear stress. Lateral inputs are influenced by stream width, which influences the amount of vegetation covering the stream, and seasonal dynamics such as air temperature.

Table 1. Biomass mass-balance equations for the state variables in the Aquatic Trophic Productivity model, where: α_{XY} is the proportion of prey type X consumed by predator Y that is assimilated. Subscript definitions: C = salmon carcass, D = detritus, E = salmon eggs, F = fish, H = nontarget fish, I = aquatic invertebrates, P = periphyton, and T = terrestrial invertebrates.

State Variable	Mass Balance Equation
Target Fish, F	$\frac{dF}{dt} = Consumption_{IF}\alpha_{IF} + Consumption_{TF}\alpha_{TF} + Consumption_{CF}\alpha_{CF} + Consumption_{EF}\alpha_{EF} - Respiration_{F} - Mortality_{F}$
Invertebrates, I	$\frac{dI}{dt} = Consumption_{PI}\alpha_{PI} + Consumption_{DI}\alpha_{DI} + Consumption_{CI}\alpha_{CI} + Upstream_{I} - Consumption_{IF} - Respiration_{I} - Mortality_{I} - Export_{I}$
Periphyton, P	$\frac{dP}{dt} = Production_{P} + Upstream_{P} - Consumption_{PI} - Decay_{I} - Export_{I}$
Terrestrial detritus, D	$\frac{dD}{dt} = Lateral_{D} + Upstream_{D} - Consumption_{DI} - Decay_{D} - Export_{D}$
Salmon carcass, C	$\frac{dS}{dt} = Marine_{C} + Upstream_{C} - Consumption_{CF} - Consumption_{CI} - Decay_{C} - Export_{C}$
Nontarget Fish, H	$\frac{dH}{dt} = Consumption_{IH}\alpha_{IH} + Consumption_{TH}\alpha_{TH} + Consumption_{CH}\alpha_{CH} + Consumption_{EH}\alpha_{EH} + Consumption_{LH}\alpha_{LH} - Respiration_{F} - Mortality_{F}$

Life cycle model

With the ATP model simulating realistic responses in biomass of trophic levels (Bellmore et al. 2017), the next step is to link it to the freshwater portion of the salmon life-cycle, and using the model to simulate how changes in freshwater conditions (and associated food webs) might influence the long-term population dynamics of anadromous salmon. To do this, we linked the ATP model to a simple life cycle model for spring Chinook salmon. The life cycle for one cohort takes four years, and considers six main life history stages: eggs, juveniles, smolts, first year ocean residency, second year ocean residency coupled with adults in migration, and adults at spawning grounds (Table 2). The focus of the linked food web and life cycle model is on the freshwater stages, and in particular the juvenile stage.

Table 2. Chinook salmon life cycle stage, duration in each stage, mortality and its source. δ is the difference between juvenile length at time *t* and reference length (100 mm). K = condition factor at time t. L = length (mm) at time t.

Stage	Duration (days)	Mortality	Source
Egg	226	0.4	Honea et al. 2009
Juvenile	365	$1-\frac{K_t^{7.5}}{K_t^{7.5}+0.45^{7.5}}$	Railsback et al. 2009,2014
		$0.01*e^{-0.04*(L_t-25)}$	Railsback et al. 2009
Early migrants	365[a]	$1-\frac{e^{-1.69+0.0329\delta}}{1+e^{-1.69+0.0329\delta}}$	Zabel and Achord 2004
Smolt	30	$1-\frac{e^{-1.69+0.0329\delta}}{1+e^{-1.69+0.0329\delta}}$	Zabel and Achord 2004
Year 1 ocean resident	365	$\frac{100-(-1.071+0.071*L_t)}{100}$	Duffy and Beauchamp 2011
Year 2 ocean resident	412[b]	0.2	Honea et al. 2009
Adult at spawning ground	62	0.1	Honea et al. 2009

[a] maximum duration of 365 if migration occurs on day of emergence; otherwise duration is dependent of migration time

[b] includes adults migrating upstream to natal habitat

The life cycle is initialized with adult salmon entering the spawning grounds on a user-specified date, and then holding in the stream a given number of days prior to spawning. For this modeling effort, identified adult salmon arriving on 01 July, holding for two months and eventually spawning on 01 September (Table 2).

The adult salmon not only seed the segment with offspring, but also deliver subsides of nutrients and organic matter (e.g., excretion, carcass material, eggs) and release benthic organism via bioturbations during redd construction. Details on how these processes are modeled have been previous documented (see Bellmore et al. 2014; Benjamin and Bellmore 2016). But briefly, the magnitude of nutrients and organic matter from marine inputs are proportional to the number of adult salmon that return to the system. Contributions of nitrogen and phosphorus from salmon are calculated using mass-specific excretion/leaching rates. During salmon spawning, salmon eggs become available for fish consumption via redd superimposition. In addition, scouring of the stream bed during redd construction detaches benthic organisms and organic matter. Once dead, salmon carcasses continue to leach nutrients and are available for invertebrate and fish consumption.

The juvenile stage starts on 15 April when fry emerge from the gravel, and occurs for 365 days. The juvenile stage of many salmon, including Chinook salmon, is split into multiple sub-stages including fry, parr, and presmolts based on physiological changes. However, we chose to leave it as one stage within the model because transitions would be based on arbitrary calendar dates.

During the juvenile stage, we simultaneously, grow the average size juvenile, account for daily abundance, estimate multiple sources of mortality, and allow individuals to migrate downstream early. We used a Wisconsin bioenergetics model, parameterized for Chinook salmon (Hanson et al. 1997; Plumb and Moffitt 2015) to grow an average size juvenile. We multiplied the number of juvenile fish by the average juvenile weight to estimate the biomass of the target fish (Chinook salmon) stock. The number of juvenile fish that could reside in the modeled reach was a function of food availability and space. We simultaneously simulated three sources of mortality: starvation; mortality related to fish size that is density independent; and predation. While growing, juveniles can experience loss in weight if bioenergetics temperature and body-size dependent costs of maintenance exceed energy intake via consumption. In extreme cases, this can lead to starvation mortality, which we account for based following Railsback et al. (2009, 2014; Table 2). We assumed that starvation mortality would indirectly mimic density dependence competition for food because more fish in the reach would translate to less food available per individual. The size of the juvenile can also influence the susceptibility to density independent causes of death (e.g., disease, environmental conditions) and predation. We assumed smaller fish were more likely to experience mortality from these sources, which we accounted for following Railsback et al. (2009). Similarly, smaller fish were more likely to be preyed upon by the non-target fish stock (Keeley and Grant 2001). For these equations that require length (mm), and those below, we estimated length (L) from weight (W) using: $L = (W*100{,}000)^{0.33}$.

Juvenile Chinook salmon can also exhibit different migratory tactics that can occur anytime from when they emerge from the gravel to the standard migratory time (Copeland and Venditti 2009). At a given time-step, we assumed the modeled stream reach can only support a certain number of juveniles owing to food availability or space, whichever is lower. We estimate the number of juveniles the system can support (N_s) by multiplying the juvenile abundance by the amount of organic matter assimilated by an average size juvenile and dividing by respiration. For spatial constraints, we divide the wetted area of the reach by the length-based territory size (Grant and Kramer 1990). The number of surplus juveniles (S) is: $S = N_j - N_s$, if $Nj > Ns$, else S

= 0, where *Nj* is the current abundance of juveniles in the modeled segment from the previous time-step. Surplus juveniles holding downstream do experience length-based mortality following Zabel and Achord (2004; Table 2). We assumed the length of the early migratory fish holding downstream would be the same as those in the modeled reach.

On April 15, one year after fry emergence, juveniles remaining in the modeled reach and those early migrants begin migrating downstream toward the ocean (smolts). Mortality rate for smolts is dependent on their length when they leave the modeled reach modified from an equation in (Zabel and Achord 2004; Table 2), which is based on a relative difference to a mean length at tagging. We assumed a similar relationship for smolts migrating downstream, but used a mean size of 100 mm, which is consistent for smolts many spring Chinook populations across the Columbia River basin (Copeland and Venditti 2009; Snow et al. 2014). Survival during the smolt stage takes into account dam passage, and ending with Bonneville Dam.

The first year in the ocean can be a critical time for the survival of salmon, and may be related to size of the juveniles entering the estuary (Beamish et al. 2004; Duffy and Beauchamp 2011). Similar to freshwater migrating smolts, we related first year ocean survival to the size of fishes when they left their rearing habitats following an empirical equations from the literature (Table 2).

The survival for the remaining the out-of-basin stages (2nd year in the ocean and adults returning) were based on empirical values (Table 2).

We allowed the model to equilibrate (burn-in), and present results for one annual year from 15 April to 15 April, which represent the one year period that juvenile Chinook in one cohort were assumed to occur in freshwater tributaries. Currently, the model is deterministic because it is still in development, therefore presenting multiple years would be redundant. The model was run on a daily time step with units of grams of ash-free dry mass for biomass, with a conversion to wet mass for juvenile weight (g). We used STELLA® 10.1 (ISEE Systems, Lebanon, N.H., USA) to construct the model and run the simulations.

Results and Discussion

In 1-km modeled reach, we simulated nine adults returning and spawning, which resulted in 794 smolts migrating. This value is approximately 2.5 times that from weekly redd surveys in the Methow River watershed (approximately 23 spawners/km; Snow et al. 2013, 2016), which we normalized to estimate the average number of redds per km and assumed two adults (female and male) per redd. Comparing the number of smolts in our modeled reach with empirical data is difficult, but we can compare smolts/adults. From model simulations we under estimated this metric (88 smolts/adult) compared to empirical estimates (approximately 900 smolts/adult). This discrepancy could be owing to lower survival estimates that were simulated compared to those experienced by the fish. For example, we simulated a survival of 25% for smolts migrating through the Columbia River, from the mouth of the Methow River and past Bonneville Dam. On average, estimates from the Comprehensive Passage Model (Zabel et al. 2008, Zabel et al. chapter 4.a) that uses empirical data suggest the survival of smolts through the Columbia River is 34%.

Multiple time periods when juvenile Chinook salmon would migrate downstream emerged from the feedbacks coded in the model. These include mid-summer and winter, as well as the timing when smolts migrate (mid-April; Figure 2A). Based on model results, downstream migration occurred when growth was stalled or negative (Figure 2B), which is owing to the reduction in energetic capacity to sustain these fish. The timing of out-of-basin movement during winter is similar to empirical data of tagged fish moving downstream past the lowest most

PIT array near the mouth of the Methow River. Tagged fish were not detected moving downstream near the mouth during mid-summer. However, juvenile Chinook salmon were captured in smolt traps near the mouth of the Twisp River and confluence of the Methow River and Chewuch River in mid-summer, which could suggest downstream movement by these juveniles (Snow et al. 2013, 2016). Copeland and Venditti (2009) also observed downstream movement of juvenile Chinook salmon in the Pahsimeroi River during late summer/early fall.

Based on model simulations, the weight of the average size smolt was 9.8 g, which is consistent with values for wild smolt migrating from the upper Methow River (9.7 g) and Twisp River (8.3 g; Snow et al. 2013). Moreover, Snow et al. (2013), observed the weight of wild juvenile Chinook salmon captured in the Methow and Twisp rivers during July and November to be approximately 2.5 g and 7.5 g, respectively. These weights are consistent with model simulations of the average sized juvenile (Figure 2B).

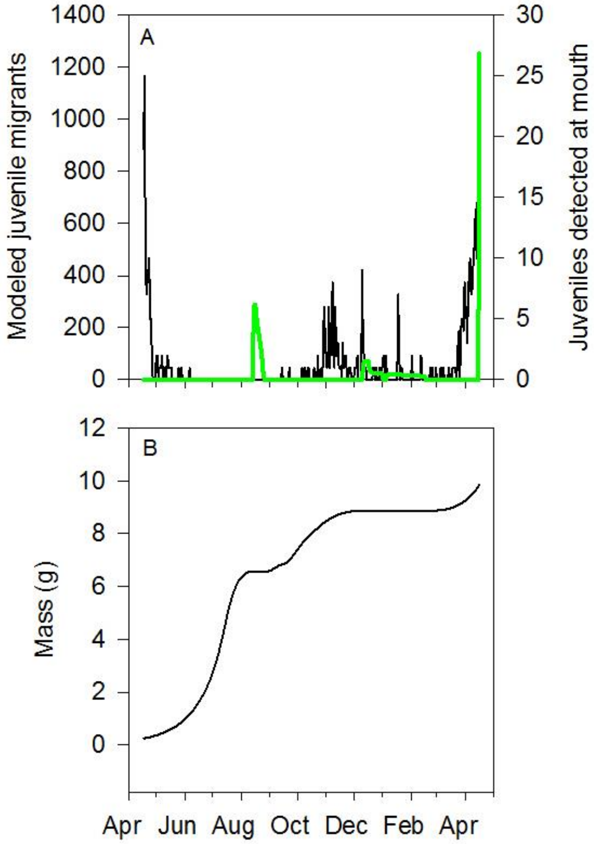

Figure 2. Modeled (green line) and observed (black line) juvenile spring Chinook salmon migration in the Methow River (A) and the mass of an average size juvenile Chinook salmon based on model simulation (B). Observed data were fish marked between 2009 and 2016 in the Methow River that passed the antenna array near the mouth.

Our intent in advancing the Aquatic Trophic Productivity model is to more completely incorporate fundamental processes driving productivity of ecosystems. By linking it to a life cycle-model we can extend these insights into understanding productivity of Pacific salmon, steelhead, and other species. The model is not intended to produce precise predictions or forecasts of fish populations, but rather to capture the important processes assumed to be at play in an explicit, model-based framework. This provides a formal and transparent description of processes believed to be driving ecosystem and fish population productivity. It also integrates a vast amount of information from individual empirical studies that can be put to work in a model-based framework to better understand stream ecosystem and fish conservation and restoration. The model itself is a dynamic process, and future additions will include: 1) addition of stochasticity surrounding life cycle dynamics, 2) sensitivity analyses to identify important parameters and uncertainties, 3) application of the model to evaluate freshwater management strategies in the Methow basin, and 4) applications of the model in other watersheds.

Moreover, the ATP model could incorporate other models presented in this report. For example, to better represent the "out-of-basin" component in the life cycle, which was beyond the scope of this modeling effort, we could link with other models that are specifically estimating different concerns that occur downstream. This could include, but not limited to, the survival during estuary and ocean residency (Burke et al. chapter 3), pinniped and avian predation (Sorel et al. chapter 6.a, Paulsen. chapter 6.b), and survival of adult migration to spawning tributaries.

Acknowledgements

We thank Jeff Jorgensen for running COMPASS model simulations to estimate out of basin survival. Funding was provided by the US Bureau of Reclamation. Any use of trade, firm, or product names is for descriptive purposes only and does not imply endorsement of the US Government.

References

Beamish, R.J., Mahnken, C., and Neville, C.M. 2004. Evidence that reduced early marine growth is associated with lower marine survival of coho salmon. Transactions of the American Fisheries Society 133:26–33.

Bellmore, J. R., C. V. Baxter, K.D. Martens, and P.J. Connolly. 2013. The floodplain food web mosaic: a study of its importance to salmon and steelhead with implications for their recovery. Ecological Applications 23:189-207.

Bellmore, J. R., A. K. Fremier, F. Mejia, and M. Newsom. 2014. The response of stream periphyton to Pacific salmon: using a model to understand the role of environmental context. Freshwater Biology 59:1437-1451.

Bellmore, J. R., J. R. Benjamin, M. Newsom, J.A. Bountry, and D. Dombroski. 2017. Incorporating food web dynamics into ecological restoration: a modeling approach for river ecosystems. Ecological Applications 27:814-832.

Benjamin, J.R., and J.R. Bellmore. 2016. The Aquatic Trophic Productivity Model- A Decision Support Model for River Restoration Planning in the Methow River, Washington: U.S. Geological Survey Open-File Report 2016-1075, p. 85.

Carpenter, S. R., S. W. Chisholm, C. J. Krebs, D. W. Schindler, and R. F. Wright. 1995. Ecosystem experiments. Science (New York, N.Y.) 269:324-7.

Copeland, T. and D.A. Venditti. 2009. Contribution of three life history types to smolt production in a Chinook salmon (*Oncorhynchus tshawytscha*) population. Canadian Journal of Fisheries and Aquatic Sciences 66:1658-1665.

Duffy, E. J. and D. A. Beauchamp. 2011. Rapid growth in the early marine period improves the marine survival of Chinook salmon (Oncorhynchus tshawytscha) in Puget Sound, Washington. Canadian Journal of Fisheries and Aquatic Sciences 68: 232-240.

Ellis, B. K., J. Stanford, D. Goodman, C. P. Stafford, D. L. Gustafson, D. Beauchamp, D. W. Chess, J. Craft, M. Deleray, and B. S. Hansen. 2011. Long-term effects of a trophic cascade in a large lake ecosystem. Proceedings of the National Academy of Sciences of the United States of America 108:1070-5.

Grant, J. W. A. and D. L. Kramer (1990). Territory size as a predictor of the upper limit to population density of juvenile salmonids in streams. Canadian Journal of Fisheries and Aquatic Sciences 47: 1724-1737.

Hanson, P.C., T.B. Johnson, D.E. Schindler, and J.F. Kitchell. 1997. Fish bioenergetics 3.0. university of Wisconsin, Sea Grant Institiute, WISCU-T-97-001, Madison.

Honea, J. M., J. C. Jorgensen, M.M. Mcclure, T.D. Cooney, K. Engie, D.M. Holzer, and R. Hilborn. 2009. Evaluating habitat effects on population status: influence of habitat restoration on spring-run Chinook salmon. Freshwater Biology 54:1576-1592.

Keeley, E. R. and J. W. A. Grant 2001. Prey size of salmonid fishes in streams, lakes, and oceans. Canadian Journal of Fisheries and Aquatic Sciences 58:1122-1132.

Naiman R.J., J.R. Alldredge, D.A. Beauchamp, P.A.Bisson, J. Congleton, C.J. Henny, N. Huntly, R. Lamberson, C. Levings, E.N. Merrill, W.G. Pearcy, B.E. Rieman, G.T. Ruggerone, D. Scarnecchia, P.E. Mouse, and C.C. Wood. Developing a broader scientific foundation for river restoration: Columbia River food webs. Proceedings of the National Academy of Sciences: 109:21201-7.

Northwest Power and Conservation Council (NPCC). 2011. Columbia River Food-Webs: Developing a Broader Scientific Foundation for Fish and Wildlife Restoration. Independent Scientific Advisory Board (ISAB) Report (ISAB 2011-1).

Palmer, M.A., E.S. Bernhardt, J.D. Allan, P.S. Lake, G. Alexander, S. Brooks, J. Carr, S. Clayton, C.N. Dahm, J. Follstad Shah, D.L. Galat, S.G. Loss, P. Goodwin, D.D. Hart, B. Hassett, R. Jenkinson, G.M. Kondolf, R. Lave, J.L. Meyer, T.K. O'Donnell, L. Pagano, and E. Sudduth. 2005. Standards for ecologically successful river restoration. Journal of Applied Ecology 42:208-217.

Plumb, J. M. and C. M. Moffitt. 2015. Re-establishing temperature-dependent consumption parameters in bioenergetics models for juvenile Chinook salmon. Transactions of the American Fisheries Society 144: 323-330.

Railsback, S. F., B. C. Harvey, and J.L. White. 2014. Facultative anadromy in salmonids: linking habitat, individual life history decisions, and population-level consequences. Canadian Journal of Fisheries and Aquatic Sciences 71:1-9.

Railsback, S.R., B.C. Harvey, S.K. Jackson, and R.H. Lamberson. 2009. InSTREAM: the individual-based stream trout research and environmental model. General Technical Report, PSW-GTR-218. Albany, CA: US Department of Agriculture, Forest Service. 254p.

Snow, C., C. Frady, A. Repp, A. Murdoch, M. Small, and C. Dean. 2013. Monitoring and evaluation of Wells and Methow hatchery programs: 2012 annual report. Prepared for Douglas County Public Utility District and Wells Habitat Conservation Plan Hatchery Committee, East Wenatchee, Washington. (Available from: http://www.dcpud.org/HCP%20HC%20Documents/2014_11_14%20Douglas%20-%20FINAL%202013%20DCPUD%20M%20and%20E%20Plan%20Report%2011-3-14.pdf)

Snow, C., C. Frady, D. Grundy, B. Goodman, and A. Murdoch. 2016. Monitoring and evaluation of the Wells Hatchery and Methow Hatchery programs: 2015 annual report. Report to Douglas PUD, Grant PUD, Chelan PUD and the Wells and Rocky Reach HCP Hatchery Committees and the Priest Rapids Hatchery Subcommittees, East Wenatchee, WA.

Wipfli, M. S., and C. V. Baxter. 2010. Linking ecosystems, food webs, and fish production: subsidies in salmonid watersheds. Fisheries 35:373-387.

Zabel, R.W., and S. Achord. 2004. Relating size of juveniles to survival within and among populations of Chinook salmon. Ecology 85:795-806.

Zabel, R. W., J. Faulkner, S. G. Smith, J. J. Anderson, C. Van Holmes, N. Beer, S. Iltis, J. Krinke, G. Fredicks, B. Bellerud, J. Sweet and A. Giorgi. 2008. Comprehensive Passage (COMPASS) Model: a model of downstream migration and survival of juvenile salmonids through a hydropower system. Hydrobiologia 609:289-300.

Zuckerman, A. 2015. Seasonal variation in empirical and modeled periphyton at the watershed scale. MS Thesis. University of Idaho, Moscow.

CHAPTER 7: Using integrated population models to evaluate natural and anthropogenic risk factors for Pacific salmon

Eric R. Buhle[1,2], Mark D. Scheuerell[3], James T. Thorson[4]

[1]Quantitative Consultants, Inc., Boise, ID 83702 USA, eric.buhle@noaa.gov

[2]Conservation Biology Division, Northwest Fisheries Science Center, National Marine Fisheries Service, National Oceanic and Atmospheric Administration, Seattle, WA 98112 USA, eric.buhe@noaa.gov

[3]Fish Ecology Division, Northwest Fisheries Science Center, National Marine Fisheries Service, National Oceanic and Atmospheric Administration, Seattle, WA 98112 USA, mark.scheuerell@noaa.gov

[4]Fisheries Resource Assessment and Monitoring Division, Northwest Fisheries Science Center, National Marine Fisheries Service, National Oceanic and Atmospheric Administration, Seattle, WA 98112 USA, james.thorson@noaa.gov

Introduction

Managing at-risk species requires an understanding of the degree to which population dynamics are governed by density dependence versus other environmental drivers. In many cases, however, the data necessary to complete a comprehensive assessment are limited over space and time, which creates unique challenges for identifying the underlying demographic causes of population declines. For example, when not addressed in an appropriate manner, errors in population censuses from incomplete surveys may cause underestimates of recruitment (Sanz-Aguilar *et al.* 2016) or overestimates of the strength of density dependence (Knape & de Valpine 2012). Similarly, imprecision in the estimated age composition of a population also biases the estimated strength of density dependence (Zabel & Levin 2002). In turn, any management decisions based on these erroneous conclusions could be misguided and thereby possibly limit recovery of the population. Therefore, proper consideration of all sources of uncertainty in the data is necessary to design robust conservation strategies.

Life cycle models are commonly used to evaluate the potential response(s) of populations to various scenarios of future conditions. Traditionally, their development follows a two-step process whereby 1) population growth rates and demographic rates are informed by multiple data sources with separate likelihoods; and 2) the estimated parameters and data are then used as inputs into population projection models or stock assessments (Schaub & Abadi 2011; Maunder & Punt 2013). Although there is nothing inherently wrong with this approach, it does suffer from two major drawbacks. First, the available raw data are used inefficiently in that information is lost when summarized, which creates problems for determining the appropriate likelihood functions and evaluating model diagnostics. Second, there is no formal assessment of the variance and covariance within and among model parameters, which requires some form of joint likelihood based on all available data. Third, failure to acknowledge the trade-offs among parameters and the fact that any given type of data (e.g., age structure) may contain information on multiple aspects of population dynamics (e.g., recruitment and survival) can lead to biased parameter estimates.

More recently, so-called integrated population models (IPMs) have been used to address these shortcomings. IPMs are based upon a joint likelihood constructed from each of the individual data likelihoods, which fully captures all of the uncertainty in the data (Schaub & Abadi 2011; Maunder & Punt 2013) and improves the precision and accuracy of parameter estimates (Tavecchia *et al.* 2009; Johnson *et al.* 2010). IPMs are closely linked to state-space models (de Valpine & Hilborn 2005), which are hierarchical models consisting of a process model (a stochastic description of the true but unobservable population dynamics) and an observation model (a model of the noisy data, conditional on the true state of the population). Furthermore, if IPMs are set up in a hierarchical fashion to model multiple populations simultaneously, information “borrowed” from data-rich populations helps to improve the precision of parameter estimates in relatively data-poor ones (Jiao *et al.* 2011; Punt, Smith & Smith 2011).

IPMs have been used in a variety of studies related to conservation of birds (Schaub *et al.* 2007; Oppel *et al.* 2014), and the management of exploited mammals (Tavecchia *et al.* 2009; Johnson *et al.* 2010) and marine fishes (Ianelli 2002; Punt *et al.* 2010), but they are less familiar in salmonid management and conservation. The IPM for Pacific salmon that we describe here shares some features with the models of Newman *et al.* (2006), Su & Peterman (2012), Fleischman *et al.* (2013), and Winship *et al.* (2014), but we expand upon previous analyses in two ways. First, we allow for the possibility that a spawning population might include hatchery-origin fish, treating their abundance as an unknown state to be estimated. Second, we extend the process model to represent an ensemble of populations with potentially correlated process errors, using a hierarchical framework.

We apply the model to 24 populations of spring/summer Chinook salmon from the Snake River basin, and compare the results to those obtained with a traditional ad hoc approach. We find that the IPM provides more conservative estimates of the strength of density-dependent compensation at low abundance. This translates into higher projected risks of quasi-extinction and more precautionary inferences about the effects of harvest or other mortality factors on population viability.

Methods

Traditional run reconstruction

The traditional approach to spawner-recruit analysis for salmonids begins by reconstructing the time series of recruits from the brood table (i.e., annual observations of spawner abundance, age structure, hatchery fraction and harvest rate). The paired values of spawners and recruits are then used as independent and dependent variables, respectively, in a regression model to estimate the production parameters. Specifically, recruits from cohort *t* are the sum of returning spawners in subsequent years weighted by age structure, inflated to include harvest, and discounted by the fraction of hatchery-origin spawners so only natural-origin recruits are counted:

$$R_t^{\text{obs}} = \sum_a \frac{S_{t+a}^{\text{obs}} q_{t+a,a}^{\text{obs}} \left(1 - p_{\text{HOS},t}^{\text{obs}}\right)}{1 - F_{t,a}^{\text{obs}}}$$

where S_t^{obs} is spawner abundance in year *t*, q_t^{obs} is the proportion of spawners of age *a*, $F_{t,a}^{\text{obs}}$ is the (possibly age-specific) harvest rate, $p_{\text{HOS},t}^{\text{obs}}$ is the proportion of hatchery-origin spawners, and the summation is over all adult ages *a*. The superscripts indicate that these are observed or measured quantities (i.e., data or summary statistics). The regression model is then

$$R_t^{\text{obs}} = f\left(S_t^{\text{obs}} \mid \boldsymbol{\theta}\right)e^{\varepsilon_t} \tag{1}$$

where *f* is the spawner-recruit function with parameter vector $\boldsymbol{\theta}$ and $\varepsilon_t \sim \text{N}(0,\sigma^2)$ is a residual error. In the case study presented below we use the Beverton-Holt model,

$$f_{\text{BH}}\left(S_t^{\text{obs}} \mid \alpha,\beta\right) = \frac{\alpha S_t^{\text{obs}}}{1+\beta S_t^{\text{obs}}} \tag{2}$$

where α is intrinsic productivity and β is the per capita strength of density dependence. The asymptotic recruitment (or "capacity") is α/β. We additionally allow serial correlation by modeling the residual errors as an AR(1) process, so that $\varepsilon_t = \rho\varepsilon_{t-1} + \nu_t$, where ρ is the autocorrelation coefficient and $\nu_t \sim \text{N}(0,\sigma^2)$ is an IID innovation term.

The basic spawner-recruit regression model can be extended to multiple populations by adopting a hierarchical framework (Clark 2005; Gelman *et al.* 2014). This entails two modifications to Eqs. 1 and 2. First, the Beverton-Holt parameters for each population *i* are assumed to follow a lognormal hyperdistribution with a common log-mean and log-variance, $\log(\alpha) \sim \text{N}\left(\mu_\alpha, \sigma_\alpha^2\right)$ and $\log(\beta) \sim \text{N}\left(\mu_\beta, \sigma_\beta^2\right)$. Second, we include a cohort effect shared among all populations and modeled as an AR(1) process, $\log(\phi_t) \sim \text{N}\left(\rho \times \log(\phi_{t-1}), \sigma_\phi^2\right)$, in addition to the IID residual error ε_{it} with common variance σ^2. Thus, the full model for cohort *t* in population *i*,

$$R_{it}^{\text{obs}} = \frac{\alpha_i S_{it}^{\text{obs}}}{1+\beta_i S_{it}^{\text{obs}}}\phi_t e^{\varepsilon_{it}} \tag{3}$$

decomposes the variation in recruitment into spatial (among-population), temporal (among-cohort), and idiosyncratic (residual) components.

Integrated population model

The traditional run-reconstruction regression (henceforth “RR”) approach treats the observed spawner abundance (the “independent variable”) as a quantity that is known precisely. By conditioning the predicted recruitment on observed spawner abundance in each cohort, it implicitly assumes that the residual deviations are due to process error alone (Hilborn & Mangel 1997), yet it is not truly a process-error model because it does not account for the biological and mathematical dependence of S_t^{obs} on the “dependent variable” R_{t-a}^{obs} in previous years. This leads to the well-known time-series and errors-in-variables biases (Ludwig & Walters 1981), which can severely affect estimates of the spawner-recruit parameters and management reference points. Furthermore, a single missing observation of any of the quantities in the brood table induces multiple missing recruitment estimates (equal to the number of adult age classes), and the regression framework simply ignores these missing values. In particular, if a_{max} is the the age of the oldest spawners, then the final $a_{\text{max}} - 1$ years of recruits will be missing because the complete cohorts have not yet returned to spawn and be counted. As a result, short-term forecasts cannot be conditioned on the most recent (and perhaps most informative) observations.

As an alternative approach, we develop an IPM to describe single life-stage (i.e., adult-to-adult) dynamics of one or more salmon populations. The process model begins with the spawner-recruit function,

$$R_t = f\left(S_t \mid \boldsymbol{\theta}\right) e^{\varepsilon_t}$$

but here the variables S_t and R_t represent the true, unknown state of the population and ε_t is interpreted as a process error deviation. As in the RR approach, we will use the Beverton-Holt model and allow autocorrelation in the process errors:

$$R_t = \frac{\alpha S_t}{1+\beta S_t} e^{\varepsilon_t} \tag{4}$$

where $\varepsilon_t = \rho\varepsilon_{t\text{-}1} + \nu_t$ and $\nu_t \sim \mathrm{N}(0,\sigma^2)$. The recruits from cohort t return to spawn in subsequent years, with the proportion of surviving adults that return at each age given by the cohort-specific vector $\mathbf{p}_t$. For example, in the case of Snake River spring/summer Chinook salmon discussed below, adults return at ages 3-5, so $\mathbf{p}_t = (p_{t3}, p_{t4}, p_{t5})$. By parameterizing the recruit age distribution conditional on survival to adulthood, we avoid the need to specify annual survival and maturation probabilities during ocean residence, which are typically not identifiable from data. The vector of age proportions in each cohort is drawn from a logistic normal distribution (Aitchison 1982) with hyperparameters $\boldsymbol{\gamma}$ and $\boldsymbol{\tau}$:

$$\log\left(p_{ta} / p_{ta_{\max}} \right) \sim \mathrm{N}\left(\gamma_a, \tau_a^2\right) \tag{5}$$

for $a \leq a_{\max} - 1$. The log ratios are then easily transformed back to the simplex space of proportions. Note that the use of $a_{\max}$ as the reference age class is arbitrary; equivalent distributions on the simplex are obtained regardless of the choice of reference class (Aitchison 1982).

The number of natural-origin (or “wild”) spawners in year t is then simply the sum over age classes of recruits minus losses to the fishery (represented by the mortality rate, F_t^{obs}) and any fish removed for hatchery broodstock (represented by the number taken, B_t):

$$S_t^{\mathrm{W}} = \left[\sum_a R_{t-a} p_{ta} \left(1 - F_t^{\text{obs}}\right) \right] - B_t\,. \tag{6}$$

In practice, we assume broodstock removals are measured without error, since these are typically small numbers of fish that are well documented. For simplicity, we also assume F_t^{obs} represents the true harvest rate, although in principle this assumption could be relaxed. The spawning population may also include hatchery-origin fish that are either deliberately or inadvertently allowed to reproduce naturally. We did not attempt to develop a process submodel describing life history trajectories of hatchery-born fish following their release as juveniles (i.e., survival to adulthood, age distribution, harvest mortality and broodstock collection, and natural dispersal or outplanting into natal or non-natal rivers). Instead we simply define $p_{\mathrm{HOS},t}$, the proportion of hatchery-origin spawners in year t, as a parameter so that

$$S_t^{\mathrm{H}} = S_t^{\mathrm{W}} p_{\mathrm{HOS},t} \big/ \left(1 - p_{\mathrm{HOS},t}\right).$$

The total spawner abundance is then $S_t = S_t^{\mathrm{W}} + S_t^{\mathrm{H}}$.

As in the RR approach, we can extend the process model to describe the dynamics of an ensemble of populations by modeling the population-specific spawner-recruit parameters as lognormal random effects and including a common AR(1) error term:

$$R_{it} = \frac{\alpha_i S_{it}}{1 + \beta_i S_{it}} \phi_t e^{\varepsilon_{it}}. \tag{7}$$

Here the parameters and their hyperdistributions are the same as in Eq. 3, but the errors are interpreted as process noise with two components: a large-scale driver common to all populations (ϕ_t), and unique, population-specific fluctuations (ε_{it}) in the underlying true dynamics. The model for the time-varying cohort age distributions (Eq. 5) also needs to be expanded in the multiple-population context. We allow each population to have its own average (on the log-ratio scale) adult age proportions $\boldsymbol{\gamma}_i$, so the age vector for cohort t is drawn from a logistic normal distribution with common standard deviation vector $\boldsymbol{\tau}$:

$$\log\left(p_{ita} \big/ p_{ita_{\max}}\right) \sim \mathrm{N}\left(\gamma_{ia}, \tau_a^2\right). \tag{8}$$

Each component of the population-level mean vector of log ratios $\boldsymbol{\gamma}_i$ is, in turn, drawn from a hyperdistribution

$$\gamma_{ia} \sim \mathrm{N}\left(\mu_{\mathbf{p}a}, \sigma^2_{\mathbf{p}a}\right) \tag{9}$$

where the mean vector $\boldsymbol{\mu}_\mathbf{p}$ represents the average age structure, on the log ratio scale, at the level of the entire population ensemble, and the vector of standard deviations $\boldsymbol{\sigma}_\mathbf{p}$ represents the among-population heterogeneity in average adult age distributions.

The observation model consists of three likelihood components. First, the observed or estimated total spawner abundance is lognormally distributed around the true abundance with observation error standard deviation σ_obs:

$$\log\left(S_t^\mathrm{obs}\right) \sim N\left(\log\left(S_t\right), \sigma^2_\mathrm{obs}\right). \tag{10}$$

Second, the observed age composition of natural-origin spawners is typically based on subsamples of carcasses or live fish handled at weirs. These sampling methods produce a vector of age frequencies, which we assume to follow a multinomial distribution,

$$\left[n^\mathrm{obs}_{ta_\mathrm{min}}, \ldots, n^\mathrm{obs}_{ta_\mathrm{max}}\right] \sim \mathrm{Multinomial}\left(\sum_a n^\mathrm{obs}_{ta}, q_{ta_\mathrm{min}}, \ldots, q_{ta_\mathrm{max}}\right) \tag{11}$$

where n^obs_{ta} is the observed count of age-*a* adults in year *t*, the sample size for the multinomial is the total number of fish aged, and the expected probability of age *a* in year *t*, q_{ta}, is found by normalizing the true number of age-*a* spawners by the true total spawner abundance (Eq. 6).

The third observation likelihood component is the frequency of hatchery- and wild-origin spawners, typically based on recovery of marks (e.g., adipose fin clips) on carcasses or fish passed over weirs. Again, these sampling methods produce counts, $n_t^\mathrm{W,obs}$ and $n_t^\mathrm{H,obs}$, which we assume to follow a binomial distribution with expected probability given by the true fraction of hatchery spawners:

$$n_t^\mathrm{H,obs} \sim \mathrm{Bin}\left(n_t^\mathrm{H,obs} + n_t^\mathrm{W,obs}, p_{\mathrm{HOS},t}\right). \tag{12}$$

Note that we make no assumptions about the age structure of hatchery-origin adults; in principle this could be incorporated into the observation model, but age frequencies of hatchery-origin fish are largely unavailable.

Parameter estimation

We estimate model parameters for both the RR and IPM in a Bayesian framework (Gelman *et al.* 2014). The joint posterior distribution is the product of (1) the prior on the hyperparameters (μ_α, σ_α, μ_β, σ_β, σ, ρ, σ_ϕ, $\boldsymbol{\mu}_\mathbf{p}$, $\boldsymbol{\sigma}_\mathbf{p}$, $\boldsymbol{\tau}$, and $\mathbf{p}_\mathrm{HOS}$), (2) the probability density of the population-specific random effects (spawner-recruit parameters and age structure means) given their hyperparameters (multi-population models only), (3) the probability density of the latent states given their hyperparameters (IPM only), (4) the prior on the initial states (IPM only), and (5) the observation likelihood (or in RR, the regression likelihood).

We used vague priors for all hyperparameters with the exception of the process error autocorrelation coefficient ρ, for which we used a power-exponential distribution that regularizes the tails of the posterior away from -1 and 1 to ensure stationarity:

$$p(\rho) \propto \exp\left[\left(\frac{|\rho|}{0.85}\right)^{50}\right]. \tag{13}$$

We explored alternate values of the shape and scale in this prior and found that they had fairly minor effects on the mean and bulk of the posterior mass. We also need to specify a prior on the initial states in the IPM. The states corresponding to the first $1{:}a_\mathrm{max}$ years of each population's data series cannot be predicted based on previous states (recruitment and age structure), so for $t = 1, ..., a_\mathrm{max}$ we assumed $\log(S_{it}) \sim \mathrm{N}(0,5^2)$ and $\mathbf{q}_{it}$, the vector of spawner age proportions in return year t, was distributed uniformly on the simplex.

For each model, we simulated 1000 draws from the posterior in each of three randomly initiated Markov chains using the Hamiltonian Monte Carlo algorithm (HMC, Monnahan, Thorson & Branch 2017) implemented in Stan v2.14.0 (Stan Development Team 2016) as run from R v3.3.3 (R Development Core Team 2017). The first 500 iterations of each chain were used as warmup and discarded, resulting in a total saved sample of 1500 draws. We assessed convergence by visual inspection of traceplots and by verifying that Gelman and Rubin's (1992) potential scale reduction factor was < 1.1 for all parameters and that there were no divergent transitions. Code for all analyses is available online as part of the R package `salmonIPM`.[1]

Forward simulation

Simulating future population trajectories under the IPM is straightforward; the process model is simply iterated for the desired number of years beyond the end of the time series of observations, generating a posterior predictive distribution of future states conditioned on the historical data. In particular, predicted future spawner abundance and age structure are conditioned on the incomplete cohorts at the end of the data series (i.e., those cohorts from which one or more older age classes have not yet returned to spawn). The IPM therefore assimilates the same information traditionally used in a so-called sibling regression (Peterman 1982), in which linear relationships between age-class abundance within cohorts are used to predict older-aged adult returns given the observed younger-aged returns. In contrast to sibling regression, however, the IPM does not assume a fixed age structure but allows the cohort age distribution to vary through time.

Under the RR approach, the estimation model is not framed as a dynamical simulation model, so additional assumptions are needed to convert the predictions (i.e., recruits) into the

---

[1] https://github.com/ebuhle/salmonIPM

state (i.e., spawners of each age) at future time steps. Because age structure is not a parameter of the model but rather an input to the data pre-processing step, we fixed the adult age structure in future cohorts at the population-specific average cohort age structure over all the available years of data. This allows the calculation of natural-origin spawners in future years using a formula analogous to Eq. 6. Those simulated spawners are then used to predict the next cohort of recruits from the spawner-recruit regression model, treating the stochastic residual error as process error.

For all of the future simulations, we set total harvest, broodstock removal, and hatchery spawner abundance to zero to represent a baseline projection of risk in the absence of either supplementation or additional mortality beyond that captured in the spawner-recruit relationship. For each simulated trajectory we determine quasi-extinction, where the quasi-extinction threshold (QET) is defined in terms of the four-year running mean of total spawner abundance. Quasi-extinction occurs if the running mean for a given population falls below the QET at least once, and the posterior predictive probability of quasi-extinction (PQE) is the proportion of such trajectories, where each trajectory corresponds to one MCMC sample from the joint posterior. For multiple-population ensemble models, we also calculate the posterior predictive probability that at least one population experiences quasi-extinction. In addition to these risk metrics, we estimate the maximum harvest (or other “extra” mortality) rate that a population *i* can sustain before the deterministic growth rate falls below replacement,

$$U_{\max,i} = 1 - \frac{1}{\alpha_i} , \tag{14}$$

as well as the corresponding quantity at the aggregate ESU level:

$$\mu_{U_{\max}} = 1 - \frac{1}{\mu_\alpha} . \tag{15}$$

Application to Snake River spring/summer Chinook salmon

As a case study, we examined 24 populations of spring/summer Chinook salmon from the Snake River Evolutionarily Significant Unit (ESU), which is listed as Threatened under the US Endangered Species Act. In total, the data set includes 1242 cases (distinct population/year combinations) spanning six decades, from 1952 to 2012. The populations and year ranges of available data are listed in Table 1. The majority of adults are age 4 or 5, with a smaller proportion of 3-year-olds (almost entirely male); 6-year-old spawners were observed in a very small number of cases (62/1242), so we omit this age class in the analysis. Spawner observations were missing in 9/1242 cases and age-frequency data were missing in 352/1242 cases, predominantly in the early years of the time series. These missing data pose no problems for the IPM approach, in which the process model automatically imputes the underlying states, but produce unusable predictor-response pairs in the RR regression (see *Run Reconstruction* above). To avoid biasing the comparison between methods by including or excluding particular eras of the time series, we imputed the missing cohort age distributions by using the population-specific time-averaged distributions in the run reconstruction step (Eq. 1).

Hatchery-origin spawners have been recorded in roughly half of the populations at some point during their history, but in most cases, there were no hatchery fish present before the mid-1980s. We therefore fixed $p_{\mathrm{HOS},t}$ at zero in the IPM except in populations and time periods when hatchery programs were known to be operational. We used estimates of the area of potential spawning habitat (in ha) in each watershed (Tom Cooney, Northwest Fisheries Science Center, unpublished data) to standardize spawner abundance among populations. That is, we used spawners/ha as the predictor or state variable in the spawner-recruit model and then multiplied by area to obtain total spawners as required for the observation model. While not strictly necessary, this approach scales β_i to standardized units of ha/spawner for all populations, removing variation due to overall population size and bolstering the assumption of exchangeability of the random effects.

Results

We focus on results from the multiple-population versions of the RR model and the IPM. The IPM did a good job of capturing the historical dynamics of Snake River spring/summer Chinook populations (examples shown in Fig. 1). The coefficient of determination between the median of the estimated log-spawners and the observed log-spawners across the entire data set was 0.85, and 98% of the observed values fell within the 95% credible interval based on the observation error distribution. Observation error in spawner abundance was greater (posterior mean and 95% CI of σ_{obs}: 0.67, 0.63-0.72) than the unique process error in recruitment (σ: 0.25, 0.21-0.30). However, overall recruitment process error was dominated by the shared cohort effect, whose standard deviation was $\sigma_{\phi} \big/ \sqrt{1-\rho^2}$ = 1.11 (0.85-1.45) and which was strongly autocorrelated (ρ: 0.77, 0.65-0.85). This can be seen in Fig. 1, where the trajectories of different populations are highly synchronous.

Importantly, the IPM and RR approaches yielded different inferences about the shape of the spawner-recruit curve (Fig. 2A). Although the credible intervals overlapped, there was a consistent tendency for higher estimates of both intrinsic productivity (Fig. 2B) and per capita density dependence (β, not shown) under the RR model, at both the population and ESU-average scale, resulting in similar capacity estimates in the two models (Fig. 2C). The effects of these differences can be seen in the simulated future trajectories (Fig. 1), where the RR model tends to project higher values of recruits per spawner than the IPM in at least some cases, and the predictive intervals on spawner abundance tend not to drop as low.

Posterior probabilities of quasi-extinction were also lower under the RR model. When the QET was set at a four-year running mean of 50 spawners per population over a 50-year time horizon, the IPM was always more pessimistic about risk, and the two models produced different rankings of relative risk among populations (Fig. 3). Similar patterns were evident at the ESU level; across a range of QETs, the risk of at least one population experiencing quasi-extinction was greater under the IPM (Fig. 4).

Because quasi-extinction can occur due to environmental stochasticity (i.e., process error) even when the average population growth rate is positive, it is informative to examine the level of additional mortality, above that embodied in the spawner-recruit relationship, that could be sustained before the long-range growth rate drops below replacement (Fig. 5). The IPM indicated that even in the absence of harvest, there is a substantial probability that some populations are already experiencing deterministic decline if relying upon natural reproduction alone (those with nonzero *y*-intercepts in Fig. 5). In contrast, the RR painted a much more optimistic picture. Comparing the distribution of observed harvest rates (Fig. 5, histogram) to these estimates, we saw that prior to 1980, the fishery posed a significant risk of deterministic decline to nearly all populations according to the IPM (but not the RR), while more recent harvest rates posed such a risk to only the least productive populations. (Note that this does not account for long-term changes in productivity as reflected in the common year effect.)

Discussion

Life cycle models are commonly used for predicting the responses of populations to potential scenarios of future conditions. As such, the degree to which they can accurately and precisely capture retrospective patterns in population dynamics is critical to evaluating how much faith one should place in any future forecasts. Although IPMs have been used much more widely in terrestrial and marine environments (Schaub & Abadi 2011; Maunder & Punt 2013), they have not yet been widely applied to studies of Pacific salmon. Here we have demonstrated how the development and application of an IPM sheds new light on the current and future status of at-risk populations. In particular, we see several advantages to this approach: 1) a unified framework for both the estimation and simulation phases of analysis; 2) a full accounting of the uncertainties inherent in the available data; and 3) unbiased, probabilistic estimates of important parameters of interest, such as quasi-extinction risks, and the abundance and productivity metrics specified under the Viable Salmon Population recovery criteria (McElhany *et al.* 2000).

Traditional approaches to salmon life cycle modeling have relied upon a variety of piecemeal approaches for assembling various data sources, estimating parameters, assessing model fits, and evaluating uncertainties (e.g., Scheuerell *et al.* 2006; Zabel *et al.* 2006; Honea *et al.* 2009). Demographic parameters are often borrowed from other systems or species, or they are assumed known and fixed at some time-invariant value. For example, it has been assumed that all adult fish in the ocean for 3+ years have a survival rate of 0.8 per year based on Ricker's (1976) seminal work, but to the best of our knowledge there is no such summary statistic in that paper. In contrast, our IPM makes no assumptions about specific demographic rates; its parameters are instead estimated solely from the data at hand. In addition, the hierarchical nature of our IPM allows us to effectively borrow information from data-rich populations to help inform parameter estimation among the data-poor populations (Jiao *et al.* 2011; Punt, Smith & Smith 2011).

Life cycle models are often used to assess a population's viability over some future time horizon. Nevertheless, quantitative population viability analyses (PVAs) for Pacific salmon are negatively affected by a number of factors that mask the true population status, including observation errors, nonstationary age composition, and hatchery supplementation (Holmes 2004). In particular, a number of meta-analyses have shown that failing to adequately address observation errors leads to overestimates of the strength of density dependence (e.g., Freckleton *et al.* 2006; Knape & de Valpine 2012), which implies greater resilience to any potential disturbance. Furthermore, statistical models such as our IPM typically outperform much more detailed mechanistic models when estimating quasi-extinction rates (Holmes *et al.* 2007) or forecasting future abundance (Ward *et al.* 2014).

Efforts are currently underway to investigate how the marked increase in adult mortality owing to pinniped predation in the lower Columbia River (see Sorel *et al.*, Sec 6a) will affect the long-term viability of upstream populations. Notably, the results from our IPM can be used to inform these efforts right now. For example, our estimates of the additional mortality that could be sustained before the long-range population growth rate falls below replacement offer a rather stark view of the current situation (Fig. 5). Already we can see several populations with non-zero risk profiles, with increasing risk to those and additional populations as the mortality from *any* source increases. Furthermore, as part of the ongoing US v Oregon litigation, NMFS is actively engaged in identifying the future prospects for recovery under various proposed harvest management plans. Our IPM already includes a means for addressing current and future harvest rates, and we are now working to adapt it for that purpose.

Our IPM is presently based upon adult data only, but there is nothing precluding an expansion of the model to also include any applicable juvenile data as well. For example, there are snorkel counts of stream-resident parr for a subset of the populations we analyzed here, which we have used successfully in other related analyses (Thorson *et al.* 2014). Nevertheless, listing decisions are based solely upon adult measures of abundance, productivity, spatial structure, and diversity. Our IPM provides estimates of the intrinsic productivity and carrying capacity at both the population and larger ESU levels, the latter of which is the domain where any (de)listing decisions are made. Thus, we see potential for the further development of IPMs and their application to salmon conservation problems throughout the Pacific Northwest.

Acknowledgments

This analysis would not have been possible without the extensive data amassed through the dedicated efforts of a large number of biologists working for tribal, state, and federal agencies in the Columbia River basin over the past 60 years. We thank Tom Cooney and Mari Williams for help with data compilation. We thank Tom Cooney, Charlie Paulsen, and Rich Zabel for helpful discussions during model development. Much of this work was funded through a grant to MDS and JTT through the NOAA Fisheries and the Environment program (#15-01).

References

Aitchison, J. (1982) The statistical analysis of compositional data. *Journal of the Royal Statistical Society. Series B,* **44,** 139-177.

Clark, J.S. (2005) Why environmental scientists are becoming Bayesians. *Ecology Letters,* **8,** 2-14.

de Valpine, P. & Hilborn, R. (2005) State-space likelihoods for nonlinear fisheries time-series. *Canadian Journal of Fisheries and Aquatic Sciences,* **62,** 1937-1952.

Fleischman, S.J., Catalano, M.J., Clark, R.A. & Bernard, D.R. (2013) An age-structured state-space stock-recruit model for Pacific salmon (*Oncorhynchus* spp.). *Canadian Journal of Fisheries and Aquatic Sciences,* **70,** 401-414.

Freckleton, R.P., Watkinson, A.R., Green, R.E. & Sutherland, W.J. (2006) Census error and the detection of density dependence. *Journal of Animal Ecology,* **75,** 837-851.

Gelman, A., Carlin, J.B., Stern, H.S., Dunson, D.B., Vehtari, A. & Rubin, D.B. (2014) *Bayesian Data Analysis,* Third edn. CRC Press, Boca Raton, Florida.

Gelman, A. & Rubin, D.B. (1992) Inference from iterative sampling using mulitple sequences. *Statistical Science,* **7,** 457-511.

Hilborn, R. & Mangel, M. (1997) *The Ecological Detective - Confronting Models with Data*. Princeton University Press, Princeton, NJ.

Holmes, E.E. (2004) Beyond theory to application and evaluation: Diffusion approximations for population viability analysis. *Ecological Applications,* **14,** 1272-1293.

Holmes, E.E., Sabo, J.L., Viscido, S.V. & Fagan, W.F. (2007) A statistical approach to quasi-extinction forecasting. *Ecology Letters,* **10,** 1182-1198.

Honea, J.M., Jorgensen, J.C., McClure, M.M., Cooney, T.D., Engie, K., Holzer, D.M. & Hilborn, R. (2009) Evaluating habitat effects on population status: influence of habitat restoration on spring-run Chinook salmon. *Freshwater Biology,* **54,** 1576-1592.

Ianelli, J.N. (2002) Simulation analyses testing the robustness of productivity determinations from West Coast Pacific ocean perch stock assessment data. *North American Journal of Fisheries Management,* **22,** 301-310.

Jiao, Y., Cortes, E., Andrews, K. & Guo, F. (2011) Poor-data and data-poor species stock assessment using a Bayesian hierarchical approach. *Ecological Applications,* **21,** 2691-2708.

Johnson, H.E., Mills, L.S., Wehausen, J.D. & Stephenson, T.R. (2010) Combining ground count, telemetry, and mark-resight data to infer population dynamics in an endangered species. *Journal of Applied Ecology,* **47,** 1083-1093.

Knape, J. & de Valpine, P. (2012) Are patterns of density dependence in the Global Population Dynamics Database driven by uncertainty about population abundance? *Ecology Letters,* **15,** 17-23.

Ludwig, D. & Walters, C.J. (1981) Measurement errors and uncertainty in parameter estimates for stock and recruitment. *Canadian Journal of Fisheries and Aquatic Sciences,* **38,** 711-720.

Maunder, M.N. & Punt, A.E. (2013) A review of integrated analysis in fisheries stock assessment. *Fisheries Research,* **142,** 61-74.

McElhany, P., Ruckelshaus, M.H., Ford, M.J., Wainwright, T.C. & Bjorkstedt, E.P. (2000) Viable salmonid populations and the recovery of evolutionarily significant units. pp. 156. U.S. Dept. Commer., NOAA Tech. Memo. NMFS-NWFSC-42.

Monnahan, C.C., Thorson, J.T. & Branch, T.A. (2017) Faster estimation of Bayesian models in ecology using Hamiltonian Monte Carlo. *Methods in Ecology and Evolution,* **8,** 339-348.

Newman, K.B., Buckland, S.T., Lindley, S.T., Thomas, L. & Fernandez, C. (2006) Hidden process models for animal population dynamics. *Ecological Applications,* **16,** 74-86.

Oppel, S., Hilton, G., Ratcliffe, N., Fenton, C., Daley, J., Gray, G., Vickery, J. & Gibbons, D. (2014) Assessing population viability while accounting for demographic and environmental uncertainty. *Ecology,* **95,** 1809-1818.

Peterman, R.M. (1982) Model of salmon age strructure and its use in preseason forecasting and studies of marine survival. *Canadian Journal of Fisheries and Aquatic Sciences,* **39,** 1444-1452.

Punt, A.E., Deng, R.A., Dichmont, C.M., Kompas, T., Venables, W.N., Zhou, S.J., Pascoe, S., Hutton, T., Kenyon, R., van der Velde, T. & Kienzle, M. (2010) Integrating size-structured assessment and bioeconomic management advice in Australia's northern prawn fishery. *Ices Journal of Marine Science,* **67,** 1785-1801.

Punt, A.E., Smith, D.C. & Smith, A.D.M. (2011) Among-stock comparisons for improving stock assessments of data-poor stocks: the "Robin Hood" approach. *Ices Journal of Marine Science,* **68,** 972-981.

R Development Core Team (2017) R: A Language and Environment for Statistical Computing. R Foundation for Statistical Computing, Vienna, Austria.

Ricker, W.E. (1976) Review of the rate of growth and mortality of Pacific salmon in salt water, and noncatch mortality caused by fishing. *Journal of the Fisheries Research Board of Canada,* **33,** 1483-1524.

Sanz-Aguilar, A., Manuel Igual, J., Oro, D., Genovart, M. & Tavecchia, G. (2016) Estimating recruitment and survival in partially monitored populations. *Journal of Applied Ecology,* **53,** 73-82.

Schaub, M. & Abadi, F. (2011) Integrated population models: a novel analysis framework for deeper insights into population dynamics. *Journal of Ornithology,* **152,** 227-237.

Schaub, M., Gimenez, O., Sierro, A. & Arlettaz, R. (2007) Use of integrated modeling to enhance estimates of population dynamics obtained from limited data. *Conservation Biology,* **21,** 945-955.

Scheuerell, M.D., Hilborn, R., Ruckelshaus, M.H., Bartz, K.K., Lagueux, K.M., Haas, A.D. & Rawson, K. (2006) The Shiraz model: a tool for incorporating anthropogenic effects and fish-habitat relationships in conservation planning. *Canadian Journal of Fisheries and Aquatic Sciences,* **63,** 1596-1607.

Stan Development Team (2016) *Stan Modeling Language: User's Guide and Reference Manual*. Version 2.12.0.

Su, Z. & Peterman, R.M. (2012) Performance of a Bayesian state-space model of semelparous species for stock-recruitment data subject to measurement error. *Ecological Modelling,* **224,** 76-89.

Tavecchia, G., Besbeas, P., Coulson, T., Morgan, B.J.T. & Clutton-Brock, T.H. (2009) Estimating Population Size and Hidden Demographic Parameters with State-Space Modeling. *American Naturalist*, **173,** 722-733.

Thorson, J.T., Scheuerell, M.D., Buhle, E.R. & Copeland, T. (2014) Spatial diversity buffers temporal variability in early juvenile survival for an endangered Pacific salmon. *Journal of Animal Ecology,* **83,** 157-167.

Ward, E.J., Holmes, E.E., Thorson, J.T. & Collen, B. (2014) Complexity is costly: a meta-analysis of parametric and non-parametric methods for short-term population forecasting. *Oikos,* **123,** 652-661.

Winship, A.J., O'Farrell, M.R. & Mohr, M.S. (2014) Fishery and hatchery effects on an endangered salmon population with low productivity. *Transactions of the American Fisheries Society,* **143,** 957-971.

Zabel, R.W. & Levin, P.S. (2002) Simple assumptions on age composition lead to erroneous conclusions on the nature of density dependence in age-structured populations. *Oecologia,* **133,** 349-355.

Zabel, R.W., Scheuerell, M.D., McClure, M.M. & Williams, J.G. (2006) The interplay between climate variability and density dependence in the population viability of Chinook salmon. *Conservation Biology,* **20,** 190-200.

Table 1. Summary of Snake River spring/summer Chinook salmon data, including the range of sampling years (some years may have missing data), spawning habitat area, and the median, 5th and 95th percentiles for both the total observed spawner abundance and the proportion of hatchery-origin spawners (p_{hos}) for those populations that received hatchery supplementation.

Population	Years	Area (ha)	Spawners	p_{hos}
Bear Valley	1957-2012	75.6	488 (57-2004)	0
Big	1957-2012	140.5	246 (19-839)	0
Camas	1960-2012	63.4	75 (8-491)	0
Catherine	1955-2011	29.2	424 (42-1969)	0.22 (0-0.79)
Chamberlain	1985-2012	74.7	424 (72-1294)	0
East Fork Salmon	1957-2012	88.7	394 (24-2234)	0.06 (0-0.36)
East Fork South Fork Salmon	1957-2009	123.3	282 (53-919)	0.08 (0-0.57)
Imnaha	1952-2011	57.2	1430 (346-3613)	0.23 (0-0.76)
Lemhi	1957-2012	148.3	281 (36-2188)	0
Loon	1957-2012	74.2	81 (8-735)	0
Lostine	1959-2011	74.7	640 (87-1522)	0.21 (0-0.75)
Lower Upper Salmon	1957-2012	612.3	181 (37-892)	0
Marsh	1957-2012	44.4	304 (20-1353)	0
Minam	1954-2012	37.8	553 (101-1525)	0.09 (0-0.5)
Pahsimeroi	1989-2012	66.7	164 (37-610)	0.44 (0-0.95)
Secesh	1957-2010	71.1	333 (72-1182)	0.02 (0-0.07)
South Fork Salmon	1958-2008	309.2	1190 (267-3086)	0.18 (0-0.58)
Sulphur	1957-2012	14.9	105 (2-578)	0
Tucannon	1979-2011	24.2	436 (62-1347)	0.33 (0-0.69)
Upper Grande Ronde	1959-2011	32.3	224 (15-1020)	0.23 (0-0.95)
Upper Salmon	1957-2012	80.1	648 (80-2974)	0.1 (0-0.4)
Valley	1957-2012	42.7	121 (12-1050)	0
Wenaha	1964-2012	49.3	471 (84-2254)	0.14 (0-0.79)
Yankee	1957-2011	52.3	90 (2-962)	0.04 (0-0.08)

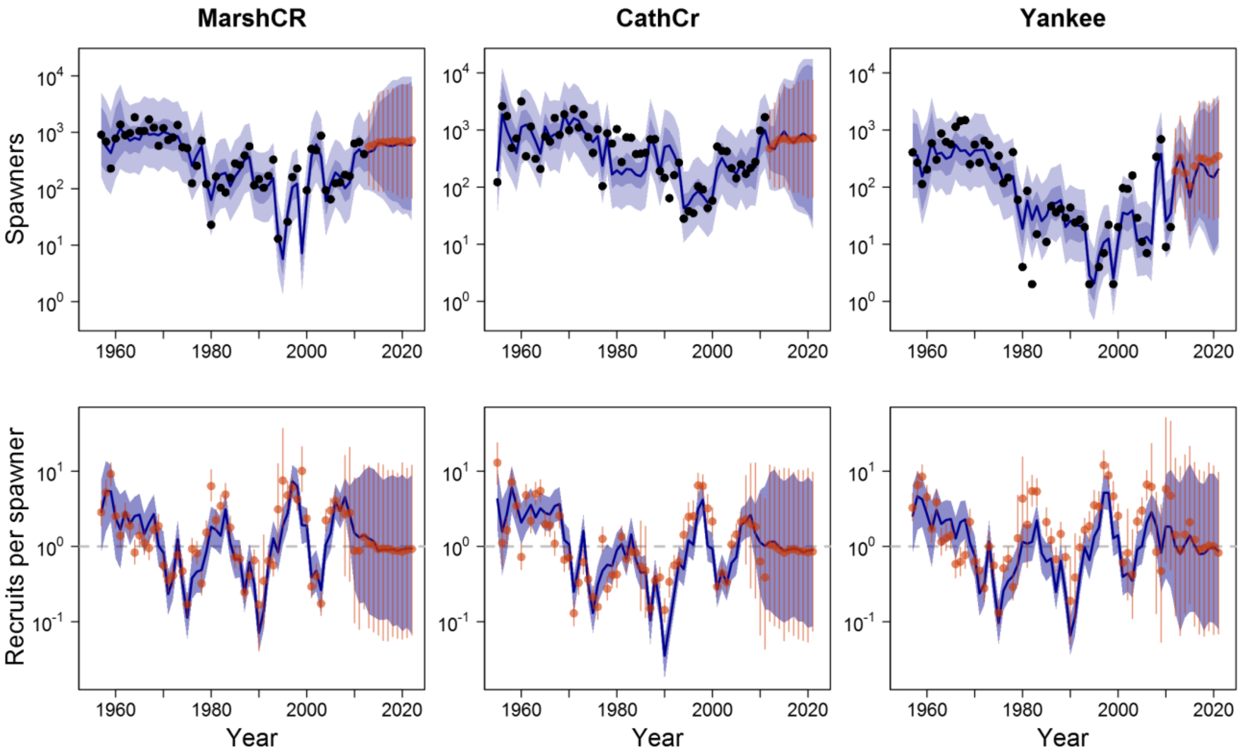

Figure 1. Top row: time series of observed spawner abundance (points) for each of three representative populations of Snake River spring/summer Chinook salmon: Marsh (left), Catherine (middle), and Yankee Fork (right). The posterior median from the IPM (solid blue line) is shown, along with 95% credible intervals accounting for process (dark shading) and observation (light shading) uncertainty. Forward simulations past the end of the data series are shown for both the IPM and the RR (orange points, posterior median; orange error bars, 95% credible intervals) models. Bottom row: time series of estimated recruits per spawner under the IPM and RR models. Symbols are as above, but only the process error credible interval is shown for the IPM because recruits per spawner is not a directly observed quantity.

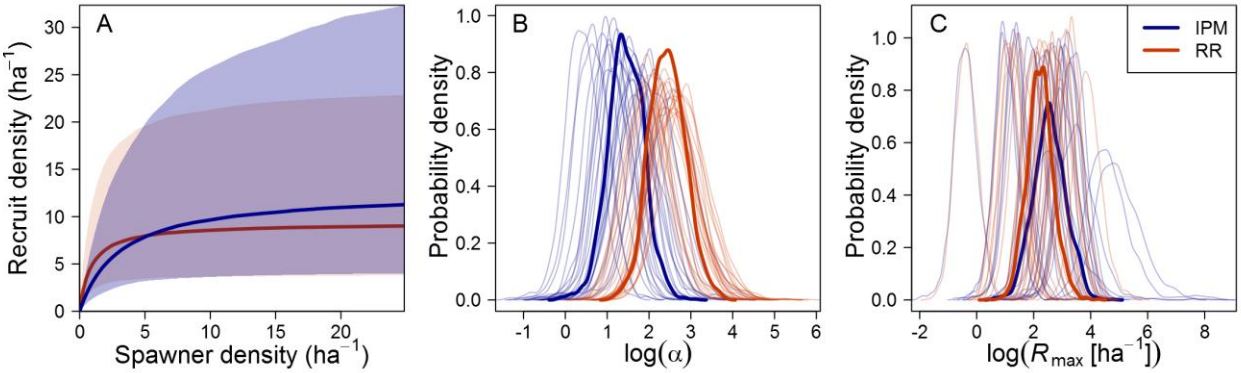

Figure 2. Estimated spawner-recruit relationships at the ESU (i.e., hyper-mean) level (A), and the posterior distributions of intrinsic productivity (B) and capacity (C) for the IPM (blue) and the RR model (red). Thick lines in (A) are the median; shaded regions represent the 95% credible intervals. Thick lines in (B) and (C) are for the ESU-level hyper-means; thin lines are for each of 24 populations.

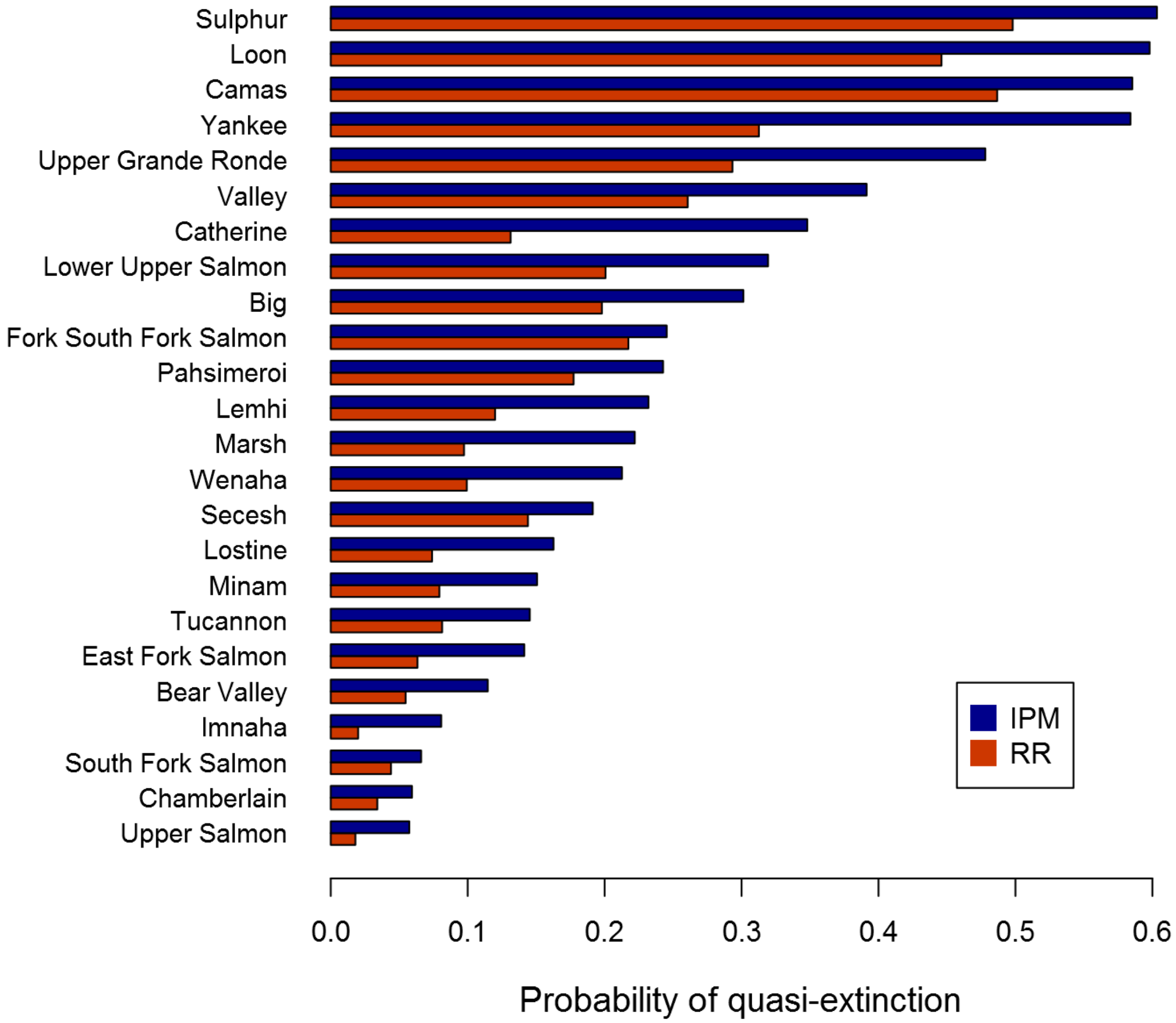

Figure 3. Posterior predictive probabilities of quasi-extinction for each of 24 populations of Snake River spring/summer Chinook salmon in the RR and IPM models. The quasi-extinction threshold is defined as a four-year running mean of 50 spawners, and risk is evaluated over a 50-year future time horizon.

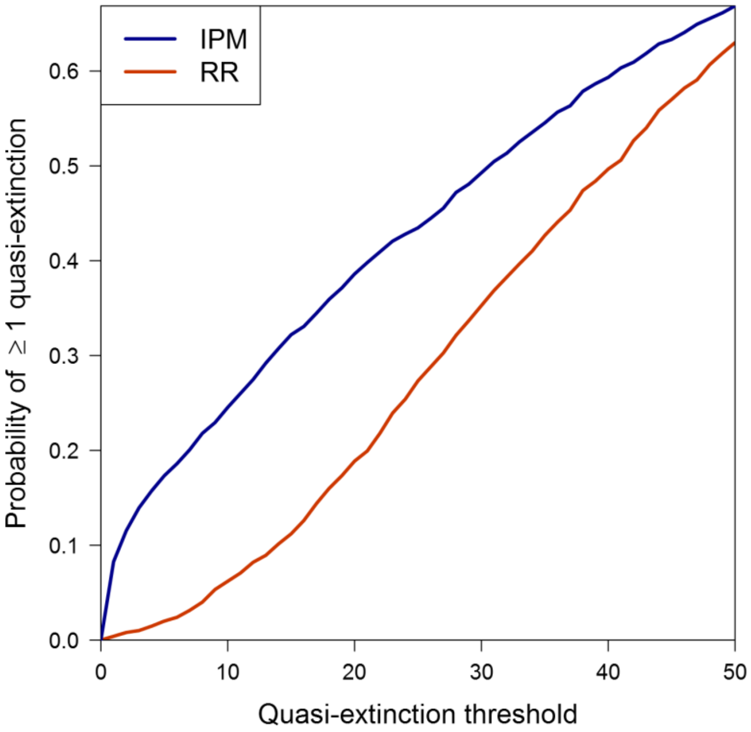

Figure 4. Posterior predictive probabilities of at least one quasi-extinction event among all populations in the ESU, as a function of the quasi-extinction threshold (defined in terms of the four-year running mean of spawner abundance).

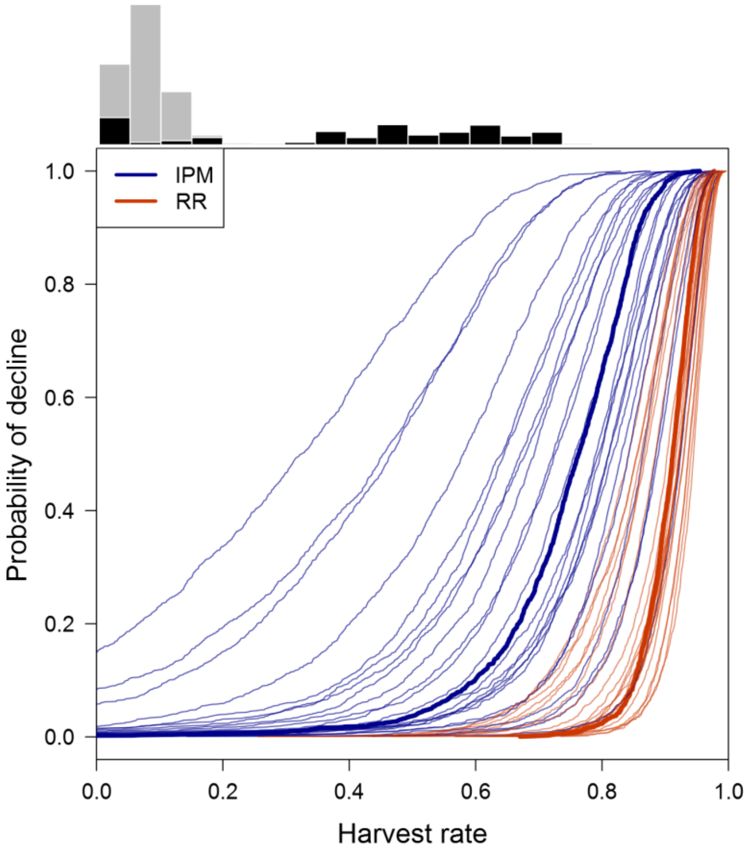

Figure 5. Cumulative probability distributions of the maximum harvest rate, defined as the level of harvest (or additional mortality from any source) above which the deterministic population growth rate would fall below replacement. Estimates are shown at the ESU level (thick curves) and for each of 24 populations (thin curves) under the IPM (blue) and RR model (red). The stacked histogram shows the distribution of observed harvest rates on all populations before (black) and after (gray) 1980.

CHAPTER 8: INTERMEDIATE MODEL

8.a Building A State-Space Life Cycle Model for Naturally Produced Snake River Fall Chinook Salmon

Russell W. Perry, John. M. Plumb, Kenneth F. Tiffan
U.S. Geological Survey, Western Fisheries Research Center, Columbia River Research Laboratory, 5501 A Cook-Underwood Road, Cook, Washington 98605 USA

William P. Connor
U. S. Fish and Wildlife Service, Idaho Fishery Resource Office, 276 Dworshak Complex Drive, Orofino, Idaho 83544, USA

Thomas D. Cooney
National Marine Fisheries Service, Northwest Fisheries Science Center, Fish Ecology Division, 525 Northeast Oregon Street, Portland, Oregon 97232-2737, USA

William Young
Nez Perce Tribe, Department of Fisheries Resources Management, Post Office Box 365, Lapwai, Idaho, 83540, USA

Introduction

In 1992, Snake River basin fall Chinook salmon (*Oncorhynchus tshawytscha*) were listed for protection under the U.S. Endangered Species Act (NMFS 1992) and the population remained below 1000 individuals until 2000. Since then, returns from natural production has rebounded to over 20,000 spawners owing to a host of factors including reduced harvest (Peters et al. 2001), stable minimum spawning flows (Groves and Chandler 1999), summer flow augmentation (Connor et al. 2003), predator control (Beamesderfer et al. 1996), hatchery supplementation (Rosenberger et al. 2017), improved juvenile passage structures (Adams et al. 2014), summer spill operations (Perry et al. 2006; Adams et al. 2008), and periods of favorable ocean conditions and food availability (Logerwell et al. 2003; Peterson et al. 2014). Given this change in abundance coincident with numerous management actions and fluctuation in environmental drivers, quantifying which factors contributed to the observed rebound in natural production can provide critical insights into future management actions for this at-risk population.

Multistage life cycle models provide a powerful analytical framework for understating how each life stage of a population contributes to population growth rate (Moussalli and Hilborn 1986; Greene and Beechie 2004). Multistage models may also be used as an analytical framework to explicitly estimate demographic parameters of a population model. This approach has an advantage over single-stage stock-recruitment models by allowing population growth rates to be partitioned among life stages rather than aggregated over an entire life cycle. Such partitioning allows for estimating 1) stage-specific density dependence, and 2) stage-specific effects of environmental factors or management actions. For example, Zabel et al. (2006) estimated parameters of a multistage model used in the context of a population viability analysis for spring/summer Chinook salmon in the Snake River, but such an approach has yet to be applied to fall Chinook salmon in the Snake River basin.

Typically, data informing estimates of abundance at particular “check points” in the life cycle determines the complexity of the multistage model that can be fit to the data. For fall Chinook salmon, we are developing a two-stage model that encompasses: 1) upstream passage of spawners at Lower Granite Dam (LGR) to the subsequent downstream passage of their progeny at the dam, and 2) downstream passage of juveniles at LGR to their subsequent return from the ocean and passage at the Dam 2–6 years later. This approach partitions the life cycle of fall Chinook salmon both spatially and temporally, which allows us to fit and compare alternative models with covariates specific to each stage. Our previous report to the ISAB (Zabel et al. 2013) detailed methods for estimating abundance of naturally produced adults and juveniles passing Lower Granite Dam, which provides the requisite data for fitting a two-stage model.

The intent of this report is to describe the structure of the two-stage life cycle model, present preliminary results from fitting the model to data, and outline future directions and developments.

As is clear from the diversity of models presented in this report, "life cycle models" range from very simple theoretically based population models (e.g., the Beverton-Holt stock-recruitment model) to very complex spatially explicit simulation models linked to hydrosystem hydrodynamic models (e.g., the COMPASS model for a single transition in a life cycle model, Zabel et al. 2008). We chose to develop a model of intermediate complexity that casts the two-stage life cycle model in a state-space framework (Newman et al. 2014). We chose to use a state-space framework implemented in a Bayesian framework because:

- It provides both a statistical estimation framework for retrospective statistical analysis and a stochastic simulation framework for prospective analysis to evaluate alternative management actions.
- Abundance estimates are uncertain. A state-space framework accounts for observation uncertainty in the abundance estimates and other data (e.g., age structure) while simultaneously estimating process uncertainty.
- It allows for missing data. By drawing missing data from an appropriate probability model, uncertainty owing to missing data can be propagated without having to omit data or assume fixed values for missing data.

Thus, a two-stage state-space life cycle model for fall Chinook salmon strikes an appropriate balance between model complexity, tractability, and applicability given the goals of performing both retrospective and prospective analysis to guide future management of this population.

Essential Features of the Life Cycle Model

It is important to note that our life cycle model is under continual development. As such, first we describe the essential features of the ideal life cycle model to be developed and then we describe the current state of the life cycle model. As illustrated in the life cycle schematic in Figure 1, the essential feature of the ideal life cycle model will include:

- <u>Natural production from three spawning aggregates</u>: A single spawning aggregate occupies Upper Hells Canyon (f_U, in Figure 1). The Lower Hells Canyon spawning aggregate includes the Lower Hells Canyon spawning area, Imnaha River lower reach, Salmon River lower reach, and Grande Ronde River lower reach (f_L in Figure 1). The Clearwater spawning aggregate includes the Clearwater River lower reach, Clearwater upper reach, SF Clearwater lower reach, MF Clearwater, and the Selway lower reach (f_C in Figure 1). Spatial structure and diversity are key aspects of Viable Salmon Populations. The contrasting thermal regimes of these spawning aggregates drive variation in juvenile outmigration strategies (early versus late) that may ultimately influence the resiliency of the aggregate population.
- <u>Age structure in juvenile outmigrants</u>. Juvenile fall Chinook salmon in the Snake River basin exhibit two outmigration strategies at Lower Granite Dam (J_0 and J_1 in Figure 1): early (March – October in brood year *y*+1), and late (November – June in brood year *y*+2). Early and late migrants experience different hydrosystem conditions that may differentially affect their survival.
- <u>Age- and outmigration strategy-specific ocean survival rates</u>.
- <u>Maturation rates by age, sex, and outmigration strategy</u>. Juveniles that pass Lower Granite Dam as subyearlings may subsequently enter the ocean as yearlings (M_1 in

Figure 1). These different outmigration strategies may help to buffer the population against unfavorable environmental conditions for a particular strategy in some years, as is evidenced by disproportionate adult returns of a given outmigration in some years.

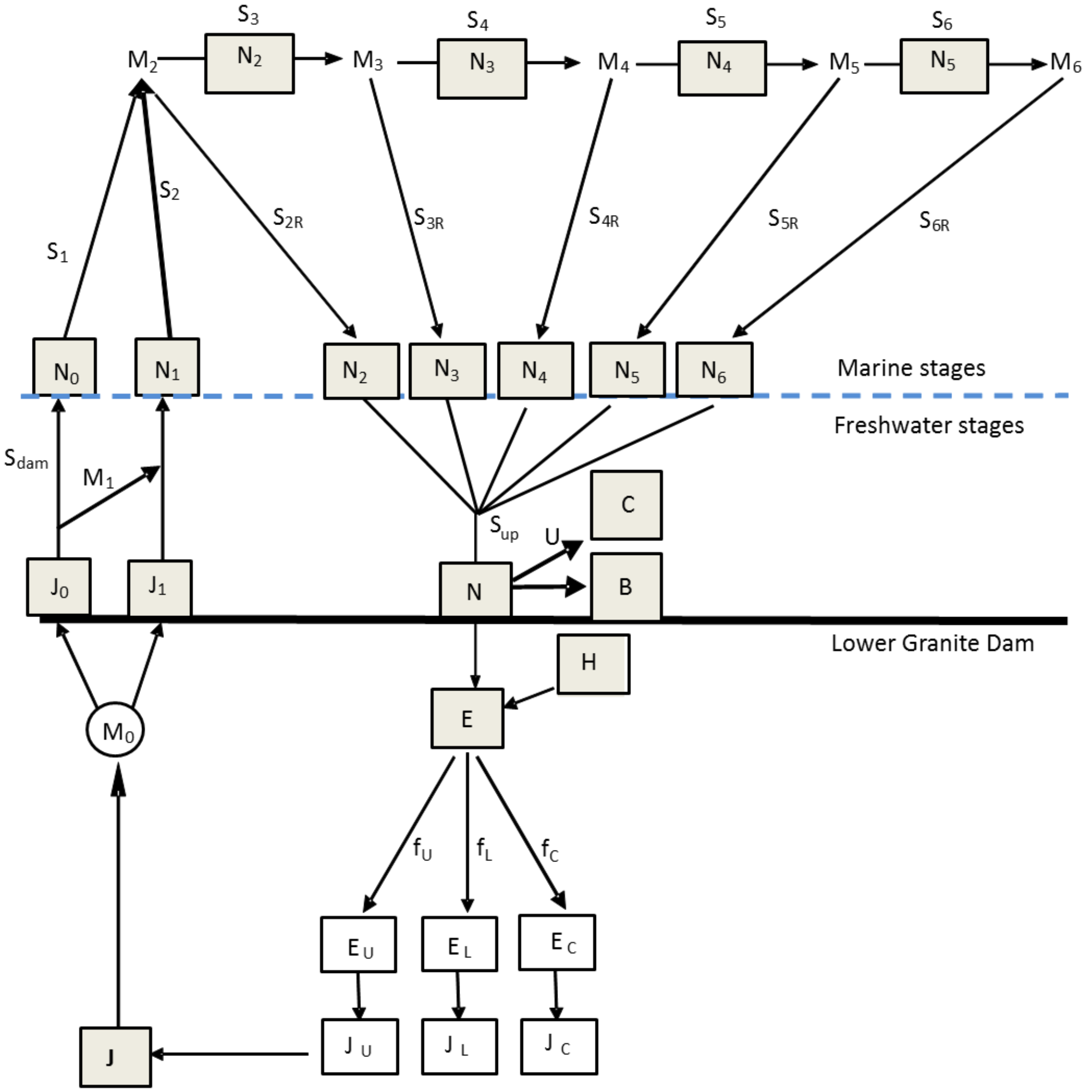

Figure 1. Schematic of the ultimate life cycle model for Snake River basin fall Chinook salmon including three spawning areas (f_U = Upper Hells Canyon, f_L = Lower Hells Canyon, f_C = Clearwater), juveniles produced within each spawning aggregate (J_U, J_L, and J_C), early (J_0) and late juvenile (J_1) juvenile migrants at Lower Granite Dam, hydrosystem survival (S_{dams}), transition of early migrants from subyearling at Lower Granite to yearlings at ocean entry ($J_0 \rightarrow N_1$), age, sex, and outmigration-specific maturation and annual ocean survival probabilities (only age structure shown for brevity), adult returns (N), and escapement (E) past Lower Granite Dam after accounting for ocean and in-river harvest (C) and supplementation of hatchery-origin fish (H), and brood stock removal (B).

- Hatchery supplementation, harvest, and hydrosystem impacts (H, C, S_{dam} and S_{up} in Figure 1).

A major goal of the ideal life cycle model is to track outmigration strategies in progeny from each spawning aggregate through the entire life cycle to understand how each spawning aggregate contributes to the diversity and resiliency of the aggregate stock complex. Although a formidable task, particularly with respect to estimating parameters of this model, this structure will allow managers to determine the best mix of management actions to maintain a viable population in perpetuity.

In Figure 2, we illustrate the structure of the current life cycle model. Critical features that will allow us to extend this model include age, sex, and outmigration strategy in adult returns, age structure in juvenile life stage, and accounting for hatchery supplementation, harvest, and broodstock removal. However, the model does not currently track outmigrant strategy through the life cycle, nor does it include the three spawning aggregates. Nonetheless, the modeling framework we present here takes an important step towards the ultimate model structure we describe above.

The Two-Stage State-Space Life Cycle Model

We formulated our two-stage state-space life cycle model for Snake River basin fall Chinook salmon by building upon the single-stage state-space framework first developed by Fleischman et al. (2013) and extended by Scheuerell et al. (In press). We extended the work of these authors by 1) breaking the life cycle into two stages and 2) including not only age structure in each stage, but also sex and juvenile out-migration strategies in the adult returns.

The state-space model consists of two parts: (1) a process model for the underlying state dynamics, and (2) an observation model that links the data to the true underlying state. The state-space model may also be thought of as a hierarchical model where the state (abundance) evolves according to a population dynamics process model (e.g., a Ricker model) with some process error, and observations on the state ("the data") are made conditional on the true but unobservable state. As a simple example, consider

$$N_t \sim \text{lognormal}\left(\mu_t, \sigma_\text{P}\right)$$

$$\hat{N}_t \mid N_t \sim \text{lognormal}\left(N_t, \sigma_\text{O}\right)$$

where N_t is the true abundance at time *t*, μ_t is the mean abundance at time *t*, σ_P is the process error, $\hat{N}_t \mid N_t$ is the observed estimate of abundance given the true abundance at time *t*, and σ_O is the observation error.

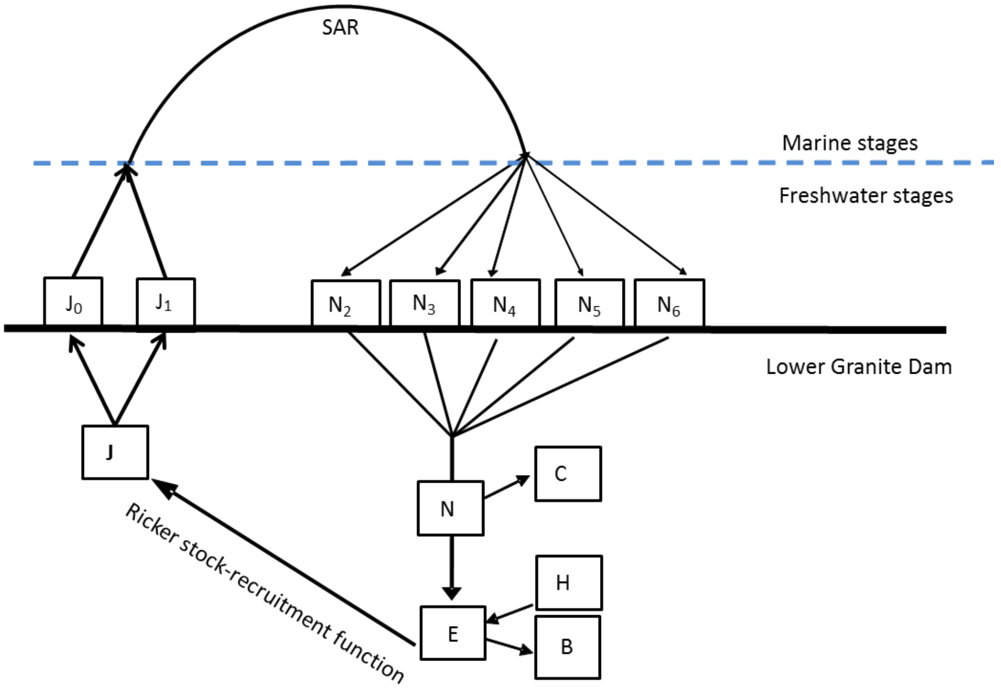

Figure 2. Schematic illustrating the structure of the current two-stage life cycle model for Snake River fall Chinook salmon. The model includes juvenile age-structure at Lower Granite Dam (J_0 = early migrants, J_1 = late migrants) and age, sex, and outmigration strategy (subyearling ocean entry, yearling ocean entry) in the adult returns (only age structure is shown for brevity). The spawner-to-juvenile transition is modeled with an aggregate Ricker function and the juvenile-to-adult transition is modeled with an aggregate smolt-to-adult return rate (SAR).

The State Model

For the adult to juvenile transition, we used the Ricker model to express the number of juveniles passing LGR as a density-dependent function of the number of female adults passing LGR in brood year *y* (Ricker 1954):

(1) $$\ln(R_{\mathrm{J},y}) = \ln(E_{\mathrm{F},y}) + \ln(\alpha) - \beta E_{\mathrm{F},y} + \varepsilon_{\mathrm{P,J},y}$$

where $R_{\mathrm{J},y}$ is the true but unobserved number of juvenile recruits produced by female adult escapement $E_{\mathrm{F},y}$ in brood year *y*, α is the productivity parameter estimating the slope at the origin (juvenile recruits per female spawner), β is the density dependence parameter where $1/\beta$ estimates the spawner level producing the maximum recruitment (S_{max}), and $\varepsilon_{\mathrm{J},y}$ is a normally distributed process error with standard deviation $\sigma_{\mathrm{P,J}}$.

For the juvenile to adult transition, we model the number of adult returns as a lognormal function of a density independent smolt-to-adult return rate (SAR):

(2) $$\ln(R_{\mathrm{A},y}) = \ln(R_{\mathrm{J},y}) + \ln(\mathrm{SAR}) + \varepsilon_{\mathrm{P,A},y}$$

where $R_{\mathrm{A},y}$ is the number of adult recruits (male and female) produced from the $R_{\mathrm{J},y}$ juveniles passing LGR that arose from female spawners in brood year *y* and $\varepsilon_{\mathrm{P,A},y}$ is a normally distributed process error with standard deviation $\sigma_{\mathrm{P,A}}$.

Given that juveniles pass LGR at ages 1-2 (from brood year not actual fish age) and adults return at ages 2-6, the initial two years of juvenile recruits and six years of adult recruits that produced returns beginning in 1992 were not linked to the two-stage stock-recruitment model. These initial state vectors were estimated as draws from common log-normal distributions with parameters $\ln\left(R_{\mathrm{J},0}\right)$, σ_{RJ0} and $\ln\left(R_{\mathrm{A},0}\right)$, σ_{RA0}, respectively for juveniles and adults.

Given juvenile recruits, the number of juveniles a_{J} passing LGR in calendar year *t* was modeled as:

(3) $$J_{t,a_{\mathrm{J}}} = R_{\mathrm{J},t-a_{\mathrm{J}}}\, p_{\mathrm{J},t-a_{\mathrm{J}},a_{\mathrm{J}}}$$

where $J_{t,a_{\mathrm{J}}}$ is the number of juvenile in year *t* of age a_{J} and $p_{\mathrm{J},t-a_{\mathrm{J}},a_{\mathrm{J}}}$ is the proportion of juvenile recruits from brood year $y = t - a_{\mathrm{J}}$ emigrating at age a_{J} (Figure 3).

Given adult recruits, we model the number of adults returning at age a_{A} of sex *s* and outmigration strategy *o* as:

(4) $$N_{t,a_{\mathrm{A}},s,o} = R_{\mathrm{A},t-a_{\mathrm{A}}}\, p_{a_{\mathrm{A}},t-a_{\mathrm{A}},s,o}$$

where $N_{t,a_{\mathrm{A}},s,o}$ is the number of adults returning in year *t* at age a_{A}, of sex *s*, and outmigration strategy *o* and $p_{a_{\mathrm{A}},t-a_{\mathrm{A}},s,o}$ is the proportion of the recruits from brood year $y = t - a_{\mathrm{A}}$ returning at a_{A}, sex *s*, and outmigration strategy *o* (Figure 3). Here, outmigration strategy refers to whether juveniles entered the ocean as subyearlings or yearlings, which differs from the proportion of brood-year juveniles passing LGR as subyearlings or yearling because fish that pass LGR as subyearlings may subsequently enter the ocean as yearlings. Given 5 adult age classes, 2 ages, and 2 outmigration strategies, the brood-year specific return probabilities, $\mathbf{p}_{\mathrm{A},y} = p_{a_{\mathrm{A}},t-a_{\mathrm{A}},s,o}$, form a vector of length 20.

Figure 3. Illustration of the reconstruction of age specific juvenile abundance (J0 and J1) and age specific returns conditional on outmigration strategy (J0 Adults, J1 Adults) from recruits generated by spawners in brood year *y*.

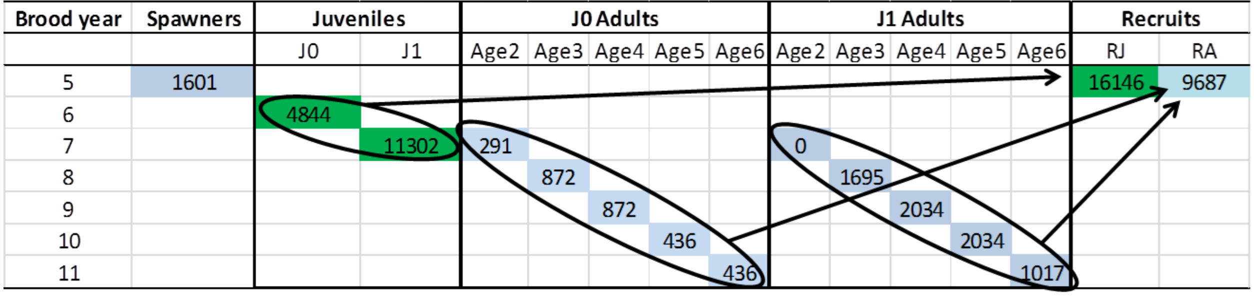

Brood year	Spawners	Juveniles		J0 Adults					J1 Adults					Recruits	
		J0	J1	Age2	Age3	Age4	Age5	Age6	Age2	Age3	Age4	Age5	Age6	RJ	RA
5	1601													16146	9687
6		4844													
7			11302	291					0						
8					872					1695					
9						872					2034				
10							436					2034			
11								436					1017		

Vectors of brood-year specific outmigration $\mathbf{p}_{\mathrm{J},y}$ and return $\mathbf{p}_{\mathrm{A},y}$ probabilities were modeled hierarchically as draws from a Dirichlet distribution:

(5) $$\mathbf{p}_{i,y} \sim \mathrm{Dirichlet}\left(\gamma_i\right)$$

where *i* = J or A and γ_i is a vector of parameters of the same length as $\mathbf{p}_{i,y}$. Under this formulation, the expected proportion of the *k*th class is

(6) $$\frac{\gamma_{k,i}}{\sum_{k=1}^{K} \gamma_{k,i}}$$

and the inverse of the sum in the denominator scales with annual variation in $\mathbf{p}_{i,y}$.

Given age-specific juvenile emigration and adult returns from brood year *y* in calendar *t*, the total number of juveniles passing LGR in calendar year *t* is the sum of the abundance-at-age over all ages:

(7) $$J_t = \sum_{a_\mathrm{J}} J_{t,a_\mathrm{J}} \ .$$

For adult returns, the total number of returning adults in year *t* is the sum of the abundances across all age, sex, and outmigration classes:

(8) $$N_t = \sum_{s} \sum_{o} \sum_{a_\mathrm{A}} N_{t,a_\mathrm{A},s,o} \ .$$

Returns of subclasses in year *t* are calculated similarly by summing over the appropriate indices. For example, the number of female returns in year *t* is

(9) $$N_{\mathrm{F},t} = \sum_{o} \sum_{a_\mathrm{A}} N_{t,a_\mathrm{A},s=\mathrm{F},o} \ .$$

In addition, the age, sex, and outmigration structure in the adult returns each calendar year is

(10) $$q_{a_{\mathrm{A}},t,s,o} = \frac{N_{a_{\mathrm{A}},t,s,o}}{N_t}$$

where $q_{a_{\mathrm{A}},t,s,o}$ is the fraction of the adults returning in year *t* at age a_{A}, sex *s*, and outmigration strategy *o*.

Escapement of spawners past LGR in calendar year *t* includes hatchery-origin adults allowed to pass LGR and spawn in the wild (H_t) plus naturally-produced spawners (N_t) that survive harvest (C_t) less naturally produced fish taken for hatchery brood stock (B_t):

(11) $$E_t = N_t - C_t - B_t + H_t \ .$$

The annual harvest rate is a composite of ocean and in-river harvest that is assumed constant across ages, sexes, and outmigration strategies of returns in a given year such that catch is:

(12) $$C_t = U_t N_t$$

where U_t is the composite harvest rate representing the fraction of returns that were harvested in year *t*.

Escapement of female spawners, which dictates juvenile recruits, is:

(13) $$E_{F,t} = N_{F,t} - q_{F,t} C_{F,t} - q_{F,t} B_t + f_{F,t} H_t$$

where $f_{F,t}$ is the fraction of hatchery-origin adults that are female and $q_{F,t}$ is the proportion of females in naturally produced returns, calculated as:

$$q_{\mathrm{F},t} = \sum_{o} \sum_{a_{\mathrm{A}}} q_{a_{\mathrm{A}},t,s=\mathrm{F},o} \ .$$

The Observation Model

Observations to inform the parameters of the state model include:

1) Estimates of age-specific (i.e., early and late migrants) abundance of naturally produced juveniles passing Lower Granite Dam for 1992 – 2014,
2) Estimates of abundance of hatchery-origin and naturally produced adults passing above Lower Granite Dam for 1992 – 2014,
3) Estimates of run composition of hatchery and naturally produced adults in terms of age, sex, and outmigration strategy for 2004 – 2014,
4) Estimates of the number of naturally produced adults removed for hatchery broodstock for 1992 – 2014, and
5) Estimates of ocean and in-river harvest rate indices for 1992 – 2007.

As this list of input data indicates, each observation component is an estimate of the true value and therefore has uncertainty associated with the estimate. This uncertainty arises from a number of sources such as sampling for only a fraction of the time fish are passing the dam (e.g., window counts for adults and bypass sample tank for juveniles) and having to estimate the fraction of unmarked fish that are of hatchery-origin (for both juveniles and adults). Although the state-space model is designed to accommodate observation error, we have yet to quantify it for a number of the inputs. Since our last report to the ISAB, we have made great strides to develop estimation techniques for estimating both juvenile abundance and the variance associated with this estimate (see Appendix). While robust estimation techniques have been developed for estimating abundance and run composition of naturally produced adults (Zabel et al. 2013), we have yet to develop variance estimators. In the observation model, we use estimates uncertainty where available and assume values for the magnitude of observation error where estimates of uncertainty are unavailable.

Estimates of naturally produced abundance of adults passing LGR were assumed to be lognormally distributed about the true abundance:

$$\hat{E}_t \sim \text{lognormal}\left(E_t, \sigma_E\right) \tag{14}$$

where $\hat{E}_t$ are the estimates of natural adults passing over LGR arising from the run reconstruction methods presented in the previous report to the ISAB (Zabel et al. 2013) and σ_E is the observation error. Since we do not have estimates of observation error, we set the value of σ_E based on a coefficient of variation (CV) of 0.12, which was the mean CV among years for the juvenile abundance estimates. CVs were converted to lognormal variance parameters according to $\sigma^2 = \ln\left(\text{CV}^2 + 1\right)$. We assumed no observation error in the estimates of hatchery-origin abundance passing LGR ($\hat{H}_t$ and $\hat{H}_{F,t}$) and in estimates of removals of naturally produced adults for hatchery broodstock ($\hat{B}_t$).

Although we had estimates of the total number of hatchery-origin adults for 1992-2014, we had information on sex structure for only 2004-2014. Therefore, we assumed that estimated year-specific female proportions arose from an over-dispersed binomial model where:

$$\begin{aligned} &\hat{H}_{F,t} \sim \text{Binomial}\left(f_{\text{F},t}, \hat{H}_t\right), \\ &\text{logit}\left(f_{\text{F},t}\right) = \mu_{\text{F}} + \omega_t, \text{ and} \\ &\omega_t \sim \text{Normal}\left(0, \sigma_f\right). \end{aligned} \tag{15}$$

Here, μ_{F} is the mean proportion of females in hatchery-origin adults across years and ω_t is a normally distributed error on the logit scale with standard deviation σ_f. The parameters of this logit-normal model were estimated from years with data (2004-2014) , and then $f_{\text{F},t}$ and $\hat{H}_{F,t}$ were drawn from this hierarchical model for years without data (1992-2003).

Age, sex, and outmigration structure in the adult return data were obtained from the run-reconstruction analysis presented in the previous report to the ISAB (Zabel et al. 2013). Run-reconstruction estimates exist only for 2004-2014. Therefore, similar to the proportion of hatchery-origin females, we drew the brood year return probabilities for 1992-2003 ($p_{y,a_{\mathrm{A}},s,o}$) from the Dirichlet distribution described previously. Parameters of the Dirichlet distribution were estimated by assuming that run-reconstruction estimates represented counts of a multinomial distribution:

$$\hat{n}_{t,a_{\mathrm{A}},s,o} \sim \text{Multinomial}\left(q_{t,a_{\mathrm{A}},s,o}, \sum_{a_{\mathrm{A}},s,o} \hat{n}_{t,a_{\mathrm{A}},s,o} \right) \tag{16}$$

where $\hat{n}_{t,a_{\mathrm{A}},s,o}$ is the estimated number of adults at age a_{A} of sex *s* and outmigration strategy *o*, and $q_{t,a_{\mathrm{A}},s,o}$ are the proportions of these groups returning in calendar year *t* that arise as functions of the brood year return probabilities $p_{y,a_{\mathrm{A}},s,o}$ in the state model. We assume no observation uncertainty in $\hat{n}_{t,a_{\mathrm{A}},s,o}$, but recognize this as an important area of future improvement for this model.

Composite harvest rates were derived from estimates of ocean and in-river harvest rate indices as follows:

$$\hat{U}_t = 1 - \left(1 - \hat{U}_{\mathrm{O},t}\right)\left(1 - \hat{U}_{\mathrm{R},t}\right) \tag{17}$$

where $\hat{U}_{\mathrm{O},t}$ and $\hat{U}_{\mathrm{R},t}$ are the fraction of fish in return year *t* harvested in ocean (O) and in-river (R) fisheries. These harvest rates are estimated as the average harvest rate across all ages, sexes, and outmigration strategies, and therefore assumes constant harvest rates across these groups. In addition, we assume these harvest rates are known without error.

Estimates of age-specific abundance of naturally produced juvenile fall Chinook salmon passing Lower Granite Dam were assumed to be lognormally distributed about the true value:

(18) $$\hat{J}_{t,a_{\mathrm{J}}} \sim \mathrm{lognormal}\left(J_{t,a_{\mathrm{J}}}, \sigma_{t,a_{\mathrm{J}}} \right)$$

where $\hat{J}_{t,a_{\mathrm{J}}}$ is the estimate of abundance for 2 age classes which we define to be early migrants (March – October in brood year *y*+1) and late migrants (November – June in brood year *y*+2). For the early migrants, $\sigma_{t,1}$ was set according to annual estimates of the CV in abundance, which ranged from 2-42% (see Appendix for estimation methods). For the late migrants, we set $\sigma_{t,2} = \sigma_{t,1}$.

Factors affecting key demographic parameters

Exogenous environmental factors can affect survival during both the adult-to-juvenile transition upstream of Lower Granite Dam, and the juvenile-to-adult transition downstream of Lower Granite Dam. Our model can be extended to allow both productivity (α) in the adult-to-juvenile transition and SAR in the juvenile-to-adult transition to be expressed as function of covariates hypothesized to influence survival:

(20) $$\ln(\alpha_y) = \mu_\alpha + \sum_{k=1}^{K} \theta_k X_k$$

(21) $$\ln(\mathrm{SAR}_y) = \mu_{\mathrm{SAR}} + \sum_{j=1}^{J} \lambda_j Z_j$$

where both annual productivity and SAR are expressed on a log scale, μ is the overall log-mean of α or SAR when covariates are centered about their mean, θ_k is the effect of the *k*th covariate X_k on α, and λ_j is the effect of the *j*th covariate Z_j. Covariates are expressed on an annual scale and may be lagged appropriately relative to brood year to represent alternative hypotheses about when a given covariate influenced a particular life stage and demographic parameter. For example, we may hypothesize that the SAR of juveniles arising from brood year *y* is influenced by spill levels in brood year *y*+1 corresponding to the time period when early migrants from brood year *y* are migrating through the hydrosystem.

For this analysis, we selected two covariates, on for α and one for SAR, to illustrate the utility of the two-stage state-space model as a tool for performing retrospective analysis in the context of statistical life cycle model. We cannot overemphasize the preliminary nature of the analysis of the covariates, and send an explicit cautionary note against the use of the results within the context of management discussions. We model juvenile productivity (α) as a function of the fraction of late-season migrants of a given brood year. We modeled SAR as a function sea surface temperature during the winter following ocean entry of subyearling juveniles. Sea surface temperature was standardized to have a mean of zero and a standard deviation of one.

Parameter estimation

All parameters and unknown states were estimated in a Bayesian framework using JAGS software (Plummer 2009) as implemented through the runjags package of the R statistical programming platform (R core team 2017). JAGS is a Bayesian estimation software package that implements Markov Chain Monte Carlo (MCMC) sampling using a Gibbs or Metropolis-Hastings sampler. Prior distributions for parameters were set according to Fleischman et al. (2013) and Scheuerell et al. (In press). We ran three independent MCMC chains each for 80,000 iterations, discarding the first 30,000 to ensure each the chain had converged to its stationary stable distribution. We then thinned the final 50,000 iterations to 1 in 50 to reduce autocorrelation, yielding a final sample of 1000 draws from each chain. Convergence of each parameter was checked visually to ensure mixing of the chains, and quantitatively by ensuring that the Rubin-Gelman statistic ($\hat{R}$) was less than 1.1. Here we present results from two models. First we present parameter and state estimates from a model fitted without covariates. Second, we fit the model with covariates on α and SAR and present results for that model.

Results

Adult and Juvenile Abundance at Lower Granite Dam

The abundance and escapement of adult salmon upstream of LGR increased over time with the lowest escapement estimated in 1994 (791 fish) and the highest in 2014 (59,747 fish; Figure 4). The escapement of hatchery-origin and naturally produced fish increased over time. Escapement of hatchery-origin fish ranged from a low of 306 fish in 1992 to 45,575 fish in 2014, and natural escapement ranged from 306 fish in 1998 to 20,638 fish 2013. The fraction of escapement comprised of hatchery-origin spawners also increased over time, ranging from 36% (306 of 855) in 1992 to 84% (1603 of 1909) in 1998.

The abundance of naturally produced and hatchery-origin juveniles passing LGR also increased overtime. Abundance of naturally produced juveniles passing LGR ranged from 23,714 fish in 1992 to 1,112,698 fish in 2004 (Figure 5). Similarly, the abundance of hatchery juveniles that passed LGR ranged from zero between 1992 and 1994 to a maximum of 2,790,611 in 2005.

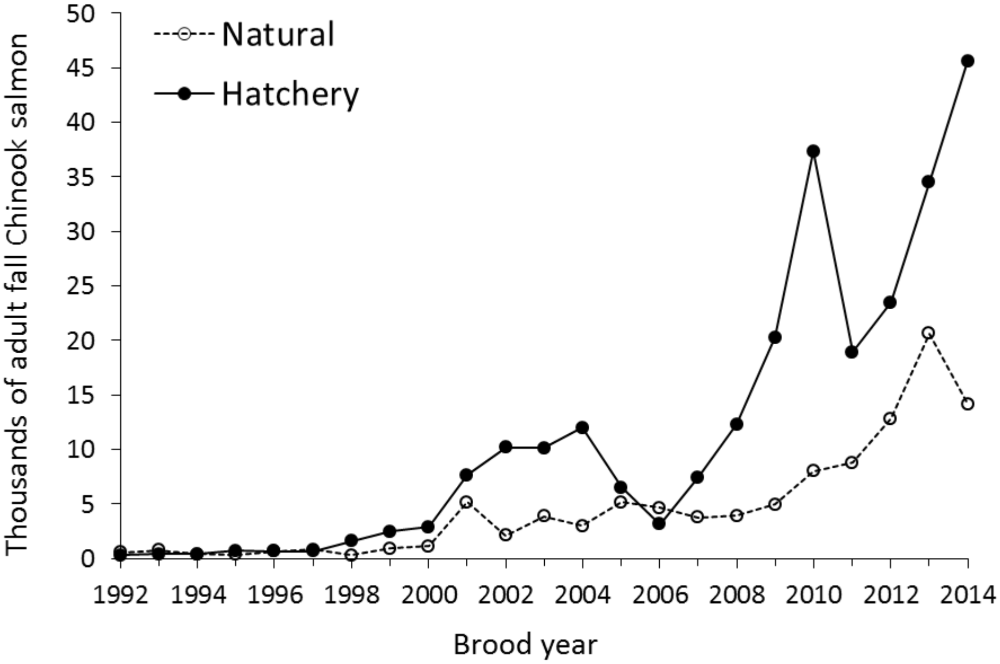

Figure 4. Time series of escapement of Snake River basin fall Chinook salmon above Lower Granite Dam.

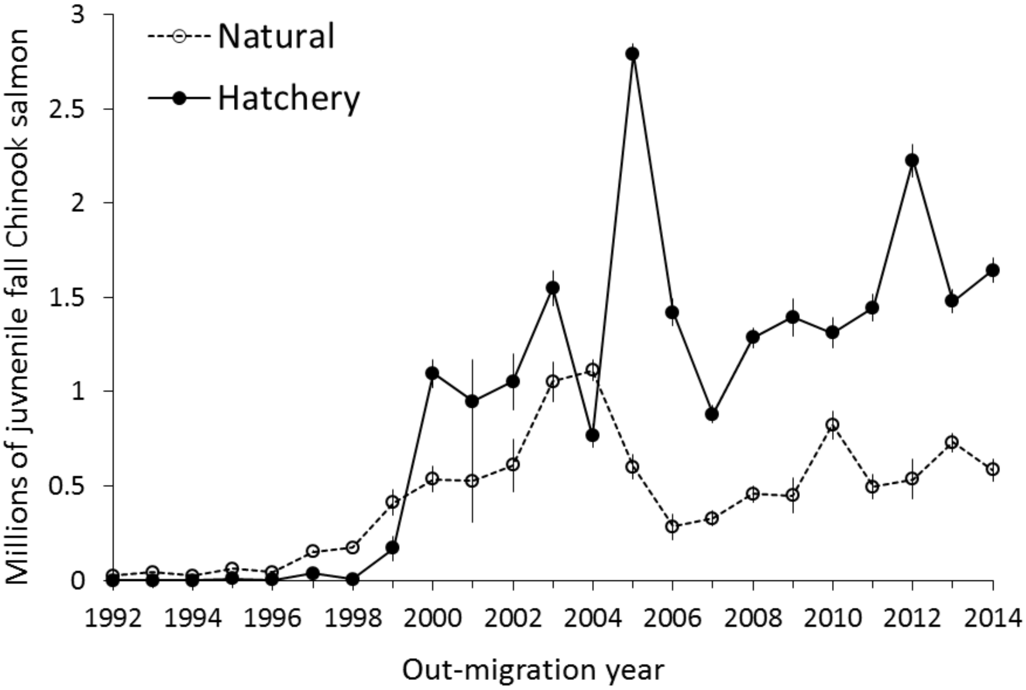

Figure 5. Time series of annual abundance of juvenile fall Chinook salmon passing Lower Granite Dam. Errors represent the 95% credible interval obtained from posteriors of the annual abundance estimates.

Parameter Estimates under the State-Space Model

Posterior distributions provide a complete representation of uncertainty about model parameters (Figure 6). The median of the posterior for mean productivity across years was 268 naturally produced juvenile recruits per female spawner (95% credible interval (CI) = 179 – 381). Given a mean fecundity of 3,750 eggs per female, this equates to a mean egg-to-juvenile survival of 7.1% at low spawner density. Median $S_{\max}$ was 7,311 female spawners (95% CI = 4,910 – 10,621), suggesting declining juvenile recruitment at spawner levels higher than $S_{\max}$ (Figure 7). For the juvenile-to-adult transition, the median estimate of the mean SAR across years was 0.020 (95% CI = 0.013 – 0.028).

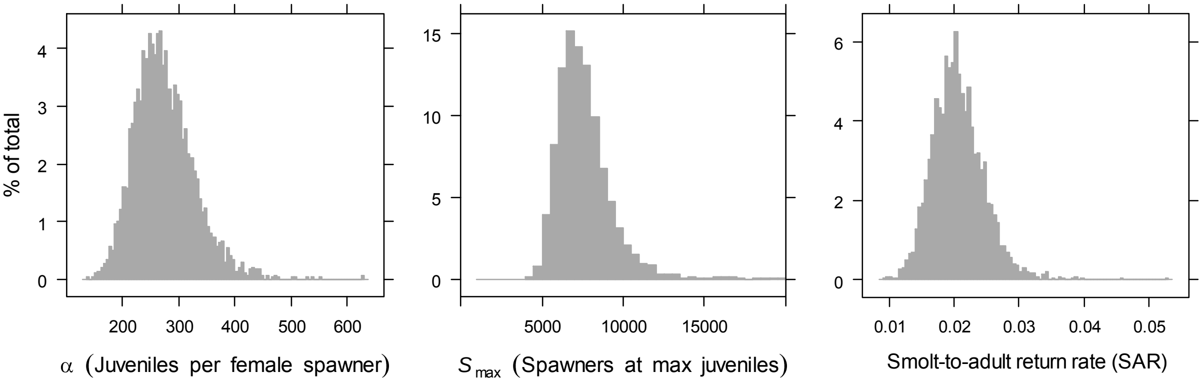

Figure 6. Posterior distributions for mean productivity, $S_{\max}$, and mean SAR of Snake River basin fall Chinook salmon.

The plot of the median Ricker curve illustrates both how recruitment of naturally produced juveniles and juvenile recruits per spawner vary as a function of the number of female spawners (Figure 7). The observations through 2014 provide evidence for overcompensation, illustrating declining recruitment at spawner levels higher than $S_{\max}$. However, this analysis is preliminary and firm conclusions regarding overcompensation should be withheld pending final analysis and inclusion of juvenile abundance estimates from brood year 2015, a high-return year.

Juvenile recruits per female spawner declined from over 500 in 1998 to less than 50 in 2010, providing strong evidence for density-dependent recruitment (Figure 7).

Owing to the hierarchical structure of the state-space model, annual variation in productivity and SAR can be estimated as random effects drawn from estimate of the lognormal process error ($\sigma_{\mathrm{P,J}}$ and $\sigma_{\mathrm{P,A}}$). Both SAR and productivity vary considerably over time, with SAR increasing considerably after 2005 and productivity declining from 1998 – 2008 before increasing to about 300 juveniles per spawner after 2008 (Figure 8). Although SARs here represent pre-fishery and brood stock removal, SARs still appear to be higher than expected relative to fall Chinook populations from the mid-Columbia region (Richards and Pearsons 2016). Prior to this analysis, we suspected our abundance estimates of naturally produced juveniles were negatively biased owing to positive bias in estimates of the daily proportion of fish collected by the juvenile bypass system. Underestimates of natural juvenile abundance would manifest as overestimates in SAR and underestimates in productivity, and we believe these estimates of SAR provide evidence of such bias. We have developed a new statistical model for estimating daily collection probability and are currently in the process of revising the juvenile abundance estimates. Although we expect revised estimates of natural juvenile abundance to increase, we expect little change in the interannual pattern in the estimates.

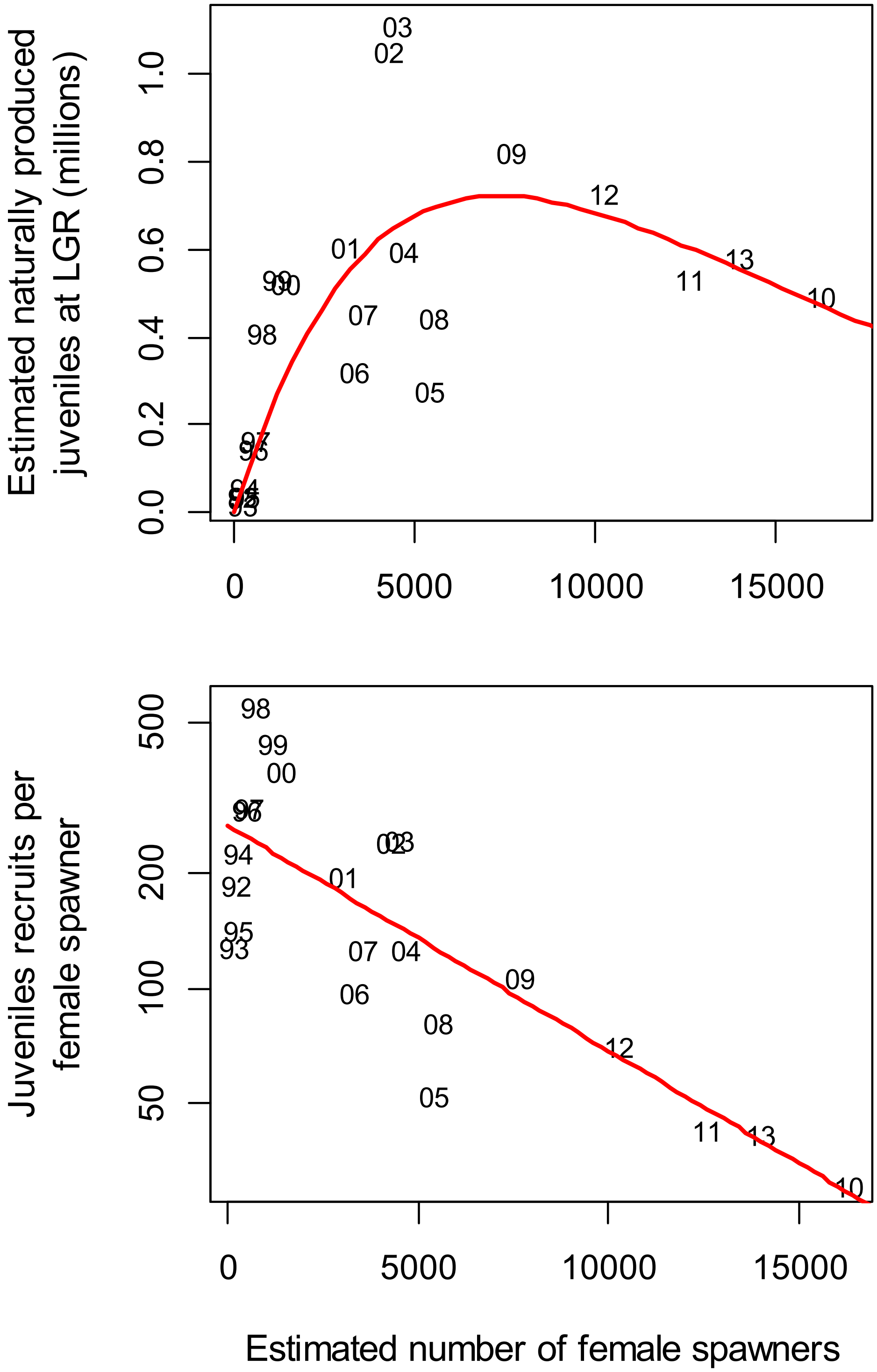

Figure 7. The fitted Ricker function based on posterior medians of parameters expressed as production of juvenile recruits (top panel) and juvenile recruits per spawner (bottom panel). Symbols represent brood years.

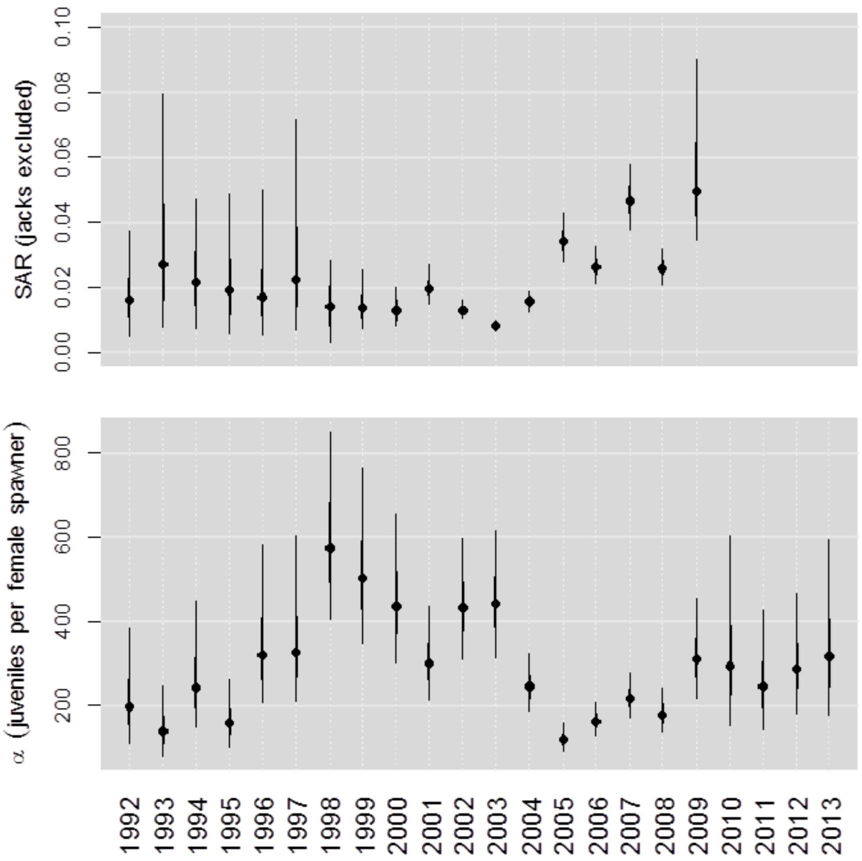

Figure 8. Annual estimates of smolt-to-adult return rate (SAR, top panel) and productivity (bottom panel). Symbols are the medians of posterior distributions, heavy lines represent the 25th-75th percentile, and the thin lines show the 90% credible interval.

Illustrating how Covariates can be Incorporated to Examine Effects on Productivity and SAR

The posteriors for covariate effects indicate strong associations with productivity an SAR when a small proportion of the posterior distributions overlap zero. First, the negative coefficient for the fraction of late season migrants indicated that productivity decreased as the fraction of late season migrants increased. This association makes sense given that survival is a time-dependent process and the longer fish remain upstream of Lower Granite Dam, the lower would be the expected number of juveniles produced per spawner. SST had a negative association with SAR, indicated the as Winter sea surface temperature increased, SAR decreased. This preliminary analysis illustrates how our two-stage space model can be used to understand factors that influence population dynamics during different stages of the life cycle of Snake River basin fall Chinook salmon.

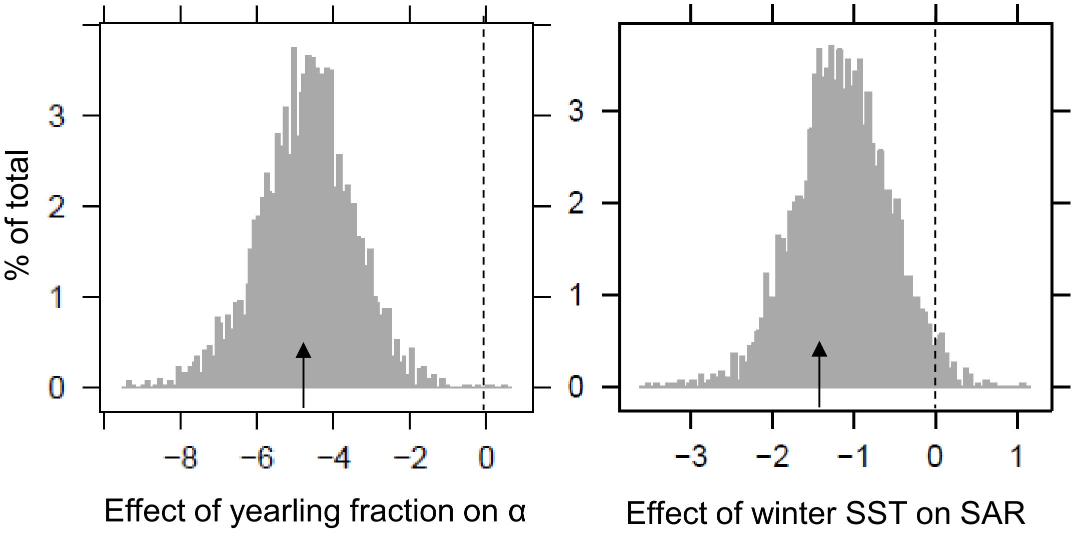

Figure 9. Posterior distributions for covariate effects on juvenile productivity (juveniles per female spawner; α). The dashed lines at zero indicate no effect of the covariate and the arrows indicate the median of the posterior distribution.

Discussion

We illustrate how a life-cycle model of intermediate complexity can be used to understand population dynamics and factors affecting different life stages of Snake River basin fall Chinook salmon. The state-space formulation of the model accounts for both observation and process error, provides estimates of uncertainty in both abundance and demographic parameters, and quantifies contributions of age, sex, and outmigration strategy to the aggregate population. Our formulation of the state-space model provides a wealth of information about population dynamics, much of which was not presented in this report, such as estimates of process uncertainty, proportions of juveniles emigrating as early and late migrants, and the brood year probabilities of returning as adults that entered the ocean as subyearlings and yearlings. For example, 85.9% of the brood year 2000 returns were comprised of juveniles that entered the ocean as yearlings (95% CI = 60.4% - 90.2%), although late migrants at Lower Granite comprised only 2.5% of the brood year 2000 juvenile migrants (95% CI = 1.8-3.4%). Subyearling juveniles from brood year 2000 emigrated during the summer of 2001, a drought year prior to summer spill operations. The disproportionate returns from yearling outmigrants suggests that either 1) subyearlings exhibited very low survival not experienced by yearlings, 2) a large proportion of subyearlings ceased migration downstream of Lower Granite and entered the ocean as yearlings, or 3) a combination of both 1 and 2 occurred. This example highlights the strengths of analyzing population dynamics using a life cycle model couched in a statistical framework such as a state-space model.

Although we have the life cycle model “up and running”, we refrain from drawing too much inference from this initial model fitting because a number of significant updates are required. First and foremost, we have developed a new statistical model that implements a fully parametric version of the Sanford and Smith (2002) method for estimating daily detection probability of PIT tagged fish passing Lower Granite Dam. This element of the juvenile abundance estimation routine is critical for expanding estimates of abundance in the juvenile bypass system to estimates of abundance passing the dam. Second, we plan to develop methods for generating bona fide estimates of uncertainty in aggregate adult abundance estimates and the run reconstruction that provides estimates of outmigration strategy-, age-, and sex-structure. A central challenge with developing a life cycle model for naturally produced fall Chinook salmon in the Snake River basin is that naturally produced fish are indistinguishable from unmarked hatchery fish. Thus, uncertainty associated with estimating abundance of natural-origin adults is non-negligible and may vary among years, and therefore, should be incorporated as observation error in the state-space model. Third, we plan to continue expanding the model's structure to add the three major spawning aggregates, hydrosystem effects, ocean survival, and move toward a structure that tracks juvenile outmigration strategies through the life cycle.

Once these changes are in place, we plan to revise the set of covariates affecting each transition and perform retrospective analysis to understand which factors most influenced population dynamics. Given the fitted model that included covariates under management control, we plan to use the model to perform prospective simulations to understand how alternative management actions or environmental conditions may have influenced past or future populations. For example, what are the chances that Snake River basin fall Chinook salmon would have rebounded (or perished) had not a hatchery supplementation program been implemented , or had improvements not been made to the hydrosystem? Given the fitted model and historic conditions, the life cycle model can be brought to bear to answer such questions.

References

Adams, N.S., J.M. Plumb, R.W. Perry , and D. W. Rondorf . 2014. Performance of a Surface Bypass Structure to Enhance Juvenile Steelhead Passage and Survival at Lower Granite Dam, Washington, North American Journal of Fisheries Management, 34:3, 576-594.

Adams, N.S., J.M. Plumb, T.W. Hatton, E.C. Jones, N. M. Swyers, M. D. Sholtis, R.E. Reagan, and K.M. Cash. 2008. Survival and migration behavior of juvenile salmonids at McNary Dam, 2006. Annual report of Research by the U.S. Geological Survey to the U. S. Army Corps of Engineers, Walla Walla District, Report number 2006, W68SBV60478899, Walla Walla, Washington.

Beamesderfer, R. C. P., D. L. Ward, and A. A. Nigro. 1996. Evaluation of the biological basis for a predator control program on northern squawfish (*Ptychocheilus oregonensis*) in the Columbia and Snake rivers. Canadian Journal of Fisheries and Aquatic Sciences 53:2898–2908.

Connor, W. P., H. L. Burge, J. R. Yearsley, and T. C. Bjornn. 2003. The influence of flow and temperature on survival of wild subyearling fall Chinook salmon in the Snake River. North American Journal of Fisheries Management 23:362–375.

DART (Data Access in Real Time). 2017. Available http://www.cbr.washington.edu/dart/dart.html. (April 2017).

FPC (Fish Passage Center). 2017. Portland, Oregon. Available: www.fpc.org. (April 2017).

Fleischman, S.J., M. J. Catalano, R. A. Clark, and D. R. Bernard. 2013. An age-structured state-space stock–recruit model for Pacific salmon (*Oncorhynchus* spp.). Canadian Journal of Fisheries and Aquatic Sciences 70: 401–414.

Greene, C.M., and T.J. Beechie. 2004. Consequences of potential density-dependentmechanisms on recovery of ocean-type Chinook salmon (*Oncorhynchus tshawytscha*)Canadian Journal of Fisheries and Aquatic Sciences 61:590-602.

Gelman, A., J.B. Carlin, H.S. Stern, and D.B Rubin. 2004. Bayesian Data Analysis. Chapman and Hall, Boca Raton.

Logerwell, E. A., N. J. Mantua, P. W. Lawson, R. C. Francis, and V. N. Agostini. 2003. Tracking environmental processes in the coastal zone for understanding and predicting Oregon coho (*Oncorhynchus kisutch*) marine survival. Fisheries Oceanography 12:554–568.

Moussalli, E. and R. Hilborn. 1986. Optimal stock size and harvest rate in multistage life history models. Canadian Journal of Fisheries and Aquatic Sciences 43:135–141.

Newman, K.B., S.T. Buckland, B.J.T. Morgan, R. King, D.L.Borchers, D.J. Cole, P. Besbeas, O. Gimenez, L. Thomas. 2014. Modeling Population Dynamics: model formulation, fitting and assessment using state-space methods. Methods in Statistical Ecology. Springer publishing. New York, USA.

NMFS (National Marine Fisheries Service). 1992. Threatened status for Snake River spring/summer Chinook salmon, threatened status for Snake River fall Chinook salmon. Federal Register 57:78(22 April 1992):14,653-14,663.

Perry, R. W., A. C. Braatz, S. D. Fielding, J. N. Lucchesi, J. M. Plumb, N. S. Adams, and D. W. Rondorf. 2006. Survival and migration behavior of juvenile salmonids at McNary Dam, 2004. Final Report of Research by the U. S. Geological Survey to the U.S. Army Corps of Engineers, Walla Walla District, Contract W68SBV40271050, Walla Walla, Washington.

Peters, C. N., D. R. Marmorek, and R. B. Deriso. 2001. Application of decision analysis to evaluate recovery actions for threatened Snake River fall Chinook salmon (*Oncorhynchus tshawytscha*). Canadian Journal of Fisheries and Aquatic Sciences 58:2447–2458.

Peterson, W.T., C.A. Morgan, J.O. Peterson, J. L. Fisher, B.J. Burke, and K. Fresh. 2014. Ocean ecosystem indicators of salmon marine survival in the Northern California current. US Department of Commerce, National Oceanic and Atmospheric Administration, National Marine Fisheries Service, Northwest Fisheries Science Center.

Plumb, J.M., W.P. Connor, K..F. Tiffan, C.M. Moffitt, R.W. Perry, and N.S. Adams. 2012. Estimating and Predicting Collection Probability of Fish at Dams Using Multistate Modeling. Transactions of the American Fisheries Society 141:1364-1373.

Plummer, M. Jags version 1.0.3 manual, Technical Report , 2009

R Development Core Team (2017), R: A language and environment for statistical computing. R Foundation for Statistical Computing, Vienna, Austria. ISBN 3-900051-00-3, http://www.Rproject.org.

Ricker, W.E. 1954. Stock and recruitment. Journal of the Fisheries Research Board of Canada 11:559-623.

Rosenberger, S., W. Young, D. Milks, B. Arnsberg and D. Wickard. 2017. Snake River Hatchery Fall Chinook Salmon Age-at-Release Performance Evaluation White Paper. http://www.nptfisheries.org/PublicationLibrary.aspx

Sandford, B. P., and S. G. Smith. 2002. Estimation of smolt-to-adult return percentages for Snake River basin anadromous salmonids, 1990–1997. Journal of Agricultural, Biological, and Environmental Statistics 7:243–263.

Scheuerell, M.D., C.P. Ruff, J.H. Anderson, and E.M. Beemer. In review. Estimating density-dependent population dynamics in a variable environment with imperfect data. Submitted to Journal of Ecological Applications.

Zabel, R. W., M. D. Scheuerell, M. M. McClure, and J. G. Williams. 2006. The interplay between climate variability and density dependence in the population viability of Chinook salmon. Conservation Biology 20:190–200.Fisheries Review 39:10–14.

Zabel, R. W., J. Faulkner, S. G. Smith, J. J. Anderson, C. Van Holmes, N. Beer, S. Iltis, J. Krinke, G. Fredricks, B. Bellerud, J. Sweet, A. Giorgi. 2008. Comprehensive passage (COMPASS) model: a model of downstream migration and survival of juvenile salmonids through a hydropower system. Hydrobiologia 609:289–300.

Zabel, R. W., and others. 2013. Life-Cycle models of salmonid populations in the interior Columbia River Basin. Report to the Independent Scientific Advisory Board.

Appendix: Estimating Juvenile Passage Abundance at Lower Granite Dam

The abundance of juvenile fall Chinook salmon passing LGR was estimated using a Bayesian hierarchical model that is informed from both daily PIT-tag detections and daily counts of marked and unmarked fish in the sample tank at the LGR juvenile fish facility (JFB). Although it is beyond the scope of this chapter to describe the model in full, the following provides a brief description of how the annual abundances of natural juveniles passing the LGR were calculated from the sample tank and PIT-tag detection data. Specifically, the annual abundance of natural juvenile fall Chinook salmon ($\hat{N}_{\mathrm{N}}$) was calculated as:

(1) $$\hat{N}_{\mathrm{N}} = \sum_{d=1}^{D} \hat{n}_{d,\mathrm{N}}$$

where D is the total number of days the JFB was sampling fish, which typically ends on October 31st (day 274) . The daily abundance of natural-origin fall Chinook salmon passing the Lower Granite Dam, $n_{d,\mathrm{N}}$, was estimated as:

(2) $$\hat{n}_{d,\mathrm{N}} = \frac{\hat{b}_{d,\mathrm{N}}}{C_d}$$

where C_d is the daily probability of collection into the bypass at the dam. A new method has been developed and soon implemented to estimate collection probabilities and juvenile abundance. This new method should alleviate critical assumptions and potential sources of bias in past methods to estimate collection probability (Sandford and Smith 2002; Plumb et al. 2014). The parameter $\hat{b}_{d,\mathrm{N}}$ is the estimated number of natural-origin juveniles that are collected into the bypass, which was estimated as:

(3) $$\hat{b}_{d,\mathrm{N}} = \frac{\hat{s}_{d,\mathrm{N}}}{r_d}.$$

Here $\hat{s}_{d,\mathrm{N}}$ is the daily number of natural-origin juvneiles in the sample tank, and r_d is the daily sample rate of fish that have entered the JFB. The daily number of natural-origin juveniles in the sample tank was estimated as:

(4) $$\hat{s}_{d,\mathrm{N}} = s_d(1 - \hat{p}_{d,\mathrm{H}})$$

where s_d is the total number of fish in the sample tank on day *d*, and $\hat{p}_{d,\mathrm{H}}$ is the estimated fraction of s_d that is hatchery-origin. The proportion of the fish in the sample tank that is hatchery-origin ($\hat{p}_{d,\mathrm{H}}$) is estimated using Bayes Theorem:

(5) $$p_{d,\mathrm{M|H}} = \frac{p_{d,\mathrm{H|M}}\, p_{d,\mathrm{M}}}{p_{d,\mathrm{H}}}$$

where $p_{d,\mathrm{M|H}}$ = the daily probability that a fish in the sample tank is marked (M), given that it is hatchery (H) origin (hereafter, the daily mark rate). Hatchery origin subyearlings can be either adipose clipped (AD) or Coded Wire-Tagged (CWT), and so $p_{d,\mathrm{M|H}}$ is the daily fraction of marked hatchery fish that are either AD or CWT. The parameter $p_{d,\mathrm{H|M}}$ = the daily probability that the fish is hatchery-origin, given the fish is marked. If a fish has been marked with either AD or CWT then it is known to be a fish of hatchery origin, and so $p_{d,\mathrm{H|M}}$ = 1. The parameter $p_{d,\mathrm{M}}$ = the daily proportion of fish in the sample tank that are marked. Setting $p_{d,\mathrm{H|M}}$ = 1 and solving for $p_{d,\mathrm{H}}$ yields:

(6) $$\hat{p}_{d,\mathrm{H}} = \frac{\hat{p}_{d,\mathrm{M}}}{\hat{p}_{d,\mathrm{M|H}}}$$

The daily fraction of marked fish in the sample ($\hat{p}_{d,\mathrm{M}}$) is straightforward to estimate from the number of marked and unmarked fish counted in the daily sample. However, the fraction of hatchery fish that are marked ($\hat{p}_{d,\mathrm{M|H}}$) is more difficult to estimate because marking rates and release dates vary among hatchery release groups, which causes $\hat{p}_{d,\mathrm{M|H}}$ to vary over the migration season. Given information provided by release group-specific PIT-tagging rates and the passage distribution of each group, $\hat{p}_{d,\mathrm{M|H}}$ can was estimated using the PIT-tag detection rates over the release groups and their subsequent detections at the dam to obtain the abundance and relative contribution of the marked and unmarked hatchery groups to the passage of juveniles at the dam.

Abundance of Late Migrants (November of year t through March of year t +1, and April through June year t +1)

If the juvenile fish bypass system and Smolt Monitoring Program at LGR were operated from November of year *t* through March of year *t* +1, the method outlined in the previous section of this write up could be applied to the data to estimate juvenile abundance at the dam during that period. However, the juvenile fish bypass was routinely dewatered from November through late March during 1992–2005 and 2007. In 2006, and after 2007, the U.S. Army Corps of Engineers extended the period of bypass water up to include the entire month of November, and a varying portion of the month of December. Efforts were also made to water the bypass up as early as possible in March. The PIT-tag detection system has been operated during those periods of water up, but the sample tank has not been operated or staffed. The present method, which is being refined, starts with the calculation of the PIT-tagging rate ($r_{\mathrm{N,PIT}}$) of natural-origin subyearlings each year:

(7) $$r_{\mathrm{N,PIT}} = \frac{n_{\mathrm{N,PIT,Oct}}}{n_{\mathrm{N,Oct}}}$$

where $n_{\mathrm{N,PIT,Oct}}$ is the number of natural-origin subyearlings that were PIT-tagged upstream of Lower Granite Dam that were subsequently detected during September and October at the dam expanded by collection probability, and $n_{\mathrm{N,Oct}}$ is the estimated abundance of natural-origin subyearlings at Lower Granite Dam during October taken from Eqs. 1—6.

Passage abundance during November was estimated by dividing the estimated passage abundance of PIT-tagged natural-origin subyearlings in November (number detected divided by collection probability) by the tagging rate from Eq. 7, and assumes a constant tagging rate over the ensuing winter out-migration period. Likewise, the same calculation was made to estimate December and March passage abundance, but the estimates for those months includes a step to expand based on the percentage of each of the months the juvenile fish bypass was in operation. Summing the abundance estimates for November, December, and March provides an abundance estimate for late migrants ($n_{\mathrm{N,Nov\text{-}Mar}}$). Those estimates can be further refined by interpolating passage abundance estimates in January and February; although existing radio-telemetry data indicate that relatively few fish pass Lower Granite Dam during those winter months.

CHAPTER 9:

9.a Grande Ronde Spring Chinook Populations: Juvenile Based Models

Thomas D. Cooney (NWFSC), Brian C. Jonasson (ODFW), Edwin W. Sedell (ODFW),
Timothy L. Hoffnagle (ODFW) & Richard W. Carmichael (ODFW retired)

Introduction

In the previous report we described development and initial applications of life cycle models for four Grande Ronde River basin spring Chinook salmon populations, each incorporating detailed functional survival and capacity relationships for freshwater stages (Figure 1) derived from ongoing monitoring and tagging efforts in each system (Cooney et al., 2013),. Derived relationships for each population were then linked with annual estimates of survival for aggregate Snake River Spring Chinook for outmigration, ocean and adult return stages (Table 1). The Grande Ronde population models were designed to incorporate alternative assumptions regarding spawning and juvenile life stages, annual patterns in estuarine/ocean survival, juvenile and adult passage through the hydropower system and harvest management strategies. Each model incorporated an adjustment to the aggregate smolt to adult survival element reflecting that comparison. Projected brood year adult returns were compared with the corresponding empirical estimates. Initial model runs incorporated previously derived ocean climate scenarios and estimates of main-stem Snake and Columbia River passage survivals. We derived empirical relationships for three sequential tributary life history stages and incorporated them into the population-specific models, including provisions for parameter uncertainty and annual variation. When expressed in terms of a standard amount of habitat, parr production per spawner estimates are relatively consistent across the four populations. The limited number of estimates of summer parr survival in the Upper Grande Ronde population prevented the development of a population specific parr production function. Density dependent effects were the strongest in the summer parr to spring out-migrant phase survival relationships for each population.

The major objectives for developing these models have been to organize available information in a quantitative life cycle model framework to provide managers with improved status assessments and analyses of the potential effects of potential management scenarios. Specific applications to these populations include identifying strategic tributary habitat restoration strategies, evaluating the effects of combinations of actions or management approaches across the life cycle, and evaluating potential contributions and impacts of natural stock supplementation programs. An additional objective is to compare results with other models, including habitat based approaches (e.g. section 9.3b) and models with less detailed inputs or structure (simple and intermediate models). Specifically, we are continuing to collaborate with the CRITFC habitat project and with their cooperators on further developments of both models with a focus on developing common approaches for translating potential tributary habitat restoration strategies or actions into model inputs.

Model Updates

The adult, juvenile and environmental data series used in determining the functional relationships incorporated into the individual Grande Ronde population models have been updated include additional years. In response to the prior ISAB review, we reviewed the density dependent relationships (spawner to summer parr, summer parr to spring migrant).to determine if they could be improved by adding environmental co-variates. While we have not been able to directly include indices in the model, we have been including consideration of addressing temperature and flow impacts in developing input sets representative of potential tributary habitat actions. We are working with CRITFC and ISEMP contractors to develop more explicit indices of temperature and flow impacts in future iterations.

The models have been expanded to include components simulating the potential impacts of ongoing hatchery supplementation programs (three of the four populations). Linkages between simple habitat change metrics and juvenile life stage survival and capacity have been added.

Functional Relationships

Updated parameter fits for the juvenile life stage functions are provided in Table (2). The most significant general change from the prior version was for the spawner to summer parr stage. The updated single variable analyses still indicated that parent spawner density was the most influential factor influencing levels of parr production. Adding the additional years to the logistic regression analyses of summer parr to spring migrant survivals resulted in minimal changes to the fitted relationships for the Catherine Creek, Minam, and Lostine River populations (Table 2). The prior fits for the limited number of Upper Grande Ronde sample pairs had a relatively high level of parameter uncertainty; the joint probability distributions included biologically unrealistic combinations. Although the parameter uncertainty levels remained higher than for the other populations, adding the three additional years improved the fit considerably (Figure 2).

We incorporated a second tributary habitat summer rearing area into the Catherine Creek model in response to recent parr survey results indicating substantial numbers of parr rearing downstream of the smolt trap in the reach extending to Davis Dam (e.g., Jonasson et al. 2016). In recent years spawning in this reach has been very low, intermittent and confined to the upstream extent. Given the relatively low rates of observed downstream passage from initial trap operations in the early spring to the fall, it is likely that these juveniles migrate downstream as fry or after a short period of rearing. That early redistribution would be prior to the initiation of large scale irrigation withdrawals. The amount of suitable rearing habitat downstream (structure and temperature) would be drastically reduced each year once large scale water withdrawals begin in early summer. In the model we assume the same density dependent relationships would apply as estimated for the above weir component. We expanded the observed densities in the reach by the estimated amount of habitat by habitat type (pool, run and fastwater) to estimate abundance relative to the population remaining above the smolt trap. We assume that the average proportion (~30%) applied to the earlier study years before systematic sampling was initiated in the downstream reaches. ODFW has expanded their ongoing summer parr tagging program to include groups in the downstream area. Initial results indicate substantially lower survivals from late summer to detection at Lower Granite Dam the following spring. To account for the downstream rearing production in our model, we assumed an average of those estimates would apply in prior years.

The updated stage specific survival functions and the resultant aggregate juvenile production relationships have been incorporated into each population life cycle model.

Tributary Habitat Linkages

The four Spring Chinook populations represent a range of habitat conditions. The Minam River is relatively pristine, although there were historical mining impacts in some parts of the drainage. The upper sections of the Lostine River are also relatively intact, the lower sections are impacted by water withdrawals and other related activities. Both Catherine Creek and the Upper Grande Ronde historical populations included extensive low gradient reaches in the Grande Ronde

Valley that likely supported a diversity of juvenile Chinook rearing patterns. Those habitats were extensively converted to agricultural use beginning in the mid to late 19th century. The draft NE Oregon Recovery Plan (link) identifies high priority limiting factors and reaches based on a combination of local expert opinion and ongoing habitat assessment efforts. High temperatures and loss of stream structure (e.g., pools) are significant limiting factors especially in downstream sections of Catherine Creek and the Upper Grande Ronde River. Specific reaches within the upper sections still supporting spawning and rearing as well as immediately downstream have been prioritized for restoration actions. In Catherine Creek, water diversions reduce flows below the town of Union (immediately downstream of current spawning) by up to 95% in most years. Further downstream additional diversions effectively remove most of the remaining flow through the summer. Both Catherine Creek and the Upper Grande Ronde populations have extensive sections with riparian impacts. In the Upper Grande Ronde River, the scouring impacts arising from historical splash dam activities combined with riparian vegetation losses has resulted in extensive channel widening and high temperatures (White et al., 2017).

Other than scaling some juvenile life stage parameters to the total amount of pool habitat within a population, our Grande Ronde MLCMs do not directly include habitat parameters. We use multipliers on life stage specific survival and capacity terms as inputs to model the impact of habitat actions or environmental changes.

The basic approach for incorporating habitat change effects starts with current life stage capacities and survival estimates derived from the 20+year juvenile series for each population. Using Catherine Creek summer parr stage as an example, we calculate the total amount of pool equivalent habitat currently supporting spawning and/or rearing. Almost all current spawning in Catherine Creek is above the juvenile screw trap and adult weir. Surveys downstream of that location have identified summer rearing of juveniles that likely emigrated downstream in early spring from spawning areas. We calculate the area of effective pool habitat available for rearing using the Oregon Aquatic Inventory data combined with the relative weightings for different reach categories (pool, run, riffle, fast water). We translate proposed actions into changes in the amount of pool equivalent habitat and express the results as a ratio of the new total to the current estimate. That ratio is used as a multiplier to increase the summer rearing capacity in the model. Life stage survivals can be increased by habitat actions in three ways; in cases where a direct survival impact is alleviated (e.g., irrigation diversion screening related mortality), a multiplier on survival weighted for the proportion of current rearing area benefiting from the action is used. Restoring riparian cover, reconnecting stream channels to associated groundwater sources or creating localized water storage (ref) can directly reduce stream temperatures. We use results from a long term habitat study in the upper sections of the Grande Ronde basin (Justice et al. 2016, White et al. 2017) as a starting point for translating potential restoration actions into temperature effects on juvenile Chinook production.

Although the MLCMs can be used to model the effects of individual reach scale habitat actions, assessment of larger scale restoration strategies is a more effective use of their capabilities. In practice, larger scale restoration strategies will take time to implement. In addition, actions such as restoring riparian habitat will take additional time to result in changes to conditions affecting juvenile or adult life stages in the reach. For example, developing canopy cover providing effective shade to adjacent stream reaches can take decades to reach full maturity. Our procedures for translating proposed actions into life stage model inputs use a simple set of assumptions to address these factors. The following Catherine Creek example illustrates the approach.

We modeled three incremental habitat action sets; 1) specific actions called for in the current draft NE Oregon Recovery Plan, expanded actions targeting priority reaches identified through the Catherine Creek Atlas project (ref) and 3)implementation of stream/riparian restoration in high and moderate priority reaches identified in Justice et al., (2016). The specific actions modeled are summarized in Table 3. .The impacts of restoring 10 cfs in flows were estimated using data from CHaMP sampling in the Union to Davis Dam reach analyzed using the U.S. Forest Service River Bathymetry Toolbox (citation). The effect of the action was expressed as a proportional increase in suitable pool habitat. The draft Recovery Plan also calls for restoring 3 miles of side channel or meander habitat. We assumed that reconnected or reconstructed channel habitats would be in the same low gradient reach (Union to Davis Dam), and that the resulting additional channel habitat would average 80% pool frequency. We assumed these actions would increase the juvenile Chinook summer rearing capacity for the population, but that temperatures would not be changed from current ranges.

The third increment of change was based on the high & moderate priority reach restoration scenario described in Justice et al. 2017 and White et al. 2017. This scenario focuses restoring stream structure and reducing temperatures through the combined effects of riparian shade and achieving natural channel structure and width/depth ratios (White et al., 2017). Most of the reaches identified as high priority for riparian restoration along Catherine Creek course through private lands. Implementing these large scale restoration actions will require extensive landowner cooperation and coordination. In some circumstances restoring natural channel structure may require direct intervention given the degree of degradation (e.g. extreme channel widening due to historical splash dam activities). Given the time requirements to get agreements in place and limitations on the resources required to actually implement large scale riparian restoration, we assumed a 20 year implementation schedule.

We estimated the potential changes in juvenile rearing capacity for restoring high and medium priority reaches in Catherine Creek by applying the mixed effects model described in Justice et al. (2017) that relates late summer juvenile densities to stream temperatures. We applied the model to each 200 m segment of stream in two priority sections of Catherine Creek (the current core spawning and rearing habitat above the town of Union, and the contiguous downstream section from Union to Pyles Creek). We combined the incremental implementation schedule with the generalized riparian response time described in Justice et. al. 2017 using a polynomial equation corresponding to their estimated response times (40% of benefits after 25 years, 85% after 75 years).

Out-migrating smolts from Catherine Creek (and to a lesser extent the Upper Grande Ronde River) are subject to relatively high mortalities either during active migration or just prior to beginning that phase (e.g., Favot et al 2010). The factors contributing to this increased mortality are not well understood. Two possible contributing mechanisms have been suggested, both at least partially driven by the unique spring flow condition at the lower end of the Grande Ronde Valley. Flows from the Upper Grande Ronde bypass the old Grande Ronde channel via the State Ditch, which begins near La Grande, Oregon well upstream of the former Catherine Creek confluence and rejoins the old main stem channel approximately 22 km below that confluence. Spring flows from the Upper Grande Ronde are backed up when they encounter the relatively confined geology at the lower end of the valley. As a result, migrants from Catherine Creek encounter slack water or even an upstream flow as they pass downstream. Reasons for the documented high levels of mortality during the transition through this reach are unclear. It is possible that migrating smolts delayed in this reach are highly vulnerable to avian or piscine predation. It also is possible that the interruption in normal migration timing is a contributing factor. An ODFW study is underway to gain an understanding of the causes and to identify strategies to reduce this documented mortality (Favrot et al, 2010). For the purposes of this modeling exercise, we assume that managers will identify and implement an approach that will reduce the mortality associated with this reach to the extent that Catherine Creek outmigrants will be equivalent to the high end of the mortality range observed for migrants from the Lostine and Minam Rivers, which enter a relatively short distance downstream.

Hatchery Supplementation

Three of the four model populations have active supplementation programs incorporating natural origin adult returns as broodstock (HGMP references). Each program has a maximum release target and a ‘sliding scale’ brood stocking and upstream release schedule. The schedules differ across the populations but include the same basic elements. The control point for capturing broodstock is an adult weir below current natural spawning reaches (the same weir used to generate the adult return counts). In general, the sliding scale management framework promotes total adult escapement at very low return levels and increases the minimum proportion of natural origin returns taken for brood stock at higher return levels. In years when returns exceed the ICTRT recommended minimum abundance threshold for a population (MAT), the proportion of hatchery fish escaping into the natural spawning area becomes controlling. As an example, we have incorporated the sliding scale schedule (Table 4) for the Catherine Creek supplementation program along with recently observed hatchery smolt production and survival rates into the life cycle model. The long-term impacts of high levels of continuous hatchery supplementation are unknown. We project scenarios under two sets of assumptions of the relative effectiveness of progeny from returning supplementation adults; an empirically derived relative survival rate from ongoing relative reproductive success studies in the Imnaha and Grande Ronde basins, and a version of the heuristic model described in Ford (2004). The two assumption sets bracket a possible range of impacts on short term performance and long-term fitness. The empirically derived reduction in return rate assumes no long-term fitness impact of the program on the natural population. The second option assumes that fitness will decline as a function of the proportions of natural returns in the hatchery broodstock and the proportional contribution of hatchery fish to natural spawning adults.

Lower Columbia River Adult Mortality

Three of the four modeled Grande Ronde populations have an early entry timing into the Columbia River and are vulnerable to increased mortality rates (Sorel this report) associated with large increases marine mammals in the lower Columbia River. We adapted the individual life cycle models to simulate increased predation rates using the PIT tag based information on adult run timing and the general predation rate analysis described in Sorel (this report). This component is implemented as an additional mortality drawn randomly from a triangular distribution representing the range in increased mortality estimated for 2011-2014. We assumed that the average mortality for the period prior to the recent increases in marine mammal presence in the lower Columbia River was part of the Bonneville to Bonneville Dam brood year SAR estimates generated from the historical juvenile and adult series. The additional mortality factor included in the model was expressed as a ratio of the more recent estimates to the historical average predation rates.

Scenario Analysis

We run 500 simulations of 100 years each for a particular scenario, drawing randomly from parameter distributions (a single 100 year simulation) and random variability elements (annually). The results are saved in arrays, the standard set includes annual spawners (total, natural origin and hatchery origin), brood year returns (natural origin) and annual adult harvest rate. For runs invoking local supplementation, annual estimates of natural origin broodstock removals, spawning area hatchery proportions and accumulated fitness effects are also stored. These arrays can be used to generate different summary statistics and graphics, both within and across scenarios.

Outputs can be summarized in ways that directly correspond to risk and recovery metrics used in status reviews, Biological Opinion evaluations and recovery planning. For example, summarizing frequency distributions of 10 year geometric mean natural origin spawners at selected years (e.g., 25, 50 or 100 years) or reporting the proportion of runs that fall below a selected quasi-extinction threshold. The ICTRT recommended using a QET of 50 fish averaged over four years as a long term recovery benchmark.

NWFSC life cycle models developed for Willamette Basin populations employ output summaries that directly correspond to the LCWTRT scoring approach for combined abundance and productivity. While the ICTRT did not use the same scoring approach to evaluate abundance and productivity components of VSP, a persistence score generated using the Willamette procedure can be used as a component in evaluating performance against the ICTRT viability criteria (Figure 5). The ICTRT recommendations have been extensively used in current status assessments and in recovery planning for listed Interior Basin populations. In common with the LCWTRT, the ICTRT approach is based on constructing a series of viability curves corresponding to different risk levels of falling below QET. The two biggest differences between the approaches: the ICTRT used a fixed QET of 50 for all populations but added a minimum abundance threshold that is a function of the historical habitat size and complexity of a population as a second 'test' in assessing viability In spite of those differences, the persistence 'score'generated by using the Willamette methodology can be combined with an estimate of th10 year geometric mean natural spawning abundance expressed as a proportion of a populations minimum abundance threshold to judge status consistent with the ICTRT viability curve.

Results

Model updates

Four additional years of juvenile and adult data were incorporated into the data series used to derive the parameters for the individual life stages in our model. The primary change resulting from these updates was to the spawner to parr relationships. Low sample sizes in several years limited the number of estimates of summer parr for the Upper Grande Ronde population, it was not possible to get a credible set of functional parameters. As an alternative, we aggregated the estimates with those for Catherine Creek to derive a spawner to parr functional relationship. We were able to generate a population specific estimate for the Upper Grande Ronde with the added years, although with relatively high parameter uncertainties.

We also reviewed and updated the estimates of pool-equivalent habitat currently supporting spawning and/or rearing for each population (Fig rf). The major changes were a reduction for the estimated amount of functional habitat above the weir & trap in the Upper Grande Ronde population and the addition of an estimate for the downstream summer rearing area recently identified in Catherine Creek.

Our models are fitted to survival and abundance estimates for a series of juvenile life stages. The median expected spawner to Lower Granite smolt estimates from our retrospective model are similar for three out of the four populations to the fitted relationships generated by an earlier version the intermediate model described in section 4A of this report (ref to R. Lessard CSS chapter).. The most significant differences are for the Upper Grande Ronde population (Fig. 4). As discussed above, we have less confidence in the spawner to summer parr function for this population. We are continuing to evaluate alternative approaches for dealing with the limited data for this population.

Pinniped Predation

Three of the four populations covered in our modeling effort have relatively early return timing patterns and are thus particularly susceptible to increased marine mammal predation in the Lower Columbia River (see M. Sobel: sec. 6a). As an example, we generated a preliminary comparative analysis using the Minam River LCM and the assumption that annual patterns in the influence of ocean and freshwater annual environmental conditions will fluctuate within recent ranges (Fig). We ran 500 simulations under three different scenarios: a) current status, b) current status with continuation of recent increases in estimated pinniped predation, and c) a two fold increase in productivity (either from survival or capacity improvements) combined with recent level pinniped impacts. The results are summarized on a persistence curve plot; the scatter of points for a given scenario represents uncertainty in the outcome for a given scenario (Fig. 6). The red point in each graphic represents the median risk outcome across the 500 simulations.

The two histograms under the outputs summarize the same results categorically for persistence risk and for a combined abundance/productivity score consistent with the ICTRT viability criteria. Each bar represents the proportion of simulation runs that fall in a particular risk category. Under a continuation of current conditions, the Minam River population persistence scores fall largely in the moderate (5-25% risk) and low risk (1 to 5% risk) bins. But the average abundance levels for all runs are well below the ICTRT recommended minimum threshold for the population. As a result the overall population abundance & productivity scores are at the low end of the moderate range. Under the current conditions with prolonged pinniped mortality increases the persistence scores over the 500 simulations shift into the moderate risk category and further towards the higher risk category for the combined score.   The third scenario illustrates that it would take approximately a doubling of stock productivity to shift the Minam population to a high persistence probability and also achieve an average combined abundance & productivity rating of viable (greater than 3).

Evaluating Tributary Habitat and Supplementation Strategies

The results of simulating the potential impacts on the Catherine Creek population of tributary habitat restoration increments combined with supplementation and increased pinniped mortality are illustrated in Figure 7 . The selected set of combinations were modeled under the three different ocean scenarios described in or previous report (poor ocean, recent ocean and historical-includes the 1960s). Two different outputs are depicted – a box & whiskers plot of the 10 year geometric means at model year100 over the 500 runs for each scenario, and a bar chart showing the proportion of runs falling below the QET standard in the first 25 years. The first metric is useful for assessing contributions towards meeting recovery abundance targets. The second is a measure of the relative risk during the action implementation and response phase.

The scenarios are grouped in order from current (no change) to implementation of natural vegetation and channel structure in high/moderate priority reaches (e.g., Justice et al. 2017, White et al. 2017). The scenarios include versions with and without hatchery supplementation. In general, the response to the short term habitat actions being currently implemented reduced short term quasi-extinction risk under all ocean scenarios. Under the supplementation options, clear bars on the lower graphic indicate that that the combined natural escapement including supplement hatchery spawners did not fall below the QET benchmark, but that the natural component alone did. Gains in average abundance are positive but relatively modest over the longer term. Successfully reducing the lower Grand Valley outmigration mortality affecting Catherine Creek and the Upper Grande Ronde to levels comparable to that observed for the two downstream populations would have a similar impact on its own on long term abundance and would result in a larger decrease in short term risk. Implementing the long term riparian and channel structure restoration in targeted high and moderate priority reaches on its own would reduce short term risk modestly, with a greater potential long term benefit to average abundance. The projected combinations of all actions have the greatest benefits to both short term risk reduction and long term abundance gains. Each the seventh and eighth components of each set represent full implementation with supplementation. The first element of the pair assumes no long term fitness impact but includes an assumed reduction in natural production from hatchery origin parents of 25%. The second of the pair includes a gradual loss in fitness. The last two pairs in each set duplicate the full implementation under the supplementation options but also add continued high pinniped predation. Comparing results across the three future ocean/environmental assumptions shows the importance of those background factors on the outcome under any of the scenarios. Substantial reductions in short term risk are possible under any of the three options, but additional improvements would be needed to meet long term minimum abundance objectives under all but the most optimistic of the ocean/environmental assumptions considered.

These results are preliminary, but they do illustrate that including implementation of longer term actions to ultimately reduce or mitigate for temperature increases and restore natural channel processes can complement short term actions in reducing short term risk. Under the assumptions included in this analysis, natural stock supplementation programs can reduce risks during recovery, but they also could have long term costs in terms of natural production levels. If estimated increases in pinniped predation rates continue, substantially higher increases in survival or capacity in other sectors would be required to achieve minimum abundance and risk objectives.

We are continuing to evolve the Grande Ronde life cycle models and the associated habitat assessments and analyses required to generate represented inputs of possible or proposed habitat strategies. We plan on continuing the cooperative work with the CHaMP/ISEMP project in general, specifically including the ongoing Grande Basin work. Next steps will include structured sensitivity analyses of the models, working to develop alternative restoration scenarios for the populations along with assumption sets for translating the potential impacts of those actions on tributary habitat into model inputs. Near term priorities include linking the hydropower passage and the ocean scenario components of the model to accommodate alternative assumption sets (e.g., section 4).

Acknowledgements

Damon Holzer (NWFSC) provided considerable GIS mapping support and analytical input into the analyses. Chris Horn (ODFW La Grande) upgraded our preliminary estimates of the potential gain in juvenile rearing habitats using detailed CHaMP survey results and the USFS River Bathymetry Tool. We thank Seth White, Casey Justice and Dale McCullough (CRITFC) for providing preliminary results from ongoing geomorphic and temperature studies as well as for critical advice on the relationships incorporated into our models.

Literature Cited

Cooney, T.,D. R.W.Carmichael B. C. Jonasson E W. Sedell & T. L. Hoffnagle. 2013. Grande Ronde Spring Chinook population models. Chap.2.1. in: Life-cycle models of salmonid populations in the Interior Columbia River Basin. June 28, 2013 draft.

Favrot, S.D., K.W. Bratcher, B.M. Alphonse, B.C. Jonasson and R.W. Carmichael. 2010. Identification and characterization of juvenile Spring Chinook Salmon overwinter rearing habitat in Upper Grande Ronde Valley. (2010). Annual Rept to the Bonneville Power Administration and U.S. Bureau of Reclimation. 54 p.

Ford MJ. 2002. Selection in captivity during supportive breeding may reduce fitness in the wild. Conserv Biol. 16:815–825

ICTRT (Interior Columbia Basin Technical Recovery Team). 2007. Viability criteria for application to interior Columbia basin salmonid ESUs. Review draft, 3/1/2007. https://www.nwfsc.noaa.gov/research/divisions/cb/genetics/trt/col/trt_viability.cfm

Jonasson, B. et al. 2016. Investigations into the Life History of Naturally Produced Spring Chinook Salmon and Summer Steelhead in the Grande Ronde River Subbasin. ODFW Annual Report 2015. BPA Project # 1992-026-04. 95p.

Justice, C., S.M. White, D.A. McCullough, D.S. Graves, and M.R. Blanchard 2017 Can stream and riparian restoration offset climate change impacts to salmon populations?. J. Envir. Mgmt 188:212-217

Lassard,R. ref to CSS report with model parameters

McElhany, P., M. H. Ruckelshaus, M. J. Ford, T. C. Wainwright, and E. P. Bjorkstedt. 2000. Viable salmonid populations and the recovery of Evolutionarily Significant Units. Technical Memorandum NMFS-NWFSC-42. United States Department of Commerce, National Oceanic and Atmospheric Administration. Seattle, WA.

Roni, P., T. Beechie, R. Bilby, F. Leonetti, M. Pollock, and G. Pess. 2002. A review of stream restoration techniques and a hierarchical strategy for prioritizing restoration in Pacific northwest watersheds. North American Journal of Fisheries Management. 22:1, 1-20

ODFW 2011. Hatchery Genetic Management Plan. Grande Ronde Basin Catherine Creek Spring/Summer Chinook Program (updated 2011). 77p. https://www.fws.gov/lsnakecomplan/reports/HGMPs/Catherine%20Creek%20CHS.pdf

ODFW (2016). 2016 Joint Staff Report: Stock status and fisheries for Spring Chinook, Summer Chinook, Sockeye, Steelhead and other species, and miscellaneous regulations. ODFW & WDFW.   January 20, 2016. 95 p.

White, S.M., C Justice, D.A. Kelsey, DA. McCullough and T. Smith 2017. Legacies of stream channel modification revealed using General Land Office surveys, with implications for water temperature and aquatic life. Elem. Sci. Anth. 5: 3 DOI:https://doi.org/10.1525/elementa.192

Tables

Table 1. Summary of model parameters

Life Stage	Function	Derivation	Parameter uncertainty	variance
Spawner to parr	Beverton Holt	R nls package	bootstrap	lognormal
fall parr to spring migrant	logistic on density	R nls package	max. likelihood	lognormal
spring migrant to LGR Dam	logistic on density	R nls package	max. likelihood	lognormal
Juvenile Col. River migration	random draw most recent 10 years	Annual system survival estimates		
Ocean: first year	Random start to fixed series with random error component	multiple regression	Poor ocn, recent ocean, long term ocean	lognormal
	pHOS multiplier	*2 options:*		
		a) 75% relative		
		b) Ford Model (H opt.=0.6)		
Ocean: years 2:5	constant	0.8	no	
Harvest	US v Oregon Sliding scale:		Management error	lognormal
Broodstocking	Cath. Creek schedule	HGMP	Management error	lognormal

Table 2. Updated model parameters for a) spawner to late summer parr stage and (lower panel) parr to spring migrant stage (logistic function).

Model	BH 'a' (se)	exp(a)	BH 'b' (se)	sigma
Catherine Creek	6.326	558.9165	9,528	0.452
	(0.258)		(5,162)	
Upper Grande Ronde River	6.287	537.5383	7279	0.439
	(0.351)		(5,269)	
Lostine River	5.918	371.6676	28,770	0.440
Minam River	6.181	483	19,640	0.542

Population	Stage	Intercept	parr density term	signif. Level	sigma
Catherine Cr.	summer to spring	-0.575	-9.61E-05	0.0058	0.420
Upper GR	summer to spring	0.100	-1.30E-04	0.0422	0.470
Lostine R.	summer to spring	-0.856	-2.89E-05	0.0004	0.182
Minam R.	summer to spring	-0.865	-5.31E-05	0.0502	0.388
Catherine Cr.	spring to LGR	-0.097	-3.66E-05	0.0938	0.299
Upper GR	spring to LGR	-0.134	1.77E-06	0.9755	0.332
Lostine R.	spring to LGR	0.780	-1.95E-05	0.1572	0.322
Minam R.	spring to LGR	0.364	-8.50E-06	0.5578	0.226

Table 3: Summary of Catherine Creek habitat scenarios in example model runs.

Action	Upstream of Union	Downstream of Union	Implementation time frame	Response time frame
Flow Restoration	2 cfs	10 cfs addition through reach	5 years	Immediate increase in rearing pool habitat
Channel structure	Km44 project + 2 more equivalent. reaches	Restore 3 miles of side channel & floodplain	Proportional over 15 years	0-5 years
Riparian restoration	High/moderate reaches:	High/moderate reaches	Proportional over 20 years	% of max. shading benefits 40% @ yr 25, 85% @ yr 85

Table 4. Catherine Creek sliding scale supplementation schedule. Excerpt from Catherine Creek HGMP.

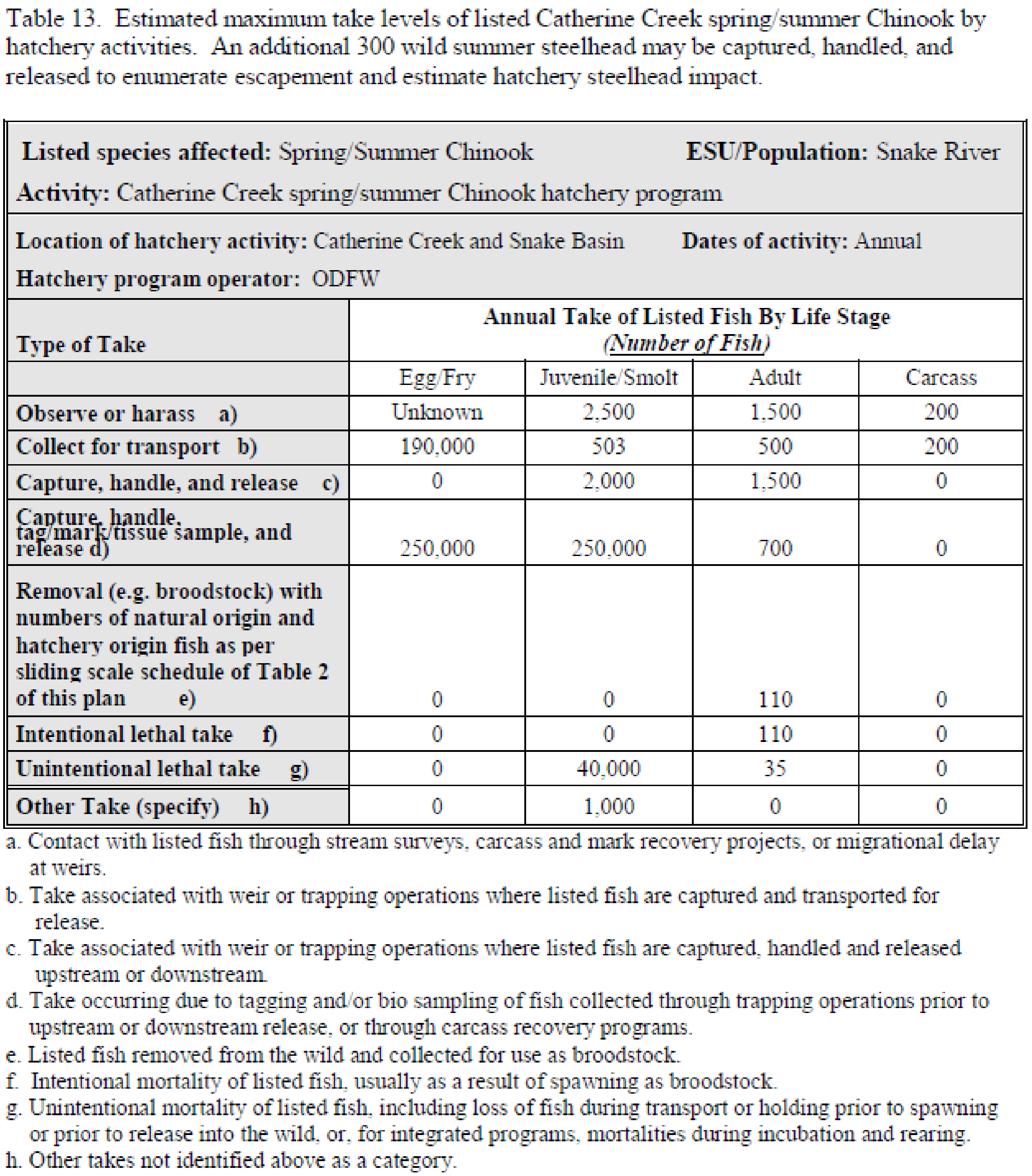

Table 13. Estimated maximum take levels of listed Catherine Creek spring/summer Chinook by hatchery activities. An additional 300 wild summer steelhead may be captured, handled, and released to enumerate escapement and estimate hatchery steelhead impact.

Listed species affected: Spring/Summer Chinook **Activity:** Catherine Creek spring/summer Chinook hatchery program			**ESU/Population:** Snake River	
Location of hatchery activity: Catherine Creek and Snake Basin **Hatchery program operator:** ODFW			**Dates of activity:** Annual	
Type of Take	**Annual Take of Listed Fish By Life Stage** ***(Number of Fish)***			
	Egg/Fry	Juvenile/Smolt	Adult	Carcass
Observe or harass a)	Unknown	2,500	1,500	200
Collect for transport b)	190,000	503	500	200
Capture, handle, and release c)	0	2,000	1,500	0
Capture, handle, tag/mark/tissue sample, and release d)	250,000	250,000	700	0
Removal (e.g. broodstock) with numbers of natural origin and hatchery origin fish as per sliding scale schedule of Table 2 of this plan e)	0	0	110	0
Intentional lethal take f)	0	0	110	0
Unintentional lethal take g)	0	40,000	35	0
Other Take (specify) h)	0	1,000	0	0

a. Contact with listed fish through stream surveys, carcass and mark recovery projects, or migrational delay at weirs.

b. Take associated with weir or trapping operations where listed fish are captured and transported for release.

c. Take associated with weir or trapping operations where listed fish are captured, handled and released upstream or downstream.

d. Take occurring due to tagging and/or bio sampling of fish collected through trapping operations prior to upstream or downstream release, or through carcass recovery programs.

e. Listed fish removed from the wild and collected for use as broodstock.

f. Intentional mortality of listed fish, usually as a result of spawning as broodstock.

g. Unintentional mortality of listed fish, including loss of fish during transport or holding prior to spawning or prior to release into the wild, or, for integrated programs, mortalities during incubation and rearing.

h. Other takes not identified above as a category.

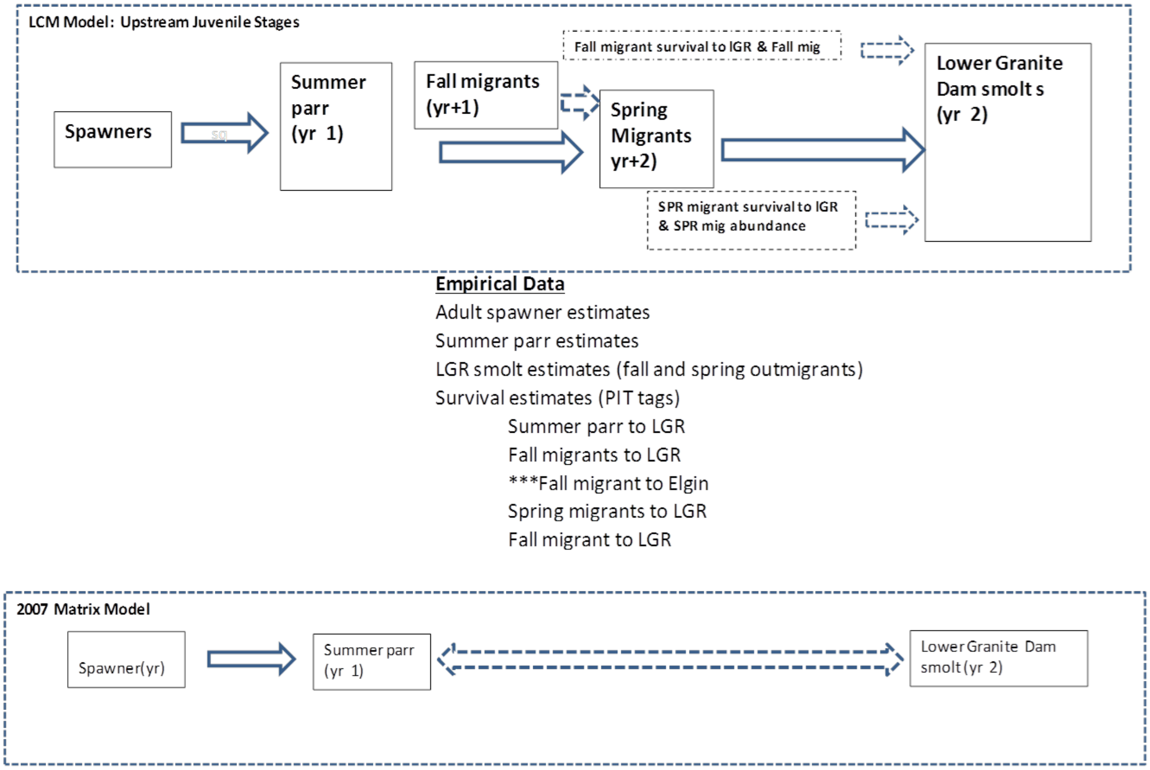

Empirical Data

Adult spawner estimates

Summer parr estimates

LGR smolt estimates (fall and spring outmigrants)

Survival estimates (PIT tags)

- Summer parr to LGR
- Fall migrants to LGR
- ***Fall migrant to Elgin
- Spring migrants to LGR
- Fall migrant to LGR

Figure 1. Schematic of Grande Ronde population life stages with abundance and survival estimates. Bottom panel represent typical summer tagging information available for several other Snake Basin populations.

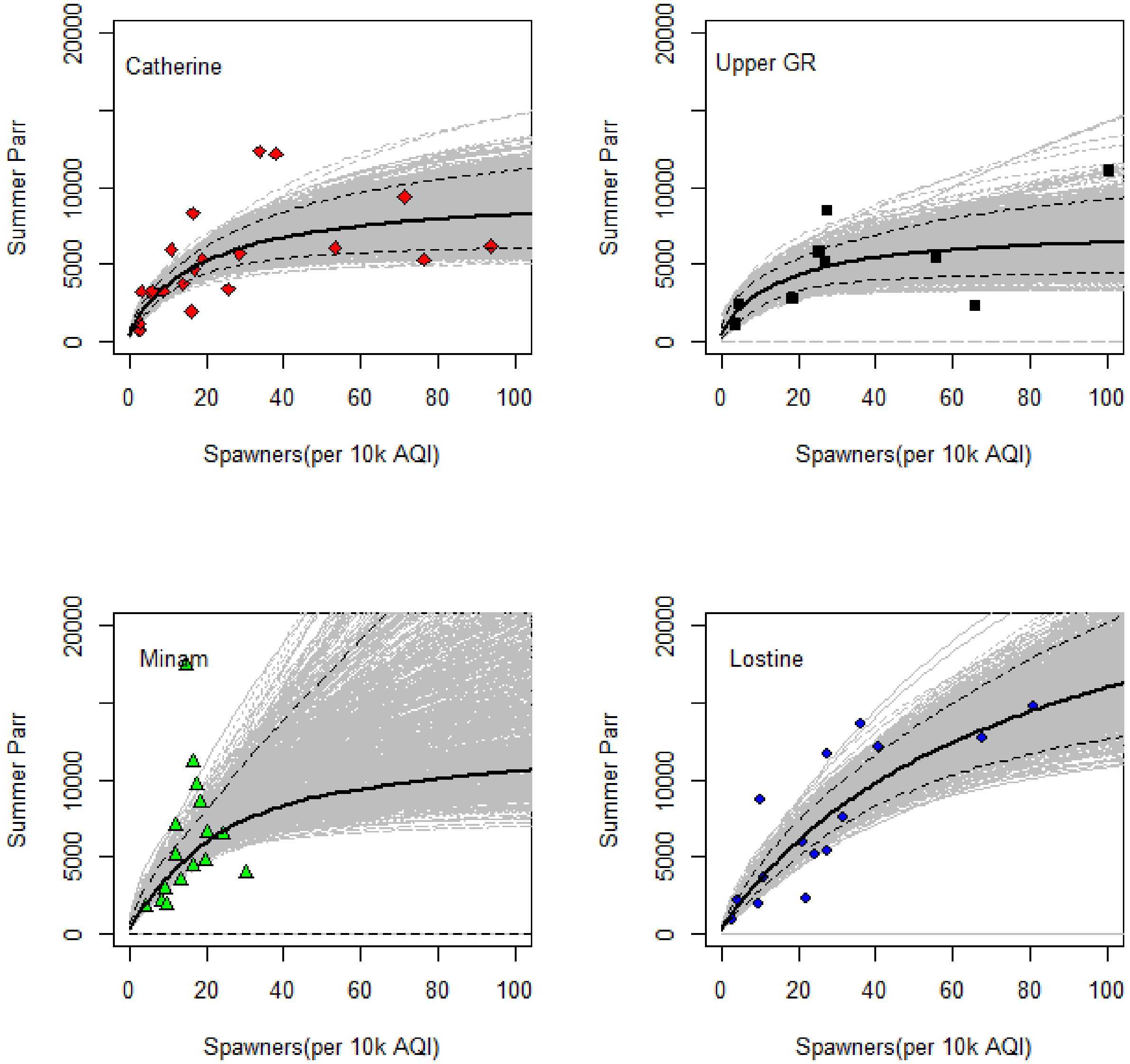

Figure 2. Updated spawner to summer parr relationships fitted to population specific estimates (points). Gray shaded zones reflect bootstrap joint parameter evaluation. Solid line: median across 4000 iterations, dashed lines contain the central 90% of results.

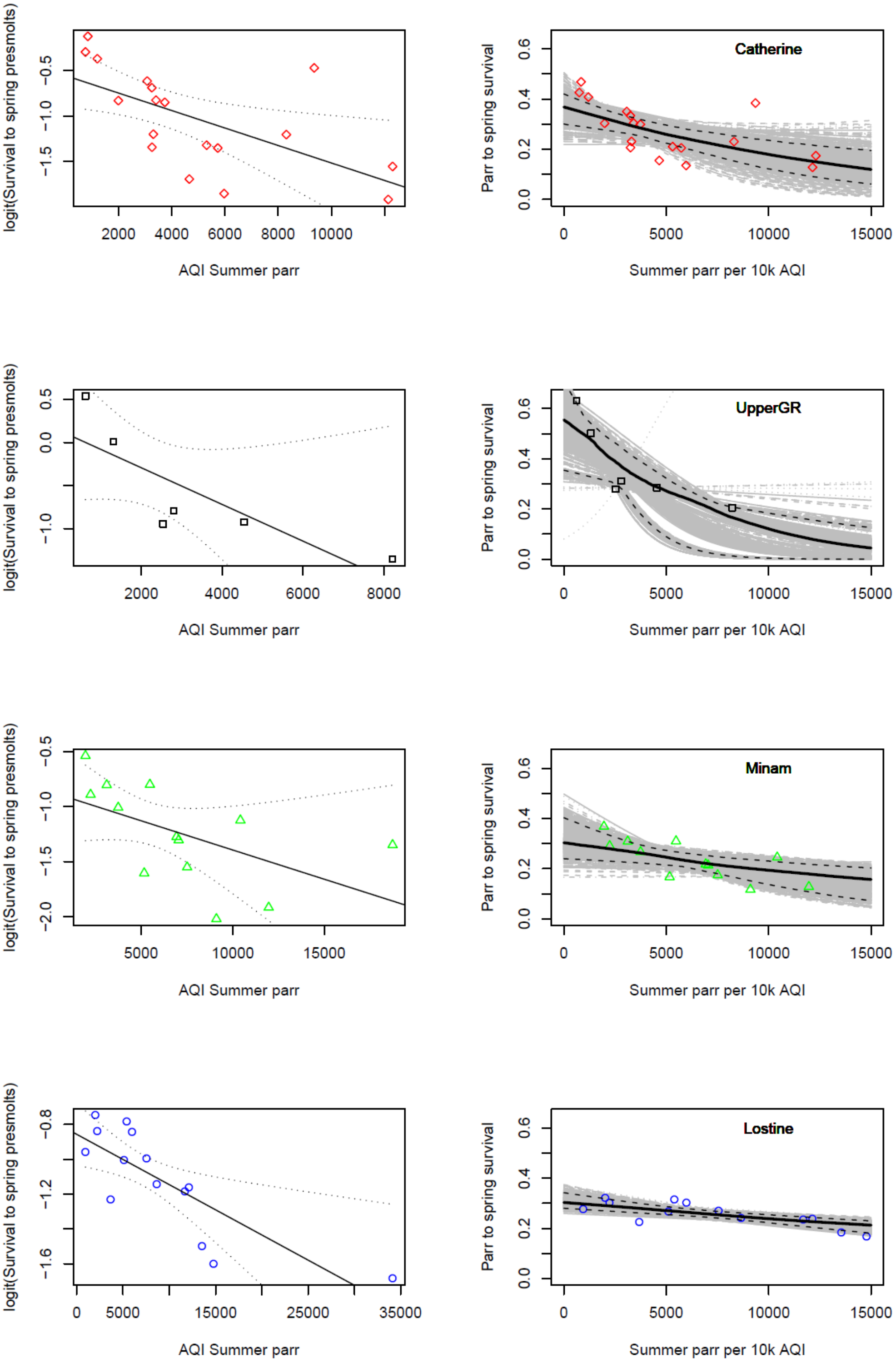

Figure 3. Summer parr to spring migrant survivals. 1992-2016 migration year estimates Gray zone represents 90% central interval for 4000 bootstrap samples.

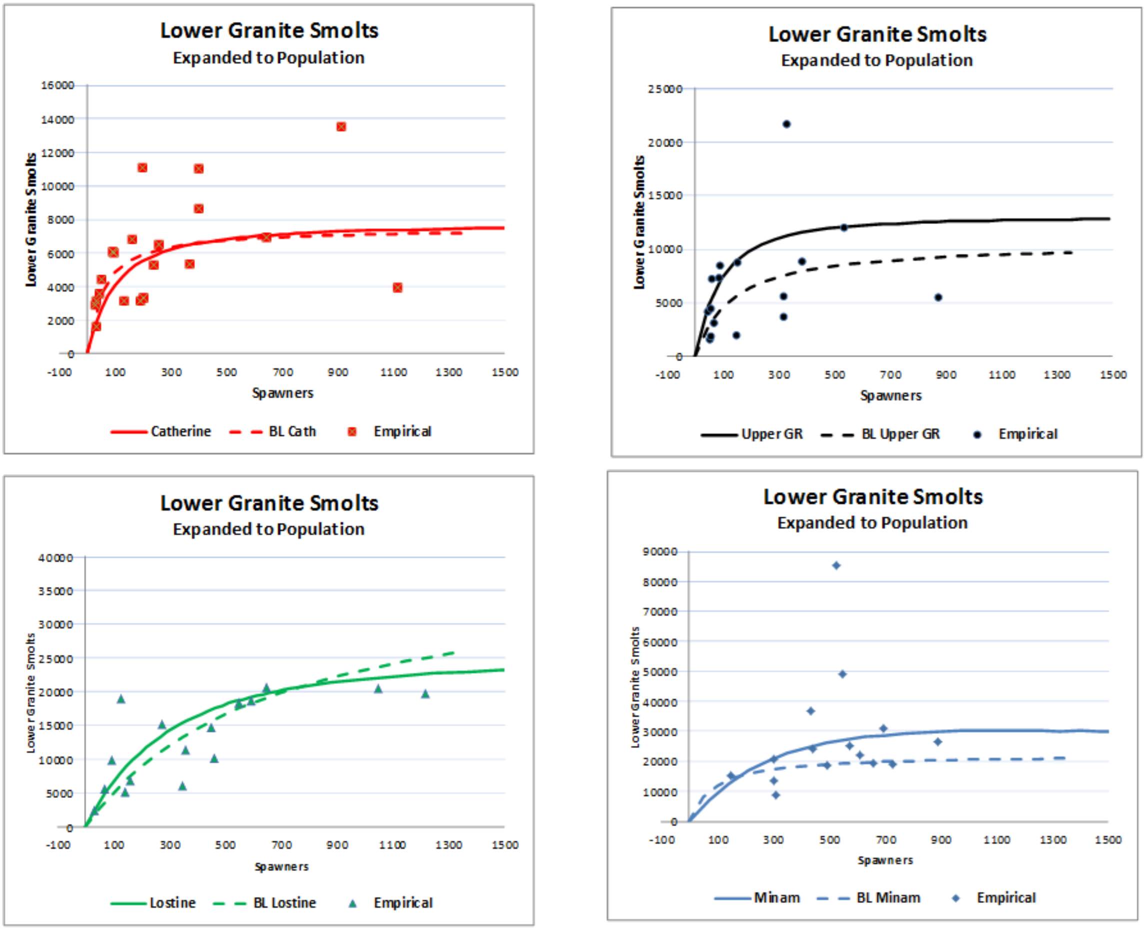

Figure 4. Comparison of Grande Ronde juvenile model estimated smolts to Lower Granite Dam for the Grande Ronde juvenile model and the 6 population intermediate model described in section 4a. Points are estimated values from ODFW tagging studies.

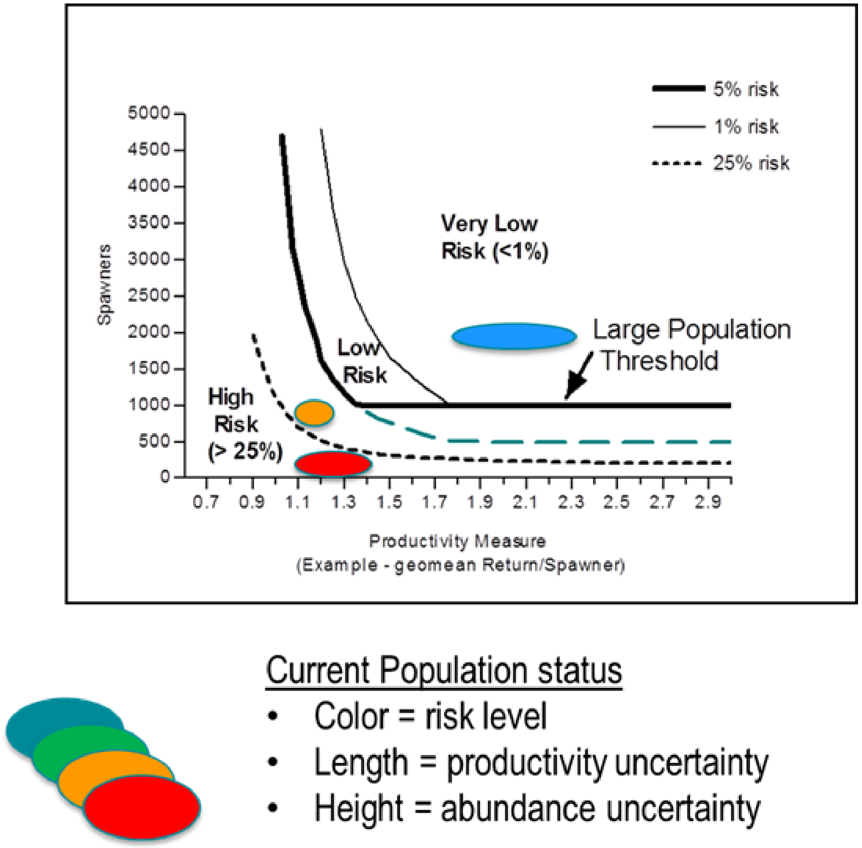

Current Population status

- Color = risk level
- Length = productivity uncertainty
- Height = abundance uncertainty

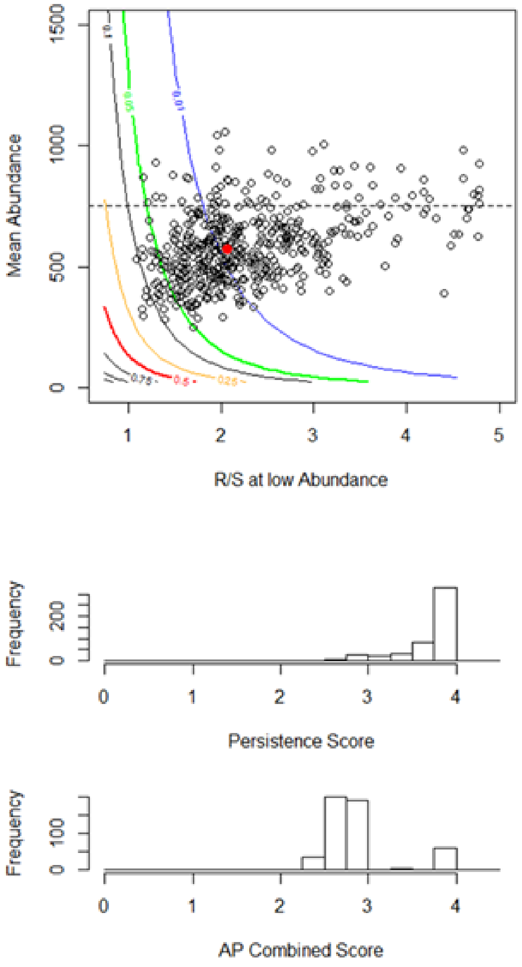

Figure 5. Interior Columbia TRT viability curve example (right panel) and an example application of Gompertz fit persistence and abundance analysis (section 1)

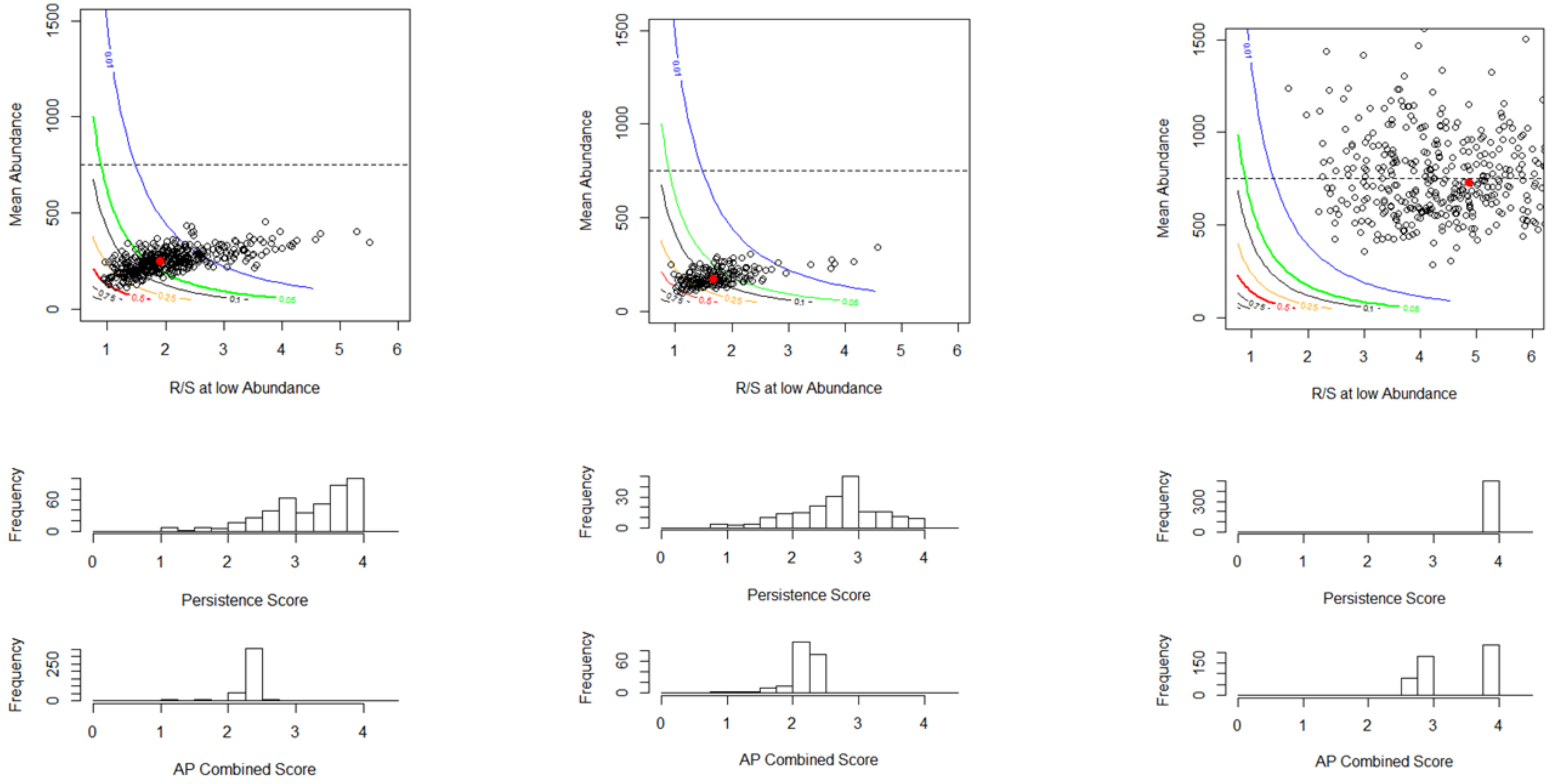

<u>Current</u>
Baseline
Lower C adult survival

<u>Current</u>
2013-2015 Increased
Lower C adult mortalities
continue

<u>Survival Increase (2X)</u>
2013-2015 Increased
Lower C adult mortalities
continue

Figure 6. Example model runs (Minam River model) with and without increased pinniped predation

Figure 7. Results from model runs (Catherine Creek) illustrating the combined effects of short and long term habitat restoration, supplementation, increased pinniped impacts and alternative future ocean scenarios. Top panel: 10 year geometric mean natural abundance at year 100. Bottom panel: proportion f 500 simulation runs infor each scenario thatfalling below a 50 fish for 4 years in a row (ICTRT QET criteria)

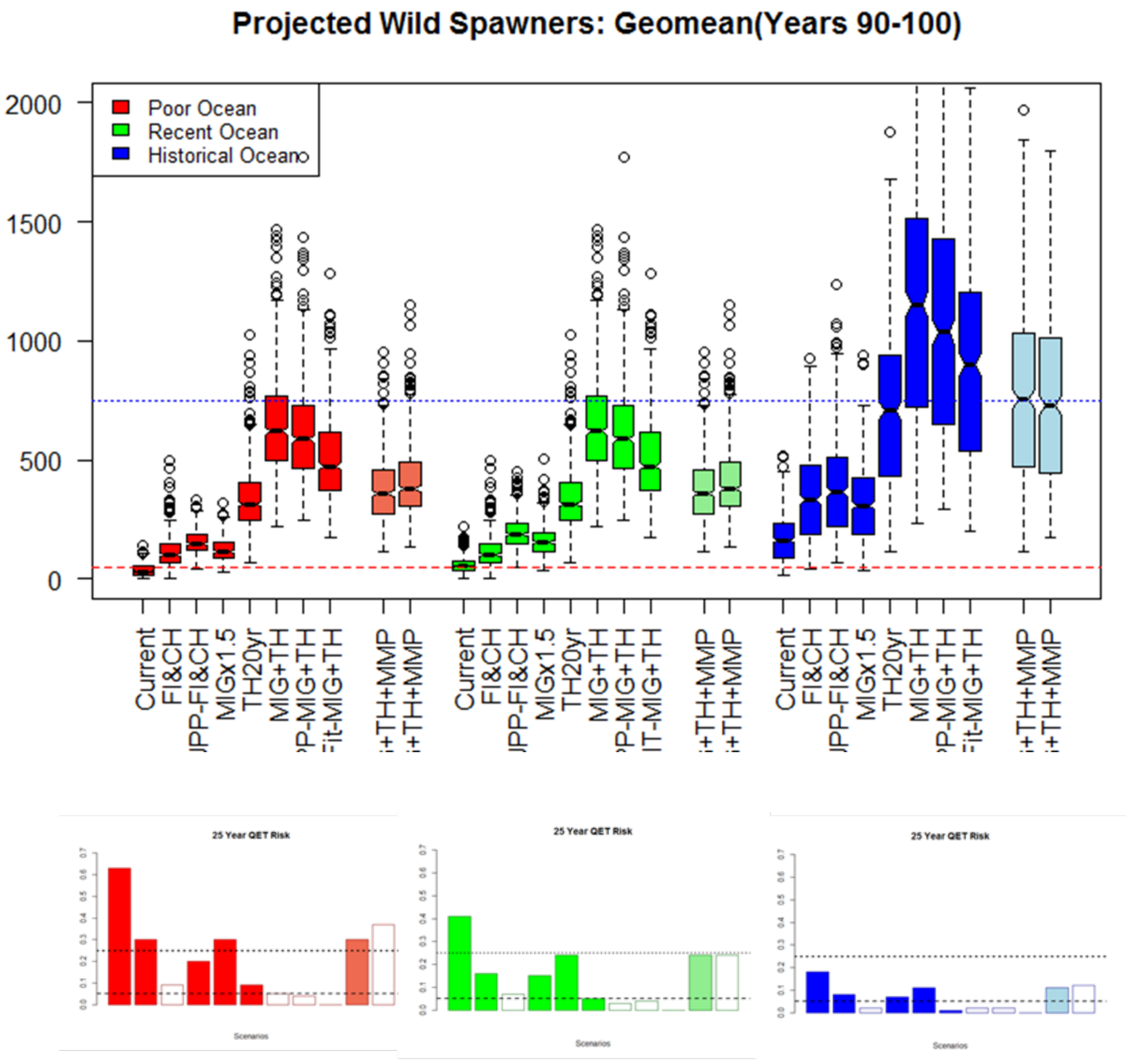

CHAPTER 9: FULL MODELS

9.b Wenatchee River spring-run Chinook salmon life-cycle model: hatchery effects, calibration, and sensitivity analyses

Jeff Jorgensen (Ocean Associates, contracted to NOAA Fisheries, NWFSC, Seattle), Andrew Murdoch (WDFW), Jeremy Cram (WDFW), Mark Sorel (Ocean Associates, contracted to NOAA Fisheries, NWFSC, Seattle), Tracy Hillman (BioAnalysts), Greer Maier (Upper Columbia Salmon Recovery Board), Charlie Paulsen (Paulsen Environmental Research), Tom Cooney (NOAA Fisheries, NWFSC, Portland), Rich Zabel (NOAA Fisheries, NWFSC, Seattle), and Chris Jordan (NOAA Fisheries, NWFSC, Newport)

Introduction

How will a salmon population respond to changes in freshwater habitat, hydrosystem operations, hatchery programs, harvest rates, and to different states of nature? What sets of combinations of management actions and conditions will help it reach recovery goals? The goal of this project is to develop a comprehensive tool to help us understand the potential population-level responses to a range of diverse management actions and environmental change. This report details several advancements that we have made to the Wenatchee River spring-run Chinook salmon life cycle model (Jorgensen et al. 2013) since its last review, and illustrates some of its potential by presenting results of a comparison of population responses to alternative combinations of several types management actions and ocean conditions. This population has been the subject of recent life cycle modeling efforts (ICTRT and Zabel 2007; Honea et al. 2009, 2016), and this model draws upon aspects of and benefits from these efforts. Also, we take advantage of extensive past and ongoing research and monitoring efforts in the basin. These datasets are invaluable for estimating population-specific vital rates and basin-specific environmental conditions.

In this report we highlight three areas of life cycle model development since its last review: hatchery effects, calibration, and sensitivity analysis. Several hatchery programs are operated in the Wenatchee basin and are directed toward buffering the population from demographic collapse. Results from a long-term study in the basin to evaluate hatchery effects on reproductive success (e.g., Ford et al. 2014) were the starting basis for building in the potential for domestication effects and understanding their population-level consequences. Calibration is an important model building step because some model parameters are estimated with a greater degree of uncertainty. We calibrated the model against observations of smolt and adult spawner abundance, giving us the opportunity to calibrate with observations at two life stages. And, sensitivity analyses allowed us to look at parameter influence on model outcomes across the suites of scenarios.

In the past review it was pointed out that there was little progress in fish-habitat relationships (ISAB 2013). We have made some progress toward incorporation of fish and habitat links and we should have more links implemented in the near future (see Discussion and the Appendix). We included a habitat scenario that was developed from the work of Bond et al. (2017) estimating population responses as a consequence of estimated changes to juvenile capacity.

What follows includes a basic description of the life cycle model, an explanation of hatchery effects, the calibration process, and the sensitivity analysis procedure. We demonstrate the model by comparing responses to several suites of management actions and environmental conditions and, finally, through sensitivity analyses we look at parameter influence across the management alternatives and ocean conditions.

Life cycle model structure

The model is an age-structured stage-based stochastic matrix-type life-cycle model and in principle it functions similarly to the traditional Leslie-style matrix structure (Leslie 1945). In this traditional formulation,

$$\mathbf{N}(t) = \begin{bmatrix} n_1 \\ n_2 \\ n_3 \\ n_4 \\ n_5 \end{bmatrix}.$$

This 5 x 1 abundance matrix tracks population numbers for five life stage classes across five ages: parr (n_1), smolts (n_2), ocean residence (from one to three years, n_3-n_5), and tributary spawners (four and five year old fish that spent two and three years, respectively, in the ocean, n_4-n_5). The number of individuals at time (t + 1) is calculated by multiplying $\mathbf{N}(t)$ by a 5 x 5 transition matrix, $\mathbf{A}(t)$:

$$\boldsymbol{N}(t+1) = \mathbf{A}(t) \cdot \mathbf{N}(t).$$

The dimensions of the transition matrix, $\mathbf{A}(t)$, reflect the five life stages incorporated into the model and its entries can change with t. The transition matrix, $\mathbf{A}(t)$, in this more simplified form, looks like this:

$$\mathbf{A}(t) = \begin{bmatrix} 0 & 0 & 0 & b_4 \cdot s_A \cdot F_4(t) & s_A \cdot F_5(t) \\ s_2 & 0 & 0 & 0 & 0 \\ 0 & s_3(t) & 0 & 0 & 0 \\ 0 & 0 & (1-b_3) \cdot s_o & 0 & 0 \\ 0 & 0 & 0 & (1-b_4) \cdot s_o & 0 \end{bmatrix}.$$

It contains demographic parameters that govern transitions from one life stage to the next. The proportion of three and four year olds leaving the ocean and returning to spawn (their breeding propensities) are noted by b_3 and b_4. Survival of adults from Bonneville dam to the spawning grounds, s_A, is a product of upstream survival through the Columbia River mainstem dam system, s_{up}, survival after in-river harvest, $(1 - h_r)$, and survival from the upper-most dam to the Wenatchee basin, s_{sb}. Fertility is denoted by the F_i terms. s_2 is the survival probability of parr to the smolt stage (moving from one-year-old fish to two years old). $s_3(t)$ is the survival probability of the transition of fish from two to three years old, the period in which fish leave freshwater and enter the estuary and ocean, corresponding to their first year of ocean residency. The s_3 term accommodates stochasticity and varies in time and according to scenarios of climatic and ocean conditions. The proportion of three and four year old fish remaining in the ocean is given by $(1 - b_3)$ and $(1 - b_4)$. s_o represents the subsequent annual probability of ocean survival. This simplified form was the basis for the ICTRT and Zabel (2007) model and from which this life cycle model comes.

Spatial structure

To account for major fish production areas (Figures 1 and 2; Jorgensen et al. 2013) the abundance array, $\mathbf{N}(t)$, has a modified form to include fish production areas as discrete spatial units,

$$\mathbf{N}(t) = \begin{bmatrix} n_{1,1} & n_{1,2} \cdots & n_{1,j} & n_{1,h1} \cdots & n_{1,hk} \\ n_{2,1} & n_{2,2} \cdots & n_{2,j} & n_{2,h1} \cdots & n_{2,hk} \\ \vdots & \vdots\ddots & \vdots & \vdots\ddots & \vdots \\ n_{5,1} & n_{5,2} \cdots & n_{5,j} & n_{5,h1} \cdots & n_{5,hk} \end{bmatrix},$$

where each $n_{x,y}$ element is indexed by age (x) and subbasin production area (y), from $y = 1$ to up to j subbasin areas. Hatchery programs (h) are included and tracked by program and objective (from $h = 1$ up to k hatcheries; see Hatchery effects section).

Because of the modification of the **N**(t) abundance array to account for each tributary of fish production and for the hatchery programs there are additional parameters required. Parameters are applied to each subbasin, j, or hatchery, h, and which are, in some cases, the same and shared among the subbasins (e.g., maturation schedule, upstream survival, fertility, and hydrosystem and ocean survivals) and, in other cases, are different to capture the unique characteristics of a subbasin (e.g., fish production functions). Adults can be collected from subbasins for broodstock to support particular hatchery programs and objectives. See the sections below for more details on parameters and functions.

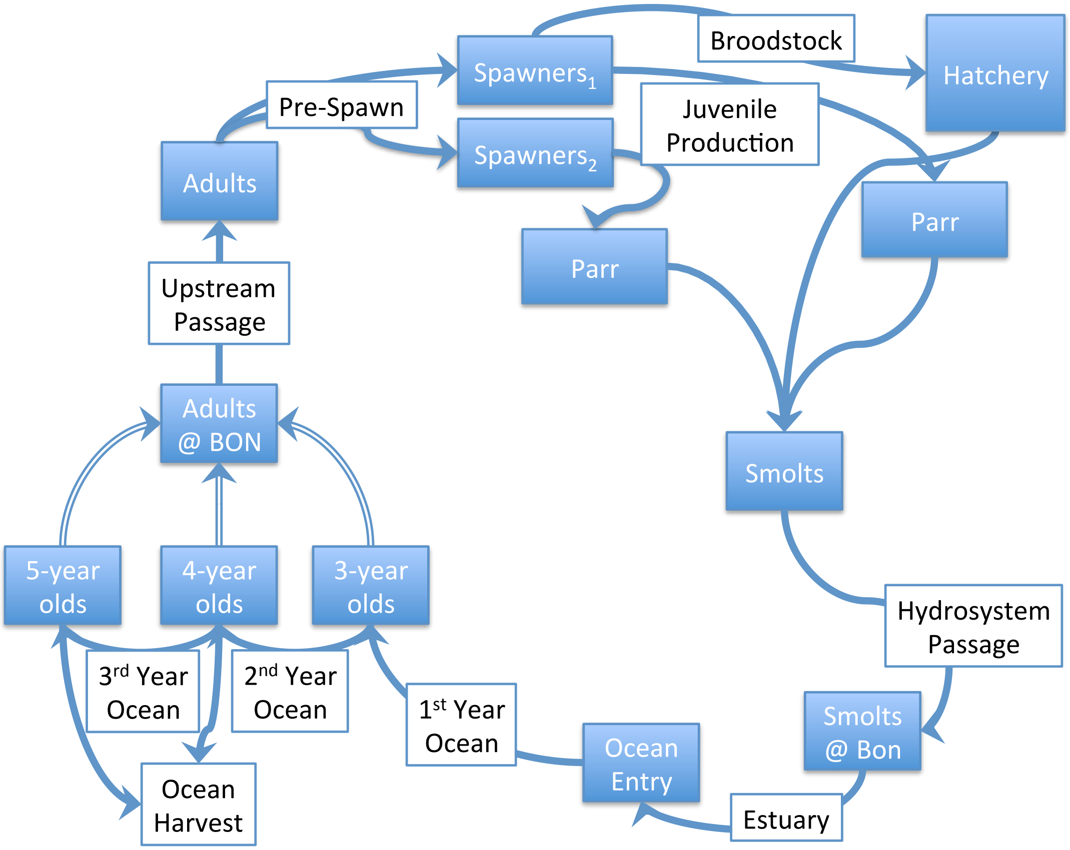

Figure 1: Diagram of the Wenatchee spring-run Chinook salmon life cycle model. Spawners with subscripts refer to the shift to model multiple juvenile production areas.

Major modifications to the life cycle model

Below, we highlight three major model changes: hatchery effects, calibration, and sensitivity.

Hatchery effects overview

Here we discuss the derivation and implementation of hatchery effects, which incorporate the potential for domestication effects on the population as a consequence of hatchery supplementation. We incorporated these effects to be able to evaluate population-level consequences of alternative hatchery management strategies. The model estimates the annual numbers of natural- and hatchery-origin adults that are collected for hatchery broodstocks, and the proportions of total spawners that are of hatchery origin (hatchery-origin returns, HORs; proportion of hatchery origin spawners, or pHOS), based on current draft management rules as well as the numbers of returning hatchery- and natural-origin adults. The hatchery programs are managed to minimize -- to the largest extent possible -- adverse ecological and evolutionary impacts to natural-origin fish from supplementation actions (HGMP Chiwawa 2009; HGMP Nason 2009; HGMP Addendum 2010). There appears to be a domestication effect as a consequence of supplementation in the Wenatchee basin: data show that hatchery-origin fish that spawn naturally in the wild (HORs) have decreased reproductive success compared to natural-origin fish that spawn in the wild (NORs) (Ford et al. 2014). We apply a domestication penalty on the progeny of HORs as a function of the 25-year (approximately 5 generations) running mean of a metric that approximates the strength of domestication selection (proportionate natural influence, pNI).

Hatchery programs

Two integrated hatchery programs supplement the Wenatchee River spring Chinook salmon population: the Chiwawa River and Nason Creek hatchery programs. The Chiwawa program commenced in 1989 while the Nason program began releasing juveniles in 2015. Each program has two parts: conservation and mitigation/safety-net elements. The conservation element's goal is to bolster the natural-origin fish and uses broodstock composed entirely of natural-origin adults. The mitigation element uses only hatchery-origin adults for broodstock, and its goal is to act as a safety-net in the event of demographic collapse and also compensates for fish lost ("no net impact") as a consequence of mortality associated with the county PUD dams. Because hatchery fish from the segregated Leavenworth National Fish Hatchery program (originally derived from out-of-basin Carson stock) are virtually nonexistent above Tumwater Dam and make no contributions to natural production we do not consider this hatchery program in the life cycle model (Pastor 2004; WDFW, unpublished data).

Broodstock collection and smolt production

The life cycle model follows procedures used by co-managers of the hatchery programs for broodstock collection according to the hatchery genetics and management plans (HGMP Chiwawa 2009; HGMP Nason 2009). Hatchery personnel identify the sub-basin of origin for returning adults in a fish ladder system at Tumwater Dam (Figure 2) using PIT tags and collect a portion of these fish for broodstock. For each of the conservation elements (Chiwawa, Nason) that use only natural-origin broodstocks, the goal is to collect up to 74 total NORs (natural-origin returns) throughout the period of adult arrivals at Tumwater Dam. The broodstock total must not exceed one-third of the expected natural-origin return. All uncollected natural-origin adults arriving at Tumwater Dam are passed above. The mitigation elements collect broodstock at Tumwater Dam and select only hatchery-origin adults.

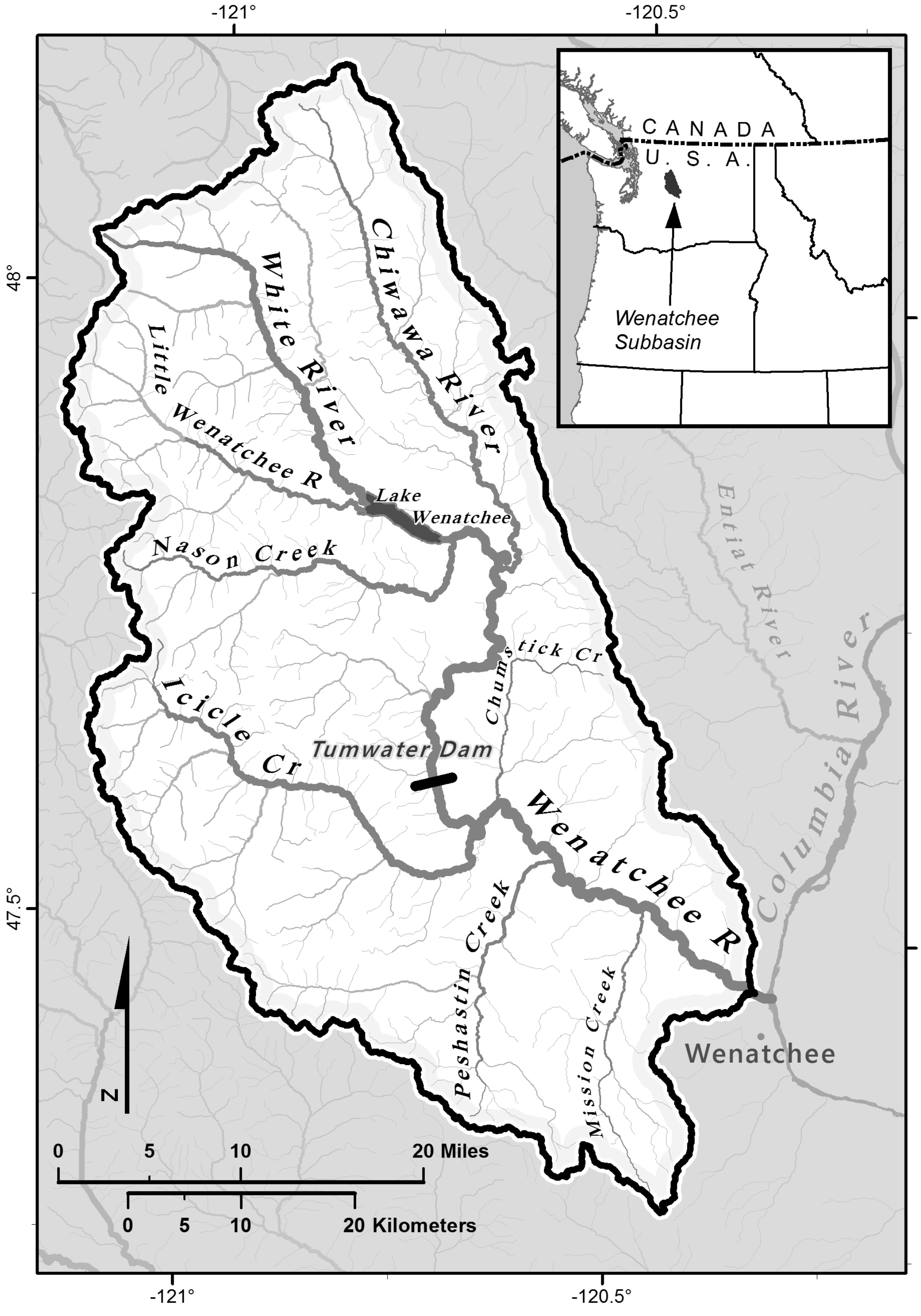

Figure 1: Map of the Wenatchee River Basin. Natural production occurs primarily in the main tributaries above Tumwater Dam: Chiwawa, White, Little Wenatchee rivers; Nason Creek (credit: D. Holzer). Integrated hatchery programs are focused in the Chiwawa River and Nason Creek.

The annual number of smolts produced from each hatchery element (conservation, mitigation) in the life cycle model was based on the assumptions of a 1:1 sex ratio, an average rate of 4,785 eggs per female, and an eggs-to-smolt survival rate of 0.8187 within the hatchery setting (HGMP Chiwawa 2009). Based on the production goals for the hatcheries, the maximum number of smolts released from each hatchery element of each program was 149,000, for a combined maximum of 298,000 smolts released from each program (HGMP Chiwawa 2009; HGMP Nason 2009).

Determining the number of hatchery-origin fish passed onto the spawning grounds

Proportionate natural influence (pNI) approximates the degree of domestication selection,

$$pNI = pNOB/(pNOB + pHOS),$$

where pNOB is the proportion of the broodstock that is of natural origin and pHOS represents the proportion of hatchery-origin spawners (some background can be found in, e.g., HSRG 2009). The conservation elements of the hatchery programs in the Wenatchee Basin have recently shifted to using only natural-origin broodstock, thus if pNOB = 1.0 then pHOS determines pNI. Theory suggests that a population is moving to a more natural state when pNI values are ≥ 0.50 (Figure 3; HSRG 2009). Therefore, the hatchery programs strive to maximize pNI by minimizing pHOS, and this depends on natural-origin returns.

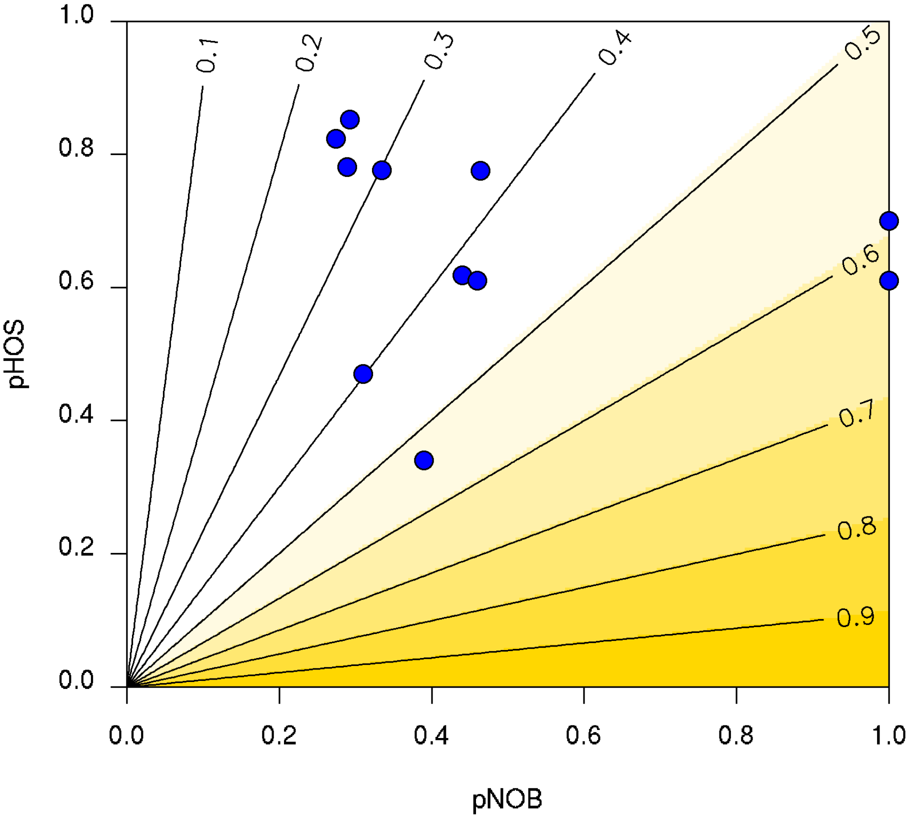

Figure 3: Isoclines of pNI for combinations of pNOB and pHOS, with pNI values ≥ 0.50 indicated by the gold shading. Points represent pNI values for the Chiwawa subbasin from 2004-2014 (from Table 5.35 in Hillman et al. 2016).

Based on the annual forecasted run sizes of natural-origin adults, hatchery co-managers identify pNI targets for each production area that guide pHOS goals. A recent draft of pNI guidance is in Table 1, which sets pNI floors for specific ranges of forecasted natural-origin returns. Targets for pNI have a lower floor when estimated returns of natural-origin adults are lower, which allows managers to have more flexibility with pHOS to increase juvenile production in the natural environment given low natural-origin returns.

Table 1: Draft guidance for co-managers that relates NOR run size to pNI objectives. Percentile represents the percent of run size of ~1213 NORs to the Wenatchee basin (sources: hatchery genetics and management plans; A. Murdoch, pers. comm.).

Percentile	**Chiwawa River**	**Nason Creek**	**Wenatchee basin**	**pNI**
>75%	>372	>350	>910	≥0.80
50% – 75%	278 – 372	259 – 349	631 – 909	≥0.67
25% – 50%	208 – 277	176 – 258	525 – 630	≥0.50
10% – 25%	176 – 207	80 – 175	400 – 524	≥0.40
<10%	<176	<80	<400	Any pNI

We developed a continuous function to predict co-managers' annual goals for pHOS as a function of the number of natural-origin adults that returned to the basin in the life cycle model and which fit within the pNI guidelines outlined in Table 1:

$$HOR = \begin{cases} HOR_{max} - HOR_{max} * \left(\dfrac{NOR}{NOR_{cutoff}}\right) & \text{if } NOR < NOR_{cutoff} \\ 0 & \text{if } NOR \geq NOR_{cutoff} \end{cases}$$

In this function, HOR_{max} represents the maximum number of HOR allowed to spawn in the wild when NOR = 0, and HOR decreases linearly with increasing NOR until reaching 0 at a threshold of $NOR_{cuttoff}$. In other words, it sets an upper maximum number of HOR in the absence of NOR, and it scales HOR down from HOR_{max} as NOR increases. It assumes that in years when NOR is large (greater than some NOR_{cutoff} level) there would be no supplementation with HORs. Given that pHOS = HOR/(HOR + NOR) and that pNOB = 1 for the conservation hatchery, the HOR function above with an HOR_{max} = 200 and NOR_{cutoff} = 1,000 produces pNI levels that are within the management guidance for the Chiwawa and Nason populations (Figure 4). We used this to represent the baseline or current management of the hatcheries. In the modeling realm, we have perfect knowledge of NOR each year and can set HOR goals to precisely match targets. In the future, we may add some noise to account for uncertainty in the annual forecasts of natural-origin returns that co-managers use to set pNI goals.

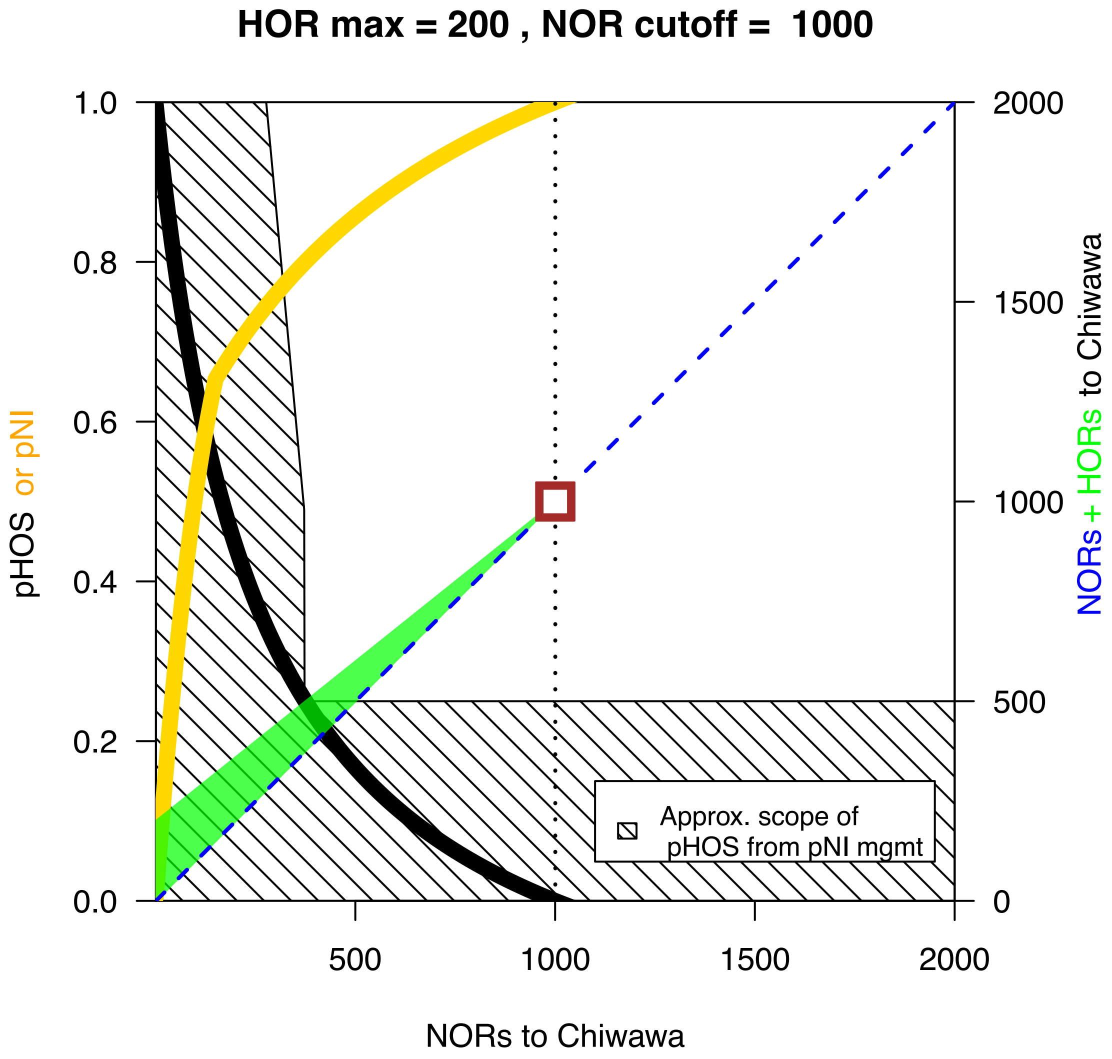

Figure 4: An illustration of how the annual numbers of NORs (dashed blue line, secondary y-axis) and HORs (green shaded area, secondary y-axis) affect pHOS (black curve, primary y-axis) and pNI (gold curve, primary y-axis) in the Chiwawa River. In this scenario that represents current management objectives, the HOR ceiling (HOR_{max}) is set to a maximum of 200 hatchery fish that are permitted to spawn in the wild when NOR abundance is zero. The number of HORs linearly decreases to zero as the number of NORs increases to the NOR_{cutoff} of 1,000. Note that the NOR abundance here is the number of NORs after broodstock are removed according to the collection guidelines.

Domestication effects and naturally spawning hatchery fish

In the Wenatchee Basin, hatchery-origin adults that spawn naturally in the riverine environment appear to produce fewer offspring per capita on average than natural-origin spawners. We take advantage of a long-term multi-generational study in this basin of reproductive success through parentage analysis, which indicates that the relative reproductive success (RRS) of hatchery-origin spawners is less than natural-origin spawners. For brood years 2004–2007 and 2010 it ranged from 0.27 to 0.85 hatchery:wild smolts per female (Ford et al. 2014).

Assuming that domestication selection is the primary driver of RRS decrements for hatchery-origin spawners within the Wenatchee Basin, we developed a preliminary model of domestication effects as a function of the 25-year (approximately five generations) running mean of pNI (as in Zabel et al. 2015; Figure 5). Results from RRS studies in the Wenatchee basin don't span the full range of pNI values to infer the shape of the functional form, so we considered reproductive success results from studies of other populations to provide some context. Estimates of reproductive success of hatchery-origin Chinook salmon and steelhead spawners in the absence of natural-origin fish (i.e., where pNI is essentially at or near 0) from studies in other basins were < 0.15 (Leider 1990; McLean et al 2003; Chilcote 2013). At the other extreme, we assumed that in the absence of supplementation that there should be no domestication effects. Given the limited number of RRS estimates across the range of possible pNI values to inform the functional form, we made a simplifying assumption of a linear relationship between domestication effects and pNI. We used 1 – RRS to generate a discount that we applied to progeny of hatchery-origin fish that spawned in the wild (Figure 5). We took a more conservative approach and set a maximum discount of 0.60 (corresponding to a RRS = 0.40) at pNI = 0 rather than the higher values suggested by Chilcote et al. (2013) and others. In the sensitivity section we tested how influential the intercept and steepness of the relationship between RSS and PNI was on population dynamics. We will explore different functions to estimate RRS in the future and we will incorporate results from additional work generated by the long-term RRS study in this basin.

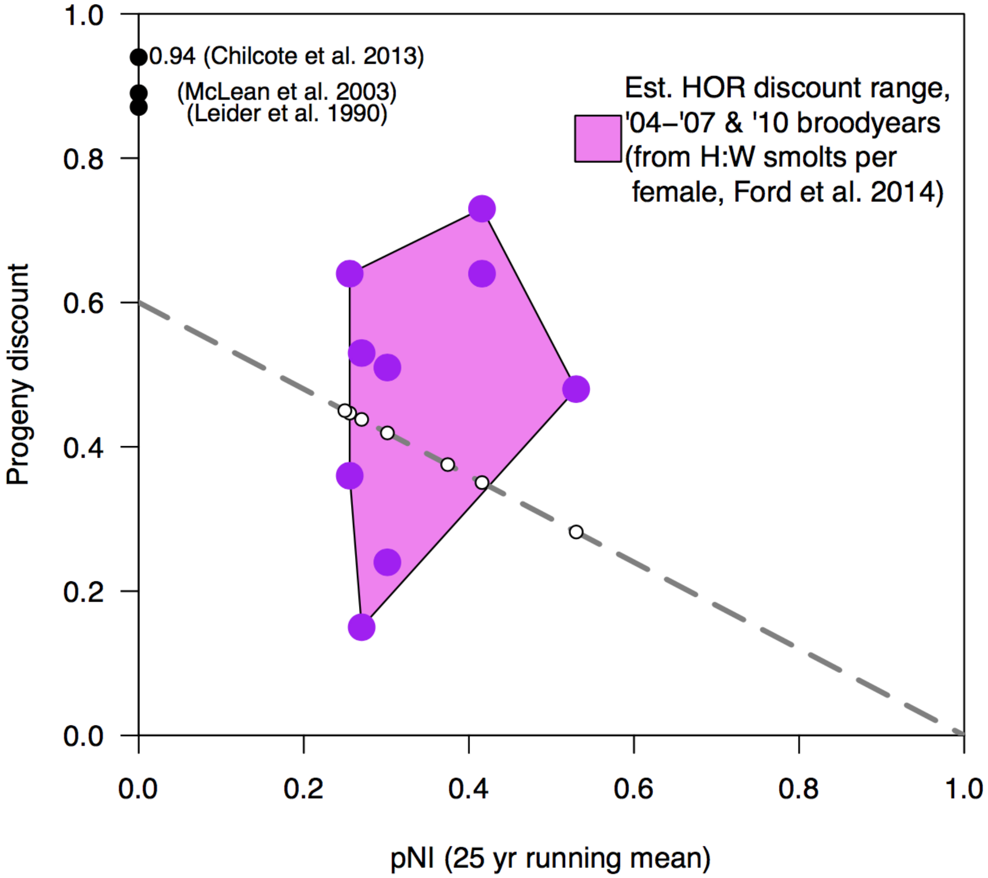

Figure 5: The domestication discount applied to progeny (smolts) of hatchery-origin fish spawning in the wild is a function of the 25 yr running mean of pNI. The discount used in the Wenatchee spring Chinook salmon life-cycle model corresponds to the dashed line with an intercept of 0.60 when the 25-yr running mean of pNI = 0. The small white points on the line are the pNI values for the brood years 2004-2007 and 2010. The light purple polygon connects the outer bounds of data points.

Calibration

To align life cycle model simulation behavior and results to observations, we initiated a parameter calibration process. The life cycle model has stochastic elements, such as in the spawner-parr fish production functions and in early ocean survival. Thus, unlike statistical-type life cycle models that are fit to data, results from simulation models like this one aren't expected to exactly match the peaks and valleys of time series of observations. Rather, we seek to identify parameter values that generate simulated data from the model that share similar characteristics as observed data.

The end product of calibration is a method or process from which to draw parameter values, where the method or process is informed from characteristics of observed data. The calibration process takes place as a step in the model building process prior to developing management scenarios for prospective simulation runs.

Calibration methods

We identified several parameters to be included in the calibration (Table 2). Their values were relatively more uncertain because there were less data available to inform them. These included estimates of parr-smolt survival, ocean survival after the first year at sea, upstream survival of adults through the mainstem to the basin, and prespawn mortality unaccounted for in the smolt-to-adult return estimates used to estimate several model parameters. The calibration procedure is flexible, easily implemented, and can be replicated as needed as model parameters are added, adjusted, deleted, and additional data become available.

To sufficiently explore the full parameter space, because we set fairly wide ranges for the parameter values for the calibration process, we ran the model many times (50,000) to construct a large number of parameter value combinations and associated life cycle model outputs. For each model run we recorded several things: the geometric mean numbers of smolts and spawners, an estimate of the AR(1) coefficient (*phi*), and the vector of parameter values that achieved these model results. Observations of juvenile and adult abundance were selected for model calibration points. These are estimated annually for the population (see below). Using two life stage points with which to calibrate the model provided two different life history benchmarks to estimate parameter likelihoods. We included a metric characterizing autocorrelation because we wanted to have a benchmark to compare across-year population dynamics. In the life cycle model we introduce autocorrelation through time series of hydrosystem smolt survivals that come from COMPASS and also in the early ocean survival functional relationship (*s*3; ICTRT and Zabel 2007; Kendall et al. 2013).

Table 2: Life cycle model parameters included in the calibration process.

Parameter	**Description**	**Calibration range**
S.ps	Parr-smolt survival	(0.2, 0.8)
So	Annual ocean survival after the first year of ocean entry	(0.2, 0.9)
S.up	Adult upstream survival to the mouth of the Wenatchee River	(0.2, 0.9)
S.sb	Prespawn survival (unaccounted for prespawning mortality)	(0.2, 0.95)

Likelihoods and joint likelihoods

The joint likelihoods were comprised of the combined density estimates from fitted distributions of three types of observations: the abundance of spawners and smolts, and autocorrelation in spawner abundance (Figure 6). Because our objective was to calibrate to current conditions, we focused on the most recent 10 years of observations of spawning adults (SPS database; https://www.webapps.nwfsc.noaa.gov/apex/f?p=261:HOME::::::) and annual smolt abundance estimates from the entire Wenatchee River Basin (WDFW, unpublished data). Adult abundance is estimated annually through redd count surveys, and smolt abundance is estimated from annual smolt trapping in the lower mainstem of the Wenatchee River. The other observation-based metric we used was the estimated first order autocorrelation coefficient (*phi*) from a fit of an AR(1) model to the entire spawning adult time series (54 years).

Table 3: Characteristics of observations used in the calibration process.

Observation	**Distributed as**
Smolt estimates near the mouth of the Wenatchee River Basin	~lognormal $(11.39, (0.467)^2)$
Natural origin spawning adult estimates	~lognormal $(6.34, (0.457)^2)$
Autocorrelation coefficient, *phi*, from an AR(1) model fit to time series of natural origin spawning adult estimates	~normal $(0.672, (0.0981)^2)$

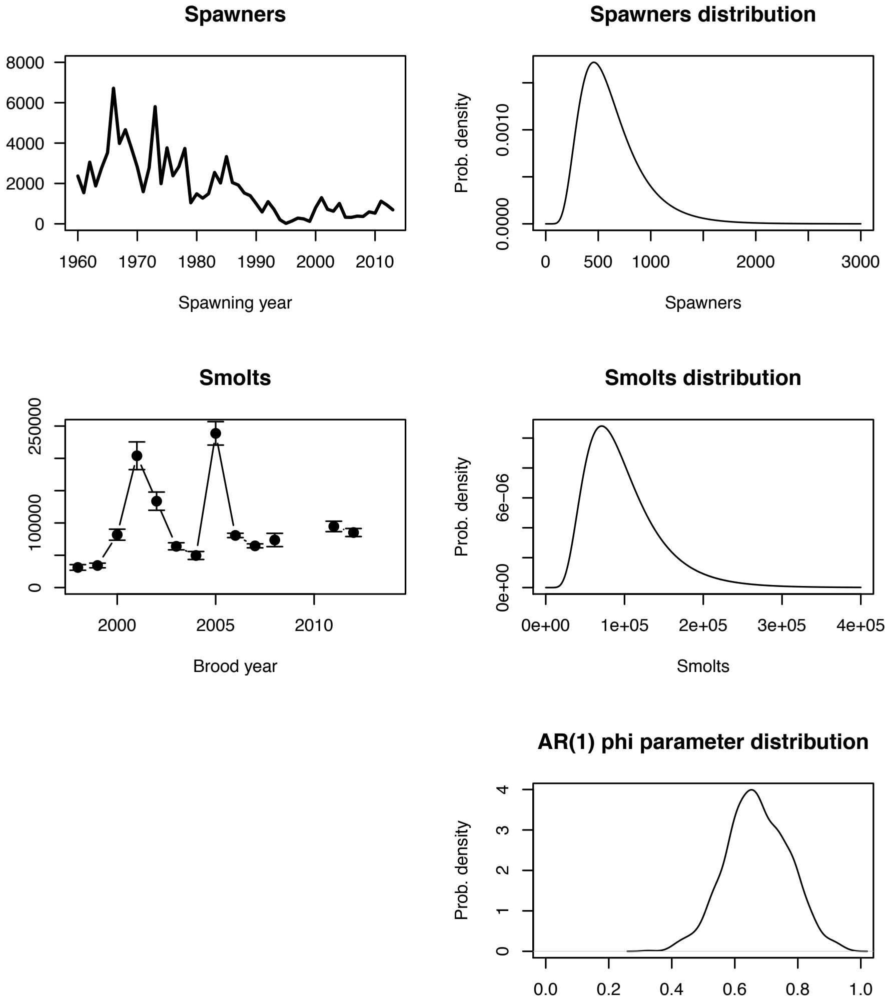

Figure 6: Characteristics of observed data used in the calibration process. Spawner observations come from the SPS database and smolts are from annual estimates by WDFW. The *phi* term comes from the estimated AR(1) coefficient fit to spawner observations.

Our first step was to compute likelihoods of model output, where the likelihoods were determined from the density distributions fitted to observed data. Observations of abundances of spawners and smolts were approximately lognormally distributed, and we made an assumption that the AR(1) autocorrelation coefficient, *phi*, of observed spawners was approximately normally distributed (Figure 6; Table 3). We fitted distributions to these observations and calculated the likelihoods of the model output. For a given model output metric and set of parameters, the individual likelihoods were for each model run, *n*, where *theta* represents a vector of parameter values, and $n = 1$ to 50,000: L{ $\text{spawners}_{\text{model},n}$ | $\textit{theta}_n$ }; L{ $\text{smolts}_{\text{model},n}$ | $\textit{theta}_n$ }; and, L{ $\text{phi}_{\text{model},n}$ | $\textit{theta}_n$ }. Likelihoods for each set of parameter combinations were approximated by the probability densities of model-generated output (spawners, smolts, and the estimated *phi*) as determined from the fitted distributions to the observed data.

The joint likelihoods, L{ ($\text{spawners}_{\text{model},n}$, $\text{smolts}_{\text{model},n}$, $\text{phi}_{\text{model},n}$) | $\textit{theta}_n$ }, were the products of the individual likelihoods for each model run, *n*. The joint likelihood for a given model run, *n*, was the product rather than the sum because the density estimates came from distributions fitted to untransformed observations.

We constructed marginal distributions for each of the parameter values along the interval (0, 1) using the joint likelihoods as a weight (Figure 7).

Importance sampling to generate parameter values

To obtain values for each of these four parameters during a prospective model run we drew values from the constructed marginal distributions of the parameters (Figure 7) by sampling according to a uniform distribution across the range (0, 1).

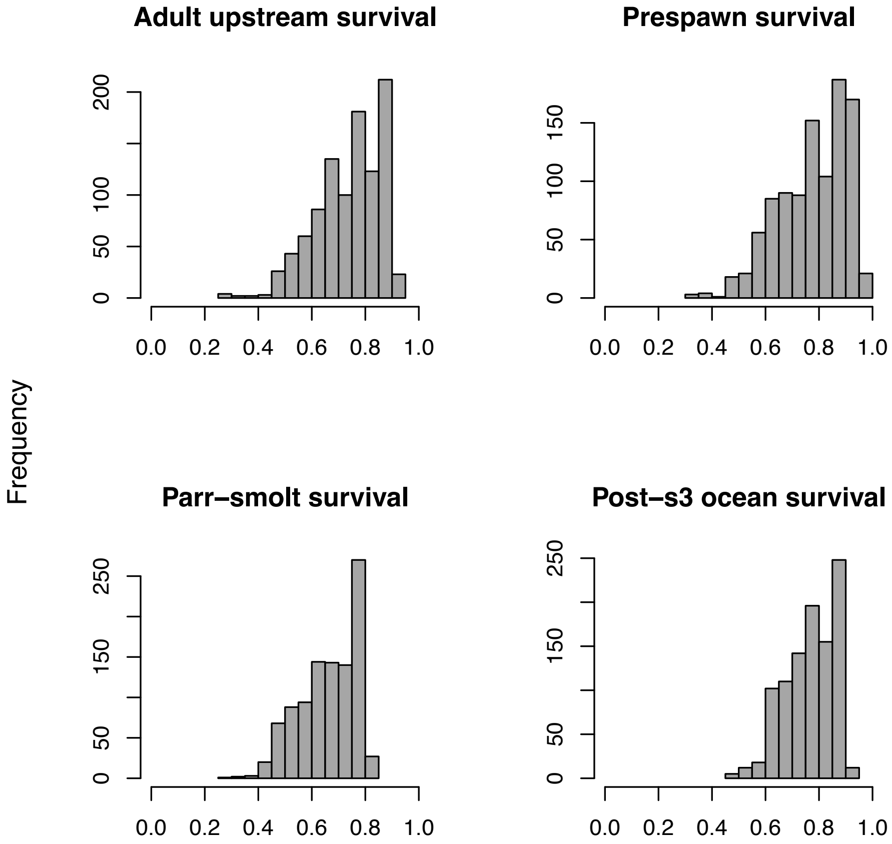

Figure 7: Histograms depicting the marginal distributions used to generate parameter values (listed in Table 2) for prospective runs of the life cycle model.

In our next steps, we will investigate the potential for correlations between parameters (Figure 8). In the above we describe a process where draws were made from each of the parameter distributions independently. We intend to compare this calibration process to one where we construct a conditional parameter distribution and to draw parameter values such that it accounts for the degree of correlation among parameters.

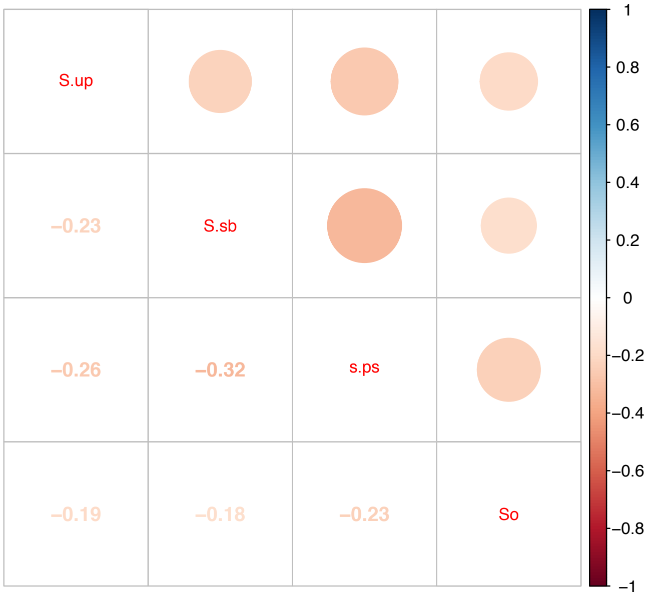

Figure 8: Correlations between centered parameters, weighted by their joint likelihoods, included in the calibration process.

Sensitivity

We conducted a sensitivity analysis of the life cycle model to understand parameter influence on model outcomes, and how influence for a given parameter might change under different states of nature or suites of scenarios. The approach we followed is similar to that described in Zabel et al. (2015). Sensitivity analyses runs were done in a separate exercise after we completed the prospective model runs.

Sensitivity analysis is the process of understanding the relationships between what goes into the model and what comes out, and which inputs are responsible for having the largest influence on model outputs (Helton et al. 2006; Storlie et al. 2009). They can be used to test assumptions about models and parameters. Sensitivity combines an examination of parameter influence with the population-level implications of uncertainty in parameter values. Results from a sensitivity analysis can help inform the focus of research and monitoring efforts, as in the case where a particular parameter may have a large influence and yet very little information informs its value. Sensitivity analyses can also suggest a population's limiting life stages.

Our focus is on so-called "global" -- rather than "local" -- sensitivity analyses because of their strengths for this type of life cycle model (McCarthy et al. 1995; Coutts and Yokomizo 2014). In a local sensitivity analysis one parameter at a time is manipulated, usually by some fixed percent, and model output is compared to average model output. This approach is insufficient for more complex models that contain stochastic elements and interactive factors. With a global sensitivity analysis all parameters of interest are manipulated simultaneously (typically independently) and their influence on model outputs are assessed relative to each other.

Among the array of global sensitivity approaches (e.g., see Helton et al. 2006) a few in particular are useful for this type of simulation model. We chose a regression-based, standardized regression coefficient (SRC), method because it is readily implemented and the results are easily interpreted (McCarthy et al. 1995; Cross and Beissinger 2001; Coutts and Yokomizo 2014). SRC has frequently been used to characterize parameter sensitivities of population viability analysis (PVA) models for many species, including those for salmon (Zabel et al. 2006; Crozier et al. 2008; Lonsdorf et al. 2016; Mortensen and Reed 2016). Another type of global sensitivity analysis sometimes used in PVA-type models assesses main and total effects of parameters using Latin Hypercube design sampling, such as Sobol' indices (e.g., Saltelli et al. 2000). We found that this designed experiment approach was difficult to implement without a major restructuring of the life cycle model code. There are methods to emulate Sobol' indices from monte carlo-type computer experiments (e.g., Gramacy and Taddy 2010) and a preliminary comparison indicated that the SRC method appeared to capture the same dynamics represented by the estimated Sobol' metrics (analyses not shown). We would like to formally compare results of these sensitivity analysis methods in the future. We present results for the SRC approach.

We followed the SRC procedure of Zabel et al. (2006; 2015) which is described below. The model was run multiple times (500) while parameters included in the sensitivity analysis were all simultaneously sampled from their identified ranges according to a random uniform distribution (Table 4). For each run of the model (out to 100 simulation years) a unique set of parameter values was drawn from specified ranges and held constant through the run. Parameter ranges from which we sampled were typically set by using the 95% confidence interval of the estimated parameter, by looking at the range in data, from the literature, or from expert opinion. Choice of parameter inclusion was driven by uncertainty in their value or by an interest to understand the magnitude of influence. Because both parameter choice and the size of the ranges sampled drive sensitivity results, we consider sensitivity to be an ongoing and evolving exercise to be conducted throughout the life cycle modeling process (model development, testing, and scenario evaluation). What is presented in this section reflects a snapshot in time during this model's evolution.

Table 4: Parameters included in the sensitivity analysis of the Wenatchee life cycle model.

Parameter	**Description**	**Range**
S.up	Adult upstream survival	(0.7, 0.9)
S.sb	Survival to spawning	(0.85, 0.95)

Parameter	**Description**	**Range**
S.ps	Parr-smolt survival	(0.5, 0.7)
HOR.domestication.discount	Survival decrement to progeny of hatchery origin fish spawning in the wild	(0.3, 0.7)
HOR max Chiwawa	Maximum number of hatchery fish allowed to spawn in the wild, Chiwawa program	(100, 200)
HOR max Nason	Maximum number of hatchery fish allowed to spawn in the wild, Nason program	(100, 200)
NOR cutoff Chiwawa	When natural origin returns reach this limit, no hatchery fish are allowed on the spawning grounds, Chiwawa program	(500, 1500)
NOR cutoff Nason	When natural origin returns reach this limit, no hatchery fish are allowed on the spawning grounds, Nason program	(500, 1500)
Beta0 (intercept)	Intercept of s3 survival function[1]	(-4.35, -3.83)
WTT	Water travel time (s3 function)[1]	(-0.89, -0.36)
Upwelling May	Coastal upwelling in May (s3 function)[1]	(-0.53, 0.004)
Upwelling April	Coastal upwelling in April (s3 function)[1]	(0.42, 0.95)
So	Ocean survival after first year	(0.7, 0.9)

[1] 95% C.I.s from the fitted s3 survival function

We used the generated dataset from the sensitivity procedure to construct SRCs for comparisons. Model outputs that we recorded for the sensitivity analysis included two metrics: the median number of spawners, and whether model runs went extinct (1 = fell below the quasi-extinction threshold, mean of 50 over a consecutive four year period; else = 0). We regressed each model output metric as the dependent variable on the parameters, which were the independent variables. In the case of extinction risk as the dependent variable, we conducted a logistic regression. Because the parameter values were sampled independently there were no collinearity concerns. We standardized the regression coefficients (divided by their standard error; and we further normalized by dividing by the largest absolute value) thereby making them more easily comparable. Coefficient values closest to or equal to plus or minus 1.0 were relatively more influential than those closer to zero. It's important to note that in cases where any particular parameter may not have been influential relative to the others (within a given scenario), it does not mean it wasn't important in the model. Rather, given the set of parameters chosen for evaluation, and given the ranges within which parameter values were being sampled, some parameters were more influential than others.

We conducted sensitivity analyses to look at parameter influence across several different combinations of scenarios (see the Sensitivity analyses section of Results).

Inputs to the life cycle model

In the sections above, we have described how we incorporate hatchery effects, the process used to calibrate the life cycle model, and the procedure for sensitivity analyses. In this section we provide some additional detail about some of the other parameters used in the life cycle model (Tables 5 and 6), and highlight some of the changes from Jorgensen et al. (2013).

Table 5: Parameters used for the Wenatchee River spring Chinook salmon life-cycle model for major production areas, which include: Chiwawa River, Nason Creek, and the White River.

Parameter	**Chiwawa River**	**Nason Creek**	**White River**
Spawner(t) -to- parr($t+1$) Beverton-Holt "a"	353.437	328.490	154.318
Spawner(t) -to- parr($t+1$) Beverton-Holt "b"	0.000298	0.005	0.005
$\sigma^2{}_1$	0.412	0.600	1.04
ϕ_1 (variance term)	0.1	---	---
Parr-smolt survival[1]	Drawn from distribution	Drawn from distribution	Drawn from distribution
Hydrosystem survival	0.525	0.525	0.525
s_3 (first ocean year)	Stochastic variable, dependent on relationship to ocean conditions	Stochastic variable, dependent on relationship to ocean conditions	Stochastic variable, dependent on relationship to ocean conditions
s_o (ocean survival for years after s_3)	Drawn from distribution	Drawn from distribution	Drawn from distribution
b_3 (propensity of 3 year olds to breed)	0.046	0.046	0.046
b_4 (propensity of 4 year olds to breed)	0.514	0.514	0.514
h_r (harvest rate)	0.09	0.09	0.09
s_{pin}	See pinniped section	See pinniped section	See pinniped section
s_u (Bonneville-to-basin survival rate)	Drawn from distribution	Drawn from distribution	Drawn from distribution
s_{sb} (pre-spawning survival rate)	Drawn from distribution	Drawn from distribution	Drawn from distribution
Initial abundance of 4 and 5 year old tributary spawners (geomean of 2008-2012)	406	148	38

[1] Parr-smolt survival measures survival from exiting the tributaries until reaching the mainstem Columbia

Table 6: Parameters used in the Wenatchee River Basin spring Chinook salmon life-cycle model for the hatchery programs in the Chiwawa River and Nason Creek (see Hatchery effects section for more details).

Parameter	**Chiwawa River program**	**Nason Creek program**
HOR.max (maximum number of hatchery fish allowed to spawn in the wild in the absence of natural-origin fish)	200	200
NOR.cutoff (natural-origin return abundance at which no hatchery fish are allowed to spawn in the wild)	1000	1000
HOR.domestication.discount (decrement on progeny of hatchery fish that spawned in the wild)	0.60	0.60

Parr capacity

The NWFSC Watershed Program has initiated efforts to characterize summer parr capacity as a function of geomorphic habitat classes. We include a scenario where capacities are changed as a consequence of conversion back to floodplain and side channel reconnections in areas with different types of land use or by removal of some small roads (see Scenarios section; Bond et al. 2017). In the near future, we will also incorporate parr capacity estimates from other methods such as quantile regression forests, which leverage fish and habitat survey data (ISEMP/CHaMP 2015).

Parr-smolt

The parr-to-smolt transition, s_2, includes three elements, parr-smolt overwinter survival (s_{ps}), migration survival through the PUD and federal dams to past Bonneville, and avian predation. Parr-smolt survival is drawn yearly from a distribution determined through a model parameter calibration routine (see Calibration section). For this presentation, we have incorporated estimated survival of two relatively recent hydro scenarios (see Scenarios section; Zabel et al. 2017b) through the hydrosystem from the COMPASS model (Zabel et al. 2008); however, the life-cycle model structure is flexible and we can accommodate migration survivals either as a time series or as an average survival across years. The model has the ability to accommodate potential avian predation management actions (see Jorgensen et al. 2013) but for this review our focus was on other suites of management actions.

We expect to change the model substantially in the juvenile life stages prior to the smolt stage as we begin to incorporate juvenile life history diversity (see Appendix).

Ocean and pinnipeds

The ocean phase of salmon in the life cycle model encompasses estuary entry and life at sea. Once smolts pass Bonneville Dam, they reach the estuary and can spend a variable number of years at sea. Survival during the first year in the ocean (s_3) is governed by a stochastic functional relationship described in Kendall et al. (2013). All subsequent survival in ocean years (s_O) is drawn from a distribution as determined through a parameter calibration process (see Calibration section). We are in the process of revising ocean survival and should have new survival estimates for Wenatchee spring-run Chinook salmon relatively soon (Burke et al. 2017).

The maturation schedule to the adult stage is set by proportions of three and four year old ocean fish returning to spawn (b_3, b_4). The model assumes that all surviving five year olds advance to the adult stage and return to spawn.

Another important component of survival during this phase for Columbia River-bound adults happens when they pass through the estuary and up through Bonneville Dam. They are vulnerable to predation by pinnipeds (s_{pin}), from which the resulting mortality rates appear to have increased since 2012 (Sorel et al. 2017; see Scenarios section).

Upstream

Survival from Bonneville Dam to the mouth of the Wenatchee River (s_{up}) is drawn yearly from a distribution determined through calibration (see Calibration section). The impacts from Columbia River fisheries (h_r) are also accounted for during the upstream migration, which is set to a constant value of 9% during prospective model runs.

Spawners

Several life history events are applied in the life-cycle model to adults that migrate upstream before becoming spawners on the spawning grounds. First, a small number of fish migrate upstream in the Columbia River and bypass the Wenatchee River, and some fish stray or disperse to nonnatal tributaries within the Wenatchee basin above and below Tumwater Dam (5% and < 3%, respectively; WDFW, unpublished data). Those below Tumwater Dam are not considered to contribute to the population and are removed from the life cycle model. The rates of bypass and below-Tumwater dispersal are applied only to HORs and can be attributed to several factors: they may be attracted to an earlier rearing location (the “Eastbank effect”), or because they may not be able to locate or may not have fully acclimated to their release site tributary, or other factors. Second, not all HORs are allowed to spawn in the wild. HORs are held at Tumwater Dam and the yearly number that are passed above and allowed to spawn is determined by annual pNI targets and by NOR abundance which govern year-to-year pHOS rates (see Hatchery effects section). Third, all fish that are on the spawning grounds experience some level of prespawn mortality (s_{sb}) which is drawn yearly from a distribution as determined through a model parameter calibration process (see Calibration section).

Scenarios

An advantage of this type of life cycle model framework is that we can evaluate population-level effects of suites of actions. For this review we focused on a few combinations to illustrate the model's capabilities (Table 7). With each scenario combination we show results of 500 model iterations of 100 years each.

Harvest

Estimates of the harvest rate suggest that the mean across years is approximately 9%. We considered two harvest rate scenarios: current, and a 25% reduction from the current rate to 6.75%.

Habitat

We used estimates of improvements to the spawner-to-parr survival from the effects of estimated by re-establishment of floodplains and reconnections to side channels by the conversion of rangeland and the removal of small roads (M. Bond and T. Nodine, NWFSC Watershed Program, unpublished data). These modifications resulted in small changes to capacity (up to a ~2% change in the White River was the largest) because the tributaries are in relatively more confined valleys which reduces the size of floodplain area and the conversion potential, and also because there has not been much modification of land for rangeland purposes in these tributaries.

Hydrosystem

We included two hydrosystem survival scenarios generated from newer outputs from COMPASS: a newly developed survival estimate from COMPASS runs simulating recent hydro operations, and a scenario that increases spill up to the gas cap at the lower Columbia River mainstem federal dams, relative to recent operations ("ORPIv2", Figure 9). Because the hydrosystem survival inputs are incorporated into the model as a time series rather than previously as a mean across the annual estimates, the life cycle model is able to link the annual hydrosystem survival water year to the seaward migration year in which the outmigrating smolts reach the estuary, thus ocean conditions of arriving smolts correspond to the in-river migration experience and water year of the hydrosystem experience.

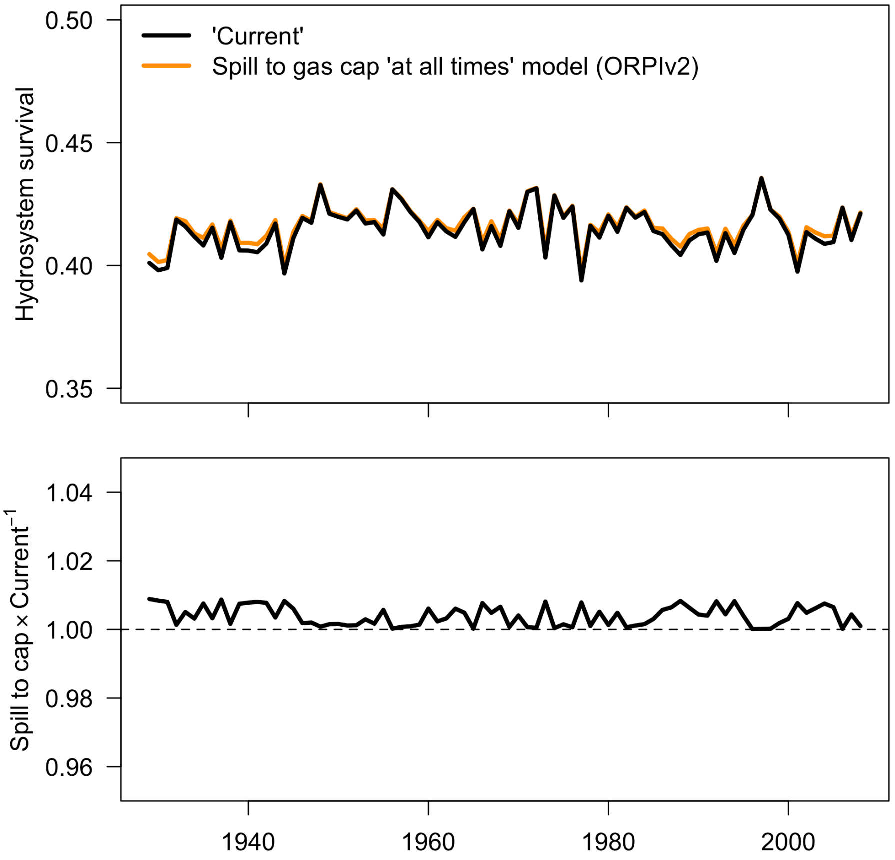

Figure 9: Hydrosystem survival estimates for flows observed in the water years 1929-2008, for Wenatchee River Basin natural-origin spring Chinook salmon, from recent COMPASS modeling. Top: estimated annual survivals based on recent dam operations (e.g., timing and degree of spill), and a scenario where spill is increased up to the gas cap as often as possible at the lower Snake River and mainstem lower Columbia River federal dams (ORPIv2). Bottom: Ratio of survival given ORPIv2 operations and current operations.

Pinnipeds

Pinniped predation intensity appears to be a growing threat for many Columbia River Basin populations (Sorel et al. 2017). We applied a pinniped predation scenario of adult survival to Bonneville Dam at levels observed in 2013 to 2015, which was 90% of the survival during the baseline period of 1998–2012. We included another scenario that assumed that survival returned to historical or background levels corresponding to predation intensity prior to the recent increase in pinniped abundance.

Hatchery

As a preliminary assumption of the current scope of the hatchery programs' levels of hatchery operations we hold HOR_{max}, the maximum number of hatchery fish allowed to spawn in the wild, at 200 and NOR_{cutoff}, the level of natural origin returns above which no hatchery fish are allowed to spawn in the wild, at 1000 (Figure 4). We explored a scenario where we cut these limits in half ($HOR_{max} = 100$, $NOR_{cutoff} = 500$) as a way to simulate effects of a scaled-back supplementation strategy.

Ocean

We used the ocean survivals as described previously (Kendall et al. 2013) generated from sampling more recent years of ocean conditions (1980 – 2012; "recent") and as a contrast we include a "bad" scenario where we sample from years representing ocean conditions unfavorable to salmon survival (1977 – 1997). In the near future we will take advantage of the work described in Burke et al. (2017) when it is expanded to include estimates of ocean survivals for Upper Columbia River spring-run Chinook salmon.

Model-input combinations for scenarios

We added scenario levels cumulatively, rather than evaluating all combinations of actions and conditions (Table 7). For example, in the first scenario we set all conditions to recent or current states except we reduced the hatchery programs. In the second scenario, all first-scenario conditions prevailed except that harvest was reduced. In the third scenario, in addition to the second-scenario conditions, juvenile survival was improved as a consequence of habitat improvements. In scenario four, a hydrosystem alternative increasing spill was added. In the fifth scenario, estuarine adult survival was reduced to historical levels in addition to conditions in scenario four. In the sixth scenario, fifth-scenario conditions prevailed except the hatchery programs were increased up to their current levels of operation. In the seventh scenario, all sixth-scenario conditions applied but ocean conditions changed to a state less favorable for salmon.

Table 7: List of suites of management actions and environmental conditions that comprised the scenarios used in this analysis. Changed conditions are indicated in italics.

Scenario #	Hatchery	Harvest	Habitat	Hydro	Pinniped	Ocean
1	*reduced*	current	current	current	2013-2015	recent
2	reduced	*reduced*	current	current	2013-2015	recent
3	reduced	reduced	*improved*	current	2013-2015	recent
4	reduced	reduced	improved	*Increased spill*	2013-2015	recent
5	reduced	reduced	improved	Increased spill	*1998-2012*	recent
6	*current*	reduced	improved	Increased spill	1998-2012	recent
7	current	reduced	improved	Increased spill	1998-2012	*bad*

Results

Model results

Population-level abundance increased and extinction risk went down as a result of simulated management actions directed at improving population viability. The biggest rise in spawner abundance occurred when estuarine adult survival increased to historical levels, as might result from reduced pinniped predation, and when the hatchery programs resumed operations to current levels (Figure 10). Extinction risk decreased as spawner abundance increased across these combinations of alternatives. Abundance dropped substantially in response to bad ocean conditions; however, extinction risk did not climb proportionally because management actions such as the hatchery programs buffered the population against extinction events.

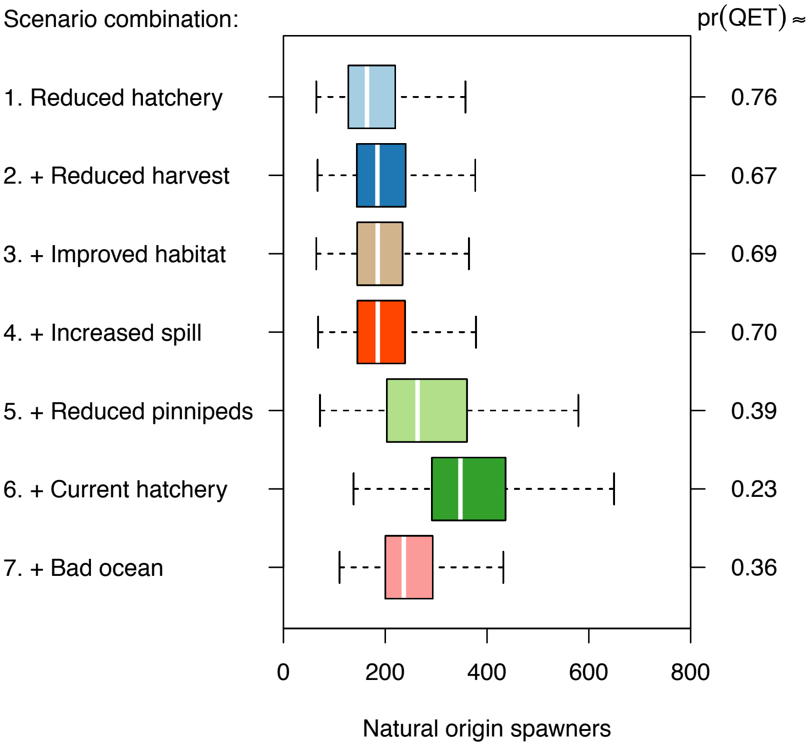

Figure 10: Population responses to the cumulative effects of several suites of management actions (Table 7). Response is measured by median spawner abundance and by estimates of the extinction risk (falling below the QET threshold).

Because we are simulating effects of supplementation on population dynamics, we also examined population measures of pHOS and pNI. The mass of the distributions of pHOS tended to move rightward when the hatchery programs were changed from a reduced level to current operational levels and when ocean conditions were unfavorable (Figure 11). Similarly, as the natural population increased as a consequence of management actions that improved survival then the population's pNI distributions tended move slightly rightward (i.e., higher pNI levels; Figure 12).

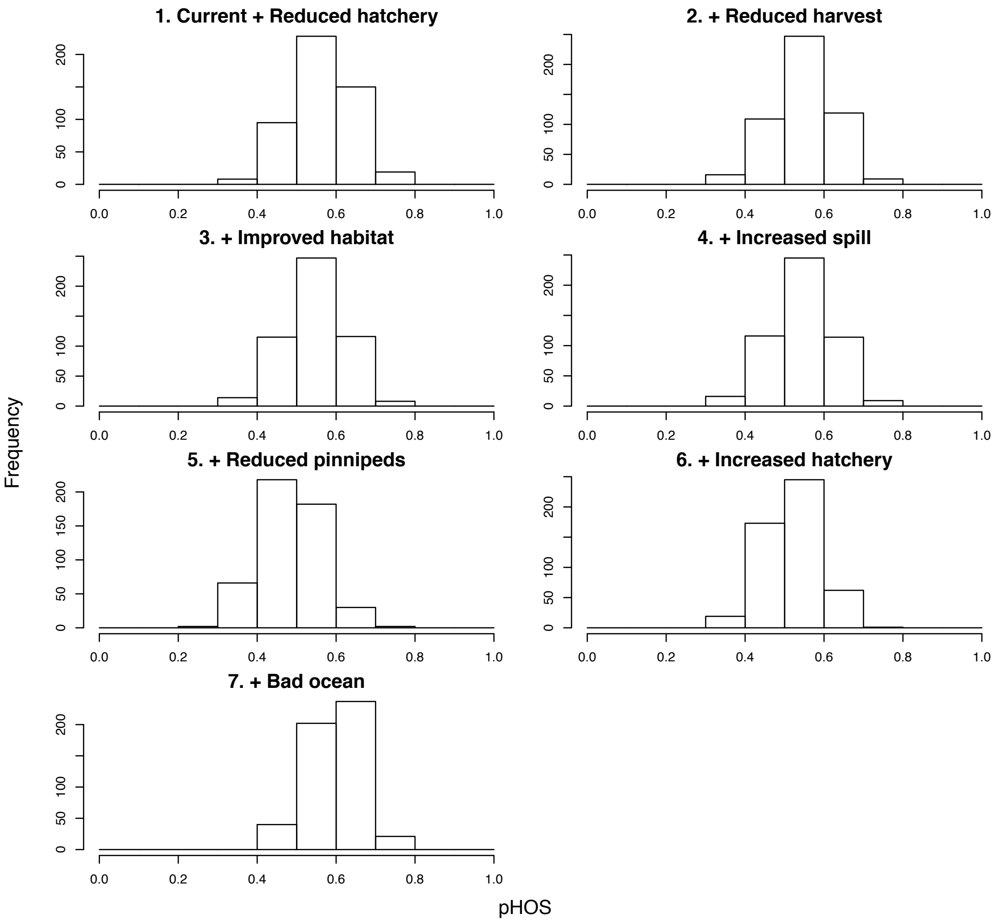

Figure 11: Distributions of the proportion of hatchery origin spawners (pHOS).

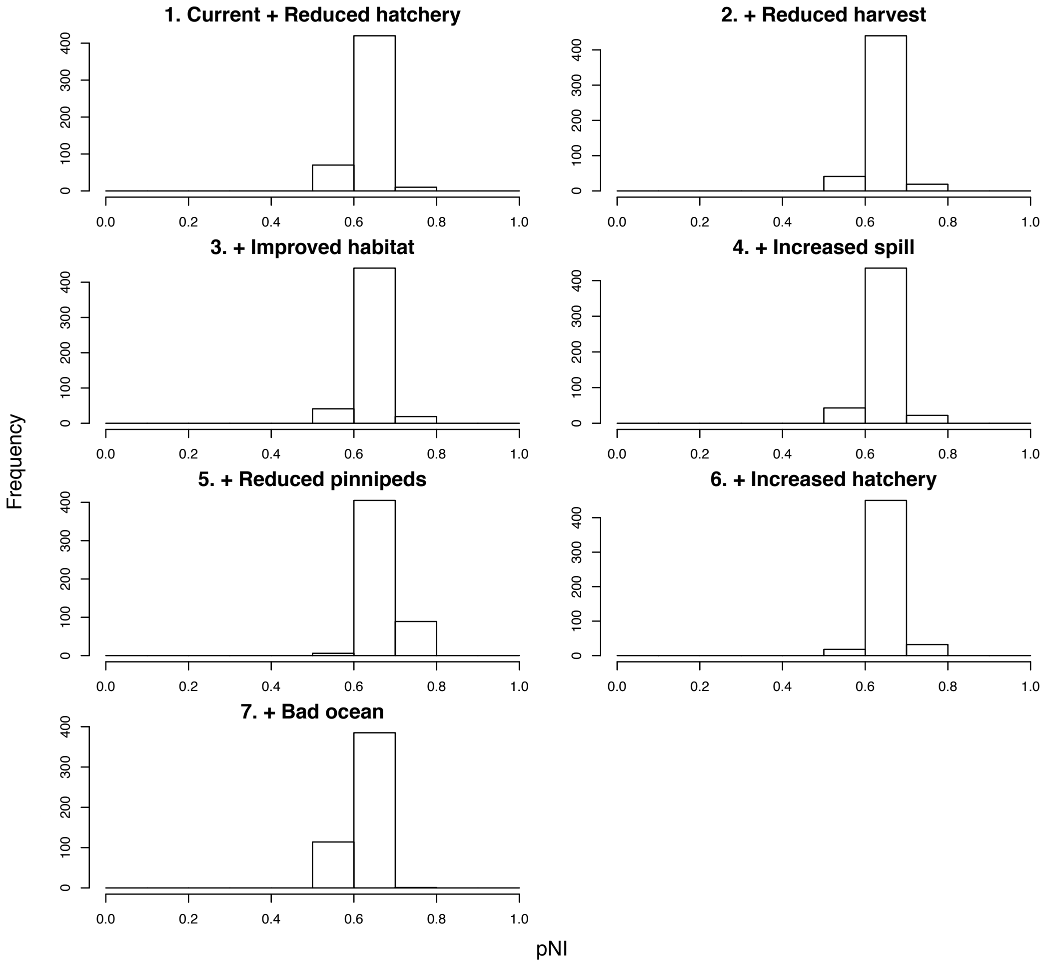

Figure 12: Distributions of proportionate natural influence (pNI).

Because the model tracks the age structure of the population we can assign returning spawners to their parent brood to calculate recruits per spawner at low abundance for generating VSP (Viable Salmonid Population) scores (Zabel et al. 2015, 2017a). The cumulative effect of the management actions generally increased productivity and abundance, and reduced extinction risk (Figure 13). As management actions accumulated, there was a rightward shift in VSP scores for abundance and productivity (Figure 14). However, unfavorable ocean conditions created a

VSP distribution similar to the initial scenario that included current conditions plus a reduced size of the hatchery programs.

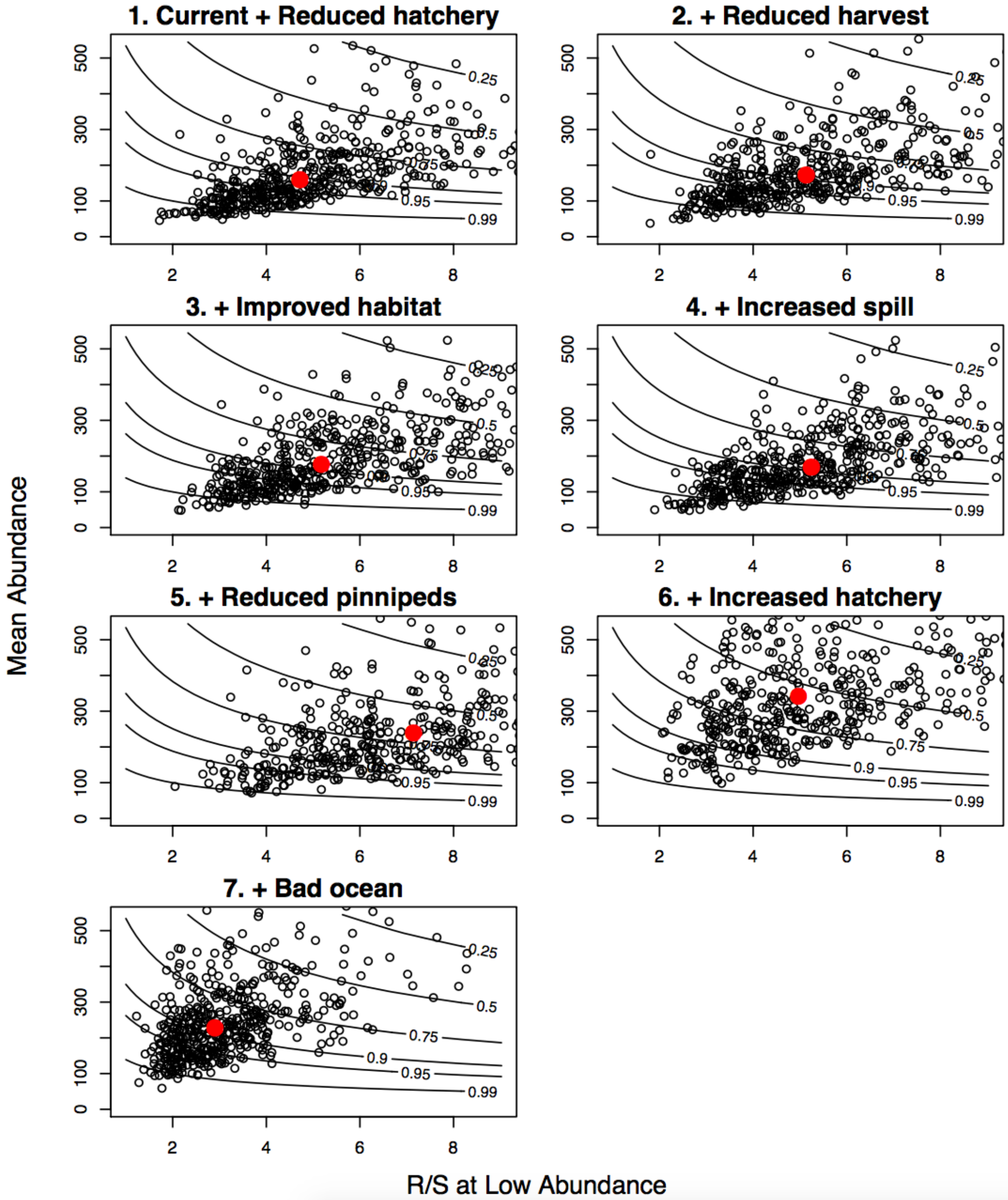

Figure 13: Productivity (recruits per spawner at low spawner abundance) and mean spawner abundance for individual model simulations (dots) of seven scenarios. The red dot is the center of the points and the isoclines represent extinction contours estimated across all seven scenarios combined.

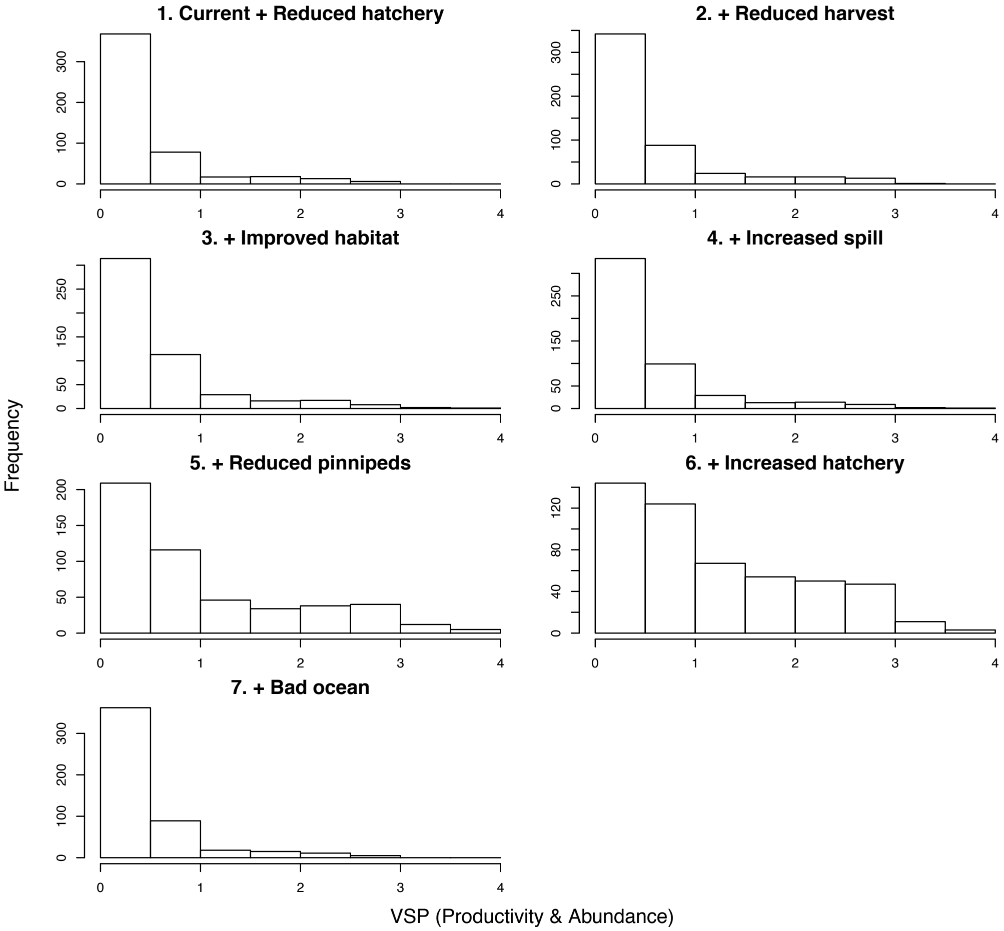

Figure 14: Distributions of estimated VSP scores for model-predicted abundance, productivity, and extinction risk across seven scenarios.

Sensitivity analyses

Sensitivity analyses showed that model outputs were most sensitive to three of the parameters examined across simulations: ocean survival after the first year, parr-to-smolt survival, and adult-upstream survival through the hydrosystem (Figure 15). Ocean survival after the first year was influential in part because it was applied multiple times for adults that remained in the ocean for more than two years. Varying parameters related to the hatchery programs had a greater influence on extinction risk than on mean spawner abundance, and these metrics sometimes responded in opposing directions to varying hatchery parameters. In most scenarios, parameters related to survival during the first year of ocean residence (coefficients for the effects of water travel time and for April and May upwelling indices) had a greater influence on extinction probability than on mean abundance. This was due to the autocorrelation in first-ocean-year survival that led to more extinction events. The coefficient for the effect of the April upwelling index was the most influential of the parameters related to first-year-ocean survival in the bad-ocean scenario.

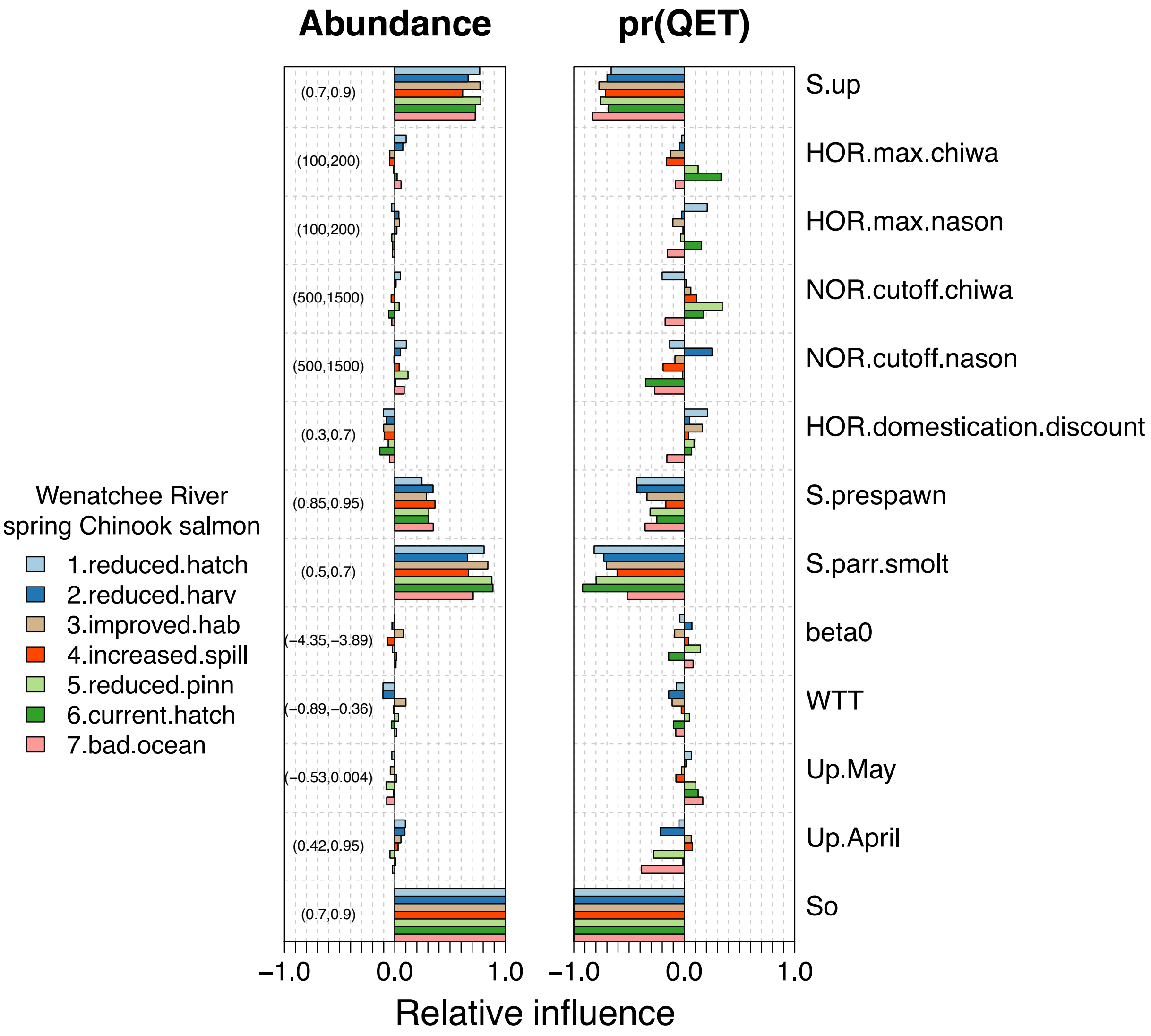

Figure 15: Parameter influence on spawner abundance and extinction risk.

Discussion

We have highlighted several significant advancements to the life cycle model: hatchery effects, calibration, and sensitivity analyses. We will continue to refine and re-adjust hatchery effects by incorporating new information as it becomes available from the ongoing reproductive success studies. Similarly, we consider calibration to be a continual process as new information to support parameter values becomes available (e.g., updated information on upstream adult survival; Crozier et al. 2016). We will continue to conduct sensitivity analyses throughout model development and scenario testing as a way to visualize model performance and to identify critical life stages and uncertainties.

We plan to incorporate fish-habitat relationships developed by ISEMP/CHaMP, the NWFSC, WDFW, and others in our model, and we are fitting relationships for life stages specific to the Wenatchee River Basin (Appendix). We will leverage results from research in the basin addressing egg-fry survival and juvenile capacity, life-history diversity, and overwinter survival. We included a scenario estimating habitat capacity increases from floodplain reconnection in rangelands and from small road removal several juvenile production areas, and will extend this analysis to include additional restoration scenarios and rearing within other mainstem and tributary habitats. We have made progress toward accounting for subbasin-specific egg-to-fry survival, downstream migrations of subyearlings out of natal tributaries, and the different survivals of juveniles that stay and rear in their natal tributary versus those that move downstream to rear in mainstem Wenatchee habitats (see Appendix for details on these developments). In addition, we are developing a functional relationship to capture the dynamics of prespawn mortality (PSM) in the Wenatchee basin. WDFW and Quantitative Consultants are re-analyzing historical carcass-recovery, redd-survey, and adult-escapement data to produce unbiased yearly estimates of PSM that we can relate to environmental variables and other factors. We are encouraged by recent modeling to describe habitat quality and quantity using remotely sensed and on-the-ground data. For example, a recent modeling effort has generated time series of spatially continuous stream temperatures in the Wenatchee and other interior Columbia basins (McNyset et al. 2015), and there are several attempts to estimate juvenile capacity in the basin through expansion of fish data based on extensive habitat modeling (Bond et al. 2017; Liermann et al. 2017; K. See, quantile regression forest methods, ISEMP/CHaMP 2015).

With more fish and habitat linkages the life cycle model will be able to more fully account for population-level responses to climate change and habitat restoration. Currently, we are limited to estimating climate effects directly for two life stages: hydrosystem survival (not evaluated in this chapter) and through alternative ocean conditions. With linkages across more life stages we could accommodate scenarios that estimate effects of climate and habitat restoration on PSM, egg-fry survival, life-history expression, juvenile rearing capacities of multiple habitat areas, and overwinter survival.

We anticipate that with additional fish-habitat relationships and other enhancements, a description of the model and a demonstration of its capabilities will be ready for submission to a peer-reviewed journal.

Acknowledgements

We are grateful to Chris Johnson (WDFW), Morgan Bond (Ocean Associates, contracted to NOAA Fisheries, NWFSC, Seattle), Jim Faulkner (NOAA Fisheries, NWFSC, Seattle), Dan Widener (OA, contracted to NOAA Fisheries, NWFSC, Seattle), Eric Buhle (QCI, Inc.), and the interior Columbia life cycle modeling group for valuable data, feedback, input, and discussions. Also, we thank the ISAB for their review of this life cycle model in 2013.

Appendix

Modeling egg-to-smolt survival that incorporates life-history diversity

Overview

Despite significant habitat restoration work, habitat monitoring, and fish monitoring conducted in the Wenatchee Basin, the relationships between habitat conditions and fish survival and movement remain highly uncertain. In order to evaluate the impacts of freshwater-habitat restoration projects, land use, and climate on spring Chinook salmon population dynamics, and the efficacy of management actions to meet delisting criteria, the life-cycle model will need to include parameters for the affected life stages and life-history strategies. Therefore, we are working to break down both the spawner-to-parr and parr-to-smolt transitions to represent how different components of the population use different habitat areas and features seasonally (life-history diversity).

A tremendous amount of data exists on juvenile Chinook salmon survival, movement, and growth in the Wenatchee basin over many years (Hillman et al. 2016). There is also a significant amount known about habitat conditions within the basin at multiple spatiotemporal scales (ISEMP/CHAMP 2015; Bond et al. 2017). We are working toward leveraging these sources of information to link habitat conditions and demographic rates within the life-cycle model to predict the effects of freshwater habitat conditions on population viability.

We are developing “fish-habitat relationships” for juvenile Chinook salmon survival and movement within the Wenatchee River Basin based on the available long-term monitoring data (Figure A1). We will relate annual survival and movement to environmental factors such as flow and thermal regimes, geomorphology, substrate, riparian condition and land use, and to ecological factors including species interactions and Chinook density to capture the effects of these factors on population dynamics (e.g. Bjornn 1971, Scheuerell et al. 2006, Copeland and Venditti 2009). We will ultimately use these relationships in combination with time series of the relevant habitat variables, including scenarios that account for habitat restoration and climate change, to predict population-level responses using the life-cycle model.

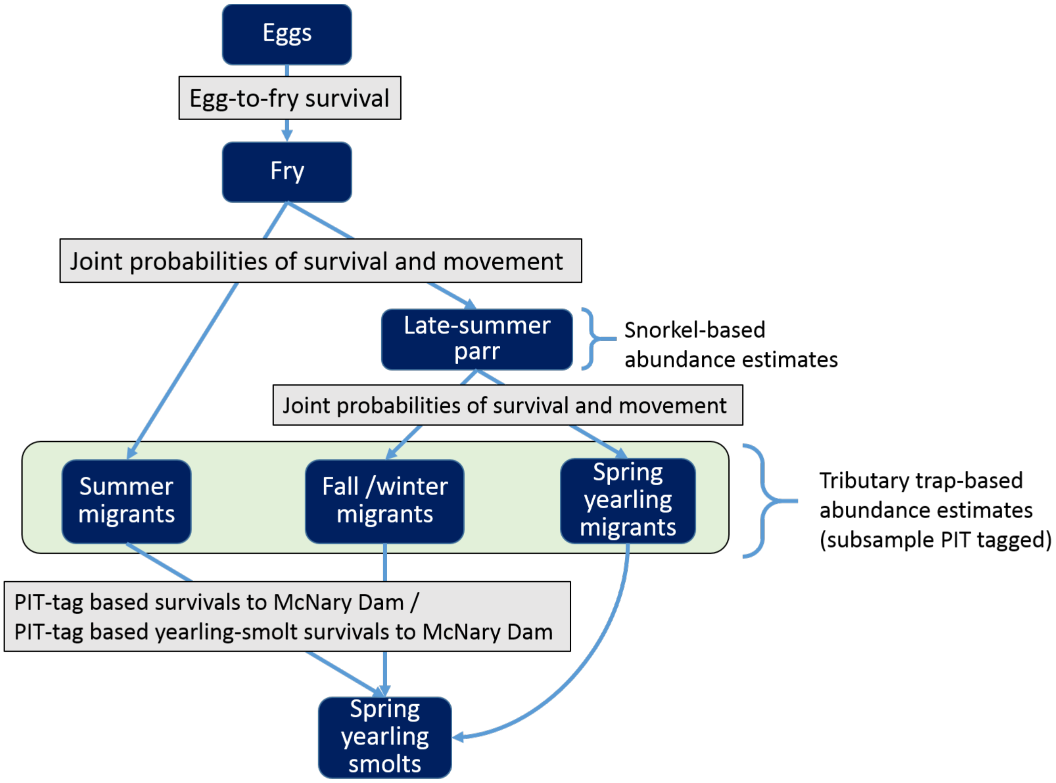

Figure A1. Proposed model structure for Chiwawa River spring Chinook salmon egg-to-smolt survival and life-history diversity, based on fish-habitat relationships (represented by arrows). We propose a similar model structure for the White River and Nason Creek Basins, except that snorkel-based abundance estimates of late-summer parr are not available, so fry will transition directly to summer, fall/winter, and spring migrants.

Specifics of individual fish-habitat relationships

We will use the product of egg deposition and egg-to-fry survival to estimate fry abundance in the model. Egg deposition will be a function of the number of adult spawners predicted by the life-cycle model, age-specific fecundity, and the proportion of total eggs deposited be the average female (egg voidance). We will fit this model to a time series of redd abundance and egg voidance, which were measured annually during spawning-ground surveys, as well as fecundity measurements of hatchery broodstock (see Hillman et al. 2016). Egg-to-fry survival models are being developed for the Wenatchee River Basin based on studies that use egg boxes and fry traps, and measure environmental conditions experienced by embryos (Johnson et al. 2012, Roni et al. 2015). Results to date suggest that egg-to-fry survival is reduced by high water temperatures, fine-sediment accumulation in redds, and scouring flows that prematurely flush eggs and alevins downstream. A predictive fish-habitat relationship for egg-to-fry survival is not yet available, but Chris Johnson (WDFW) is currently developing one (Table A1; Chris Johnson, unpublished data).

Table A1. Average egg-to-fry survival within production areas in the Wenatchee River Basin (Chris Johnson, WDFW, unpublished data). Annual averages for each production area are means of egg-box survivals within each stream reach, weighted by redd densities in each reach. "Mean Survival" is the average survival across years for each production area. "Mean Standard Deviation" represents the weighted mean standard deviation for survival in individual egg boxes within reaches.

Production Area	Years	Mean Survival	Mean Standard Deviation
Little Wenatchee	2014-2015	0.29	0.18
Upper Wenatchee	2014-2015	0.21	0.10
Nason Creek	2014-2015	0.24	0.16
White River	2014-2015	0.27	0.09
Chiwawa River	2010-2012	0.55	0.10

We are developing predictive models of the joint probabilities of fry surviving and migrating from their natal tributaries at different times of year. Subyearlings (parr) emigrate from natal tributaries throughout the summer, potentially in response to declining flows and increasing fish sizes that lead to competition for food and space (Figure A2; Richards and Cernera 1989, Williams et al. 2016). In contrast, a second pulse of emigration occurs in fall and is seemingly triggered by declining temperatures and fall rain events (Bjornn 1971). The final pulse of emigration occurs in spring, when 1-year-old smolts that remained in their natal basin initiate seaward migration. For modeling, we plan to partition migrants into seasonal groups that reflect the habitat variables driving their movements (e.g. fry density, invertebrate drift, flow, temperature, wood and substrate cover). Rotary screw traps operated near the mouths of the Chiwawa, Nason, and White Basins capture migrants, and their abundances are estimated with release-recapture methods to inform trap efficiencies (Williams et al. 2016). Washington Department of Fish and Wildlife and Yakama Nation Biologists are updating the time series of migrant abundances to account for interannual variability in migration timing, and missing data, and to incorporate the most recent years.

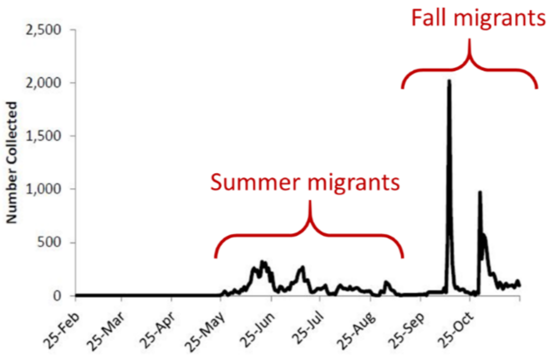

Figure A2. Daily catch of subyearling spring Chinook salmon >50 mm in a rotary screw trap operated near the mouth of the Chiwawa River in 2015, from Williams et al. (2016). The general pattern of subyearling migration across years and basins is a steady but declining rate from roughly June through August, followed by episodic increases in September–November.

Preliminary data suggest that the joint probabilities of fry surviving and leaving natal tributaries during summer (currently defined as 1 July–31 August) are density independent or positively density dependent (Figure A3). We will investigate the ability of habitat and ecological variables, such as invertebrate drift and flow, to predict these transition probabilities in combination with fry densities. A relatively small proportion of fry also migrate from their natal basins in spring, but we do not currently have data to evaluate their contribution to smolt production, which is believed to be negligible. Therefore, we will ignore these fry migrants in our modeling until data become available.

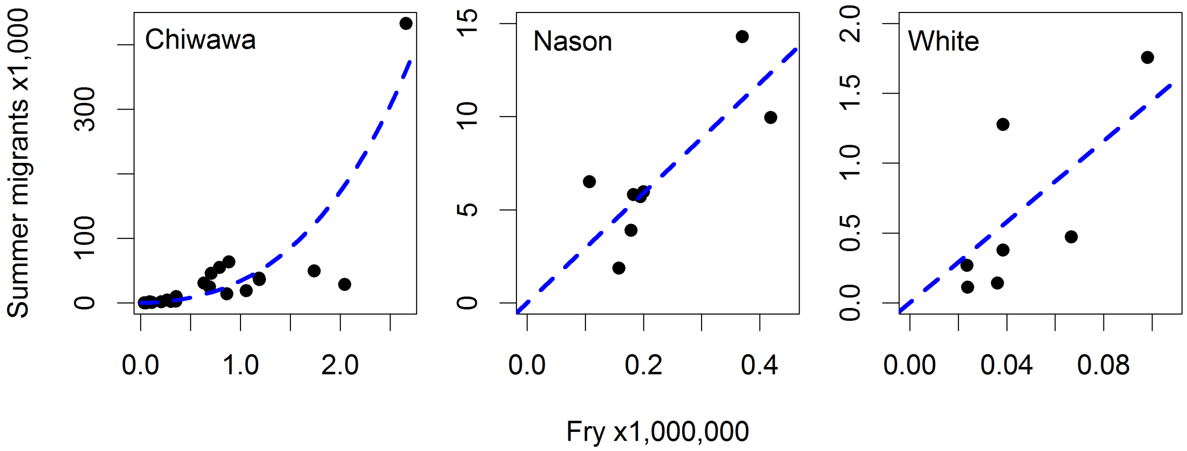

Figure A3. Annual estimates of subyearling migrants between 1 July and 31 August of 1993–2013 in the Chiwawa, and 2007–2013 in the Nason and White, as functions of estimated fry abundances (Andrew Murdoch, WDFW, unpublished data). **Note the different axes scales for the different basins.** The blue-dashed line for the Chiwawa represents an exponential-power function; however, the highest migrant estimate is a highly influential point. The data in these plots are currently being revised so these results are preliminary.

We will model the transition from fry to parr that remain within the Chiwawa basin through at least late summer based on a 25-year time series of abundance estimates generated by expanding snorkel-survey counts by habitat areas (Hillman et al. 2016). The data suggest that the transition is negatively density dependent, which we will approximate with a Beverton-Holt, Ricker, Hockey Stick, or Cushing Model (Figure A4). The density dependence suggests that habitat and food availability limit the combined probability of fry surviving and remaining in the Chiwawa through late summer when densities are high. We will investigate whether habitat variables explain additional interannual variability in the transition probability that we cannot predict with fish densities alone.

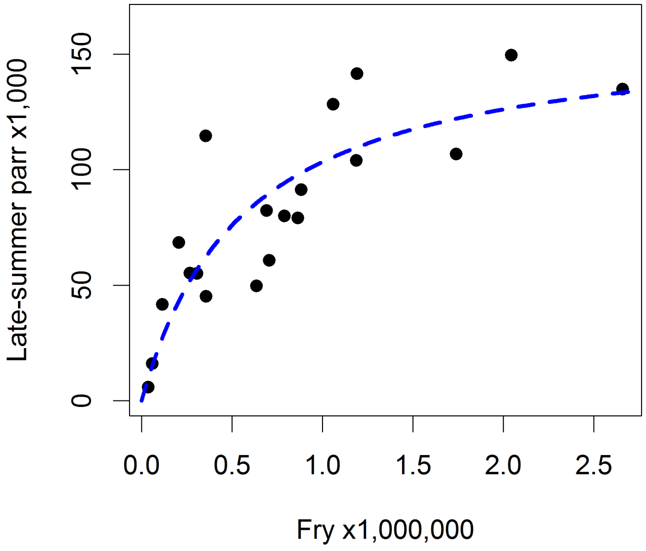

Figure A4. Annual estimates of late-summer parr residing within the Chiwawa River Basin based on snorkel surveys conducted in late August of 1993–2013, as a function of estimated fry abundances (Hillman et al. 2016; Andrew Murdoch and Chris Johnson, WDFW, unpublished data). The blue-dashed line represents a Beverton-Holt model, which suggests a negatively density dependent relationship as might result from habitat limitation.

Following summer, additional pulses of migration from natal habitats occur in fall and spring. We will predict the transition probabilities of late-summer parr in the Chiwawa, and fry in the Nason and White, to fall and spring migrants using migrant estimates from rotary screw traps (Figure A5). Screw traps cannot operate during the winter due to ice; however, parr are PIT tagged throughout the basin in late summer and we will use their subsequent detections on in-stream antennae and other recapture/detection sites to estimate migration rates during winter. The winter migrants appear to be relatively uncommon and will be added to the fall migrants for simplicity.

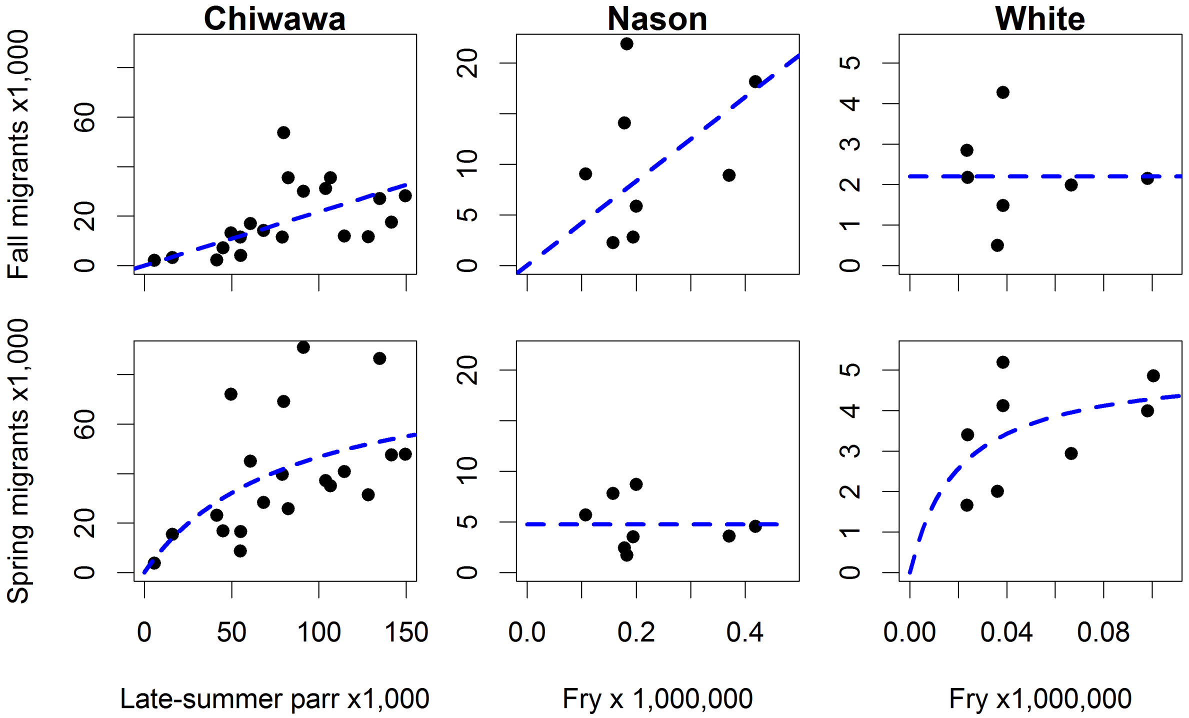

Figure A5. Annual fall- and spring migrant abundances as functions of late-summer parr or fry abundances from the same brood years. **Note the different axes scales for the different basins.** All data and models, which are represented by blue-dashed lines, are highly preliminary and likely to change once data are updated and habitat variables are incorporated. The models are included simply to suggest some of the density (in)dependent relationships that we may see. The Nason River appears to have a lower ratio of spring to fall migrants than the Chiwawa and White River Basins.

We will model the subsequent survival of summer and fall/winter migrants during the remainder of their freshwater rearing with a mark-recapture model of PIT-tagged individuals.

Parr have been PIT-tagged at screw traps when leaving their natal basins for >10 years. We will estimate their survival rates to McNary Dam, the first significant PIT-tag interrogation site encountered, the following spring with Cormack-Jolly-Seber (CJS) models using the *marked* package in the program R (Figure A6; Laake et al. 2013, R Core Team 2017). We will partition these survival rates into two components: one to represent mortality incurred while rearing, and another for mortality incurred while migrating through the upper Columbia River as smolts. We will estimate the survival of smolts migrating through the upper Columbia with CJS models of fish that were PIT-tagged at a screw trap operated at the mouth of the Wenatchee in spring. The survival rates during late-summer and overwinter rearing will be related to fish and habitat variables to generate predictive models, which will be used to generate time series that explore different scenarios for life-cycle modeling. Spring migrants from natal basins will be considered smolts, assuming negligible mortality between exiting their natal tributaries and exiting the Wenatchee River. We will test this assumption by comparing their survival to McNary Dam with that of smolts tagged in the lower Wenatchee River.

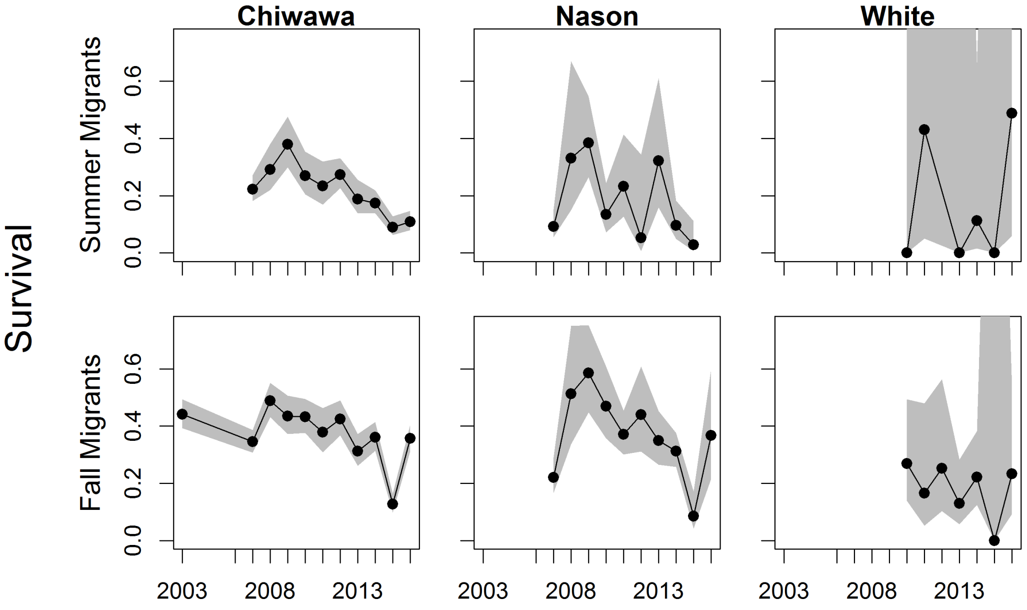

Figure A6. Preliminary estimates of survival for summer and fall emigrants between leaving their natal basins in summer (top row) or fall (bottom row) and initiating seaward migration the following spring. We estimated survival between leaving natal basins as parr and passing McNary Dam as smolts using Cormack-Jolly-Seber models of PIT-tagged migrants. We divided these estimates by 0.4, assuming 60% mortality incurred by smolts en route to McNary Dam based on preliminary analysis of the survival of smolts tagged in the lower Wenatchee River. Note that survival was inestimable for migrants from the White River in some years due to low sample sizes. We will relate survival rates to habitat and ecological variables for use in the life-cycle model.

Discussion

This model will leverage the extensive body of work in the Wenatchee Basin to understand how habitat conditions effect movement and survival, and ultimately population dynamics. We plan to incorporate in our analysis much of the available data from sources such as ISEMP, CHaMP, Bond et al. (2017), USGS flow gauges, and studies of fish species composition, abundance, and distribution by local agencies, tribes, and other entities. By combining previous work, we hope to identify the habitat and ecological drivers of survival and movement at critical times, adding context and management implications to existing studies.

Parts of the model might be useful in other basins as well, where less information is available than in the Wenatchee. Mortality in the Chiwawa Basin following the late-summer snorkel census is the ratio of combined fall/winter and spring migrants to late-summer parr, assuming that all fish smolt as spring yearlings. Such estimates of overwinter mortality are relatively rare in the literature; relating them to habitat variables would be beneficial within and outside the Wenatchee Basin for evaluating the relative importance of summer and overwinter mortality on smolt production (See Liermann et al. 2017).

There are limitations to the data that we will have to work with. For example, the transition probabilities of fry to spring migrants in the Nason and White Basins integrate over relatively long periods of roughly one year, during which fish rear in multiple different microhabitats within their natal basins. Multiple significant fish-habitat relationships, which drive summer and overwinter survival, are confounded within these transition probabilities. Despite this, we hope to identify the primary drivers of these transitions using multiple regression. We can also draw on the fish-habitat relationships observed for fry-to-fall/winter parr transitions, and overwinter mortality in the Chiwawa Basin, to make inferences about the relative roles of different habitat factors driving fish survival and movement observed in the Nason and White Basins. Uncertainties in our modeling should suggest future studies to fill knowledge gaps.

Our work characterizing fish-habitat relationships that drive life-history diversity and survival should be extremely valuable when prioritizing management actions that target specific freshwater habitats and life-stages. For example, if there were less scope for habitat actions to improve the capacity for late-summer parr in the Chiwawa than to improve survival or capacity in other life stages or areas, then it would be prudent to devote effort where recovery potential is greatest. Opportunities to increase survival of summer and fall/winter migrants within the mainstem Wenatchee could have compounding benefits, if more fish emigrate from natal tributaries earlier in response to higher spawner and fry abundances. Integrating fish-habitat relationships within the life-cycle model will be valuable for predicting the implications of such management actions for increasing population viabilities toward delisting.

References

Bjornn, T. C. 1971. Trout and salmon movements in two Idaho streams as related to temperature, food, stream flow, cover, and population density. Transactions of the American Fisheries Society 100:423-438.

Bond, M., et al. 2017. This volume. 2a. Review of capacity methods.

Burke, B., et al. 2017. This volume. 3. Estuary/ocean survival based on PIT tag data.

Chilcote, M.W., Goodson, K.W. and Falcy, M.R. 2011. Reduced recruitment performance in natural populations of anadromous salmonids associated with hatchery-reared fish. Canadian Journal of Fisheries and Aquatic Sciences 68(3):511-522.

Chilcote, M.W., Goodson, K.W. and Falcy, M.R. 2013. Corrigendum: Reduced recruitment performance in natural populations of anadromous salmonids associated with hatchery-reared fish. Canadian Journal of Fisheries and Aquatic Sciences 70(3):513-515.

Cooney, T., et al. 2017. This volume. 9a. Grande Ronde life cycle modeling.

Copeland, T and Venditti, D.A. 2009. Contribution of three life history types to smolt production in a Chinook salmon (*Oncorhynchus tshawytscha*) population. Canadian Journal of Fisheries and Aquatic Sciences 66:1658-1665.

Copeland, T., Venditti, D.A., and Barnett, B.R. 2014. The importance of juvenile migration tactics to adult recruitment in stream-type Chinook salmon populations. Transactions of the American Fisheries Society 143:1460-1475.

Coutts, S.R. and Yokomizo, H. 2014. Meta-models as a straightforward approach to the sensitivity analysis of complex models. Population Ecology 56:7-19.

Cross, P.C. and Beissinger S.R. 2001. Using logistic regression to analyze the sensitivity of PVA models: a comparison of methods based on African wild dog models. Conservation Biology 15:1335-1346.

Crozier, L., E. Dorfmeier, T. Marsh, B. Sandford, & D. Widener. 2016. Refining our understanding of early and late migration of adult Upper Columbia spring and Snake River spring/summer Chinook salmon: passage timing, travel time, fallback and survival. NWFSC Report. Seattle, WA.

Crozier, L. G., R. W. Zabel, and A. F. Hamlett. 2008. Predicting differential effects of climate change at the population level with life-cycle models of spring Chinook salmon. Global Change Biology 14:236-249.

Ford, M.J. 2002. Selection in captivity during supportive breeding may reduce fitness in the wild. Conservation Biology 16(3):815-825.

Ford, M.J., Murdoch, A.R., and Hughes, M.S. 2014. Monitoring the reproductive success of naturally spawning hatchery and natural spring Chinook salmon in the Wenatchee River, 3/1/2014 - 2/28/2015 Annual Report, 2003-039-00. Annual project report to BPA (BPA Project # 2003-039-00).

Gramacy, R.B. and Taddy, M. 2010. Categorical inputs, sensitivity analysis, optimization and importance tempering with tgp version 2, an R package for treed Gaussian process models. Journal of Statistical Software 33, issue 6.

Hamann, E. J., and B. P. Kennedy. 2012. Juvenile dispersal affects straying behaviors of adults in a migratory population. Ecology 93:733-740.

Helton, J.C., Johnson, J.D., Sallaberry, C.J., and Storlie, C.B. 2006. Survey of sampling-based methods for uncertainty and sensitivity analysis. Reliability Engineering & System Safety 91:1175-1209.

(HGMP Chiwawa) Hatchery genetics and management plan. 2009. Wenatchee Upper Columbia River spring Chinook: Chiwawa River spring Chinook.

(HGMP Nason) Hatchery genetics and management plan. 2009. Upper Columbia Spring-run Chinook salmon – Nason Creek Supplementation Program.

(HGMP Addendum). Hatchery genetics and management plan. 2010. Spring Chinook Adult Management in the Wenatchee River Basin. Addendum to the Wenatchee River Hatchery Genetic Management Plans.

Hillman, T., M. Miller, C. Willard, S. Hopkins, M. Johnson, C. Moran, J. Williams, M. Tonseth, B. Ishida, C. Kamphaus, T. Pearson, and P. Graf. 2016. Monitoring and evaluation of the Chelan and Grant county PUDs hatchery programs: 2015 annual report. Report to the HCP and PRCC Hatchery Committees, Wenatchee, WA.

Honea, J.M., Jorgensen, J.C., McClure, M.M., Cooney, T.D., Engie, K., Holzer, D.M. and Hilborn, R. 2009. Evaluating habitat effects on population status: influence of habitat restoration on spring-run Chinook salmon. Freshwater Biology 54(7):1576-1592.

Honea, J.M., McClure, M.M., Jorgensen, J.C. and Scheuerell, M.D. 2016. Assessing freshwater life-stage vulnerability of an endangered Chinook salmon population to climate change influences on stream habitat. Climate Research 71(2):127-137.

HSRG (Hatchery Science Review Group). 2009. White Paper 1: Predicted fitness effects of interbreeding between hatchery and natural populations of Pacific salmon and steelhead. Appendix A *in*, Columbia River hatchery reform system wide report [http://hatcheryreform.us/wp-content/uploads/2016/05/4_appendix_a_1_interbreeding_fitness_effects.pdf]

ICTRT (Interior Columbia Technical Recovery Team), and Zabel, R.W. 2007. Assessing the impact of environmental conditions and hydropower on population productivity for Interior Columbia River stream-type Chinook and steelhead populations. NWFSC Draft Technical Report, Seattle, WA. https://www.nwfsc.noaa.gov/research/divisions/cb/genetics/trt/col/trt_ic_viability_survival.cfm

ISAB (Independent Scientific Advisory Board). 2013. Review of NOAA Fisheries' life-cycle models of salmonid populations in the interior Columbia River Basin (June 28, 2013 draft). Northwest Power and Conservation Council, Portland, OR. https://www.nwcouncil.org/fw/isab/isab2013-5/

(ISEMP/CHaMP) Integrated Status and Effectiveness Monitoring Program (ISEMP) and Columbia Habitat Monitoring Program (CHaMP) Annual Combined Technical Report, January 2015 – December 2015, BPA Projects 2003-017-00 and 2011-006-00.

Johnson, C. L., P. Roni, and G. R. Pess. 2012. Parental effect as a primary factor limiting egg-to-fry survival of spring Chinook salmon in the Upper Yakima River Basin. Transactions of the American Fisheries Society 141:1295-1309.

Jorgensen et al. 2013. 2.3: Upper Columbia River spring Chinook salmon. *In* Life-cycle models of salmonid populations in the interior Columbia River Basin. NWFSC Report, Seattle, WA. https://web.archive.org/web/20160826141522/https://www.nwfsc.noaa.gov/trt/lcm/index.cfm

Kendall, N., et al. 2013. 5.2 Ocean conditions. *In* Life-cycle models of salmonid populations in the interior Columbia River Basin. NWFSC Report, Seattle, WA. https://web.archive.org/web/20160826141522/https://www.nwfsc.noaa.gov/trt/lcm/index.cfm

Laake, J.L., Johnson, D.S. and Conn, P.B. 2013. marked: an R package for maximum likelihood and Markov Chain Monte Carlo analysis of capture–recapture data. Methods in Ecology and Evolution 4(9):885-890.

Leider, S.A., Hulett, P.L., Loch, J.J. and Chilcote, M.W. 1990. Electrophoretic comparison of the reproductive success of naturally spawning transplanted and wild steelhead trout through the returning adult stage. Aquaculture 88(3-4):239-252.

Liermann, M. et al. 2017. This volume. 2c Juvenile capacity modeling.

Leslie, P.H. 1945. On the use of matrices in certain population mathematics. Biometrika 33:183-212.

Linley, T. J., E. J. Krogstad, M. K. Nims, and R. B. Langshaw. 2016. Geochemical signatures in fin rays provide a nonlethal method to distinguish the natal rearing streams of endangered juvenile Chinook Salmon *Oncorhynchus tshawytscha* in the Wenatchee River, Washington. Fisheries Research 181:234-246.

Lonsdorf, E.V., Thogmartin, W.E., Jacobi, S., Aagaard, K., Coppen, J., Davis, E., Fox, T., Heglund, P., Johnson, R., Jones, M.T., Kenow, K., Lyons, J.E., Luke, K., Still, S., Tavernia, B. 2016. A generalizable energetics-based model of avian migration to facilitate continental-scale waterbird conservation. Ecological Applications 26:1136-1153.

McCarthy, M.A., Burgman, M.A., and Ferson, S. 1995. Sensitivity analysis for models of population viability. Biological Conservation 73:93-100.

McLean, J.E., Bentzen, P. and Quinn, T.P. 2003. Differential reproductive success of sympatric, naturally spawning hatchery and wild steelhead trout (*Oncorhynchus mykiss*) through the adult stage. Canadian Journal of Fisheries and Aquatic Sciences 60(4):433-440.

McNyset, K.M., Volk, C.J., and Jordan, C.E. 2015. Developing an effective model for predicting spatially and temporally continuous stream temperatures from remotely sensed land surface temperatures. Water 7:6827-6846.

Mortensen, J. and Reed, J.M. 2016. Population viability and vital rate sensitivity of an endangered avian cooperative breeder, the White-Breasted Thrasher (*Ramphocinclus brachyurus*). PLoS ONE 11(2): e0148928. doi:10.1371/journal.pone.0148928

Pastor, S. M. 2004. An Evaluation of Fresh Water Recoveries of Fish Released from National Fish Hatcheries in the Columbia River Basin, and Observations of Straying. Pages 87-98 *in* Propagated Fish in Resource Management. American Fisheries Society Symposium No. 44.

R Core Team. 2017. R: A language and environment for statistical computing. R Foundation for Statistical Computing, R Foundation for Statistical Computing, Vienna, Austria.

Richards, C., and P. J. Cernera. 1989. Dispersal and abundance of hatchery-reared and naturally spawned juvenile chinook salmon in an Idaho stream. North American Journal of Fisheries Management 9:345-351.

Roni, P., C. Johnson, T. De Boer, G. Pess, A. Dittman, and D. Sear. 2015. Interannual variability in the effects of physical habitat and parentage on Chinook salmon egg-to-fry survival. Canadian Journal of Fisheries and Aquatic Sciences 73:1047-1059.

Saltelli, A., Chan, K. Scott, E. 2000. Sensitivity Analysis. New York: Wiley.

Scheuerell, M. D., R. Hilborn, M. H. Ruckelshaus, K. K. Bartz, K. M. Lagueux, A. D. Haas, and K. Rawson. 2006. The Shiraz model: a tool for incorporating anthropogenic effects and fish–habitat relationships in conservation planning. Canadian Journal of Fisheries and Aquatic Sciences 63:1596-1607.

Sorel, M., et al. 2017. This volume. 6a Pinniped predation.

Storlie, C.B., Swiler, L.P., Helton, J.C., and Sallaberry, C.J. 2009. Implementation and evaluation of nonparametric regression procedures for sensitivity analysis of computationally demanding models. Reliability Engineering & System Safety 94:1735-1763.

Williams, J., A. Repp, and M. Johnson. 2016. Monitoring Juvenile Salmonids in the Wenatchee River Subbasin: Activities in the Chiwawa and Lower Wenatchee during 2015. Report to the PUD No. 1 of Chelan County, Wenatchee, WA and PUD No. 2 of Grant County HCP and PRCC Hatchery Committees, Ephrata, WA.

Zabel, R. W., M.D. Scheuerell, M.M. McClure, and J.G. Williams. 2006. The interplay between climate variability and density dependence in the population viability of Chinook salmon. Conservation Biology 20:190-200.

Zabel, R.W., Faulkner, J., Smith, S.G., Anderson, J.J., Van Holmes, C., Beer, N., Iltis, S., Krinke, J., Fredricks, G., Bellerud, B. and Sweet, J. 2008. Comprehensive passage (COMPASS) model: a model of downstream migration and survival of juvenile salmonids through a hydropower system. Hydrobiologia 609(1):289-300.

Zabel, R., Myers, J., Chittaro, P., and Jorgensen, J. 2015. Willamette River VSP modeling of spring Chinook and steelhead. Draft report, NWFSC, Seattle, WA.

Zabel et al. 2017a. This volume. 1. Introduction.

Zabel et al. 2017b. This volume. 4b. Hydrosystem modeling.

CHAPTER 9

9.c Themes of climate impacts on Columbia Basin salmon: multiple limiting factors, correlation in climate drivers, and cumulative life cycle effects

Lisa Crozier (NWFSC), Rich Zabel (NWFSC), Brian Burke (NWFSC)

Introduction

Most populations of salmon within the California Current large marine ecosystem are expected to be negatively affected by climate change (Cheung et al. 2015; Ford et al. 2016). However, individual species and populations differ in their relative vulnerability to climate change, depending on their physiological tolerances, life histories, and geographic locations. Here we explore how populations of Snake River spring/summer Chinook might be differentially susceptible to projected climate changes.

Vulnerability is typically separated into two aspects, biological sensitivity and climate exposure (IPCC 2014). Biological sensitivity can differ among populations within a geographic region depending on factors such as life history variation due to local adaptation and habitat characteristics. The general approach applied here is to represent differential population sensitivity by exploring a range of parameter values from positive to negative for two potential limiting factors (temperature and flow). The importance of these limiting factors for the juvenile stage likely depends mostly on local habitat (Crozier and Zabel 2008). We also examine how adult run-timing leads to differential sensitivity to river temperature.

The second component of vulnerability is exposure, which refers to the extent of climate change that actually occurs. Variation in exposure results from different human emissions behavior, different global or regional climate sensitivity to rising greenhouse gases, represented by multiple climate models, and/or the time frame into the future for our projections. In this analysis, we explore a relatively continuous surface of potential warming scenarios by using a climate scalar to intensify warming in the simulations.

An important feature of climate change that has not been addressed in previous quantitative models of Pacific salmon is the simultaneous effect of annual climatic conditions in multiple life stages. Life cycle models are particularly suitable for comparing the impacts of various processes that affect multiple life stages, especially when there is autocorrelation within and between these processes. Climate has a major impact on growth and survival throughout the life cycle, with interactions between stages. Temporal autocorrelation in marine survival has already been shown to increase population extinction risk beyond that expected based on mean conditions (Zabel et al. 2006). For this analysis, we developed scenarios in which multiple life stages experienced correlated climate effects. Future work will manipulate this covariation to explore its significance.

To explore differential sensitivity and exposure to climate change, we used an existing life cycle model for 9 populations of Salmon River spring/summer Chinook salmon. This model was first developed for the ESU by Zabel et al. (2006), and modified by Crozier and Zabel (Crozier and Zabel 2013; Crozier et al. 2008) to the population level. The key features of this model are 1) population-specific spawner to smolt productivity, 2) population-specific smolt carrying capacities limited by climatic conditions, 3) upstream and downstream survival through the hydrosystem, 4) variable marine survival driven by climate. Additions to the model described in current work include climate-sensitive upstream survival and a change in the ocean climate drivers such that they are more closely related to climate change projections for climate scenario exploration, and fit directly using PIT-tag data from wild fish in this ESU.

The goal of this effort is to model the vulnerability of populations to climate change across life stages and across a range of future climate change scenarios. We tested existing model parameters on juvenile production with independent data from pit-tagged fish to demonstrate the utility of the model. We developed the model with a relatively general structure that can be applied to other salmon populations. Nearly all salmon will be affected by rising temperature and changing hydrologic regimes, although each population has own specific pathway linking these phenomena. We focus on understanding the relationships between sensitivities and vulnerability, rather than validating the exact mechanism that links the climate driver to the response in any particular population. In principle, a wide variety of different mechanisms are possible that could produce the same population-level response. We aim to identify the types of sensitivities that have the greatest impact on population vulnerability.

Objectives

Our objectives in this report are threefold. First, we sought to improve our characterization of population sensitivity by modifying or adding sensitivity to climate in additional life stages based on new data. Second, we sought to improve our characterization of exposure to climate change by utilizing climate model projections for sea surface temperature, and incorporating the covariance structure of climate drivers in multiple life stages into our scenarios. Third, we sought to represent vulnerability across a more continuous set of warming scenarios. This is meant to guide management priorities by ordering expected extinction risk along a roughly temporal gradient.

Methods

Life-cycle model structure

We applied the life cycle model developed originally in Zabel et al (2006) and modified in Crozier and Zabel (2013). The model is explained in detail elsewhere (Chapter 1, ICTRT and Zabel 2007) and thus we describe it briefly here. This is a stochastic, age-structured model where multiple life stages can be included in a given annual step. We modified the upstream and ocean survival functions, but used the same assumptions and parameter estimates for spawner-to-parr and parr-to-smolt transition stages (Figure 1), including assumptions of a fixed propensity to mature at a given age and age-adjusted adult fertility as in previous analyses. We acknowledge upfront that these original parameter estimates need to be refit now that we are using new marine survival estimates. Nonetheless, we have made progress in model development and approach.

The matrix has the form:

$$A(t) = \begin{matrix} 0 & 0 & 0 & b_4 \cdot s_A \cdot F_4(t) & s_A \cdot F_5(t) \\ s_2(t) & 0 & 0 & 0 & 0 \\ 0 & s_3(t) & 0 & 0 & 0 \\ 0 & 0 & (1-b_3)\cdot s_o & 0 & 0 \\ 0 & 0 & 0 & (1-b_4)\cdot s_o & 0 \end{matrix} \qquad [1]$$

where s_i determines the survival rate at age or stage i and might be a stochastic process or depend on environmental or anthropogenic conditions, indexed by year t. The stages are defined as follows. Age 1 begins when fish enter the river and includes adult migration upstream, in-river harvest, prespawn survival, egg deposition, and survival through the parr stage. Age 2 includes parr and smolt stages and downstream migration survival. Ocean entry occurs at age 3 and describes most of the variation in ocean survival, which depends on migration and early ocean conditions. The variable s_o describes later ocean survival, which is a constant in these scenarios

(0.8). Salmon spawn at a variety of ages, captured in the propensity to breed term, b_i, which governs the fraction of the cohort that spawns at age 3, 4 and 5 years old. The fertility term, $F(t)$, describes the production of parr from adults (or the number of eggs times first year survival) in year t, which is part of our spawner-to-smolt productivity function.

Spawner-to-smolt productivity

The life-cycle model separates the spawner-to-smolt productivity into two transition steps: the spawner-to-parr, and the parr-to-smolt. The model was fit by minimizing the combined likelihood of two forms of this equation, as described in Crozier and Zabel (2013). The two stages were solved simultaneously in the form described by Moussalli and Hilborn (1986):

$$R_{smolts} = \frac{p_1 \cdot p_2 \cdot S}{1 + \left(\frac{p_1}{c_1} + \frac{p_1 \cdot p_2}{c_2} \right) \cdot S}, \qquad [2]$$

where R is the number of recruits (in this case, smolts), S is the number of spawners, p_1 and p_2 are the productivity parameters from the spawner to parr stage and from the parr to smolt stage, respectively (actual parameter estimates shown in Figure 1). c_1 and c_2 are the asymptotic (maximum) recruitment parameters for the parr and smolt stages, respectively, which we refer to as “capacity” parameters. The data used in model fitting consisted of 1) an expanded estimate of spawners, based on redd counts in index reaches of each population, age distributions and harvest rates from 1962- 2008 from the Northwest Fisheries Science Center Salmon Population Summary (SPS) Database (available online at *https://www.webapps.nwfsc.noaa.gov/sps*), 2) parr-smolt survival from PIT-tag data (Lamb et al. 2017), and 3) an estimate of smolt production based on brood-reconstruction and Lower Granite to Lower Granite aggregate smolt to adult survival estimates using estimates from the Technical Recovery Team (ICTRT and Zabel 2007).

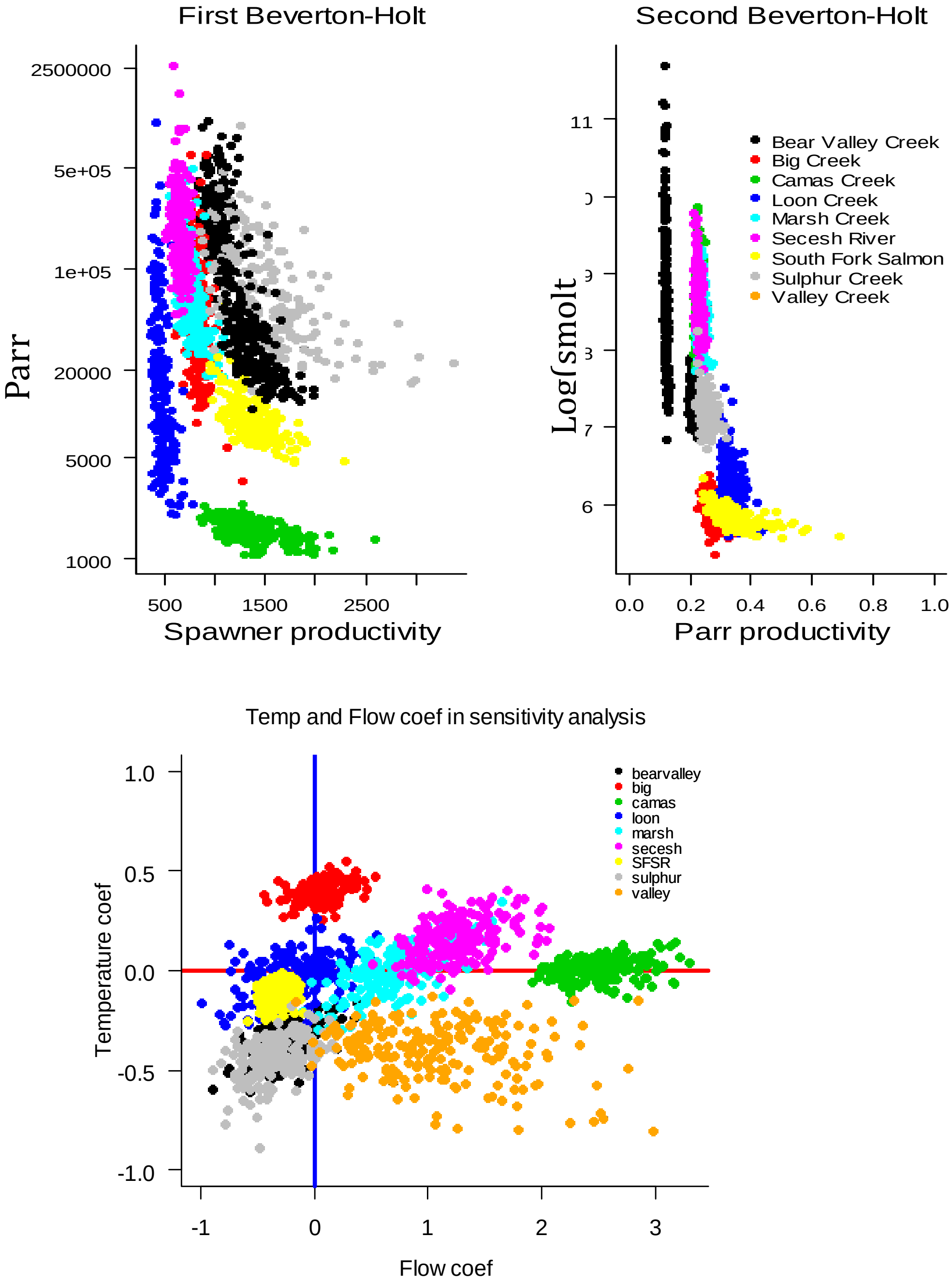

Figure 1. Posterior parameter estimates from the two-stage Beverton-Holt equation (equation 2). In the upper-left plot, spawner productivity (p1) is plotted versus parr capacity (c1). Populations are differentiated by different colors. In the upper-right plot, parr productivity (p2) is plotted versus smolt capacity (c2). The bottom plot represents the posterior parameter estimated from the relationship between smolt capacity (c2) and temperature and flow, as described in equation 3.

We further fit the smolt capacity term as a function of basin-aggregate climatic conditions

$$c_2 = \exp(\beta_0 + \beta_F F + \beta_T T). \qquad [3]$$

where the *βs* are fitted regression coefficients, *F* is mean September-October monthly flow at Salmon River, Idaho, and *T* is mean monthly air temperature in the Salmon River Basin from May to August. Placement of the temperature and flow covariates in the capacity term was based on model selection, in which we compared either placing them in the parr productivity term p_2, or dropping one or both environmental drivers (Crozier and Zabel 2013).

We used basin-aggregate indicators of climate (i.e., temperature and flow indices that reflect the entire Salmon River Basin instead of individual creeks) in this equation to match the spatial and temporal range of this life stage. The fish were tagged in headwater streams in July and August as parr, and they moved downstream at various times from fall to spring the following year. Even within a population there was a diversity of outmigration timing (Lamb et al. 2017), analogous to the fall migrants and spring migrants referred to in the Grand Ronde chapter (Cooney et al., chapter 9a). The fish were detected at Lower Granite dam the following spring. We do not know when or where the majority of the mortality occurs. The strong correlations in both space and time in climatic variables require caution to avoid overfitting. Nonetheless, we will conduct additional exploration of these relationships when we re-fit these parameters.

The primary mechanism assumed to link summer temperature with overwinter survival is the density-dependent relationship between spawner abundance and parr size documented in (Crozier et al. 2010). Size at tagging as parr is strongly associated with overwinter survival

(Crozier and Zabel 2013; Lamb et al. 2017). Thus we reasoned that parsimonious treatment of the two environmental variables in the parr to smolt stage was the best approach.

The Bayesian hierarchical model fitting process produced posterior samples of parameter estimates for each population. We used 7500 of these parameter sets per population as input vectors of parameters in our life cycle model. In every simulation, we randomly selected a stored iteration and applied the associated vector of seven parameters in equations 2 and 3.

Downstream survival

As juveniles migrate downstream a variable proportion of them are transported in barges through the hydropower system and released below Bonneville Dam. Transported fish have different rates of adult return than fish that migrate in-river, which we account for with a multiplier *D*, which is applied to the survival during transport p_t. All parameters values in this scenario are drawn from Crozier and Zabel (2013). We drew *D* from a lognormal distribution with a mean of 0.46 and a standard deviation of 1.4, fit from PIT-tag data. 80% of the fish were assumed to be transported. Survival of in-river migrants was drawn from a lognormal distribution with mean 0.472 and SD= 0.134. Total downstream survival, s_d, is as follows:

$$s_d(t) = D(t) \cdot p_T \cdot s_T + (1 - p_T) \cdot s_I \qquad [4]$$

where $s_d(t)$ is survival of downstream migrants, $p_T\,(t)$ is the portion of fish arriving at the uppermost dam that were transported (Marmorek et al. 1998; Williams et al. 2005), $s_T(t)$ is the survival of transported fish, and $s_I(t)$ is the survival of in-river migrants (ICTRT and Zabel 2007).

Marine survival and age at maturity

We used a new ocean survival module based on PIT-tag data, described in Burke et al., chapter 3 (Figure 2). The model we selected was very similar to the top model in AIC (dAIC=0.87), but the top model included a principal component axis of a number of variables, which we could not project into the future. The 2nd best model based on AIC comparison is composed of sea surface temperature (SST) off the coast of Washington in summer and an index of sea surface temperature in an arc along the eastern edge of the Pacific in winter (SSTarc, Johnstone and Mantua 2014). Both of these variables are related to SST, which has a lengthy historical time series and can be projected under climate change scenarios.

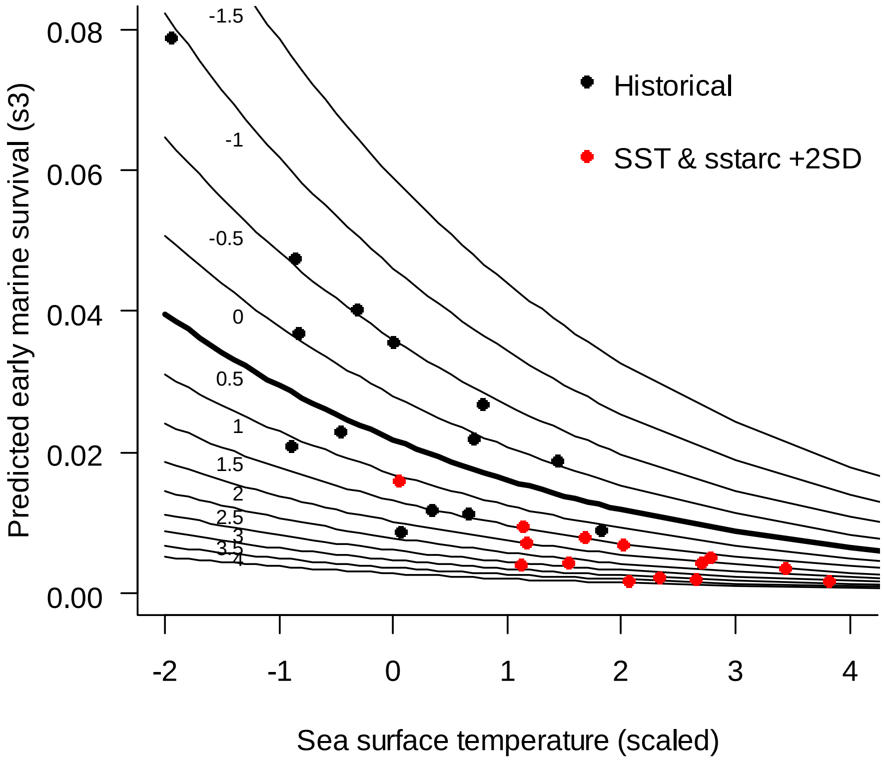

Figure 2. Predicted third-year survival (y-axis, s_3) versus SST (x-axis) and SSTarc (contour lines), from Burke et al. (Chapter 3). The contour lines represent values of SSTarc, which are labeled on the plot. The black points represent predicted survival during migration years 2000-2015. The red points represent predicted survival with 2 standard deviations (SD) of each index added to the observed values.

SST and SSTarc are also related to the variables used in previous early-ocean survival models: upwelling and the Pacific decadal oscillation. Upwelling affects nearshore temperature in the early summer, which is reflected in the nearshore SST index. The Pacific decadal oscillation captures spatial heterogeneity in temperature across the north Pacific, which is also reflected in SSTarc.

Salmon survival in this life stage is a complex interplay of conditions upon arrival in the estuary (timing, body condition), ocean prey base (driven largely by ocean conditions the previous winter and upwelling) but also predation rates, which are highly uncertain. Maturation rates also vary with environmental conditions, but we are not confident in future trends at this time. Larger smolts often return at younger ages than smaller smolts. Warmer ocean conditions can sometimes improve growth, which could produce younger spawners. Fishing pressure may also have selected against older-maturing fish. Thus a coast-wide trend across multiple salmon species has been observed toward younger age at reproduction, but whether this trend will continue is not known. We will explore the implications of this trend in future modeling, but for this version we assumed the same propensity to mature at age as in previous versions of the model.

Marine survival estimated by pit tags was lower than that estimated by the fish count smolt-to-adult data used in original model fitting. As a temporary solution, we added a multiplier on early-ocean survival (s_3) to account for the difference in estimates. We selected the multiplier by comparing mean spawner counts from 2000-2015 that were observed and those predicted by the model, with pit-tag estimates of s_3.

Effects of mainstem temperature on upstream survival

Snake River spring-summer Chinook salmon typically migrate through the mainstem Columbia River April through June, and reach high-elevation tributaries before summer temperatures reach their peak. Therefore, historically exposure to stressful temperatures in the mainstem Columbia River was apparently rare (Keefer et al. 2005). However, higher mortality has occurred in recent years, especially in the summer-run populations, and is well explained by temperature (Crozier et al. 2016). Only 41% of fish that passed Bonneville Dam when temperatures exceeded 16˚C reached Lower Granite Dam from 2004-2015 (Figure 3), compared with 76% survival at lower temperatures. Because higher temperatures are expected in the future, we explored the implications of temperature-induced mortality during the upstream migration.

To model how future temperatures will alter upstream survival, we needed to account both for run timing and temperature projections at a monthly time step, rather than the daily time step used in Crozier et al. (2016). To approximate this relationship, we correlated annual estimates of survival based on the daily model with monthly June temperature at Bonneville Dam (Figure 3). This assumes that run timing stays constant over time. However, because we derived separate correlations for spring and summer-run, this could be considered a bounding scenario for summer-run under the optimistic assumption that summer-run shifts toward current spring-run timing: actual survival might be lower than modeled if migration timing shifts earlier, as has been observed in Columbia River sockeye (Crozier et al. 2011). For the daily model, we assumed run timing was lognormally distributed with mean on May 11 and sd = 0.13 (in Julian days) for spring run (Grand Ronde, Upper Salmon, and Middle Fork Salmon 2004-2015), and mean=Jun 1 and sd = 0.1 for summer run (South Fork Salmon, Pahsimeroi, and Imnaha). Most of the populations in this report are modeled as spring run, but Secesh, South Fork Salmon River, and Valley Creek were modeled as summer run.

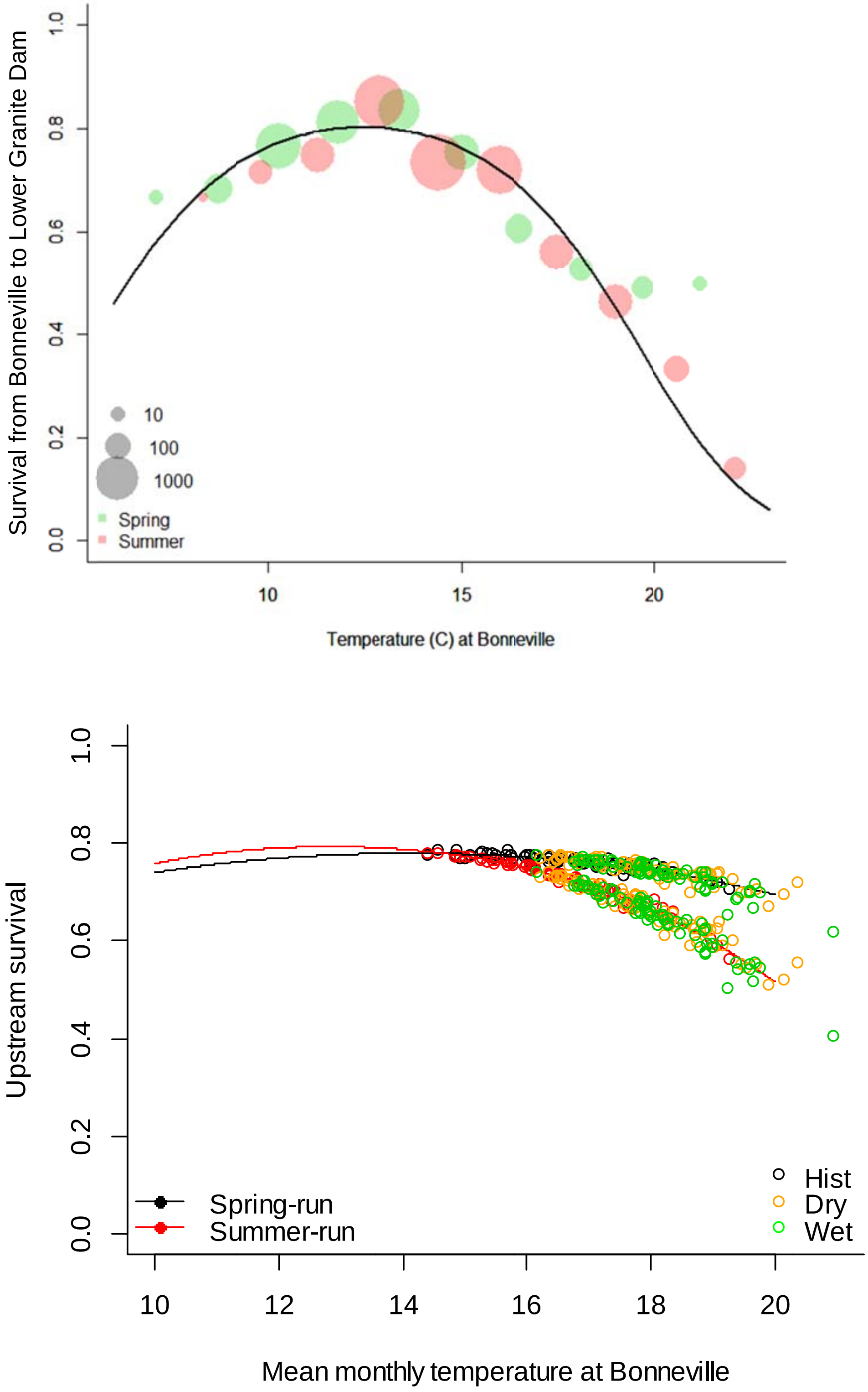

Figure 3. Crozier et al. 2017, Figure 9. Survival of Snake River spring- and summer-run Chinook salmon from Bonneville to Lower Granite Dam as a function of daily mean temperature

at Bonneville Dam on the day of passage. Fish are grouped by temperature or travel time. Circle size is proportional to the number of fish in each group. The bottom figure shows the results of the model with daily temperature inputs compared to output from a model that used a separate monthly temperature for spring and summer runs. The colors of the circles represent separate climate-change scenarios, and the solid lines are fits between survival and the model output from the monthly model.

The daily model is fit to observed survival of PIT-tagged Snake River spring/summer Chinook adults from Bonneville to Lower Granite Dam (see Crozier et al. 2016 and 2017 for specifics about the fish in the database). We extracted the temperature component of the model as the only covariate driving variation, but mean survival includes harvest and other factors (e.g., fallback, transportation, hatchery vs wild origin, age distribution, etc.). We therefore are assuming in our scenarios that these other factors continue to have the same average net impact as they did 2004-2015.

Environmental data and climate change sources

Historical environmental data

Monthly mean flow records (Table 1 for mean and SD) for Salmon River, ID were downloaded from USGS (2017). Daily and monthly mean temperatures at Bonneville Dam were collected by Army Corps of Engineers and accessed through the Columbia River Basin website (DART 2017).

Recent records for summer mean air temperature (mean monthly May-August temperature) were not available from the three meteorological stations used in the original analysis (McCall, Grangeville, and Warren, ID). We therefore switched sources to the PRISM database (PRISM Climate Group). This database has the important advantage of being complete and able to cover the spatial heterogeneity of the Salmon River Basin more systematically. It is also more compatible with climate projections, which are similarly based on a climatological model rather than raw observations. We downloaded monthly average temperature for the grid cell that contained the upper Middle Fork (Lat: 44.4068, Lon: -115.3520, Elev: 6404ft). During the period over which the parr to smolt data was fit (1993 to 2010), PRISM data was highly correlated with weather station data (r=0.89). Because the model coefficients were fit to standardized data, we applied the same coefficients to the new (standardized) temperature data.

We downloaded SST data and calculated the summer mean from June, July, and August temperatures (https://www.ncdc.noaa.gov/data-access/marineocean-data/extended-reconstructed-sea-surface-temperature-ersst-v3b accessed via http://cci-reanalyzer.org/Reanalysis_monthly/tseries.php (using E1: 237.1335, E2: 233.9523, N: 48.50611, S: 46.05009). SSTarc was obtained directly from Jim Johnstone, who published the details in Johnstone and Mantua (2014)

Simulating Environmental Covariates

When creating future climate scenarios, our aim is to maintain the statistical properties of the environmental data driving survival in the various life stages. However, another important aspect of these data are the covariances across drivers. For example, if large-scale oceanic and atmospheric drivers are impacting both the marine environment and the freshwater environment, such that a good or bad year in one environment is often paired with a good or bad year in other environments, our climate scenarios should express this same relationship.

To estimate variances and covariances of six environmental datasets (air temperature, Bonneville temperature, fall flow, spring flow, SST and SSTarc), we truncated the beginning of each to begin in 1960 and used data through 2015. We included spring flow for future use as a predictor of smolt survival and timing. We analyzed the data with the MARSS package in R (a multivariate time series package) (Holmes et al. 2014). Using just the process equation, this is the same as estimating an autoregressive process (AR1) with mean reversion.

$$\mathbf{x}_t = \mathbf{b} \cdot \mathbf{x}_{t-1} + \mathbf{w} \quad [5]$$

where $\mathbf{x}_t$ is a vector of the environmental data at time t, $\mathbf{b}$ is a vector that represents the strength of the mean reversion for each covariate, and $\mathbf{w}$ is multivariate normal (0, $\mathbf{Q}$). Here, the diagonal elements of $\mathbf{Q}$ are the estimated variances of the individual time series and the off-diagonal elements are the covariances between covariates.

Climate scenarios

Our objective was to explore specifically how the relationships among the various climate drivers interacted with population sensitivities to shape population trajectories. To do this, we first simulated 1000 time series of 100 years of baseline environmental conditions that followed the observed covariance relationships in the historical record using MARSS.

Second, we modified these baseline conditions systematically. The maximum rate of change expected in each variable was based on projections for mid-century from the latest round of global climate models (CMIP5) whenever possible. If these were not available, we used projections from an earlier model comparison project (CMIP3). We focused on mid-century for our initial scenarios, because even this level of climate change was sufficient to drive most of our populations extinct. Furthermore, more distant projections were not available for all variables.

We perturbed the baseline time series by adding a climate scalar. The climate scalar ranges from 0 (historical conditions) to the maximum expected change (1) for each variable by mid-century in increments of 0.01. The same scalar is applied to all variables simultaneously.

We compared population performance across climate scenarios after running 2000 replicate simulations per scenario, across the 100 increments of warming. In each replicate, we randomly drew one of 1000 environmental time series and one of 7500 spawner-to-smolt parameter sets per population. We fixed the maximum change at 2 standard deviations (SD) for Bonneville temperature, SST and SSTarc, and 5 SD for air temperature. For each of these temperature scenarios, we explored 4 flow scenarios from -1 to +2 SD change in the mean in increments of 1 SD. Each scenario was run at the designated increment for 100 years.

Sea surface temperature

Our projection of sea surface temperature comes from the NOAA Earth System Research Laboratory Climate Change Web Portal (https://www.esrl.noaa.gov/psd/ipcc/ocn/)/ We selected a grid from 46.027˚S to 48.05˚N and -125.09˚W to -123.42˚E using the business-as-usual emissions scenario, representative concentration pathway (RCP) 8.5. On average, across 37 different global climate models, temperature across this entire grid space increased by approximately 1˚C for the July-August-September period in the 2006-2055 time period compared with the historical (1955-2005), and 2.8-2.9˚C across the domain for the 2050-2099 period. There is no change in modeled standard deviation between periods, and historical SD is 0.58-0.62 across the spatial domain. Thus the scaled projections are 1.7 SD for mid-century, and 4.5-5 SD for late century. In our scenarios, we modeled changing SST and SSTarc from 0 to 2 SD. Although it is possible to calculate SSTarc directly from these SST projections, these are not yet finished. Instead, we made the simplifying assumption that SSTarc warms at the same rate (in SD) as SST. We note that seasonal definitions vary across sources. Because this was a sensitivity analysis rather than a specific projection, we simply used the closest period available.

Air temperature

For air temperature, we used RCP 8.5 emission scenario for 2040-2069 centered in the upper Middle Fork Salmon River Basin from the Integrated Scenarios project (http://climate.nkn.uidaho.edu/IntegratedScenarios/model_products.php). For the mid-century, individual global climate models (GCM) projections for the June-August period range from 2-5.5˚C above the historical mean temperature. The average projection change across 20 GCMs is 3.9˚C. The SD in our historical dataset was 0.86, so the scaled expected change from the model mean was 4.5 SD. In our scenarios, we modeled a change from 0 to 5 SD.

Flow

Hydrological models based on the CMIP5 GCMs are still being finalized. We therefore used products from the CMIP3 modeling exercise (Hamlet et al. 2013). This effort focused on more moderate emissions scenarios (B1 and A1B), and thus might be expected to somewhat underestimate forthcoming results for the RCP 8.5. However, there is still a large amount of variation across GCMs in precipitation projections regardless of the emissions scenario (Abatzoglou and Brown 2012). So we explored a wide range of flow scenarios across all of the temperature scenarios. Modeled changes in flow for the Salmon River, at Salmon, Idaho projected changes in mean flow for September and October from 90% to 150%. The variation in flow increased as well in many individual GCMs, which could have an independent biological impact from changes in the mean (Ward et al. 2015). In our scenarios, we explored a drier scenario at 1 SD below historic, and 2 wetter scenarios (1 SD and 2 SD increases). We doubled the variance in both wetter scenarios.

Temperature at Bonneville Dam

Bonneville Power Administration modeled two managed-flow scenarios for the hydrosystem based on the University of Washington naturalized-flow products for water years 1929-1998 (Brekke et al. 2010). Using the method developed by Yearsley et al. (2012; 2009) we added temperature to these two flow scenarios. This daily temperature time series was used to model upstream migration survival under historical and the two climate change scenarios (ECHO_G 3.2 B1 and MIROC 3.2 A1B, IPCC 2007). Under these projections, mean June temperature at Bonneville Dam increased by 1.3˚C and 1.5˚C in two scenarios, respectively. The historical SD was 1.1˚C, producing an estimated future increase of 1.2 -1.4˚C in the scaled mean. We explored a change of 0-2 SD to fully capture these projections and the slightly warmer climate that would occur under the RCP 8.5 scenario.

Analyses

The most rigorous test of a model is whether it performs well in fitting data outside the range to which it was fit. Validating the role of temperature and flow in influencing parr to smolt survival is especially important for exploring climate-change scenarios. We lack mechanistic models for these relationships for several reasons. First, habitat models have traditionally focused on a static estimate of summer rearing capacity, which does not necessarily capture interannual variation in capacity. Second, habitat models have not focused on overwinter capacity limitations, which presumably differ from summer constraints. We are working on developing habitat models that can explain the relationships we have observed in these populations, but at this point we rely on statistical correlations that have been robust over time.

We tested the robustness of the spawner to smolt model parameters (from Crozier and Zabel 2013) by comparing model-predicted parr-to-smolt survival against 5 years of new pit tag data, given annual spawner estimates and environmental observations. We examined three metrics: first, whether the 95% CI of observed data fell within the range predicted by our model simulations, and second, whether the observed interannual pattern was highly correlated with model predicted interannual pattern. Finally, we compared the linear regression slopes of parr-smolt survival as a function of temperature and flow, respectively, generated from the model predictions versus those from observations.

Population performance in each scenario was summarized by 1) geometric mean spawner abundance over each simulation, and 2) the proportion of runs that fell below the quasi-extinction threshold, defined as the proportion of simulations in which the 4-year running mean abundance dropped below 50 spawners. To describe the rank order of vulnerability to extinction, we identified the climate scalar at which all runs went extinct.

Results

Testing model parameters

Model simulations tracked the annual pattern of observed parr to smolt survival for most populations (Figure 4): model estimates fell within the confidence interval of observations in 84% of year by population comparisons. The raw correlation coefficients between modeled and observed time series ranged from 0.53-0.84 for all but 1 population (South Fork Salmon River, SFSR 0.25, Figure 5). SFSR had very weak climate forcing parameters (Figure 1), so it is not surprising that climate was not the major factor driving parr to smolt survival in this population.

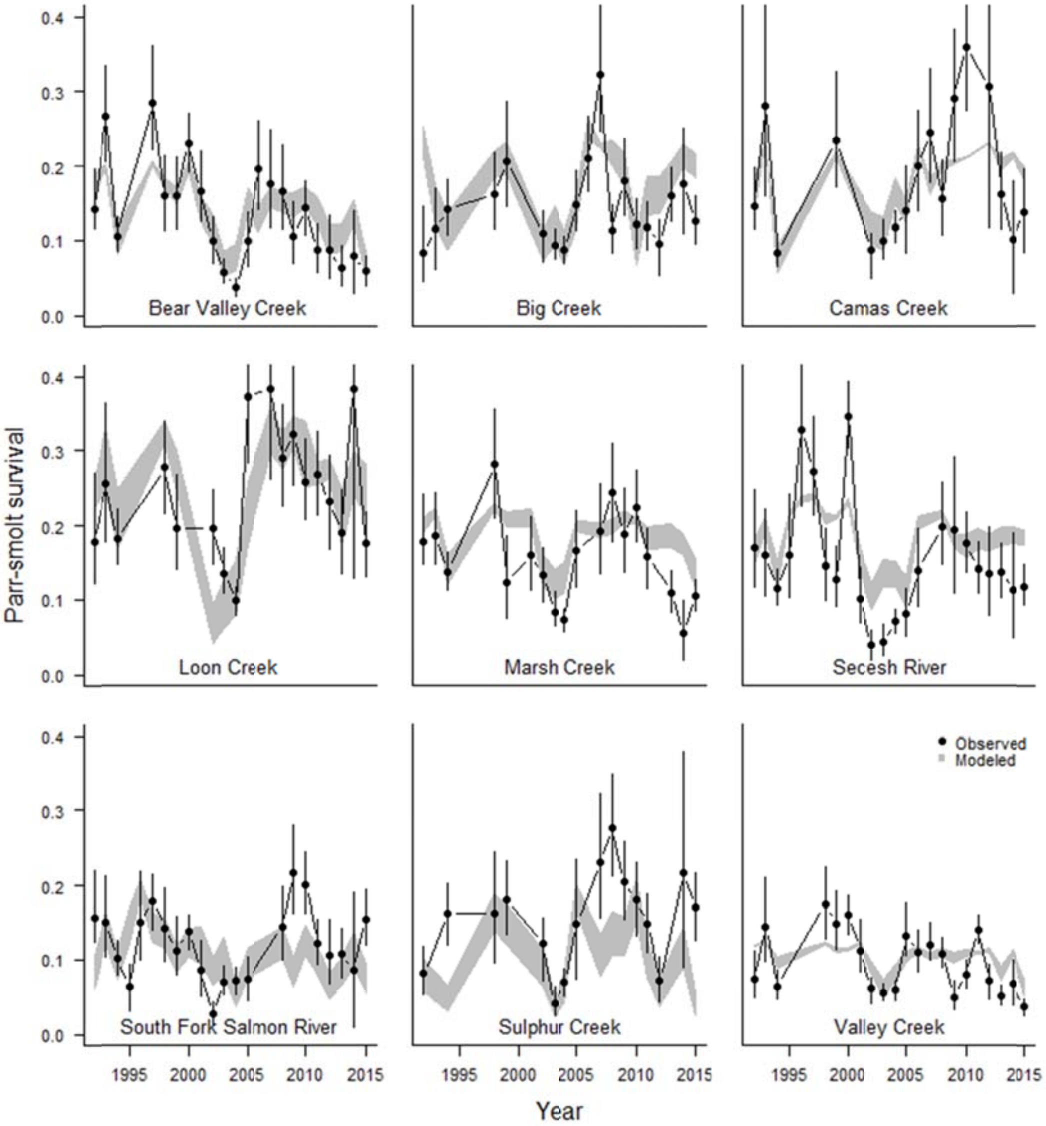

Figure 4. Modeled (grey) versus estimated parr-smolt survival (black points with 95% CI represented as vertical lines). The gray area was derived by running the model repeatedly using the posterior distributions of parameter estimates, and then representing the 95% CI of the modeled runs.

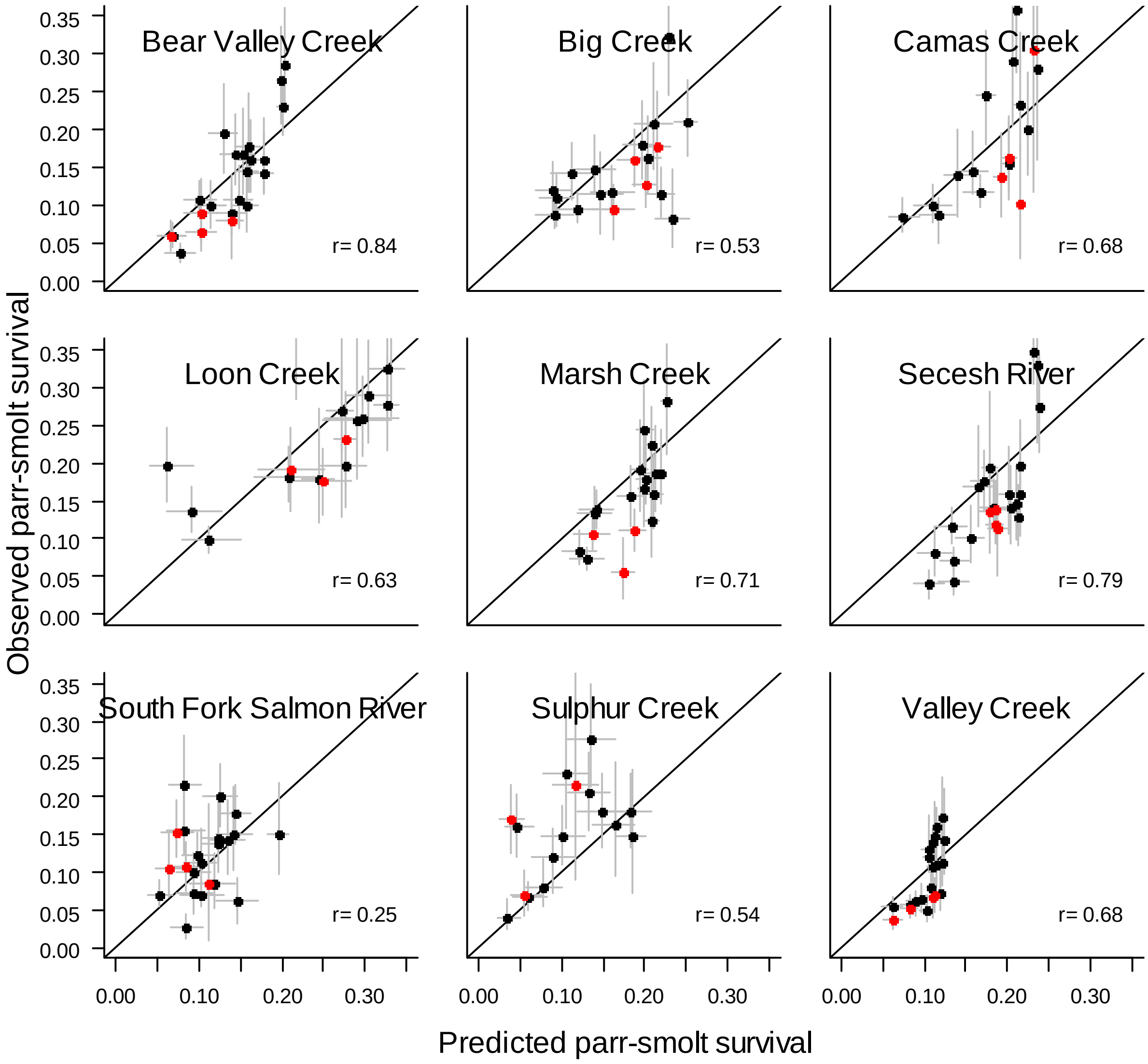

Figure 5. Qqplots of modeled and observed parr-smolt survival. Grey lines show 95% confidence limits. Model confidence limits represent the range of 95% of simulations. Red dots show the new datapoints (2012-2016). Pairwise correlation coefficient between observed and predicted survival shown in bottom right of each plot.

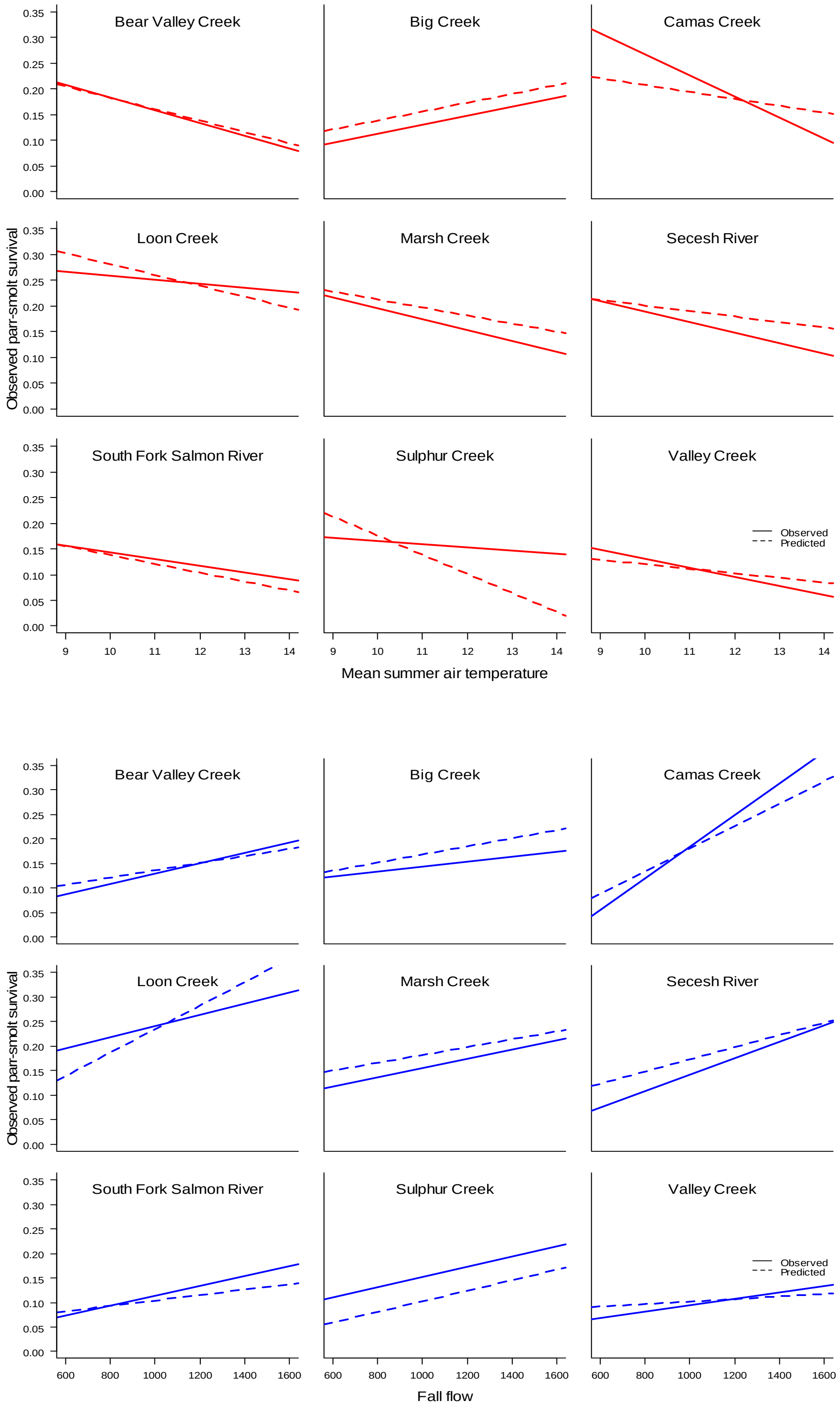

Figure 6. Linear regression fits of parr-to-smolt survival as a function summer air temperature (top) and flow (bottom) for observations (solid lines) and model-predicitons (dotted lines).

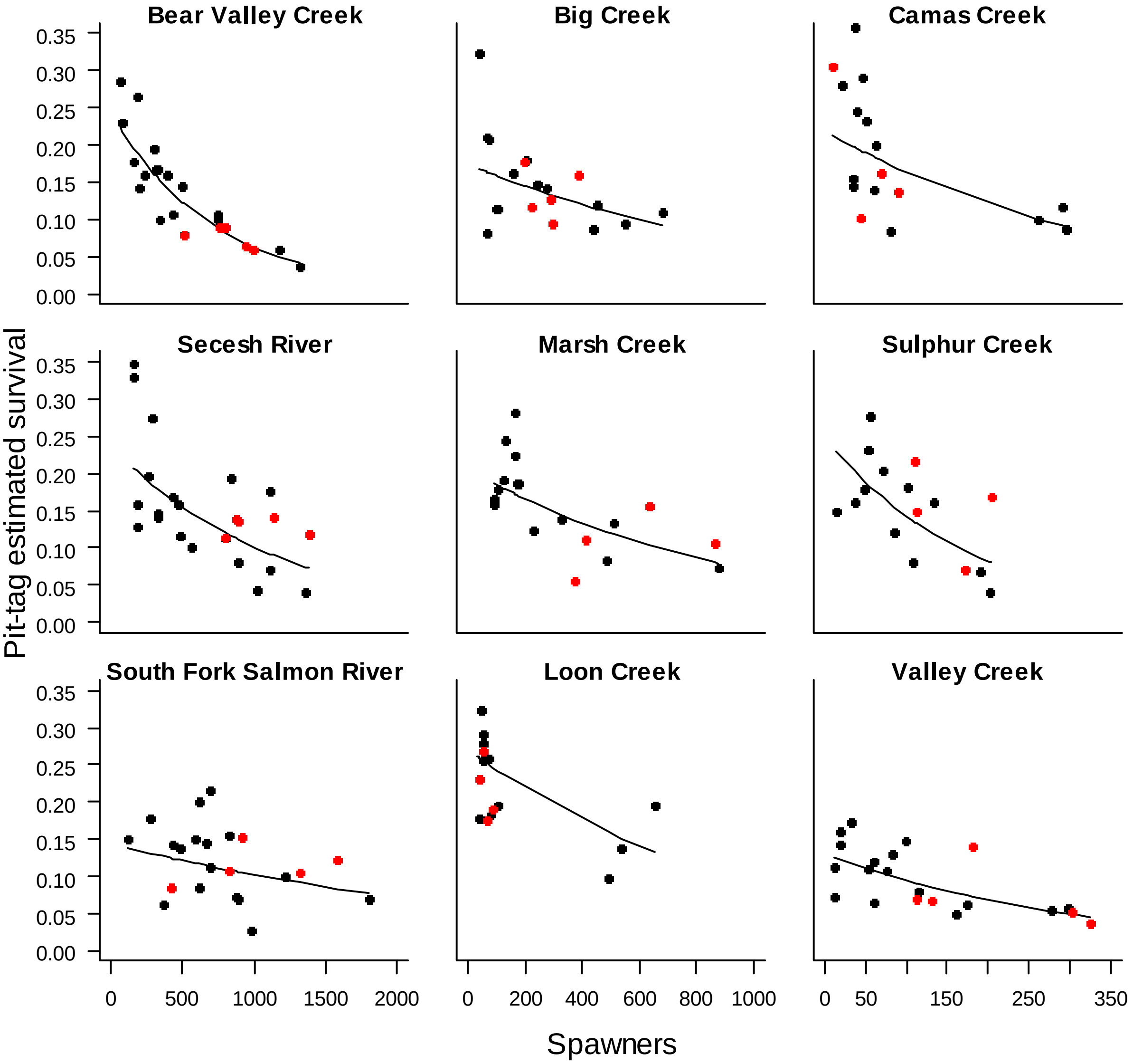

Figure 7. Relationship between observed parr-to-smolt survival and spawner abundance, by population. The line represents a regression fit (to log abundance). The original data is shown with black points. The red points are the new independent data that were not used in the spawner-smolt paramter fitting.
`

However, the most important test is that the basic trend of predictions as a function of temperature and flow compares favorably to observations. To examine these patterns, we fit simple regression models to observed parr to smolt survival as a function summer temperature and fall flow. All populations had negative slopes with temperature except for Big Creek (Figure

6, top). All populations had positive slopes in relation with fall flow (Figure 6, bottom). Recent data was very consistent with previous data for both relationships. Thus the general relationships we modeled, particularly populations expected to have strong relationships with temperature and flow, continue to show these relationships in recent data.

Furthermore, density dependence affecting this life stage is still apparent when parr to smolt survival is plotted against spawner counts (Figure 7). Simulated spawner counts from 1000 simulations are shown with gray lines in Figure 8, with the observed time series overlaid in black.

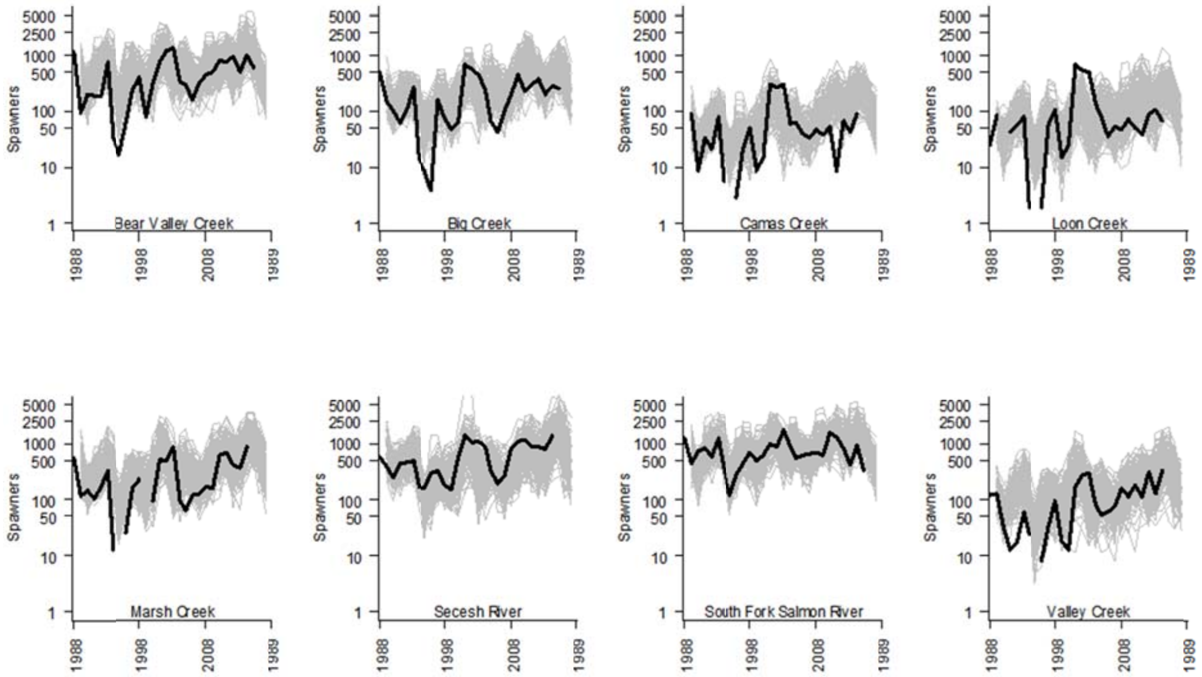

Figure 8. Spawner counts by population on the log scale. The dark line represents observed data. The grey lines represent realizations of the fully calibrated model, included adjusted s_3 values.

Climate scenarios

The covariance analysis identified weak but significant correlations among climate factors. The strongest relationship was between air temperature in the Salmon Basin and water temperature at Bonneville (r=0.45, Table 1), followed by links between Bonneville temperature and the two ocean temperature indices (r=0.35 and r=0.38). Finally, summer air temperature and fall flow displayed a negative correlation (r=-0.35). These relationships were maintained, with extensive noise, in the simulations.

Table 1. Covariance matrix with mean and standard deviation of the environmental drivers.

	Fall flow	Tair	Tbonn	SSTarc	Mean	SD
Fall flow (cfs)					1157	271
Tair (°C)	-0.35				11.53	0.86
Tbonn (°C)	-0.21	0.45			15.66	1.28
SSTarc	-0.17	0.1	0.35		-0.016	0.32
SST (°C)	-0.07	0.15	0.38	0.14	13.79	0.63

Under climate conditions expected to be typical in the second half of this century, all populations went extinct (climate scalar=1, Figure 9 top). The populations with the largest population sizes under the historical climate generally persisted the longest (e.g., SFSR, Figure 9), but several populations changed rank (in terms of extinction risk) in warmer scenarios. Big Creek, in particular, persisted longer than expected based on mean current population size (Figure 9, bottom).

Changing flow conditions either increased or decreased tolerance of warming, depending on the population (Figure 10). Camas and Valley Creeks both responded positively to increased flow, which affected them almost immediately because under historical flow conditions, they went extinct very quickly. Sulphur had the opposite response, with a negative response to increased flow.

Life stage-specific survival rates all changed with climate (Figure 11). Comparing historical conditions to the full extent of warming expected (climate scalar of 1), parr per spawner and parr to smolt survival both went up, due largely to release from density dependence at low spawner abundance. Upstream migration survival dropped from 0.75 to 0.64 for summer-run populations. Early ocean survival plummeted from about 0.05 to 0.01.

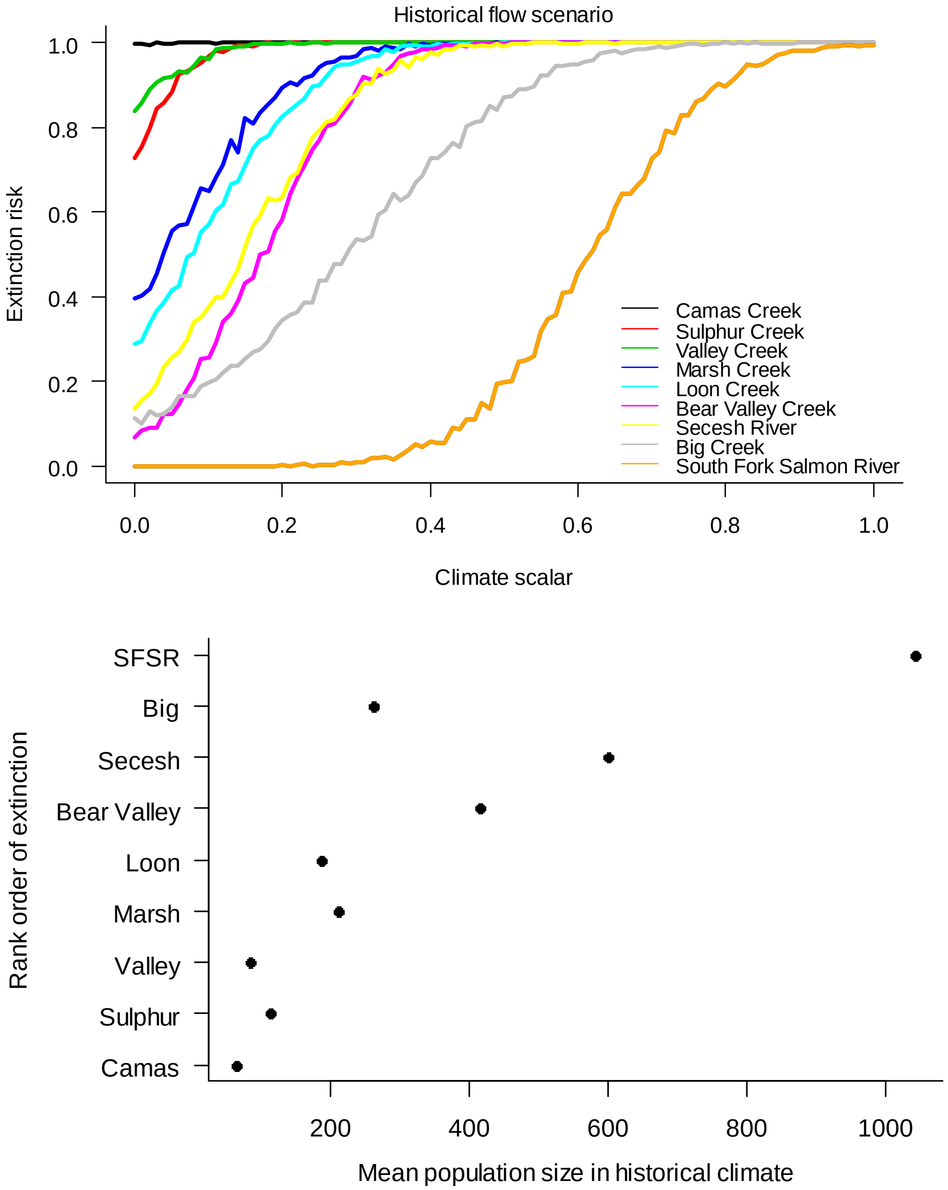

Figure 9. Extinction risk versus climate scalar by population (top) under the historical flow scenario. A climate scalar of 0 represents current conditions, and a scalar of 1 represents the most extreme climate change assumptions. The scalar was varied from 0 to 1. The rank order of when each population had a 100% percent chance of falling below the quasi-extinction threshold was plotted against the mean population abundance (bottom).

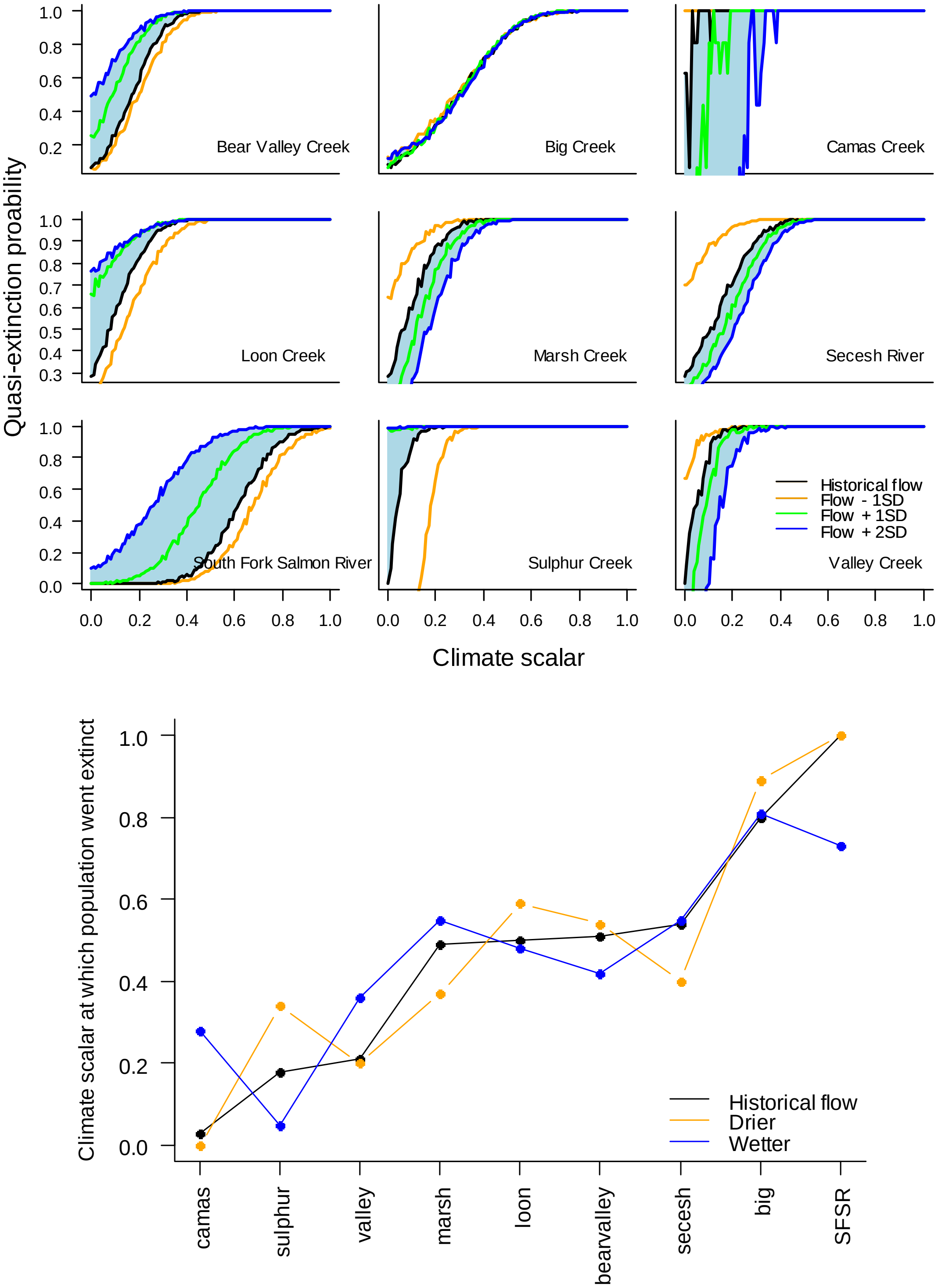

Figure 10. Quasi-extinction probability versus climate scalar under different flow scenarios (top plot). The greyed area represents the difference between the historical flow and the flow + 2 SD scenario. The orange line represents a scenario with 1 SD subtracted from historical flow. If the orange line falls to the right of the shaded area, that means the population has a negative relationship with flow. If the orange line falls to the left of the shaded area, that

means the population has a positive relationship with flow. The bottom plot shows the relationship between the temperature climate scalar at which the population had a 100% chance of going extinct under various flow scenarios.

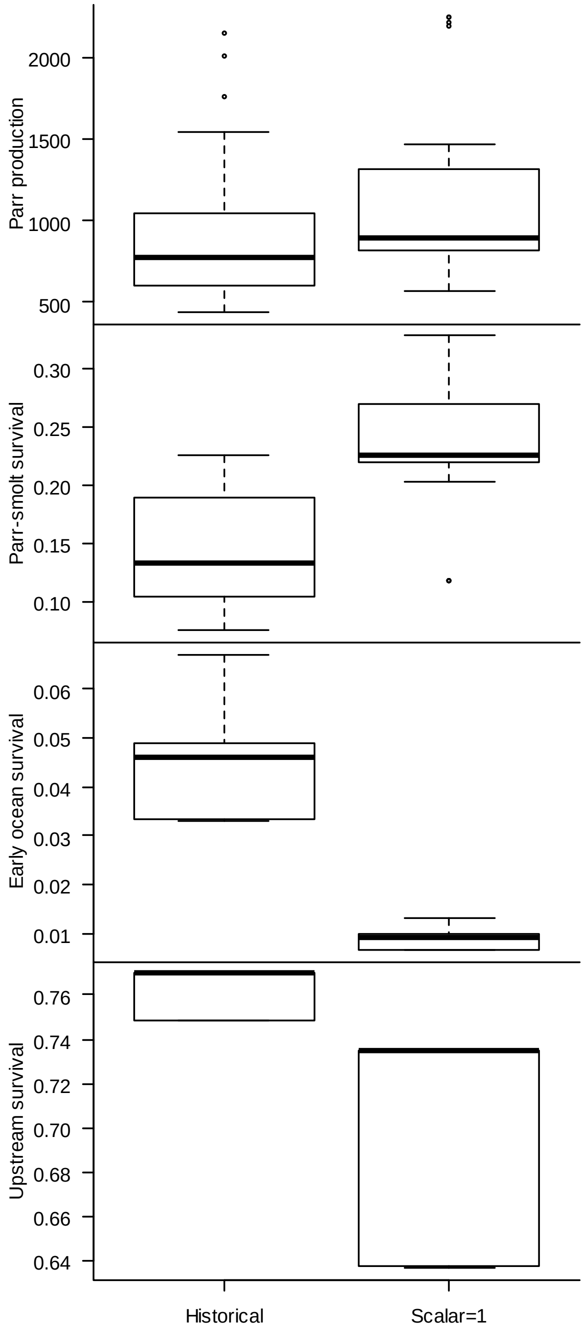

Figure 11. Comparison of several life-stage survival estimates under historical conditions (left hand side) and under assumptions about climate change by mid-century (right side) (see text). The bar plot represents the median value (horizontal dark line) the 25th and 75th percentiles (outer edges of box) and the 5th and 95th percentiles are represented by the whiskers.

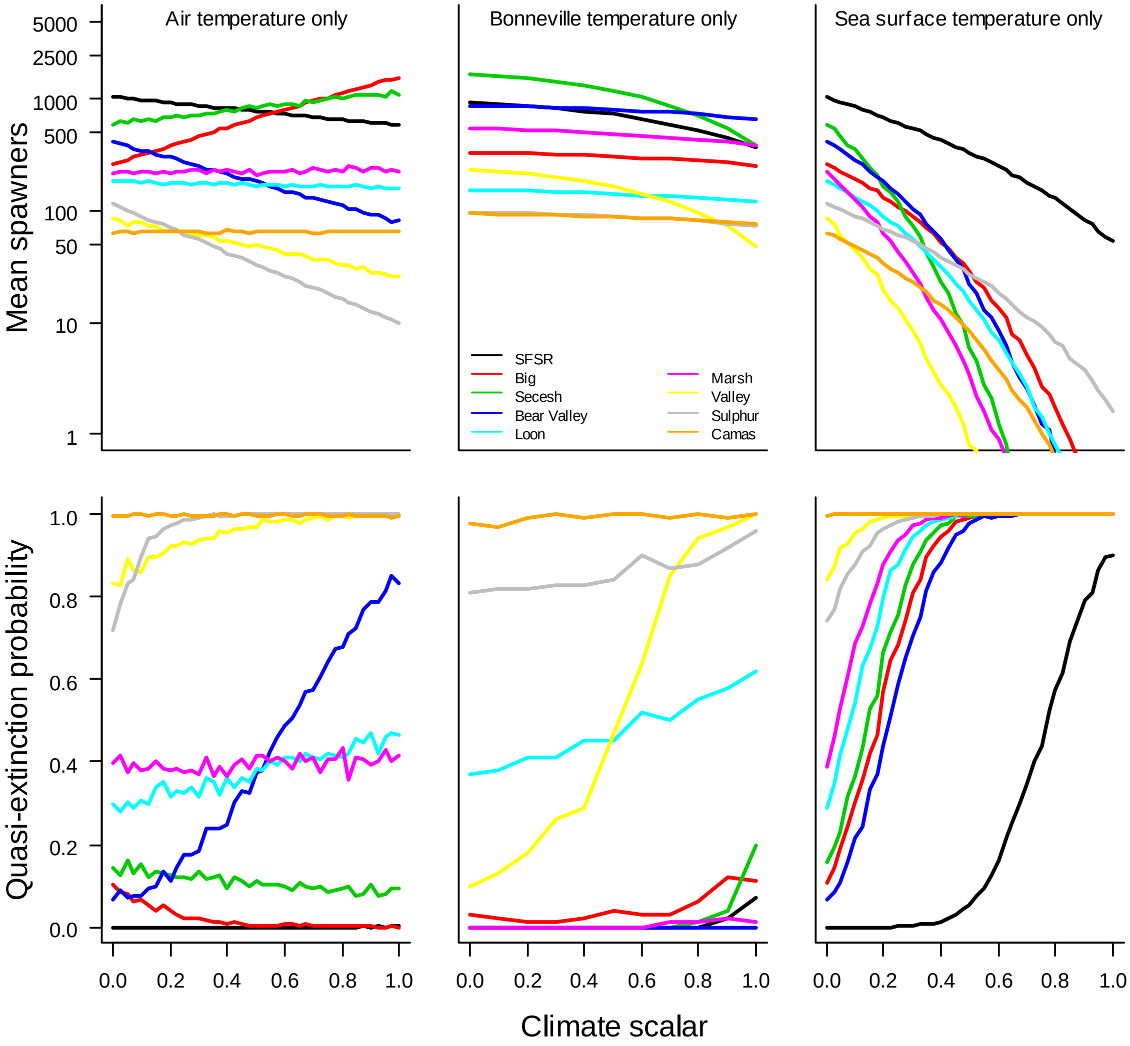

Figure 12. Single-factor perturbation experiments. Mean spawners (top row) and quasi-extinction risk (bottom row) as climate was modified incrementally in just one life stage.

The largest single factor that caused populations to decline was sea surface temperature. The climate scalar of 0.5 corresponds to 0.6˚C (Figure 12). The population most affected by temperature perturbations in both the headwaters and mainstem was Valley Creek. This was because of its negative response to temperature in the parr to smolt stage (Figures 1 and 6), and because of the portion of its population that migrates upstream relatively late, following the summer-run life history.

Discussion

Integrating climate change into vulnerability analyses is a major management objective (Link et al. 2015). Qualitative climate vulnerability assessments are being conducted across the nation (Crozier et al. 2017; Haltuch et al. 2017; Hare et al. 2016). Results from qualitative assessments have put spring Chinook in the Columbia River Basin in the highest risk category, along with Snake River sockeye, California's Central Valley Chinook and Central California Coast coho. The advantage of a qualitative assessment is that many factors can be considered, despite very limited data on their potential effects. Quantifying risk is more difficult because large unknowns exist. Nonetheless, one major concern for these populations in Crozier et al. (2017) was that high exposure to summer temperature associated with the spring/summer life history of these ESUs would eventually put the characteristic life history itself at risk.

We have improved on previous life cycle modeling efforts by addressing two major needs. First, we have increased the number of links between climate drivers and life-stage specific survival. Unfortunately, a large suite of factors influences how climate drivers affect populations, such that considering all potentially important factors is unfeasible. However, cumulative effects of multiple interacting factors can be collapsed into net responses that are positive, negative or neutral for a particular life stage. By exploring many combinations of positive and negative responses to temperature and flow in the parr to smolt stage, we have considered the influence on viability across a wide range of possible limiting mechanisms.

A second key improvement is that the current model form allows a shared general climate driver, such as temperature, to affect multiple life stages and potentially accumulate over the life cycle. We have begun analyzing the correlation among climate drivers in different life stages, and simulating future climates that reflect this correlation structure. In addition, by modeling both spring-run and summer-run sensitivities to summer temperature, we have allowed the same correlation in exposure to temperature to be filtered through different population sensitivities, which in this case depends on life-history characteristics (i.e., migration timing). Although our results are still preliminary pending model re-fitting, some general patterns and management recommendations have emerged.

Importance of intrinsic potential and current carrying capacity

An important theme in our results was that the vulnerability to climate change was correlated with current population size (Figure 13). In most cases, a higher carrying capacity in the current climate provided resilience to perturbations due to climate change. Although our model was fit exclusively to population abundance estimates, previously developed estimates of habitat quantity and quality, as characterized by intrinsic potential (ICTRT and Zabel 2007), nearly matched our rank order of extinction risk (r=0.89, Figure 13). These basic habitat features are well understood, and already used in recovery planning.

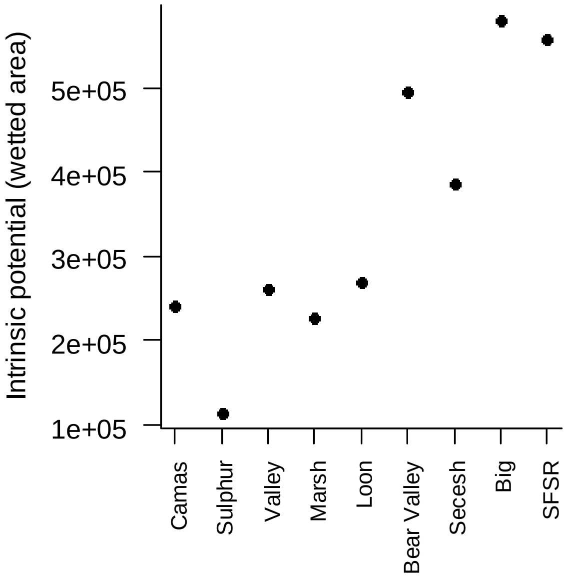

Figure 13. Relationship between Intrinsic potential and rank order of extinction risk in the historical flow scenarios shown in Figure 9.

Climate sensitivities affected outcomes

There were some exceptions to the general relationship with habitat capacity that offer some guidance in recovery planning specifically for climate change. One population in our analysis displayed a strong positive response to temperature, which has continued since the model parameters were first fit. Big Creek has been studied specifically by the University of Idaho at Taylor Ranch. The relationship between survival and temperature in Big Creek is complicated, as described by Crowell and Kennedy (2011). Nonetheless, it appears that cumulatively, productivity goes up in warmer years sufficiently to support the added metabolic needs of the fish, which correlates with higher overwinter survival (Lamb et al. 2017). A constructive avenue for future efforts would be to explain why this location appears to have more growth potential than other streams. But it is specifically this characteristic that greatly improved population outcomes in our climate change scenarios.

Most other populations showed differential vulnerability to climate change, depending on whether precipitation goes up or down. Future precipitation patterns are less certain than for temperature, but whether the climate becomes drier or wetter does affect the rank order of climate vulnerability within this ESU. In addition to affecting parr to smolt survival as modeled here, changes in precipitation also could affect other life stages. As suggested for Chinook in other locations, more intense fall precipitation could reduce egg survival through scouring of redds (Battin et al. 2007); or changes in summer precipitation and flows might cause adults to spawn in the thalweg, with implications for egg survival as suggested by Ward et al. 2015. The Salmon River Basin sits at higher elevation and in a more arid climate compared with Puget Sound and other coastal populations, reducing the relative risk of scour. Furthermore, atmospheric rivers, which are an important driver of storm intensity along the coast, do not strongly influence this region. Nonetheless, in the future, intense storms could alter the general relationships described here between mean flow and survival. The habitat features that reduce the risk from scouring floods are well known, and could therefore be examined in these populations. Regardless, additional factors beyond what we have considered here will certainly arise, and require additional inquiry. That is a key element of adaptive management, which is particularly important with respect to climate change. But the range of parameter values explored in this analysis captures numerous potential phenomena such as these.

Overwintering habitat for parr continues to limit all of these populations, shown by the persistent density-dependent relationship of parr-smolt survival (Figure 6). The mechanism for this limitation continues to be speculative. We explored whether estimates of specific types of habitat, such as bank, bar or midstream, were correlated with any of our model parameters or general results. We hypothesized that midstream habitat might be an index for fall migration or overwintering limitations, and hence be limited in flow-sensitive populations. Although there was a loose trend toward higher flow coefficients for populations with less midstream habitat, it was not strong or statistically significant. However, these habitat estimates are currently static and not specifically focused on winter habitat, and thus do not capture the interannual variation that appears key. Identifying specific limitations will be complicated by multiple behavioral strategies for overwintering location, as observed in the Grand Ronde. Thus understanding why flow affects overwinter survival likely requires understanding why some fish stay at high elevation over winter, while others move downstream. We recommend more tracking of parr migrants, and more pit-tagging of parr that remain higher in the tributaries over winter to better estimate the fitness consequences and dependence on climate of different behaviors.

The two dominant features of climate change are that temperatures are going up and precipitation may become more variable. Summer flows will likely decline in the Columbia Basin (Vano et al. 2015), which will probably exacerbate the temperature limitations we have modeled. Any management actions that can increase habitat quality, especially protecting cool groundwater storage in large marshes, would likely help these populations. Although these locations are relatively pristine compared with others across the Columbia River Basin (Paulsen and Fisher 2001), there is still anthropogenic water withdrawal, agricultural impingement with pesticides and other toxic chemicals eliminating much needed food resources, and directly inhibiting fish. Riparian habitat degradation also elevates stream temperatures. We expect that with a healthy invertebrate community, these streams could be more productive in a warmer climate. Therefore, maintaining the integrity of the invertebrate communities, underground storage of cool water and hyporrheic exchange would be a good strategy to improve climate resilience.

Updates to the model

We have improved estimates of marine survival using pit-tag data, which reduces the potential for error propagation caused by having to account for upstream and downstream survival in the process of estimating marine survival, as was done previously (Crozier and Zabel 2013). Sample sizes are still too low to conclude that populations within the ESU differ in their marine survival, although existing data are consistent with that hypothesis. The annual variation in the new estimates is similar to our previous model predictions that were based on the PDO, upwelling, and travel time. However, our previous model allowed wider confidence intervals that resulted in higher marine survival. We plan to re-fit all parameters using a multiple likelihood framework that includes pit-tag data from all the major transitions.

Although data specific for wild populations of known origin and in-river juvenile migration is still limited, we did identify a strong interannual signal in survival that can be associated with climate. By identifying a strong link with sea surface temperature, we can now make quantitative projections from GCM scenarios. However, the mechanism linking SST to survival is presumably mediated through foodweb interactions (Daly et al. 2009), and the relationship we described could be disrupted by major transformations of community dynamics, as well as ocean acidification and other factors. Our longer term goal is to improve our understanding of how climate affects marine survival using high resolution oceanographic models of current transport and productivity, community models of prey and predator interactions, and salmon growth and propensity to mature given a tradeoff with survival. But ultimately, regardless of how “mechanistic” the modeled relationship is, net relationships can change over time as other limiting factors arise or are released.

One advance of this model is incorporation of thermal constraints in the upstream migration stage. Recent years of high temperatures and high migration mortality are a grave concern. Three major factors – temperature, spill, and harvest, all hit summer-run populations harder than spring run. The suspected harvest on these ESA-listed summer-run populations was over 20% in 2014 and 2015 (Crozier et al. 2017), much higher than the average of 7% we have assumed in previous models. Although we did not explore the impact of harvest explicitly in these scenarios, it could be a management lever that could ameliorate some of the future losses to high temperature, and it will be explored further in future scenarios. We have also worked on scenarios that elevate smolt migration survival to reflect several years of high survival that occurred recently. However, these results were not finished in time to include them in this report. But in the future we will include the smolt stage in our environmental correlation matrix.

Literature cited

Abatzoglou, J. T., and T. J. Brown. 2012. A comparison of statistical downscaling methods suited for wildfire applications. International Journal of Climatology 32(5):772-780.

Battin, J., and coauthors. 2007. Projected impacts of climate change on salmon habitat restoration. Proceedings of the National Academy of Sciences of the United States of America 104(16):6720-6725.

Brekke, L., B. Kuepper, and S. Vaddey. 2010. Climate and Hydrology Datasets for Use in the RMJOC Agencies' Longer-Term Planning Studies: Part 1 - Future Climate and Hydrology Datasets.

Cheung, W. W. L., R. D. Brodeur, T. A. Okey, and D. Pauly. 2015. Projecting future changes in distributions of pelagic fish species of Northeast Pacific shelf seas. Progress in Oceanography 130:19-31.

Cromwell, K. J., and B. P. Kennedy. 2011. Diel distribution, behaviour and consumption of juvenile Chinook salmon (Oncorhynchus tshawytscha) in a Wilderness stream. Ecology of Freshwater Fish 20(3):421-430.

Crozier, L., E. Dorfmeier, T. Marsh, B. Sandford, and D. Widener. 2016. Refining our understanding of early and late migration of adult Upper Columbia spring and Snake River spring/summer Chinook salmon: passage timing, travel time, fallback and survival. Report of research by Fish Ecology Division, Northwest Fisheries Science Center.

Crozier, L., and coauthors. 2017. A Climate Vulnerability Assessment for West Coast Salmon ESUs. Plos One in prep.

Crozier, L., R. W. Zabel, S. Achord, and E. E. Hockersmith. 2010. Interacting effects of density and temperature on body size in multiple populations of Chinook salmon. Journal of Animal Ecology 79:342-349.

Crozier, L. G., M. D. Scheuerell, and R. W. Zabel. 2011. Using time series analysis to characterize evolutionary and plastic responses to environmental change: A case study of a shift toward earlier migration date in sockeye salmon. American Naturalist 178(6):755-773.

Crozier, L. G., and R. W. Zabel. 2013. Population responses of spring/summer Chinook salmon to projected changes in stream flow and temperature in the Salmon River Basin, Idaho. R. W. Zabel, T. D. Cooney, and C. E. Jordan, editors. Life cycle models of interior Columbia River populations. NWFSC Draft Technical Report, Seattle, WA.

Crozier, L. G., R. W. Zabel, and A. F. Hamlett. 2008. Predicting differential effects of climate change at the population level with life-cycle models of spring Chinook salmon. Global Change Biology 14(2):236-249.

Daly, E. A., R. D. Brodeur, and L. A. Weitkamp. 2009. Ontogenetic Shifts in Diets of Juvenile and Subadult Coho and Chinook Salmon in Coastal Marine Waters: Important for Marine Survival? Transactions of the American Fisheries Society 138(6):1420-1438.

DART. 2017. Columbia River Data Access in Real Time. http://www.cbr.washington.edu/dart/dart.html, accessed June 2007 and Jan 2011.

Ford, M. J., and coauthors. 2016. 2015 Status Review Update for Pacific Salmon and Steelhead Listed under the Endangered Species Act: Pacific Northwest. National Marine Fisheries Service, Northwest Fisheries Science Center. Available at: https://www.nwfsc.noaa.gov/publications/scipubs/display_doctrack_allinfo.cfm?doctrackmetadataid=8623.

Haltuch, M. A., and coauthors. 2017. A California Current Fish Stock Climate Vulnerability Assessment. Plos One in prep.

Hamlet, A. F. M. M. E., G. Mauger, S. Y. Lee, and I. Tohver. 2013. An Overview of the Columbia Basin climate change scenarios project: approach, methods, and summary of key results. Atmosphere-Ocean (in print).

Hare, J. A., and coauthors. 2016. A Vulnerability Assessment of Fish and Invertebrates to Climate Change on the Northeast U.S. Continental Shelf. Plos One 11(2):e0146756.

Holmes, E. E., E. J. Ward, and M. D. Scheuerell. 2014. Analysis of multivariate time-series using the MARSS package. Northwest Fisheries Science Center, NOAA, Seattle, WA, USA.

ICTRT, and R. W. Zabel. 2007. Assessing the Impact of Environmental Conditions and Hydropower on Population Productivity for Interior Columbia River Stream-type Chinook and Steelhead Populations. NWFSC Technical Report.

IPCC. 2007. Climate Change 2007: The Physical Science Basis, http://www.ipcc.ch/, accessed March 2007.

IPCC. 2014. Climate Change 2014: Synthesis Report. Contribution of Working Groups I, II and III to the Fifth Assessment Report of the Intergovernmental Panel on Climate Change. IPCC, Geneva, Switzerland.

Johnstone, J. A., and N. J. Mantua. 2014. Atmospheric controls on northeast Pacific temperature variability and change, 1900-2012. Proceedings of the National Academy of Sciences of the United States of America 111(40):14360-14365.

Keefer, M. L., and coauthors. 2005. Escapement, harvest, and unknown loss of radio-tagged adult salmonids in the Columbia River - Snake River hydrosystem. Canadian Journal of Fisheries and Aquatic Sciences 62(4):930-949.

Lamb, J. J., and coauthors. 2017. Monitoring the migrations of wild Snake River spring/summer Chinook salmon juveniles, 2015-2016.

Link, J. S., R. Griffis, and S. Busch, editors. 2015. NOAA Fisheries Climate Science Strategy. U.S. Dept. of Commerce, NOAA Technical Memorandum NMFS-F/SPO-155.

Moussalli, E., and R. Hilborn. 1986. OPTIMAL STOCK SIZE AND HARVEST RATE IN MULTISTAGE LIFE-HISTORY MODELS. Canadian Journal of Fisheries and Aquatic Sciences 43(1):135-141.

Paulsen, C. M., and T. R. Fisher. 2001. Statistical relationship between parr-to-smolt survival of Snake River spring-summer Chinook salmon and indices of land use. Transactions of the American Fisheries Society 130:347-358.

PRISM Climate Group. Oregon State University, http://prism.oregonstate.edu, accessed March, 2017.

USGS, W. R. 2017. Surface-water data for Idaho, http://waterdata.usgs.gov/id/nwis/. Cited April 2005.

Vano, J. A., B. Nijssen, and D. P. Lettenmaier. 2015. Seasonal hydrologic responses to climate change in the Pacific Northwest. Water Resources Research 51(4):1959-1976.

Ward, E. J., J. H. Anderson, T. J. Beechie, G. R. Pess, and M. J. Ford. 2015. Increasing hydrologic variability threatens depleted anadromous fish populations. Global Change Biology 21(7):2500-2509.

Yearsley, J. 2012. A grid-based approach for simulating stream temperature. Water Resources Research 48(3):W03506.

Yearsley, J. R. 2009. A semi-Lagrangian water temperature model for advection-dominated river systems. Water Resources Research 45(12):W12405.

Zabel, R. W., M. D. Scheuerell, M. M. McClure, and J. G. Williams. 2006. The interplay between climate variability and density dependence in the population viability of Chinook salmon. Conservation Biology 20(1):190-200.

CHAPTER 9: FULL MODELS

9.d ISEMP/CHaMP Life-cycle models – Entiat, John Day, Lemhi, Habitat Actions

W. Carl Saunders (Department of Watershed Sciences and Eco Logical Research), Nick Weber (Eco Logical Research), Nicolaas Bouwes (Eco Logical Research), Pete McHugh (Eco Logical Research), Eric Buhle (Quantitative Consultants Inc.), Kevin See (Quantitative Consultants Inc.), Braden Lott (Quantitative Consultants Inc.), Chris Beasley (Quantitative Consultants Inc.), and Jody White (Quantitative Consultants Inc.), Shubha Pandit (Terraqua), Pamela Nelle (Terraqua), Tom Desgroseillier (U.S. Fish and Wildlife Service), Keith van den Broek (Terraqua), Mark Armour (Southfork Research), Matt Nahorniak (Southfork Research), Chris Jordan (NOAA-NMFS-NWFSC).

Table of Contents

Generic Stage- or Age-structured Life-cycle Model 1

Middle Fork John Day Steelhead Life-cycle model Application: Evaluation of Riparian and Aquatic Habitat Restoration Actions 4

Entiat Chinook Life-cycle model: Evaluation of Instream Habitat Improvement Actions 21

Lemhi Chinook Adult-to-Smolt Parameter Estimation and Restoration Scenario Analysis 33

References 45

Generic Stage- or Age-structured Life-cycle Model

The Integrated Status and Effectiveness Monitoring Program (ISEMP; BPA Project 2003-017-00) in conjunction with the Columbia Habitat Monitoring Program (CHaMP; BPA Project 2011-06-00) has developed a life-cycle model (LCM) for salmon population dynamics to support the application of LCMs to salmonid management situations in the Columbia River basin. Three applications of the model have been developed as part of the AMIP Life-cycle Modeling Project, all focused on exploring the impacts of tributary restoration actions and providing an analytical framework for habitat action effectiveness monitoring. In this chapter, we present the generic model and two full implementations of the model (Middle Fork John Day steelhead and Entiat River Chinook), as well as initial parameterizations for a Lemhi River Chinook model.

The ISEMP Watershed Model is implemented in the R programming language, an open source software package, and is freely available by download from the ISEMP website (www.isemp.org). This model is an improvement and enhancement of the Visual Basic QCI (2006) model "Salmon ISEMP Watershed Model Development: Adding Stochasticity to the Life History Model Structure" and the stage-based Yuen and Sharma (2005) model, and implements the Beverton-Holt spawner-recruit salmon population dynamics model (Beverton and Holt 1957). Many inputs are user specified, including inputs describing one or more sites within a watershed, initial salmonid populations and survival estimates by life stage, measures of uncertainty in parameter estimates, and estimates of natural parameter spatial, temporal, and pure variability. Hatchery fish introductions into a watershed, and parameters describing the relative robustness and fecundity of hatchery fish and their descendants, can also be user specified. The model calculates fish populations by life stage for each subsequent year up to a user- specified number of years.

The model also includes the option of user-specified levels of stochasticity for input parameters. This stochasticity serves two functions: 1) estimation of uncertainty of model results stemming from uncertainty of input parameters; and 2) estimation of temporal, spatial, and pure variability in the results stemming from temporal, spatial, and pure variability in the input parameters. Stochasticity is structured so as to give rise to natural correlations among input parameters. These correlation structures enable a stochastic model much more reflective of natural processes than could be achieved by assuming independence across all parameters.

Also included in the model is the ability to include time-based trends or step function changes for all user-specified parameters. Such changes may reflect, for example, changes in watershed management that lead to gradual increases in forested lands within a watershed, or discrete changes, such as a change in dam management, leading to a step function shift in seasonal water flows.

Multiple sites may be modeled simultaneously, where "sites" refer to a user-defined spatial scale over which the user wishes to define the input parameters. A site may be a reach within a tributary, a tributary within a watershed, a watershed within a subbasin, etc. The advantages of concurrent modeling of multiple sites, as opposed to modeling one site at a time, are three-fold: first, the model accounts for lack of independence among sites within a watershed (e.g., a low water year for a single site is likely a low water year for all sites within a watershed); second, modeling multiple sites concurrently allows for inclusion of cross-site migration, where fish at various life stages have some user-specified non-zero probability of migrating to a different site within a watershed; and third, modeling multiple sites concurrently allows summarization of results at whatever spatial level chosen after the completion of the simulation (i.e., results may be summarized by site, stream, river, watershed, etc.).

The model has been primarily designed for stream-rearing Chinook and steelhead but is structured such that it is flexible enough to handle different species of salmonids (although they cannot be modeled simultaneously). The modeling environment does support sufficient life history variability to capture simultaneous and resident / anadromous forms, as would be necessary for a general *O. mykiss* population model.

In order to run the model, the user has to prepare a precisely defined set of input files, for which templates are provided:

- **Header File** (provided as "Watershed_Header_File.csv). This file provides a template for the user to enter high-level data inputs for the simulation.
- **Site Level Input File** (provided as "Example_Inputs.csv"). This file provides a template for detailed user inputs for required modeling parameters such as fish survival probabilities by life stage, land use and habitat information, and inputs for temporal trends; as well as input describing stochasticity of these parameters. Multiple copies, saved under separate filenames, of this file may be used when modeling step changes in input parameters. At least one site-level input file is required for each site included in the watershed model.
- **Initial Values File (**provided as "Example_InitialValues.csv"). These files are used to specify initial values for fish counts, by life stage. One file is required for each site modeled.
- **Cross Site Migration File** (provided as Cross_Site_Migration_T1.csv"). This file allows the user to specify the probability by life stage of a fish migrating from one site to another within a watershed. For example, while a spawner generally returns to the same site from which it smolted, the user may specify a probability that it returns to a different site to spawn.

A stage-by-stage description of the model and the input and output files are provided in the ISEMP Watershed Model Version 3.0. User's Guide. User guide and software downloads are available from: www.isemp.org/products/tools.

Middle Fork John Day Steelhead Life-cycle model Application: Evaluation of Riparian and Aquatic Habitat Restoration Actions

Study system and model population

The Middle Fork John Day River (MFJD) drains the highlands of north central Oregon and is a primary tributary to the John Day River (**Figure 1**). Its basin is moderate in size (*ca*. 2100 km^2; average base flow 7.2 $m^3 \cdot s^{-1}$) and spans habitats ranging from near-alpine at its crest (*ca*. 2200 m) to sagebrush steppe near its confluence with the North Fork John Day River (*ca*. 650 m) (O'Brien et al. 2017). The climate of the MFJD basin is semi-arid, characterized by cool, wet winters (i.e., highland snow, lowland rain) and dry, hot summers. The MFJD hydrograph is thus snowmelt-driven, and both low-flow and warm-temperature extremes are currently ubiquitous during the summer months (Torgersen et al. 1999). Contemporary thermal limitations, combined with other legacy effects of historic land-use practices, are the focus of an ongoing experimental restoration effort coordinated by the MFJD Intensively Monitored Watershed (IMW) working group (Bennett et al. 2016). Restoration efforts aim to improve the status of anadromous salmonids by reducing summer temperatures, reducing fine sediment loading, and increasing in-stream habitat availability and complexity. Unless noted otherwise, this assessment focuses exclusively on the anadromous fish-bearing extent upstream of the MFJD juvenile migrant trap.

We focused on MFJD steelhead, an independent population of the Middle Columbia River steelhead evolutionarily significant unit classified as 'threatened' under the U.S. Endangered Species Act (ESA; ICTRT 2003). These fish express a life history pattern typical of Columbia River summer-run steelhead. First, premature adults enter the Columbia River during summer, hold in mainstem rivers through the fall and winter, and spawn in tributaries in the following spring (Quinn et al. 2015). Thus, nearly a year elapses between the time adult steelhead exit the Pacific Ocean and when spawning occurs. Three distinct life stages (i.e., eggs, fry, age-0 parr) occur thereafter (spring – winter) but before the next year begins. After their first spring out of the gravel (i.e., as age-1 pre-smolts), a portion of individuals undergo smoltification and emigrate downstream to the ocean as age-1 smolts; remaining ocean-bound juveniles typically depart the following spring as age-2 smolts, but some emigrate as age-3 smolts. The emigrant age composition for smolts produced by a typical MFJD brood is *ca*. 10% age 1, 75% age 2, and 15% age 3 (Bare et al. 2015). Smolts reside briefly in the estuary before undergoing a 1 – 3 year residence in the ocean. Relative to other summer steelhead populations, the majority of MFJD steelhead return to freshwater after one year at sea (ocean age 1, OA1), with fewer ocean age-2 and ocean age-3 individuals (the typical ocean-age composition for a cohort is ca. 65% OA1, 35% OA2, and <1% OA3; McCann et al. 2014). In total, it takes a single cohort (i.e., brood year) eight calendar years to complete this life history, barring the possibility of repeat spawning, and involves discrete stages that span annual (age-1+ pre-smolt and adult stages) and sub-annual (eggs, fry, age-0 parr, smolts) periods.

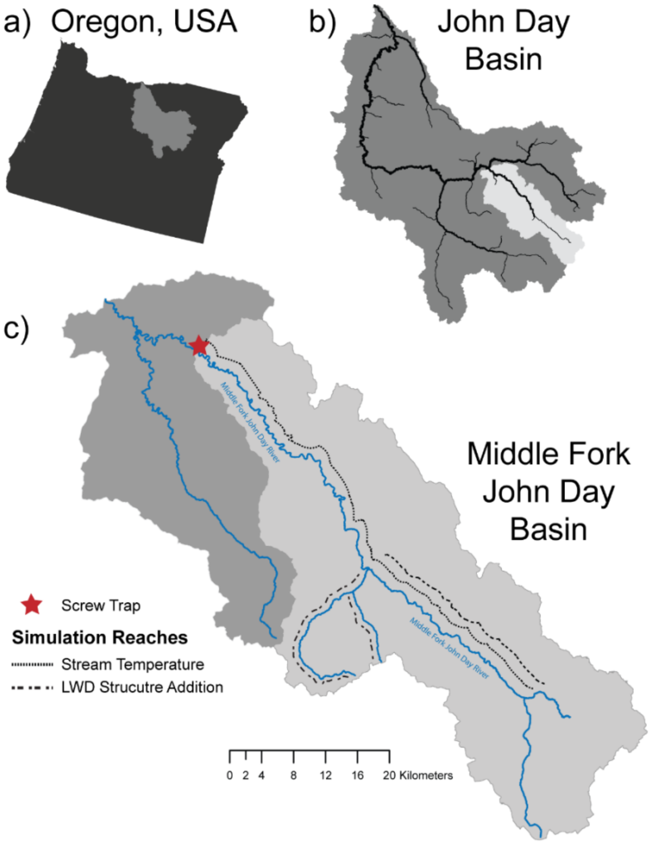

Figure 1. The location of the Middle Fork John Day River basin within (a) Oregon, (b) the John Day basin, and (c) the portion of the catchment upstream of the juvenile outmigrant rotary screw trap near Ritter, Oregon (light gray subbasin) covered by the life-cycle model, as well as the portion of the river network used in restoration scenarios (stream temperature [riparian restoration] = dash; large woody debris (lwd) structure additions = dot-dash).

In the MFJD, anadromous *O. mykiss* (steelhead) co-occur with non-anadromous *O. mykiss* (redband trout, resident rainbow trout, or resident O. mykiss, hereafter; e.g., McMillan et al. 2012). Although the factors governing life history expression remain uncertain, evidence to date suggests that both forms can give rise to one another (see Kendall et al. 2014 for a recent review) and, additionally, that females tend towards anadromy more than males (Ohms et al. 2014, Sloat et al. 2014). MFJD redband trout are not (and generally cannot be) enumerated separately from anadromous steelhead juveniles (but see Ohms et al. In Review, for potential methods); however, they are present, probably at modest levels, and contribute reproductively to the aggregate *O. mykiss* population (e.g., based on presence of mature age-1+ males [McMillan et al. 2012]).

Modeling Framework

The modeling framework we used is built on three components: (1) reach-scale hydraulic and habitat models that inform capacity input needs; (2) published demographic parameter estimates (i.e., stage-specific survival, fecundity, emigration/maturation probabilities) for steelhead and resident *O. mykiss*; and (3) the LCM for simulating population dynamics given these data.

The model was parameterized using stage-specific productivity (p_i) values estimated from published survival estimates (S_i) from John Day Basin (e.g., Bouwes et al. 2016) or other relevant monitoring studies (see Saunders et al. Chapter 2.d). The MFJD's capacity (c_{spawner}, c_{juvenile}) to support spawning and juvenile rearing (i.e., age-0 parr and age-1+ pre-smolts/resident *O. mykiss*) was estimated using mechanistic habitat models applied at the reach scale (i.e., survey sites) and upscaled to the population level (discussed below). Whereas parr/pre-smolt and spawner life stages were modeled according to density-dependent functions, other life stages (i.e., fry, smolts, ocean rearing stages) were assumed to behave in a density independent manner. In addition to the parameters c_i and p_i, this LCM requires insight on smolting probabilities (e_i) for freshwater juveniles, maturation probabilities (m_i) for adults at sea (and resident *O. mykiss*, described below), and fecundity (f_i) for relevant life stages.

Relative to its precursor (i.e., Sharma et al. 2005), this adaptation incorporates three important changes to accurately capture the MFJD's diversity of *O. mykiss* life histories. The first change enables pre-smolts to remain in natal tributaries as resident rainbow trout, whilst contributing reproductively to the mixed anadromous/resident population. Secondly, the model allows for this anadromy/residency 'decision' to be made on a gender-specific basis. Thirdly, mature *O. mykiss* can survive after spawning and make multiple reproductive contributions over a lifetime.

Reach-scale spawning and rearing capacity estimation

Steelhead population dynamics were estimated using reach-scale estimates of spawning and rearing capacity generated using mechanistic habitat models (**Figure 2**). Between 2011 – 2014, CHaMP collected the topographic, surface roughness, and discharge data necessary to construct digital elevation models (DEMs) and parameterize hydraulic models (Delft3D; Deltares 2010) at *n* = 54 river reaches (120 – 600 m in length) from across the MFJD basin sampled according to a probability-based, spatially balanced design (for a review of the survey design, see Nahorniak et al. 2015). Hydraulic modeling result were then used as inputs for two habitat models: (1) a net rate of energy intake (NREI) model (for a recent review of NREI models, see Rosenfeld et al. 2014), used to estimate juvenile capacity; and (2) a spawning habitat suitability index (HSI) model (see Ahmadi-Nedushan et al. 2006, for a review of HSI models), used to estimate spawner capacity (in egg equivalents, described below).

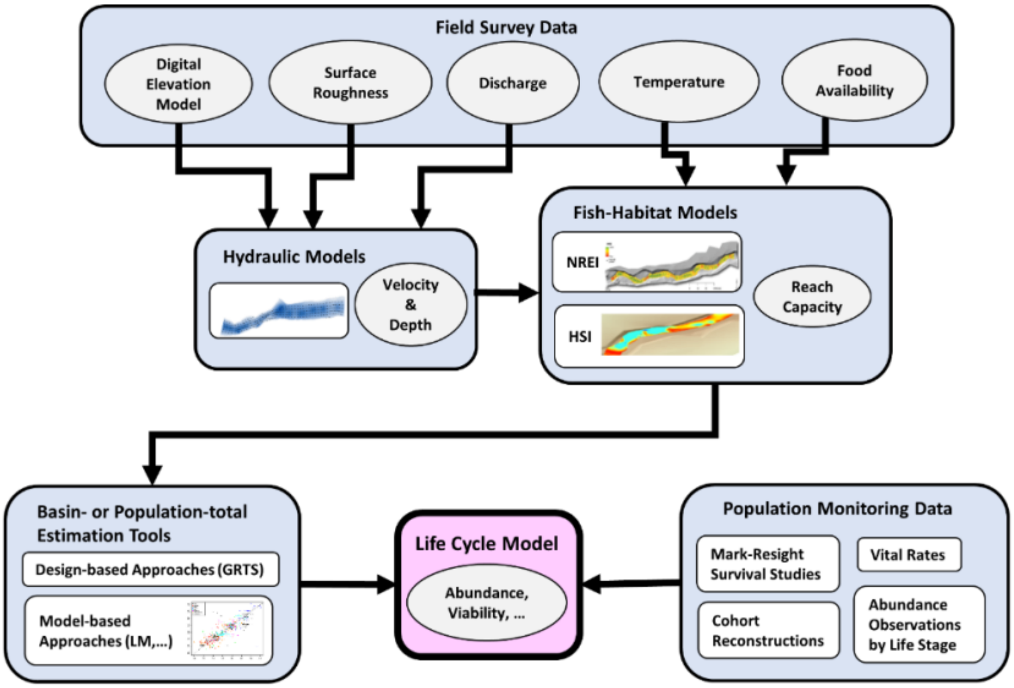

Figure 2. Relationships among components contributing to the Middle Fork John Day River steelhead LCM framework. Field data collected by Columbia Habitat Monitoring Program crews were used to parameterize hydraulic and fish-habitat models that informed key LCM inputs (i.e., juvenile rearing and adult spawning capacity). Other LCM inputs were acquired or estimated from basin- or species-specific population monitoring studies.

The NREI model consists of two sub-models, a foraging model and a bioenergetics model which, given information about ambient food availability (i.e., invertebrate drift), water temperature, hydraulic conditions (depth and velocity, output from hydraulic model), and an average fish size, provide spatially explicit predictions of the energy costs (swimming costs) and benefits (gross energy intake) associated with occupying different locations in survey reaches. These predictions are then translated into an estimate of juvenile rearing capacity using a fish placement algorithm and a minimum NREI threshold (0.0 $J \cdot s^{-1}$). Similar to NREI, the HSI model provides a spatially explicit depiction of the quality of spawning habitat within modeled reaches. Its primary inputs are depth and velocity (see above), as well as geo-referenced field observations of substrate size (i.e., gravel, cobble, etc.). These data, in conjunction with the steelhead spawning habitat suitability criteria used by Maret et al. (2005), were used to compute a spawning HSI score for every 10-cm raster cell within a survey reach. Scores were then combined into a composite HSI score, and translated into a reach-scale estimate of available spawning habitat, weighted by its suitability.

Upscaling from reach to basin capacity

Reach-scale estimates of juvenile rearing and adult spawner carrying capacity had to be scaled up from individual sampled reaches to all reaches in the drainage network. For the MFJD model, upscaling was based on relationships between reach-level capacity estimates and globally available (GIS) variables (i.e., model-based extrapolation, **Figure 2**), which allowed integration of environmental variables (e.g., temperature) likely to be shaped by habitat restoration. For both juvenile rearing and spawning capacity, upscaling proceeded in three steps that included: (1) assembling relevant GIS layers at *ca.*1-km (L_i) segments for the MFJD IMW presently used by steelhead (ODFW 2013); (2) fitting statistical models that relate capacity (y_i, normalized to fish per linear m) to GIS predictors ($x_1, x_2, \ldots, x_p$); and (3) using these models to predict capacity ($\widehat{y_i}$) at all locations within the occupied river network (i.e., $Total\ capacity = \sum \widehat{y_i} * L_i$).

Five candidate GIS variables were used to develop a juvenile capacity network extrapolation model: (1) average maximum July – August temperature (TEMP; McNyset et al. 2015); (2) aquatic gross primary production (Saunders et al. In Review); (3) bankfull width (BFW; Beechie and Imaki 2014); (4) valley bottom width (Gilbert et al. 2016); and (5) riparian condition (Macfarlane et al. 2016). Two of these variables (*TEMP* and *BFW*) proved to be significant predictors of reach-level capacity (**Figure 3**). The spawning capacity extrapolation model considered variables 3 – 5 above; *BFW* was the only significant predictor of reach-scale spawning capacity.

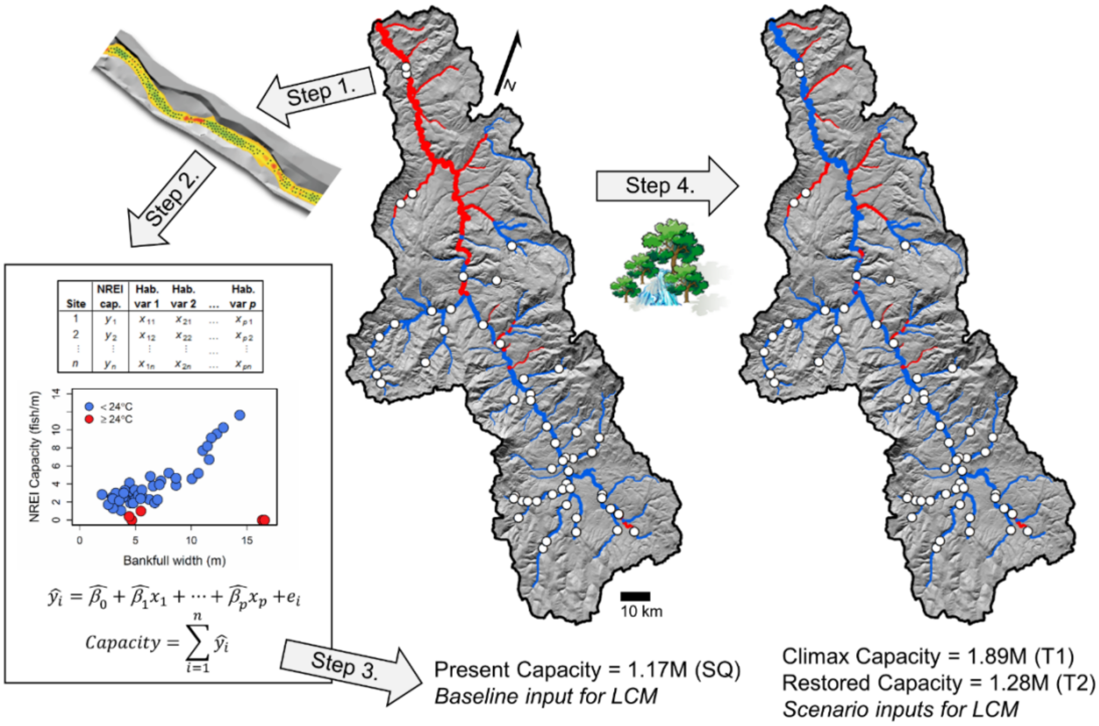

Figure 3. Conceptual illustration of the process followed to link site-scale estimates of juvenile rearing capacity to basin-scale total capacity for baseline simulations. During step 1, NREI-based estimates of juvenile capacity were estimated for Columbia Habitat Monitoring Program monitoring sites (white circles on basin maps). In step 2, relationships between site-level NREI predictions and globally available environmental predictors (GIS variables) were estimated; fitted relationships were then used to predict capacity at all locations within the river network and summed accordingly to estimate basin-total capacity (step 3). During step 4, basin-scale capacity was recomputed given the network-scaling relationship estimated in step 3 but using the stream temperatures predicted under different riparian restoration scenarios (see text for details).

LCM Simulations

Each LCM scenario was based on $n = 200$ Monte Carlo simulations spanning 60 years, of which the first 20 years were removed from the analysis as a model burn in period. Population performance for all scenarios was based on three metrics: (1) *Abundance*: as the geometric mean spawning escapement for the assessed time horizon; (2) *Productivity*: as the ratio of juvenile outmigrants (smolts) to parent (brood) year spawners. Smolts/spawner only offers meaningful insight on inter-scenario differences in resilience when populations are below carrying capacity (e.g., Moussalli and Hilborn 1986), so we computed/compared this statistic for low adult run size years only (i.e., total spawners <1,200, the ca. 25th percentile of spawner abundance based on preliminary runs). Productivity for the baseline scenario (current conditions) as spawners per spawner was also used to ground truth the model against sampling data; and (3) *Quasi-extinction Risk* (QER): which assumed quasi-extinction occurred whenever the steelhead spawning population fell below 226 in a given year (i.e., fewer than 1 spawner per 2 km within the modeled portion of the MFJD basin, after Chilcote (2001)) and computed QER as the proportion of all simulations in which this was the case.

Uncertainty in parameter estimates due to observation error and natural process variability were modeled as beta random variables. The LCM's capacity inputs were modeled as invariant given the lack of empirical data on inter-annual variability for these parameters.

For validation purposes, model-generated values and field monitoring estimates were compared for two key population parameters, abundance and productivity. For abundance, simulated values were compared to the Oregon Department of Fish and Wildlife's (ODFW) sampling estimates for the most recent eight-year record (2008 – 2015), subset to the IMW portion of the MFJD only (K. Bliesner, ODFW, unpublished data). For productivity, estimates of the number of steelhead spawners produced in subsequent years per parent-year spawner for each simulated spawning event were compared to ODFW's field sampling analog. Field spawner-to-spawner estimates were summarized for the 10 most recent complete broods (1999 – 2008; note the upper bound corresponds to all recruits through 2015).

Restoration scenario development and implementation

Model scenarios were developed to evaluate the effects of 'doing nothing' and two general classes of habitat restoration on the abundance, productivity, and viability of MFJD steelhead (**Table 1**). The first (SQ or 'status quo' hereafter) entailed simulating the population under the base model parameterization (see above). The second (T1) and third (T2), evaluated the effects of improved (i.e., reduced) mainstem MFJD summer temperatures resulting from riparian planting and shading on juvenile steelhead capacity and productivity. T1 or 'climax thermal restoration' hereafter ('natural thermal potential' scenario [ODEQ 2010]) provides a best-case riparian revegetation, channel adjustment, and in-stream flow acquisition effort, whereas T2 ('post-restoration' scenario [ODEQ 2010]) considers only the thermal benefits resulting from the maturation of riparian plantings on the ground in 2008. In the fourth scenario (W1), the population response to juvenile rearing capacity increases resulting from the targeted placement of in-stream wood structures in a major tributary sub-basin (Camp Creek and Lick Creek; 57 anadromous fish-accessible km) and along the upper MFJD mainstem (34 anadromous fish-accessible km). See **Figure 1** for details on the geographic extent of these scenarios.

To translate thermal restoration into a numerical change in capacity and productivity parameters for Scenarios T1 and T2, we re-ran the network extrapolation exercise described previously using temperature predictions from ODEQ (2010)[1]. Reduced estimates of maximum temperatures and the statistical model relating NREI-based juvenile capacity to GIS variables (described above, **Figure 3**) were used to compute revised basin-total capacity inputs for T1 and T2. We simulated a benefit to survival/productivity using a simple scalar approach (e.g., $p_{S2} = p_{S1}\,\lambda$, where $\lambda = S_{S2temp} / S_{S1temp}$) consistent with the shift expected from a published *O. mykiss* temperature-survival curve (i.e., S predicted from Bear et al. 2007). Finally, to gain insight on what portion of the T1 and T2 population response was due to improved capacity versus improved productivity, the two scenarios were run with enhanced capacity inputs only (indicated by the suffix 'a' in scenario names, i.e., T1a and T2a).

---

[1] ODEQ (2010) made spatially explicit predictions of mainstem MFJD temperatures using Heat Source (Boyd and Kasper 2003).

Table 1. Scenarios evaluated using the MFJD steelhead life-cycle model and the derivation of their associated inputs.

Scenario Category	Abbrev.	Name	Brief Description	Data/Scenario Sources
Base case	SQ	Status quo (also baseline, 'do nothing')	Assumes current habitat conditions persist into the future; simulations rely on base model parameters	N/A
Riparian (thermal) restoration	T1	Maximum thermal potential	Best-case scenario thermal state; capacity inputs generated assuming the summer temperature reduction of the 'NTP' scenario of ODEQ (2010); productivity scaled using survival-temp. curve of Bear et al. (2007)	ODEQ (2010); Bear et al. (2007)
	T1a	Maximum thermal potential, with capacity benefit only	Same as T1 but with a modeled capacity increase only	ODEQ (2010)
	T2	Current riparian vegetation restoration	Temperature improvements consistent with the shading benefits expected from current restoration projects once they mature (20 – 40 yrs into future); capacity inputs generated assuming the 'restored' scenario of ODEQ (2010); productivity scaled as in T1	ODEQ (2010); Bear et al. (2007)
	T2a	Current riparian vegetation restoration, with capacity benefit only	Same as T2 but with a modeled capacity increase only	ODEQ (2010)
Enhance habitat complexity	W1	Woody structure additions	Woody structures added to all anadromous fish-accessible stream within the upper MFJD mainstem and Camp/Lick Creek drainage; capacity increase estimated after Wall et al. (2016) and productivity scaled proportionally	Wall et al. (2016)
	W1a	Woody structure additions, with capacity benefit only	Same as W1 but with a modeled capacity increase only	Wall et al. (2016)

Scenario W1 assessed the benefits of increasing in-stream habitat complexity via woody structure addition using the approach of Wall et al. (2016). In brief, we modified the channel form (i.e., DEM) around simulated wood structures for mainstem (n = 8) and tributary (n = 9) reaches and reran the NREI model with the original parameters (temperature and drift) but representing woody structures as porous topography so that changes in NREI capacity resulting from this type of restoration can be approximated (**Figure 4,** see McHugh et al. 2017 for details). Scenario specifications (i.e., structure frequency, number·km^{-1}; depth of aggradation, degradation) were informed by restoration targets (e.g., wood frequency targets; Fox and Bolton 2007) and post-monitoring observations (Duffin 2015), as well as results from similar structure placement efforts (Wall et al. 2016). NREI capacity estimates were computed for modeled reaches and extrapolated to the target restoration area to compute a new population-level capacity input for running W1. In the absence of a mechanistic link between survival increases resulting from wood additions, we assumed that the improvement in survival (i.e., relative to the base input) was proportional to the population-level increase in capacity. The effect of including versus excluding a survival benefit for W1 was assessed in a capacity-only variant (i.e., W1a).

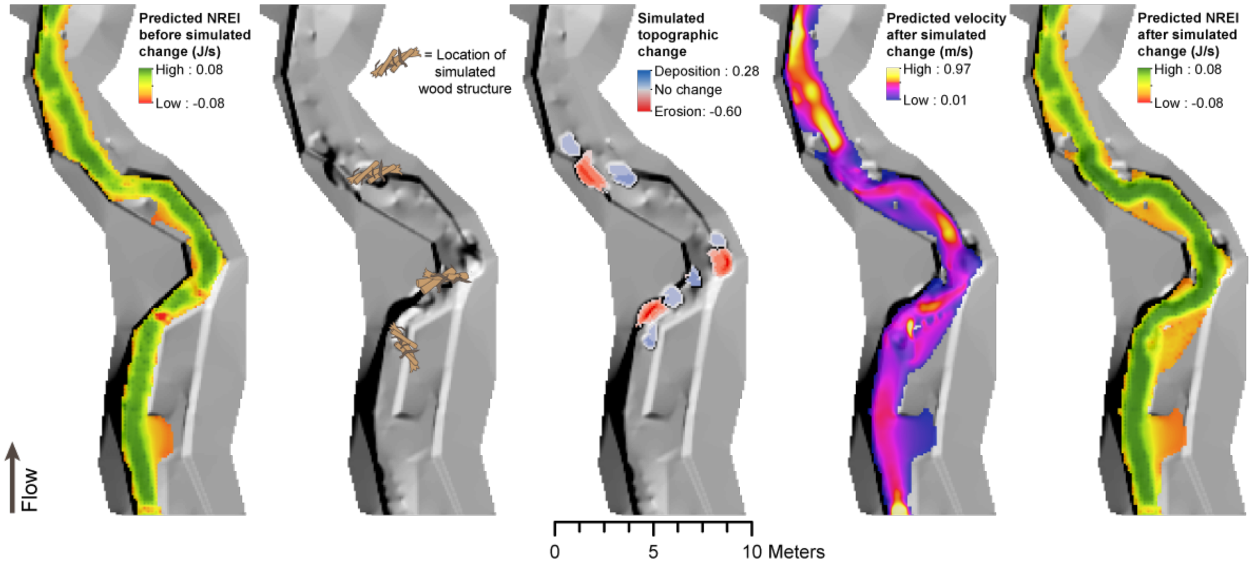

Figure 4. Example illustration of the modeling workflow used to represent woody structure additions. From left to right, the panels represent (a) the pre-restoration distribution of NREI values within the reach, (b) the location of simulated structures added to the site, (c) the post-restoration projection of topographic change resulting from structure-related deposition and erosion, (d) the change in hydraulics resulting from the combined structure addition and topographic change, and (e) the post-restoration distribution of NREI values. This combination of changes resulted in a 6% increase in rearing capacity for this reach. Results

Baseline Scenario Validation and Results

The base (SQ) LCM parameterization produced abundance dynamics consistent with recent observations for MFJD steelhead. Escapement from baseline simulations ranged from 489 to 5,482, whereas sampling estimates ranged from 811 to 5,859 (**Figure 5**). Total life cycle productivity (spawner-to-spawner) values computed from SQ simulation results (range: 0.02 to 14.30) spanned a range similar to sampling estimates for the 10 most recent completed broods (range: 0.10 to 15.21). In both cases, however, modeled distributions had a lower central tendency than field data, both for escapement (LCM grand mean of years/reps = 2,084; sampling mean = 3,199) and spawner-to-spawner estimates (LCM mean = 1.25; sampling mean = 4.14). Across simulations, several other characteristics of the virtual steelhead population mirrored those of the real MFJD population. For example, the spawning population was female skewed (57% female on average) and dominated by ocean-age 1 individuals (60% OA1, 38% OA2, 2% OA3). Simulations also retained a modest population of resident *O. mykiss* population segment that was overwhelmingly male (>90%), although these fish contributed little to annual abundance (<1% of reproductive output in a year, on average). Across the 40-year assessment horizon, steelhead escapements averaged *ca*. 1,800 to 1,900 spawners, freshwater productivity averaged 65 smolts per spawner, and the probability of falling below the quasi-extinction threshold was 12.5%, consistent with a 'vulnerable' (>10% QER in 100 years, although 40 years was assessed) classification under IUCN Red List Category E criteria (**Table 2**, **Figures 5 and 6**).

Table 2. Summary statistics for abundance (geometric mean escapement for the simulated time horizon), freshwater productivity (smolts per spawner), and quasi-extinction risk (QER) for modeled scenarios from *n* = 200 Monte Carlo trials of each scenario. SQ = base/status quo; T1 = maximum thermal potential; T1a = T1 without survival benefit; T2 = thermal benefits of current restoration; T2a = T2 without survival benefit; W1 = woody structure additions; W1a = W1 without survival benefit.

	Abundance			Productivity			
Scenario	Mean	Median	SD	Mean	Median	SD	QER
SQ	1,790	1,797	507	65	65	14	12.5%
T1	3,869	3,872	833	94	89	32	0.0%
T1a	2,953	2,903	803	74	72	23	1.5%
T2	2,080	2,111	570	68	69	17	6.5%
T2a	2,041	2,052	518	66	65	12	9.0%
W1	1,897	1,846	518	65	66	12	6.5%
W1a	1,940	1,939	507	66	65	12	6.5%

Riparian Restoration Scenarios

Scenarios T1, T1a, T2, and T2a explored the effects to restoration-related temperature reductions on population performance, mediated by increases in capacity (T1, T1a, T2, T2a) and productivity (T1, T2) (**Table 1**). Both scenarios caused temperatures to change for 89 km of the mainstem MFJD, resulting in temperature reductions of −4.0°C on average (range: +0.1 to −7.0°C) for T1/T1a and −1.0°C (range: +0.1 to −5.2°C) for T2/T2a. Averaged across modeled reaches and relative to SQ, these changes correspond to decreases from 25°C (SQ) to 21°C (T1/T1a) and 24 °C (T2/T2a), respectively. Relative to baseline (SQ) juvenile rearing capacity (1.17M), these temperature shifts equated to a 60% (1.87M) and 9% (1.28M) increase in capacity for scenarios T1/T1a and T2/T2a respectively (**Figure 3**). Further, productivity increased by 13% (λ = 1.13) and 2% (λ = 1.02) for the T1 and T2 scenarios in response to these temperature shifts.

Capacity and productivity increases associated with thermal restoration benefitted the abundance, productivity, and viability of MFJD steelhead (**Figures 5 and 6**). Under climax riparian conditions (T1, T1a), for example, abundances ranged 60% to more than 100% greater than baseline (SQ) conditions, with lower values when only modeling a capacity increase (i.e., T1a <T1). The thermal benefits of current projects at a mature state (T2, T2a) also yielded abundance benefits, with increases over the current status simulated by SQ ranging *ca.* 15% (**Table 2**). In every case, the population benefits of thermal restoration were sufficient to reduce QER below 10% (**Table 2**). Finally, overall freshwater productivity (i.e., smolts/spawner at low spawner abundance) increased by *ca.* 15 – 45% under climax riparian conditions.

Structural Addition Scenarios

We quantified the population-level benefits of large woody debris (LWD) additions, which were modeled to increase juvenile summer rearing capacity (W1, W1a) and productivity (W1 only). In total, restoration treatments were implemented at 17 survey sites (*n* = 9 in Camp/Lick Creeks; *n* = 8 in upper mainstem MFJD), ‘treating’ a total of 3.4 km of modeled stream, by placing on average *ca.* 15 and 30 structures per km (i.e., *ca.* 3 – 5 structures per survey site) at mainstem and tributary sites, respectively (**Figure 4**). Virtual wood additions resulted in a relatively modest increase in juvenile rearing capacity within treated reaches, averaging 2% overall and ranging from essentially no increase to a 15% increase. Upon extrapolating these results to the overall treatment area (i.e., mainstem and Camp/Lick), the new population-total capacity (W1, W1a) was estimated to be *ca*. 10,000 (+1%) juvenile steelhead greater than the base (SQ) value; given the assumption that the survival benefit of LWD addition was proportional to the capacity increase, the productivity parameter was also negligibly increased (i.e., by 1%) for the W1 scenario.

Despite the scope of manipulation, the effects of wood addition on the abundance and productivity of the MFJD steelhead population were minimal, relative to SQ, and given the small survival benefit that was modeled there was little to no difference between W1 (capacity and productivity benefits) and W1a (capacity benefits only) (**Table 2; Figures 5 and 6)**. At best, a spawner abundance increase on the order of 7% may be feasible (**Table 2**). However, the modest increase in spawner abundance associated with LWD addition did translate into reduced quasi-extinction risk, below the 'vulnerable' benchmark of 10%, for the model population.

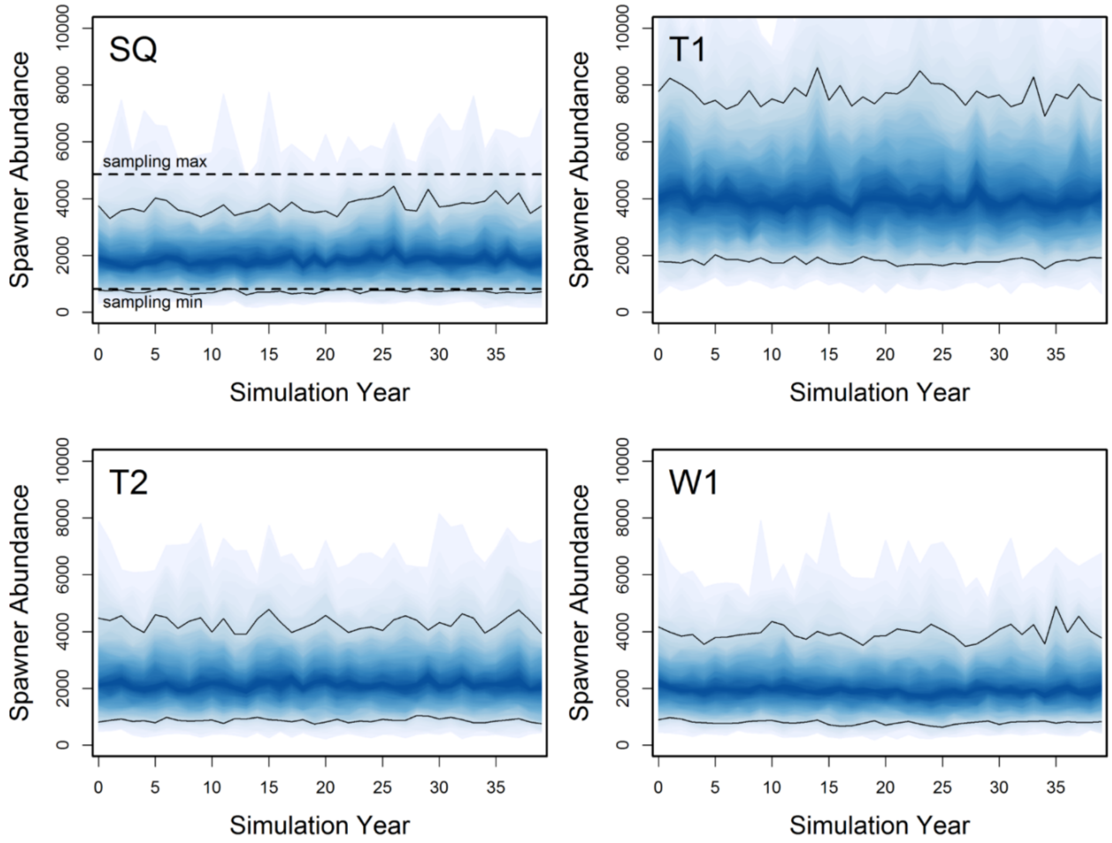

Figure 5. Time series of spawner abundance for scenarios: (SQ) Baseline current conditions scenario (status quo); (T1) Best-case thermal restoration scenario; (T2) Thermal restoration given that all on-the-ground (currently existing) riparian restoration projects reach maturity; and (W1) Structure (large woody debris) additions to mainstem

MFJD and Camp/Lick Creeks. Note, in panel SQ, the solid horizontal line and upper/lower dashed lines correspond to recent average abundance observations and min/max, respectively.

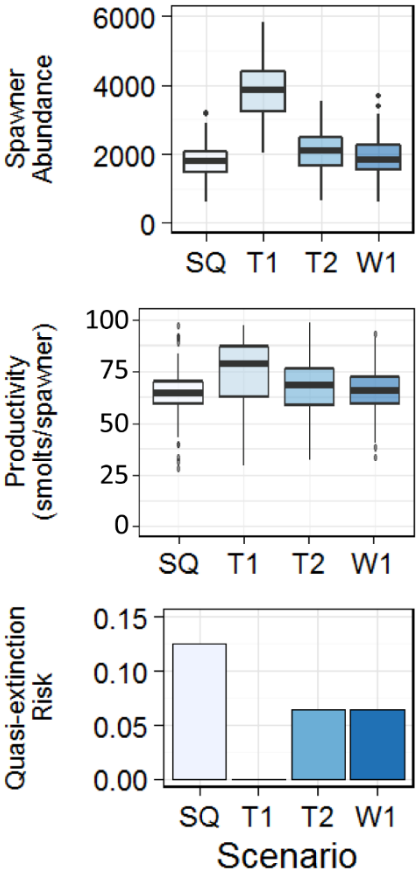

Figure 6. Population performance metrics (a) Abundance (geometric mean escapement), (b) Productivity (smolts per spawner) across scenarios, and (c) Quasi-extinction risk. See **Table 1** for scenario descriptions.

To support comparison of the MFJD modeling framework to LCM efforts within the CRB, we generated quasi-extinction response surfaces and viable salmonid population (VSP) scores consistent with methods established by the Interior Columbia Technical Recovery Team. Below, we summarize the probability that the modeled MFJD steelhead populations would fall below a quasi-extinction threshold QET of 100 spawners. The results reported here contrast with results provided in the main body of the chapter where QET = 1 spawner per km (i.e., 226) was used to calculate the MFJD quasi-extinction risk (QER) summary (see **Figure 6**).

In general, interpretation of response surfaces and VSP (**Figure 7**) yield inference about the MFJD steelhead population that are consistent with QER estimates for each restoration scenario. Specifically, under current conditions (i.e., SQ – base scenario), few model runs (ca. 4%)

exceeded the 0.1 isocline of extinction probability, and nearly all individual model runs exceeded a VSP score of 2.5. These results support the conclusion that the MFJD steelhead population has a relatively low extinction risk. Furthermore, extinction risk declined under each of the restoration scenarios that either reduced high stream temperatures (T1 and T2) or increased instream habitat complexity (W1, **Table 1, Figure 7**), with the greatest reduction in extinction risk occurring under the maximum vegetation restoration scenario (T1). However, these inferences are based on the assumption that the status quo and restoration scenarios modeled here represent truth, but in reality they fail to consider many other potential threats (e.g., non-native species, climate change, etc.). Therefore, our estimates of extinction risks should be considered conservative (see McHugh et al. 2017).

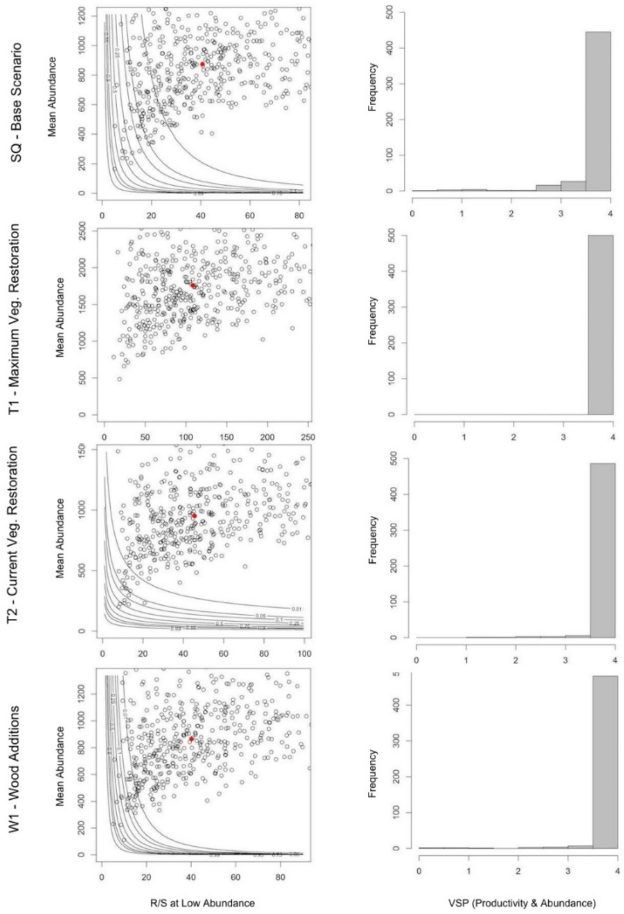

Figure 7. Response surface (left panels) with individual runs (points, n = 500) for the baseline (SQ), reduced summer water temperature (T1 and T2) and wood addition (W1) scenarios for MFJD steelhead. QET was set at 100 spawners. Right panels show translation of the response surface to a histogram of VSP scores for productivity and abundance (see McElhany et al. 2000).

Discussion

This analysis offers several insights relevant to the management of habitat for steelhead within the Middle Fork John Day River basin. Firstly, based on an independent analysis and using a different set of criteria (i.e., IUCN 2001), the status quo simulation results corroborate recent assessments (e.g., Ford 2011) concluding that the MFJD steelhead population continues to warrant conservation attention. For example, although simulated escapements often met recovery targets, quasi-extinction risk remained non-trivial (>10%), suggesting that continued restoration actions are indeed necessary. However, when evaluated at a lower quasi-extinction threshold, n = 100 spawners, used in other LCM applications in the CRB to facilitate comparison among other salmon and steelhead populations, steelhead in the MFJD likely serve as a stronghold in the region, demonstrating a relatively low risk of extinction. Secondly, among restoration measures considered, the population's response to reduced summer temperatures resulting from increased riparian shading were particularly strong in this system. Although the most favorable response was to T1 (climax riparian), an ambitious restoration target, this scenario combined with T2 (current projects, matured) defines the scope of riparian-related thermal benefits that could be realized in the future, albeit in the absence of climate change considerations. Lastly, large wood additions (W1) offered only marginal benefits to the modeled population, despite being simulated over an extensive area (approximately a third of the modeled domain). These results suggest that warm summer water temperatures are a primary limiting factor for steelhead in the MFJD, and that restoration of instream habitat via the addition of woody structures would likely need to occur at much higher densities that currently implemented to have meaningful impacts on steelhead populations. Importantly, these results were generated by a model grounded in empirical, basin-specific data and that was shown to yield dynamics that were qualitatively similar to those exhibited by the real MFJD steelhead population.

This work also represents a considerable advance over past attempts at quantifying the benefits of habitat restoration for threatened salmonid populations using LCMs. Reconciling fine- (i.e., habitat models) and coarse-scale (i.e., population dynamics models) modeling traditions, which was attempted here, is recognized as an emerging but overdue research focus (e.g., Matthiopoulos et al. 2015). This effort incorporates the benefits of specific restoration actions, tied to particular places within drainage networks and translated into a demographic response by upscaling the results from reach-scale mechanistic models, whereas past investigations have pursued habitat restoration questions largely as a sensitivity analysis exercise (i.e., how might a population respond to a hypothetical survival increase of x%, assumed to be achievable through restoration? e.g., Kareiva et al. 2000). Although the latter approach has proven useful, this framework offers a more powerful means for sorting through restoration possibilities. By combining modeling strengths from disciplines focused at disparate spatial scales (i.e., ecohydraulics [0.01 to 10+ m^2] and population dynamics [100 to 1000+ km^2]), it provides a means to quantify the benefits of habitat restoration in a more realistic manner than has been tried previously. Specifically, scenarios can be developed across a network in which each reach's capacity can be bounded by its current condition and recovery potential (Fryirs 2015, O'Brien et al. 2017). This approach is also sufficiently flexible to model scenarios of varying specificity, ranging from cases informed by actual restoration plans (e.g., a set of reaches with georeferenced design specifications) to the more generalized 'what if' scenario approach common to salmonid LCM work of the past. Notably, these advances stem as much from developments in the areas of habitat surveying and ecohydraulic modeling as from population modeling developments: namely, the adoption and broad implementation (i.e., 100s of sites per year) of a topographic survey approach by CHaMP, which in turn has given rise to scalable hydraulic and ecohydraulic modeling tools (e.g., HSI, NREI).

Entiat Chinook Life-cycle model: Evaluation of Instream Habitat Improvement Actions

Introduction

The Entiat River watershed is an intensively monitored watershed (IMW) designed to assess the effectiveness of current and future instream habitat improvement actions on ESA-listed spring Chinook and steelhead populations. As a result of the IMW there are data available on abundance, survival and growth that can be used in species-specific LCMs. We have developed an Entiat River Chinook LCM to predict population trends for juvenile abundance and adult returns over time, as a function of habitat capacity. This model helps us to identify potential life-cycle bottlenecks and the effectiveness of current and proposed habitat improvement actions on Chinook population dynamics. Here we describe how the major parameters have been derived or estimated for the Entiat Chinook LCM, and the results of initial model runs predicting the population's long-term response to habitat actions implemented to date.

Background

The Entiat River drains approximately 1,100 km^2 of the eastern slope of the central Cascade Mountains in Washington State, and is a tributary to the Columbia River (**Figure 8**). Wildfire, flooding, mass soil and debris movement, and land use have been the primary historic disturbance processes. Impacts have included floodplain and river channel modification projects and structures such as channel straightening/widening and diking, streamside vegetation disturbance, grazing, roads, agriculture, timber harvest, log driving, flash damming, irrigation and hydropower damming, residential development, and recreation. These land use actions have resulted in simplified channel conditions and created limiting factors for spring Chinook and steelhead populations.

The Entiat River subbasin has three ESA-listed fish populations: Upper Columbia River ESU spring Chinook (*Oncorhynchus tshawytscha*), Upper Columbia River DPS steelhead (*O. mykiss*), and Columbia River DPS bull trout (*Salvelinus confluentus*). The Upper Columbia Spring Chinook and Steelhead Recovery Plan (Recovery Plan; UCSRB 2007) has determined that these populations have a high risk of extinction (more than 25% in 100 years), low abundance and productivity, and are at risk for poor diversity and spatial structure. Efforts to restore salmon and steelhead habitat in the Upper Columbia Basin are guided by the Recovery Plan, which states that effectiveness monitoring coupled with adaptive management is required to assist in the identification of limiting factors, to assess the effects of habitat actions, and to recover the listed species in the Entiat River subbasin. The Recovery Plan recommends the use of instream structures (such as boulders and large wood) as immediate, short-term actions to increase habitat diversity in the Entiat River subbasin. The Entiat IMW was launched in 2011 to determine the effectiveness of these instream habitat improvement actions and, as secondary benefit to the effectiveness monitoring occurring under a rigorous Before-After-Control-Impact design, has provided a rich data source for parameterizing a LCM.

A tributary assessment (USBR 2009) divided the lower 26 miles of the Entiat mainstem into geomorphic reaches defined based on changes in the channel gradient and geologic features that control channel morphology, with 17 geomorphic reaches nested within three valley segments, plus the lower Mad River (**Figure 8**). The geomorphic reaches distinguish sections of river with unique physical characteristics and provide a context for customizing river restoration strategies based on specific characteristics of each reach.

- Valley Segment 1 (VS1) extends from the mouth of the Entiat to the Potato Creek moraine (river mile 0 to 16.1) and marks a change from a high-gradient mostly single-threaded channel with low sinuosity to a predominately low gradient high sinuosity meandering channel.
- Valley Segment 2 (VS2) extends from the Potato Creek moraine to the Dill Creek alluvial fan (river mile 16.1 to 21.1) and marks a change in slope from the low gradient of VS2 to a slightly higher gradient in VS3.
- Valley Segment 3 (VS3) extends from river mile 21.1 to river mile 26.0, at the boundary of USFS land and has greater influence from tributary alluvial fans.

These valley segments act as natural breaks for evaluation of spatially discrete restoration actions, and may provide information on the influence of geomorphic reach types on the ability of instream structures to provide benefits (i.e., slow meandering sections may respond differently to certain actions than more confined higher gradient reaches). Habitat and population monitoring have been implemented annually since 2011 using the CHaMP protocol, as well as a seasonal mark-recapture tagging study (summer and winter) that generates data on abundance, survival, growth and movement. A rotary screw smolt trap is also operated at the mouth of the Entiat River by the U.S. Fish and Wildlife Service from March through November annually.

The Entiat River supports two runs for Chinook – spring and summer. Genetic analysis conducted by USFWS recently has suggested traditional methods used to distinguish between spring and summer Chinook (size in the summer and timing and size at the RST at the mouth of the river) are reliable and for this reason we are calling this a Chinook model until such times as there is more information available to help us parse out the two runs.

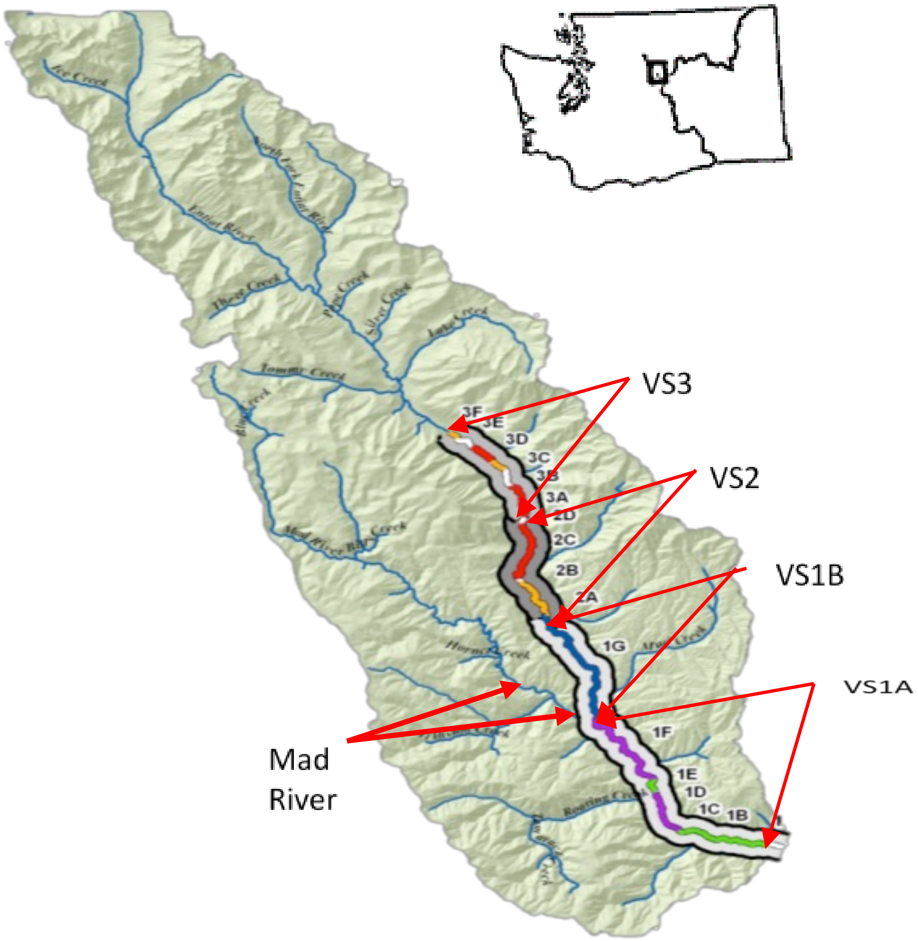

Figure 8. Location of the Entiat River subbasin in Washington State (insert map) and location and extent of the geomorphically distinct valley segments and the Mad River, the major tributary to the Entiat River, in the Entiat Intensively Monitored Watershed.

Methods

Entiat Chinook LCM Framework and Parameterization

Similar to the MFJD model, we built the Entiat Chinook LCM on three components: (1) reach-scale hydraulic and habitat models that inform capacity input needs; (2) published or empirical demographic parameter estimates (i.e., stage-specific survival, fecundity, emigration/maturation probabilities) for Chinook; and (3) the LCM for simulating population dynamics using these data. The data flow and relationships for the analysis outlined in **Figure 2** for the MFJD also apply to the Entiat LCM.

We have parameterized the ISEMP LCM for Entiat Chinook by:

1) Estimating watershed habitat capacity before and after habitat improvement actions by upscaling site-level habitat capacity derived through hydraulic and habitat models (e.g., Net Rate of Energy Intake [NREI] and Habitat Suitability Index [HSI]); and
2) Estimating population-level demographic parameters such as life stage-specific survival and abundance, fecundity, and movement probabilities, etc. based on empirical or published data.

Habitat Capacity

The Entiat River's capacity (c_{spawner}, c_{juvenile}) to support Chinook spawning and juvenile rearing was estimated using mechanistic habitat models applied at the reach scale (i.e., survey sites) and upscaled to the population level. We estimated habitat capacity at the site scale for Chinook spawning using HSI and for juvenile rearing using NREI. Both NREI and HSI models were parameterized using the hydraulic outputs of depth and velocity from a DELFT-3D model (Deltares 2010), macroinvertebrate drift data, stream temperature data, and fish size for all sites sampled. We estimated the spawning and rearing habitat capacity for all available sites using the average summer temperature (July – August) at base flow. We upscaled the site capacity estimates to the valley segment and watershed scale using site weights generated from a Generalized Random Tessellation Stratified (GRTS, Stevens and Olsen 2004) sampling design.

Survival Probability

The model was parameterized using stage-specific productivity (p_i) values estimated from survival estimates (S_i) of juvenile Chinook by life stage obtained using a combination of literature-derived values and empirical data. Egg-to-fry survival probability was estimated using a temperature model (Honea et al. 2009), whereas spawner to egg survival probability was taken from the literature (Gebhard 1961). Annual parr survival probability was estimated using a mark-recapture dataset collected as part of the effectiveness monitoring for the Entiat IMW for the years 2010 – 2015 by season and at various spatial scales when data permitted (i.e., valley segment, watershed [Entiat versus Mad River] and subbasin) using the Barker model (Barker 1997, White and Burnham 1999, Barker and White 2001; see survival estimation chapter for detailed description). For these initial model runs we are reporting estimates at the watershed scale.

Residence Period, Fecundity and Proportion of Females

We determined the residence period for Entiat Chinook based on empirical data as the time between tagging and the last detection at an instream PIT-tag detection array, the rotary screw trap, or during a mark-recapture event. Fecundity was estimated using average annual wild female fork length taken from spawner carcasses by year, from which we estimated the number of eggs laid by multiplying fecundity by the proportion of females in the returning adults, also based on literature values (Roni et al. 2014) combined with spawner escapement estimates from redd surveys.

Ocean Adult Survival and Maturation Probability

The LCM requires age-specific estimates of survival and maturation to accurately simulate the cohort/age structure of the mature run of Chinook returning to the Columbia River Basin during each time period. In general, aggregate survival estimates integrating these two processes across ages are available (e.g., the Comparative Survival Study's [CSS] smolt-to-adult return rates [SARs], McCann et al. 2014). However, the lack of information on the abundance or maturation status of tag groups during ocean life stages means that information is only available for marked fish when they are released (or last detected) as juveniles (N_{smolt}) and upon return (N_{OA1}, N_{OA2}, N_{OA3}), after survival and maturation processes have occurred (see, McHugh et al. 2017). Thus, in a statistical sense these quantities are not uniquely identifiable and therefore the observed age-at-return-at-age data can be reasonably described by multiple combinations of $S_{\mathrm{OA}a}$ and m_{a} values. To overcome this limitation, we used a Bayesian estimation approach following McHugh et al. (2017) to identify the set of $S_{\mathrm{OA}a}$ and m_a estimates that best describe published estimates of SARs (2008 – 2011 migration year; McCann et al. 2014) (**Table 3**).

Table 3. Rocky Reach Dam to Bonneville Dam SAR estimates for Entiat/Methow wild Chinook (data taken from McCann et al. 2014).

Year	N Smolts	N OA1	N OA2	N OA3	SAR (%)	Age comp (% BON by age) p OA1	p OA2	p OA3
2008	9309	16	96	47	1.71	10	60	30
2009	3253	3	31	5	1.20	8	79	13
2010	5292	4	42	18	1.21	6	66	28
2011	1361	2	3	1	0.44	33	50	17
				Mean	1.14	14	64	22

Hatchery and Harvest Effects

For the purposes of this simulation of the Entiat Chinook LCM we have assumed that effect of hatchery and harvest are minimal on wild Chinook population dynamics and have not accounted for their potential effects in the LCM. However, it should be noted that the Entiat National Fish Hatchery has been operating on the Entiat River since 1940, during which time it has raised and released a variety of species, and is currently producing summer Chinook. Strays are detected entering the Entiat River watershed and downriver harvest could also have potential deleterious effects on wild Entiat Chinook populations.

Entiat Chinook LCM Simulations

Each LCM scenario was based on *n* = 300 Monte Carlo simulations spanning 150 years, of which the first 50 years were removed from the analysis as a model burn in period. Other user-specified parameters are provided in **Table 4**.

As described by Zabel et al. (Chapter 1), we also calculated the VSP (abundance and productivity) score as measure of risk (probability of extinction) using a probability of quasi-extinction threshold P(QET) following McElhany et al. (2000). A score of 0 indicates a population is either extinct or at a very high risk of extinction, 4 indicates a population has very low risk of extinction in 100 years, and 1, 2, and 3 indicate relatively high risk, moderate risk and low risk of extinctions in 100 years, respectively (see Zabel et al., Chapter 1, this report).

For validation purposes, model-generated values and field monitoring estimates were compared for spring Chinook spawning ground surveys. We developed model scenarios to evaluate the effects of no habitat improvement actions (baseline), a subset of actions that have been implemented, and the effect of those actions plus a 2% increase in Chinook survival on the abundance, productivity, and viability of Entiat River Chinook.

Scenario 1:Baseline

We simulated baseline conditions in the Entiat River using CHaMP habitat data collected at untreated sites upscaled to the watershed scale and Chinook population inputs based on empirical and literature-derived data (**Table 4**).

Scenario 2: Habitat Improvement Actions

As mentioned earlier, instream habitat has been monitored under the Entiat IMW using the CHaMP protocol since 2011. Habitat improvement actions targeting instream complexity (addition of large wood and boulders) and side channel creation/enhancement were implemented along the Entiat River mainstem in 2012 and 2014. To estimate the change in habitat carrying capacity at base flow accruing from a subset of the 2012 actions, we used the same approach as in the MFJD (we modified the channel form [i.e., DEM] around simulated wood structures and boulders for mainstem (n = 4) reaches and reran the NREI model with the original parameters [temperature and drift] but representing woody structures as porous topography and boulders as changes in the streambed so that changes in NREI capacity resulting from this type of restoration can be approximated; **Figure 4,** see McHugh et al. 2017 for details. To estimate habitat capacity at the watershed scale after the restoration actions were implemented, we used the habitat capacity estimates generated using the modified DEMs with carrying capacity estimates generated from unaltered DEMS at non-restored sites, and extrapolated the site-level capacity estimates at base flow for all available sites across the watershed using the GRTS-based site weights. We measured the rate of change of habitat capacity before and after restorations at both scales (site and watershed).

Scenario 3: Habitat Improvement Actions plus Increase in Survival

We have also hypothesized that habitat restoration actions are not only able to increase habitat capacity, but may also improve juvenile Chinook survival probabilities. Indeed, analysis of the empirical survival data has shown higher juvenile Chinook over-winter survival in valley segments 2 and 3, which have better habitat (lower gradient, multi-thread channel, more pools and wood, and greater access to the floodplain and off-channel habitat) compared to valley segment 1. In the absence of a mechanistic link between survival increases resulting from habitat improvement actions, we tested the effects of improving survival probabilities on the Chinook population by increasing the survival probability of juvenile Chinook by a conservative estimate of 2%, in addition to the changes in carrying capacity estimated in Scenario 2.

Table 4. User-specified parameters by life stage used in the Entiat River Chinook LCM.

Components	Life stage	Value	References
Survival probability	Spawner-Egg	0.423	Gebhards 1961
	Egg-Fry	0.492	Computed using temperature model (Honea et al., 2009 & McHugh et al., 2004)
	Fry to Parr	0.419	Computed using temperature model (Honea et al., 2009 & McHugh et al., 2004)
	Subyearling/Yearlings	0.408	Computed using capture-recaptures Model (Barker)
	Adult Age 0	0.088	Computed using Bayesian Approach (McHugh et al., 2017)
	Adult Age 1	0.484	
	Adult Age 2	0.530	
Harvest	Mean Harvest	0	
	Hatchery Fish Annual introductions	0	
Fecundity	Age1	2530	Computed using average annual wild female fork length taken from spawned carcasses by year
	Age2	3926	
	Age 3	5067	
Ocean Capacity	Ocean Age 1	Infinity	
	Ocean Age2	Infinity	
	Ocean Age 3	Infinity	
Habitat capacity/m	Egg	309.03	Estimated using HSI
	Fry	152.14	
	Parr	30.75	Estimated using NREI (Wall et al., 2015)
	Yearling/subyearlings	12.66	
Age specific maturation probabilities	Prob. maturing at Ocean Age 1 (OA1)	4.22%	Computed using Bayesian Approach (McHugh et al., 2017)
	Prob. maturing at Ocean Age 2 (OA2)	52.33%	
	Prob. maturing at Ocean Age 3 (OA3)	100.00%	

Results

Scenario 1: Baseline Conditions

Long-term annual spring Chinook redd data (Hamstreet 2012; Fraser and Hamstreet 2015) shows that on average 257 spring Chinook have spawned in the Entiat River over the last 21 years (1994 – 2014; **Figure 9**), well below the target of 500 spawners established by the Recovery Plan (UCSRB 2007).

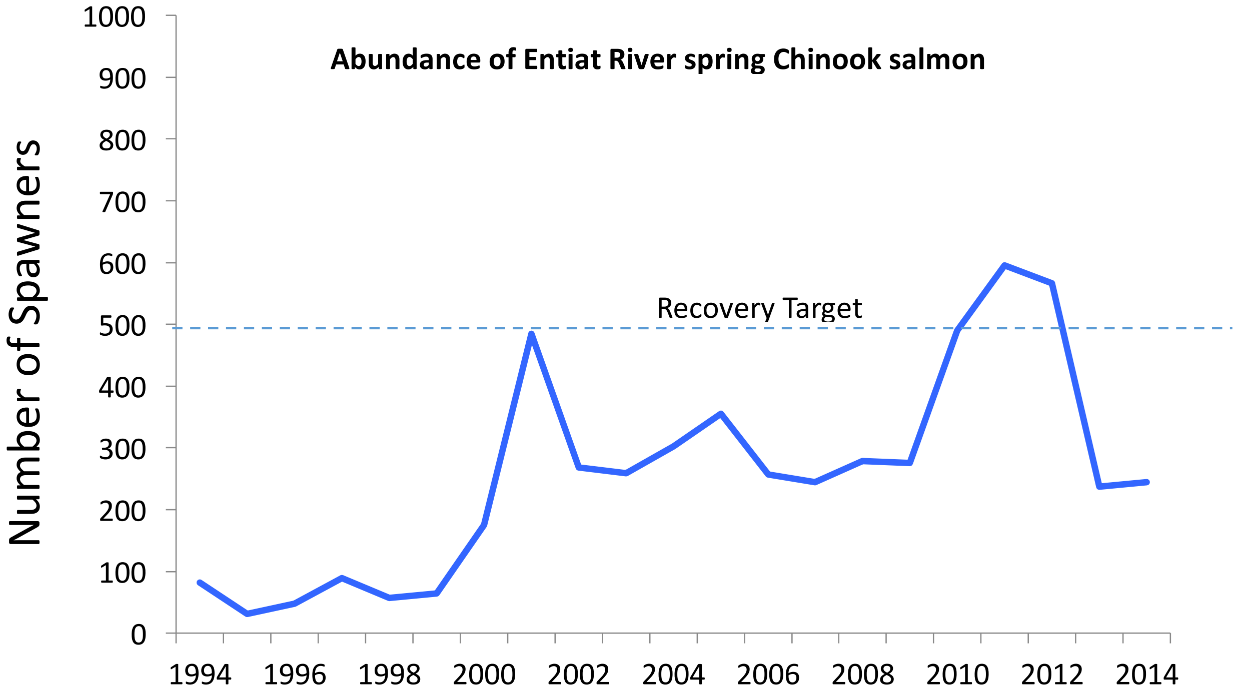

Figure 9. Time series of observed Entiat River spring Chinook salmon spawner abundance (data from Hamstreet [2012] and Fraser and Hamstreet [2015]; number of spawners was estimated using a 2.4 fish per redd ratio from Hamstreet [2012]).

The baseline simulation produced spawner abundance estimates slightly lower than the observed spring Chinook spawning ground surveys, with the LCM estimating an average of 231 spawners in the Entiat River, but both are below the target 500 spawners needed to reach recovery goals (**Figure 10**). The population experienced quasi-extinction and the VSP score for productivity and abundance for the baseline scenario ranged from 0 – 4 (**Figure 11, Panel A**) but skews heavily towards 0, indicating high probability of extinction in 100 years under the baseline scenario.

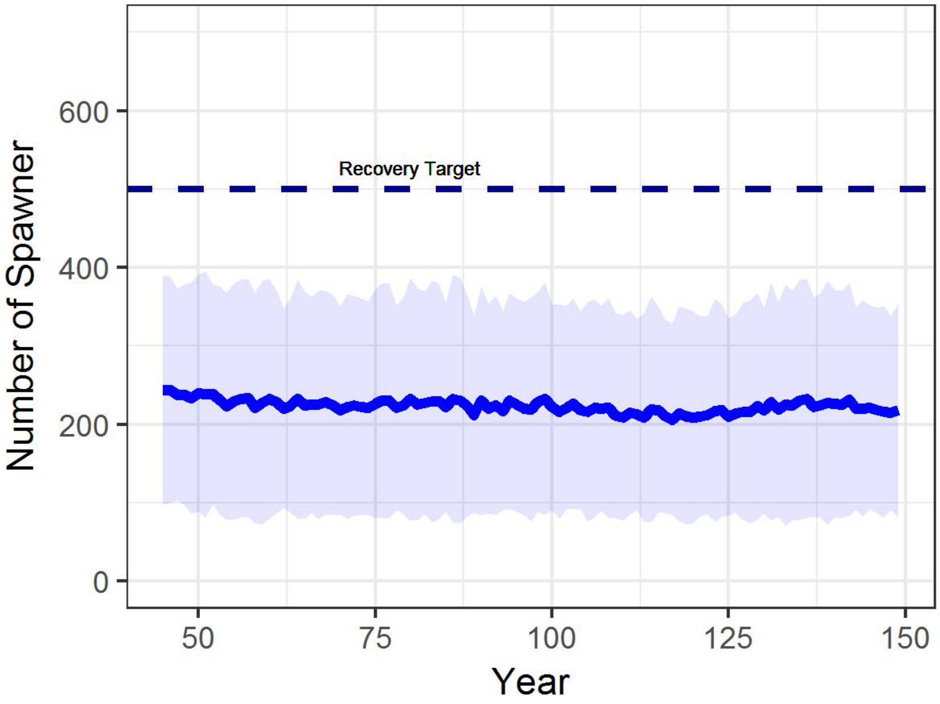

Figure 10. Time series of Chinook spawner abundance in the Entiat watershed under baseline conditions.

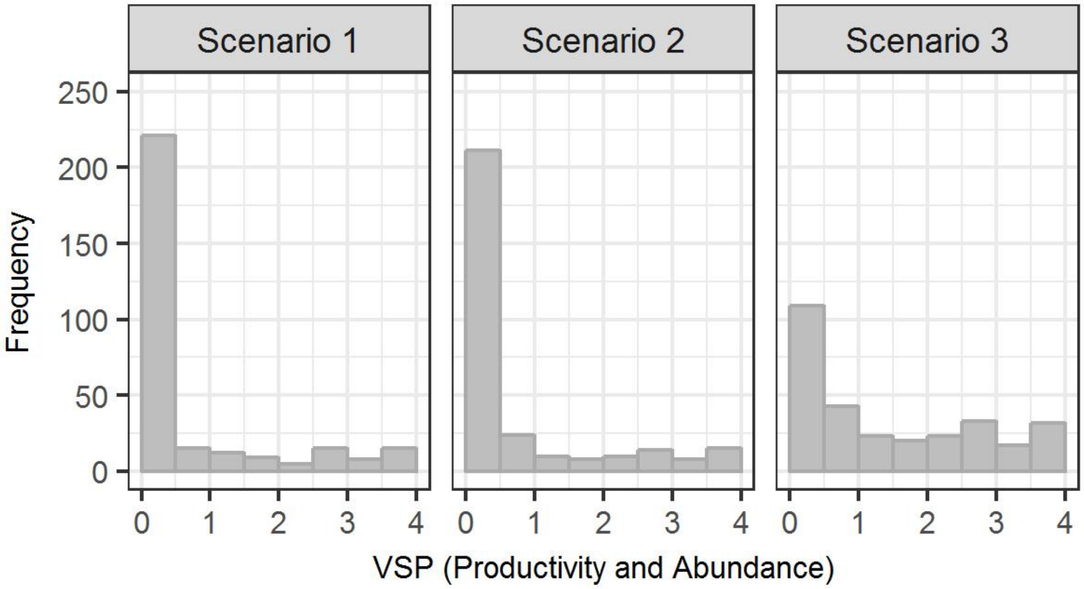

Figure 11. Histogram of VSP scores for productivity and abundance for three scenarios: (A) Scenario 1 Baseline conditions; (B) Scenario 2: effect of increased juvenile rearing capacity only; and (C) Scenario 3: effect of increased juvenile rearing capacity plus increased juvenile survival probability by 2%.

Scenario 2: Habitat Improvement Actions

The limited amount of habitat improvement actions available for this simulation resulted in a relatively modest increase in juvenile rearing capacity within treated reaches, averaging 7% overall across the sites and ranging from 0% to a 35% increase. Extrapolating these results to the watershed scale resulted in an increase in the watershed carrying capacity of less than 1%. Parameterizing carrying capacity in the LCM based on these estimates resulted in a small increase in the number of Chinook spawners predicted to return to the Entiat River (middle panel, **Figure 12**) but the probability of extinction was still skewed toward 0 (middle panel, **Figure 11**), indicating a high probability of extinction in 100 years.

Scenario 3: Habitat Improvement Actions with an Increase in Survival

Scenario 3, improved carrying capacity plus a 2% increase in survival, resulted in an even greater increase in the number of spawners (right panel, **Figure 12**), although neither scenario 2 nor 3 resulted in spawner numbers meeting or exceeding the recovery target. Among the three scenarios, the probability of extinction was lowest under scenario 3 where the frequency of the VSP score was distributed among the classes and relatively more group 4 scores compared with scenarios 1 and 2 (right panel, **Figure 11**).

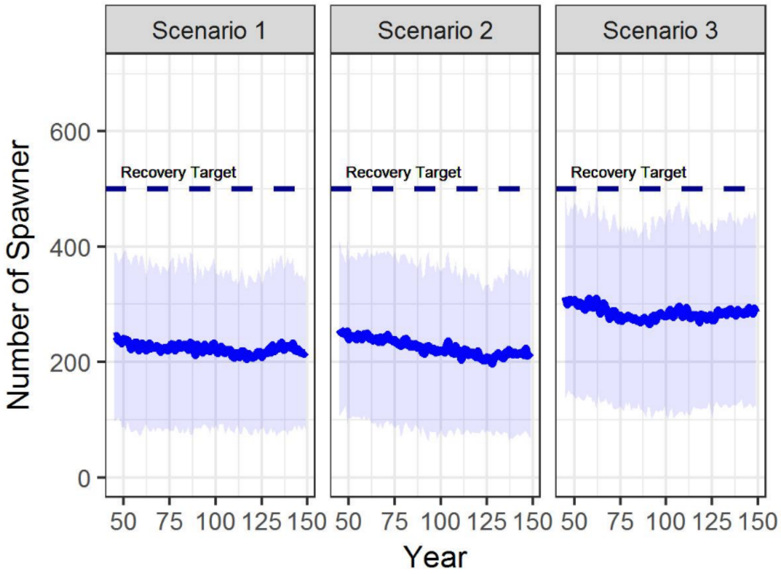

Figure 12. The number of Chinook spawners predicted by the Entiat Chinook LCM for Scenario 1: baseline conditions; Scenario 2: effect of increased juvenile rearing capacity only; and Scenario 3: effect of increased juvenile rearing capacity plus increased juvenile survival probability by 2%.

Discussion and Next Steps

Baseline simulations of the Entiat Chinook LCM model at the watershed scale produced biologically feasible spawner predictions against which various habitat improvement/increases in survival scenarios could be compared. Similar to the MFJD and Lemhi River, these results were generated by a model grounded in empirical, basin-specific data which yielded spawning dynamics qualitatively similar to observed spring Chinook spawning population.

Although the response for either the increased habitat capacity or increased habitat capacity with improved survival was not large, these simulations were based on modeling a subset of the habitat improvement actions that have gone in to date. Ongoing work includes modifying more DEMs for the remainder of the implemented habitat improvement actions to more accurately reflect the full impact of the actions to date. We also plan to run the hydraulic model at sites before and after restoration at various flows (e.g., low, medium and high) to gauge the effectiveness of habitat improvement actions at different flows based on preliminary analysis that shows an increase in the effectiveness of habitat improvement actions at low to medium flows but which is “washed out” at high flows. We will continue to explore the level of change needed in habitat capacity and survival in order for Entiat Chinook to reach the target recovery goal thereby providing project sponsors with targets for the level of restoration needed. We are also concurrently developing a similar LCM for Entiat River steelhead.

Lemhi Chinook Adult-to-Smolt Parameter Estimation and Restoration Scenario Analysis

Introduction

Spring/summer Chinook salmon in the Lemhi River basin have declined significantly from their historical abundance. Loss of access to important spawning and rearing habitats in tributaries to the Lemhi is believed to be one of the major obstacles to recovery. Although the basin is primarily (81%) federal and state land, private ownership constitutes the majority of the mainstem and lower portions of tributaries. This has led to channelization of portions of the lower river and disconnection of most tributaries, with the exception of Hayden Creek (**Figure 13**), due to irrigation water withdrawals. At the inception of ISEMP, 29 of 31 major tributaries were continuously or seasonally disconnected from the mainstem Lemhi River. Suggested restoration actions therefore include enhancing spawning and rearing habitat in the mainstem and reconnecting tributaries (Trapani et al. 1994).

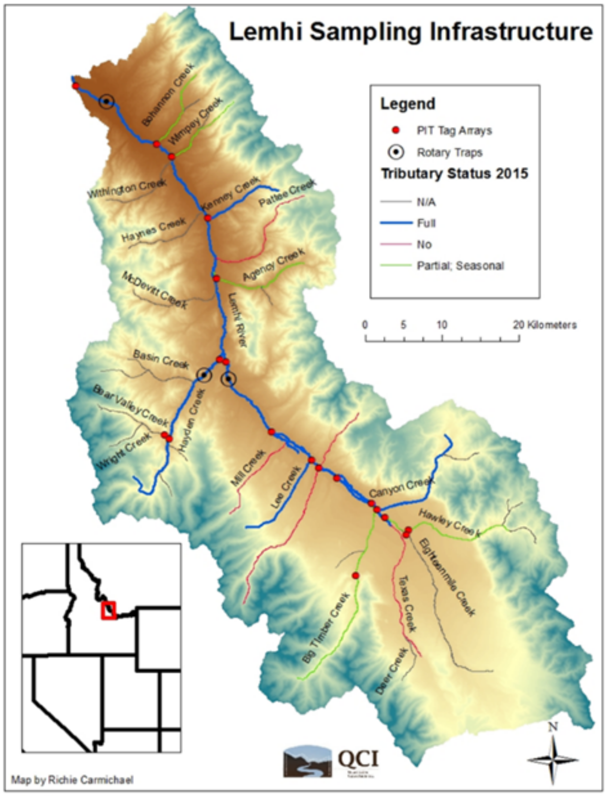

Figure 13. The Lemhi River basin with major tributaries and fish sampling infrastructure.

The monitoring strategy for Lemhi spring/summer Chinook is designed to assess the effectiveness of habitat restoration actions intended to increase freshwater productivity (i.e., smolts per spawner). In particular, evaluations at the population scale are focused on determining whether restoration actions will be sufficient to achieve the 7% improvement in freshwater productivity identified in the NOAA (2008) Biological Opinion process.

Here we describe a simple model of the freshwater portion of the life cycle for spring/summer Chinook salmon and parameterize the model using data from the Lemhi River basin. This is a minimal, empirical model, including only life stages whose abundance or survival can be directly observed. Thus we consider spawners, parr (juveniles rearing in their natal basin during the first summer of life), and smolts (operationally defined as juvenile emigrants passing Lower Granite Dam [LGR]). The spatial scale is the entire Lemhi basin; we do not distinguish among subbasins or reaches, and thus there is no dispersal or movement beyond the directed migration implicit in the parr-to-smolt transition. By using habitat-based information to constrain key stage-specific parameters, we show how the model can be used to simulate the effects of past or future tributary reconnection projects.

Methods

Study System and Sampling Design

The mainstem Lemhi is divided into upper and lower reaches by the confluence of Hayden Creek (**Figure 13**). The lower mainstem is highly channelized, does not currently support spring/summer Chinook salmon spawning, and provides limited opportunities for juvenile rearing. Approximately two-thirds of total spawning occurs in the upper mainstem, which also provides substantial juvenile rearing habitat. Hayden Creek has retained a permanent connection with the mainstem and supports approximately one-third of spring/summer Chinook salmon spawning.

Rotary screw traps (RSTs) are deployed at the mouth of Hayden creek, in the upper mainstem just upstream of the confluence with Hayden Creek, and in the lower mainstem ~5 km above the confluence with the Salmon River (**Figure 13**). In-stream PIT tag Detection System (IPTDS) arrays are located near each RST. Remote-site juvenile enumeration and tagging surveys have been used to estimate the abundance and distribution of juvenile salmonids beginning in 2009.

Surveys are distributed throughout the area of the watershed occupied by anadromous salmonids using a GRTS design (Stevens and Olsen 2004). Additionally, a continuous sampling design was initiated in 2013 to resolve issues arising from fish movement into and out of sample reaches between mark and recapture events. Spatially explicit locations were recorded for every tagged, recaptured or resighted fish using mobile PIT tag equipment.

Model Structure and Data

Transitions between successive stages are described by the Beverton-Holt model:

$$N_{a+1,t} = \frac{p_{a,a+1} N_{a,t}}{1 + \frac{p_{a,a+1}}{c_{a,a+1}} N_{a,t}} \qquad (1)$$

where $N_{a,t}$ is the abundance of stage a in brood year t, $p_{a,a+1}$ is the intrinsic productivity, and $c_{a,a+1}$ is the asymptotic maximum production of stage $a + 1$ (henceforth called "capacity" but not to be confused with carrying capacity, which is a stable equilibrium point of a full life-cycle model such that $N_{a,t+1} = N_{a,t}$).

To estimate the parameters in the spawner-to-parr and parr-to-smolt Beverton-Holt functions, we require observations of the state variables ($N_{a,t}$ and $N_{a+1,t}$), the realized transition probabilities (e.g., survival $s_{a,a+1,t} = N_{a+1,t}/N_{a,t}$), or both, along with associated estimates of uncertainty. We first describe these data before considering the statistical approach used to match the model to the data.

Total adult escapement estimates for 2010 – 2015 were based on a branching model of adult PIT-tag detections, coupled to a model of adult passage at LGR. The model is implemented in a Bayesian framework, and the posterior distribution of total Lemhi escapement is summarized here by its mean and standard deviation. For years prior to 2010, escapement estimates were taken from the Salmon Population Summary database[2] compiled by the Interior Columbia Technical Recovery Team, and standard errors were based on an assumed 30% observation error CV.

---

[2] https://www.webapps.nwfsc.noaa.gov/apex/f?p=261:1:

Summer parr abundance in the mainstem Lemhi and Hayden Creek in 2009 – 2012 was estimated using multi-pass electrofishing surveys done in CHaMP reaches, and the estimates were scaled up using GRTS design weights (Stevens and Olsen 2004). Estimates for subsequent brood years were produced using the Stratified Population Analysis System (SPAS) software[3] based on continuous mark-recapture sampling. Total parr abundance is the sum of Hayden and the mainstem Lemhi, and the variance of the sum is calculated assuming independent observation errors.

Smolts from the Lemhi basin are not directly enumerated, but we can estimate the survival of parr tagged during the summer prior to outmigration until they pass LGR the following spring. We assume all juveniles that survive to the smolt stage migrate past LGR as yearlings. These overall parr-to-LGR survival estimates and associated standard errors are produced using TribPIT software (Buchanan et al. 2015), which models a cohort of juveniles assumed to follow the same migration route, albeit perhaps at different times. In our case, the cohorts consist of parr tagged in Hayden Creek and in the Upper Lemhi River, respectively. The overall survival is based on pooling cohorts from these two locations.

Finally, we used independent estimates of parr capacity as an informative prior to help constrain the model fits. These estimates are derived from quantile random forest (QRF) models that predict parr abundance as a function of habitat variables (see Chapter 2 in this document). For the baseline scenario, prior to tributary reconnection, we include only the Upper and Lower mainstem and Hayden Creek, so the prior median of total parr capacity is the sum of these three values (**Table 5**).

---

[3] http://www.cs.umanitoba.ca/~popan/

Table 5. Parr capacity estimates derived from habitat-based quantile random forest (QRF) models, in various tributaries or mainstem reaches of the Lemhi River basin. Tributaries that were reconnected to the mainstem in recent restoration efforts are indicated.

Stream	Reconnected	Length (km)	Parr capacity (thousands)
Lower Lemhi	no	52	131
Upper Lemhi	no	40	80
Hayden	no	24	43
Big Timber	yes	31	48
Bohannon	yes	15	25
Canyon	yes	21	30
Kenney	yes	8	18
Little Springs	yes	7	11

Parameter Estimation

We now consider the stochastic elements that will allow us to confront the model with data. The state variables are the numbers of spawners (S_t), parr (J_t), and smolts (M_t) in brood year t. We specify priors on S_t and on the stage-specific intrinsic productivity and capacity parameters described previously:

$$\begin{aligned} S_t &\sim N\left(\hat{S}_t, \hat{\sigma}^2_{S_t}\right) T\left(0, \infty\right) \\ p_{SJ} &\sim \text{Unif}\left(0, 10^6\right) \\ \log\left(c_{SJ}\right) &\sim N\left(\log\left(\hat{c}_{\text{QRF}}\right), 0.1^2\right) \\ p_{JM} &\sim \text{Unif}\left(0, 1\right) \\ c_{JM} &\sim \text{Unif}\left(0, \hat{c}_{\text{QRF}}\right). \end{aligned} \tag{2}$$

The prior on escapement is the posterior from the PIT-tag branching model, where the $T(L,U)$ notation indicates a truncated distribution with lower bound L and upper bound U. The prior on spawner-to-parr capacity is centered on the QRF estimate with a CV of 10%. The prior on parr-to-smolt capacity has an upper bound equal to the QRF parr capacity estimate, on the grounds that the watershed is unlikely to support more smolts than parr. The other priors are uninformative. Note that for transitions from stages other than spawners, intrinsic productivity is a survival, so cannot exceed 1.

The likelihood has two components: observations of (1) parr abundance and (2) parr-to-smolt survival, each with associated observation error variances. We assume observed parr abundance follows a truncated normal distribution:

$$\begin{gathered} J_t = \frac{p_{SJ} S_t}{1 + \frac{p_{SJ}}{c_{SJ}} S_t} \\ J_t^{\text{obs}} \sim N\left(J_t, \hat{\sigma}_J^2\right) T\left(0, \infty\right). \end{gathered} \tag{3}$$

Likewise, observed parr-to-smolt survival has a truncated normal distribution centered on predicted survival:

$$\begin{gathered} s_{JM,t} = \frac{p_{JM}}{1 + \frac{p_{JM}}{c_{JM}} J_t} \\ s_{JM,t}^{\text{obs}} \sim N\left(s_{JM,t}, \hat{\sigma}_{JM}^2\right) T\left(0, 1\right). \end{gathered} \tag{4}$$

The truncated normal distributions are used for convenience, given that uncertainty in the estimates generated by SPAS and TribPIT is reported as standard errors under asymptotic normality. In principle, a lognormal distribution (for abundance) and beta or logistic normal distribution (for survival) would be more appropriate.

Because the models for the two stage transitions are coupled, they use the same estimated "true" parr values, ensuring internal consistency through the composite spawner-to-smolt model. The parameter estimates will marginalize over uncertainty in the predicted values of the state variables, given the observation error variances. However, note that this is an "observation error only" likelihood (Hilborn and Mangel 1997). We could also include process error (deviation of the true state variables from their underlying deterministic relationships), but since this is not a state-space time-series formulation (i.e., the model does not close the loop from spawners back to spawners) the process error variances would be non-identifiable without some prior information.

We fit the model using JAGS 4.2.0 (Plummer 2003) via R 3.3.3 (R Development Core Team 2017) to perform Gibbs sampling on the joint posterior distribution of the unknown parameters and state variables. We ran three parallel chains of 10,000 iterations each, discarded the first

2000 iterations as burn-in, and saved every 8th sample to reduce autocorrelation. Convergence was assessed by inspecting traceplots and the Gelman-Rubin potential scale reduction factor.

Tributary Reconnection Scenario

Between 2009 and 2012, several tributaries that were previously inaccessible to Chinook, mainly due to seasonal dewatering in the lower reaches, were reconnected to the main channel (**Table 5**). Juvenile Chinook have not yet been observed using these tributaries, so any increase in rearing capacity is not reflected in the data used to fit the model. To assess the potential effect of these restoration actions on overall freshwater productivity, we replaced the empirical posterior distribution of total parr capacity by a lognormal distribution with the same CV but a log-mean based on QRF predictions that included the reconnected tributaries. This assumes that juveniles will eventually occupy all accessible areas and that intrinsic productivity does not change.

Results

Posterior distributions of stage-specific intrinsic productivity and capacity are shown in **Figure 14**. The posterior for parr capacity is strongly determined by the prior, whose CV was chosen arbitrarily; however, the other parameter estimates are robust to values of $\sigma_{\hat{c}_{\mathrm{QRF}}}$ as high as 0.5. As the lognormal prior on c_{SJ} becomes more diffuse and thus more skewed, the posterior mean increases, but the posterior median changes very little and the remaining parameters are stable. Overall, the estimates appear biologically reasonable.

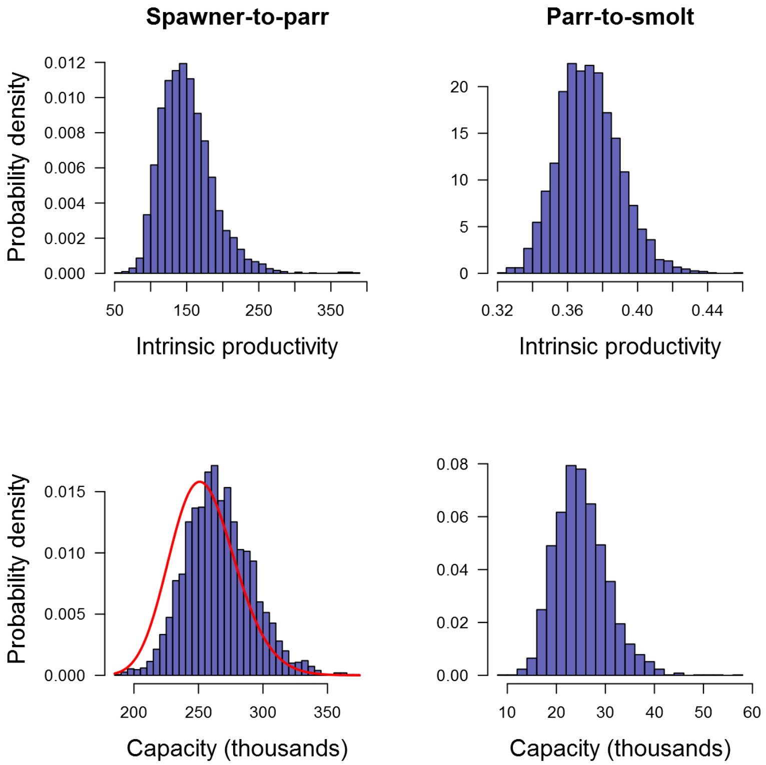

Figure 14. Posterior distributions of intrinsic productivity and capacity in the spawner-to-parr and parr-to-smolt Beverton-Holt transition functions. Priors were uniform over the range of the posterior except in the case of parr capacity (lower left), where the informative prior based on QRF predictions is shown in red.

Comparing observed and fitted values of parr abundance demonstrates the importance of observation uncertainty (**Figure 15**). The model attributes three exceptionally high observed values to measurement noise based on the associated standard errors, resulting in a more conservative estimate of the slope of the spawner-to-parr relationship at low spawner abundance (i.e., intrinsic productivity). **Figure 16** also explains why the prior on parr capacity is so informative: the model infers that none of the observed escapements have come close to saturating the system with parr. In contrast to the spawner-to-parr relationship, there is not much evidence of density dependence in the parr-to-smolt transition based on the raw data. After shrinkage of the measurement errors, the estimated intrinsic productivity (i.e., maximum parr-to-smolt survival) is around 0.37.

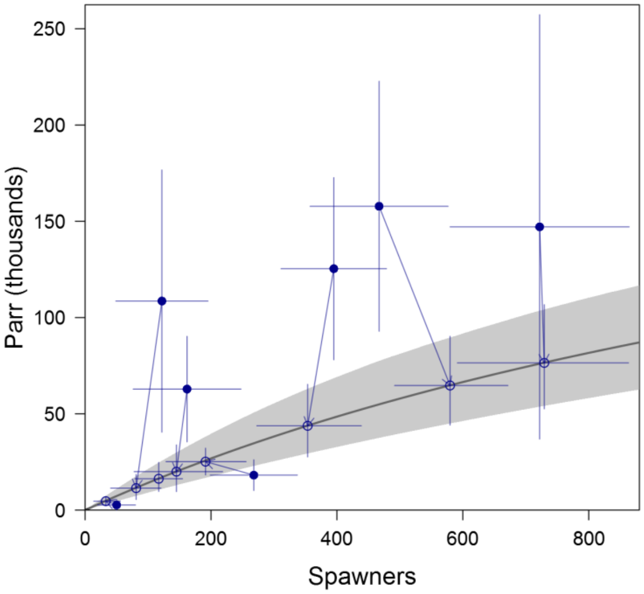

Figure 15. Estimated spawner-to-parr Beverton-Holt function (black line: posterior mean, gray envelope: 95% credible interval). The observed data (solid points, with error bars indicating observation SEs) are connected by arrows to the corresponding fitted values (open circles, with error bars indicating 95% credible intervals).

The model predicts a fairly modest increase in population-scale smolt production due to tributary reconnection, both in absolute terms (an average 10% increase in smolts per spawner) and relative to uncertainty (**Figure 17**). It is possible that this simple scenario analysis underestimates the true improvement; for example, if the reconnected tributaries have higher intrinsic productivity than the previously accessible subwatersheds, then the increase would be apparent at lower spawner abundance. Even in this case, however, the asymptotic difference between baseline and reconnection scenarios (that is, at high spawner abundance) would remain the same.

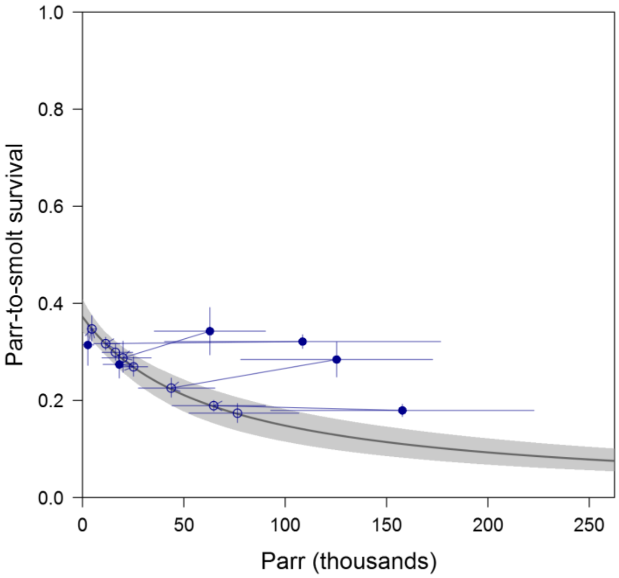

Figure 16. Estimated parr-to-smolt Beverton-Holt function, expressed as a relationship between abundance and survival (black line: posterior mean, gray envelope: 95% credible interval). The observed data (solid points, with error bars indicating observation SEs) are connected by arrows to the corresponding fitted values (open circles, with error bars indicating 95% credible intervals).

Conclusions and Next Steps

Our analysis shows that it is possible to recover biologically plausible estimates of stage-specific transition functions (e.g., Beverton-Holt parameters) from sparse, noisy data, but in some cases auxiliary information (in this case, parr capacity predicted by QRF) is needed to constrain the estimates. This simple two-stage model of freshwater juvenile production suggests there is moderate density dependence in the spawner-to-parr transition and weak density dependence in parr-to-smolt survival. The former incorporates any habitat constraints on egg deposition, as well as habitat effects on fry and summer parr rearing, while the latter includes the effect of overwintering habitat.

This analysis also illustrates how habitat-derived metrics such as QRF capacity predictions, when used as prior information in a Bayesian statistical framework, provide a mechanism to simulate habitat restoration actions. In this case, we simulated an increase in total parr rearing habitat due to tributary reconnection by increasing the prior median on parr capacity in accordance with QRF estimates. The estimated population-level freshwater productivity (smolts per spawner) increased roughly 10% on average, but this effect was largely obscured by parameter uncertainty. This result emphasizes the importance of a formal accounting of uncertainty in model outputs used to provide management advice (Harwood and Stokes 2003). Similarly, Roni et al. (2010) showed that given typical levels of habitat restoration, the signal (population response of juvenile salmonids) is often undetectable given the noise.

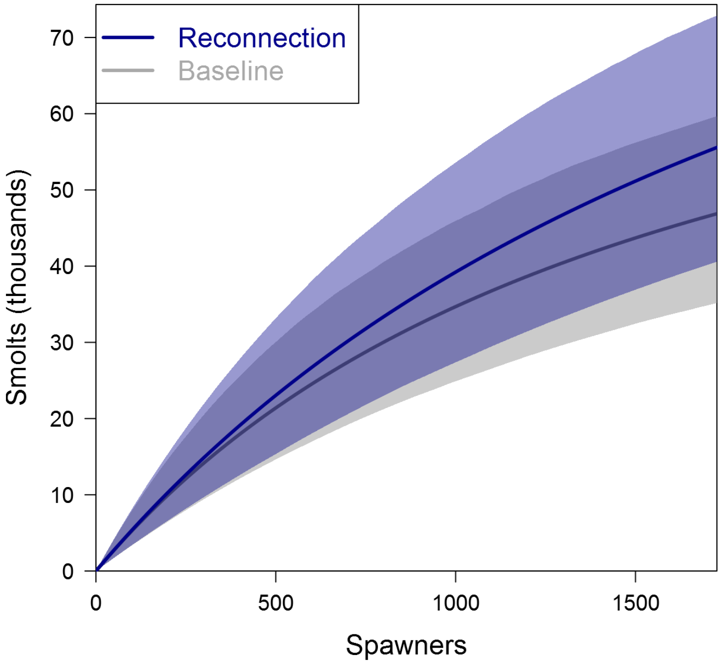

Figure 17. Composite Beverton-Holt curves for spawner-to-smolt production, under baseline conditions and after tributary reconnection. Lines show posterior means and shading indicates 95% credible intervals.

The model presented here is not yet a full LCM; it does not "close the loop" from smolts back to spawners. To do so, we plan to embed the freshwater production model within a stage-structured integrated population model (IPM; see Chapter 7 in this volume) that incorporates long-term monitoring data on spawner escapement and age structure. The much longer available time series of escapement observations, compared to juvenile data, should increase the precision of overall life-cycle productivity and capacity estimates, helping to constrain the estimates of the stage-specific juvenile parameters (Schaub and Abadi 2011). We also plan to explore the addition of within-basin spatial structure to the IPM framework to provide finer-grained estimates of population parameters and their dependence on habitat during summer rearing as well as overwintering. This will require a model structure capable of accommodating two known features of spring/summer Chinook ecology in the Lemhi basin. First, as noted by Bjornn (1978) and seen in our own data, a large number of juveniles migrate downstream as fry shortly post-emergence. RSTs capture fry migrants, but the abundance estimates are highly imprecise and there is no information on pre-migratory standing stocks. Second, given the PIT-tag study design and detection infrastructure in the Lemhi, it is possible to estimate the joint probability that parr tagged during the first summer remain in their natal reach (or migrate downstream) and survive the winter, but the separate survival and movement probabilities are non-identifiable (Buchanan et al. 2015). These data therefore cannot be used to parameterize the commonly used Shiraz framework (Scheuerell et al. 2006), which assumes that stage-specific survival and movement probabilities are known, so a different parameterization of space is needed.

Another possibility for future work is to extend a stage-structured IPM from a single population such as the Lemhi to an ensemble of multiple populations, as described for the adult-to-adult model in Chapter 7 of this document. Doing so would offer several advantages, including a formal mechanism for extrapolating information from data-rich systems to data-poor ones (Punt et al. 2011, Jiao et al. 2011). In addition, this would enable the use of mechanistic or statistical habitat-derived metrics (e.g., NREI, HSI, or QRF predictions) as covariates of stage-specific parameters. Here, we used the QRF prediction of parr capacity directly as a prior on the corresponding model parameter, but if multiple populations are analyzed simultaneously, habitat-based metrics could be incorporated into regression relationships to be estimated jointly with the other parameters, relaxing the need to assume a direct 1:1 correspondence between bottom-up metrics based on small-scale local information and emergent population-dynamic parameters at larger scales (Bentley 2015). For an example of this approach, see Chapter 2 Section c in this document.

References

Ahmadi-Nedushan, B., A. St Hilaire, M. Bérubé, É. Robichaud, N. Thiémonge, and B. Bobée. 2006. A review of statistical methods for the evaluation of aquatic habitat suitability for instream flow assessment. River Research and Applications **22**:503-523.

Bare, C. M., K. B. S. DeHart, J.A., J. L. Latshaw, J. J. Rogers, I. A. Tattam, J. R. Ruzycki, and R. W. Carmichael. 2015. Escapement and productivity monitoring of summer steelhead and spring Chinook salmon in the John Day River. 2014 Annual Report **BPA Contract # 1998-016-00**:89 pp.

Barker, R.J. 1997. Joint modeling of live-recapture, tag-resight, and tag-recovery data. Biometrics, 53, 666–677.

Barker, R. J. and G. White. 1999. Joint analysis of live and dead encounters of marked animals. Program MARK, http://www.cnr.colostate.edu/~gwhite/mark/mark.htm.

Bear, E. A., T. E. McMahon, and A. V. Zale. 2007. Comparative Thermal Requirements of Westslope Cutthroat Trout and Rainbow Trout: Implications for Species Interactions and Development of Thermal Protection Standards. Transactions of the American Fisheries Society **136**:1113-1121.

Beechie, T., and H. Imaki. 2014. Predicting natural channel patterns based on landscape and geomorphic controls in the Columbia River basin, USA. Water Resources Research **50**:39-57.

Bennett, S., G. Pess, N. Bouwes, P. Roni, R. E. Bilby, S. Gallagher, J. Ruzycki, T. Buehrens, K. Krueger, W. Ehinger, J. Anderson, C. Jordan, B. Bowersox, and C. Greene. 2016. Progress and Challenges of Testing the Effectiveness of Stream Restoration in the Pacific Northwest Using Intensively Monitored Watersheds. Fisheries **41**:92-103.

Bentley, N. 2015. Data and time poverty in fisheries estimation: potential approaches and solutions. Ices Journal of Marine Science 72:186–193.

Bjornn, T. C. 1978. Survival, production, and yield of trout and chinook salmon in the Lemhi River, Idaho.

Bouwes, N., N. Weber, C. E. Jordan, W. C. Saunders, I. A. Tattam, C. Volk, J. M. Wheaton, and M. M. Pollock. 2016. Ecosystem experiment reveals benefits of natural and simulated beaver dams to a threatened population of steelhead (Oncorhynchus mykiss). Scientific Reports **6**.

Boyd, M., and B. Kasper. 2003. Analytical methods for dynamic open channel heat and mass transfer: Methodology for heat source model Version 7.0. Oregon Department of Environmental Quality, Portland, Oregon. Web site: http://www. deq. state. or. us/wq/TMDLs/tools. htm.

Buchanan, R. A., J. R. Skalski, G. Mackey, C. Snow, and A. R. Murdoch. 2015. Estimating cohort survival through tributaries for salmonid populations with variable ages at migration. North American Journal of Fisheries Management 35:958–973.

Chilcote, M. W. 2001. Conservation assessment of steelhead populations in Oregon. Unpublished report.(Available from Oregon Department of Fish and Wildlife, Fish Division, 3406 Cherry Drive NE, Salem, OR 97303.).

Deltares. 2010. Delft3D FLOW User Manual. Deltares, Delft.

Duffin, J. 2015. Effects of Engineered Log Jams on Channel Morphology, Middle Fork of the John Day River, Oregon.

Ford, M. J. 2011. Status review update for Pacific salmon and steelhead listed under the Endangered Species Act: Pacific Northwest. US Department of Commerce, National Oceanic and Atmospheric Administration, National Marine Fisheries Service, Northwest Fisheries Science Center.

Fox, M., and S. Bolton. 2007. A Regional and Geomorphic Reference for Quantities and Volumes of Instream Wood in Unmanaged Forested Basins of Washington State. North American Journal of Fisheries Management **27**:342-359.

Fraser, G. S. and C. O. Hamstreet. 2015. Chinook salmon spawning ground surveys on the Entiat River, 2014. U. S. Fish and Wildlife Service, Leavenworth, Washington.

Fryirs, K. A. 2015. Developing and using geomorphic condition assessments for river rehabilitation planning, implementation and monitoring. Wiley Interdisciplinary Reviews: Water **2**:649-667.

Gebhard, S.V. 1961. Emergence and mortality of Chinook salm- on fry in a natural redd. Progressive Fish-Culturist. 23:91.

Gilbert, J. T., W. W. Macfarlane, and J. M. Wheaton. 2016. The Valley Bottom Extraction Tool (V-BET): A GIS tool for delineating valley bottoms across entire drainage networks. Computers & Geosciences **97**:1-14.

Hamstreet, C.O. 2012. Spring and summer Chinook salmon spawning ground surveys on the Entiat River, 2011. U. S. Fish and Wildlife Service, Leavenworth Washington.

Harwood, J., and K. Stokes. 2003. Coping with uncertainty in ecological advice: lessons from fisheries. Trends in Ecology & Evolution 18:617–622.

Hilborn, R., and M. Mangel. 1997. The Ecological Detective. Princeton University Press, Princeton, New Jersey, USA.

Honea, J.M., Jorgensen, J.C., McClure, M.M., Cooney, T.D., Engie, K., Holzer, D.M., and Hilborn, R. 2009. Evaluating habitat effects on population status: Influence of habitat restoration on spring-run Chinook salmon. Freshw. Biol. 54(7): 1576–1592. doi: 10.1111/j.1365-2427.2009.02208.x.

Interior Columbia Technical Recovery Team (ICTRT). 2003. Independent populations of Chinook, steelhead, and sockeye for listed Evolutionarily Significant Units within the Interior Columbia River Domain. Northwest Fisheries Science Center, Seattle, WA. July.

IUCN. 2001. International Union for Conservation of Nature Red List Categories and Criteria.

Jiao, Y., E. Cortes, K. Andrews, and F. Guo. 2011. Poor-data and data-poor species stock assessment using a Bayesian hierarchical approach. Ecological Applications 21:2691–2708.

Kareiva, P., M. Marvier, and M. McClure. 2000. Recovery and management options for spring/summer chinook salmon in the Columbia River Basin. Science **290**:977-979.

Kendall, N. W., J. R. McMillan, M. R. Sloat, T. W. Buehrens, T. P. Quinn, G. R. Pess, K. V. Kuzishchin, M. M. McClure, and R. W. Zabel. 2014. Anadromy and residency in steelhead and rainbow trout (Oncorhynchus mykiss): a review of the processes and patterns. Canadian Journal of Fisheries and Aquatic Sciences **72**:319-342.

Macfarlane, W. W., J. T. Gilbert, M. L. Jensen, J. D. Gilbert, N. Hough-Snee, P. A. McHugh, J. M. Wheaton, and S. N. Bennett. *In Press*. Riparian vegetation as an indicator of riparian condition: detecting departures from historic condition across the North American West. Journal of Environmental Management Volume & Issue TBD.

Maret, T. R., J. E. Hortness, and D. S. Ott. 2005. Instream flow characterization of upper Salmon River basin streams, central Idaho, 2004. **2328-0328**.

Matthiopoulos, J., J. Fieberg, G. Aarts, H. L. Beyer, J. M. Morales, and D. T. Haydon. 2015. Establishing the link between habitat selection and animal population dynamics. Ecological Monographs **85**:413-436.

McCann, J., Chockley, B., Cooper, E., Schaller, H., Haeseker, S., Lessard, R., Petrosky, C., Tinus, E., Van Dyke, E., Ehlke, R., 2014. Comparative Survival Study of PIT-tagged Spring/Summer/Fall Chinook, Summer Steelhead, and Sockeye. 2014 Annual Report BPA Contract # 19960200.

McElhany, P., M. Ruckelshaus, M. Ford, T. Wainwright, and E. Bjorkstedt. 2000. Viable salmonid populations and the recovery of evolutionarily significant units. US Dept. Commer. NOAA Tech. Memo. NMFS-NWFSC **42**:156.

McHugh, P., Budy, P., and Schaller, H. 2004. A model-based assessment of the potential response of Snake River spring–summer Chinook salmon to habitat improvements. Trans. Am. Fish. Soc. 133(3): 622–638. doi: 10.1577/T03-097.1.

McHugh, P. A., W. C. Saunders, N. Bouwes, C. E. Wall, S. Bangen, J. M. Wheaton, M. Nahorniak, J. R. Ruzycki, I. A. Tattam, and C. E. Jordan. 2017. Linking models across scales to assess the viability and restoration potential of a threatened population of steelhead (Oncorhynchus mykiss) in the Middle Fork John Day River, Oregon, USA. Ecological Modelling **355**:24-38.

McMillan, J. R., J. B. Dunham, G. H. Reeves, J. S. Mills, and C. E. Jordan. 2012. Individual condition and stream temperature influence early maturation of rainbow and steelhead trout, Oncorhynchus mykiss. Environmental Biology of Fishes **93**:343-355.

McNyset, K. M., C. Volk, and C. E. Jordan. 2015. Developing an effective model for predicting spatially and temporally continuous stream temperatures from remotely sensed land surface temperatures. Water **7**:19.

Moussalli, E., and R. Hilborn. 1986. Optimal Stock Size and Harvest Rate in Multistage Life-History Models. Canadian Journal of Fisheries and Aquatic Sciences **43**:135-141.

Nahorniak, M., D. P. Larsen, C. Volk, and C. E. Jordan. 2015. Using Inverse Probability Bootstrap Sampling to Eliminate Sample Induced Bias in Model Based Analysis of Unequal Probability Samples. PloS one **10**:e0131765.

O'Brien, G. R., J. Wheaton, K. Fryirs, P. McHugh, N. Bouwes, G. Brierley, and C. Jordan. 2017. A geomorphic assessment to inform strategic stream restoration planning in the Middle Fork John Day Watershed, Oregon, USA. Journal of Maps **13**:369-381.

Ohms, H. A., C. E. Jordan, and D. A. Lytle. In Review. Estimating the proportions of migrants and residents in partially migratory species using sex ratio balancing. Submitted to Ecology.

Ohms, H. A., M. R. Sloat, G. H. Reeves, C. E. Jordan, and J. B. Dunham. 2014. Influence of sex, migration distance, and latitude on life history expression in steelhead and rainbow trout (Oncorhynchus mykiss). Canadian Journal of Fisheries and Aquatic Sciences **71**:70-80.

Oregon Department of Environmental Quality (ODEQ). 2010. John Day River basin total maximum daily load (TMDL) and water quality management plan (WQMP). Page 177 *in* State of Oregon Department of Environmental Quality, editor., Portland, OR.

Oregon Department of Fish and Wildlife (ODFW). 2013. Oregon Fish Habitat Distribution.*in* Oregon Department of Fish and Wildlife (ODFW), editor.

Plummer, M. 2003. JAGS: A program for analysis of Bayesian graphical models using Gibbs sampling. Proceedings of the 3rd International Workshop on Distributed Statistical Computing. Vienna, Austria.

Punt, A. E., D. C. Smith, and A. D. M. Smith. 2011. Among-stock comparisons for improving stock assessments of data-poor stocks: the "Robin Hood" approach. Ices Journal of Marine Science 68:972–981.

Quinn, T. P., P. McGinnity, and T. E. Reed. 2015. The paradox of "premature migration" by adult anadromous salmonid fishes: patterns and hypotheses. Canadian Journal of Fisheries and Aquatic Sciences **73**:1-16.

R Development Core Team. 2017. R: A language and environment for statistical computing. R Foundation for Statistical Computing, Vienna, Austria.

Roni, P., G. Pess, T. Beechie, and S. Morley. 2010. Estimating changes in coho salmon and steelhead abundance from watershed restoration: how much restoration is needed to measurably increase smolt production? North American Journal of Fisheries Management 30:1469–1484.

Roni, P., Beechie, T., Pess, G., Hanson, K., 2014. Wood placement in river restoration: fact, fiction, and future direction. Can J Fish Aquat Sci 72, 466-478

Rosenfeld, J., N. Bouwes, C. E. Wall, and S. Naman. 2014. Successes, failures, and opportunities in the practical application of drift-foraging models. Environmental Biology of Fishes **97**:551-574.

Saunders, W. C., N. Bouwes, P. McHugh, and C. E. Jordan. In Review. A network model for primary production highlights linkages between riverine fish populations and autochthonous resources. Submitted to Ecosphere.

Schaub, M., and F. Abadi. 2011. Integrated population models: a novel analysis framework for deeper insights into population dynamics. Journal of Ornithology 152:227–237.

Scheuerell, M. D., R. Hilborn, M. H. Ruckelshaus, K. K. Bartz, K. M. Lagueux, A. D. Haas, and K. Rawson. 2006. The Shiraz model: a tool for incorporating anthropogenic effects and fish-habitat relationships in conservation planning. Canadian Journal of Fisheries and Aquatic Sciences 63:1596–1607.

Sharma, R., A. B. Cooper, and R. Hilborn. 2005. A quantitative framework for the analysis of habitat and hatchery practices on Pacific salmon. Ecological Modelling **183**:231-250.

Sloat, M. R., D. J. Fraser, J. B. Dunham, J. A. Falke, C. E. Jordan, J. R. McMillan, and H. A. Ohms. 2014. Ecological and evolutionary patterns of freshwater maturation in Pacific and Atlantic salmonines. Reviews in Fish Biology and Fisheries **24**:689-707.

Stevens, D. L. and A. R. Olsen. 2004. Spatially-balanced sampling of natural resources. Journal of American Statistical Association 99(465):262-278.

Torgersen, C. E., D. M. Price, H. W. Li, and B. A. McIntosh. 1999. Multiscale thermal refugia and stream habitat associations of Chinook salmon in northeastern Oregon. Ecological Applications **9**:301-319.

Trapani, J., M. Champie, and K. Slavin. 1994. Upper salmon basin watershed project: stream habitat inventory report. 64p.

USBR (United States Bureau of Reclamation). 2009. Entiat Tributary Assessment. Available at www.usbr.gov/pn/programs/fcrps/thp/ucao/entiat/tribassmt/index.html

Upper Columbia Spring Chinook Salmon and Steelhead Recovery Plan. 2007 (accessed at http://www.westcoast.fisheries.noaa.gov/publications/recovery_planning/salmon_steelhead/domains/interior_columbia/upper_columbia/uc_plan.pdf

Wall, C.E., Bouwes, N., Wheaton, J.M., Saunders, W.C., Bennett, S.N., 2015. Net rate of energy intake predicts reach-level steelhead (Oncorhynchus mykiss) densities in diverse basins from a large monitoring program. Canadian Journal of Fisheries and Aquatic Sciences **73:** 1081-1091.

Wall, C. E., N. Bouwes, J. M. Wheaton, S. N. Bennett, W. C. Saunders, P. A. McHugh, and C. E. Jordan. 2016. Design and monitoring of woody structures and their benefits to juvenile steelhead trout (Oncorhynchus mykiss) using a net rate of energy intake model. Canadian Journal of Fisheries and Aquatic Sciences **74:** 727-738.

White, G.C. & Burnham, K.P. (1999) Program MARK: survival estimation from populations of marked animals. Bird Study, 46, 120–138.

Yuen, H. and Sharma, R. 2005. Using simulation techniques to estimate management parameters on Snake River steelhead: Declines in productivity make rebuilding difficult. North Am. Jr. of Fish Mgt 25: 446-463.

CHAPTER 9: FULL MODELS

9.e Yakima River *Oncorhynchus mykiss* populations

Neala Kendall (Washington Department of Fish and Wildlife) and Chris Frederiksen (Yakama Nation Fisheries)

Introduction

Life-cycle models can be used to better understand life history strategies and dynamics of *O. mykiss* and evaluate their population dynamics both spatially and temporally (Roff 1992). Specifically, with such models, parameters associated with fish characteristics, such as survival and growth, and environmental features, such as temperature and carrying capacity, can be modified to understand how habitat modifications and environmental conditions will affect fish abundance and characteristics at different stages.

Oncorhynchus mykiss display a wide variety of life history strategies, including partial migration (where a portion of a common population migrates to the ocean while another portion matures in freshwater; Jonsson and Jonsson 1993). Rainbow trout remain in freshwater their whole lives and are not listed under the Endangered Species Act (ESA) whereas steelhead trout perform an anadromous migration to the ocean and are listed. Resident and anadromous *O. mykiss* coexist in sympatry throughout the Columbia and Snake River basins, including in the Yakima River basin.

Partial migration has been well documented in a variety of salmonid species (Jonsson and Jonsson 1993). Individuals are more likely to mature in freshwater when their physical needs are met; if not, they will smolt and make an anadromous migration to the ocean (Kendall et al. 2015; Thorpe et al. 1998). The expression of anadromy and residency in *O. mykiss* is genetically controlled to some degree and has been correlated with several physical and biological factors including (but not limited to) water temperature and flow, productivity, hydrology and geomorphology, spawning habitat conditions such as substrate size, fish density, cost of migration to and from the ocean, and mortality in the ocean (Kendall et al. 2015).

To better understand and accurately predict the complexity of O.mykiss population dynamics, one must assess the production of both resident and anadromous life history and the abiotic and biotic factors affecting them. One challenge with life-cycle models is having adequate empirical data with which to populate the models. One of the most unique and robust dataset available for *O. mykiss* in the interior Columbia River is from the Yakima River basin in central Washington State, USA. This basin, and the upper portion in particular, provides a unique study case and opportunity in which to advance the development of life-cycle models for partially migratory *O. mykiss* populations. Two life-cycle models currently exist specifically for Yakima River *O. mykiss* (Courter et al. 2009; Courter et al. 2010) and another life-cycle model has been developed for anadromous Interior Columbia River basin salmonids (McClure et al. 2007; Zabel et al. 2013). Another *O. mykiss*-specific model has been developed for California fish (Satterthwaite et al. 2009; 2010). We will integrate these models in order to better understand resident and anadromous sympatric population dynamics, how these dynamics affect abundance trends over time, and the relative proportions of anadromous vs. resident individuals produced. This model will improve our ability to understand the population bottlenecks affecting Yakima River anadromous and resident *O. mykiss* production, predict the numbers of anadromous and resident individuals in newly accessible habitat, and understand the consequences, in terms of population abundance and viability, of changes in mortality at different life stages.

Study site

The Yakima River Steelhead major population group (MPG) is comprised of four distinct steelhead (anadromous *O. mykiss*) populations including Upper Yakima, Naches, Toppenish, and Satus, all of which are listed as threatened under the Endangered Species Act (ESA). The Upper Yakima River steelhead population is regarded by NMFS as one of the most depressed (relative to its historical levels) independent steelhead populations in the Columbia River basin. Rainbow trout (resident *O. mykiss*) are abundant in the Upper Yakima River basin and support a popular wild trout fishery, and their abundance has been stable since monitoring on these fish began in 1990. Multiple time a year and each year since 1991, Upper Yakima River juvenile O. mykiss have been captured via electrofishing, PIT tagged, and measured for size (Temple et al. 2016). Data from recaptured fish in subsequent sampling events provides data on fish growth and survival. Less information is available about resident *O. mykiss* in other regions of the Yakima River basin. Hatchery fish have not been released into the Yakima River main stem since 1984 and tributary stocking has not occurred since the mid-1990s. Genetic analysis indicated that resident trout are similar to native steelhead and quite distinct from hatchery stocks (Busack et al. 2005; Pearsons et al. 2007).

The Yakima River basin collects runoff from streams draining the eastern slopes of the Cascade Mountains. The river flows through the arid and irrigated Yakima Valley and joins the Columbia River 541 km upstream of the Pacific Ocean. The amount and type of precipitation (snow vs. rain) varies greatly between the upper and lower basins. Therefore, increasing temperatures associated with global warming and subsequent changes in snow vs. rain precipitation could have a significant effect on the hydrology in the basin and thus the fish living there.

9.e Yakima River O. mykiss *populations*

Anadromous adult steelhead bound for the Yakima basin cross Prosser Dam at river kilometer (rkm) 74 and those bound for the Upper Yakima River basin must cross Roza Dam at rkm 201. Downstream-migrating smolts are sampled at the Chandler Juvenile Facility located just below Prosser Dam. Distribution and spawn timing of adult steelhead in the Yakima River basin have been determined by a combination of redd surveys and radio-telemetry studies (C. Frederiksen, unpublished data). The spatial scale of steelhead spawning is smaller than that of rainbow trout but is within the geographic range of rainbow trout spawning. Resident rainbow trout and steelhead spawn timing is similar (in the spring). Yakima River rainbow and steelhead trout interbreed when their spawning areas overlap spatially and temporally and are capable of producing offspring of the other type (Courter et al. 2013).

Main stem river flows in both the Naches and Upper Yakima River basins are altered from their natural regimes. Specifically, the Upper Yakima main stem experiences high flows from three separate headwater reservoirs during the summer months spanning mid-June through the end of August. The Naches River experiences a less severe regulated hydrograph, with a constrained medium to high water release spanning the months of mid-August through mid-October provided by two storage reservoirs. Releases from the reservoirs augment flows from mid-June through late August to meet downstream irrigation demands and support agriculture in the Yakima Valley. This alteration in flow regime has increased river depths and velocities while reducing the thermal profile in the upper Yakima River. These physical alterations are thought to favor resident production or, to some degree, allow the resident life history type to thrive in the Upper Yakima main stem (Courter et al. 2009).

Existing models

Stochastic population dynamics life-cycle model to estimate O. mykiss abundance trends

The first model we will utilize is a stochastic population dynamics life-cycle model that estimates population abundance trends of resident and anadromous *O. mykiss* in the Upper Yakima River basin (Figure 9.e.1; Courter et al. 2010). Resident and anadromous abundances differ greatly, with residents averaging about 13,000 annual spawners and steelhead surveyed at 550 spawners in 2016 (G. Temple, WDFW, pers. comm.). The model reconstructs trends from a 25-year dataset (1992-2016) of steelhead and rainbow trout abundance, age structure, life history tactic, and maturation status. It captures breeding and competition interactions between anadromous and resident *O. mykiss* in areas where temporal and spatial overlap are known to occur, incorporates density-dependent dynamics, and predicts the spawner abundance trends and their life history tactic over time.

Figure 9.e.1. Diagrammatic representation of the Upper Yakima basin *O. mykiss* population dynamics model (Courter et al. 2010). Am=anadromous males, Af=anadromous females, Rf=resident females, and Rm=resident males.

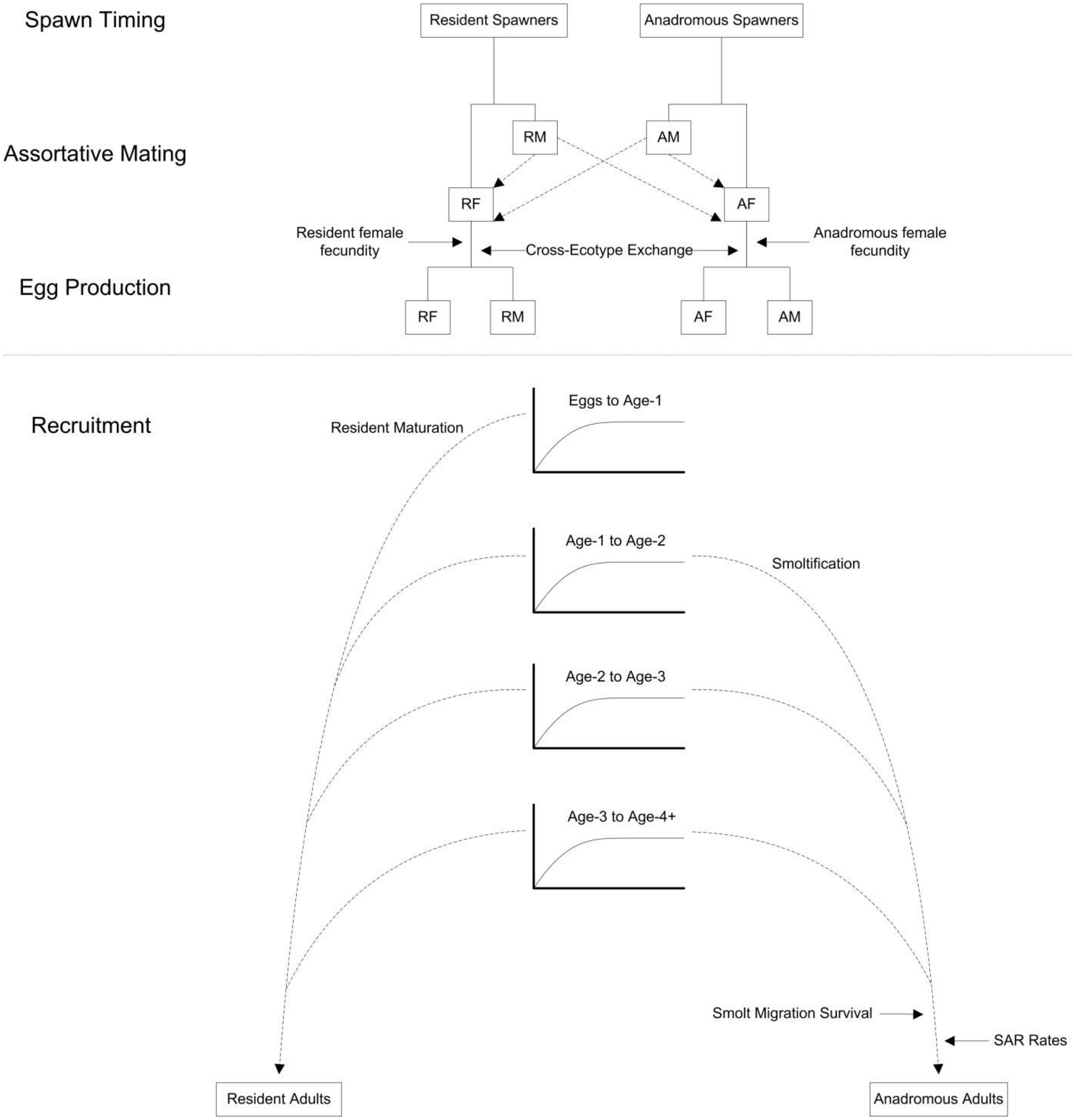

For a given model run, the number of resident rainbow trout and steelhead of brood years 0 and 1 were seeded with spawner abundances (life history tactic, sex, and age). Spawner abundance in subsequent years was a function of returning adult steelhead and mature resident rainbow trout available each year, determined via an empirically-based maturation schedule. The frequency of anadromous breeding pairs observed in the Upper Yakima River basin (Karp et al. 2009) along with observational data from the Olympic Peninsula of Washington state (McMillan et al. 2007) were used to determine rates of interbreeding between resident and anadromous fish. For the model runs, three pairing events were simulated annually: anadromous males spawned preferably with anadromous females, resident females spawned with resident males, and 21-25% of anadromous females were fertilized by resident males. Sex ratios of anadromous and resident spawners were computed and compared to observed data.

Rates of juvenile production were assumed to be directly related to spawner abundance, but productivity rates differed between steelhead and resident rainbow trout. Female steelhead are known to have higher fecundity compared to their resident counterparts. A constant female fecundity rate for each phenotype was estimated using a length-fecundity model previously developed for Yakima River Basin *O. mykiss* (Murdoch 1995; Pearsons et al. 1993). A length-fecundity model was developed for steelhead based on adults sampled at Prosser Dam between 1986 and 1987 (C. Frederiksen, unpublished data). Mean fecundity estimates were generated for both steelhead that had spent one and two years in the ocean using length and age data from fish sampled at Roza Dam (bound for the Upper Yakima).

The expression of residency or anadromy for mature spawners was determined automatically for female and male progeny produced from each of the four potential breeding crosses (anadromous female (Af) x anadromous male (Am), Af x resident male (Rm), resident female (Rf) x Rm, Rf x Am). The determination was based on data from breeding studies in the

Grande Ronde River basin, Oregon (Ruzycki et al. 2009), and Sashin Creek, Alaska (Thrower et al. 2004; Thrower and Joyce 2004).

Data collected on juvenile *O. mykiss* abundance in freshwater revealed strong density-dependent effects (G. Temple, WDFW, unpublished data). Beverton-Holt stock-recruitment curves were fit to the abundance data and to estimate survival between juvenile age classes and resident adult production. Specifically, recruitment and survival between egg deposition and age 1, age 1 and 2, 2 and 3, and 3 and 4 were estimated. The juvenile sampling data used in these estimations were assumed to represent the abundance of both juvenile steelhead and resident rainbow trout. Thus, density-dependent effects were also affected by emigration and maturation. Both anadromous and resident juveniles of a similar age are likely to compete for similar habitat and the locations sampled were within known distributions occupied by fish displaying both life history tactics. Therefore, age class-specific carrying capacity estimates derived from Beverton-Holt recruitment functions were assumed to represent aggregated estimates for combined steelhead and rainbow trout.

Yakima River steelhead emigration, smolt migration survival, and smolt-to-adult return (SAR) rates were estimated based on smolt and adult counts enumerated at Prosser and Roza dams, respectively (Frederiksen et al. 2014; Kock et al. 2016). Emigration survival from Roza to Prosser Dam was estimated from survival data on coho and spring Chinook salmon (Frederiksen et al. 2014; Neeley 2012). Steelhead and spring Chinook salmon emigration survival were positively correlated ($r^2 = 0.98$) during common years. The geometric mean of emigrating steelhead survival from Roza to Prosser Dam was 57% (SD ±18.7%). Steelhead SAR rates averaged 2.9% for the period of record available at the time of model development. Steelhead counts and ocean age varied by freshwater age at smolting and sex. Age structure was informed by scale samples collected from returning adults at Roza Dam.

Past telemetry studies (Hockersmith et al. 1995) showed that older and larger rainbow trout prefer rearing and spawning habitat types in the Yakima River main stem over those in higher-elevation tributaries. In addition, juvenile age structures and size at age, along with adult steelhead age at maturation, differed between the majority of tributary and main stem rearing locations. Thus, demographic differences between tributary and main stem reaches required partitioning main stem and tributary spawning and recruitment dynamics in the model.

The model operates on an annual time step with certain parameters varying stochastically to account for observed temporal variability, including production rate of progeny with different life history tactics, freshwater recruitment parameters (i.e., environmental variability affecting habitat productivity), smolt survival rates, and SAR rates.

***Life-cycle simulation model of temperature and flow on relative abundance of* O. mykiss**

The second model developed specifically for the Yakima River basin is a deterministic life-cycle simulation model (Figure 9.e.2; Courter et al. 2009). It examines the influence of temperature and flow on the growth and survival of steelhead and rainbow trout. Specifically, this model examines how freshwater rearing capacity in multiple reaches, combined with growth, survival, and breeding interactions between anadromous and resident *O. mykiss*, influence the relative reproductive success and thus proportion of resident vs. anadromous spawners.

Figure 9.e.2. Flow chart showing key inputs and relationships within the Yakima basin *O. mykiss* life-cycle simulation model (Courter et al. 2009).

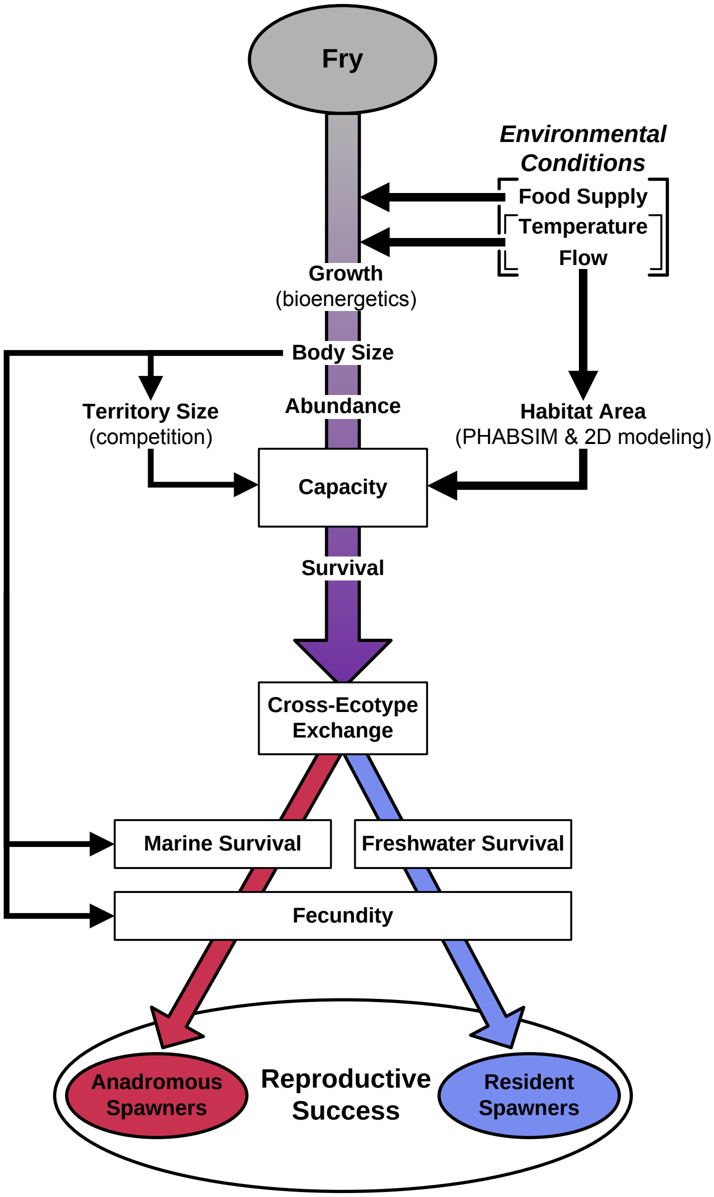

Freshwater environmental conditions such as flow are important drivers of population abundance trends and life history tactic expression (e.g., Mills et al. 2012). Because the Yakima River is flow regulated by upstream storage reservoirs, understanding how flow management affects the production of anadromous and resident *O. mykiss* is a priority. In particular, researchers and managers are interested in whether and how flow affects the production of steelhead (rainbow trout [resident *O. mykiss*] are not listed under the Endangered Species Act).

Courter et al. (2009) hypothesized that environmental conditions influence survival tradeoff between freshwater residency and anadromy. Specifically, they predicted that flow regimes providing cool water temperatures and maintaining water depth and velocities necessary to provide ideal adult rainbow trout habitat throughout the summer and fall results in higher residency rates and fewer steelhead trout. Furthermore, tributary and Columbia River main stem migration mortality, poor ocean survival, and fisheries will contribute to further reductions in the number of steelhead. The model predicted that steelhead would be more prevalent in tributary habitats and resident rainbow trout would be more common in the main stem Yakima River, principally because tributary habitats tend to provide poor growing conditions (low summer flows and high stream temperatures) for resident trout relative to main stem habitats.

Nine spatial units, or reaches, in the Yakima River basin were modeled: four tributary reaches (Satus, Toppenish mid, Toppenish upper, Taneum) and five main stem reaches (Easton, Kittitas, Union Gap, Wapato, and Naches). These represented reaches within each of the four Yakima basin independent steelhead populations where sufficient data were available to parameterize the model. Fish habitat estimates from habitat-hydrological models, Physical Habitat Simulation (PHABSIM) or two-dimensional models (2D), had been created previously for each spatial reach (Frederiksen pers. comm.; Pacheco pers. comm.; Bovee et al. 1998), which provided information necessary to quantify the effects of flow on freshwater habitat area for juvenile and adult life-stages. Daily temperature and flow data were also available from the PHABSIM and 2D models for each reach. Flow and temperature conditions differed dramatically among reaches, especially between main stem and tributary sites.

This model operates on a daily time step. In each step, flow and temperature are specified for each stream reach, which influences growth, survival, and available habitat area for fry (age 0), juveniles (age 1), and resident adults (ages 2-5). The predicted habitat areas were adjusted based on a temperature suitability index (Sullivan et al. 2000) to account for negative effects of high temperatures on rearing capacity. Based on predicted fish length and age, the required territory size per fish was estimated (Grant and Kramer 1990). Each reach's carrying capacity for fry, juveniles, and resident adults was estimated by dividing habitat area by fish territory size. Because many factors influencing habitat area and carrying capacity were not included, this modeling approach produced relative indices of carrying capacity among reaches rather than absolute measures.

A generalized bioenergetics growth model (based on Mangel and Satterthwaite 2008; Thorpe et al. 1998) was used to estimate the influence of environmental conditions on *O. mykiss* freshwater growth. Growth was a function of modeled food availability and stream temperature (and thus is density dependent). The growth model was calibrated to data separately for main stem and tributary habitats and applied to the five model reaches. Growth predictions fit length-at-age data well, explaining ~76% of variation in individual fish length in main stem sites.

Freshwater survival during winter was assumed to be density independent and size dependent (Ebersole et al. 2006; Quinn and Peterson 1996; Smith and Griffith 1994) and thus was modeled as a size-dependent logistic function. An additional 30% mortality due to predation and other factors was added to account for observed survival rates of *O. mykiss* in the Upper Yakima River (C. Frederiksen, Yakama Nation Fisheries, unpublished data). March to October freshwater survival was calculated on a daily basis, based on fish age, as a function of carrying capacity and fish abundance.

Fall juvenile dispersal from tributary to main stem habitats was incorporated into the model. Observations suggest that a portion of age-1 and age-2 juvenile fish leave tributary habitats, prior to smolt transformation, and continue rearing in main stem habitats. Although downstream parr migrants are commonly observed in *O. mykiss* populations, the proportion of juveniles adopting this strategy is thought to be controlled by a complex set of environmental and genetic mechanisms, and data describing fall juvenile dispersal behavior in the Yakima Basin are limited (Conley et al. 2009). Fixed proportions of fall migrants were approximated using data from the Grande Ronde River basin (R. Carmichael, ODFW, pers. comm.). Fall parr (migrants) and resident main stem parr were tracked separately within “holding reaches.” Flow and temperature in these holding reaches were assumed to be the same as conditions in the nearest main stem reach. Survival was modeled as density independent and a function of stream temperature.

In this model, a fish’s “decision” to mature in freshwater or initiate smolt transformation was determined by parental life history tactic and breeding crosses; it was not environmentally influenced. Smolt age was estimated as a function of fish size on May 1 of a given year. Fish that reached a threshold size (150 mm; D. Lind, Yakama Nation Fisheries, pers. comm.) by that date migrated to the ocean; otherwise they continued rearing in freshwater until the next spring when size was reassessed.

Smolt-to-adult survival for anadromous individuals was dependent on smolt size at emigration and migration distance. Outmigrating smolt survival was based on SAR data estimated at Prosser and Roza dams (Frederiksen et al. 2014; Kock et al. 2016) and an assumed relationship between smolt size at emigration and marine survival using a logistic function. A function developed for coastal Vancouver Island, BC, Canada (Ward et al. 1989) was modified to account for increased migration mortality for Yakima River steelhead. Different relationships were developed for the lower and upper Yakima basin reaches because of increased migration mortality (43.3% from the Upper Yakima River to Roza Dam) for fish in the upper basin. Upper and lower Yakima Basin reaches' functions were calibrated so that the SAR for an average-sized smolt (175 mm) was equal to the geometric mean of the estimated SAR for steelhead smolts outmigrating between 1985 and 2002.

Age-at-maturation and sex ratios of anadromous fish were also based on empirical data, collected at Prosser Dam (for Satus, Toppenish, and Naches populations) and Roza Dam (for the upper Yakima Population) between 2002 and 2005 (Conley et al. 2009). Age-at-maturation for resident females was estimated based on data collected in the Upper Yakima River main stem (above Roza Dam) between 1990 and 1993 (Pearsons et al. 1993).

For the adults that made it back to the spawning grounds, mate selection (of anadromous vs. resident individuals based on a fish's life history tactic) was modeled using an asymptotic function to be influenced by fish size and abundance and based on observational studies on the Olympic Peninsula of Washington state (McMillan et al. 2007). When the ratio of steelhead to rainbow trout males was 1:1, anadromous females were estimated to spawn with an anadromous male 76% of the time (fidelity rate). This fidelity rate was scaled proportionally to the observed ratio of steelhead to rainbow trout male spawners.

Fecundity of both resident and anadromous females (number of eggs) is size-dependent. The relationship differs between resident and anadromous fish with steelhead producing more eggs than resident trout. Female fecundity was modeled as a function of length from steelheads captured at Prosser Dam (Conley et al. 2009) and residents sampled in tributary and main stem habitats of the Upper Yakima River basin (Pearsons et al. 1993).

The production of anadromous offspring by resident spawners and vice-versa was modeled as a fixed proportion based on observed data from the Grande Ronde River basin (Ruzycki et al. 2009). Egg-to-fry survival was assumed to be 20% for all *O. mykiss* (anadromous and resident) based on data from the Olympic Peninsula of Washington state (Bley and Moring 1988). For rainbow trout, post-spawning survival rate of 55% was estimated based on data from a Yakima River tributary (Wydoski and Whitney 2003). A repeat spawning rate of 50% was estimated based on observations in the Deschutes River of Oregon (Schroeder and Smith 1989), whereas the anadromous fish repeating spawning rate was 5.4% based on Yakima River-specific observations (Conley et al. 2009).

The model predicts relative reproductive success values as the ratio of total anadromous egg production to total resident egg production. For a given scenario (specified set of flow and temperature conditions), the model is run for ten or more brood years to allow spawner abundance to reach equilibrium. Relative reproductive success in the tenth year was evaluated and compared among reaches.

***State-dependent life-cycle model of* O. mykiss**

As noted above, there are several limitations to the existing Yakima basin-specific life-cycle models (Courter et al. 2009; Courter et al. 2010). In particular, environmental conditions do not influence the rates of expression of anadromy and residency, which is known to be the case (Hendry et al. 2004; Thorpe et al. 1998). An existing tool that can be used to understand how proximate (physiological) and ultimate (reproductive success) considerations predict life history strategies of female *O. mykiss* is a state-dependent model developed by Satterthwaite et al. (2009; 2010) for coastal and central California streams. This model framework has also been applied to Methow River *O. mykiss* of Washington State (Benjamin et al. 2013). This model predicts whether a fish will remain in freshwater as a resident or undergo the smolt transformation and migrate to the ocean as an anadromous individual and at what age the smolt transformation occurs.

In the Satterthwaite et al. (2009; 2010) model (Figure 9.e.3), annual freshwater survival was estimated to be constant for age 1+ fish (Bley and Moring 1988). Freshwater growth rates were based on emergence date, season, and fish age (Hayes et al. 2008). Fecundity of adult resident fish (Shapovalov and Taft 1954) and marine survival of outmigrating smolts (Bond et al. 2008; Shapovalov 1967; Shapovalov and Taft 1954) were modeled based on a fish’s body length. Returning anadromous fish were assigned a constant “lifetime fecundity value” (to account for the fact that most anadromous fish spawned once while a few were iteroparous). Several parameters were used to describe a fish’s condition and model its fitness (including emergence timing, survival, length at age, and growth rates) during an annual maturation decision window in April and a smolting decision window from November-December. Based on this state-dependent fitness estimation, a fish is predicted to mature or not in the spring and then undergo smolt transformation or not in the fall.

Figure 9.e.3. Timeline of the Satterthwaite et al. (2009) model of *O. mykiss* life history. The intervals are designated according to their corresponding survival rates (s_p, where p is a given period).

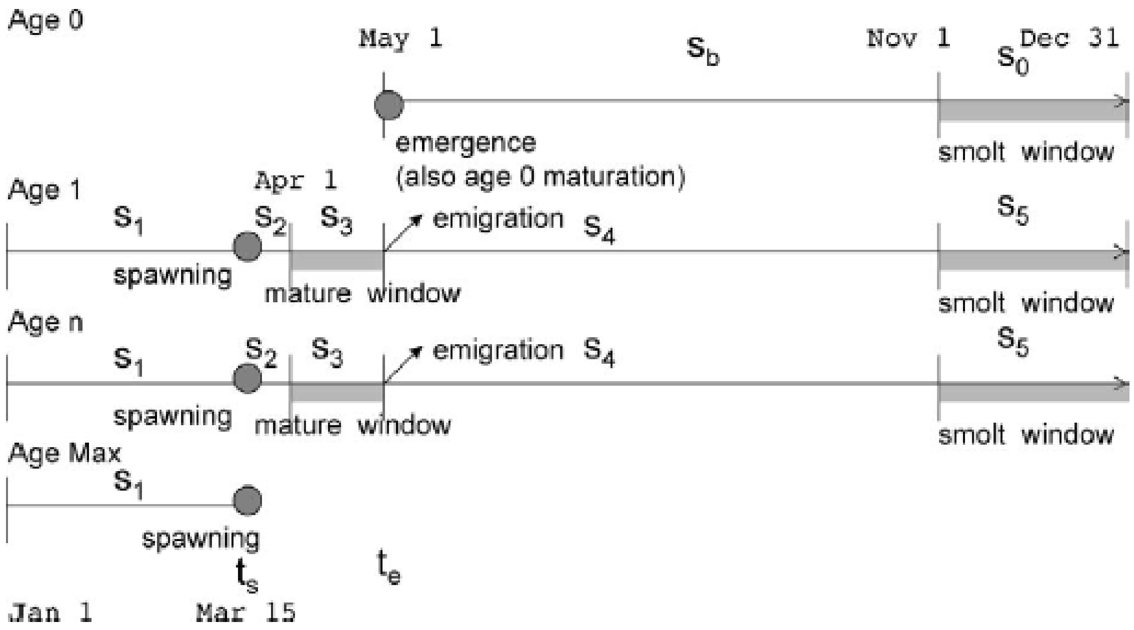

Congruence between model predictions and observed life history strategies (smolting, maturing in freshwater, and delayed adoption of a life history) in the California streams (Satterthwaite et al. 2009; 2010; Satterthwaite et al. 2012) emphasize the notion that body length and growth early in life, which is influenced by both genetic and enviornmental factors, have proximate and ultimate consequences for life history expression in female *O. mykiss*.

Life-cycle matrix model of Interior Columbia steelhead trout

Including in our life-cycle model ways to assess how Interior Columbia River steelhead abundance is associated with out-of-basin impacts improves our ability to document population bottlenecks and understand how climate change and other factors influencing survival will affect the fish. These out-of-basin impacts including smolt and adult migration survival (including dam passage), ocean survival, harvest, and adult overwintering survival. This can be done by incorporating components of the ICTRT life-cycle matrix model (Figure 9.e.4; McClure et al. 2007; Zabel et al. 2013), which is utilized by many other life-cycle models described in this document.

Figure 9.e.4. Flow chart showing key life stages of salmonids in the Interior Columbia River basin and factors influencing them at different stages that will be modeled by the ICRTRT life-cycle matrix model (McClure et al. 2007; Zabel et al. 2013).

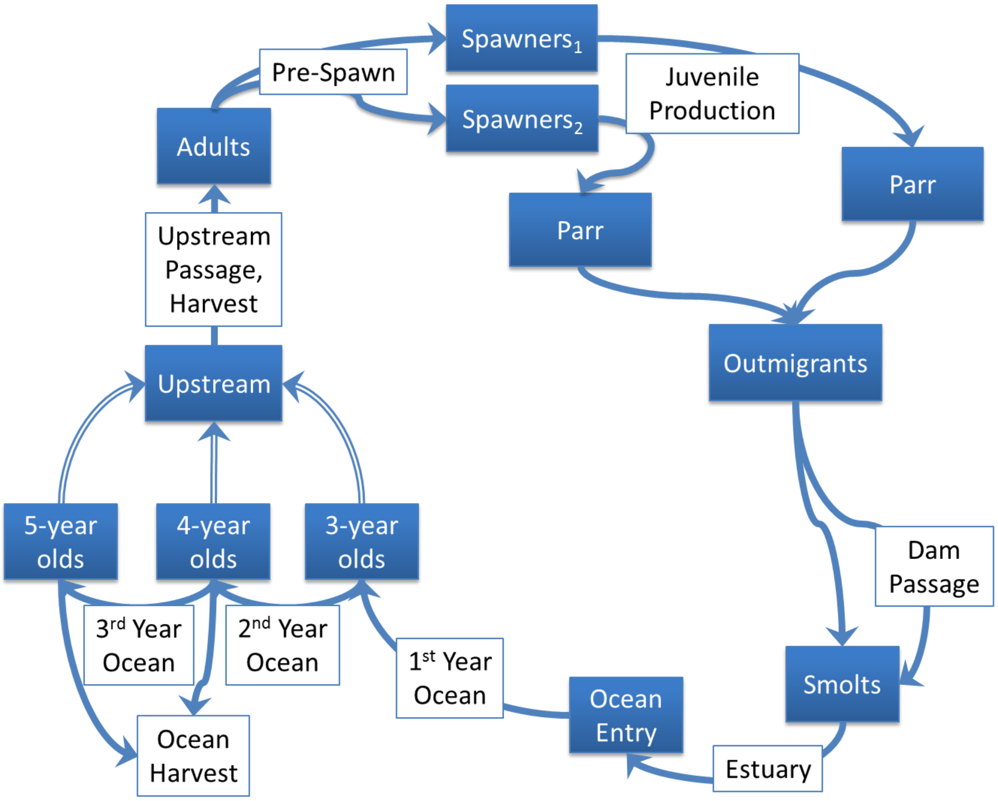

This model is a stochastic, density-dependent Leslie matrix age-structured population models for eight steelhead populations in multiple Evolutionarily Significant Units (ESUs) of the interior Columbia River by modifying the general structure of an ESU-level model developed by Zabel et al. (2006) for Snake River spring/summer Chinook. This model currently only considers anadromous steelhead trout; it does not incorporate resident *O. mykiss* (rainbow trout) and their potential spawning contribution to the anadromous population.

The model structure is based on the life history of steelhead. Differing from Chinook salmon, steelhead exhibit multiple smolt ages and a freshwater overwintering period prior to spawning. Thus, their matrix covers three distinct life stages: juveniles in freshwater (ages 1-4), ocean residence, and freshwater overwintering (where prespawning mortality occurs) of adults. Spawning occurs in spring so the age classes are delineated from spring to spring. Age classes are enumerated at the end of a year.

The primary data for the models are population-specific spawner counts and their age structure, which provide the basis for annual estimates of productivity and temporal trends in abundance and variability. Additional data such as smolt counts and age composition and smolt-to-adult return rates (SARs) allow the models to be partitioned into two major components: spawner-to-smolt survival and smolt-to-adult survival. Survival within each component is partitioned further as available data allowed. Specifically, model inputs can include juvenile and adult migration survival, estuarine and early-ocean survival, and adult later ocean survival. This modeling approach translates life-stage-specific survival changes into metrics of population abundance, productivity, and viability.

Future work

We currently have funding from the Yakama Nation to complete this model integration work. Our first step is to flesh out and finalize the scenarios for which we will run the model, as this will shape the components of the model. For example, if mortality in certain areas (e.g., through Roza Dam, in the estuary, or in the ocean) or due to certain causes (e.g., hydropower projects, pinniped or avian predation, or climate change) are of particular interest, we will work to build a model that can important these factors. We are in the process of meeting with stakeholders to understand how they would like to use the models and shaping the scenarios around this information.

The following scenarios occurring within the Yakima River basin will be modeled:

- Freshwater rearing environment temperature changes due to climate change scenarios (Isaak et al. 2011; Isaak et al. 2012) which would impact *O. mykiss* growth in freshwater and thus potentially the number of residents and the age structure of both smolts and residents. Smolt age and size changes could have downstream impacts, potentially affecting SARs.
- The opening of habitat in the Manastash River (due to the removal of the Reed Diversion Dam) and Lake Cle Elum and upstream tributaries for steelhead to spawn in. Will anadromy be the primary life history observed or will residency predominant?

The following scenarios occurring outside of the Yakima River basin will be modeled:

- Water flow scenarios affecting the survival of smolts from Roza to McNary dams (Sean Gross, NOAA Fisheries, pers. comm.).
- Variation in SARs due to ocean conditions, such as pre- vs. post-PDO shift in 1999 and expected survival in a warmer ocean with different upwelling and other patterns due to climate change (Chapter 3 of this document).
- Changes in smolt outmigration timing, affecting steelhead SARs based on smolt arrival time at Bonneville Dam (J. Gosselin, Columbia Basin Research, unpublished data).

- Steelhead smolt downstream migration survival through the Columbia River dams due to different dam spills scenarios assessed with the COMPASS model (COMPASS 2007; Zabel et al. 2008; Chapter 4.b of this document).
- Changes in smolt survival through the Columbia River estuary as a result of changes in avian predation in the Columbia River estuary due to changes in management actions (Chapter 6.b of this document).
- Changes in smolt survival through the Columbia River estuary as a result of changes in pinniped predation due to changes in management actions (Chapter 6.a of this document).

We are also currently working to code the stochastic population dynamics life-cycle model specific to the Yakima River basin (Courter et al. 2009) in the program R (R development core team 2015), giving us the capability and flexibility to run sensitivity analyses and a variety of scenarios that cannot be done in Excel (the platform in which this model currently exists). We will then integrate this model with the state-dependent life-cycle model (Satterthwaite et al. 2009; 2010) and the life-cycle matrix model (McClure et al. 2007; Zabel et al. 2013) in the program R. Males and females will be modeled separately because of their differential expression of anadromy (Hendry et al. 2004; Jonsson and Jonsson 1993).

Once a complete model is available in the program R, we will need to “ground truth” it with known data. Specifically, we will parameterize the model with known data to confirm that it predicts the number of resident and anadromous individuals that have actually been observed. We will also run sensitivity analyses of the model to understand which life stages drive variation in the rates of anadromy and residency along with abundance trends. We will also assess confounding among parameters with these sensitivity analyses. Specifically, SARs and proportion of steelhead produced by crosses are likely confounded. Additional sensitivity analyses are needed to see what other relationships are confounded. We will assess what data would be needed to inform the confounded relationships.

We will then run the model under the various different scenarios described above. Model results will inform management actions, including those taken as part of the Yakima River Biological Opinion, the Yakima River Integrated Water Resource Management Plan, and the Climate Adaptation Plan for the Territories of the Yakama Nation.

Ultimately, we would like to create a model that can be used for other *O. mykiss* populations beyond the Upper Yakima River and other Yakima River basin populations that also contain both anadromous and resident individuals. However, it is important to consider the basic environmental setting of the various interior Columbia River basin streams and rivers where *O. mykiss* populations reside. Few of these settings are similar to the Upper Yakima River basin, which encompasses major tributaries and main stem reaches representing a range of environmental settings. Freshwater habitats for most other interior Columbia River basin *O. mykiss* populations do not have the extensive main stem habitats with relatively long annual periods of temperature conditions supportive of juvenile *O. mykiss* growth. Instead, most of these populations are more like the Naches River or Toppenish Creek in the Yakima River basin. Given the functional relationships between habitat conditions and *O. mykiss* capacities and stage transitions, the potential for relatively strong resident populations may be substantially less in other populations than in the Upper Yakima River. In addition, interior Columbia River basin steelhead populations occur across a wide range of elevations. Higher-elevation populations in the Snake River ESU, for example, are likely subject to substantially shorter growing seasons and more severe overwintering conditions. Thus, they are also less likely to have strong a strong resident trout component.

Literature cited

Benjamin, J.R., Connolly, P.J., Romine, J.G., and Perry, R.W. 2013. Potential effects of changes in temperature and food resources on life history trajectories of juvenile *Oncorhynchus mykiss*. Trans. Am. Fish. Soc. **142**(1): 208-220.

Bley, P.W., and Moring, J.R. 1988. Freshwater and ocean survival of Atlantic salmon and steelhead: a synopsis Biological report 88 (9). Prepared for U. S. Fish and Wildlife Service.

Bond, M.H., Hayes, S.A., Hanson, C.V., and MacFarlane, R.B. 2008. Marine survival of steelhead (*Oncorhynchus mykiss*) enhanced by a seasonally closed estuary. Can. J. Fish. Aquat. Sci. **65**: 2242-2252.

Bovee, K.D., Lamb, B.L., Bartholow, J.M., Stalnaker, C.B., Taylor, J., and Henriksen, J. 1998. Stream habitat analysis using the instream flow incremental methodology Information and Technology Report USGS/BRD-1998-0004. U. S. Geological Survey, Biological Resources Division.

Busack, C.A., Frye, C., Kassler, T., Pearsons, T., Schroder, S.L., Von Bargen, J., Young, S.F., Knudsen, C.M., and Hart, G. 2005. Yakima/Klickitat fisheries project genetic studies Annual Report. Prepared for the U.S. Department of Energy, Bonneville Power Administration, Project number 1995-063-25.

COMPASS. 2007. Modeling evaluating the effects of proposed hydropower actions Available at: http://www.salmonrecovery.gov/biological_Opinions/FCRPS/biop_remand_2004/Docs/2007/draft_prop_action/Biological%20Analysis_052107_Final[1].pdf.

Conley, A., Freudenthal, J., Lind, D., Mees, P., and Visser, R. 2009. Yakima steelhead recovery plan. Yakima Basin Fish and Wildlife Recovery Board.

Courter, I., Justice, C., and Cramer, S. 2009. Flow and temperature effects on life history diversity of *Oncorhynchus mykiss* in the Yakima River basin. Cramer Fish Sciences, Gresham, OR.

Courter, I.I., Child, D.B., Hobbs, J.A., Garrison, T.M., Glessner, J.J.G., and Duery, S. 2013. Resident rainbow trout produce anadromous offspring in a large interior watershed. Can. J. Fish. Aquat. Sci. **70**(5): 701-710.

Courter, I.I., Frederiksen, C.R., Teply, M.E., Cramer, S.P., Justice, C., Temple, G.M., Thrower, F.P., and Child, D.B. 2010. Influence of resident rainbow trout on abundance of steelhead in the upper Yakima River basin.

Ebersole, J.L., Wigington, P.J., Baker, J.P., Cairns, M.A., Church, M.R., Hansen, B.P., Miller, B.A., LaVigne, H.R., Compton, J.E., and Leibowitz, S.G. 2006. Juvenile coho salmon growth and survival across stream network seasonal habitats. Trans. Am. Fish. Soc. **135**(6): 1681-1697.

Frederiksen, C.R., Fast, D.E., Bosch, W.J., and Temple, G.M. 2014. Yakima Steelhead VSP Project: Yakima River Steelhead Population Status & Trends Monitoring, 10/15/2011 - 10/14/2013 Annual Report, 2010-030-00. Yakama Nation Fisheries and Washington Department of Fish and Wildlife.

Grant, J.W.A., and Kramer, D.L. 1990. Territory size as a predictor of the upper limit to population density of juvenile salmonids in streams. Can. J. Fish. Aquat. Sci. **47**(9): 1724-1737.

Hayes, S.A., Bond, M.H., Hanson, C.V., Freund, E.V., Smith, J.J., Anderson, E.C., Ammann, A.J., and MacFarlane, R.B. 2008. Steelhead growth in a small central California watershed: upstream and estuarine rearing patterns. Trans. Am. Fish. Soc. **137**: 114-128.

Hendry, A.P., Bohlin, T., Jonsson, B., and Berg, O.K. 2004. To sea or not to sea? Anadromy versus non-anadromy in salmonids. *In* Evolution illuminated: salmon and their relatives. *Edited by* A.P. Hendry and S.C. Stearns. Oxford University Press, Oxford. pp. 92-125.

Hockersmith, E., Vella, J., and Stuehrenberg, L. 1995. Yakima River radio-telemetry study of rainbow trout, annual report 1993 U. S. Department of Energy, Bonneville Power Administration, Divison of Fish and Wildlife, Project number 89-089, Contract number DE-AI79-BP00276.

Isaak, D.J., Wenger, S.J., Peterson, E.E., Ver Hoef, J.M., Hostetler, S., Luce, C.H., Dunham, J.B., Kershner, J., Roper, B.B., Nagel, D., Horan, D., Chandler, G., Parkes, S., and Wollrab, S. 2011. The NorWeST stream temperature database and model for mapping thermal habitats and predicting vulnerability of aquatic species to climate change across the Great Northern Landscape Conservation Cooperative Great Northern Landscape Conservation Cooperative Grant. U.S. Fish and Wildlife Service.

Isaak, D.J., Wollrab, S., Horan, D., and Chandler, G. 2012. Climate change effects on stream and river temperatures across the northwest U.S. from 1980 – 2009 and implications for salmonid fishes. Clim. Change **113**: 499=-524.

Jonsson, B., and Jonsson, N. 1993. Partial migration: niche shift versus sexual maturation in fishes Rev. Fish Biol. Fish. **3**: 348-365.

Karp, C., Larrick, W., Johnston, M., and Dick, T. 2009. Steelhead movements in the upper Yakima River basin, fall 2002-spring 2006. United States Bureau of Reclaimation, Denver, CO.

Kendall, N.W., McMillan, J.R., Sloat, M., R., Buehrens, T.W., Quinn, T.P., Pess, G.R., Kuzishchin, K.V., McClure, M.M., and Zabel, R.W. 2015. Anadromy and residency in steelhead and rainbow trout (*Oncorhynchus mykiss*): a review of the processes and patterns. Can. J. Fish. Aquat. Sci. **72**: 319-342.

Kock, T.J., Perry, R.W., and Hansen, A.C. 2016. Survival of juvenile Chinook salmon and coho salmon in the Roza Dam fish bypass and in downstream reaches of the Yakima River, Washington, 2016. U. S. Geological Survey.

Mangel, M., and Satterthwaite, W.H. 2008. Combining proximate and ultimate approaches to understand life history variation in salmonids with application to fisheries, conservation, and aquaculture. Bull. Mar. Sci. **83**(1): 107-130.

McClure, M., Cooney, T., Baldwin, C., Carmichael, R., Hassemer, P., Howell, P., Petrosky, C., Schaller, H., Spruell, P., Utter, F., and Zabel, R.W. 2007. Assessing the impact of environmental conditions and hydropower on population productivity for interior Columbia River stream-type Chinook and steelhead populations Interior Columbia Technical Recovery Team

McMillan, J.R., Katz, S.L., and Pess, G.R. 2007. Observational evidence of spatial and temporal structure in a sympatric anadromous (winter steelhead) and resident rainbow trout mating system on the Olympic Peninsula, Washington State. Trans. Am. Fish. Soc. **136**(3): 736-748.

Mills, J.S., Dunham, J.B., Reeves, G.H., McMillan, J.R., Zimmerman, C.E., and Jordan, C.E. 2012. Variability in expression of anadromy by female *Oncorhynchus mykiss* within a river network. Environ. Biol. Fishes **93**: 505-517.

Murdoch, A.R. 1995. The effects of spawning bridgelip suckers (*Catostomus columbianus*) on the reproductive success of rainbow trout (*Oncorhynchus mykiss*) in Umtanum Creek, Washington, Central Washington University, Ellensburg, WA.

Neeley, D. 2012. Prosser-Passage Estimation Issues. Yakama Nation Fisheries, Toppenish, WA.

Pearsons, T.N., McMichael, G.A., Bartrand, E.L., Fisher, M., Monahan, J.T., Leider, S.A., Strom, G.R., and Murdoch, A.R. 1993. Yakima species interactions study, 1992 annual report. Washington Department of Fish and Wildlife.

Pearsons, T.N., Phelps, S.R., Martin, S.W., Bartrand, E.L., and McMichael, G.A. 2007. Gene flow between resident and anadromous rainbow trout in the Yakima River basin: ecological and genetic evidence, pp. 56-64.

Quinn, T.P., and Peterson, N.P. 1996. The influence of habitat complexity and fish sire on over-winter survival and growth of individually marked juvenile coho salmon (*Oncorhynchus kisutch*) in Big Beef creek, Washington. Can. J. Fish. Aquat. Sci. **53**(7): 1555-1564.

R development core team. 2015. R: a language and environment for statistical computing. R Foundation for Statistical Computing, Vienna.

Roff, D.A. 1992. The evolution of life histories: theory and analysis. Chapman and Hall, New York, NY.

Ruzycki, J.R., Clarke, L.M., Flesher, M.W., Carmichael, R.W., and Eddy, D.L. 2009. Performance of progeny from steelhead and rainbow trout crosses. Oregon Department of Fish and Wildlife, Fish Research and Development, NE Region.

Satterthwaite, W.H., Beakes, M.P., Collins, E.M., Swank, D.R., Merz, J.E., Titus, R.G., Sogard, S.M., and Mangel, M. 2009. Steelhead life history on California’s Central Coast: insights from a state-dependent model. Trans. Am. Fish. Soc. **138**: 532-548.

Satterthwaite, W.H., Beakes, M.P., Collins, E.M., Swank, D.R., Merz, J.E., Titus, R.G., Sogard, S.M., and Mangel, M. 2010. State-dependent life history models in a changing (and regulated) environment: steelhead in the California Central Valley. Evol. Appl. **3**: 221-243.

Satterthwaite, W.H., Hayes, S.A., Merz, J.E., Sogard, S.M., Frechette, D.M., and Mangel, M. 2012. State-dependent migration timing and use of multiple habitat types in anadromous salmonids. Trans. Am. Fish. Soc. **141**(3): 781-794.

Schroeder, R.K., and Smith, L.H. 1989. Life history of rainbow trout and effects of angling regulations in the Deschutes River, Oregon Information report (fish) 89-6. Oregon Department of Fish and Wildlife, Portland, OR.

Shapovalov, L. 1967. Biology and management of steelhead trout in California Inland Fisheries Administrative Report 67-7. California Department of Fish and Game, Sacramento, CA.

Shapovalov, L., and Taft, A.C. 1954. The life histories of the steelhead rainbow trout (*Salmo gairdneri gairdneri*) and silver salmon (*Oncorhynchus kisutch*) with special reference to Waddell Creek, California, and recommendations regarding their management. Fish Bulletin Fish Bulletin 98.

Smith, R.W., and Griffith, J.S. 1994. Survival of rainbow trout during their first winter in the Henrys Fork of the Snake River, Idaho. Trans. Am. Fish. Soc. **123**(5): 747-756.

Sullivan, K., Martin, D.J., Cardwell, R.D., Toll, J.E., and Duke, S. 2000. An analysis of the effects of temperature on salmonids of the Pacific Northwest with implications for selecting temperature criteria. Sustainble Ecosystems Institute, Portland, OR.

Temple, G.M., Fifield, R., Steele, R., Frederiksen, C., Mays, Z., and Seamons, T. 2016. Yakima Steelhead VSP Project: Resident/Anadromous Interactions Monitoring, 1/1/2016 – 12/31/2016. Washington Department of Fish and Wildlife and Yakama Nation Fisheries.

Thorpe, J.E., Mangel, M., Metcalfe, N.B., and Huntingford, F.A. 1998. Modelling the proximate basis of salmonid life-history variation, with application to Atlantic salmon, *Salmo salar* L. Evol. Ecol. **12**: 581-599.

Thrower, F.P., Hard, J.J., and Joyce, J.E. 2004. Genetic architecture of growth and early life-history transitions in anadromous and derived freshwater populations of steelhead. J. Fish Biol. **65**(Supplement A): 286-307.

Thrower, F.P., and Joyce, J.E. 2004. Effects of 70 years of freshwater residency on survival, growth, early maturation, and smolting in a stock of anadromous rainbow trout from southeast Alaska. Am. Fish. Soc. Symp. **44**: 485-496.

Ward, B.R., Slaney, P.A., Facchin, A.R., and Land, R.W. 1989. Size-biased survival in steelhead trout (*Oncorhynchus mykiss*): back-calculated lengths from adults' scales compared to migrating smolts at the Keogh River, British Columbia. Can. J. Fish. Aquat. Sci. **46**: 1853-1858.

Wydoski, R.S., and Whitney, R.R. 2003. Inland fishes of Washington. University of Washington Press, Seattle, WA.

Zabel, R.W., Cooney, T., Jordan, C.E., Carmichael, R.W., Jonasson, B.C., Sedell, E.W., Hoffnagle, T.L., White, J.L., Beasley, C., Nahorniak, M., McGrath, C., Benjamin, J.R., Jorgensen, J., Murdoch, A.R., Cram, J., Paulsen, C., Crozier, L.G., Kendall, N.W., Connor, W.P., Young, W., Perry, R.W., Tiffan, K.F., Newsom, M., Bellmore, R., Snow, C.G., Lessard, R.B., Justice, C., Courter, I., Frederiksen, C.R., Buhle, E., Fullerton, A.H., Moran, P., Van Doornik, D., Ward, E.J., and Scheuerell, M.D. 2013. Life-cycle models of salmonid populations in the interior Columbia River Basin.

Zabel, R.W., Faulkner, J., Smith, S.G., Anderson, J.J., Van Holmes, C., Beer, N., Iltis, S., Krinke, J., Fredricks, G., Bellerud, B., Sweet, J., and Giorgi, A. 2008. Comprehensive passage (COMPASS) model: a model of downstream migration and survival of juvenile salmonids through a hydropower system. Hydrobiologia **609**: 289-300.

Zabel, R.W., Scheuerell, M.D., McClure, M., and Williams, J.G. 2006. The interplay between climate variability and density dependence in the population viability of Chinook salmon. Conserv. Biol. **20**: 190-200.

Chapter 9.f. Catherine Creek Spring Chinook Life Cycle Model

Peter McHugh[1], Casey Justice[2], Seth White[2], Dale McCullough[2], and Nicolaas Bouwes[1]

[1]Eco Logical Research, Inc., Logan, UT

[2]Columbia River Inter-Tribal Fish Commission, Portland, OR

Introduction

Report overview

This document provides an overview of progress towards a life cycle model (LCM) based assessment of restoration opportunities within the Catherine Creek (CC) and Upper Grande Ronde River (UGR) watersheds. The specific goals of our project were to (1) parameterize two Chinook salmon (*Oncorhynchus tshawytscha*) LCMs, one for Catherine Creek and the other for the Upper Grande Ronde River (UGR) and (2) extend UGR and CC LCMs to assess the effects of several different habitat restoration treatments, varying in specificity, on the performance of model populations. Through March of 2017, we made progress in several areas:

(1) We reviewed available demographic data for the UGR and CC populations and successfully parameterized LCMs for both populations. However, we present only CC results here as an initial draft.

(2) We made LCM code modifications to support the modeling of the hatchery supplementation strategies currently in place for CC and UGR Chinook salmon. We initially hoped to avoid modeling hatchery programs; however, doing so was necessary because preliminary analyses projected rapid extinction with only natural production regardless of initial abundance conditions. Additionally, while our LCM allowed for the

modeling of simple supplementation scenarios, Catherine Creek's 'sliding scale' style supplementation management necessitated coding changes.

(3) We simulated population performance under seven different scenarios that consider alternative future water temperature regimes arising from restoration of key habitat conditions (channel width and potential natural vegetation) under current and future climate change projections modeled by Justice et al. (2017).

In the following pages, we review progress on items 1-3 in detail, summarize findings in general terms, and end with several suggestions for further developing this work.

Relevance to ODFW-NOAA life cycle modeling in the Upper Grande Ronde basin

This work is intended as an alternative model in collaboration with the ODFW-NOAA spring Chinook Salmon life cycle model for the upper Grande Ronde basin (Chapter 9.a) in the interest of testing multiple approaches to predicting recovery benefits to restoration actions. We foresee selecting a short list of common restoration scenarios and evaluating the degree of similarity in outcomes, in terms of benefit to fish, of the different models. In the same way that AMIP supports the development of various LCM frameworks, we see benefit in applying multiple LCMs for the same fish population to increase our understanding of how model differences affect interpretations, and ultimately management decisions.

Modeling framework

Life cycle modeling framework

Chinook salmon population performance under alternative habitat scenarios was assessed using a life cycle modelling framework. A life cycle model (LCM) is simply a mathematical representation of a Pacific salmon's life history (**Figure 1**) that, given relevant inputs (e.g., stage-specific productivity, capacity), can be used to simulate population dynamics. LCMs are particularly well suited for addressing habitat scenarios because they can simulate population trajectories as a function of the same demographic parameters that management aims to modify (e.g., summer rearing capacity, overwinter survival, etc.), all while considering uncertainty in model inputs. More specifically, the LCM used here (i.e., McHugh et al. In Press) is a stage-structured, stochastic projection model, adapted from Sharma et al. (2005) and implemented in the R statistical computing language (R Core Team 2014). This LCM propagates cohorts across a complete life cycle according to a series of stage-specific Beverton-Holt 'spawner' (N_i) and 'recruit' (N_{i+1}) relationships (after Moussalli and Hilborn 1986), each of which is governed by stage-specific capacity (c_i) and productivity (p_i, maximum recruits per spawner) parameters,

Equation 1. $N_{i+1} = \frac{N_i}{\frac{1}{p_i}+\frac{1}{c_i}N_i}$

Although this functional form implies that density dependence occurs at all life stage transitions, density independent assumptions can also be modeled here simply by setting capacity to an infinitely large value and using empirical estimates of survival (S_i) as the productivity input (p_i). Otherwise, realized survival ($S_i = N_{i+1} / N_i$) is a function of both the capacity and productivity for a given population or segment thereof. Note that these parameters form the basis for representing management scenarios; we discuss parameter sourcing in further detail below (see *Base model parameterization*).

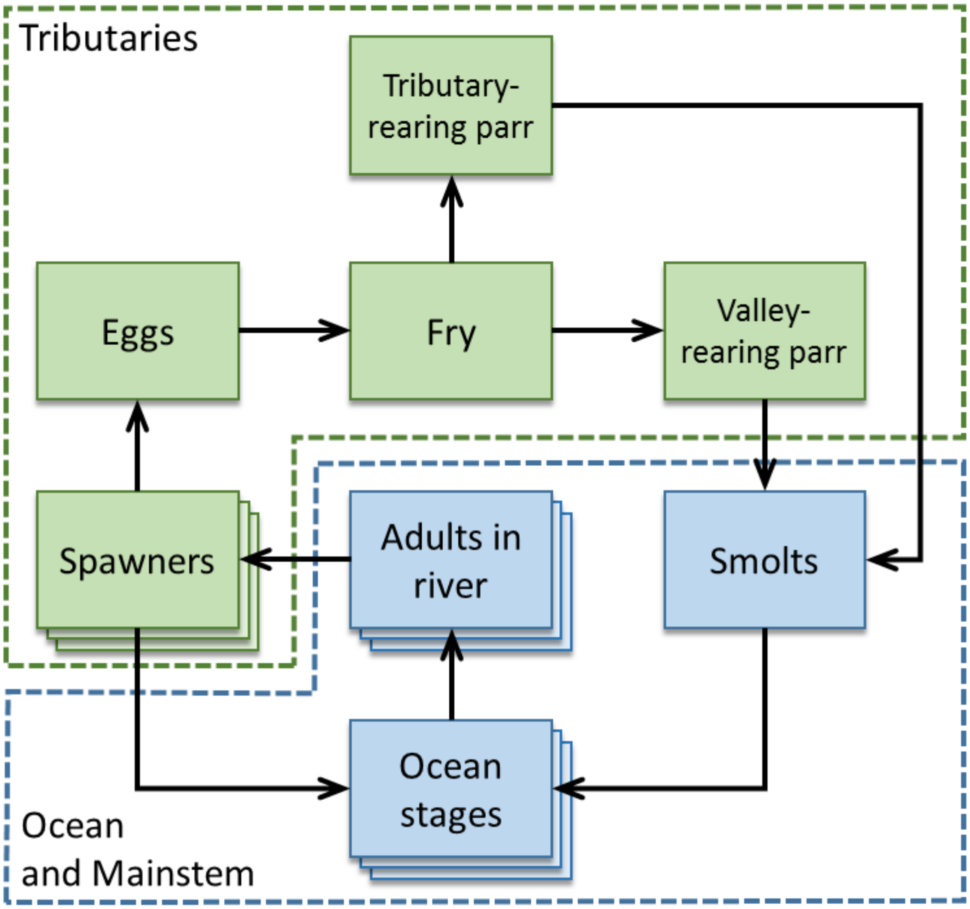

Figure 1. Conceptual diagram of the life cycle model (LCM) framework used to assess restoration scenarios in Catherine Creek. Stacked boxes represent life stages for which multiple ages exist and are tracked accordingly. In our LCM, parr can 'choose' to migrate downstream and overwinter in the Grande Ronde Valley ('Valley') or remain in the upper mainstem and tributaries of Catherine Creek ('Tributary'). Otherwise, the LCM's smolts are enumerated at Lower Granite Dam (LGD), where 'ocean stages' begin and are modeled via LGD-to-LGD smolt-to-adult return rates.

Study system overview

For modeling purposes, Catherine Creek Chinook Salmon express two life history trajectories which occur over three different spatial strata (**Figure 1**). All fish spawn in late summer, hatch in spring, and rear through the bulk of their first summer out of the gravel within the upper mainstem and tributaries of Catherine Creek, above the primary location at which state and tribal agencies enumerate abundance via ‘fish in-fish out’ sampling (i.e., juvenile trap, adult weir). In the autumn of their first year, parr diverge into one of two life histories: parr either (a) move down river and overwinter in the Grande Ronde Valley (‘Valley’ life history), before moving downstream towards Lower Granite Dam (LGD) as smolts in the spring, or (b) remain in the upper mainstem/tributaries of Catherine Creek (‘Tributary’ life history) for the winter, and migrate to LGD as smolts in the subsequent spring. Thereafter, both life history pathways begin the mainstem–ocean segment of their life cycle before returning in 1 to 3 years to the upper mainstem/tributary stratum as prespawners/spawners.

Base model parameterization

In most LCM applications, capacity and productivity parameters appropriate for the species or system of interest are difficult to obtain, as these parameters are rarely estimated as part of routine monitoring programs. Here, however, a combination of entities monitors populations and habitats in such a way that estimating these parameters using population-specific data or models is possible; the Oregon Department of Fish and Wildlife (ODFW), Confederated Tribes of Umatilla Reservation (CTUIR), Columbia River Inter-Tribal Fish Commission (CRITFC), and other parties, collect the data needed to estimate spawner, parr, and smolt abundance and/or survival each year. Additionally, as part of the Columbia Habitat Monitoring Program (CHaMP) and Integrated Status and Effectiveness Monitoring Program (ISEMP), population-specific habitat data are collected and analyzed in such a way that permits the estimation of adult and juvenile carrying capacities as a function of current habitat conditions. More specifically, both egg-to-parr (late summer) and parr-to-smolt (at Lower Granite Dam, LGD) survival inputs were based on estimates generated by ODFW’s ‘Early Life Histories’ monitoring program. ‘Ocean’ (i.e., smolts passing LGD downstream to adults passing LGD upstream) survival and adult maturation schedules were estimated using age-specific smolt-to-adult return rate estimates (SARs) generated by the Fish Passage Center (McCann et al. 2016), similar to those used in B. Lessard's LCM (McCann et al. 2016)[1]. We additionally included carrying capacity terms for two freshwater tributary life stages, summer parr and adult spawners (expressed in terms of eggs), respectively: (a) juvenile capacity was estimated using an empirical model that predicts parr carrying capacity as a function of habitat variables (i.e., a quantile random forest model; K. See, unpublished manuscript), and (b) adult carrying capacity was predicted using habitat suitability index models after McHugh et al. (In Press). Where necessary, other LCM parameters were informed by literature values where necessary. Complete details on our base/status quo (scenario 'Curr' in **Table 1**) Catherine Creek LCM parameterization, including assumptions about stochasticity, are presented in **Appendix A**.

Beyond the basic numerical and life history parameter details associated with our LCM, other parameterization decisions were made to represent population dynamics as accurately as possible in space and time given the data available, including:

(1) Although the LCM allows fish to exhibit separate Tributary and Valley life history trajectories, and at the frequency with which they occur in sampling data, the current model implementation assumes they share a similar overwinter survival in both places. In other words, the current life history trajectory construct is simply a placeholder for future evaluation and comparisons of spatially distinct scenarios affecting overwintering

---

[1] Note that here we model SARs assuming a single 'average' outmigrant experience and make no attempt to distinguish transported vs. in-river migrants; thus, our assumption is that conditions during the 2001-2014 smolt migration years provide reasonable insight on average future mainstem/ocean conditions.

survival, and the LCM preserves total survival from the summer parr stage to LGD smolts in a manner consistent with available data.

(2) Upon return, adults are recognized perfectly by production type and passed over the weir or taken to the hatchery according to the Catherine Creek supplementation program's sliding scale rule set (see **Appendix B**). In practice, weir management is more difficult due to the fact that collection decisions are made in real time with imperfect knowledge about the total run size. Note additionally that supplementation is handled in the model through the annual release of 150,000 smolts (less if broodstock needs are not met in year y - 2, see **Appendix B**) and it is assumed that supplementation fish home perfectly back to the natal basin.

Management scenarios

We modeled several scenarios for Catherine Creek Chinook (**Table 1**). First, we modeled the population under 'current conditions', i.e., based on recent averages for demographic parameters (**Appendix A**). This scenario provides insight on performance under a 'do nothing' case and also provides an opportunity to verify that population dynamics are consistent with those of the actual CC Chinook population. In addition to the base case ('Curr'), we considered six different scenarios based on the recent temperature modeling work of Justice et al. (2017). Specifically, we modeled the population-level effects of alternative temperature/habitat futures ranging from a scenario that considered the effects of global warming, manifested as increased water temperature and decreased streamflow, in the absence and presence of habitat restoration (i.e., scenarios 'Clim', 'ClimVeg', 'Clim…', etc.) to scenarios that considered the effects of riparian restoration under current thermal conditions (e.g., scenario 'PNV'). Two scenarios ('WidPNV' and 'ClimVegWid') included narrowing stream widths to their historical condition as estimated from 19th century General Land Office surveys (White et al. 2017). Benefits/changes were expressed via a simple proportional change in summer parr rearing capacity, based on the abundance changes that Justice et al. (2017) predicted under each scenario. Note also that changes are imposed at the outset of simulations; thus scenarios/results do not account for the differing time scales required for changes to be realized in practice.

Beyond habitat restoration, we explicitly modeled the CC hatchery supplementation strategy according to the ‘sliding scale’ weir management system described in Carmichael et al. (2011) and in **Appendix B**. In brief, the passage (to spawning grounds) or collection (for spawning in hatchery) of hatchery (i.e., adult returns from releases of supplementation smolts) and natural adults reaching the CC weir are managed to maintain the overall genetic integrity of the population while offering the abundance-boosting benefits of hatchery spawning. Thus, the adult trap is used to manage three aspects of escapement that are pertinent to supplementation goals: (i) $P_{NOS\text{-}R}$ (i.e., the proportion of the total natural-origin returns that is retained for the hatchery), (ii) P_{HOS} (i.e., the proportion of natural spawners that is of hatchery origin), and (iii) P_{NOB} (i.e., the proportion of hatchery broodstock/egg-take that is of natural origin). Although our LCM could be used to look at the effects of varying supplementation strategies, here we modeled all scenarios assuming the same operation, which is described in **Appendix B**. Thus, although it is embedded herein as a ‘management strategy,’ it is consistent across each of the seven scenarios described in **Table 1**.

Lastly, although harvest scenarios can also be addressed using our model, we do not explicitly model harvest management here. This modeling decision is reasonable for ocean fisheries because they minimally affect interior Columbia Basin spring Chinook stocks. However, future analyses should consider whether the differential impact of mark-selective freshwater sport and net fisheries on hatchery (i.e., the basis for SAR estimation; **Appendix A**) relative to natural fish affects the relative performance of model populations across habitat and/or supplementation scenarios.

Table 1. Scenarios modeled using the CC LCM, after Justice et al. (2017). For LCM inputs, each scenario is represented as a proportional increase or decrease in summer parr rearing capacity.

Scenario Abbreviation	Description	Proportional Δ in Capacity
Curr	Baseline model calibrated using 2010 temperature, climate, vegetation, and hydrologic conditions	0.00
PNV	Vegetation across the entire model extent set to potential natural vegetation (PNV) cover and height, assuming climax conditions (i.e., 300-year cover and height).	0.61
HiPr	Vegetation in high priority areas set to PNV and other areas set to current conditions.	0.30
WidPNV	Channel width set to historic conditions and vegetation set to PNV.	0.67
Clim	Air temperature and streamflow set to 2080s climate projections.	-0.36
ClimVeg	2080s climate projections and vegetation set to potential cover and height at 75 years.	0.20
ClimVegWid	2080s climate projections, vegetation set to potential cover and height at 75 years, and channel width set to historic conditions.	0.37

Simulation specifications and performance metrics

To evaluate population performance across different scenarios (**Table 1**), we simulated dynamics for a 30-year period (i.e., 40 years, less a 10-year burn-in period) for N = 100 separate Monte Carlo iterations for each of the seven habitat scenarios. All models were initialized with 1,000,000 natural-origin fry and 150,000 hatchery-origin smolts. Supplementation releases were tracked as hatchery (H1) fish until their death; all progeny spawned in the wild were tracked and treated as being ‘natural’, regardless of parentage (e.g., H1 x H1 = natural, natural x H1 = natural, …). Although LCM results can be summarized in innumerable ways, here we focus on one metric, the natural-origin adult run size (‘abundance’) returning to CC. More specifically, abundance for each Monte Carlo trial in terms of the geometric mean natural-origin run size returning to the adult trap (i.e., pre-sliding scale management) for the modeled 30-year time horizon. Although we considered other summary metrics, such as quasi-extinction risk, we determined that this metric is less relevant here due to the continuously bolstering effect of the heavy supplementation component that was modeled for CC. Additionally, although a metric such as the proportion of fish spawning naturally that is of natural origin (i.e., P_{NOS}, or its corollary P_{HOS}) may be informative, in this case it is simply a mathematical rearrangement of our abundance metric given the consistent release of 150,000 hatchery-reared smolts. Beyond abundance, we conducted initial simulations using base model (scenario ‘Curr’) parameters to verify that the overall LCM properly captured freshwater productivity (i.e., smolts/spawner and its dependence on adult density), age structure (returning adult), SARs, and life history expression (i.e., Tributary vs. Valley) as intended.

Assumptions, limitations, and uncertainties

Although the CC and UGR population and habitat monitoring cases are perhaps best-case scenarios for LCM development (i.e., in temporal and stage coverage), simplifying assumptions were nonetheless made in order to make LCM-based scenario evaluations tractable. Perhaps the most noteworthy of these are the following:

1. First-generation hatchery fish and subsequently produced natural fish (and back-crosses thereof) have similar fitness. Although studies show fitness differences for wild- and

hatchery-origin fish, as well as captive-reared fish and parent wild populations spawning naturally, little information exists for representing these effects numerically in a LCM for spring Chinook in the Grande Ronde Basin in particular. Further, previous analyses suggest that where differences may exist, they are either inconsistent and on average compensating (e.g., the larger size of hatchery smolts offsets the acclimatization advantage held by natural fish). For these reasons, we used the same (species-specific) survival, fecundity, and maturation inputs for all fish, regardless of origin.

2. Habitat benefits are realized instantaneously. Whereas riparian revegetation and associated thermal benefits may take decades to centuries to be realized, here scenarios assume that they are realized at the outset of model runs. Thus, we provide a comparative view of population performance that has inherent uncertainty regarding if/how other pertinent factors might change in the future. At a minimum, future phases of modeling may wish to consider phasing in restoration-related benefits over appropriate time scales and perhaps consider alternative population metrics (e.g., does the population 'wink out' before benefits are established?).

Results and discussion

Overall, our base parameterization (i.e., 'Curr') appeared to accurately capture both the stage-specific (i.e., freshwater vs. marine) and total life cycle productivity of spring Chinook salmon in Catherine Creek—despite being developed from disparate and somewhat independent datasets in a piecewise fashion (e.g., freshwater survivals from long-term monitoring datasets vs. a habitat-based parr capacity model that predicts how many fish a basin can produce). For example, the relationship between smolts per female spawner in our modeled dataset closely mirrors the relationship evident in ODFW's 20-year sampling dataset (**Figure 1**). Similarly, natural-origin fish reaching CC were well within recent average values (i.e., those summarized in Carmichael et al. 2011). Given these patterns, we believe that our base LCM parameterization (‘Curr’) reasonably captured the demographics of the intended composite hatchery–natural population. Accordingly, we used this model, with the capacity modifications described in **Table 1** to assess the effects of the Justice et al. (2017) scenarios on total spawner abundance. While no attempt is made to infer meaning here, LCM simulation results (summarized in **Table 2** and **Figures 3-5**) illustrate the following:

- The proportional changes in juvenile carrying capacity reflecting the Justice et al. (2017) habitat scenarios translated into a natural origin adult abundance response that was similar on a rank-order basis. However, the magnitude of adult increase/decrease, while proportional to the juvenile capacity manipulation, was approximately 25-40% lower in magnitude. In other words, adult abundance did not respond on a one-to-one basis.
- Overall, the ‘PNV’ and ‘WidPNV’ scenarios, which assume maximum cooling of stream temperatures in the absence of climate change effects, showed the greatest response, with an approximate 30-40% increase in spawner abundance. On the other hand, ‘doing nothing’ vegetation/restoration wise in the face of the anticipated effects of climate change on conditions in CC (scenario ‘Clim’) translated into a 30% reduction in spawner abundance. Scenarios considering the positive effects of restoration and negative effects of climate change showed an intermediate response.
- Finally, a scenario testing the effects of ceasing all supplementation efforts after 20 years (all other inputs set to ‘Curr’ values), illustrated that natural origin extinction was a virtual certainty under current freshwater and marine capacity/productivity assumptions in the absence of hatchery support.

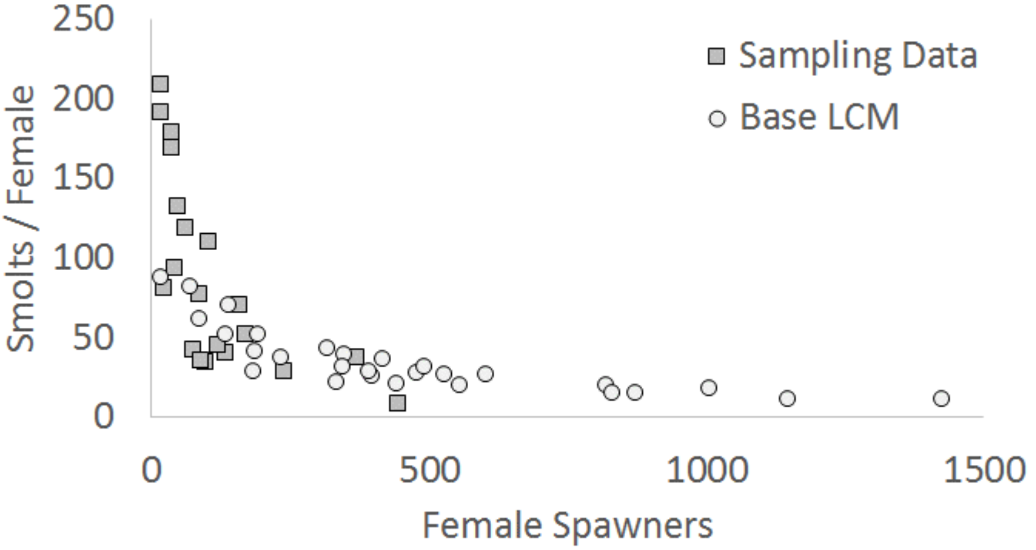

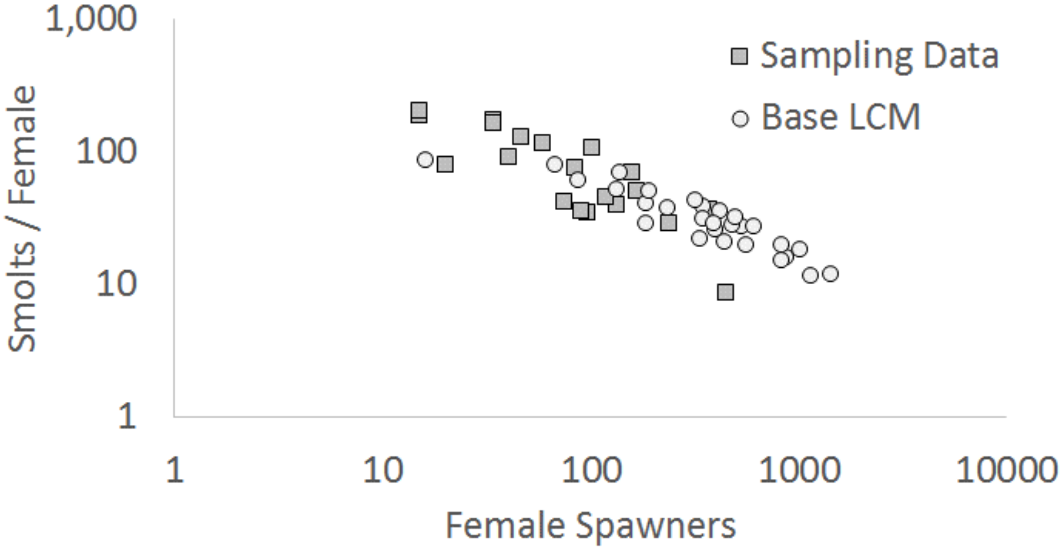

Figure 2. Comparison of simulated ('Base LCM') and observed ('Sampling Data') estimates of freshwater productivity relative to spawner abundance, plotted on untransformed (upper panel) and $\log_{10}$ (lower panel) axes. Sampling data are brood year 1993-2012 estimates of smolts per female, where smolts are in LGD equivalents and a "female spawner" assumes one female per redd, whereas LCM data are one realization of smolts and females from a 30-year simulation period given (a) sampling estimates of freshwater productivity, (b) Habitat model-based estimates of spawner and juvenile carrying capacities, and (c) Beverton-Holt-type density dependence (See **Appendix A** for further details on all).

Table 2. Summary statistics for natural-origin adult returns to the Catherine Creek adult trap from N = 100 Monte Carlo trials, by scenario. See Table 1 for scenario descriptions. Values represent summary statistics on the trial-level abundance metric (i.e., geometric mean abundance from each 30-year simulation).

Scenario Abbreviation	Mean	Median	SD	Range	Proportional Δ rel. to 'Curr'
Curr	81	95	21	42-125	0.00
PNV	114	133	26	68-233	0.39
HiPr	104	119	22	51-159	0.25
WidPNV	112	124	27	45-204	0.30
Clim	57	70	14	32-101	-0.27
ClimVeg	95	108	24	34-172	0.13
ClimVegWid	97	116	27	51-193	0.21

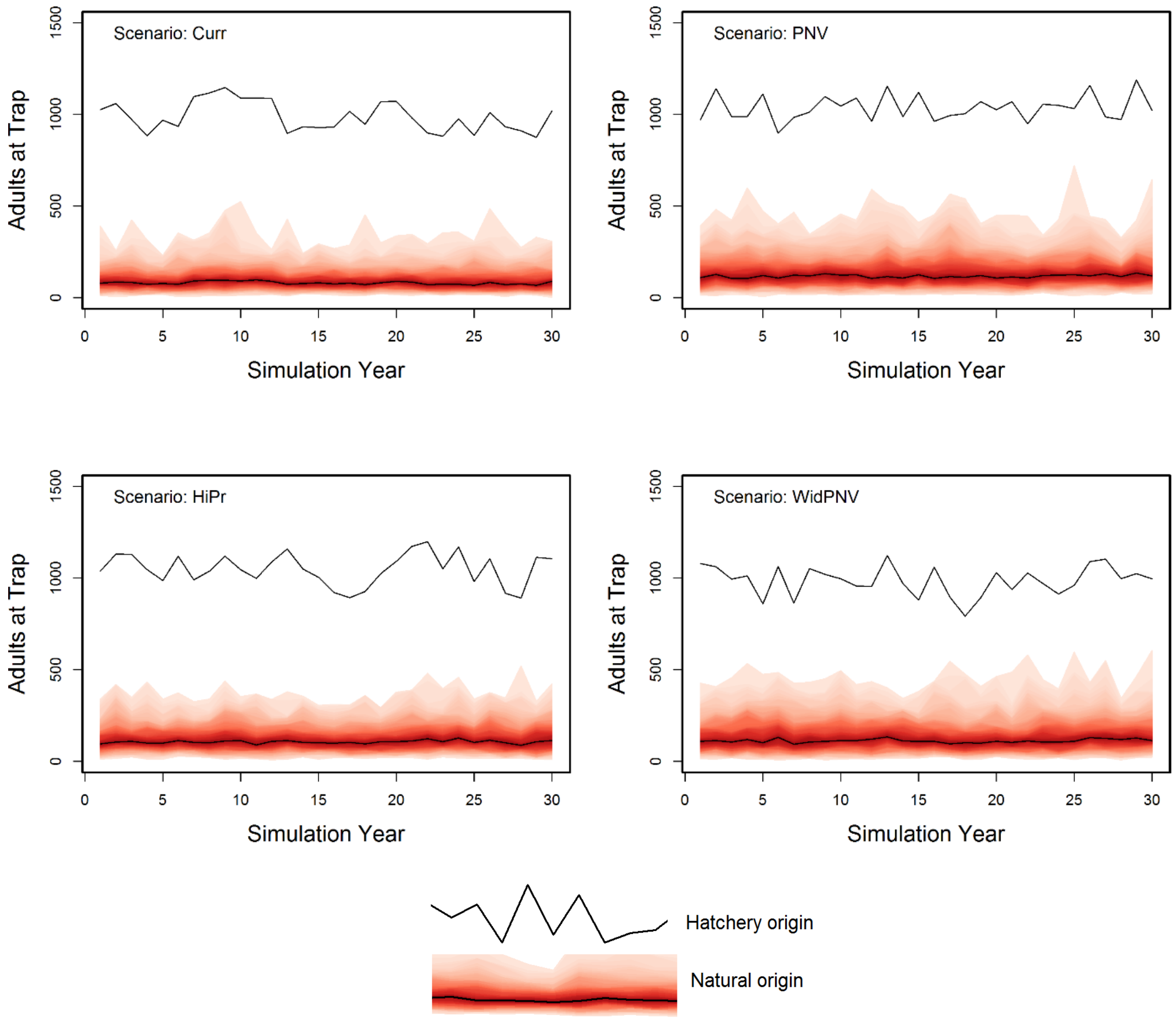

Figure 3. Time series density plots of natural-origin Chinook salmon returns to the Catherine Creek adult trap over a 30-year simulation for each of seven scenarios. In each plot, the higher thin black line is the median abundance of hatchery-origin returns whereas the second black line (flanked by red shading) represents the median abundance of natural-origin returns (i.e., natural-origin fish or progeny of H1 [or otherwise] spawning in wild); shading reflects the density of abundance observations across the N = 100 Monte Carlo trials.

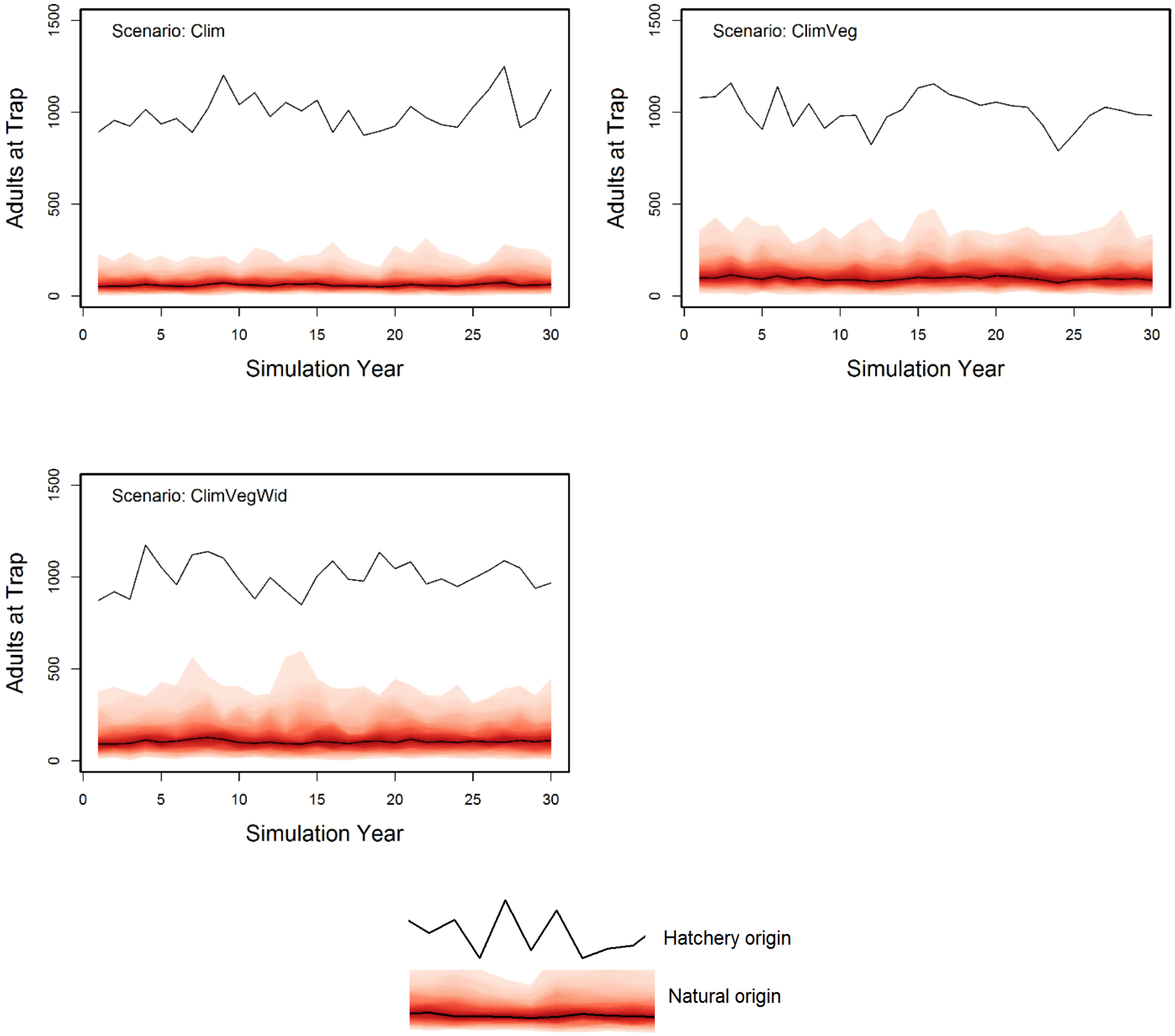

Figure 3. Continued.

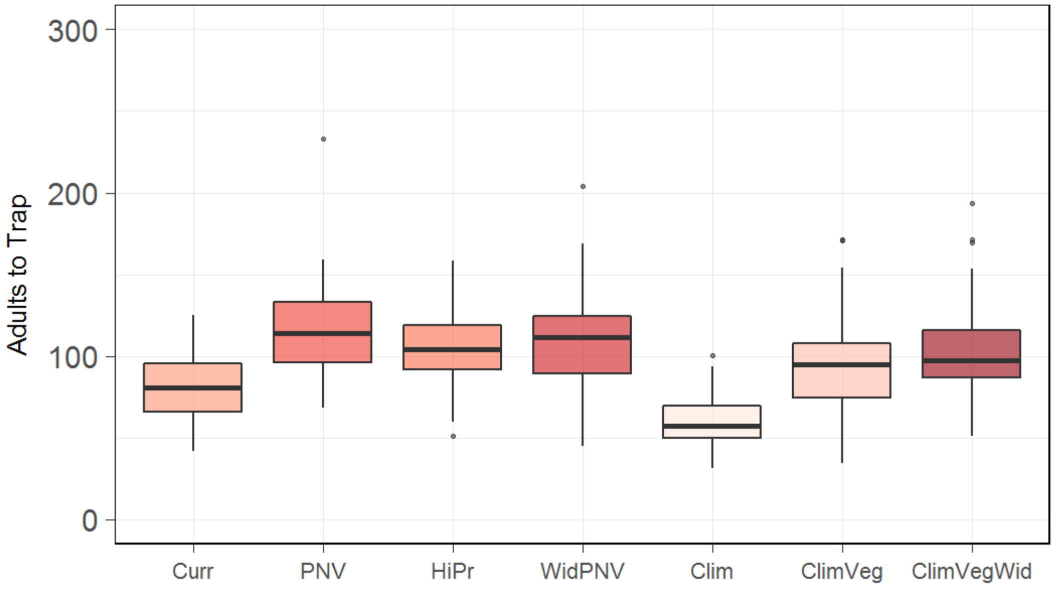

Figure 4. Box-and-whisker plots of natural-origin adult returns to the Catherine Creek adult trap, by scenario (based on N = 100 Monte Carlo trials). See Table 1 for scenario definitions.

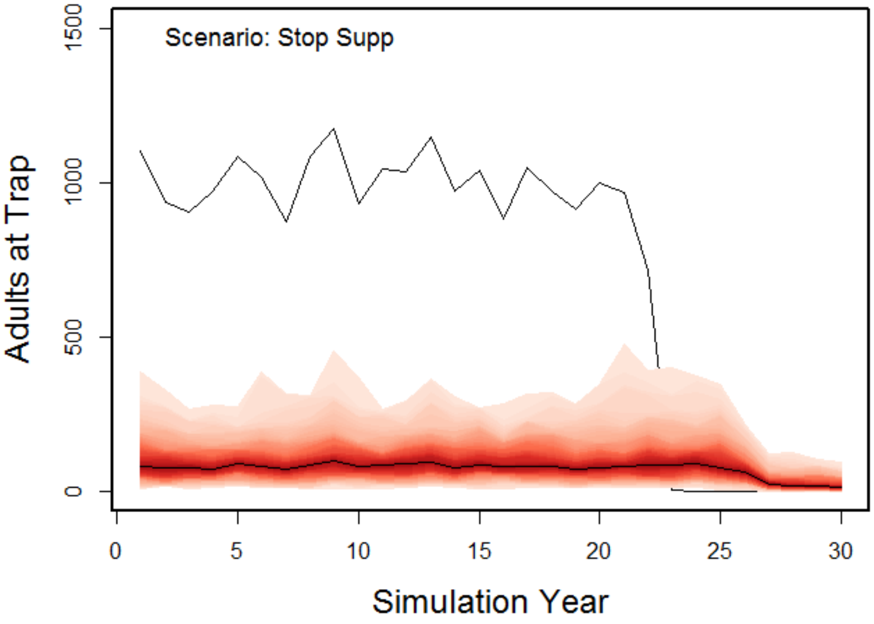

Figure 5. Time series density plots of natural-origin Chinook salmon returns to the Catherine Creek adult trap over a 30-year simulation for a scenario considering the effects of ceasing supplementation activities after 20 years under the base model parameterization (i.e., 'Curr' scenario). The higher thin black line is the median abundance of hatchery-origin returns whereas the second black line (flanked by red shading) represents the median abundance of natural-origin returns (i.e., natural-origin fish or progeny of H1 [or otherwise] spawning in wild); shading reflects the density of abundance observations across the N = 100 Monte Carlo trials.

Future considerations & next steps

Although the preceding analyses lend insight of immediate relevance, scenario inputs can be further refined so that the LCM framework's utility is maximized relative to the needs of stakeholders working to recover spring Chinook in the Grande Ronde Basin. Based on the work summarized here, future analyses and model updates might consider the following tasks:

(1) *Revisit the demographic parameters used to model tributary life stages*. Additional data sources may improve the accuracy of our base model parameterization. Additionally, although inputs selected here yielded results with qualitative similarities to monitoring data collected for the actual CC population, reviewing model inputs in collaboration with other basin partners will help achieve buy-in/agreement on future modelling results.

(2) *Expand the analysis to include the Upper Grande Ronde spring Chinook population*. As noted in the introduction, we had hoped to include UGR Chinook here and thus view this as a top priority for future phases of modeling. Thus, in concert with pursuing item 1 for CC Chinook, the data review associated with an updated/final parameterization should be pursued simultaneously for both the UGR and CC populations.

(3) *Consider alternative parameterizations for modeling the Justice et al. (2017) scenarios.* For example, here we represent scenarios via proportional changes in juvenile carrying capacity. Perhaps there is a basis for inferring a parr productivity benefit as well, or even a response for other life stages.

(4) *Consider modeling alternative supplementation scenarios*. For example, although this work includes a feedback between adult run sizes and the availability of smolts for release in subsequent years, no attempt was made to model a life span for

supplementation programs (e.g., phasing it out based on some time or abundance threshold).

(5) *As new data become available, consider modeling hatchery vs. natural survival differentials for various life stages*. Due to the highly integrated status of the supplementation programs, and due to other considerations (noted above), we assumed equivalent survival/fitness for hatchery and natural fish in the wild.

(6) *Integrate habitat modeling scenarios/hypotheses with model runs that address management actions affecting other life stages*. For instance, downstream passage scenarios could be developed to represent different smolt transportation protocols embodied in different SAR inputs (e.g., results of B. Lessard's chapter in McCann et al. 2016). Alternatively, temperature projections associated with different restoration scenarios could be used to inform growth predictions that influence smolt survival or SARs given size–survival linkages.

(7) *Do more MC trials.* While the relative findings here are adequate to gauge inter-scenario differences, additional MC iterations will minimize the influence of random variation on general patterns.

(8) *Consider other performance metrics*, in addition to abundance, that are relevant to heavily supplemented populations and reassess LCM results. Although natural-origin spawner abundance is perhaps the most relevant response, there are likely other metrics that will be useful to managers for assessing inter-scenario differences. Additionally, evaluations that consider how supplementation programs interact with other actions to shape spawner abundance (e.g., by turning hatchery programs 'on' or 'off', as in **Figure 5**)

(9) *Model the outcomes of more realistic restoration scenarios.* For example, access to private land is limited in some important portions of the basin and therefore restoration may not be possible in the near future. In addition, current restoration scenarios assumed that riparian restoration actions were implemented instantaneously across the whole stream network, when in reality, tree planting and fencing projects occur gradually over time as dictated by landowner permission and availability of funding. For the current modeling work, these issues were ignored because of the need to begin with a simple model. Future work could include evaluating the consequences of not being able to restore critical private lands, and where restoration is possible, applying a more realistic implementation schedule for restoration (e.g., average rates of riparian planting and protection).

(10) *Explore alternative fish-habitat model as a scalar to carrying capacity*. In this version of our model, carrying capacity of parr was adjusted proportionally according to the restoration scenarios in Justice et al. (2017). Future work will involve using an alternative fish-habitat model incorporating local- and landscape-scape habitat conditions, such as the structural equation model (SEM) presented in Chapter 2.a.

Acknowledgements

We thank Rishi Sharma and Tom Cooney, NOAA, and Gene Shippentower, CTUIR, for their direction and support for this work. Additionally, we thank Bob Lessard, CRITFC, as well as Joseph Feldhaus, Chris Horn, and Ted Sedell, ODFW, for sharing insights on population monitoring and demographic data for spring Chinook in the Grande Ronde Basin. Lastly, support from CHaMP and ISEMP program partners, particularly Matt Nahorniak, Carol Volk, Kevin See, and Matt Reimer, was instrumental in developing habitat model-based estimates of habitat capacity and variability. This work was funded under the Columbia Basin Fish Accords (BPA Project No. 2009-004-00).

References

Carmichael and coauthors. 2011. Catherine Creek spring Chinook salmon hatchery progam review. Oregon Department of Fish and Wildlife report to Lower Snake Comp. Program. https://www.fws.gov/lsnakecomplan/Reports/ODFW/Eval/CatherineCreekSpringChinookSalmonHatcheryReviewFINAL.pdf

Justice, C., White, S.M., McCullough, D.A., Graves, D.S., Blanchard, M.R., 2017. Can stream and riparian restoration offset climate change impacts to salmon populations? Journal of Environmental Management 188, 212-227.

Kareiva, P., Marvier, M., McClure, M., 2000. Recovery and management options for spring/summer chinook salmon in the Columbia River Basin. Science 290, 977-979.

McCann, J., and coauthors. 2016. Comparative Survival Study of PIT-tagged Spring/Summer/Fall Chinook, Summer Steelhead, and Sockeye. 2015 Annual Report BPA Contract # 19960200. http://www.fpc.org/documents/CSS/CSS_2016_Final.pdf

McHugh, P., and coauthors. In Press. Linking models across scales to assess the viability and restoration potential of a threatened population of steelhead (*Oncorhynchus mykiss*) in the Middle Fork John Day River, Oregon, USA. Submitted to Ecological Modelling.

Moussalli, E., and R. Hilborn. 1986. Optimal stock size and harvest rate in multistage life-history models. Canadian Journal of Fisheries and Aquatic Sciences 43(1):135-141.

R Core Team, 2014. R: A language and environment for statistical computing. R Foundation for Statistical Computing, Vienna, Austria.

Sharma, R., A. B. Cooper, and R. Hilborn. 2005. A quantitative framework for the analysis of habitat and hatchery practices on Pacific salmon. Ecological Modelling 183(2-3):231-250.

White, S. M., C. Justice, D. A. Kelsey, D. A. McCullough, and T. Smith. 2017. Legacies of stream channel modification revealed using general land office surveys, with implications for water temperature and aquatic life. Elem Sci Anth 5 (3):1-18. doi:10.1525/elementa.192.

Appendix A. Base parameterization and references for Catherine Creek spring Chinook salmon.

Input category	Life stage(s)	Parameter	Value(s)	Stochasticity	Source(s)	Comments
survival/ productivity	egg-to-parr	egg-to-summer parr productivity	0.26	target CV: 40%	B. Jonasson, ODFW, monitoring spreadsheet	Computed from ODFW estimates of late summer parr, relative to ODFW's redd counts (above trap), assuming 1 female/redd and average fecundity; modeled using 75th% value to reflect productivity (rather than survival) model usage
	summer parr-to-smolt	summer parr-to-smolt survival	0.12	target CV: 70%	B. Jonasson, ODFW, monitoring spreadsheet	survival from fall to LGD as a smolt; computed for entire cohort of summer parr rather than via separate Tributary vs. Valley overwintering component
	ocean rearing stages [by ocean age (oa)]	survival by ocean age, Soa1, Soa2, Soa3, …	Soa1 = 0.02, Soa2 = 0.32, Soa3= 0.56	target CV: 50, 30, 30%, respectively	Based on CSS age-specific smolt-to-adult return rates (McCann et al. 2016)	Survival inputs & maturation probabilities (below) yield adult return age composition of Catherine Creek Acclimation Pond releases oa1 = 23%, oa2 = 75%, oa3 = 3%
	spawners	prespawn survival (on spawning grounds)	0.97	target CV < 10%	J. Feldhaus, ODFW, and T. Bowerman prespawn mort summaries	Because this is a pre-spawn 'productivity' in Beverton-Holt sense, used higher value. Note also that losses between LGD and the spawning grounds are assumed to be negligible; violation of this assumption introduces a positive bias in adult survival
capacity	summer parr	total capacity	159,708	n/a (static)	K. See (2016), unpublished	Quantile random-forest carrying capacity prediction for CC.
	adult (spawners)	total capacity	12,578	n/a (static)	Habitat suitability index model-based female spawner (redd) capacity, CHaMP	Modeled in units of eggs assuming average spawner age structure and age-specific fecundity [~48M eggs]

Input category	Life stage(s)	Parameter	Value(s)	Stochasticity	Source(s)	Comments
other life history or mgmt parameters	fall/early winter parr	probability of moving downstream to overwinter	e = 0.76	n/a (static)	B. Jonasson, ODFW, monitoring spreadsheet	Allows for spatial redistribution of fish in fall, in manner reflective of obs'd fall vs. spring migrant abundance
	ocean rearing stages [by ocean age (oa)]	maturation probability, Moa1, Moa2, Moa3, …	Moa1 = 0.11, Moa2 = 0.95, Moa3= 1.00	target CV: 80, 15, 0, respectively	Estimated from SARs data (see note for marine survival above)	see McHugh et al. (In Press) appendix for details estimation approach
	fecundity, by total age	f3, f4, f5, …	f3 = 3,257, f4 = 4,095, f5= 5,149	n/a (static)	Kareiva et al. (2000) values as preliminary input	Replace with basin-specific values; note, however, that these yield average fec (age-weighted) within 100 eggs of CC-specific means
	smolts	supplementation releases	150,000	n/a (static)	n/a	Current management target; varies in LCM as f(run size) if hatchery broodstock req's aren't met.

Appendix B. Overview of the approach taken to model hatchery supplementation programs.

The Catherine Creek (CC) and the Upper Grande Ronde River (UGR) populations of spring Chinook are presently supplemented by the annual release of approximately 150K (CC) and 250K (UGR) hatchery-reared smolts ($N_{sm\text{-}sup}$), which are released into acclimation ponds near the spawning grounds in both systems. As surplus production permits, additionally, modest numbers of eyed eggs are occasionally released into specific tributaries (UGR = Meadow and Sheep creeks; Catherine = Indian Creek). Adults returning from supplementation releases (HOR) are meant to home to the spawning grounds and spawn naturally, in tandem with natural-origin (NOR) fish. Similarly, a fraction of the natural-origin fish returning to spawn in the wild are retained for spawning in the hatchery to support an integrated hatchery program. To help maintain genetic integrity while offering abundance benefits, weirs and adult traps situated in both streams are used to manage three aspects of escapement that are pertinent to supplementation goals: (i) $P_{NOS\text{-}R}$ (i.e., the proportion of the total natural-origin returns that's retained for the hatchery), (ii) P_{HOS} (i.e., the proportion of natural spawners that is of hatchery origin), and (iii) P_{NOB} (i.e., the proportion of hatchery broodstock/egg-take that's of natural origin). Because supplementation efforts influence abundance dynamics in both CC and UGR populations, measures were taken to accurately represent this management strategy in life cycle model (LCM) simulations, which we describe here.

Several simplifying assumptions were made in order to represent a mixed, supplemented hatchery-natural population for each the CC and UGR case:

1. Beyond hatchery-reared stages (i.e., smolt+), we assume that survival and life history differences for natural and supplementation (i.e., hatchery) fish are negligible. This means that common rates were used, regardless of fish origin, including (i) survival rates from tributaries to Lower Granite Dam (LGD), (ii) LGD-to-LGD smolt-to-adult return rates (SARs), and (iii) adult maturation schedules. [*Note, this can be revised using tributary-to-LGD outmigrant survival and/or LGD-to-LGD SAR differentials, e.g., based on C. Justice's survival analyses, etc.*].
2. We assume that all hatchery-reared fish are produced from supplementation fish captured in the wild and reared according to conventional hatchery practices; thus, we do not model a captive broodstock component, due to its discontinued status and previously documented life history differences.
3. To model a feedback between total (HOR+NOR) adult returns ($N_{AD\text{-}tot} = N_{AD\text{-}h}+N_{AD\text{-}N}$, adults eligible for retention as broodstock (N_{BS}), and $N_{sm\text{-}sup}$ in year y+2, we assumed an egg take requirement of 85 females to produce 250K smolts (M. McLean, CTUIR, pers. comm.); or an equivalency of 1,470 smolts per adult, assuming a 50:50 sex ratio. Thus, $N_{sm\text{-}sup}$ in year y+2 is determined as noted below, where N_{BS} is determined according to stream-specific rules below. Hatchery broodstock goals for UGR and CC are 170 and 103 adults (fem+male), respectively.

If N_{BS} in year y >= hatch. Goal { $N_{sm\text{-}sup}$ in y+2 = smolt goal (i.e., 150K CC, 250K UGR) }

```
    Else { $N_{sm\text{-}sup} = N_{BS}$ in year y+2 = $N_{BS} * 1{,}470$ }
```

Catherine Creek. In CC (rule type = 4 in input files), where adult trapping operations span the entire run, the management of hatchery and natural fish on the spawning grounds and in hatchery broodstock follows a 'sliding scale' framework under which target levels for $P_{NOS\text{-}R}$, P_{HOS}, and P_{NOB} vary across three levels of run size ($N_{AD\text{-}tot}$), <250, 250-500, and >500 (Carmichael et al. 2011). At low abundance, $P_{NOS\text{-}R}$ is capped at 40% and there are no constraints on P_{HOS}, and P_{NOB}, and hatchery fish are otherwise retained to meet egg-take requirements. At high abundance, P_{HOS} is minimized (max allowed = 50%), P_{NOB} is maximized (target >= 30%), and is $P_{NOS\text{-}R}$ more tightly constrained (max allowed = 20%). At moderate abundance, $P_{NOS\text{-}R}$ is similarly constrained (20% cap) and there is tolerance for higher P_{HOS} (max allowed = 70%) and lower P_{NOB} (target >= 20%). While this rule set is straightforward, there are cases for which it is impossible to meet all constraints simultaneously, which made implementing it in code somewhat complicated. Consider for example a case in which returns fall between 250 and 500, but are almost exclusively (say 80+%) of hatchery origin. In this case, it's quite likely that egg take needs will not be met if weir management strictly follows the sliding scale's P_{NOB} and $P_{NOS\text{-}R}$ constraints; nor is it clear what passage goals (to spawning grounds) should be in cases for which returns exceed the scale's upper abundance threshold but are based predominantly on hatchery origin returns. Thus, to operationalize the CC sliding scale, several additional 'rules' were imposed, via the following pseudo-code:

```
Case 1 (in the low abundance tier)
If $N_{AD\text{-}tot}$ < lower threshold (i.e., <250 adults, H+N) then … {
        If $N_{AD\text{-}N} > 0$ … {
    Retain up to 40% of the natural run for hatchery broodstock
    Make up the balance of broodstock needs with hatchery fish
} Else (i.e., case for which $N_{AD\text{-}N}$ is 0, but $N_{AD\text{-}h}$ is > 0) … {
    Collect hatchery fish up to the broodstock goal
}
Rescale H and N run sizes to account for fish taken to hatchery
Pass everything that wasn't collected to the spawning grounds
        If adult collections < broodstock goals {
            Recompute smolt releases for year y+2 as function of fish retained (i.e., per #3 above)
```

```
}
}

Case 2 (in the mid abundance tier)
If lower threshold < $N_{AD-tot}$ < upper threshold (i.e., 250-500 adults) then … {
        If $N_{AD-N} > 0$ … {
    Retain up to 20% of the natural run for hatchery broodstock
    Make up the balance of broodstock needs with hatchery fish
} Else (i.e., case for which $N_{AD-N}$ is 0, but $N_{AD-h}$ is > 0) … {
    Collect hatchery fish up to the broodstock goal
}
Rescale H and N run sizes to account for fish taken to hatchery
Determine $P_{HOS}$ would be if remaining fish were allowed to spawn
If $P_{HOS} > 70\%$ {
    If you can meet $P_{HOS}$ goal without dropping into lower abundance tier {
        Remove hatchery fish until you meet $P_{HOS}$ goal
    } Else { Don't worry about it }
}
Rescale H run size to account for removals
Pass remaining fish to spawning grounds
        If adult collections < broodstock goals {
            Recompute smolt releases for year y+2 as function of fish retained (i.e., per #3 above)
}
}

Case 3 (in the high abundance tier)
If $N_{AD-tot}$ > upper threshold (i.e., 500 adults) then … {
```

```
        If $N_{AD-N} > 0$ … {
    Retain up to 20% of the natural run for hatchery broodstock
    Make up the balance of broodstock needs with hatchery fish
} Else (i.e., case for which $N_{AD-N}$ is 0, but $N_{AD-h}$ is > 0) … {
    Collect hatchery fish up to the broodstock goal
}
Rescale $N_{AD-h}$ and $N_{AD-N}$ run sizes to account for fish taken to hatchery
Determine $P_{HOS}$ would be if remaining fish were allowed to spawn
If $P_{HOS} > 50\%$ {
    If you can meet the system total escapement goal with natural fish alone {
        Pass only natural fish to the spawning grounds ($P_{HOS} = 0$)
    } Else If $N_{AD-N}$ / upper threshold >= 50% {
Remove hatchery fish until you're at or under $P_{HOS} = 50\%$
    }
}
Rescale H run size to account for removals
Pass remaining fish to spawning grounds
        If adult collections < broodstock goals {
            Recompute smolt releases for year y+2 as function of fish retained (i.e., per #3 above)
}
}
```

As the above pseudo-code illustrates, we made no attempt to constrain the modeled supplementation program based on the stated hatchery P_{NOB} goals, because (a) as doing so introduced additional coding complications (i.e., due to exceptions and circular dependencies), and (b) was virtually impossible to meet under the natural population's current life cycle productivity/capacity assumptions.

Upper Grande Ronde River. In the Upper Grande Ronde (rule type = 5 in input files), the management of HOS/NOS on the spawning grounds and HOB/NOB at the hatchery is less formalized than in Catherine Creek, due to the fact that the weir is typically pulled before the majority of the run makes its way through to the spawning grounds and because its supplementation program is generally less restrictive regarding target $P_{NOS\text{-}R}$, P_{HOS}, and P_{NOB} values. In brief, the main constraint imposed on weir/program management is that no more than 50% of the natural run can be retained for hatchery broodstock. This is executed in code according to the following pseudo-code:

```
        If $N_{AD\text{-}N} > 0$ … {
    Retain up to 50% of the natural run for hatchery broodstock
    Make up the balance of broodstock needs with hatchery fish
} Else (i.e., case for which $N_{AD\text{-}N}$ is 0, but $N_{AD\text{-}h}$ is > 0) … {
    Collect hatchery fish up to the broodstock goal
}
Rescale H and N run sizes to account for fish taken to hatchery
Pass everything that wasn't collected to the spawning grounds
        If adult collections < broodstock goals {
            Recompute smolt releases for year y+2 as function of fish retained (i.e., per #3 above)
}
```

Chapter 10: Assessing salmon spatial structure and metapopulation dynamics

Aimee Fullerton, Chris Jordan, Tom Cooney, Rich Zabel and Mike Ford (NOAA, Northwest Fisheries Science Center)

Three points were brought up during the review of our work by the ISAB in 2013. Reviewers asked for (1) a comprehensive literature review on what is known about salmon metapopulations and the critical issues and priorities for further work; (2) a clearer picture of how we would develop a metapopulation model; and (3) a more concrete description of how our spatial analyses relate to the broader life cycle modeling effort. This chapter is organized into 5 sections that address each of these questions. Specifically, we discuss our motivation and the broad context rationale for assessing salmon spatial structure; provide a conceptual overview of metapopulations (in general and for salmon specifically) and key information needs; and review the guidance produced by and used in the recovery planning process. We then summarize our earlier research (phase I), now published, and outline some ideas about analytical options for completing remaining research objectives (phase II).

Context and Motivation

Pacific salmon are structured and managed across a spatial hierarchy defined by freshwater habitats, life history diversity, and genetic attributes. Endangered Species Act (ESA) listings are made at the level of an Evolutionarily Significant Unit (ESU Waples 1991). Stocks comprising an ESU are typically managed as populations that are, in many cases, synonymous with river watersheds (e.g., ICTRT 2003, 2005). In some regions, an intermediate level of spatial organization is also recognized that aggregates similar populations into Major Population Groups (MPG). MPGs are geographically and genetically cohesive groups of populations that are critical components of ESU-level spatial structure and diversity. Although within-population spatial structure is likely important in many cases, we focus in this chapter on processes at spatial scales larger than populations. Specifically, our analyses target spatial structure within MPGs and ESUs, and interactions among their component populations. Subpopulation-level spatial structure and diversity are addressed by some population life cycle models (e.g., Lemhi, Wenatchee; see Chapter 4, this document).

The need to consider spatial structure and metapopulation processes when evaluating salmon status and viability was recognized and described during the recovery planning process (McElhany et al. 2000, ICTRT 2007a, 2007b). We will review concepts relevant for persistence of ESUs and MPGs in the 'Spatial Structure and Diversity in Recovery Planning' section. A call for spatial analyses was specifically highlighted in the FCRPS Adaptive Management Implementation Plan (AMIP 2009, p. 22, III.A.5.):

> *"Analyses will be developed to assess the degree of geographic concordance among populations. Establishing spatial patterns by which populations co-vary will enhance our ability to identify similarities and differences in their responses to variability in freshwater and marine productivity, differing levels of habitat restoration across watersheds, and influences of total hatchery composition on the wild component of the species, among others. In addition, spatially explicit metapopulation models will be developed for MPGs. Such models can help to identify populations that are especially vulnerable to extinction due to spatial isolation. Taken together, these modeling efforts can inform the spatial structure metric of viable salmonid populations."*

The recent Endangered Species Act status review for Pacific Northwest salmonids also underscored the need to evaluate metapopulation processes (NWFSC 2015, p. 56). More broadly, our motivation comes from a desire to use information about population structure in a common way for future ESA status reviews, jeopardy analyses, and recovery planning activities. At the ESU scale, conservation activities can be better prioritized if there is a clear understanding of how individual populations contribute to MPG and ESU viability. At the population scale, robust conservation strategies will account for spatial dynamics among production areas.

Literature Review and Research Needs

Spatial distribution of populations across a landscape can promote resilience by reducing the likelihood that all populations will experience the same disturbances (Kallimanis et al. 2005, Good et al. 2008). Spatial structure also increases genetic diversity through local adaptation and reduced genetic exchange, which in turn can increase the long- term resilience of the species (Fox 2005). Therefore, a portfolio of diverse, semi-related populations is better equipped to survive disturbances over many years (Schindler et al. 2010, Anderson et al. 2013, Griffiths et al. 2014, Moore et al. 2014, Thorson et al. 2014, Anderson et al. 2015), provided the population dynamics are not too synchronous (Moore et al. 2010, Yeakel et al. 2014, Satterthwaite et al. 2015).

Definitions and Terminology

Conceptualization of dynamics among spatially structured populations often invokes the term "metapopulation". In the classic sense (Levins 1970, Hanski 1998), a metapopulation is a collection of populations that interact such that the long-term viability of the metapopulation is greater than the viability of any individual population. That is, one population may become depressed or go extinct, but is rescued or recolonized by neighboring populations. Metapopulations can exhibit source–sink relationships, wherein populations with a net demographic surplus support those with net deficits (Pulliam 1988). Since its conception, the term "metapopulation" has expanded to include a variety of classes of metapopulations, varying in the amount to which populations are connected by dispersal and in the strength of source-sink relationships among populations (**Figure 1**).

However, it is not always clear when a group of populations (say, a salmon MPG) functions as a metapopulation. For one, population dynamics may be correlated for multiple populations because they are all influenced similarly by factors encountered in shared environments, even if they do not exchange individuals (**Figure 2**). Second, Primmer et al. (2006) suggested that population structure may have evolved as a consequence of selective forces promoting accurate homing, which would result in local adaptation and strong spatial structure without the need to invoke the metapopulation concept. Third, observation of metapopulation processes may depend on the spatiotemporal lens used to evaluate dynamics. For instance, Schtickzelle and Quinn (2007) argue that in a metapopulation, dispersal occurs at relatively short time scales (ecological time) affecting population dynamics, whereas the spatial structure observed may be due to genetic processes operating at longer timeframes (evolutionary time). Whereas Rieman and Dunham (2000) suggest that metapopulation dynamics are likely important at finer spatial scales, but that the dynamics may play out over centuries rather than years or decades.

Salmon as Metapopulations

Spatially structured populations and homing behavior in salmonids have been recognized for decades (Quinn et al. 1991, Schlosser and Angermeier 1995). Researchers began discussing spatial structuring for salmon in terms of metapopulation theory around the turn of the century (Policansky and Magnuson 1998, Cooper and Mangel 1999, Young 1999). Rieman and Dunham (2000), McElhany et al. (2000), and Schtickzelle and Quinn (2007) all argued that salmon could be considered metapopulations because they met three criteria: (1) spawning occurs at discrete locations, (2) some asynchrony in population dynamics exists, and (3) some dispersal among populations occurs. In addition, extinctions are a natural part of metapopulation dynamics (Mangel and Tier 1994). Gustafson et al. (2007) estimated that nearly one-third of 1400 historical populations of Pacific salmonids have been extirpated since Euro-American contact. However, the causes of extinctions, including reduced habitat availability and altered thermal and hydrologic regimes (Fukushima et al. 2011, Zeug et al. 2011) suggest that these extinctions may not represent natural stochastic extinction and colonization dynamics.

Spatial structure has been identified and portrayed in metapopulation terms for anadromous, semi-anadromous, and resident salmonids, and many other stream fishes. Anadromous species evaluated as metapopulations include Atlantic salmon (aka sea trout, Baltic trout) on multiple continents (Fontaine et al. 1997, McKinnell and Karlstrom 1999, Garant et al. 2000, Primmer et al. 2006, Freamo et al. 2011, Sandlund et al. 2014), coho salmon (Bradford 1999), Chinook salmon (Isaak et al. 2003, Neville et al. 2006b, Schick and Lindley 2007), chum (Petrou et al. 2014, Small et al. 2014), and steelhead (Fullerton et al. 2011, Hand et al. 2016). Metapopulations have been described for many resident salmonids including bull trout (Dunham and Rieman 1999, Spruell et al. 1999), cutthroat trout (Rieman and Dunham 2000, Neville et al. 2006a), brook charr (Fraser et al. 2004, Gomez-Uchida et al. 2013, Kazyak et al. 2016), gila trout (Fagan 2002), and white-spotted charr (Yamamoto et al. 2004). Many other freshwater fishes may be structured as metapopulations, including semi-anadromous splittail (Feyrer et al. 2015), galaxiids (Galeotti 2013, Jones and Closs 2015), and a variety of non-anadromous species (Schlosser and Angermeier 1995, Gotelli and Taylor 1999, Fagan et al. 2005, Falke and Fausch 2010, Whitney et al. 2015).

Isolation by distance (IBD) has been postulated as a structuring mechanism, whereby individuals near in space are more closely related due to the higher likelihood of dispersers reaching new breeding locations over shorter distances. IBD patterns of genetic relatedness vs. geographic distance (typically using stream distance rather than Euclidean distance) have been identified for a number of salmonid populations (Primmer et al. 2006, Petrou et al. 2014, Small et al. 2014, Fullerton et al. 2016). Neville et al. (2006b) found genetic structure among female, but not male, Chinook salmon in the Middle Fork Salmon River, suggesting factors other than distance are also likely to influence spatial structuring. The spatial organization of habitats within landscapes (e.g., the field of landscape genetics (Manel et al. 2003)), seascapes (Quéméré et al. 2016), and stream network structure (Fagan 2002, Muneepeerakul et al. 2007, Seymour and Altermatt 2014, Yeakel et al. 2014, Erős and Campbell Grant 2015, Heino et al. 2015) may all influence metapopulation structure and dynamics.

Many factors influence dispersal, including sex, physical habitat, landscape features, environmental conditions, rearing history, age, size, etc. (Blankenship et al. 2011, Keefer and Caudill 2013, Peterson et al. 2016). Westley et al. (2013) found that Chinook salmon strayed at higher rates than coho or steelhead, and that ocean-type Chinook strayed at higher rates than spring/summer Chinook (in the study, "stray" indicated probability of dispersal, as measured by tagged and recaptured hatchery fish). Similarly, stray rates may be stronger in certain geographic locations or under particular conditions. Westley et al. (2015) found that rates of straying by Chinook salmon were plastic, and were influenced by factors such as temperature experienced in different environments, conspecific density, and migration distance.

The difficulties of empirical estimation of dispersal rates are myriad. For one, if stray rates are low, there is a very small chance that the few fish that do stray also happen to be tagged fish that survive to adulthood (i.e., we are unlikely to detect and measure stray events). Second, capturing a spawner in a non-natal river does not necessarily mean that the fish intended to spawn there, or that its offspring will be successful. Third, even if we perfectly captured stray rates with tag-recapture technology, it does not mean that fish would not stray at much higher rates during a large disturbance, such as happened with the explosion of Mt. St. Helens in 1980 (Whitman et al. 1982, Bisson et al. 2005). Indeed, stray rates likely differ from year to year because they are influenced by so many factors. New technologies, such as parentage-based estimates of straying (Ford et al. 2015) will help by providing more accurate short-term estimates of straying, but capturing episodic straying events will remain experimentally difficult.

The scale of observation is likely to influence whether or not spatial structure is observed (Cushman and Landguth 2010). Spatial structuring of populations has been identified at multiple spatial scales and can be hierarchical (Rieman and Dunham 2000, Fraser et al. 2004, Matthaeus 2016). Several studies have found spatial structure even at very fine spatial scales (< 1 km) (Hendry et al. 1995, Neville et al. 2006b, Quinn et al. 2012, Kelson et al. 2015) or even meters (Kuligowski et al. 2005). Temporal consistency of spatial structure depends on scale as well. Some studies have found instability over short periods (Garant et al. 2000, Kitanishi et al. 2017), whereas long-term stability has been inferred when analyzing longer-term datasets or datasets that combine data from different years across broad spatial extents. Different types of genetic data can represent processes over different temporal horizons (Neville et al. 2006b).

In addition to the issues raised about scale, population structure will best be understood with a comprehensive “demogenetics” approach; that is, considering both ecological connectivity (i.e., demographic processes) and evolutionary connectivity (i.e., genetic processes) (Zavorka et al. 2015, Hawkins et al. 2016, Landguth et al. 2016). Whitlock and McCauley (1999) caution that it is rare that estimates of genetic variance among populations can be directly translated into the number of dispersers (and vice versa). Using both types of information can yield insights otherwise unavailable. For instance, Peterson et al. (2014) found that reproductive success of dispersers differed for two groups of sockeye: in one group, fish strayed from one stream to another, and in another group, fish strayed from beaches to streams. Had they not confirmed which fish produced viable offspring, estimates of successful dispersal would have been inaccurate. On the other hand, Ford et al. (2015) found that direct estimates of gene flow and dispersal of Chinook salmon among spawning areas within the Wenatchee River were correlated, indicating that in this case patterns of genetic variance were a good predictor of homing and straying. Life history diversity may represent the convergence of ecological and evolutionary connectivity. For example, timing of maturation and spawning is highly heritable, leading to discrete life history types (Hendry et al. 1995, Bentzen et al. 2001, Hendry 2004, Crozier et al. 2008).

Recent studies have evaluated conservation approaches for salmon that incorporate spatial structure and metapopulation processes into planning (Schick and Lindley 2007, Good et al. 2008, Fullerton et al. 2011, Johnson et al. 2012, Pess et al. 2012, Anderson et al. 2013, Anderson et al. 2014, Anderson et al. 2015). These studies have addressed questions such as appropriate conditions for reintroduction, opening new habitats, or assisted migration; prioritization of habitat restoration activities; and management of hatchery activities to avoid synchronization of population dynamics.

Research Needs and Guiding Questions

Some key questions remain that may help focus future research efforts and inform prioritization of recovery efforts for salmon. Across scales but particularly important within populations, key questions include: (1) How does habitat structure (variance in habitat quality and its configuration) influence population viability? (2) What are the sources and sinks of productivity? (3) Is it ever a good idea to deliberately prevent access to low quality habitats? and (4) What is the temporal variance in habitat quality/use and how important is unoccupied habitat?

At the ESU or MPG scale, key questions include: (1) When and where are spatial processes likely to be important? (2) Do spatial structure and diversity criteria developed during the recovery planning process (next section) adequately preserve metapopulation processes? (3) In cases where spatial processes are important, how would this knowledge influence the way recovery planning and management are implemented? and (4) Will climate change or other factors alter metapopulation dynamics in some unexpected way?

We will use these questions to guide our analyses to ensure efficient use of time and resources. The degree that spatial processes influence population dynamics likely differs across species, geographic locations, environmental conditions, and spatiotemporal scale. Understanding the context under which spatial processes are likely to substantially influence population, MPG, or ESU viability may highlight obvious conservation strategies. Conversely, knowing when and where spatial processes are unlikely to be important should simplify evaluation of the effect of management activities on long-term viability. Comparison of viability scenarios with and without spatial processes could highlight their relative influence on reaching conservation targets. This would give a sense of how management might be misguided if potentially important structure was missed. It could also help in prioritizing and sequencing actions over short and long planning horizons.

Spatial Structure & Diversity in Recovery Planning

During the recovery planning process, McElhany et al. (2000) and the Technical Recovery Teams (TRT) developed guidance for determining long term conservation status for salmon that included assessment of abundance, productivity, spatial structure and diversity; the "viable salmonid population" (VSP) parameters. Their guidelines were intentionally general, given the broad spectrum of life history diversity, habitat conditions, and metapopulation structures represented in the region. They surmised that ESUs may function as metapopulations over the long term (centuries), and likely did so historically. They stated that in relating VSPs to a viable ESU, planners would need to consider 1) catastrophic events, 2) long-term demographic processes, and 3) long-term evolutionary potential. The ESU guidelines suggested maintenance of multiple viable populations, geographically widespread so that not all experience the same environmental conditions but close enough to each other to allow for rescue effects following disturbance; that there be a diversity of life history and phenotypes represented; and that some populations should exceed other VSP requirements to enable functional source-sink processes.

Consistent with these general criteria, the Interior Columbia TRT (ICTRT) developed and recommended population level criteria for abundance and productivity along with hierarchical criteria for spatial structure and diversity (ICTRT 2007b). The ICTRT described criteria for assessing ESU and MPG viability status in terms of the status of component populations. Their ESU-level criteria required that all extant MPGs and any extirpated MPGs critical for proper functioning of the ESU should be at low risk. Their MPG-level criteria depended on the number, spatial arrangement, and diversity of component populations (described below). Population-level criteria were also established; those are not discussed here.

MPG criteria were designed to both ensure robust metapopulation functioning and mitigate risk of catastrophic loss, and ensure that an ESU could survive adverse fluctuations in the environment while maintaining long-term adaptive potential. The TRT believed that MPGs likely functioned historically as metapopulations. At the time the TRT developed their criteria, there was insufficient information on exchange rates among populations to directly model MPGs as metapopulations. Instead, they developed a suite of criteria intended to ensure preservation of the historical metapopulation processes. These included (1) genetic exchange across populations within an ESU over a long time frame; (2) opportunity for neighboring populations to serve as source areas in the event of local population extirpations; and (3) populations distributed within an ESU so that they are not all susceptible to a specific localized catastrophic event.

Their MPG-level criteria included five elements:

1. **Minimum Number Represented**: > Half of populations historically within an MPG (minimum of 2) meeting viability standards
2. **Include Highly Viable Populations**: > 1 population "Highly Viable"
3. **Population Sizes Represented**: Some populations "Very Large", "Large" or "Intermediate", with biggest at or above historical abundance
4. **Major Life History Patterns Represented**: All major life history strategies (e.g. run-timing) that were present historically represented by populations meeting viability requirements
5. **Maintained Populations**: Maintain populations not meeting viability standards to support viability of MPG

Phase I Research Completed

To date, we have completed two analyses that partially addressed the spatial objectives called for by the AMIP. Here, we briefly review major findings from those analyses before moving on to outline options for additional research.

To address the first AMIP objective of assessing the degree of geographic concordance among populations, Jorgensen et al. (2016) evaluated the similarity between temporal trends in spawner abundance for populations in the Upper Columbia and Snake River ESUs of spring/summer Chinook salmon. They fit abundance time series of 24 populations with dynamic factor analysis models. They found support in the data for grouping the time series according to five common latent variables. The top data-supported model included summer and autumn seasonal metrics of the Pacific Decadal Oscillation. Assignment of populations to the latent variables matched the ICTRT's population structure at the ESU level (i.e., all 3 Upper Columbia River ESU populations were more associated with each other than with Snake River ESU populations). At finer scales among and within MPGs, some relatively distant populations from different MPGs grouped together and some populations near in geographic space were better associated with distantly located populations. It is likely that the correspondence in abundance trends between the distant populations was due to shared exogenous influences rather than to exchange of individuals (e.g., **Figure 2**).

To address the second AMIP objective of identifying which populations are at risk due to isolation and for parameterizing a metapopulation model, Fullerton et al. (2016) assessed the spatial structure of the Snake River spring/summer Chinook salmon ESU. Their assessment used multiple data sources for estimating dispersal among populations (tag-recaptures, genetics, and models). This analysis provided a snapshot of spatial structure for the present and estimates of how spatial structure would change under various scenarios (e.g., past abundance levels, future management strategies). Their estimate of the present-day ESU spatial structure was congruent with previous findings, where populations within MPGs shared more connections than populations between MPGs, and interactions were strongest for populations near in space. The authors proposed which populations were most (and least) independent or isolated, those best (and worst) connected, and the strongest (and weakest) sources. A major finding was that missing or inaccurate data for some populations had substantial influences on estimated metapopulation structure. They suggested that data gaps (i.e., data missing for some populations) and uncertainty in dispersal estimates had the greatest potential to influence results (more so than uncertainty in abundance estimates). They proposed that an ensemble of available data (empirical and modeled) may be best when there are data gaps. Using an ensemble dispersal dataset, they evaluated potential response in spatial structure to a variety of management scenarios, and proposed the types of actions that are likely to be safe bets and which are riskier.

Phase II Analytical Options

The two phase I analyses described present-day geographic concordance and spatial structure for the Snake River spring/summer Chinook salmon ESU. Findings from these analyses are an informed starting point for considering how spatial processes within the ESU might influence recovery planning strategies. With phase II analyses, our aim is to advance these concepts to complement what we learn from individual life cycle models, and to expand our consideration to include other species. Specifically, our objectives are to use models to (1) assess whether adherence to the ICTRT MPG-level criteria conserves metapopulation processes as intended; and (2) evaluate how the viability/persistence of ESUs and MPGs would differ with and without recognition of metapopulation processes. We have conceived of three ways to accomplish these objectives, and are soliciting feedback about which one or more of these approaches would be most useful. The first option involves a collective assessment of results across the set of existing life cycle models comprising an MPG to see if the MPG as a whole is meeting spatial structure and diversity targets, without explicitly modeling dispersal among component populations. The second and third options involve building two different types of metapopulation model that include dispersal. We recognize that in some cases within-population spatial processes may be as important or more important than spatial processes at broader scales. Thus, it may be a priority to assess which populations would benefit from integration of spatial processes into life cycle models.

Option 1: Assess life cycle model outputs collectively against ICTRT's MPG-level criteria

Population-level life cycle models of varying scales of resolution are becoming available for a majority of populations within the Snake River Spring/Summer ESU and for other ESUs (see other chapters in this report). To date, those models do not directly incorporate dispersal among populations. One analysis option would be to use outputs from these existing population-level life cycle models to collectively assess whether an MPG as a whole is likely to be viable over some time horizon (e.g., in 50 or 100 years) under commonly modeled scenarios. As noted above, the ICTRT's MPG-level criteria were not developed with an explicit quantitative metapopulation analysis, but collectively they were intended to reflect an underlying metapopulation framework.

This would be strictly a post-hoc analysis; we would not model inter-population dispersal or metapopulation dynamics. We would use abundance, productivity, and viability predictions for each population within an MPG (produced by separate life cycle models) to assess whether the MPG as a whole meets the ICTRT's MPG-level criteria for spatial structure and diversity (**Table 1**). We would assess the first four of these criteria by asking: (1) how many of the populations historically present are predicted to be viable?; (2) what proportion of populations are predicted to be highly viable?; (3) what proportion of population are predicted to be large?; and (4) how many of the life history strategies present historically in the MPG are predicted to remain present? The last criterion (5) is more difficult to evaluate directly from life cycle model outputs and would require further thought. Life cycle models are not developed for every population in an MPG; thus, we would need to employ an approach for estimating their dynamics and therefore contribution to the MPG-level score.

Option 2: Develop a metapopulation model with simplified life cycle model elements (Chinook)

A second and more involved option is to develop a metapopulation model that is built on the constructs and principles of existing life cycle models but which would also incorporate dispersal among populations. These constructs include commonly used stock-recruitment functions that predict recruits per spawner annually, as well as approaches for estimating survival through the mainstem hydropower system and in the ocean. This could take the form of a spatially explicit integrated population model that fits common parameters simultaneously (e.g., see Buhle et al., Chapter 7). More simply, it could link dynamics for individual populations using relatively simple population-specific life stage production/survival elements from existing life cycle models and allow demographic exchange among populations. This approach imposes some degree of spatial structure initially (e.g., population boundaries, presumed dispersal rates). The model would require spawner abundance by age for each population in each year (estimates are available for many populations); survival of recruits back to their natal populations (some data and methods for estimating this exist); and population-specific dispersal (stray) rates. Estimates of dispersal rates are notoriously sparse, especially for wild fish, but can be approximated (e.g., using distance decay functions) (Fullerton et al. 2016).

For this type of model, we would likely target one of the MPGs within the Snake River spring/summer Chinook ESU because data are available, and because previous analyses have suggested the presence of spatial structure. For instance, the residual covariance matrix from an integrated population model across 24 populations in this ESU retained spatial structure that was not accounted for by other factors in the model (Eric Buhle, pers. comm.). Plotting this residual covariance matrix against hydrologic distance between populations suggested a weak relationship over a portion of the dataset. One aim would be to evaluate what amount of that spatial structure may be due to demographic processes that could be explained by a metapopulation model. The Middle Fork Salmon River seems a likely candidate; there, we have redd counts, some PIT tag and genetic data, and populations are least likely to be influenced by hatcheries (none are operated there).

The resulting multiple population model could then be used to evaluate how achieving the ICTRT's MPG-level viability criteria – e.g., through comprehensive habitat restoration, good ocean conditions, reintroductions, reduced harvest, hatchery management, or a combination of these or other strategies – would change risk levels relative to the current status. That is, we could run simulations in which these two baseline scenarios ("status quo" or "restored to meet viability criteria") would be subjected to stochastic effects such as catastrophic extirpation of one or more populations, climate change and variability, or changing conditions in shared environments such as the mainstem, estuary, or ocean. In this way, we could evaluate whether achieving the ICTRT's MPG-level viability criteria was sufficient for the MPG to maintain viability when faced with stochastic stressors. We would also conduct sensitivity analyses to evaluate the extent to which results might differ under a range of dispersal hypotheses. This would allow us to consider whether MPG viability would differ with and without explicit estimation of metapopulation dynamics. Similarly, additional simulations could evaluate alternative ways of achieving the baseline status of "restored to meet viability criteria". Specifically, how results would change given different sets or different sequencing of activities including habitat restoration, reintroductions, etc. Such a model would not be presumed to predict the way metapopulation dynamics will actually occur; rather, it could inform users as to the range of ways the MPG could be expected to behave under different conditions.

Option 3: Develop a metapopulation model with mechanistic behavioral rules (steelhead)

A third option is to develop an individual-based metapopulation model in which individual fish behave according to rules for interacting with their environment. In an individual-based model (IBM), metapopulation processes and spatial structure, if they exist, will be emergent properties arising from the collective decisions of many individuals. An individual-based model could be used to evaluate the same kinds of scenarios described in the previous section: specifically, whether the ICTRT's MPG-level criteria sufficiently protect an MPG in spite of stochastic stressors, and whether explicit consideration of metapopulation dynamics is warranted.

For this option, we would use HexSim, a free, versatile, multi-species, life history simulator ideal for building models of animal and plant population viability interactions, and responses to disturbance. HexSim is a multi-species spatially-explicit and individual-based life history simulator written in a C-sharp and C++ and built for a Windows platform. It includes a sophisticated graphical user interface (GUI) and built-in tools for inputting spatial data, defining populations, creating and running scenarios, and analyzing the results. It is ideal for building models of animal population viability, interactions, and responses to disturbance. A detailed HexSim user guide and download can be found at: http://www.hexsimhelp.com/Help/help.htm.

A population model and the modeling environment within HexSim consists of several distinct components.

Landscape

HexSim simulations are built around a user-defined landscape that can be either a 2-dimensional grid of hexagons, or a branching, directional network consisting of segments and nodes. In either case, the landscape represents the topology within which individuals interact with space, such as through movement or resource acquisition. The grid-based landscape is the most general, and thus most powerful way in which space can be represented. However, there are specific properties of networks, such as directionality and branching order, which are commonly used in landscape ecology. These features could be approximated within a grid-based system, but are much more efficient when performed on a true network. The work-flow for developing population simulations on grid vs. network landscapes are fundamentally the same, though the details differ sufficiently that a user should carefully weigh the pros and cons of the two approaches prior to initiating the workspace and scenario construction process. Any specific HexSim workspace can include both grid and network topologies.

For populations that are to be simulated on a network, the HexSim workspace contain a single network file and one or more spatial data time step update files. Network files describe the basic landscape topology, such as the size of network reaches, and the spatial arrangement of reaches relative to a designated "upstream" or "downstream" location. The property files that can accompany HexSim networks each define properties and their values for a specific range of time steps.

Populations

HexSim simulations must include at least one population. When multiple populations are present, individuals from the different populations may interact with each other, and they may compete for resources. HexSim populations are of two types - grid or network. All events that are assembled into a scenario for each population must match the population type.

Scenario

A HexSim scenario (programmed by the user within HexSim) is an XML file that contains all of the information necessary to run a HexSim simulation. Scenarios include population definitions, spatial data requirements, an event list, and event parametrization. Populations and events have sophisticated parameterization windows, but most of the model's complexity can be ignored if desired. Events can be set up to trigger once, only within a temporal window, periodically, or randomly. The model has tools for building in environmental stochasticity and for controlling density dependence. Individuals from the same, or from different populations can interact, compete for resources, and so on. Because all of this information is stored in a single scenario file, it can be quickly retrieved and used to run a new simulation. Scenario files are small in size and easily shared.

Event List

A HexSim scenario consists of an ordered sequence of events. The sequence is run a defined number of times (each iteration is a "time step"), and each event can be set up to "trigger" (run or not run) at particular time steps.

Each HexSim event has a unique purpose, interface, and parameter set. Events can be run on all individuals, or a specific subset of individuals. Events are what cause individuals to be born, to move, to die, to mate, to grow, to interact with their environment, etc.

HexSim has been used to develop models for salmonid (O. mykiss) populations in the John Day River basin (Chris Jordan, Kris McNyset, Chris Beasley, Mark Armour, Carol Volk, and Jason Neuswanger). Because a HexSim scenario contains the biological rule set for a population, and we think that these rules are species specific, but not strictly population or geographically unique, it is a relatively straightforward extension to model suites of populations simultaneously by expanding the size of the stream network over which fish can move.

We are developing a HexSim model for six populations of steelhead in the upper Salmon River basin – the populations in the watersheds above the confluence of the Middle Fork Salmon with the mainstem Salmon River. Using the biological rule set for resident and anadromous O. mykiss based on results from the Bridge Creek IMW in the Lower John Day steelhead population (Middle Columbia Steelhead DPS) and a stream network for the upper Salmon River, we are modeling multiple populations with the intent of supporting large-scale habitat restoration planning.

It will be important to apply multiple modeling approaches to the "metapopulation" scenario presented by supporting watershed and land-use planning on a spatial extent as large as the Upper Salmon. IPM and other process based parameter estimation methods can be used to parameterize the exchange between populations, if adequate abundance time series exist; however, including complex fish-habitat relationships, especially at fine spatial scales is not possible with these methods. Stage based LCMs offer an approach that can be appropriate at intermediate spatial resolution (population down to subpopulation), but it will become unwieldly when applied at finer scales; however, the population dynamics that emerge from habitat structure at these extents is critical to capture, and can serve to bound simulation results from IPM or IBM methods, or, if abundance or distribution data are available at these scales, can be use to verify or calibrate population modeling efforts of all froms. IBM based approaches emphasize population dynamics based on the fine-scale, spatially explicit components of population processes. Movement is the most obvious example of this since movement events in a spatially explicit framework consist of a distribution of movement distances, but the same is true for growth potential (determinant of survival rates) and capacity, as the spatial distribution of habitat features can determine population dynamics (Heinrichs et al 2016). However, this resolution comes at considerable cost in terms of computational time (single iterations requiring 10s of hours to complete). Therefore, balancing across multiple methods based on the management scenario being addressed is necessary to develop the most technically robust, yet efficient, decision support product.

Summary and Next Steps

In this chapter, we reviewed some basic metapopulation biology concepts and illustrated how this framework has been useful for thinking about spatially-structured salmon populations. We summarized the results from initial research (phase I; now published) that partially addressed the objectives described in the AMIP. We reviewed the history of metapopulation thinking that permeated the early recovery planning guidance, and specifically, the MPG-level spatial structure and diversity criteria laid out by the ICTRT. We then outlined several options for completing remaining research (phase II) to address the AMIP objectives: (1) collectively assessing existing individual life cycle model outputs against the ICTRT's MPG-level criteria; (2) building a metapopulation model for a Chinook salmon MPG that employs many of the elements of population-level life cycle models to assess MPG viability under a variety of scenarios; (3) expanding an existing individual-based model for steelhead to evaluate metapopulation processes; and (4) focusing more effort on spatial processes within populations (as opposed to among-population interactions).

Before we decide on an approach or a set of approaches, we are seeking guidance about the most useful way to spend our efforts. Specifically, are we focusing on the right questions? What spatial scale seems most important to study spatial processes? Do our analysis ideas seem reasonable, or might there be alternatives we haven't considered? Our intention is to maximize the information provided by these analyses for multiple management activities including recovery planning, habitat restoration, status assessments, and climate adaptation planning.

Literature Cited

Anderson, J. H., G. R. Pess, R. W. Carmichael, M. J. Ford, T. D. Cooney, C. M. Baldwin, and M. M. McClure. 2014. Planning Pacific salmon and steelhead reintroductions aimed at long-term viability and recovery. North American Journal of Fisheries Management **34**:72-93.

Anderson, S. C., A. B. Cooper, N. K. Dulvy, and D. Hodgson. 2013. Ecological prophets: quantifying metapopulation portfolio effects. Methods in Ecology and Evolution **4**:971-981.

Anderson, S. C., J. W. Moore, M. M. McClure, N. K. Dulvy, and A. B. Cooper. 2015. Portfolio conservation of metapopulations under climate change. Ecological Applications **25**:559-572.

Bentzen, P., J. B. Olsen, J. E. McLean, T. R. Seamons, and T. P. Quinn. 2001. Kinship analysis of Pacific Salmon: insights into mating, homing, and timing of reproduction. The Journal of Heredity **92**:127:136.

Bisson, P. A., C. M. Crisafulli, B. R. Fransen, R. E. Lucas, and C. P. Hawkins. 2005. Responses of Fish to the 1980 Eruption of Mount St. Helens

Ecological Responses to the 1980 Eruption of Mount St. Helens. Pages 163-181 *in* V. H. Dale, F. J. Swanson, and C. M. Crisafulli, editors. Springer New York.

Blankenship, S. M., M. R. Campbell, J. E. Hess, M. A. Hess, T. W. Kassler, C. C. Kozfkay, A. P. Matala, S. R. Narum, M. M. Paquin, M. P. Small, J. J. Stephenson, K. I. Warheit, and P.

Moran. 2011. Major Lineages and Metapopulations in Columbia RiverOncorhynchus mykissAre Structured by Dynamic Landscape Features and Environments. Transactions of the American Fisheries Society **140**:665-684.

Bradford, M. J. 1999. Temporal and Spatial Trends in the Abundance of Coho Salmon Smolts from Western North America. Transactions of the American Fisheries Society **128**:840-846.

Cooper, A. B., and M. Mangel. 1999. The dangers of ignoring metapopulation structure for the conservation of salmonids. Fishery Bulletin **97**:213-226.

Crozier, L. G., A. P. Hendry, P. W. Lawson, T. P. Quinn, N. J. Mantua, J. Battin, R. G. Shaw, and R. B. Huey. 2008. Potential responses to climate change in organisms with complex life histories: evolution and plasticity in Pacific salmon. Evolutionary Applications **1**:252-270.

Cushman, S. A., and E. L. Landguth. 2010. Scale dependent inference in landscape genetics. Landscape Ecology **25**:967-979.

Dunham, J. B., and B. E. Rieman. 1999. Metapopulation structure of bull trout: Influences of physical, biotic, and geometrical landscape characteristics. Ecological Applications **9**:642-655.

Erős, T., and E. H. Campbell Grant. 2015. Unifying research on the fragmentation of terrestrial and aquatic habitats: patches, connectivity and the matrix in riverscapes. Freshwater Biology **60**:1487-1501.

Fagan, W. F. 2002. Connectivity, fragmentation, and extinction risk in dendritic metapopulations. Ecology **83**:3243-3249.

Fagan, W. F., C. Aumann, C. M. Kennedy, and P. J. Unmack. 2005. Rarity, fragmentation, and the scale dependence of extinction risk in desert fishes. Ecology **86**:34-41.

Falke, J. A., and K. Fausch. 2010. From metapopulations to metacommunities: linking theory with empirical observations of the spatial population dynamics of stream fishes. American Fisheries Society Symposium **73**:207-233.

Feyrer, F., J. Hobbs, S. Acuna, B. Mahardja, L. Grimaldo, M. Baerwald, R. C. Johnson, S. Teh, and A. Fisk. 2015. Metapopulation structure of a semi-anadromous fish in a dynamic environment. Canadian Journal of Fisheries and Aquatic Sciences **72**:709-721.

Fontaine, P. M., J. J. Dodson, L. Bernatchez, and A. Slettan. 1997. A genetic test of metapopulation structure in Atlantic salmon (*Salmo salar*) using microsatellites. Canadian Journal of Fisheries and Aquatic Science **54**:2434-2442.

Ford, M. J., A. Murdoch, and M. Hughes. 2015. Using parentage analysis to estimate rates of straying and homing in Chinook salmon (*Oncorhynchus tshawytscha*). Molecular Ecolology **24**:1109-1121.

Fox, G. A. 2005. Extinction risk of heterogeneous populations. Ecology **86**:1191-1198.

Fraser, D. J., C. Lippe, and L. Bernatchez. 2004. Consequences of unequal population size, asymmetric gene flow and sex-biased dispersal on population structure in brook charr (Salvelinus fontinalis). Molecular Ecology **13**:67-80.

Freamo, H., P. O'Reilly, P. R. Berg, S. Lien, and E. G. Boulding. 2011. Outlier SNPs show more genetic structure between two Bay of Fundy metapopulations of Atlantic salmon than do neutral SNPs. Molecular Ecology Resources **11 Suppl 1**:254-267.

Fukushima, M., H. Shimazaki, P. S. Rand, and M. Kaeriyama. 2011. Reconstructing Sakhalin taimen *Parahucho Perryi* historical distribution and identifying causes for local extinctions. Transactions of the American Fisheries Society **140**:1-13.

Fullerton, A. H., S. Anzalone, P. Moran, D. M. Van Doornik, T. Copeland, and R. W. Zabel. 2016. Setting spatial conservation priorities despite incomplete data for characterizing metapopulations. Ecological Applications **26**:2558–2578.

Fullerton, A. H., S. T. Lindley, G. R. Pess, B. E. Feist, E. A. Steel, and P. McElhany. 2011. Human influence on the spatial structure of threatened Pacific salmon metapopulations. Conservation Biology **25**:932-944.

Galeotti, D. M. 2013. Metapopulation theory explains back-stripe minnow (Pisces: Galaxiidae, Galaxiella nigrostriata) distribution in seasonal wetlands in south-west Western Australia. Edith Cowan University, Joondalup, Western Australia.

Garant, D., J. J. Dodson, and L. Bernatchez. 2000. Ecological determinants and temporal stability of the within-river population structure in Atlantic salmon (Salmo salar L.). Molecular Ecology **9**:615-628.

Gomez-Uchida, D., F. P. Palstra, T. W. Knight, and D. E. Ruzzante. 2013. Contemporary effective population and metapopulation size (N e and meta-N e): comparison among three salmonids inhabiting a fragmented system and differing in gene flow and its asymmetries. Ecol Evol **3**:569-580.

Good, T. P., J. Davies, B. J. Burke, and M. H. Ruckelshaus. 2008. Incorporating catastrophic risk assessments into setting conservation goals for threatened Pacific Salmon. Ecological Applications **18**:246-257.

Gotelli, N. J., and C. M. Taylor. 1999. Testing metapopulation models with stream-fish assemblages. Evolutionary Ecology Research **1**:835-845.

Griffiths, J. R., D. E. Schindler, J. B. Armstrong, M. D. Scheuerell, D. C. Whited, R. A. Clark, R. Hilborn, C. A. Holt, S. T. Lindley, J. A. Stanford, and E. C. Volk. 2014. Performance of salmon fishery portfolios across western North America. Journal of Applied Ecology **51**:1554-1563.

Gustafson, R. G., R. S. Waples, J. M. Myers, L. A. Weitkamp, G. J. Bryant, O. W. Johnson, and J. J. Hard. 2007. Pacific salmon extinctions: quantifying lost and remaining diversity. Conservation Biology **21**:1009-1020.

Hand, B. K., C. C. Muhlfeld, A. A. Wade, R. P. Kovach, D. C. Whited, S. R. Narum, A. P. Matala, M. W. Ackerman, B. A. Garner, J. S. Kimball, J. A. Stanford, and G. Luikart. 2016. Climate variables explain neutral and adaptive variation within salmonid metapopulations: the importance of replication in landscape genetics. Molecular Ecology **25**:689-705.

Hanski, I. 1998. Metapopulation dynamics. NATURE **396**:41-49.

Hawkins, S. J., K. Bohn, D. W. Sims, P. Ribeiro, J. Faria, P. Presa, A. Pita, G. M. Martins, A. I. Neto, M. T. Burrows, and M. J. Genner. 2016. Fisheries stocks from an ecological perspective: Disentangling ecological connectivity from genetic interchange. Fisheries Research **179**:333-341.

Heino, J., A. S. Melo, T. Siqueira, J. Soininen, S. Valanko, and L. M. Bini. 2015. Metacommunity organisation, spatial extent and dispersal in aquatic systems: patterns, processes and prospects. Freshwater Biology **60**:845-869.

Heinrichs, J.A., Lawler, J.J., and N.H. Schmaker. 2016. Intrinsic and extrinsic drivers of source-sink dynamics. Ecology and Evolution **6**(4):892-904

Hendry, A. P. 2004. Selection against migrants contributes to the rapid evolution of ecologically dependent reproductive isolation. Evolutionary Ecology Research **6**:1219-1236.

Hendry, A. P., F. E. Leonetti, and T. P. Quinn. 1995. Spatial and temporal isolating mechanisms: the formation of discrete breeding aggregations of sockeye salmon (*Oncorhynchus nerka*). Canadian Journal of Zoology **73**:339-352.

ICTRT (Interior Columbia Technical Recovery Team). 2003. Independent populations of Chinook, steelhead, and sockeye for listed Interior Columbia ESUs, working draft. http://www.nwfsc.noaa.gov/trt/col/trt_pop_id.cfm.

ICTRT (Interior Columbia Technical Recovery Team). 2005. Updated population delineation. Addendum to the working draft, Independent populations of Chinook, steelhead, and sockeye for listed Interior Columbia ESUs. http://www.nwfsc.noaa.gov/trt/col/trt_pop_id.cfm.

ICTRT (Interior Columbia Technical Recovery Team). 2007a. Current status assessments and status updates for Snake River spring/summer Chinook populations. Workgroup Draft. http://www.nwfsc.noaa.gov/trt/col/trt_snake_ss_chinook_esu.cfm.

ICTRT (Interior Columbia Technical Recovery Team). 2007b. Viability criteria for application to Interior Columbia Basin salmonid ESUs. Review Draft, March 2007. http://www.nwfsc.noaa.gov/trt/col/trt_viability.cfm.

Isaak, D. J., R. F. Thurow, B. E. Rieman, and J. B. Dunham. 2003. Temporal variation in synchrony among chinook salmon (Oncorhynchus tshawytscha) redd counts from a wilderness area in central Idaho. Canadian Journal of Fisheries and Aquatic Sciences **60**:840-848.

Johnson, R. C., P. K. Weber, J. D. Wikert, M. L. Workman, R. B. MacFarlane, M. J. Grove, and A. K. Schmitt. 2012. Managed metapopulations: do salmon hatchery 'sources' lead to in-river 'sinks' in conservation? PLoS ONE **7**:e28880.

Jones, P. E., and G. P. Closs. 2015. Interspecific differences in larval production and dispersal in non-migratory galaxiids: implications for metapopulation structure. Marine and Freshwater Research **67**:1479-1492.

Jorgensen, J. C., E. J. Ward, M. D. Scheuerell, and R. W. Zabel. 2016. Assessing spatial covariance among time series of abundance. Ecol Evol **6**:2472-2485.

Kallimanis, A. S., W. E. Kunin, J. M. Halley, and S. P. Sgardelis. 2005. Metapopulation extinction risk under spatially autocorrelated disturbance. Conservation Biology **19**:534-546.

Kazyak, D. C., R. H. Hilderbrand, T. L. King, S. R. Keller, and V. E. Chhatre. 2016. Hiding in Plain Sight: A Case for Cryptic Metapopulations in Brook Trout (Salvelinus fontinalis). PLoS ONE **11**:e0146295.

Keefer, M. L., and C. C. Caudill. 2013. Homing and straying by anadromous salmonids: a review of mechanisms and rates. Reviews in Fish Biology and Fisheries **24**:333-368.

Kelson, S. J., A. R. Kapuscinski, D. Timmins, and W. R. Ardren. 2015. Fine-scale genetic structure of brook trout in a dendritic stream network. Conservation Genetics **16**:31-42.

Kitanishi, S., T. Idkeda, and T. Yamamoto. 2017. Short-term temporal instability in fine-scale genetic structure of masu salmon. Freshwater Biology.

Kuligowski, D. R., M. J. Ford, and B. A. Berejikian. 2005. Breeding structure of steelhead inferred from patterns of genetic relatedness among nests. Transactions of the American Fisheries Society **134**:1202-1212.

Landguth, E. L., A. Bearlin, C. C. Day, J. Dunham, and J. Travis. 2016. CDMetaPOP: an individual-based, eco-evolutionary model for spatially explicit simulation of landscape demogenetics. Methods in Ecology and Evolution.

Levins, R. 1970. Extinction. Pages 77-107 *in* M. Gerstenhaber, editor. Mathematical problems in biology. American Mathematical Society, Providence, Rhode Island, USA.

Manel, S., M. K. Schwartz, G. Luikart, and P. Taberlet. 2003. Landscape genetics: combining landscape ecology and population genetics. Trends in Ecology & Evolution **18**:189-197.

Mangel, M., and C. Tier. 1994. Four facts every conservation biologists should know about persistence. Ecology **75**:607-614.

Matthaeus, W. J. 2016. Investigation of fine spatial scale population genetic structure in two Alaskan salmonids. Baylor University, Waco, TX.

McElhany, P., M. H. Ruckelshaus, M. J. Ford, T. C. Wainwright, and E. P. Bjorkstedt. 2000. Viable salmonid populations and the recovery of evolutionarily significant units. NOAA Technical Memorandum NMFS-NWFSC-42. Seattle, WA.

McKinnell, S. M., and O. Karlstrom. 1999. Spatial and temporal covariation in the recruitment and abundance of Atlantic salmon populations in the Baltic Sea. ICES Journal of Marine Science **56**:433-443.

Moore, J. W., M. McClure, L. A. Rogers, and D. E. Schindler. 2010. Synchronization and portfolio performance of threatened salmon. Conservation Letters **3**:340-348.

Moore, J. W., J. D. Yeakel, D. Peard, J. Lough, and M. Beere. 2014. Life-history diversity and its importance to population stability and persistence of a migratory fish: steelhead in two large North American watersheds. Journal of Animal Ecology.

Muneepeerakul, R., S. A. Levin, A. Rinaldo, and I. Rodriguez-Iturbe. 2007. On biodiversity in river networks: A trade-off metapopulation model and comparative analysis. Water Resources Research **43**.

Neville, H. M., J. B. Dunham, and M. M. Peacock. 2006a. Landscape attributes and life history variability shape genetic structure of trout populations in a stream network. Landscape Ecology **21**:901-916.

Neville, H. M., D. J. Isaak, J. B. Dunham, R. F. Thurow, and B. E. Rieman. 2006b. Fine-scale natal homing and localized movement as shaped by sex and spawning habitat in Chinook salmon: insights from spatial autocorrelation analysis of individual genotypes. Molecular Ecology **15**:4589-4602.

NWFSC (Northwest Fisheries Science Center). 2015. Status review update for Pacific salmon and steelhead listed under the Endangered Species Act: Pacific Northwest.

Pess, G. R., R. Hilborn, K. Kloehn, T. P. Quinn, and M. Bradford. 2012. The influence of population dynamics and environmental conditions on pink salmon (*Oncorhynchus gorbuscha*) recolonization after barrier removal in the Fraser River, British Columbia, Canada. Canadian Journal of Fisheries and Aquatic Sciences **69**:970-982.

Peterson, D. A., R. Hilborn, and L. Hauser. 2014. Local adaptation limits lifetime reproductive success of dispersers in a wild salmon metapopulation. Nat Commun **5**:3696.

Peterson, D. A., R. Hilborn, and L. Hauser. 2016. Exploratory behavior of dispersers within a metapopulation of sockeye salmon. Behavioral Ecology **27**:126-133.

Petrou, E. L., J. E. Seeb, L. Hauser, M. J. Witteveen, W. D. Templin, and L. W. Seeb. 2014. Fine-scale sampling reveals distinct isolation by distance patterns in chum salmon (*Oncorhynchus keta*) populations occupying a glacially dynamic environment. Conservation Genetics **15**:229-243.

Policansky, D., and J. J. Magnuson. 1998. Genetics, metapopulations, and ecosystem management of fisheries. Ecological Applications **8**:S119-S123.

Primmer, C. R., A. J. Veselov, A. Zubchenko, A. Poututkin, I. Bakhmet, and M. T. Koskinen. 2006. Isolation by distance within a river system: genetic population structuring of Atlantic salmon, Salmo salar, in tributaries of the Varzuga River in northwest Russia. Molecular Ecology **15**:653-666.

Pulliam, H. R. 1988. Sources, sinks, and population regulation. The American Naturalist **132**:652-661.

Quéméré, E., J.-L. Baglinière, J.-M. Roussel, G. Evanno, P. McGinnity, and S. Launey. 2016. Seascape and its effect on migratory life-history strategy influences gene flow among coastal brown trout (Salmo trutta) populations in the English Channel. Journal of Biogeography **43**:498-509.

Quinn, T. P., R. S. Nemeth, and D. O. Mcisaac. 1991. Homing and Straying Patterns of Fall Chinook Salmon in the Lower Columbia River. Transactions of the American Fisheries Society **120**:150-156.

Quinn, T. P., H. B. Rich, D. Gosse, N. Schtickzelle, and J. Grant. 2012. Population dynamics and asynchrony at fine spatial scales: a case history of sockeye salmon (Oncorhynchus nerka) population structure in Alaska, USA. Canadian Journal of Fisheries and Aquatic Sciences **69**:297-306.

Rieman, B. E., and J. B. Dunham. 2000. Metapopulations and salmonids: a synthesis of life history patterns and empirical observations. Ecology of Freshwater Fish **9**:51-64.

Sandlund, O. T., S. Karlsson, E. B. Thorstad, O. K. Berg, M. P. Kent, I. C. Norum, and K. Hindar. 2014. Spatial and temporal genetic structure of a river-resident Atlantic salmon (Salmo salar) after millennia of isolation. Ecol Evol **4**:1538-1554.

Satterthwaite, W. H., S. M. Carlson, and I. Bradbury. 2015. Weakening portfolio effect strength in a hatchery-supplemented Chinook salmon population complex. Canadian Journal of Fisheries and Aquatic Sciences **72**:1860-1875.

Schick, R. S., and S. T. Lindley. 2007. Directed connectivity among fish populations in a riverine network. Journal of Applied Ecology **44**:1116-1126.

Schindler, D. E., R. Hilborn, B. Chasco, C. P. Boatright, T. P. Quinn, L. A. Rogers, and M. S. Webster. 2010. Population diversity and the portfolio effect in an exploited species. NATURE **465**:609-612.

Schlosser, I. J., and P. L. Angermeier. 1995. Spatial variation in demographic processes of lotic fishes: conceptual models, empirical evidence, and implications for conservation. Pages 392-401 *in* J. L. Nielsen, editor. EVOLUTION AND THE AQUATIC ECOSYSTEM: DEFINING UNIQUE UNITS IN POPULATION CONSERVATION. American Fisheries Society Symposium.

Schtickzelle, N., and T. P. Quinn. 2007. A metapopulation perspective for salmon and other anadromous fish. Fish and Fisheries **8**:297-314.

Seymour, M., and F. Altermatt. 2014. Active colonization dynamics and diversity patterns are influenced by dendritic network connectivity and species interactions. Ecology and Evolution **4**:1243-1254.

Small, M. P., T. H. Johnson, C. Bowman, and E. Martinez. 2014. Genetic assessment of a summer chum salmon metapopulation in recovery. Evol Appl **7**:266-285.

Spruell, P., B. E. Rieman, K. L. Knudsen, F. M. Utter, and F. W. Allendorf. 1999. Genetic population structure within streams: microsatellite analysis of bull trout populations. Ecology of Freshwater Fish **8**:114-121.

Thorson, J. T., M. D. Scheuerell, E. R. Buhle, and T. Copeland. 2014. Spatial variation buffers temporal fluctuations in early juvenile survival for an endangered Pacific salmon. Journal of Animal Ecology **83**:157-167.

Waples, R. 1991. Pacific salmon, *Oncorhynchus* spp., and the definition of 'species' under the endangered species act. Marine Fisheries Review **53**:11-22.

Westley, P. A. H., A. H. Dittman, E. J. Ward, and T. P. Quinn. 2015. Signals of climate, conspecific density, and watershed features in patterns of homing and dispersal by Pacific salmon. Ecology **96**:2823-2833.

Westley, P. A. H., T. P. Quinn, A. H. Dittman, and B. Jonsson. 2013. Rates of straying by hatchery-produced Pacific salmon (*Oncorhynchus* spp.) and steelhead (*Oncorhynchus mykiss*) differ among species, life history types, and populations. Canadian Journal of Fisheries and Aquatic Sciences **70**:735-746.

Whitlock, M. C., and D. E. McCauley. 1999. Indirect measures of gene flow and migration: F-ST not equal 1/(4Nm + 1). Heredity **82**:117-125.

Whitman, R. P., T. P. Quinn, and E. L. Brannon. 1982. Influence of suspended volcanic ash on homing behavior of adult chinook salmon. Transactions of the American Fisheries Society **111**:63-69.

Whitney, J. E., K. B. Gido, T. J. Pilger, D. L. Propst, and T. F. Turner. 2015. Metapopulation analysis indicates native and non-native fishes respond differently to effects of wildfire on desert streams. Ecology of Freshwater Fish **25**:376-392.

Yamamoto, S., K. Morita, I. Koizumi, and K. Maekawa. 2004. Genetic differentiation of white-spotted charr (Salvelinus leucomaenis) populations after habitat fragmentation: Spatial-temporal changes in gene frequencies. Conservation Genetics **5**:529-538.

Yeakel, J. D., J. W. Moore, P. R. Guimaraes, Jr., and M. A. de Aguiar. 2014. Synchronisation and stability in river metapopulation networks. Ecology Letters **17**:273-283.

Young, K. A. 1999. Managing the decline of Pacific salmon: metapopulation theory and artificial recolonization as ecological mitigation. Canadian Journal of Fisheries and Aquatic Sciences **56**:1700-1706.

Zavorka, L., P. Horky, J. Kohout, L. Kalous, and O. Slavık. 2015. Demogenetic structure of brown trout *Salmo trutta* Linnaeus, 1758 populations in mountain headwaters: implications for conservation management. Journal of Applied Ichthyology **31**:501-508.

Zeug, S. C., L. K. Albertson, H. Lenihan, J. Hardy, and B. Cardinale. 2011. Predictors of Chinook salmon extirpation in California's Central Valley. Fisheries Management and Ecology **18**:61-71.

Table 1. The Interior Columbia Technical Recovery Team's spatial structure and diversity viability criteria for major population groups (MPG), and potential metrics for evaluating these criteria using outputs from the AMIP life cycle models.

TRT's MPG Criteria	What We Could Measure
Minimum number (#1): at least two populations meeting abundance & productivity goals	Proportion of historical populations viable over a given time horizon
High viability (#2): at least one highly viable population needed	Proportion of historical populations that are highly viable
Population size (#3): need some large populations	Proportion of historical populations that are large
Life history patterns (#4): all historical major life history patterns represented	Proportion of: • adult migration strategies (late/early) • juvenile migration strategies (parr, yearling) • resident vs. anadromous • natural origin vs hatchery spawners
Maintained populations (#5): maintain "supporting" populations	Fraction of sources (sinks), connected (isolated)
Combined spatial structure & diversity score	Geomean of the 5 component scores

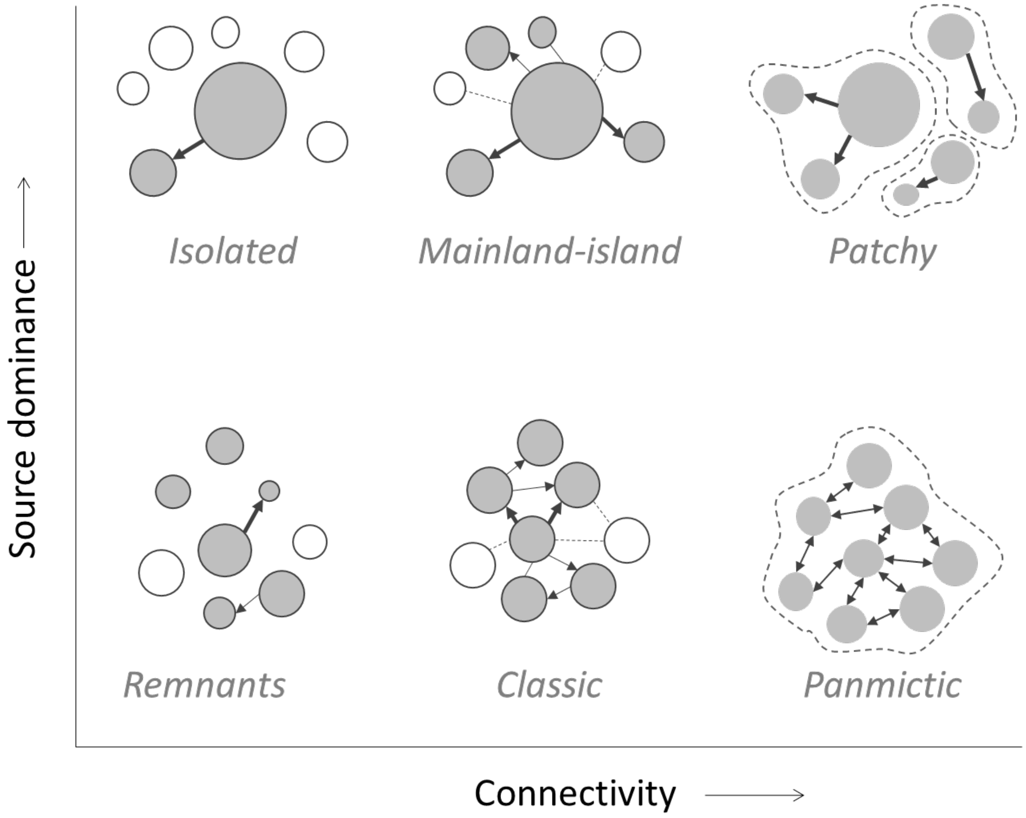

Figure 1. Characterization of various forms of metapopulations. From Fullerton et al. 2016; adapted from Harrison and Taylor 1997.

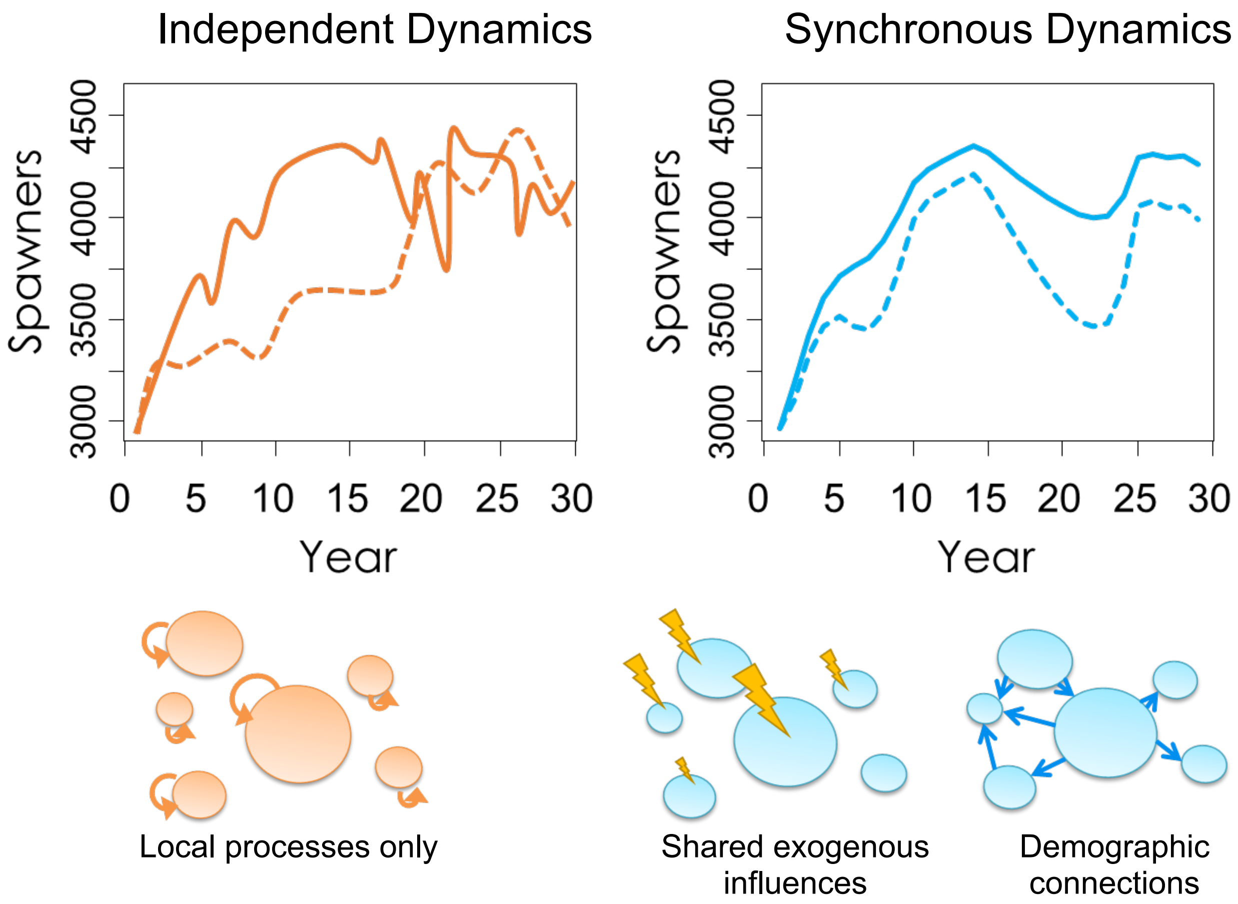

Figure 2. Population dynamics can be unrelated across a suite of independent populations (left) or dynamics can be correlated (right). Correlated dynamics may be driven by shared experiences (i.e., conditions in the ocean and mainstem environments), dispersal of individuals from one population to another, or both.

Chapter 11: Communication with Managers

Introduction

Translating complex scientific and technical information between research scientist and natural resources managers, policy makers and funders (collectively referred to as decision makers, hereafter) is a critical step in advancing theory and study into "on-the-ground" application. In the case of life cycle modeling for salmon and steelhead, this process is especially acute given the considerable policy and social implications of these Endangered Species Act listed fish, a vast northwest-wide and international electrical system with national implications, long term recovery planning and vast financial investments including future revenue impacts. The Adaptive Management Implementation Plan (AMIP) workgroup that is focused on developing, testing and deploying life cycle models (LCMs) has recently added an 'Outreach to Management' subcommittee to begin drafting products, messages and a strategy for communicating outwardly about the progress made to date. The following provides a summary of the subcommittee's basis, approach and draft materials.

Hurdles to Communication

Translating complex research concepts to decision makers and the challenges within such an endeavor are not unique to the Columbia River basin LCM effort. Adapted from Lee and Belohlav 2014 - the fundamental lack of communication between researchers and policymakers serves as a major barrier to understanding. The simple fact of 'running in different circles' and few opportunities to interact on any regular or frequent interval creates a natural void of understanding. It is not uncommon for research and policy timelines to be misaligned or even at cross purposes simply due to different drivers and expectations that are not inherently shared.

In any profession, a certain dialect or vernacular emerges from the environment with the regularity of issues and day-to-day interactions that occurs. In the cases of policy and science, these differences can verge on the appearance, at least, of different languages altogether. It can be inconvenient and at times even counterproductive to a decision maker to grapple with or utilize information that is filled with uncertainty, inconclusive or even contradictory results. These can lead to distrust and the devaluing of what is otherwise very valid research given these are a natural byproduct of rigorous scientific exploration.

Staff turnover due to political processes and term-limits (etc.) as well as turnover in the pool of scientists can serve to erode confidence and relationships that are necessary building blocks to breaking down the barriers to effective communication.

All of these challenges make it increasingly difficult for both parties to: facilitate productive exchange of ideas and information; identify, frame, and relay actionable messages that are appropriate for the intended audiences; and, measure/evaluate the impact of research evidence on decision making.

Figure 1.

Salmon and Steelhead LCM Case Study

In the case of salmon and steelhead LCMs, a communication effort with decision makers is especially confounded by several fundamental aspects of the species' life history. Given that there are several different species of salmon, seven life cycle stages, numerous life history strategies, migration over the course of as many as five years-crossing state boundaries and into the ocean and back to freshwater tributaries, and a massive hydro-electric dam and river management system on the Columbia and Snake rivers to navigate, it is not surprising that many questions arise about how and to what extent LCMs will account for these factors.

Other complexities that are built into the replication of the fishes' experiences in LCMs include habitat conditions, harvest by humans, predations by mammals and birds, toxics and other water quality factors, water quantity and river operations, all within a changing climate. Figure 1 attempts to depict many of these influences and challenges relative to the salmon and steelhead life cycle-from egg to returning adult.

AMIP Subcommittee Approach

The subcommittee and associated entities it is comprised of has developed a multi-pronged approach to enhancing the opportunities for communication about both the LCMs as well as their results. The following outline depicts the fundamental principles and goals that the group has employed:

- Ensure opportunities for personal contact between researchers and policymakers. *Several presentations have been given to policymaking and other decision making bodies by the co-leaders of the AMIP LCM workgroup. Other opportunities are anticipated over the coming year.*
- Purposely plan the timelines and focus of the LCM effort to maximize the relevance of the research. *The AMIP process was a direct outgrowth of regulatory mandates and processes related to the Federal Columbia River Power System Biological Opinion and the topics and focal areas of the LCMs are designed to be specifically used in that framework as well as for Recovery Planning. In addition, the LCM framework and the manner in which the component parts will be used together are structured to tackle key management questions in both major processes. The timeline of development, testing and generating outputs from the LCMs is structured around the needs of the regulatory timeline. The review requested of the ISAB also assists significantly toward both attaining the timeline goal as well as sharpening the relevance questions.*
- Develop materials that contain discrete messages geared toward specific audiences. *The workgroup elected to begin drafting 3 tiers of 'fact sheets' that are designed for different audiences trending from simple to more in-depth messages. In addition maps have been drafted to assist with depicting where life cycle models area available, for what species and where there are gaps.*

  Tier 1 messages (Simple overview fact sheet):

  - What are they?
  - How are they an advancement from before?
  - What are they used for?
  - How are they used all together?

  Tier 2 messages (Integration and more detailed fact sheet):

  - More detail about how life cycle models work together
  - More on outputs
  - Move away from single populations to meta-populations

  Tier 3 messages (Detailed fact sheet for each model/geography): - - -

  - Overview of individual models
  - Focus on parameters
  - Outputs & relationship to other models
  - Knowledge gaps

  - Uncertainties

- Inclusion of a summary with clear recommendations. *The request of the ISAB to review the LCMs and the framework as well as through this composite report, in combination, will be significant contributions toward attaining this goal.*

Draft Products

- Attachment 1 depicts the draft Tier 1 fact sheet designed to introduce LCMs to the reader and to deliver *high level overview* messages.

- The figure below depicts the life cycle models that have been developed for Chinook salmon and the type of model within each basin.

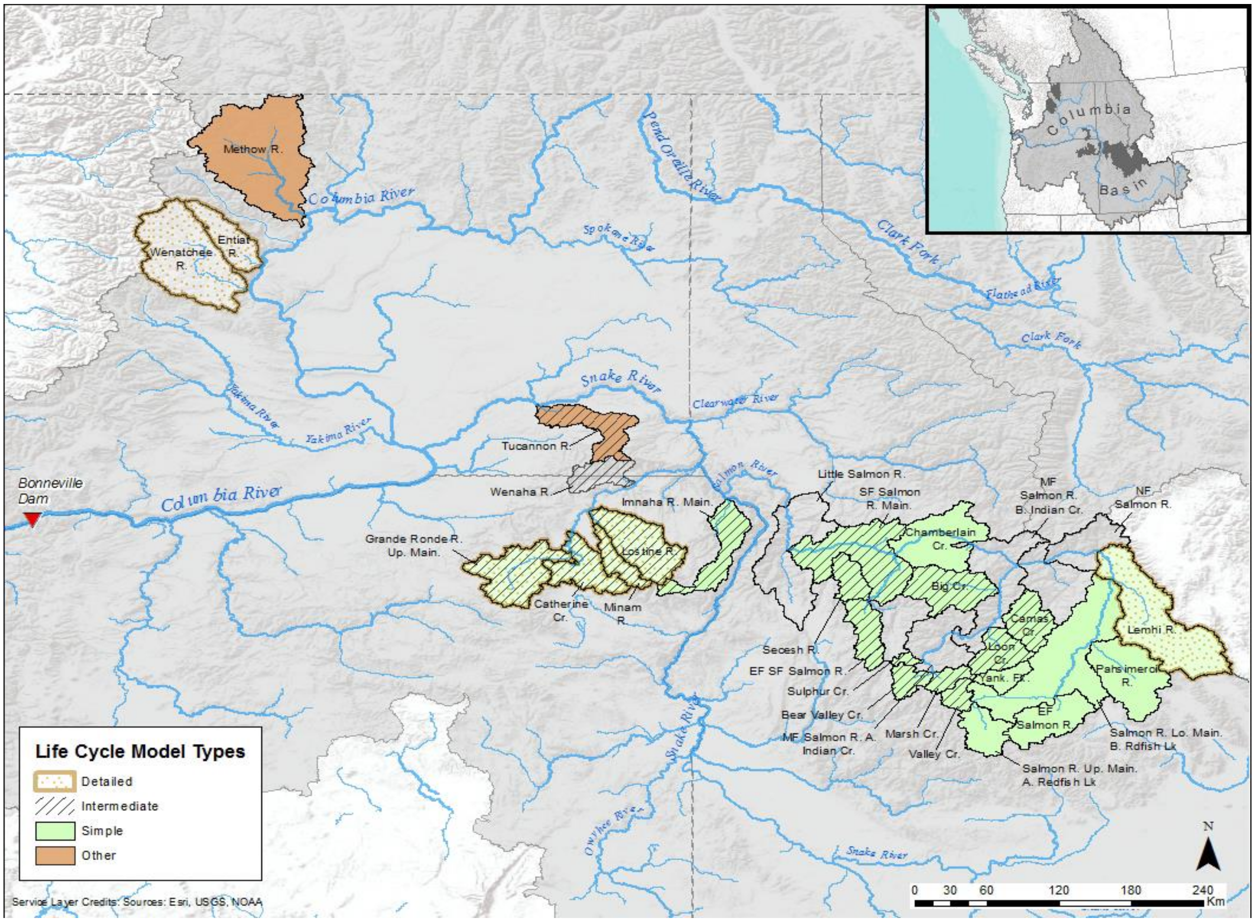

Figure 3.

- Figure below depicts the life cycle models that have been developed for Steelhead and the type of model within each basin.

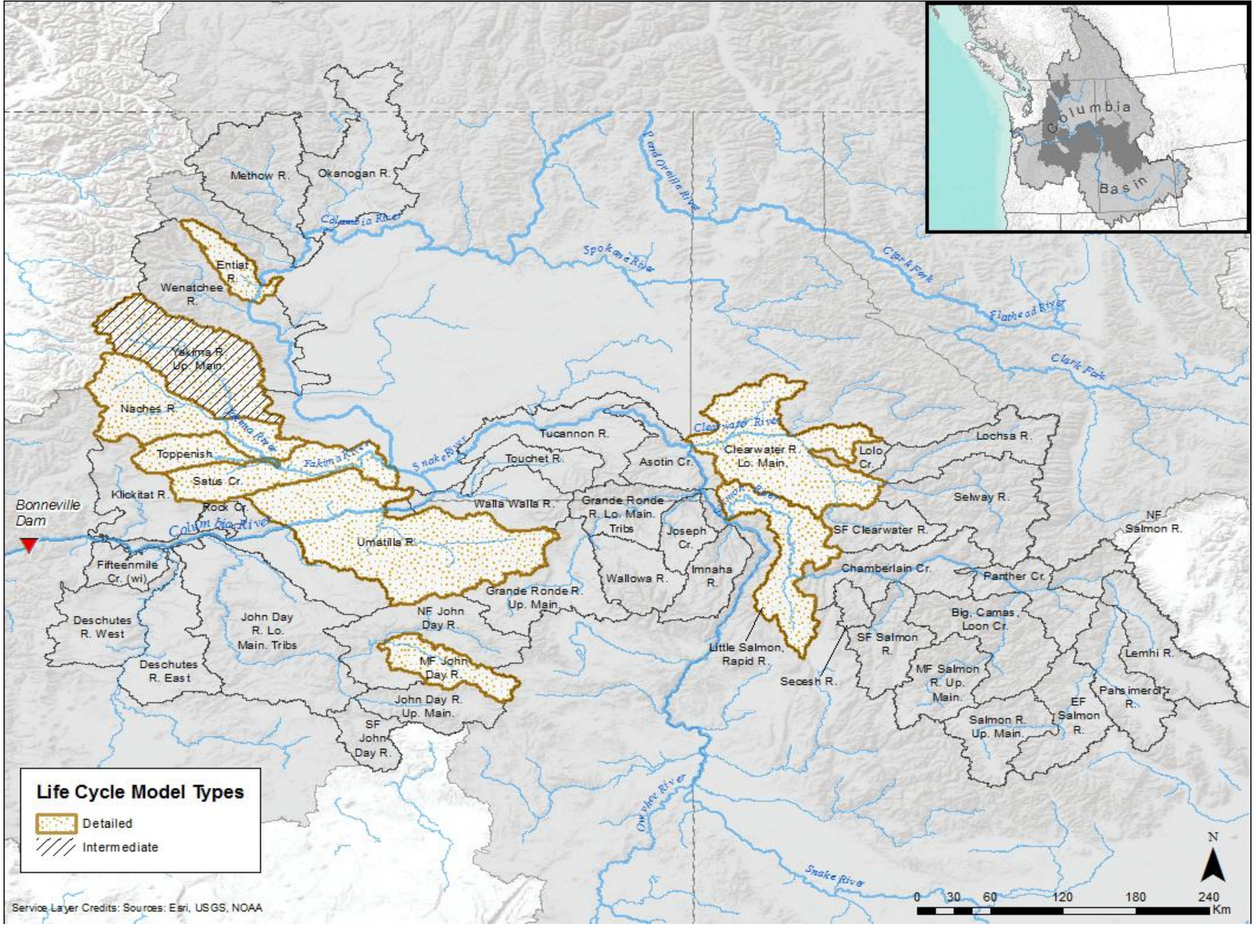

Figure 4.

Next Steps and Request of ISAB

The Northwest Fisheries Science Center developed a specific list of questions that are requested of the ISAB, under accompanying letterhead, to delve into when reviewing this report. Due to the ISAB's expertise and experience in developing observation and advice for the Northwest Power Conservation Council and other bodies in other arenas, we welcome observations and recommendations about the concepts and approaches outlined above describing the current efforts of the AMIP workgroup.

Presently, we have the following questions that have either already been raised by decision makers and those that are familiar with the LCM program or we anticipate these to be on the near horizon.

Questions from decision makers:

- How many models do we need?
- Geographically speaking, where are they? Where are they not?
- How will the models be used together?
- What are the indications that the models are an advancement of past work/types of analyses?
- What role will the models play in Recovery Plan implementation and the FCRPS Biological Opinions?
- Can the models assist in evaluating progress toward or limitations in attaining accomplishments?
- Will the models be helpful in prioritizing actions?

Given the ISAB's role and breadth of its membership, we anticipate additional added value and thank you, in advance, for any feedback that could be used to help in adequately and effectively placing the LCMs in the hands of policymakers, natural resources managers, and funders.

References

Lee, M. and K. Belohlav 2014. Communicating Research to Policymakers: Researchers' Experiences. Population Reference Bureau, Washington, DC. 9 pp.

Attachment 1.